



UNIVERSITY OF
LIVERPOOL

**INVESTIGATIONS ON THE EFFECT OF FASTING
ON LIVER FUNCTION AND THE RESPONSE TO
ACETAMINOPHEN OVERDOSE IN TWO MOUSE MODELS**

Thesis submitted in accordance with the requirements of the University of Liverpool
for the degree of Doctor in Philosophy

By

Nur Fazila Binti Saulol Hamid

March 2016

AUTHOR'S DECLARATION

Apart from the help and advice acknowledged, this thesis represents the unaided work of the author

.....

Nur Fazila Binti Saulol Hamid

March 2016

This research was carried out in the Department of Infection Biology, Institute of Infection and Global Health, the Department of Pharmacology and Therapeutics, Institute of Translational Medicine, and the School of Veterinary Science, University of Liverpool

LIST OF CONTENTS

ABSTRACT	iv
ACKNOWLEDGEMENTS	vi
LIST OF FIGURES	vii
LIST OF TABLES	xi
LIST OF ABBREVIATIONS	xiv
CHAPTER ONE Introduction	1
CHAPTER TWO Materials and Methods	44
CHAPTER THREE Results	64
CHAPTER FOUR Discussion and Conclusions	194
CHAPTER FIVE Bibliography	229
CHAPTER SIX Appendix	250

ABSTRACT

Investigations on the effect of fasting on liver function and the response to acetaminophen overdose in two mouse models

Hamid NF^{1,2,3}, Williams D², Antoine D², Benson C², Webb H², Starkey-Lewis P², Kipar A^{1,2,3}
¹*Department of Infection Biology, Institute of Infection and Global Health,* ²*Department of Pharmacology and Therapeutics, Institute of Translational Medicine, and* ³*School of Veterinary Science, University of Liverpool, UK*

Laboratory mice are widely used in biomedical research as models for human diseases and also to provide insight into the toxicity of various xenobiotics. Fasting of mice prior to dosing is common practise in toxicological studies to ensure uniform drug absorption. However, many studies ignore the potential effect of fasting on parameters that are affected by the circadian rhythm. Model hepatotoxicants like acetaminophen (APAP) are commonly used to provide better insight into, for example, chemical structure, drug metabolism and the response of cells to toxicants. The APAP mouse model has been extensively used for studies on pathogenesis and intervention of drug induced liver injury (DILI) based on the CYP450 mediated formation of N-acetyl-p-benzo-quinoneimine (NAPQI). More recently, it also served for the identification of new biomarkers for liver injury. In addition, it can also serve to gain further insight into liver regeneration, the mechanisms of which need to be further elucidated. So far, liver regeneration has mainly been studied in partial hepatectomy (PHx) models, which could have a different mechanism than regeneration after DILI. The work presented in this thesis has used two mouse models, out-bred CD-1 and in-bred C57BL/6J mice to investigate the differences in their response to APAP overdose and the effect of fasting prior to dosing. This was done over a time course expected to cover both acute liver injury and regeneration.

The results on saline dosed control mice show that fasting alone significantly reduces the body weight (up to 12%) with onset of the fasting period during day time (16:00 to 18:45). Interestingly, C57BL/6J mice have higher basic hepatic GSH levels than CD-1 mice. While the hepatic GSH content followed a circadian rhythm in fed mice, it overshot in animals refed after fasting. In contrast, the restitution of ATP after feeding was slow in CD-1 mice where even after 24 hours of refeeding the ATP levels were still lower than in fed mice. In fasted C57BL/6J mice, however, they returned to control animal levels within 20 hours of refeeding. Surprisingly, after 10 hours of refeeding, the GSH levels showed a significantly higher fold increase than the ATP levels in both strains. Fasting did not induce any histopathological changes, however there was evidence of complete hepatocellular glycogen depletion after fasting and full glycogen restitution within 1 hour of refeeding in C57BL/6J mice but 4 hours in CD-1 mice. Fasting neither had an effect on the transcription of cytokines TNF- α , IL-6, and IL-10 nor on hepatocellular proliferation, assessed on the basis of NF-kB and cyclin-D1 transcription and in situ PCNA expression.

The determination of the hepatic GSH and ATP content, serum ALT levels and the histopathological changes with an established scoring system served to assess the extent of liver injury following APAP overdose. A reduction of the GSH content was observed as early as 1 hour post dosing (hpd) in CD-1 mice and at 3 hpd in C57BL/6J

mice; after that the levels increased gradually again until the end of the study period. In fasted CD-1 mice, GSH levels returned to control levels with delay; this was variable in C57BL/6J mice until the levels were similar to those of control animals at 36 hpd. ATP levels remained lower in fasted mice of both strains over the entire time course. In both strains, APAP overdose resulted in a progressive increase in serum ALT activity with significantly higher levels in fasted mice at the later time points. This was matched by the histological findings, i.e. centrilobular hepatocyte loss. In fed mice, cell death via apoptosis was initially seen and most abundant at 3 and 5 hpd in CD-1 mice. However, in C57BL/6J, only a few individual apoptotic hepatocytes were seen in the affected centrilobular areas at 5 hpd, whereas they were abundant in the same location at 24 hpd. The first sign of liver damage was the centrilobular loss of hepatocellular glycogen, a feature that remained obvious until the pathological changes resolved. Fasting of mice prior to APAP overdose led to similar, though more severe changes, whereby cell death was almost exclusively via necrosis with a variably intense centrilobular neutrophil infiltration. At 15 hpd, histology showed that the damage had subsided in fed CD-1 mice, in association with increased proliferation and evidence of full regeneration including complete glycogen reconstitution at 24 hpd. In C57BL/6J mice, there was prolonged evidence of centrilobular hepatocyte degeneration and death, by both apoptosis and coagulative necrosis, which declined but was still present at 36 hpd. In fasted mice of both strains, there was evidence of substantial ongoing hepatocyte death and neutrophil recruitment until the end of the study at 24 and 36 hpd, respectively, together with delayed hepatocyte proliferation.

The extent of the inflammatory response after APAP-induced DILI and the regenerative capacity of the liver were assessed via the quantitative assessment of the transcription of the cytokines TNF- α , IL-6 and IL-10, and the transcription factor NF- κ B and cell cycle protein, cyclin-D1 in the liver and, for TNF- α and IL-6, the spleen, using RT-qPCR. Fed animals showed early upregulation of hepatic TNF- α , obvious at 5 hpd in CD-1 and at 10 hpd in C57BL/6J mice, with levels dropping thereafter. In fasted mice, a further increase was seen after these time points, correlating also with the more pronounced neutrophil influx. Splenic TNF- α transcription seemed to follow the hepatic transcription alongside serum protein levels that were continuously elevated at the later time points, suggesting systemic effect. Fed mice, and in particular CD-1 mice, showed higher hepatic and splenic IL-6, IL-10, NF- κ B and cyclin-D1 mRNA levels than fasted mice, correlating with effective liver regeneration. In fasted mice of both strains, the transcription of these markers started to increase only towards the end of the study period. The quantitative assessment of hepatocyte proliferation, based on the in situ expression of PCNA, confirmed the earlier onset and faster liver regeneration in fed animals, with an earlier onset also in fed CD-1 mice than in fed C57BL/6J mice.

In conclusion, the results of the present study confirm circadian rhythms for body weight and hepatic GSH and ATP content, features that could interfere with study outcomes. They also provide definite evidence that fasting prior to APAP overdose does not only modulate the resulting liver injury, but has further effects, i.e. the induction of an inflammatory response and a delay in the subsequent liver regeneration. Finally, they confirm that the inbred C57BL/6J mice are more susceptible to APAP-induced DILI when fed prior to dosing, but show that both strains react in a similar way when dosed after a period of fasting.

ACKNOWLEDGEMENTS

It has been a great opportunity for me to pursue the study for a PhD degree in the University of Liverpool, UK. To be honest, living and studying in a country with a different language (Scouse), weather and food is quite challenging, but the support and help from a large number of individual people and organisations eased my PhD journey up to the end.

First and foremost, I would like to express my deep sense of gratitude to my supervisors, Prof Anja Kipar, Dr Dominic Williams, Prof James Stewart and Dr Daniel Antoine for their valuable supervision and guidance through all steps of my PhD works, especially Prof Anja Kipar for her hard work in critically reading and directing me in thesis writing, I shall never forget those favours.

My heartfelt thanks also for all the people in Department of Pharmacology and Therapeutics, especially Phil Starkey Lewis, Hayley Webb, Craig Benson, Aine Norton, Alison Rodrigues, Phil Roberts, and Sophie Regan who helped me a lot by providing skills and scientific knowledge involving laboratory mouse experiments. Also, special thanks to Julie Haigh for spending many hours, days and nights at the BSU, collecting samples with me.

I am indebted to staff in the Histology Laboratories in the School of Veterinary Science at Leahurst campus who have put up with me for three years, especially Valerie Tilston and again Julie Haigh. I would also like to acknowledge the people in the Department of Infection Biology who have encouraged and supported me throughout the laboratory work, and any assistance I needed, especially Nathifa Moyo and Catherine Hartley for being so helpful. Special thanks also to Adina Najwa that provide guidance in statistical analysis.

A heartfelt thank you to my friends for their friendship and scientific support including Juriah, Zuliza, Kittichai, Sarah, Patrick, Dashty and many others, who made my stay in Liverpool joyful and full of happy memories. I appreciate the multiple scientific discussions we had over the years and the time they have taken to help me progress.

I am profoundly grateful to the Ministry of Higher Education Malaysia for financially supporting my studentship and University Putra Malaysia, especially the Dean of the Faculty of Veterinary Medicine, for allowing me to pursue my doctorate studies in the UK during the entire tenure of my study.

Last but not least, a very special thank you to my husband, Kamarulnizam, and kids, Amyra and Adam, for being by my side through all the highs, lows and in-betweens of my PhD journey. Finally, I greatly thank my beloved parents, Saulol Hamid and Faridah, siblings, Manja and Faizal, and the rest of my big family (Che Tom's family) and also my family-in-law, whose unwavering love and support made this goal in my life possible. Without all their encouragement and advice, it would be impossible to make my study journey this far.

LIST OF FIGURES

Figure 1.1. Schematic diagramme of the effect of food restriction in the laboratory mouse.	8
Figure 1.2. Acetaminophen induced hepatocellular injury.	18
Figure 1.3. Metabolism of APAP-induced hepatotoxicity.	21
Figure 1.4. Pathogenesis of APAP hepatotoxicity.	28
Figure 1.5. The role of NF-kB in liver regeneration.	35
Figure 1.6. PCNA cell-cycle phases.	40
Figure 3.1.1. Percentage of body weight loss in male CD-1 and C57BL/6J mice after fasting, in relation to the time of day at the onset of the fasting period.	69
Figure 3.1.2. Hepatic GSH content in fed CD-1 and C57BL/6J mice at different times of day.	70
Figure 3.1.3. Hepatic GSH content in male CD-1 (A) and C57BL/6J (B) mice that had been fed ad libitum or fasted for 16 h or 24 h and then refed for variable time spans.	72
Figure 3.1.4. Hepatic ATP levels in saline dosed male CD-1 and C57BL/6J mice.	75
Figure 3.1.5. Hepatic GSH and ATP content (fold changes in comparison to fed mice) in male CD-1 and C57BL/6J mice.	77
Figure 3.1.6. Serum ALT levels in fed and fasted CD1 and C57BL/6J mice.	79
Figure 3.1.7. Histological features and glycogen content in fed and fasted CD-1 and C57BL/6J mice.	81
Figure 3.1.8. Hepatocellular glycogen content in CD-1 and C57BL/6J mice that have been refed for 30 and 60 minutes.	82
Figure 3.1.9. Hepatic TNF- α , IL-6 and IL-10 transcription in saline dosed CD-1 and C57BL/6J mice (delta Ct method).	84
Figure 3.1.10. Hepatic TNF- α , IL-6 and IL-10 transcription in fasted saline dosed CD-1 and C57BL/6J mice (fold change method).	85
Figure 3.1.11. Serum TNF- α and IL-6 levels in fed and fasted CD-1 and C57BL/6J mice.	88
Figure 3.1.12. Changes in hepatic transcription of NF-kB and cyclin-D1 in fasted compared to fed male CD-1 and C57BL/6J mice.	90
Figure 3.1.13. PCNA expression pattern in hepatocytes.	91
Figure 3.2.1. Hepatic GSH levels (nmol/mg) in fed male CD-1 mice after APAP treatment.	94
Figure 3.2.2. Hepatic GSH levels (nmol/mg) in fasted male APAP dosed CD-1 mice.	95
Figure 3.2.3. Comparison of hepatic GSH levels (nmol/mg) in fed and fasted male APAP dosed CD-1 mice.	96
Figure 3.2.4. Hepatic ATP levels (nmol/mg) after APAP dosing of fed and fasted CD-1 mice.	98
Figure 3.2.5. Hepatic ATP and GSH levels in male CD-1 mice after APAP overdose.	100
Figure 3.2.6. Serum ALT levels (U/L) after APAP overdose in male fed CD-1 mice.	101

Figure 3.2.7. Serum ALT levels (U/L) after APAP-induced liver injury in fasted CD-1 mice.	102
Figure 3.2.8. Serum ALT levels (U/L) after APAP-induced liver injury in CD-1 mice.	102
Figure 3.2.9. Histological scoring in CD-1 mice after APAP overdose.	108
Figure 3.2.10. Assessment of histopathological features and glycogen content in fed and fasted male CD-1 mice at 3 h post APAP (530 mg/kg) treatment.	109
Figure 3.2.11. Assessment of histopathological features and glycogen content in fed and fasted male CD-1 mice at 5 h post APAP (530 mg/kg) treatment.	110
Figure 3.2.12. Assessment of histopathological features and glycogen content in fed and fasted male CD-1 mice at 10 h post APAP (530 mg/kg) treatment.	111
Figure 3.2.13. Assessment of histopathological features and glycogen content in fed and fasted male CD-1 mice at 24 h post APAP (530 mg/kg) treatment.	112
Figure 3.2.14. Assessment of liver damage in male fed and fasted CD-1 mice following APAP dosing.	114
Figure 3.2.15. Hepatic TNF- α , IL-6 and IL-10 transcription levels after APAP dosing of fed and fasted male CD-1 mice.	116
Figure 3.2.16. Hepatic TNF- α , IL-6 and IL-10 transcription levels in fed and fasted male CD-1 mice after APAP dosing.	118
Figure 3.2.17. Hepatic TNF- α , IL-6 and IL-10 transcription levels in fed and fasted male CD-1 mice after APAP dosing.	120
Figure 3.2.18. Splenic TNF- α and IL-6 transcription in male CD-1 mice that had been either fed or fasted prior to APAP dosing.	122
Figure 3.2.19. Splenic TNF- α and IL-6 transcription of in APAP dosed CD-1 mice.	123
Figure 3.2.20. Serum TNF- α and IL-6 levels in control and APAP dosed male CD-1 mice.	125
Figure 3.2.21. Hepatic NF- κ B transcription in control and APAP dosed CD-1 mice.	127
Figure 3.2.22. Hepatic transcription of cyclin-D1 in male CD-1 mice.	129
Figure 3.2.23. Immunohistological demonstration of PCNA expression in the liver of fed and fasted APAP dosed male CD-1 mice.	131
Figure 3.2.24. Assessment of proliferating hepatocytes, based on the expression of proliferating cell nuclear antigen (PCNA).	132
Figure 3.2.25. Assessment of hepatocytes exhibiting cytoplasmic PCNA expression.	133
Figure 3.2.26. Assessment of hepatocytes exhibiting PCNA expression.	134
Figure 3.2.27. Assessment of liver regeneration in fed and fasted male CD-1 mice.	136
Figure 3.3.1. Hepatic GSH levels (nmol/mg) in fed male C57BL/6J mice after APAP treatment and comparison to fed CD-1 mice.	139
Figure 3.3.2. Hepatic GSH levels (nmol/mg) in fasted male C57BL/6J after APAP treatment and comparison to fasted CD-1 mice.	141
Figure 3.3.3. Hepatic ATP levels (nmol/mg) in fed male C57BL/6J mice after APAP treatment and comparison to fed CD-1 mice.	143
Figure 3.3.4. Hepatic ATP levels (nmol/mg) in fasted male C57BL/6J mice after APAP treatment and comparison to fasted CD-1 mice.	144

Figure 3.3.5. Hepatic ATP and GSH levels in male C57BL/6J mice after APAP overdose and comparison to CD-1 mice.	147
Figure 3.3.6. Serum ALT levels (U/L) in male fed C57BL/6J mice after APAP overdose and comparison to fed CD-1 mice.	149
Figure 3.3.7. Serum ALT levels (U/L) in fasted male C57BL/6J mice after APAP overdose and comparison to fasted CD-1 mice.	150
Figure 3.3.8. Histological scoring in fed C57BL/6J mice after APAP overdose and comparison to the scores in CD-1 mice.	154
Figure 3.3.9. Histological scoring in fasted male C57BL/6J and CD-1 mice after APAP overdose.	156
Figure 3.3.10. Assessment of histopathological features and glycogen content in fed and fasted C57BL/6J mice with comparison to CD-1 mice at 3 hours post APAP (530 mg/kg) treatment.	157
Figure 3.3.11. Assessment of histopathological features and glycogen content in fed and fasted C57BL/6J mice at 24 h post APAP (530 mg/kg) treatment.	158
Figure 3.3.12. Assessment of histopathological features and glycogen content in fed C57BL/6J and CD-1 mice at 24 hours post APAP (530 mg/kg) treatment.	159
Figure 3.3.13. Assessment of histopathological features and glycogen content in fasted C57BL/6J and CD-1 mice at 24 hours post APAP (530 mg/kg) treatment.	160
Figure 3.3.14. Assessment of histopathological features and glycogen content in fed and fasted C57BL/6J at 36 hours post APAP (530 mg/kg) treatment.	161
Figure 3.3.15. Assessment of liver damage in fed and fasted male C57BL/6J and CD-1 mice after APAP dosing.	163
Figure 3.3.16. Hepatic TNF- α , IL-6 and IL-10 mRNA levels in control and APAP dosed fed and fasted male C57BL/6J mice over 1-36 hpd.	164
Figure 3.3.17. Fold changes in hepatic TNF- α transcription levels in fed and fasted APAP dosed C57BL/6J mice and comparison to CD-1 mice.	166
Figure 3.3.18. Fold changes in hepatic TNF- α transcription levels in fed and fasted APAP dosed C57BL/6J mice and comparison to CD-1 mice.	167
Figure 3.3.19. Fold changes in hepatic IL-6 transcription levels in fed and fasted APAP dosed C57BL/6J mice and comparison to CD-1 mice.	168
Figure 3.3.20. Fold changes in hepatic IL-6 transcription levels in fed and fasted APAP dosed C57BL/6J mice and comparison to CD-1 mice.	169
Figure 3.3.21. Fold changes in hepatic IL-10 transcription levels in fed and fasted APAP dosed C57BL/6J mice and comparison to CD-1 mice.	171
Figure 3.3.22. Fold changes in hepatic IL-10 transcription levels in fed and fasted APAP dosed C57BL/6J mice and comparison to CD-1 mice.	172
Figure 3.3.23. Fold change in splenic TNF- α and IL-6 transcription levels after APAP dosing in C57BL/6J mice and comparison to CD-1 mice.	173
Figure 3.3.24. Serum TNF- α level in fed male C57BL/6J mice.	175
Figure 3.3.25. Serum TNF- α level in C57BL/6J mice, and comparison to CD-1 mice.	177
Figure 3.3.26. Serum IL-6 levels in fed male C57BL/6J mice.	178
Figure 3.3.27. Serum IL-6 levels in C57BL/6J mice, and comparison to CD-1 mice.	180

Figure 3.3.28. Hepatic NF-kB transcription in fed and fasted C57BL/6J mice and comparison to CD-1 mice.	182
Figure 3.3.29. Hepatic NF-kB transcription in APAP dosed male C57BL/6J mice.	183
Figure 3.3.30. Hepatic cyclin-D1 transcription in fed and fasted C57BL/6J mice and comparison to CD-1 mice.	185
Figure 3.3.31. Hepatic cyclin-D1 transcription in APAP dosed C57BL/6J mice and comparison to CD-1 mice.	186
Figure 3.3.32. Immunohistological demonstration of PCNA expression in the liver of fed and fasted male C57BL/6J and CD-1 mice at 24 hpd.	188
Figure 3.3.33. Assessment of proliferating hepatocytes, based on the expression of proliferating cell nuclear antigen (PCNA) and comparison to CD-1 mice.	189
Figure 3.3.34. Assessment of hepatocytes exhibiting cytoplasmic PCNA expression and comparison to CD-1 mice.	190
Figure 3.3.35. Assessment of hepatocytes exhibiting PCNA and cytoplasmic PCNA expression in C57BL/6J and CD-1 mice after APAP dosing.	191
Figure 3.3.36. Assessment of liver regeneration in male fed and fasted C57BL/6J and CD-1 mice after APAP dosing.	193
Figure 4.1. Schematic diagramme of mechanisms involved in APAP induced toxic liver injury and subsequent regeneration.	224

LIST OF TABLES

Table 1.1. Experimental models of APAP-induced liver toxicity and regenerative response.	37
Table 2.1. Serum ALT dilution measurement	48
Table 2.2. Standards for the glutathione assay	49
Table 2.3. Standard of Lowry assay	50
Table 2.4. Standard of ATP assay	51
Table 2.5. Scoring of histological changes in murine livers	53
Table 2.6. Antigen retrieval methods	54
Table 2.7. Summary of antibodies used, antigen retrieval methods, detection systems and the staining result	55
Table 2.8. Primer sequences for the detection of TNF- α , IL-6, IL-10, cyclin-D1, NF-kB and GAPDH by PCR and real-time PCR	60
Table 2.9. Cycling condition, temperature and time used for qPCR analysis.	62
Table 3.1.1. Mean body weight (g) of fed male CD-1 and C57BL/6J mice at different times of day, immediately prior to saline dosing.	69
Table 3.1.2. Mean body weight loss (g), standard deviation and p-value of fasted male CD-1 and C57BL/6J mice prior and immediately after the fasting period, at different times of day.	69
Table 3.1.3. Mean hepatic GSH levels (nmol/mg) in fed male CD-1 and C57BL/6J mice.	71
Table 3.1.4. Hepatic ATP levels (nmol/mg) in fed and fasted CD-1 mice at the different time points post saline application.	73
Table 3.1.5. Hepatic ATP levels (nmol/mg) in fed and fasted C57BL/6J mice at the different time points post saline application and comparison to time matched CD-1 mice.	74
Table 3.1.6. Hepatic GSH and ATP content after fasting in CD-1 and C57BL/6J mice.	76
Table 3.1.7. Serum ALT levels (U/L) in fed and fasted male CD-1 mice.	78
Table 3.1.8. Serum ALT levels (U/L) in fed and fasted C57BL/6J mice.	78
Table 3.1.9. Pooled serum ALT levels at all time points in saline dosed CD-1 and C57BL/6J mice.	80
Table 3.1.10. Relative transcription levels of TNF- α , IL-6 and IL-10 in fed or fasted CD-1 and C57BL/6J mice using the comparative Ct value method (fold change).	85
Table 3.1.11. Comparison of relative transcription levels ($2^{-\Delta\Delta Ct}$) and fold change ($2^{-\Delta\Delta Ct}$ fasted/fed) of TNF- α and IL-6 in the spleen of fed and fasted male CD-1 mice over a 24 h time period after i.p. application of 0.9% saline (and refeeding).	86
Table 3.1.12. Comparison of relative transcription levels ($2^{-\Delta\Delta Ct}$) and fold change ($2^{-\Delta\Delta Ct}$ fasted/fed) of TNF- α and IL-6 in the spleen of fed and fasted male C57BL/6J mice over a 24 h time period after i.p. application of 0.9% saline (and refeeding).	86
Table 3.1.13. Serum TNF- α and IL-6 levels (pg/mL) in fed and fasted male CD-1 mice.	87

Table 3.1.14. Serum TNF- α and IL-6 levels (pg/mL) in saline dosed C57BL/6J mice.	87
Table 3.1.15. Comparison of serum TNF- α and IL-6 levels (pg/mL) in fed and fasted CD-1 and C57BL/6J mice.	89
Table 3.1.16. Comparison of the amount of proliferating hepatocytes (nuclear and cytoplasmic PCNA expression; "PCNA +") and hepatocytes that were prior to/in mitosis (cytoplasmic PCNA expression; "cytopl +") in CD-1 and C57BL/6J mice that had been fed ad libitum or fasted, immediately after saline dosing (0 hours of refeeding).	92
Table 3.2.1. Comparison of mean GSH levels (nmol/mg) in fed control and APAP dosed mice over a 24 hour period.	94
Table 3.2.2. Comparison of mean GSH levels (nmol/mg) in mice that had been fasted for 16 h (24 h) and then dosed with APAP or 0.9% saline (control mice) and fed ad libitum again, over a 24 hour period.	95
Table 3.2.3. Comparison of mean GSH levels (nmol/mg) in mice that had been fed or fasted prior to APAP dosing, over a 24 hours period.	96
Table 3.2.4. Hepatic ATP levels (nmol/mg) in fed CD-1 mice with p-value at the different time points post saline application (control) and APAP dosing.	97
Table 3.2.5. Hepatic ATP levels (nmol/mg) in fasted CD-1 mice with p-value at the different time points post saline application (control) and APAP dosing.	98
Table 3.2.6. Comparison of fold changes in hepatic GSH and ATP levels in fed and fasted, APAP dosed male CD-1 mice.	99
Table 3.2.7. Mean serum ALT levels (U/L) with standard deviation (SD) in fed control (0.9% saline) and APAP dosed mice at different times post dosing.	100
Table 3.2.8. Mean serum ALT levels (U/L) with standard deviation (SD) in fasted control (0.9% saline) and APAP dosed mice at 5 and 24 hpd.	101
Table 3.2.9. Mean serum ALT levels (U/L) with standard deviation (SD) in fed and fasted APAP dosed mice at 5 and 24 hpd.	102
Table 3.2.10. Histological findings in APAP dosed fed male CD-1 mice (time course).	104
Table 3.2.11. Histological scores in APAP dosed fed CD-1 mice (time course).	105
Table 3.2.12. Histological findings in APAP dosed fasted male CD-1 mice (time course).	106
Table 3.2.13. Histological scores in APAP dosed fasted CD-1 mice (time course).	107
Table 3.2.14. Comparison of histological scores in APAP dosed fed and fasted male CD-1 mice (time course).	107
Table 3.2.15. Comparison of GSH, ATP, ALT fold changes and DILI scores in male fed and fasted CD-1 mice following APAP insult.	113
Table 3.2.16. Comparison of serum TNF- α and IL-6 levels in control and APAP treated fed and fasted CD1 mice. Data is given as mean SD of 4 mice per group.	124
Table 3.2.17. Fold change of the levels of TNF- α , IL-6, IL-10, NF-kB, cyclin-D1 and PCNA expression in male fed and fasted CD-1 mice following APAP dosing.	136
Table 3.3.1. Mean GSH content (nmol/mg) with standard deviation (SD) in fed control (saline dosed) and APAP dosed male C57BL/6J mice at different times post dosing, with a comparison to the values obtained in CD-1 mice.	138

Table 3.3.2. Mean hepatic GSH content (nmol/mg) with standard deviation (SD) in control and APAP treated fasted C57BL/6J at different times post dosing, with p-value to CD-1 APAP dosed mice.	140
Table 3.3.3. Hepatic ATP content (nmol/mg) with standard deviation (SD) in fed control (saline) and APAP dosed mice at different time points post dosing.	142
Table 3.3.4. Hepatic ATP content (nmol/mg) with standard deviation (SD) in fasted control (saline) and APAP dosed C57BL/6J mice at different times post dosing (10-36 hpd).	144
Table 3.3.5. Comparison of GSH and ATP levels in fed and fasted male C57BL/6J mice after APAP overdose and comparison to CD-1 mice.	146
Table 3.3.6. Mean serum ALT levels (U/L) with standard deviation (SD) in fed control (saline) and APAP dosed male C57BL/6J mice at different times post dosing, including comparison to values in CD-1 mice.	148
Table 3.3.7. Mean serum ALT levels (U/L) with standard deviation (SD) in fasted control (saline) and APAP dosed C57BL/6J mice at different times post dosing and comparison to CD-1 mice.	150
Table 3.3.8. Histological findings in APAP dosed fed C57BL/6J mice (time course).	152
Table 3.3.9. Histological scores in APAP dosed fed C57BL/6J mice (time course) and comparison to CD-1 mice.	153
Table 3.3.10. Histological findings in APAP dosed fasted C57BL/6J mice (time course).	155
Table 3.3.11. Histological scores in APAP dosed fasted C57BL/6J mice (time course) and comparison to CD-1 mice.	156
Table 3.3.12. Comparison of GSH, ATP, ALT and DILI score in male C57BL/6J and CD-1 mice in animals that had been fed or fasted prior to APAP dosing using comparative value, assessing fold change relative to control animals.	162
Table 3.3.13. TNF- α serum levels (pg/mL) in control and APAP treated fed C57BL/6J mice with p-value and comparison to levels in fed CD-1 mice.	174
Table 3.3.14. TNF- α serum levels (pg/mL) in control and APAP treated fasted C57BL/6J mice with p-value and comparison to levels in fasted CD-1 mice.	176
Table 3.3.15. IL-6 serum levels (pg/mL) in control and APAP treated fed C57BL/6J mice with p-value and comparison to levels in fed CD-1 mice.	178
Table 3.3.16. IL-6 serum levels (pg/mL) in control and APAP treated fasted C57BL/6J mice with p-value and comparison to levels in fasted CD-1 mice.	179
Table 3.3.17. Range and average amount (%) of PCNA-positive, proliferating cells in fed control mice at 0 h and in APAP dosed C57BL/6J mice at different time points post dosing. The values were also compared to those obtained in CD-1 mice.	187
Table 3.3.18. Average amount (%) of hepatocytes with cytoplasmic PCNA expression in fed and fasted APAP dosed male C57BL/6J mice and comparison to the amount in CD-1 mice.	190
Table 3.3.19. Assessment of liver regeneration of the levels of TNF- α , IL-6 IL-10, NF- κ B, cyclin-D1 and PCNA expression in the liver by comparative value, assessing the fold change relative to pooled control animals.	192

LIST OF ABBREVIATIONS

-COOH	Carboxylic acids
-NH ₂	Primary amines
-OH	Hydroxyl groups
-SH	Sulphydryl
ABC	ATP binding cassette
ADR	Adverse drug reactions
AILI	APAP-induced liver injury
ALF	Acute liver failure
ALT	Alanine aminotransferase
APAP	Acetaminophen; paracetamol
AST	Aspartate aminotransferase
ATP	Adenosine triphosphate
bp	base pair
BSA	Bovine serum albumin
BSU	Biomedical Service Unit
°C	Degrees centigrade
Ca ²⁺	Calcium ion
CaCl ₂	Calcium chloride
Caspases	Cascade of cysteine-aspartate proteases
C/EBPβ	Controlled Amino Acid Therapy/Enhancer binding protein beta
CC3	Cleaved caspase-3
CCl ₄	Carbon tetrachloride
cDNA	Complementary DNA
CL	Centilobular
CN	Coagulative necrosis
CV	Central vein
CO ₂	Carbon dioxide
COX	Cyclooxygenase
Ct	Cycle threshold
CuSO ₄ .5H ₂ O	Copper(II) sulfate pentahydrate
CYP2E1	Cytochrome P4502E1
CYP450	Cytochrome P450
Cyto	Cytoplasmic

DAB	Diaminobenzidine-tetrahydrochloride
DAMP	Damage-associated molecular pattern molecules
DC	Dendritic cell
dH ₂ O	Distilled water
DILI	Drug-induced liver injury
DMSO	Dimethyl sulfoxide
DNA	Deoxyribonucleic acid
DNase	Deoxyribonuclease enzyme
dNTP	Deoxynucleotide
DTNB	5,5'-Dithio-bis (2-nitrobenzoic acid) or Ellman's reagent
E	Efficiency
EDTA	Ethylenediaminetetraacetic acid
EGF	Epidermal growth factor
ELISA	Enzyme-linked immunosorbant assay
EtOH	Ethanol
FasL	Fas ligand
FDA	Federal Drug Administration
g	Gram
GAPDH	Glyceraldehyde-3-phosphate dehydrogenase
GCLC	Glutamyl cysteine ligase catalytic subunit
GdCl ₃	Gadolinium chloride
gp130	Glycoprotein 130
GSH	Reduced glutathione
GSSG	Oxidised GSH
GST	Glutathione-S-transferase
h	Hour/hours
HCl	Hydrochloric acid
HD	hydropic degeneration
HE	Hematoxylin and eosin
HGF	Hepatocyte growth factor
HMGB1	High mobility group box-1
H ₂ O	Water
H ₂ O ₂	Hydrogen peroxide
HPA	Hypothalamus-pituitary-adrenal
hpc	hepatocytes
hpd	hours post dosing
hps	hours post saline
HRP	Horseradish peroxidase

HSPs	Heat-shock proteins
IFN- γ	Interferon gamma
IHC	Immunohistochemistry
I κ B	Inhibitor κ B
IKKs	I κ B kinases
IL	Interleukin
IM	Infiltrating macrophages
IRF-1	Interferon Regulatory Transcription Factor 1
i.p	Intraperitoneal administration
IPA	Isopropyl alcohol
JAK/STAT	Janus Kinase/Signal Transducer and Activator of Transcription
JNK	c-Jun-N-terminal
K	Kappa
kb	Kilobases
KCl	Potassium chloride
KCs	Kupffer cells
KH ₂ PO ₄	Monopotassium phosphate
KO	Knock-out
L	Litres
LPCs	Liver progenitor cells
LPS	Lipopolysaccharide
M	Molar
MCP-1	Monocyte chemoattractant protein-1
mg	Miligrams
μ g	Micrograms
MgCl ₂	Magnesium chloride
MIF	Macrophage migration inhibitory factor
min	Minute/minutes
ml	Mililitres
μ l	Microlitres
mM	Milimolar
μ M	Micromolar
MPT	Mitochondrial permeability transition
mRNA	messenger Ribonucleic acid
MRP	Multi-resistant proteins

n	Number of animals used per group
NAC	N-acetyl-cysteine
NaCl	Sodium chloride
Na ₂ CO ₃	Sodium carbonate
NADPH	Nicotinamide adenine dinucleotide phosphate
Na ₂ HPO ₄	Sodium hydrogen phosphate
NaOH	Sodium hydroxide
NAPQI	N-acetyl-p-benzoquinoneimine
NATs	N-acetyltransferases
NF-KB	Nuclear factor kappa B
NHAIR	No histological abnormality is recognised
NHS	National Health Service
NKs	Natural killer (NK) cells
NKT	Natural killer T
NL	Neutrophilic leukocytes
nm	Nanometer (wavelength)
nM	Nanomolar
NO	Nitric oxide
NPC	Non-parenchymal cells
Nrf2	NF-E2-related factor 2
NS	Not significant
NTCP	Sodium taurocholate cotransporting polypeptide
O ₂	Molecular oxygen
OAT	Organic amine transporters
OCT	Organic cation transporters
PAS	Periodic Acid Schiff
PBS	Phosphate-buffered saline
PCNA	Proliferating cell nuclear antigen
PCR	Polymerase chain reaction
PFA	Paraformaldehyde
PGE2	Prostaglandin E2
PHx	Partial hepatectomy
PMN	Polymorphonuclear cells
qPCR	Quantitative polymerase chain reaction
rDNase	recombinant DNase
RNA	Ribonucleic acid
ROS	Reactive oxygen species
rpm	revolutions per minute

RT	Reverse transcription
RT-PCR	Reverse transcriptase-polymerase chain reaction
SCN	Suprachiasmatic nucleus
SD	Standard deviation
sec	second/seconds
SLC	Solute carrier
SOD	Superoxide dismutase
SOCS-3	Suppressor of cytokine signalling-3
SOP	Standard operating protocol
SPF	Specific pathogen free
SSA	5-sulfosalicylic acid
STAT-3	Signal Transducer and Activator of Transcription-3
Std	Standard
SULTs	Sulfotransferases
SW mice	Swiss Webster mice
TAE	Tris base + acetic acid + EDTA
TBS	Tri buffered saline
TBST	TBS buffer with 0.05% Tween 20
TGF- α	Transforming growth factor- α
TLR	Toll-like receptors
TNF- α	Tumour necrosis factor alpha
TNFR	TNF receptor
ToD	Time of day
U	Units
UDP	Uridine 5' diphosphate
UGTs	UDP-glucuronyltransferases
UV	Ultraviolet
V	Volts
v/v	volume/volume
w/v	weight/volume

CHAPTER ONE

INTRODUCTION

CONTENTS

1.1	THE LABORATORY MOUSE AS AN ANIMAL MODEL FOR HUMAN LIVER DISEASES	4
1.1.1	The use of the laboratory mouse as an animal model	4
1.1.2	The laboratory mouse as a model for APAP-induced acute liver injury	4
1.1.3	Effect of food restriction on the laboratory mouse	6
1.1.4	Hepatic regenerative capacity in mice	9
1.2	DRUG INDUCED LIVER INJURY (DILI)	10
1.2.1	Mechanism of DILI	11
1.2.1.1	Phase I drug metabolism	12
1.2.1.2	Phase II drug metabolism	12
1.2.1.3	Phase III drug metabolism	13
1.2.2	Adverse drug reactions (ADRs)	14
1.2.3	Sterile inflammation and damage-associated molecular pattern molecules (DAMP) induced by ADRs	15
1.3	APAP-INDUCED LIVER INJURY	16
1.3.1	Role of drug metabolism in APAP-induced liver injury	18
1.3.2	Mode of cell death after APAP intoxication	20
1.3.2.1	APAP-induced hepatocellular apoptosis	22
1.3.2.2	APAP-induced hepatocellular necrosis	23
1.3.3	Liver regenerative response after APAP insult	24
1.4	EFFECT OF FASTING ON APAP-INDUCED LIVER INJURY	25
1.4.1	Effects of fasting on mouse hepatotoxicity	25
1.4.2	Effects of fasting on liver regeneration after APAP overdose	26

1.5	CYTOKINES INVOLVED IN ASSOCIATION WITH APAP-INDUCED LIVER TOXICITY AND LIVER REGENERATION	27
1.5.1	Role of Kupffer cell (KC)	29
1.5.2	Role of natural killer (NK) and natural killer T (NKT) cells	29
1.5.3	Role of cytokines in APAP-induced liver injury and regeneration	30
1.5.3.1	Role of TNF- α	30
1.5.3.2	Role of IL-6	32
1.5.3.3	Role of IL-10	33
1.5.3.4	Role of NF-kB	34
1.5.3.5	Role of cytokines network in hepatic regeneration	36
1.5.4	Role of liver regeneration after APAP overdose: markers and mediators	38
1.5.4.1	Role of cyclin-D1	38
1.5.4.2	Proliferating cell nuclear antigen (PCNA) and HE staining	38
1.6	AIMS OF THESIS	41
1.6.1	Effects of fasting on the liver of untreated (i.e. saline dosed, control) mice	41
1.6.2	Effects of fasting on the development and extent of APAP-induced DILI and the regeneration thereafter	42
1.6.3	Differences between C57BL/6J and CD-1 mice in their response to fasting and APAP overdose	43

1.1 THE LABORATORY MOUSE AS AN ANIMAL MODEL FOR HUMAN LIVER DISEASES

1.1.1 The use of the laboratory mouse as an animal model

Animal models are important tools in biomedical research since the 16th century, for scientific discovery including genetics, medicine and other disciplines (Hedrich Hans, 2012). The laboratory mouse, species *Mus musculus*, is most commonly used in human-oriented research as the animals are easy to handle, inexpensive to raise and maintain, and due to the fact that 99% of mouse genes have human counterparts. Basically, by examining the physiology, anatomy and metabolism of a mouse, scientists can gain valuable insight into how humans function. Mice reproduce in a short time period, therefore enable researchers to study generations of offspring within a reasonable period of time at minimal cost. In drug safety development, the laboratory mouse is an important human model to understand the effectiveness and the toxicities of various xenobiotics (Jacksons, 2010).

1.1.2 The laboratory mouse as a model for APAP-induced acute liver injury

Previous studies have shown that the mouse is both a clinically relevant and experimentally convenient species for the study of APAP hepatotoxicity. Similar to humans, it can exhibit mitochondrial damage and nuclear DNA fragmentation in response to APAP overdose, different from rats which are resistant to APAP toxicity due to reduced mitochondrial protein adducts and dysfunction, which prevents the oxidative stress (McGill et al., 2012b; Mitchell et al., 1973). Furthermore, other studies have shown that the mechanisms of APAP toxicity in humans are similar to those in mice which render the laboratory mouse the preferred species for mechanistic studies (Knight et al., 2001; McGill et al., 2012b; Muldrew et al., 2002). Although the basic mechanism of APAP toxicity is similar, hepatotoxic responses are variable in different animal models, including dog (Francavilla et al., 1989; Gazzard et al., 1975) and pig (Miller et al., 1976). The incidence of sudden death due to methaemoglobinaemia is a notable recurrent problem when using these models

(Gazzard et al., 1975; Henne-Bruns et al., 1988). Although the large animal models are useful to determine the haemodynamic parameters including intracranial pressure, cardiac output, systemic vascular disturbance and many more, the laboratory mouse is still a good candidate to understand the pathogenic outcome of hepatocellular damage and the immune response due to widely available antibodies and immune markers in this species that provide better understanding of mechanism for APAP-induced liver injury (Mossanen and Tacke, 2015).

Laboratory mice are bred and maintained in a tightly controlled environmental setting, without the confounding influence of any other factors. CD-1 and C57BL/6J mice are commonly used in toxicity studies. CD-1 mice are the most common out-bred mice used when the inter-individual genetic variability that mimics the genetic variation in humans is supposed to be considered and where this may be beneficial in toxicology research (Chia et al., 2005). They are therefore widely used in toxicology and pharmacology studies, particularly for product safety testing (Chia et al., 2005). They also serve as models in acetaminophen toxicity studies (Antoine et al., 2010; Goldring et al., 2004; Hart et al., 1994). However, C57BL/6J are mostly used in studies of APAP hepatotoxicity and the mechanism of toxicity in these animals is well understood (McGill et al., 2012c). C57BL/6J mice are an in-bred strain that is considered as genetically homogeneous or identical (Beck et al., 2000). They are used as physiological and pathological models for in vivo experiments that aim to obtain consistent data; this allows reproducible studies especially to establish novel drugs (Festing, 2010). The use of C57BL/6J mice as a model of APAP hepatotoxicity is well documented and proven to produce results significant to humans (Festing, 2010). Meanwhile, other relevant and susceptible strains have been used in APAP toxicity studies, like ICR mice (Jaeschke, 1990), C3Heb/FeJ mice (Cover et al., 2005), and B6C3F1 mice (Agarwal et al., 2011). All these studies consistently reported mitochondrial dysfunction, oxidative stress and peroxynitrite formation after APAP insult.

APAP toxicity studies frequently use male C57BL/6J mice because they are more susceptible to APAP hepatotoxicity than females (Botta et al., 2006; Dai et al., 2006; McConnachie et al., 2007). This is also evident by the higher levels of serum ALT and

hepatocellular damage in male compared to female CD-1 mice following APAP overdose (Botta et al., 2006).

Different mouse strains with their specific genetic backgrounds can potentially show different degrees of immune cell activation after APAP administration. Due to different genetic profiles, liver injury induced by APAP may require dose adjustments to achieve a similar response (Mossanen and Tacke, 2015). A previous study has shown more intense liver damage in C57BL/6J mice, together with higher TNF- α expression, compared to BALB/c mice (Masubuchi et al., 2009). This was considered a consequence of a more intense innate immune response, due to a more intense specific Th1-dominant response of T-helper cells in C57BL/6J mice (Masubuchi et al., 2009). Although numerous published studies have explored APAP toxicity in mouse models, comparative studies to assess APAP toxicity in different mice, such as out-bred CD-1 vs. in-bred C57BL/6 mice, as a means to allow the choice of the optimal mouse model, have not been performed.

1.1.3 Effect of food restriction on the laboratory mouse

Food availability affects the basal metabolism and therefore the function of the liver as the major metabolic organ. Fasting of mice changes several physiological parameters and moreover, these changes are depending on a variety of environmental factors (Jensen et al., 2013). In experimental settings, fasting is primarily used as a way to ensure uniform drug absorption and minimise the variability in basal blood glucose levels. Both is helpful in toxicology tests and pharmacokinetics studies in general and helps to reduce the number of animals per dosing group to achieve statistical significance (Ellacott et al., 2010; Kim et al., 2006; Kinoshita et al., 2000; Strubelt et al., 1981b).

Mice lost significantly more weight after 18 hours of fasting compared to 5 hours, 16% and 5% respectively, with significantly lower gastrointestinal tract weights than in fed mice (Ayala et al., 2006; Heijboer et al., 2005). Fasting can also lead to a reduction of the basal metabolic rate, which can even persist after food re-

introduction, while the body weight is returning to a value within the normal range as in pre-fasting state (Bj et al., 1982; Penicaud and Le Magnen, 1980). The metabolic state of fasting mice can be described as catabolic or post-absorptive, and it is characterised by mobilisation of glycogen to maintain the necessary blood glucose levels (Ayala et al., 2006). A study has reported that the amount of hepatic glycogen is significantly reduced after a 18 hours fasting period compared to 5 hours of fasting (Ayala et al., 2006). Furthermore, in mice fasted for 24 hours, muscle glycogen was reduced to half the level of fed mice (Gavrilova et al., 1999).

In the liver, glutathione (GSH) acts as an antioxidant in hepatocytes to detoxify free radicals and oxygen species (Pompella et al., 2003). After a 16 or 24 hour fasting period, the amount of GSH in the liver is significantly decreased, which reduces the detoxification capacity of hepatocytes (Brooks and Pong, 1981; Strubelt et al., 1981b). No significant difference in the CYP450 level was seen after 12 hours of fasting, but it was significantly lower (about 33%) after 24 hours of fasting in mice (Walker et al., 1982). This is interesting since a lack in CYP450 can minimise the toxification of acetaminophen (Strubelt et al., 1981b). Several factors, such as food intake, overnight fasting and disease conditions, affect the function of hepatic phase II enzymes and are thus able to influence the formation of reactive metabolites (Howell and Klaassen, 1991; Walker et al., 1982). During the feeding period of mice, peak GSH levels were noted at the end of dark period or in the early morning (i.e. when mice are most active) while the GSH levels were lowest when the mice were normally asleep (i.e. at the end of a prolonged period of light) (Schnell et al., 1984). Also, the susceptibility of mice to APAP toxicity has shown to follow a circadian rhythm in hepatic glutathione levels (Howell and Klaassen, 1991; Schnell et al., 1984). Therefore, the importance of feeding regime and circadian variations in hepatic GSH levels needs to be considered when animal models are used to investigate the relationship between drug metabolism and toxicity.

In C57BL/6J mice, the histological examination of the liver did not reveal any evidence of a reduction in the number of liver cells, and the zonal architecture including periportal and pericentral regions of the lobules remained unaffected after 12 and 24 hours of fasting (Sokolovi et al., 2008). Staining for active caspase-3,

a marker of apoptosis, did not indicate an increase in apoptotic cell death even after 72 hours of fasting. In agreement with this, the microarray data for apoptosis genes showed no significant expression in fasted and fed mice (Sokolovi et al., 2008).

Fasting can be expected to cause stress, aggressive behaviour and reduction in body weight (Ayala et al., 2006; Strubelt et al., 1981b), body temperature (Webb et al., 1982) and glucose levels (Tsuneki et al., 2002) as well as enhance sympathetic nervous system activity (Jensen et al., 2013). However, the association of all these changes between strains is still poorly defined, and the study on the metabolic response of mice upon food re-introduction after fasting is limited (Jensen et al., 2013). Figure 1.1 illustrates in a schematic diagramme of the changes in the feeding pattern which influence various responses including body weight (%), and the level of hepatic GSH and ATP contents (Froy and Miskin, 2010; Jensen et al., 2013).

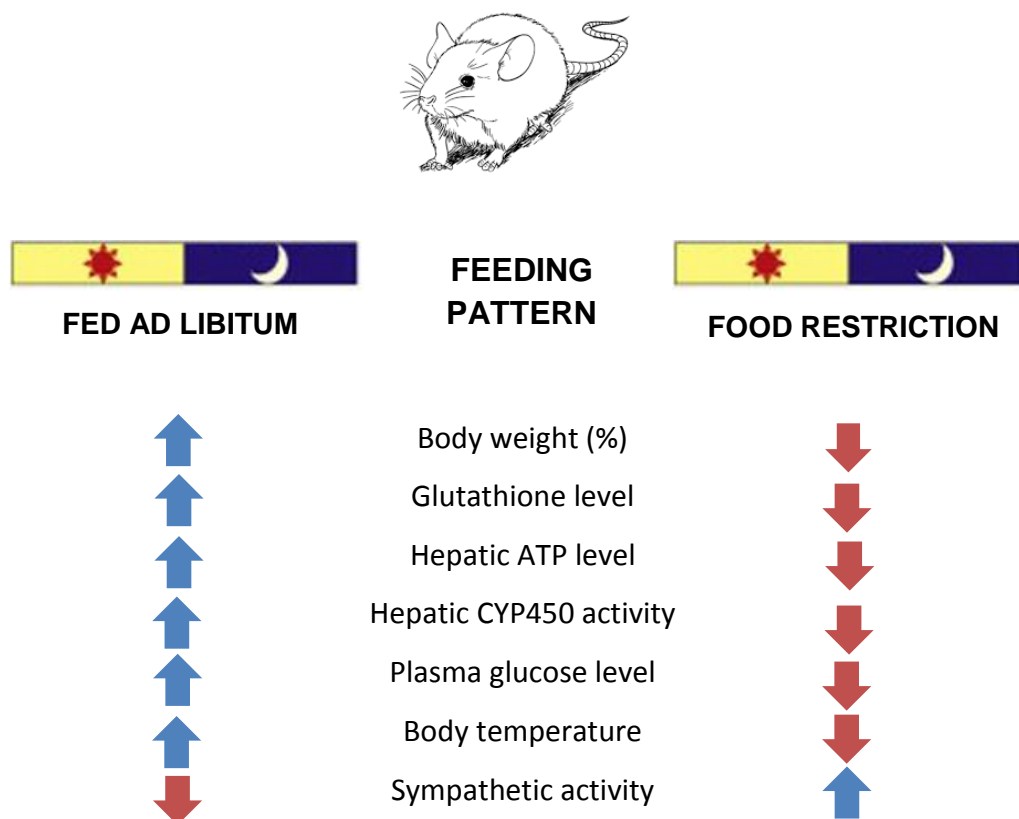


Figure 1.1. Schematic diagramme of the effect of food restriction in the laboratory mouse. The effects of ad libitum feeding and fasting on body weight, hepatic glutathione, ATP, CYP450, plasma glucose level, body temperature and sympathetic activity in mice are shown (Jensen et al., 2013).

The effect of food deprivation is greatest in the scotophase, when the animals are most active. A study has argued that overnight fasting of mice is not comparable with the overnight fasting of humans as mice have a nocturnal circadian rhythm and a higher metabolic rate compared to man. Fasting of mice for 5-6 hours instead of overnight (16-18 hours) might offer a better comparison to humans, who are usually fasted overnight for toxicology testing (Jensen et al., 2013).

1.1.4 Hepatic regenerative capacity in mice

The process of liver regeneration is complicated and relies on various factors including the type, aetiology and severity of liver injury, and the clinical conditions (Kvittingen et al., 1994). Hepatocytes are capable of regeneration and to fully reconstitute damaged livers multiple times (Kvittingen et al., 1994). Previous studies in rats have suggested that new hepatocytes are formed in the periportal region and then slowly migrate towards the centrilobular area (Friedman and Kaestner, 2011; Zajicek et al., 1985). During normal liver turnover or in response to mild injury, the liver mass is maintained by self-duplicating hepatocytes (Malato et al., 2011). However, when an injury is severe or the proliferative capability of hepatocytes is impaired, liver progenitor cells (LPCs) located in the periportal areas provide a backup system for hepatocyte regeneration (Malato et al., 2011). During liver regeneration, hepatocyte clusters are formed, followed by proliferation of hepatic stellate cells and fenestrated sinusoidal endothelial cells; this process also re-establishes the normal vascularisation (Martinez-Hernandez and Amenta, 1995). In the healthy liver, hepatocytes are in the G0 phase of the cell cycle (i.e. the quiescent state) and respond only minimally to growth factors (Fausto, 2000). Briefly, the kinetics of liver regeneration can be divided into three closely related phases, initiation, progression and termination. During initiation, quiescent hepatocytes are primed to enter the cell cycle also through cytokine-mediated signalling. Once primed, hepatocytes respond more intensely to mitogens, such as growth factors (Apte et al., 2015). During progression, they then undergo several

cell cycle rounds to improve liver structure and restore its function. Termination of liver regeneration takes place once cell proliferation stops.

Evidence of liver regeneration as a compensatory response and final outcome of hepatotoxicity has been provided in various hepatotoxicant mouse models, such as acetaminophen (APAP), carbon tetrachloride (CCl₄), chloroform, thioacetamide (TA), trichloroethylene (TCE) and allyl alcohol (AA); this provides relevant information for the risk assessment of toxic exposure (Mangipudy et al., 1995; Mehendale, 2005). Analysis of cell proliferation after prolonged exposure to various toxic insults has shown that high doses inhibit cell cycle progression by suppression of cytokine or growth factor-mediated signalling followed by cyclin-D1 reduction (Shankar et al., 2003).

1.2 DRUG INDUCED LIVER INJURY (DILI)

DILI can affect parenchymal or non-parenchymal cells within the liver, leading to a variety of pathological conditions which include acute or chronic hepatitis, hepatic vascular damage and cirrhosis (Larrey, 2000; Martinez-Hernandez and Amenta, 1995). Acute hepatitis and cholestasis are two predominant forms of DILI which is characterised by a pronounced increase in alanine aminotransferase (ALT) activities and liver necrosis that could be seen histologically (Gunawan et al., 2004). DILI is a major contribution towards patient mortality and morbidity (Lee et al., 2005). A main concern for the pharmaceutical industry and regulatory authorities are DILI, causing a significant issue for withdrawal of an approved drug (Jaeschke et al., 2002). In the United States, approximately 50% of drug-induced liver toxicity contributes to the cause of acute liver failure, with over 800 drugs associated with hepatotoxicity (Dossing and Sonne, 1993; Ostapowicz et al., 2002). Liver is the main organ to metabolise endogenous and exogenous compounds and thereby is a major target for toxic insults. It plays an indispensable role to metabolise xenobiotics into hydrophilic metabolites to assist their excretion via urine or bile. Although the actual mechanisms are still being studied, it is well accepted that the formation of reactive metabolites contributes to cellular damage as an outcome of oxidative

stress. In order to examine the mechanism of hepatotoxicity, acetaminophen (paracetamol, APAP) serves as one of the classically studied drugs, is also characterised as an ideal hepatotoxicant (Ostapowicz et al., 2002).

1.2.1 Mechanism of DILI

Drug metabolism is the complex process by which a drug was chemically biotransformed by several enzymatic reactions into more hydrophilic metabolites to ease their excretion. Principally, liver is the main organ and most important site of drug metabolism. Most xenobiotics have characteristic of non-polar and lipophilic chemical compounds that are readily absorbed in the gastrointestinal tract. Xenobiotics need to be metabolised to increase their hydrophilicity and facilitate their excretion in the urine or bile. Drug metabolism can be divided into three different phases; phase I (functionalization/bioactivation), phase II (conjugation/detoxification), and phase III (transport/excretion) (Pachkoria et al., 2007). Phase I reactions involve the exposure or incorporation of a functional group. Then, it serves as a target for phase II conjugation reactions to form a highly polar conjugate (Guengerich and Shimada, 1991). It should also be noted that a drug can be metabolised by phase II metabolism without having previously been involved in phase I metabolism, provided the parent compound carries a suitable functional group. Meanwhile, drug conjugates that are transported across the membranes are involved in phase III metabolism (Pachkoria et al., 2007). Metabolism does not only result in detoxifying process, however, some drugs are bioactivated to reactive and potentially toxic metabolites (Grillo et al., 2003). An imbalance of these three different phases could also promote an accumulation of reactive metabolites, resulting in liver injury (Pachkoria et al., 2007).

1.2.1.1 Phase I drug metabolism

Phase I metabolic reactions are also known as functionalization reactions and involve functional groups, such as hydroxyl groups (-OH), primary amines (-NH₂), sulphhydryl (-SH) and carboxylic acids (-COOH) by oxidation, reduction, hydrolysis or hydration reactions to facilitate phase II reactions (Gibson, 2001). Phase I drug metabolism enzymes include CYP450, an enzyme that is highly expressed at the innermost layer of the mitochondrial membrane or in the endoplasmic reticulum of hepatocytes are able to catalyse the majority of phase I oxidation reactions (Guengerich, 2003; Meyer and Meyer, 1996). CYP450 is known to have a mixed functional role, with the predominant role to detoxify the metabolites from endogenous and exogenous compounds. However, there is a chance that the newly generated metabolite catalysed by CYP450 is more active than the parent compound in some ways, resulting in hepatocellular damage. Basically, the metabolism of drugs can potentially produce free radicals and reactive oxygen species (ROS), resulting in oxidative stress to cellular macromolecules such as proteins, DNA and RNA, by covalent interactions. The functional modification of these cellular macromolecules has the potential to cause a variety of toxic changes, such as necrosis, apoptosis, chemical carcinogenesis and hypersensitivity (Hinson et al., 1981; Park et al., 2005).

1.2.1.2 Phase II drug metabolism

A second hepatic drug metabolism pathway is represented by the processing of electrophilic metabolites initially formed by phase I reactions in order to raise polarity and water solubility to facilitate excretion (Timbrell, 2000). The phase II drug-metabolising enzymes include uridine 5' diphosphate-glucuronyltransferases (UGTs), N-acetyltransferases (NATs), sulfotransferases (SULTs), glutathione S-transferases (GSTs) and several methyltransferases (McCarver and Hines, 2002). These are responsible for the detoxification of reactive metabolites generated during phase I, enabling their excretion via urine or bile. Phase II reactions are generally considered detoxification reactions which include glucuronidation,

sulphation, acethylation, acetylation, methylation, amino acid conjugation and GSH conjugation (Zamek-Gliszczynski et al., 2006). In the liver, ROS and free radicals can be detoxified by GSH conjugation. GSH is an endogenous tripeptide (γ -glutamylcysteinylglycine) consisting of glutamate, cysteine and glycine amino acids, plays an indispensable role as antioxidant and scavenger within the cells (Hayes et al., 1999). Basically, GSH exists in an oxidised (GSSG) and a reduced (GSH) form. GSH is able to conjugate with a reactive electrophilic species, or by facilitation through GST, an enzyme located in the cytosol and microsomes, to form a thioether bond between the cysteine residue of GSH and electrophiles (Coles et al., 1988). If highly reactive metabolites are exposed and exceed the amount of GSH available, other thiol groups and especially critical proteins such as γ -glutamyl cysteine ligase catalytic subunit (GCLC), glyceraldehyde-3-phosphate dehydrogenase (GAPDH) and $\text{Ca}^{2+}/\text{Mg}^{2+}$ ATPase, undergo subsequent oxidation, cross-linking and formation of covalent adducts. It is well known that depletion of GSH is a prerequisite for the onset of toxicity (Mitchell et al., 1973). For example, newly generated GSH is unable to replace GSH used by GSSG conjugation or oxidation during APAP hepatotoxicity (Mitchell et al., 1973). There is still a potential for bioactivation to occur, although phase II metabolism is principally a detoxification pathway (Zhou et al., 2005).

1.2.1.3 Phase III drug metabolism

Phase III involves a series of hepatic drug transporter proteins (Ishikawa, 1992). A study characterised plasma membrane-bound hepatocyte transporters and illustrated that drugs enter and exit hepatocytes by using energy dependent transporters (Mizuno et al., 2003), which are responsible to transport and remove endogenous as well as exogenous compounds (Borst et al., 2002). The predominant solute carrier (SLC) transporter superfamily that is responsible for drug uptake or efflux is found on the basolateral (sinusoidal) membrane that lies between hepatocytes (Jose, 2012). The hepatic sinusoidal plasma membrane plays a role to transport organic/inorganic cations and/or anions for the efflux from cell into circulation (Yabuuchi et al., 1998). Examples of these transporters are organic amine

transporters (OAT), organic cation transporters (OCT) (Zhang et al., 1998) and sodium taurocholate cotransporting polypeptide (NTCP) (Hagenbuch and Meier, 1994). The excretion of drugs and their metabolites involve the ATP binding cassette (ABC) transporter superfamily which mediates the excretion of drugs into the bile or the sinusoidal membrane and also mediates the efflux back into the bloodstream (Dean et al., 2001; Kerb et al., 2001).

1.2.2 Adverse drug reactions (ADRs)

Adverse drug reactions (ADRs) are a major concern for patient health. In 1994, it was estimated that over 100,000 patients died from ADRs in the United States alone (Lazarou et al., 1998). Three out of five drugs were removed from the market within two years, between 1997 and 1998 (Lasser et al., 2002). ADRs have been responsible for the post-market withdrawal of more than 75 drugs/drug products in the USA between 1969 and 2002 and have also become a major reason for attrition in the drug development (Lasser et al., 2002). A 6 month prospective study from two hospitals in Merseyside, UK revealed that 6.5% (1,225 out of 18,820) patients were admitted during 2001-2002 for the case of ADRs, and 2.3% died due to the reaction (Pirmohamed et al., 2004).

ADRs can be classified as 'on target' or 'off target' reactions. On target reactions can be predicted from the known compound of the drug, and the pharmacological side effect of the drug can usually be avoided by dose reduction without life-threatening outcome (Park et al., 2005). In contrast, off target ADRs are often dose-independent due to lack of toxicological knowledge; accordingly, the response in patients is unpredictable as it follows their levels of tolerance. Off-target ADRs, also known as idiosyncratic ADRs, can therefore be severe and life-threatening (Park et al., 2005; Uetrecht, 2003). ADRs are known to affect every organ system, but particularly liver and kidney (McNaughton et al., 2014). DILI represents a major proportion of the ADRs observed in drug development as a consequence of poor predictive models in understanding of the mechanism responsible for cell death (Roberts et al., 2004).

1.2.3 Sterile inflammation and damage-associated molecular pattern molecules (DAMP) induced by ADRs

First response of an organism upon cellular injury is inflammation. It is characterised by increasing blood flow, with extravasation of both nucleated blood cells and fluid from vessels into the affected tissue. Neutrophils are recruited to damaged areas, as a response to intruding microorganisms or with sterile inflammation induced by necrotic cells, and to clear the debris, they are later followed by macrophages (Raucci et al., 2007). Inflammation has a dual and contradictory role, one that can repair and another that can produce damage. It is a part of the physiological processes to repair tissue after damage, however, when this process is not controllable and inflammation spreads, it may cause severe damage (Aller et al., 2006; Kumar and Robbins, 2007; Nathan et al., 2002).

In liver inflammation, molecules that are initially generated to kill microbes, such as ROS and proteases, leak from dying hepatocytes or leukocytes and subsequently kill surrounding healthy cells (Rock et al., 2008). Dying cells trigger inflammation also in the absence of pathogens (Dumitriu et al., 2005; Rock and Kono, 2008). Such a sterile inflammation occurs in response to intracellular proteins released by necrotic cells, known as damage-associated molecular patterns (DAMPs) which attract neutrophils. Following cellular injury, DAMPs are recruited to initiate an inflammatory response (Ishida et al., 2006; Jaeschke, 2006a; Laskin et al., 1986). They include heat-shock proteins (HSPs) (Quintana and Cohen, 2005; Vabulas et al., 2001), DNA fragments (Jahr et al., 2001), ATP (Mariathasan et al., 2006) and high mobility group box-1 (HMGB-1) (Hori et al., 1995; Tian et al., 2007; Yu et al., 2006). Meanwhile, under physiological circumstances, DAMPs commonly remain intracellularly and undetectable by innate immune cells. However, in acute hepatotoxicity, DAMPs (i.e. HMGB-1) are released from necrotic cells and trigger an inflammatory and an immune response (Miller et al., 1976; Rubartelli et al., 2007).

The role played by inflammatory response and the innate immune system in the modulation of liver injury remains disputed (Adams et al., 2010). DILI can be initiated by bioactivation of drugs to chemically reactive metabolites, which allows

them to interact with cellular macromolecules, leading to cellular dysfunction. The impairment of hepatocellular function can lead to cell death and ultimately liver failure. Hepatocellular dysfunction and death after mitochondrial peroxidation due to oxidative stress can initiate an immunological response and trigger both an innate and adaptive immune response. Hepatocyte damage results in the release of signals that stimulate the activation of particularly innate immune cells, including Kupffer cells (KCs), natural killer cells (NKs) and natural killer T (NKT) cells (Jaeschke, 2006b; Liu et al., 2006). These can all contribute to the progression or regression of liver injury as they can produce pro-inflammatory or anti-inflammatory mediators and chemokines to inhibit or recruit inflammatory cells, like neutrophils, to the liver (Ishida et al., 2006; Jaeschke, 2006a; Laskin et al., 1986; Liu et al., 2004; Luster et al., 2001). Moreover, a balance between pro- and anti-inflammatory mediators produced after activation of the innate immune response could determine the susceptibility towards liver injury after a toxic insult (Gardner et al., 2003). Therefore, in hepatotoxicity studies, knock-out (KO) animals with depletion of specific cell types are widely used to highlight their critical role in innate immune response (B. Yee et al., 2007; Bourdi et al., 2002; Masubuchi et al., 2003b).

1.3 ACETAMINOPHEN INDUCED LIVER INJURY

APAP is commonly used as an analgesic and anti-pyretic drug that is safe at therapeutic doses of 4 g/day in healthy patients (Evans and Evans, 1993) but with overdosing can induce acute liver failure (ALF) due to massive centrilobular cell loss. It continues to be a major contributing factor to acute liver failure in the United Kingdom and United States (Larson et al., 2005; Ostapowicz et al., 2002). Intriguingly, APAP-induced hepatotoxicity has been widely studied as it provides a clinically relevant tool to study toxicological consequences of drug metabolism in vitro and in vivo models. Over the last 4 decades, rodent models have been widely used in order to understand the mechanism of APAP hepatotoxicity in toxicological studies (McGill et al., 2012a).

APAP hepatotoxicity is well-characterised in animal models. Toxicity is initiated through the formation of a reactive metabolite called N-acetyl-p-benzoquinonimine (NAPQI) (Mitchell et al., 1973; Raucy et al., 1989), which depletes hepatic GSH, an antioxidant and scavenger within hepatocytes (Knight et al., 2001). NAPQI initiates covalent binding to cellular macromolecules, leading to mitochondrial dysfunction and oxidative stress which results in hepatocellular damage and, ultimately, death (Jaeschke et al., 2003). Previous studies provided evidence that different laboratory mouse strains respond differently to APAP overdose, with some in-bred strains showing a higher susceptibility than others (i.e. B6C3F1/J > DBA/2J > C57BL/6J > SM/J > CAST/EiJ). These also suggested that genetic factors could independently influence APAP-induced liver damage and ALT release into the serum, and indicated that CD44 is involved in the modulation of susceptibility (Harrill et al., 2009). Although no strain difference has been identified with regards to the metabolism of APAP, C57BL/6J mice tend to be more susceptible than those of Balb/c (Masubuchi et al., 2009) and SW mice (Williams et al., 2011).

For the assessment of liver damage, the measurement of serum liver enzymes, released once the reactive metabolites inhibit the functions of various critical proteins within hepatocytes and lead to hepatocyte cell death, is used. Alanine aminotransferase (ALT) activity has long been established as a reliable tool for the detection of hepatotoxicity. ALT is released during severe liver damage, when levels exceeding 1000 U/L can be reached (Becketta et al., 1985). Serum ALT is an important marker and used in a plethora of studies ranging from preclinical animal studies until patient monitoring (Amacher, 1998). However, a major limitation of this enzyme as a marker of liver toxicity is that it is not an early indicator, as it is only elevated once liver necrosis and toxicity has occurred. It then slowly returns to baseline levels which it may only reach when the damage has already been resolved (Kim et al., 2008a). Subsequently, the cellular damage can trigger the activation of other cells, which can initiate an inflammatory response as shown in Figure 1.2. This event may overwhelm the capacity of the liver to regenerate, thereby contributing to the pathogenesis of hepatic injury (Bhushan et al., 2014; James et al., 2003b).

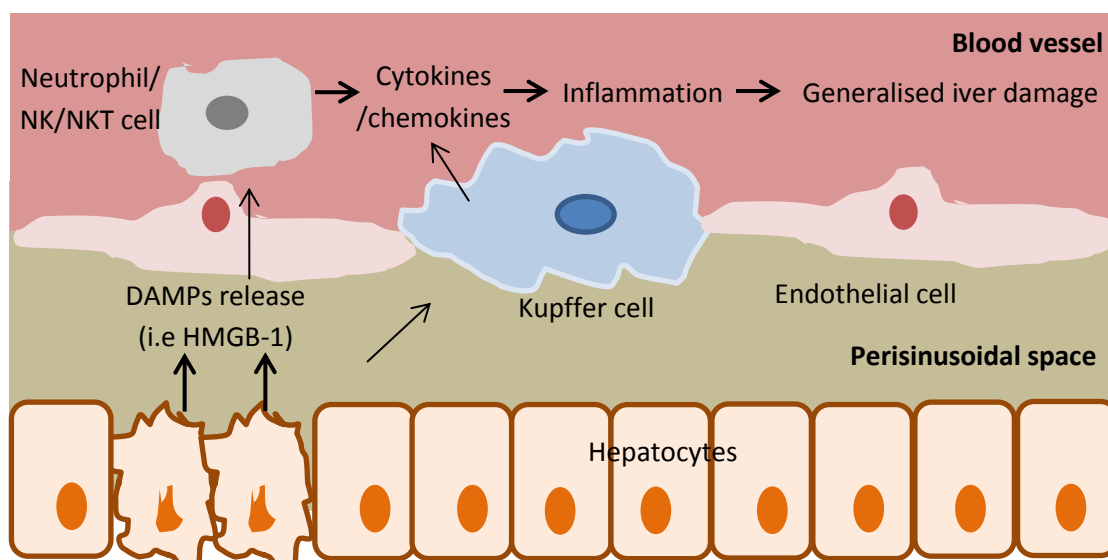


Figure 1.2. Acetaminophen induced hepatocellular injury.

In APAP overdose, released DAMPs into extracellular space and blood, are recognised by KC and then become activated. Upon activation, KCs secrete cytokines and chemokines to attract monocytes and neutrophils, which induce inflammation and sensitize hepatocytes to undergo apoptosis and/or necrosis, and further enhancing inflammation. Neutrophils also secrete cytokines to phagocytose apoptotic bodies and cell debris. Activation of innate immune cells (KCs, neutrophils and NK/NKT cells) modulate an overall pathogenesis of ALLI. DAMPs – damage-associated-molecular patterns; KCs – Kupffer cells; NK – Natural killer cell; NKT – natural killer T cell.

1.3.1 Role of drug metabolism in APAP-induced liver injury

APAP is extensively metabolised in the liver (Lee et al., 1996; Mitchell et al., 1973). Around 55% and 30% of APAP at therapeutic doses is bioactivated to glucuronide and sulphate conjugates, by UDP-glucuronosyltransferase (UGT) and sulfotransferase (SULT), respectively (Howie et al., 1977). However, these metabolites are rapidly excreted in the urine (Nelson, 1990). At therapeutic doses, only a small proportion of APAP (5-10%) is bioactivated to the reactive metabolite, NAPQI, by some CYP450s, including CYP2E1, CYP1A2, CYP3A4, and CYP2D6 yields the generation of NAPQI (Raucy et al., 1989; Thummel et al., 1993). NAPQI, which is react either spontaneously or via catalysis by GST with GSH, leading to detoxification process, and subsequently excreted as cysteine and mercapturate conjugates in the urine (Mitchell et al., 1973).

Saturation of the glucuronidation and sulphation pathways in APAP overdose forces a larger amount of APAP to become metabolised via the oxidative pathway.

Consequently, it promotes the production and accumulation of NAPQI, exceeding the hepatic GSH storage and the amount of newly synthesised GSH, leading to subsequent GSH depletion (Dahlin et al., 1984; Davies, 1986; Jollow et al., 1973; Lee et al., 1996; Mitchell et al., 1973). Hepatic GSH depletion enables NAPQI to covalently modify and suppress the function of various hepatocytes cellular proteins, leading to cellular dysfunction and ultimately cell death. The covalent modification or functional suppression of critical proteins such as glutamyl cysteine ligase catalytic subunit (GCLC) (Kitteringham et al., 2000), glyceraldehyde-3-phosphate dehydrogenase (GAPDH) (Dietze et al., 1997) and $\text{Ca}^{2+}/\text{Mg}^{2+}$ ATPase (Tsokos-Kuhn et al., 1988) can severely impair hepatocyte function. NAPQI is responsible to modify these proteins that has been hypothesised to lead to mitochondrial dysfunction and disturbance of ATP and Ca^{2+} homeostasis (Jaeschke et al., 2003). Therefore, NAPQI was believed to be a crucial step in cell death development after APAP overdose. NAPQI has been shown to be capable of binding to cellular proteins (Guengerich et al., 1985). In APAP hepatotoxicity, the covalent modification of proteins is mentioned to correspond with the oxidation of protein thiols (Bartolone et al., 1988; Davis et al., 1974; Roberts et al., 1987).

When NAPQI covalently binds to mitochondrial proteins, mitochondrial respiration can be inhibited, thereby promoting oxidative stress and peroxynitrite formation. This causes opening of the mitochondrial membrane permeability transition (MPT) pore, lysis of the outer membrane and swelling of the matrix. Consequently, the mitochondrial membrane potential and thereby the synthesis of ATP is suppressed, which further increases ROS production and cellular damage (James et al., 2003, Jaeschke et al., 2003). ROS inhibits the pro-survival transcription factor NF- κ B and subsequently initiates autophosphorylation and activation of c-Jun N-terminal kinase (JNK). JNK activation will lead to the production of more ROS and, subsequently, to mitochondrial permeability, dysfunction, which ultimately causes hepatocyte necrosis, followed by the release of DAMPs. HMGB-1 is one of the most notable DAMPs recognised by KCs and dendritic cells (DCs), subsequently leading to further activation of immune cells. N-acetylcysteine (NAC) is known as a standard treatment for APAP intoxication. In fact, NAC is responsible to replace intracellular

stores of GSH, which allows the detoxification of NAPQI (Hazelton et al., 1986). Without NAC, NAPQI would not only contribute to more tissue injury (David Josephy et al., 2005) but it also activates the cellular defence response (Park et al., 2005). NAC is most beneficial if administered within 16 hours after APAP overdose (Bari and Fontana, 2014) and is less effective for delayed cases (Kerr et al., 2005; Whyte et al., 2007). The mechanism of APAP-induced liver injury is presented in Figure 1.3.

1.3.2 Mode of cell death after APAP intoxication

Reactive metabolites resulting from APAP contribute to cell damage in a variety of ways which result in reversible or irreversible injury; the latter consequently leads to cell death. The reactive metabolite can irreversibly attach to cellular macromolecules and generate oxidative stress after massive depletion of hepatic GSH stores. Ultimately, the macromolecule binding contributes to damage and dysfunction of mitochondria, the cell organelles that are mainly responsible for ATP synthesis through metabolic conversion by glycolysis and oxidative phosphorylation (Boelsterli and Lim, 2007). Damage to mitochondria results in uncoupling of oxidative phosphorylation, suppressed ATP synthesis and opening of mitochondrial permeability transition (MPT) pore due to compromise of membrane potential, and subsequently cell death through generation of ROS and the disruption of electron transport systems and ATP production (Bossy-Wetzel and Green, 1999; Gross et al., 1999). These changes are mediated either via apoptosis or necrosis, or a combination of both. However, the actual mechanisms leading to drug-induced cell death are still being investigated. Some studies believed that evidence of apoptosis or necrosis is dependent on ATP levels within the cell (Leist et al., 1997; Nicotera et al., 1998). If MPT occurs as a result of damage to a few mitochondria within the cells or without severe ATP depletion, apoptosis occurs, but if marked ATP depletion takes place during this process then necrosis will intervene (Leist et al., 1997; Lemasters, 1999; Lemasters et al., 1999). Mitochondrial injury can gradually accumulate while being silent, which eventually leads to liver dysfunction and explains the delay of liver recovery by weeks or months (Boelsterli and Lim, 2007).

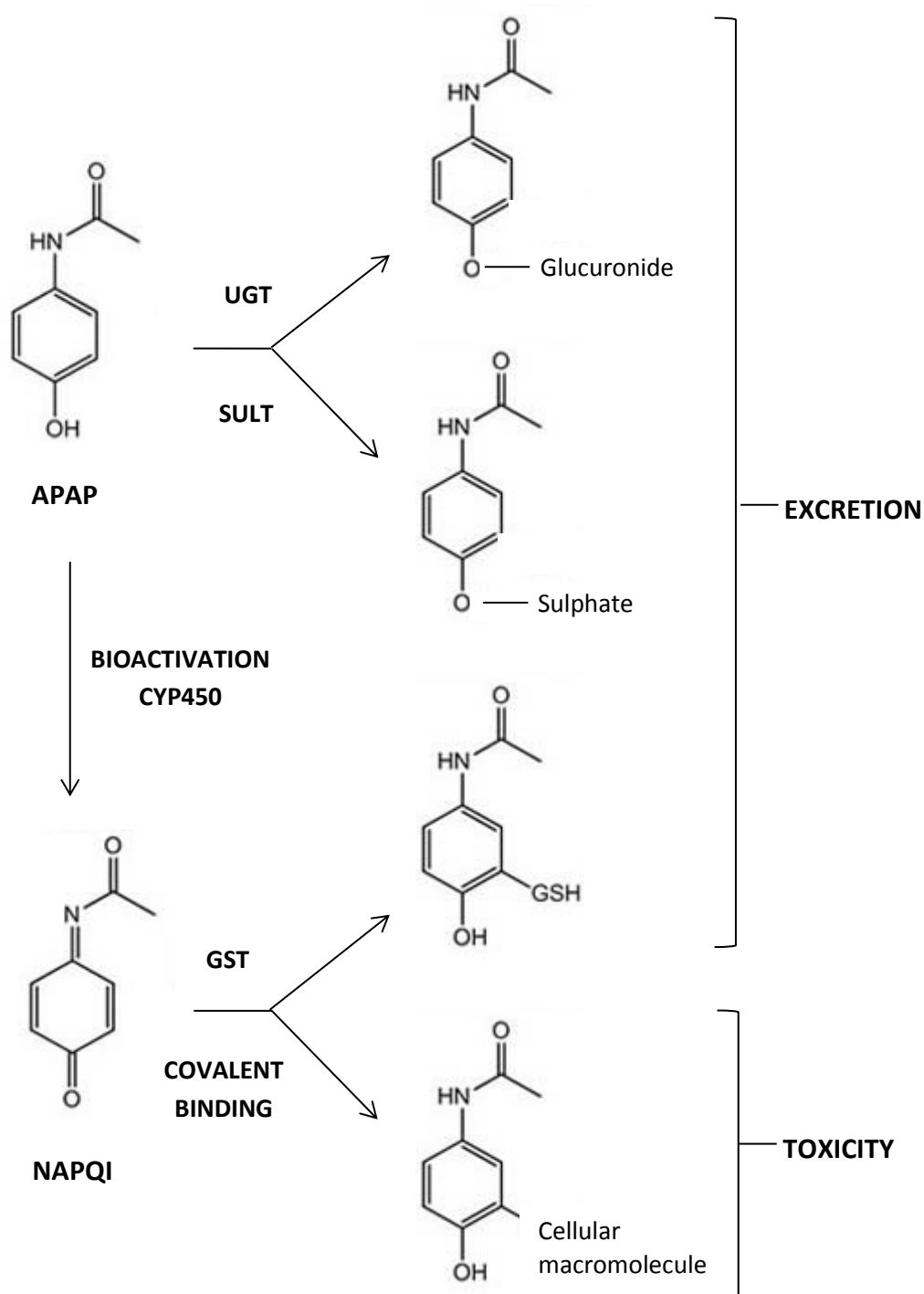


Figure 1.3. Metabolism of APAP-induced hepatotoxicity.

Generally, APAP is detoxified to glucuronide and sulphate metabolites in hepatocytes. CYP450 converts APAP to the chemically reactive metabolite NAPQI which is then conjugated by GSH stored in the liver, and detoxified. With APAP overdose, glucuronide and sulphate metabolites will saturate which promotes NAPQI production. When intracellular GSH is depleted, NAPQI is oxidised and can covalently bind to cellular macromolecules resulting in toxicity (James et al., 2003b). APAP - Acetaminophen; SULT - sulfotransferase; UGT - UDP-glucuronyltransferases; GST - Glutathione-S-transferase; GSH - reduced glutathione; NAPQI - N-acetyl-p-benzoquinoneimine.

1.3.2.1 APAP-induced hepatocellular apoptosis

Apoptosis is a mechanism of programmed cell death that is executed during the normal, i.e. physiological regulation of cell numbers (Kerr et al., 1972). It takes place if hepatocytes are injured beyond repair to avoid the spread of damaged DNA to other healthy cells and stop the damaged or abnormal DNA from dividing (Kerr et al., 1972). Apoptosis is characterised by membrane blebbing, cell shrinkage, chromatin condensation and DNA fragmentation (Robertson et al., 2000). Apoptotic bodies which represent cell fragments surrounded by an intact cell membrane are phagocytosed by adjacent cells and macrophages, for lysosomal degradation. This minimises the leakage of cellular components into the extracellular space and prevents the initiation of subsequent inflammatory responses (Savill et al., 2003). Many stimuli can initiate apoptosis. Among these are tumour necrosis factor alpha (TNF- α) and Fas ligand (FasL) which engage with death receptors on the cell surface (Ashkenazi et al., 1998; Latta et al., 2000). These stimuli can activate a cascade of cysteine-aspartate proteases (caspases) that are commonly expressed in most cells and once activated can usually release other procaspases, allowing initiation of a protease cascade. Some of the procaspases are able to aggregate and autoactivate (Elmore, 2007). Moreover, activation of other caspases are capable to amplify the apoptotic signalling pathway, they cleave cellular proteins after an aspartate residue, thereby leading to rapid cell death (Cohen, 1997; Elmore, 2007).

1.3.2.2 APAP-induced hepatocellular necrosis

Necrosis is another form of cell death that occurs as a consequence of acute cellular injury. It is characterised by mitochondrial swelling, loss of plasma membrane integrity and random nuclear DNA cleavage as a consequence of cellular degradation. This results in damage of the cell membrane and subsequent release of intracellular contents into the surrounding tissue. This release can trigger an inflammatory response, leading to exacerbation of injury and further damage (Robertson et al., 2000). Many studies had reported that necrotic hepatocyte cell death is a result of APAP overdose (Gujral et al., 2002; Jaeschke et al., 2003; Malhi et al., 2006).

Generally, it has been accepted that necrosis is the final and ultimate form of hepatocyte death in APAP-induced hepatotoxicity in animals as well as man (Jaeschke et al., 2003). However, some studies claimed that intracellular events following APAP insult may result in hepatocyte apoptosis (Ferret et al., 2001; Henderson et al., 2007; Kon et al., 2007). These mechanisms are largely dependent upon mitochondrial pathways, such as the induction of the MPT and the release of cytochrome C after mitochondrial rupture (Buki et al., 2000). Other reports support the role of apoptosis in the modulation of APAP-induced liver damage (El-Hassan et al., 2003; Ray et al., 1996). However, the role played by apoptosis following APAP in man and in experimental animals is so far not clear. Some reports suggest that apoptosis may not be a feature of APAP hepatotoxicity due to overwhelming oxidative stress and rapid depletion of hepatocyte ATP, conditions not favourable for caspase activation (Gujral et al., 2002; Gunawan et al., 2006). Antoine et al. have reported that fasting of mice for 24 hours prior to APAP dosing can inhibit APAP-induced caspase activation through depletion of basal ATP, thereby switching the mode of cell death to necrosis, which promotes the induction of an inflammatory response (Antoine et al., 2010). The process of apoptosis and necrosis during liver damage forms a mixture of events associated with cell death that can occur in parallel or sequentially (Raffray and Cohen, 1997).

1.3.3 Liver regenerative response after APAP insult

Hepatic regeneration following APAP intoxication plays an indispensable role in determining the outcome of liver injury (Bhushan et al., 2014). Other studies also suggested that liver regeneration is stimulated in a timely manner leading to improved survival after stimulation by stem cell factor (Hu and Colletti, 2008) and vascular endothelial growth factor (Donahower et al., 2010). Although models of partial hepatectomy (PHx) have been extensively studied in the past in order to understand the mechanism of liver regeneration, the link from PHx to APAP overdose is still questionable because PHx is not associated with tissue injury and inflammation. After PHx, hepatocytes enter the cell cycle phases simultaneously and undergo mitosis together whereas the cell cycle is not synchronised following chemical injury as the time, duration and signals required for cell proliferation may differ (Apte, 2009; Bhushan et al., 2014). While the mechanism of APAP induced liver injury has been studied widely over the last three decades, the mechanisms underlying the subsequent liver regeneration are still poorly understood (Pritchard and Apte, 2015). In hepatotoxicity studies, it has been suggested that the extent of liver regeneration is associated with the dose response until a threshold level is reached (Bhushan et al., 2014). When a threshold dose is exceeded, liver regeneration would be impaired due to inhibition of the pro-regenerative signalling pathway, resulting in enhanced liver damage (Anand et al., 2003; Mangipudy et al., 1995; Mehendale, 2005). Each increment of a toxic dose corresponds to a delay in the onset of liver recovery (Mangipudy et al., 1995). Due to dose dependency of the response, it is important to carry out preliminary toxicity studies in order to gather the information the optimal dose and the time course of liver regeneration in an animal model (Pritchard and Apte, 2015).

1.4 EFFECT OF FASTING ON APAP-INDUCED LIVER INJURY

1.4.1 Effects of fasting on mouse hepatotoxicity

The effects of food availability or deprivation on liver damage and function after APAP administration are yet to be further elucidated. A recent study suggested a standard operating protocol (SOP) for APAP toxicity studies, which included fasting a mice for 12 to 16 hours prior to APAP administration, with an adjustment for the different mouse strains, sex, age and dosage (Mossanen and Tacke, 2015). Furthermore, an overview of many studies that reveal the effects of fasting on the examined parameters in pharmacological research has been given in the past (Claassen, 1994). Fasting of animals prior to APAP dosing can profoundly affect the toxicological response to the drug by decreasing hepatic GSH (Shimizu et al., 1992) and ATP (Lee et al., 1988), altering CYP450 expression (Hu et al., 1995) and downregulating gene expression related to apoptosis (Matthias et al., 2004). Theoretically, GSH depletion is known to be a prerequisite for the onset of toxicity as it is required to detoxify the reactive metabolite (Jollow et al., 1973). A reduction of intracellular hepatic GSH levels due to fasting results in a markedly increased susceptibility to the toxic effects of APAP (Pessayre et al., 1979). A reduction of hepatic GSH has been documented in chronic alcoholic patients following therapeutic doses of APAP (Jewell et al., 1986; McClain et al., 1980; Seeff et al., 1986). Hence, malnourished individuals have a compromised detoxification capacity due to reduced hepatic GSH levels, and thereby become more susceptible to APAP-induced liver injury (Larson, 2007; Price et al., 1987).

A 6 hour duration of study showed that mice fasted for 12 hours overnight had a higher prevalence of hepatic centrilobular necrosis and a mortality rate of up to 20% compared to 4-6 hours fasting mice prior to APAP administration. Also, the fasted mice developed a significantly increased liver weight/body weight ratio after APAP treatment compared to non-fasted mice (Walker et al., 1982). A recent study has histologically confirmed the depletion of hepatocellular glycogen in fasted mice, coupled with significantly decreased basal hepatic ATP and GSH levels in these animals (Antoine et al., 2010). Overnight fasting of mice prior to APAP

administration can cause hypothermia, more intense liver necrosis and hepatic congestion, with significantly higher covalent binding of APAP or its reactive metabolite, thereby enhancing the mortality rate (Walker et al., 1982).

1.4.2 Effects of fasting on liver regeneration after APAP overdose

Mice that have been treated with 300 mg/kg APAP underwent liver regeneration similar to that observed in the PHx model (James et al., 2003a). A recent study revealed that liver regeneration is inhibited and sustained injury up to 96 hours at high doses of APAP (600 mg/kg) in C57BL/6J mice because of active restriction of cell progression and/or reduced pro-regenerative signal pathways compared to 300 mg/kg treated animals that underwent complete recovery at 48 hours, as evidenced by reduced serum ALT and lack of necrosis (Bhushan et al., 2014). This study also revealed a significantly higher amount of total PCNA positive cells and cyclin-D1 in low dose than high dose APAP treatment. It also demonstrated that liver regeneration involves Wnt/ β -catenin and NF- κ B mediated signalling (Bhushan et al., 2014). However, these studies have all been performed in mice that had been fasted for 12 hours prior to APAP dosing, and there is no information on animals that have been fed ad libitum. Overnight fasting of mice is known to generate hepatic CYP2E1 levels which potentially have an effect on liver injury or/and regeneration (Pritchard and Apte, 2015). A study in CD-1 mice showed liver regeneration had taken place within 24-48 hours after APAP-induced liver injury subsided. Regenerating hepatocytes were estimated by percentage of S-phase in PCNA analysis, but it did not mentioned the condition (fed or fasted) of animals prior to dosing (Apte et al., 2009b).

1.5 CYTOKINES INVOLVED IN ASSOCIATION WITH APAP-INDUCED LIVER TOXICITY AND LIVER REGENERATION

The innate immune system acts as the first line defence mechanism against any invading pathogens. The liver is also an immune organ and plays a pivotal role in the innate immune response, as non-parenchymal cells including KCs, NK cells, NKT cells and DCs show their own specific responses towards invading pathogens (Mackay, 2002). The immune response can also contribute to severity and progression of APAP-induced hepatotoxicity, through recruitment of inflammatory cells into the liver and production of cytokines downstream of bioactivation (Blazka et al., 1995; Laskin et al., 2001; Liu et al., 2004). The production of inflammatory mediators including cytokines released by KCs and macrophages have been implicated in APAP hepatotoxicity by exacerbating cell damage as a result of an aggressive inflammatory response (Liu et al., 2004; Luster et al., 2001). Cytokines are soluble protein mediators produced by almost all cell types in response to various stimuli. There are many cytokines including IL-1, TNF- α and IL-6 which play a role as key mediators of APAP hepatotoxicity (Blazka et al., 1995). An understanding of the cytokine response is beneficial to the future development of novel therapies for APAP-induced liver injury (Galun and Axelrod, 2002).

Tissue repair is an important determinant of the final outcome of toxicant-induced liver injury. Since hepatocytes are mostly in a quiescent state (G₀ phase of the cell cycle), pro-inflammatory mediators such as TNF- α and IL-6 are needed for their priming (Fausto, 2000). This renders the cells more responsive to growth factors which results in the expression of cell cycle proteins (Michalopoulos, 2013). Meanwhile, the gene expression is widely studied during liver regeneration because the changes are rapid and transcribe within minutes after PHx or DILI and the production of gene transcription continues throughout the time course of liver regeneration (Michalopoulos, 2013; Taub, 1996, 2004). Many factors including nutrition and metabolic status may influence liver regeneration. After the loss of a large number of parenchymal cells, the metabolic response of surviving hepatocytes is increased to generate more ATP for both maintenance of homeostasis and

regeneration in APAP overdose (Yang et al., 2009b). Figure 1.4 illustrates the pathogenesis of APAP hepatotoxicity.

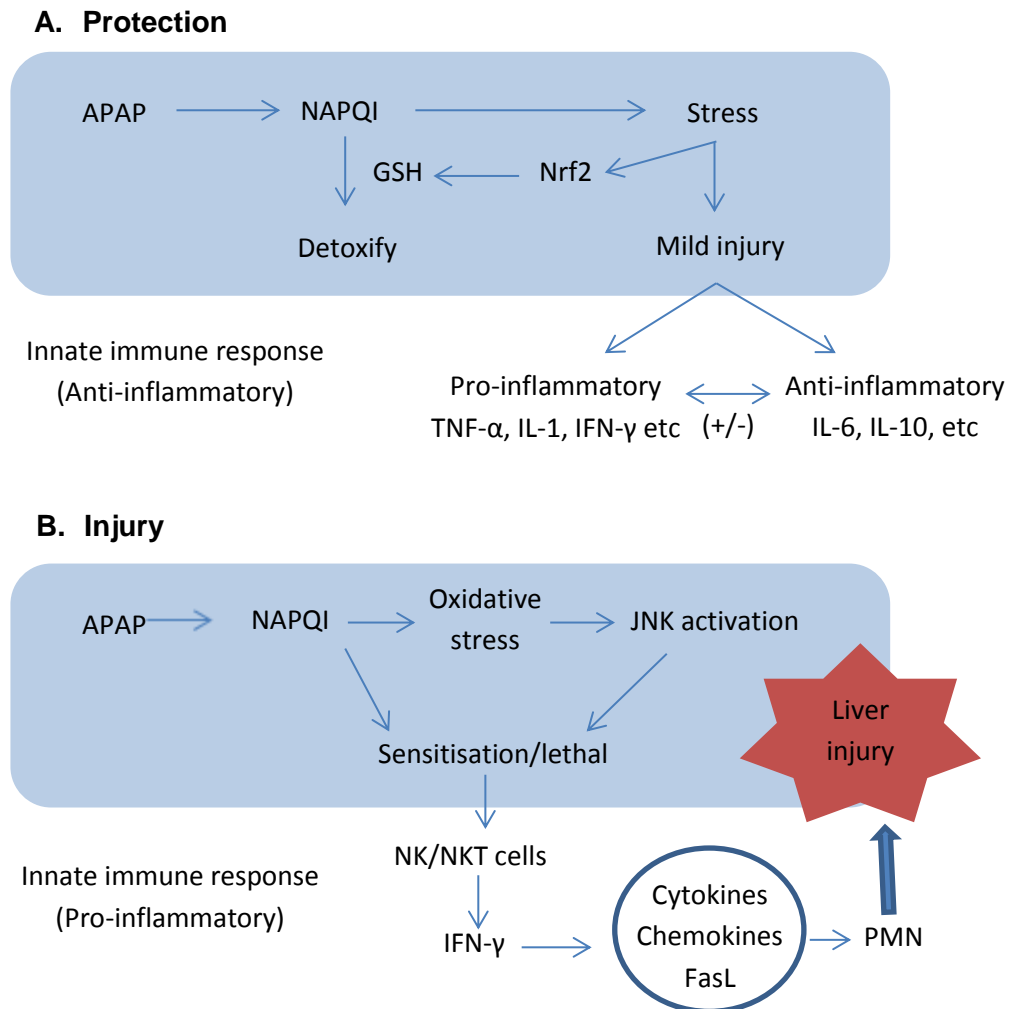


Figure 1.4. Pathogenesis of APAP hepatotoxicity.

A. APAP is metabolised by CYP450 to the toxic metabolite NAPQI, but GSH detoxifies NAPQI with the aid of Nrf2, which protects against toxicity. Intracellular injury initiated at this stage activates simultaneously pro and anti-inflammatory cascades and the balance between them determines the outcome of toxicity. B. With GSH depletion, NAPQI triggers cellular oxidative stress that activates JNK and thereby activates more NK/NKT cells to release IFN- γ to stimulate FasL expression, and promotes production of pro-inflammatory cytokines and chemokines leading to severe APAP hepatotoxicity. APAP - acetaminophen; FasL - Fas ligand; GSH - glutathione; JNK - c-Jun-N-terminal; NAPQI - N-acetyl-p-benzoquinone-Imine; NK - natural killer cells; NKT - natural killer T cells; Nrf2 - NF-E2-related factor 2; PMN - polymorphonuclear cells (Liu and Kaplowitz, 2006).

1.5.1 Role of Kupffer cells (KCs)

KCs are the liver macrophages and constitute up to 90% of tissue macrophages in the body; they are localised in the periportal and centrilobular regions (Mackay, 2002). Upon activation, KCs can functionally differentiate into M1 and M2 macrophage subsets (Yang et al., 2012a). Release of type 1 cytokines including TNF- α , IL-6 and IFN- γ is associated with M1 macrophage activation which contributes to the induction of pro-inflammatory cytokines that further promote a T helper cell response. However, activation of M2 macrophages is responsible for the excretion of IL-4, IL-10 and IL-13; these inhibit the inflammatory response and stimulate liver regeneration. Some studies have reported that activated KCs release cytokines and thereby contribute to APAP-induced hepatotoxicity (Ito et al., 2003; Laskin et al., 1986). In contrast, another experiment demonstrated the hepatoprotective role of KCs (Ju et al., 2002). These contradictory reports highlight the complexity of the Kupffer cell function to either inhibit or promote liver damage following APAP overdose which depends on types or doses of agents used (Ju et al., 2002).

1.5.2 Role of natural killer (NK) and natural killer T (NKT) cells

Natural killer (NK) and natural killer T (NKT) cells, which account for 20-50% of isolated liver leukocytes, produce a variety of immunoregulatory mediators after the cells have been infected, transformed or stressed (Liu et al., 2000). Infected cells trigger NK/NKT cells to kill the cells directly or generate cytokines and chemokines which then stimulate immune system components (Biron et al., 1999). NK and NKT cells were shown to become activated and play a crucial role in the progression of hepatotoxicity following APAP overdose. Meanwhile, neutralisation of NK and NKT cells by anti-NK1.1 was discovered to downregulate the expression of IFN- γ and monocyte chemoattractant protein-1 (MCP-1) mRNA (Liu et al., 2004). It subsequently minimises the susceptibility of mice in APAP toxicity as evidenced by low serum ALT levels, reduced hepatic necrosis and increased survival rate (Liu et al., 2004). In contrast, APAP solubilisation by dimethyl sulfoxide (DMSO) enhanced

the NK and NKT cell response and further increased the sensitivity to APAP-induced cell damage (Masson et al., 2008). Activated Kupffer cells release cytokines TNF- α , IL-12 and IL-18 which may activate NK/NKT cells (Gao et al., 2009). Activated NK/NKT cells increase the production of IFN- γ , which in turns promote further activation of macrophages, stimulates Fas ligand (FasL) expression and increases the production of chemokines and cytokines that could further stimulate the recruitment of neutrophils into the liver (Gunawan et al., 2006; Yuko et al., 2002). Innate immune cells like KCs, NK/NKT cells and neutrophils that express the FasL effector on their surface can induce the death of Fas-expressing hepatocytes via apoptosis (Gunawan et al., 2006; Imamura et al., 2004). Depletion of NK/NKT cells resulted in the inhibition of APAP-promoted upregulation of hepatic FasL expression at both mRNA and protein levels (Liu et al., 2004). It should be noted that FasL also plays a inflammatory role as it induces inflammatory cytokines/ chemokines that are responsible for progression of APAP-induced liver injury (Faouzi et al., 2001; Imamura et al., 2004; Liu and Kaplowitz, 2006; Park et al., 2003).

1.5.3 Role of cytokines in APAP-induced liver injury and regeneration

1.5.3.1 Role of TNF- α

TNF- α is the mainly produced by KCs after inflammatory stimulation and is also known as cachectin (Decker et al., 1990). Currently, the role of TNF- α in APAP toxicity appears to be controversial because it is considered to have diverse effects in different phases. It has been shown that TNF- α production during early events of hepatic injury triggers the release of a cascade of cytokines, therefore recruiting and activating inflammatory cells (Bradham et al., 1998). However, continuous production of TNF- α induces necrosis of hepatocytes and can increase the infiltration of inflammatory cells, by promoting recruitment and adhesion of neutrophils to endothelial cells (Fiers, 1991). The effect of TNF- α is mediated by two receptors, TNFR1 and TNFR2, which are involved in different distinct signalling pathways (Tartaglia et al., 1993; Tartaglia et al., 1991). TNF- α signalling via TNF- α

receptor 1 (TNFR1) which is heavily released and expressed by Kupffer cells is the main signalling pathway leading to an inflammatory response (Douni et al., 1998; Peschon et al., 1998). TNF- α can act directly on hepatocytes via both receptors TNFR1 and TNFR2 to induce direct toxicity, leading to hepatocyte apoptosis and necrosis (Bour et al., 1996; Wang et al., 1995). Several previous studies reported that TNF- α plays a role in the exacerbation of liver damage and it has been shown that its secretion contributes to the hepatotoxicity in APAP overdose (Blazka et al., 1996a; Blazka et al., 1995; Goldin et al., 1996). A recent study demonstrated significantly higher serum TNF- α levels in fasted mice treated with APAP than in fed mice (Antoine et al., 2010). Blazka and co-authors have demonstrated the secretion of TNF- α between 4 and 24 hours after APAP overdose; the APAP-induced liver injury was attenuated after administration of antibodies targeted against TNF- α (Blazka et al., 1995). However, another study showed that antibody-mediated neutralisation of TNF- α had no effect on APAP hepatotoxicity (Simpson et al., 2000). Likewise, TNF- α KO mice and wild-type mice showed similar response in APAP hepatotoxicity (Boess et al., 1998).

It has also been reported that TNF- α plays a role in liver regeneration after PHx (Diehl, 1995) and APAP-induced liver injury (Bhushan et al., 2014). In addition, deletion of TNF- α receptor (TNFR1) also showed delayed liver proliferation (Yamada et al., 1997). Therefore, TNF- α has been implicated to play a dual role in tissue repair and tissue damage in hepatotoxicity after APAP challenge, depending on the balance and kinetics of TNF- α production as well as other mediators in the liver (Gardner et al., 2003). Gardner et al. also suggested that the contradictory results regarding the role of TNF- α are due to the variability in the APAP doses and the sensitivity of the different mouse strains to APAP (Gardner et al., 2003). Michalopoulos concluded that TNF- α should not be viewed as initiator of liver regeneration, but as one contributor signal during the early response because TNF- α has no direct mitogenic effects on hepatocytes. This study also showed that TNF- α is unable to induce DNA synthesis both in cell culture and *in vivo* (Michalopoulos, 2013). Although the major source of TNF- α are KCs, production by other cells cannot not been ruled out; i.e increased TNF- α levels in the plasma after PHx may

be induced by another stimulus like endotoxin, produced by bacteria from gut (Michalopoulos and DeFrances, 1997).

1.5.3.2 Role of IL-6

IL-6 is mainly produced by macrophages and T cells and has both pro- and anti-inflammatory properties that regulate acute phase immune responses and inflammation (Heinrich et al., 2003; Hirano, 1998). IL-6 also plays a role in liver regeneration (Cressman et al., 1996; Trautwein et al., 1996). It has been calculated that almost 40% of the immediate early genes expressed in the regenerating liver may be IL-6 dependent, suggesting that the role of IL-6 in this process is complex (Fausto, 2000). A role of IL-6 is probably in proliferation, as IL-6 KO mice showed a significant reduction of liver regeneration due to delayed STAT-3 activation, a major signal transduction factor that is important for the activation of a large number of genes in hepatocyte regeneration (Cressman et al., 1996). Likewise, IL-6 deficient mice showed a reduced capacity of liver regeneration compared to wild-type mice following PHx and 30 minute ischaemia; hepatocyte proliferation improved when the animals were pre-treated with recombinant IL-6 (Selzner et al., 1999). In animal models of autoimmune diseases such as insulin-dependent diabetes mellitus (Rabinovitch, 1998), inflammatory bowel disease (Mudter and Neurath, 2007) and rheumatoid arthritis (Srirangan and Choy, 2010), IL-6 has a pathogenic pro-inflammatory effect. In contrast, it is protective and anti-inflammatory in liver damage caused by ethanol (Hong et al., 2002), carbon tetrachloride (CCl₄) (Kovalovich et al., 2000), and APAP (James et al., 2003a; Masubuchi et al., 2003c). A few studies have reported an increase in IL-6 production after APAP-induced liver damage in mice (Bourdi et al., 2002; James et al., 2003a). In addition, it has been suggested that IL-6 is relevant for hepatocyte regeneration and that liver damage following APAP overdose is pronounced in the absence of IL-6 due to lack of cytoprotective hepatic heat-shock protein expression compared to wild-type mice (James et al., 2003a; Masubuchi et al., 2003c).

Significantly elevated IL-6 serum levels together with evidence of hepatic regeneration were seen in APAP treated fed mice (Antoine et al., 2010). IL-6 was claimed to play a pathogenic role when overexpressed in a model of APAP-induced liver injury which indicates that the dual, pro- and anti-inflammatory role of IL-6 may be determined by its level of expression (Bourdi et al., 2002). The same study also showed that even though the level of IL-6 is high in IL-10/IL-4 KO mice, these animals were highly sensitive to APAP. Administration of an anti-IL-6 antibody reduced the degree of APAP-induced liver damage and was followed by decreasing IL-6 levels. Based on this, the authors concluded that although the production of IL-6 was high in the absence of IL-10 and IL-4, mice were still susceptible to hepatotoxicity following APAP overdose because IL-6 alone is unable to stimulate hepatocyte regeneration in vivo (Bourdi et al., 2002).

1.5.3.3 Role of IL-10

Similar to IL-6, IL-10 plays a protective role in APAP hepatotoxicity (Bourdi et al., 2002). It has been reported that IL-10 KO mice are more susceptible to APAP liver injury due to suppression of monocytes activation by downregulating NF- κ B, and also increased the release of pro-inflammatory cytokine production (TNF- α , IL-1 and IFN- γ) (Bourdi et al., 2002). However, a study has demonstrated that liver regeneration in PHx model is also enhanced in IL-10 deficient mice, due to capability of IL-10^{-/-} mice to increase inflammatory response-associated STAT-3 activation (Yin et al., 2011). It is strongly believed that the anti-inflammatory role of IL-10 is mediated by activation of STAT-3 signaling pathway in macrophages or neutrophils (Bazzoni et al., 2010), as deletion of STAT-3 in IL-10^{-/-} mice inhibited liver regeneration (Yin et al., 2011).

1.5.3.4 Role of NF- κ B

NF- κ B is a transcription factor that is strongly activated by TNF- α (Guicciardi and Gores, 2009) and has pleiotropic effects in various events, including inflammation and injury, cell survival, proliferation, and apoptosis (Karin et al., 2002). Under normal conditions, NF- κ B remains in the cytoplasm through the influence of the inhibitor κ B (I κ B) (Wajant et al., 2003). When I κ B undergoes phosphorylation, ubiquitination and degradation, the NF- κ B pathway is activated. I κ B kinases (IKKs) are the enzymes important for I κ B phosphorylation (Tacke et al., 2009). Once the I κ B complex has lost various subunits after phosphorylation through the IKKs, NF- κ B is released and translocates to the nucleus (Perkins, 2000). A study demonstrated that in mice after PHx, the primary activation of NF- κ B in the liver occurs in KCs rather than in hepatocytes (Yang et al., 2005). Depletion of KCs resulted in reduced NF- κ B activation and reduced regeneration of the liver in PHx model (Abshagen et al., 2007). NF- κ B provides signals to the cells, resulting in transcription of inflammatory cytokines, such as TNF- α and IL-6 (Karin et al., 2002; Yamada et al., 1997). It also acts as a regulator of inflammation; its activation can induce the expression of survival genes, including BCL_{XL} and A1, that are strongly linked to liver regeneration after cell injury (Fausto, 2000; Malhi et al., 2006). Some studies provide evidence that NF- κ B induces the inflammatory response that is involved in the progression of hepatotoxicity (Tsung et al., 2005; Ulloa et al., 2002). Others concluded that NF- κ B is not critical in the process of liver regeneration after PHx (Laurent et al., 2005). Another study has shown that inhibition of NF- κ B results in pronounced hepatocyte cell death and thereby worsens liver injury and increases the mortality in a PHx model (Malato et al., 2012). It has also been demonstrated that enhanced NF- κ B activation diverts intracellular pathways involved in inflammation and cell death to other mechanisms that activate a pro-regenerative response (Sun and Karin, 2008). This is supported by another study which suggests that enhanced NF- κ B binding is associated with improved liver regeneration during the late phase of APAP hepatotoxicity (Yang et al., 2012b; Yang et al., 2011), and decreased NF- κ B binding is associated with impaired liver regeneration (Yang et al., 2009a). A more recent study also demonstrated the production of NF- κ B during liver regeneration

(Bhushan et al., 2014). Although NF- κ B was shown to be activated both during hepatic regeneration after PHx and in the APAP toxicity model, its overall contribution to hepatocyte proliferation is yet to be determined (Robinson and Mann, 2010). Therefore, NF- κ B activation during liver regeneration can have an upregulating or downregulating effect or none at all on regeneration and/or apoptosis, it is influenced by many factors including various specific target of cell types which induced by different agent or model used (Nejak-Bowen and Monga, 2015). The role of NF- κ B played in liver regeneration as it is known so far is illustrated in Figure 1.5.

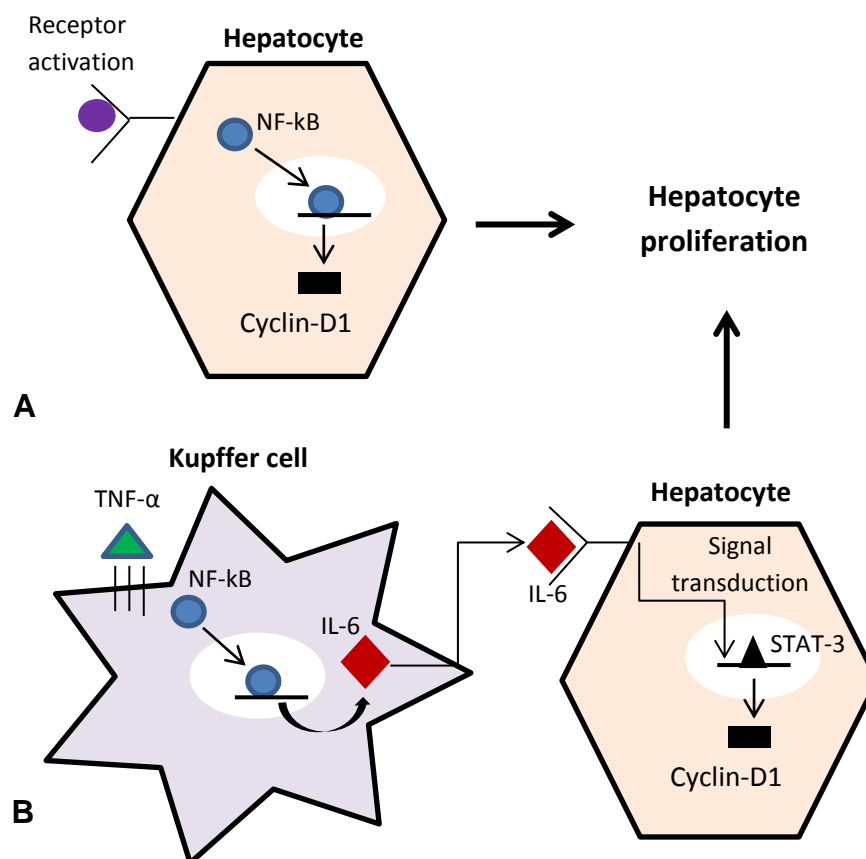


Figure 1.5. The role of NF- κ B in liver regeneration.

(A) NF- κ B is activated in hepatocytes to drive regeneration, (B) Activation of NF- κ B cell in Kupffer cells that are capable to secrete cytokines that trigger the proliferation of hepatocytes. Activation of TNF- α , LPS or other cytokines on KCs surface are able to induce NF- κ B production, thereby further release of IL-6 and TNF- α . Subsequently, these cytokines can stimulate adjacent hepatocytes to proliferate via activation of signal transducer and activator of STAT-3 transcription (Nejak-Bowen and Monga, 2015).

1.5.3.5 Role of cytokine networks in hepatic regeneration

The process of liver regeneration involves activation of two distinct pathways, a growth factor and a cytokine-regulated pathway (Fausto, 2000). The importance of cytokines for liver regeneration is due to the fact that certain cytokines can prime resting hepatocytes for cell division (Fausto, 2000). Before hepatocytes fully respond to growth factors, such as hepatocyte growth factor (HGF), transforming growth factor alpha (TGF- α) and epidermal growth factor (EGF), they need to be primed by cytokines like TNF- α and IL-6. Also, transcription factors including NF- κ B, STAT-3, AP1 and C/EBP β which are proteins responsible for binding to specific recognition sites in target genes are crucial for the initiation of liver proliferation. The precise role played by these individual cytokines and transcription factors is still needs further clarification. In PHx and CCl₄-induced liver injury, the TNF- α signal transduction pathway plays an important role, with the following sequence: TNF- α - TNFR1 - NF- κ B - IL-6 - gp130 - STAT-3 (Fausto, 2000).

The cytokine network is initiated by binding of TNF- α to TNFR1, leading to activation of NF- κ B by removal of the inhibitory I κ B through phosphorylation, mediated by the kinase IKK, and the subsequent proliferative response by preventing further cell death (Yamada and Fausto, 1998; Yamada et al., 1997). TNF-R1 KO mice show a lack of NF- κ B activation due to blockage of cell cycle progression at the G1 and S phase, and are ultimately depleted of IL-6 serum levels and show impaired DNA synthesis in the liver (Yamada et al., 1997). Induction of NF- κ B by TNF- α can promote production of IL-6 and its release from hepatocytes, which activates the Jak/STAT pathway, an important stimulator in the early phase of liver regeneration (Liebermann and Baltimore, 1990). Binding of IL-6 to a soluble circulating receptor, which then binds to the cell-surface receptor gp130 will initiate the signals for STAT-3 activation (Cressman et al., 1996; Wuestefeld et al., 2003). An important STAT-3 target is Suppressor of cytokine signalling-3 (Socs3), which acts in a feedback loop by preventing ongoing activation of IL-6 signalling through inhibiting STAT-3 phosphorylation (Riehle et al., 2008). The activation of IL-6/STAT-3 signalling is a pivotal mediator of pro-survival factors for liver regeneration (Kovalovich et al.,

2001). STAT-3 activation acts together with transcription factors C/EBP β and AP1 to increase expression of other additional factors such as NF-IL-6.c-myc, c-fos, IRF-1, to enable cell progression from G1 to S phase (Galun and Axelrod, 2002).

Taking together, this indicates that the induction of cytokine signalling activates pro-survival factors that are important in protecting the liver against further damage and promote liver recovery (Kovalovich et al., 2001). However, the balance between pro-inflammatory and anti-inflammatory cytokines produced by the liver is important to determine the development towards toxicity or regeneration of the liver (Galun and Axelrod, 2002). Deletion of certain cell gene or types in KO animals has been substantially used to highlight the role played by the innate immune cells in APAP hepatotoxicity and regenerative response (listed in Table 1.1).

Table 1.1. Experimental models of APAP-induced liver toxicity and regenerative response.

Experimental model	References
Increased susceptibility	
IL-6 (-/-) mice	(Masubuchi et al., 2003c)
TNFR1(-/-) mice	(Yamada et al., 1997)
IL-10 (-/-) mice	(Bourdi et al., 2002)
Kupffer cell depletion	(Ju et al., 2002)
GSH depletion	(Jollow et al., 1973)
Decreased susceptibility	
IL-6 administration	(Masubuchi et al., 2003c)
NK and NKT cell depletion	(Liu et al., 2004)
Neutrophil depletion	(Liu and Kaplowitz, 2006)
FasL-deficient mice	(Liu et al., 2004)
Increased regeneration	
HMGB-1 blockade	(Yang et al., 2012b)
IL-6 administration	(Masubuchi et al., 2003b)
Decreased regeneration	
IL-6 (-/-) mice	(Cressman et al., 1996)
TNFR1 (-/-) mice	(Chiu et al., 2003)
STAT-3 deletion in IL-10(-/-) mice	(Yin et al., 2011)

1.5.4 Liver regeneration after APAP overdose: markers and mediators

1.5.4.1 Role of cyclin-D1

Cyclin-D1 is cell cycle protein that believed to be a reliable marker of proliferating hepatocytes in the G1 phase. Hepatocytes express cyclin-D1 once they have passed the G1 restriction point and started DNA replication (Fausto, 2000). A few recent studies revealed that after Ringer's lactate solution and anti-HMGB1 treatment, cyclin-D1 was highly expressed during liver recovery, at the late phase of APAP hepatotoxicity (Yang et al., 2012b; Yang et al., 2011). In addition, other previous studies have demonstrated that EP therapy and prolonged treatment with NAC reduce cyclin-D1 expression after liver regeneration is inhibited (Yang et al., 2009a; Yang et al., 2012c). Based on these reports, cyclin-D1 is concluded to be a reliable marker to detect liver regeneration after APAP induced hepatotoxicity (Yang et al., 2009b; Yang et al., 2012c).

1.5.4.2 Proliferating cell nuclear antigen (PCNA) and HE staining

Proliferating cell nuclear antigen, commonly known as PCNA, is a 36-kDa auxiliary protein that acts as a processivity factor that measures the average number of nucleotides added by a DNA polymerase enzyme in eukaryotic cells (Bravo et al., 1987). It is an example of a DNA clamp since it achieves this processivity by encircling the DNA, thus creating a topological link to the genome. PCNA is found in the nucleus and is a cofactor of DNA polymerase delta that is involved in the coordination of cell cycle progression. Since DNA polymerase delta is involved in the resynthesis of excised damaged DNA strands during DNA repair, PCNA is important for both DNA synthesis and DNA replication (Bravo et al., 1987). Many proteins are involved in the process of cell cycle replication, including cyclins and cyclin-dependent kinases that are important in the regulation of cell transition at different phases; G1, where cells increase in size and become ready to divide; S, where genome duplication occurs; G2 where cells check for completion of DNA replication; and M where the mitosis takes place (Pritchard and Apte, 2015). Under normal

circumstance, the majority of hepatocytes are in a quiescent state, i.e. in the G0 phase and not within the cell cycle (Kurki et al., 1986). However, DNA damage induced by chemicals, disease or aging leads to the production of p21 protein that blocks the transition from the G1 to the S phase, by inhibiting the activity of cyclin-dependent kinases. PCNA expression is induced in the late G1 phase, peaks in the S phase and stops thereafter (Kurki et al., 1986).

The in situ demonstration of PCNA by immunohistology is a well-known method to assess hepatic regeneration and the clone the most commonly used is PC10, as it can detect PCNA in formalin-fixed tissues (Hall and Woods, 1990). By this method, individual hepatocytes at each time point when the liver was removed can be assessed to determine which phase of cell cycle is dominant during liver regeneration (Eldrige et al., 1993; Greenwell et al., 1991). Figure 1.6 provides detailed information on how the cell-cycle phase can be evaluated using PCNA immunostaining. However, some authors claimed that PCNA is an unreliable indicator for the quantitative assessment of hepatocyte regeneration during APAP hepatotoxicity in C57BL/6J mice, because the specificity of the first antibody used markedly influence the results (Yang et al., 2012b; Yang et al., 2011; Yang et al., 2014). The studies indicate that PCNA is expressed in the liver at 24 hours post APAP administration, but without positive PCNA immunostaining. Also, after 48 hours, PCNA staining was seen extensively in areas of marked liver damage, with larger areas of necrosis exhibiting larger numbers of PCNA positive cells, while improved liver damage with smaller areas of necrosis exhibited a lower number of PCNA positive cells; this was considered as a potential false result (Yang et al., 2011; Yang et al., 2014). A conclusion comes from the finding that the pattern of hepatocyte regeneration as indicated in HE stained slides does not match the pattern of liver proliferation suggested by the distribution of PCNA-positive cells (Yang et al., 2012b; Yang et al., 2011; Yang et al., 2014). Although HE staining is not widely used for the assessment of early hepatocyte regeneration, it can be a reliable method in determining late recovery of hepatocytes in C57BL/6J mice during APAP-induced liver injury as it confirms the improvement of the hepatic architecture, the lower numbers of necrotic cell death and the reduced recruitment

of inflammatory cells (Bhushan et al., 2014). Although these studies suggested that the immunohistological demonstration of PCNA does not provide reliable results for the assessment of liver regeneration after APAP toxicity, a most recent study demonstrated that PCNA immunostaining is indeed an effective tool for the quantification of cell proliferation in cancer risk assessment (Wood et al., 2015).

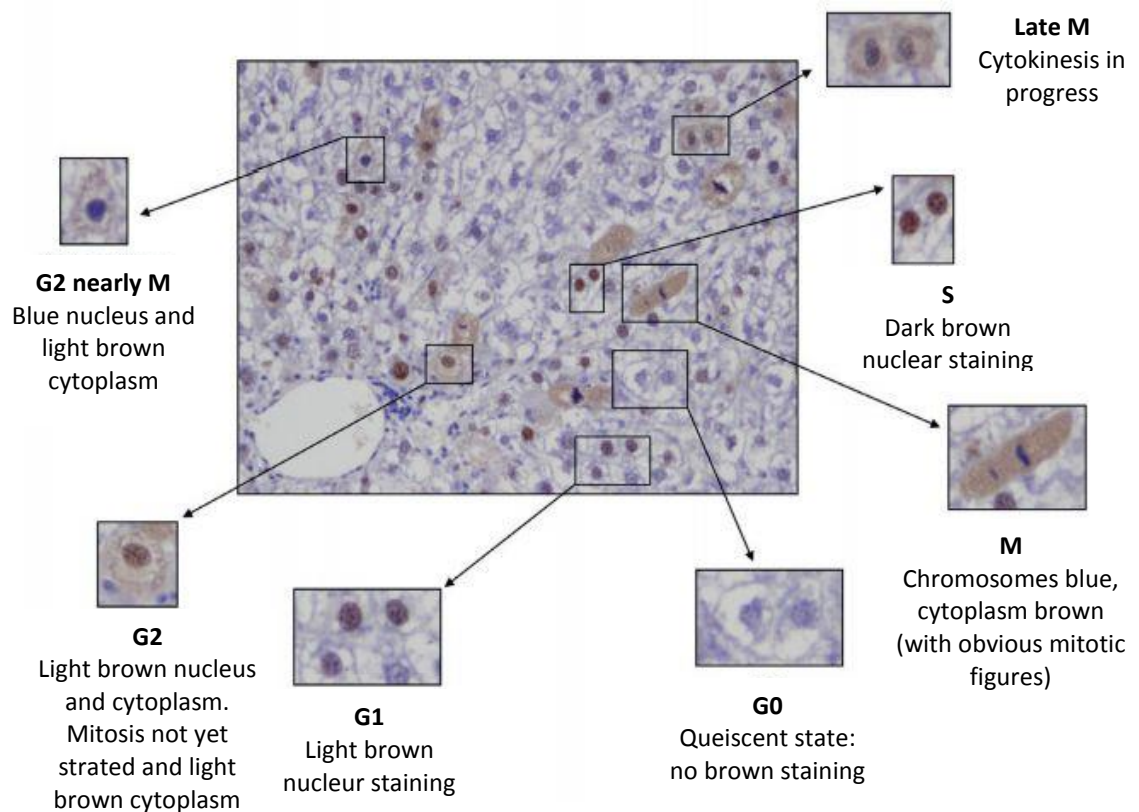


Figure 1.6. PCNA cell-cycle phases.

G0 or quiescent cells; no brown staining. Cells in the G1 phase exhibit a light brown nuclear staining, while cells in the S phase exhibit dark to nearly black nuclear staining; cells in both G1 and S cells do not show cytoplasmic staining. When cells enter the G2 phase, a reaction is seen both in nucleus and cytoplasm, while mitotic cells exhibit a light brown cytoplasmic reaction and a negative nucleus (Pritchard and Apte, 2015).

1.6 AIMS OF THESIS

1.6.1 Effects of fasting on the liver of untreated (i.e. saline dosed, control) mice

Despite the extensive use of fasting in toxicity studies, and in particular also in acute drug induced liver injury (DILI) studies, only limited information is available on the effect of fasting on a range of relevant liver parameters that could potentially also affect the outcome of DILI studies. Furthermore, the effect of refeeding on the liver has not been examined, and this has not been looked at in the context of the circadian rhythms. The hypothesis was that both fed and fasted control CD-1 and C57BL/6J mice have similar basic levels after a certain time period prior to and after the onset of refeeding.

The aims of this part of the thesis are therefore:

- To gather reliable baseline data that allow better interpretation of the results from DILI studies in mice;
- To understand the effect of fasting on hepatocyte function, by assessing hepatic GSH content, serum ALT levels, hepatic ATP levels, cytokine levels, and the extent of hepatocyte proliferation as well as the morphological features of the liver including the hepatocellular glycogen content.

For this purpose, male CD-1 and C57BL/6J mice that had been consistently fed ad libitum or had been fasted for 16 or 24 hours and then refeed for different time spans thereafter were used.

Answers to the following questions were sought:

- What is the effect of fasting in untreated mice?
- Do CD-1 and C57BL/6J mice show the same type and degree of fasting effects?

1.6.2 Effects of fasting on the development and extent of APAP-induced DILI and the regeneration thereafter

Despite intensive research, inconsistencies and conflicting reports remain on the extent of the role of innate immune, inflammatory and regenerative response in APAP-induced hepatotoxicity. The aim of the thesis was to assess the influence of fasting on hepatocyte regeneration after the toxic insult and on the inflammatory response that contributes to either progression or regression of APAP-induced liver injury. The hypothesis was that fasting of mice prior to APAP overdose results in higher susceptibility to APAP hepatotoxicity and subsequent delayed capability of hepatocytes to regenerate after the damage has subsided.

The aims of this thesis were to answer the following questions:

- To investigate the influence of fasting on the outcome of APAP-induced liver damage which include serum ALT, hepatic ATP and hepatic GSH content.
 - What effect has fasting animals on the extent of hepatocyte damage (serum ALT level) and the detoxifying capacity of hepatocytes (GSH level)?
 - Does fasting influence the type and extent of drug induced cell death (hepatic ATP content)?
- To assess the degree of hepatocellular injury and the glycogen content microscopically to identify any effect of fasting on APAP-induced liver injury.
 - Does fasting exacerbate liver damage and delayed regeneration following APAP overdose?
- To further explore the signalling cascade triggered by DILI by investigating the degree of expression of inflammatory cytokines, such as TNF- α , IL-6 and IL10 transcription in liver and spleen, and TNF- α and IL-6 in the serum.
 - Does fasting affect the expression and secretion of cytokines?
 - When after DILI are these cytokines expressed most intensely?

- To further evaluate the effect of fasting on the degree and speed of hepatocyte regeneration, as indicated by the hepatocellular expression of PCNA and the transcription of NF- κ B and cyclin-D1 in the liver following APAP-induced liver damage.
 - Does DILI induce NF- κ B and cyclin-D1 expression?
 - Does DILI induce hepatocellular proliferation, and when after injury?
 - Can a quantification of NF- κ B and cyclin-D1 transcription and/or PCNA expression be used as indicators for the extent of hepatic regeneration following APAP overdose?

1.6.3 Differences between C57BL/6J and CD-1 mice in their response to fasting and APAP overdose.

- Due to conflicting data obtained in toxicological studies, we wanted to explore the effect of fasting on acute APAP toxicity and the subsequent liver regeneration, comparing the two strains, CD1 and C57BL/6J mice, using the same APAP dose (530 mg/kg).
 - Do the two strains respond differently to an APAP overdose of 530 mg/kg? If yes, what are the differences? It is postulated that the extent of APAP-induced liver injury and/or regeneration differs between fed and fasted groups, however, both strains are expected to respond in a similar fashion to APAP treatment.

The studies in this thesis have been undertaken in an attempt to provide more information on the effect of fasting on the response of mice to APAP induced acute hepatotoxicity. The overall objective was to provide information on baseline data of liver parameter after fasting, since these appear to be often ignored. Furthermore, this study also wants to raise the awareness on how important it is to carefully choose the mouse strain and the experimental protocol during the planning of toxicity studies in vivo. This study also provides data that might allow researchers to optimise their experimental settling to maximise the scientific outcome and secure better scientific data without compromised animal welfare.

CHAPTER TWO

MATERIALS AND METHODS

CONTENTS

2.1	Experimental animals	46
2.2	Experimental and sampling protocols	46
2.3	Assessment of serum alanine transaminase (ALT) levels	47
2.4	Determination of hepatic glutathione (GSH) levels	48
2.4.1	Glutathione assay	49
2.4.2	Lowry assay	50
2.4.3	Quantification of glutathione levels	50
2.5	Determination of hepatic ATP content	51
2.6	Histology and immunohistochemistry for the assessment of hepatotoxicity and regeneration in the liver	52
2.6.1	Preparation of specimens for histological and immunohistological examinations	52
2.6.2	Histological examinations	52
2.6.3	Immunohistological examinations	54
2.6.3.1	Quantitative analysis of immunohistological stains	56
2.7	Assessment of cytokine expression in serum, liver and spleen	57
2.7.1	Measurement of serum cytokine levels by ELISA	57
2.7.2	Determination of cytokine transcription levels in liver and spleen	58
2.7.2.1	RNA extraction	58
2.7.2.2	DNase treatment	59
2.7.2.3	Reverse transcription (RT)	59
2.7.2.4	Conventional PCR	60
2.7.2.5	Quantitative Real time PCR (qPCR)	61
2.8	Statistical analysis	63

2.1 Experimental animals

All protocols described were undertaken in accordance with criteria outlined in a licence granted under the Animals (Scientific Procedures) Act 1986 and approved by the University of Liverpool Animal Welfare Committee. All CD-1 and C57BL/6J mice were obtained from Charles River Laboratories (Canterbury, England), were housed at the Biomedical Service Unit (BSU), University of Liverpool, UK, and had a 7 day acclimatisation period prior to experimentation. They were maintained in a 12 hours light/dark cycle with free access to a commercial diet (Source: Special diet services (SDS) - carbohydrate 77%, amino acids 11.5%, fatty acids 2.7%) and drink.

2.2 Experimental and sampling protocols

The study was performed on male CD-1 and C57BL/6J mice (body weight: 25-35 g) that had been grouped randomly for each strains which either had free access to food and water throughout the entire experiment or were fasted for 16 or 24 hours with free access to water prior to dosing. The body weight of individual animals was determined before and upon completion (i.e. immediately prior to dosing) of the fasting period in the fasted group and immediately before dosing in the fed group for both CD-1 and C57BL/6J mice.

Acetaminophen (APAP) solution (Sigma, St Louis, MO, 30 mg/ml) was freshly prepared with 0.9% saline (9 g NaCl / 1 L dH₂O) and incubated at 42 °C for 15 min with intermittent agitated using a vortex machine. In groups of 4 or 6 animals, mice were intraperitoneally administered 530 mg/kg of acetaminophen in 0.9% saline. Food was returned immediately after APAP administration in the fasted mouse groups. Control animals received 0.9% saline intraperitoneally instead.

Animals were euthanized at different time points; 0, 0.5, 1, 2, 4, 5, 10, 15, 20, 24, 30 and/or 36 hours post APAP and saline administration, respectively. Animals were euthanised by CO₂ inhalation followed by exsanguination. Blood was collected by cardiac puncture. Blood samples were stored at 4 °C and allowed to clot overnight to obtain serum.

Subsequently, animals were dissected and livers removed, rinsed in ice cold saline and fixed in 4% paraformaldehyde (PFA) [4 g paraformaldehyde in 100 ml PBS] for histology processing, or snap frozen at -80°C until further analysis.

Animals originated from 3-5 experiments undertaken either specifically for the current PhD project or as part of other PhD and/or postdoctoral research projects at the MRC CDSS, Institute of Translational Medicine (ITM), University of Liverpool, UK. In all experiments, the same mouse strains (CD-1 or/and C57BL/6J mice) from the same source (Charles River) were used, the same APAP dose (530 mg/kg APAP in 0.9% saline) and the same application protocol was applied (Appendix Table 6.1), using a minimum of 4 animals per group. The same procedure was performed on each individual mouse, including the euthanasia technique and the procedures for blood and tissue sample collection. This approach served to keep animal numbers at a minimum and avoid unnecessary repetitive experimentation. The time of fasting, dosing and endpoint as well as the tests carried out on the different groups of mice from the different studies are listed in Appendix (Tables 6.2 to 6.5).

2.3 Assessment of serum alanine transaminase (ALT) levels

Serum alanine transaminase (ALT) levels were determined and served as a measurement of hepatotoxicity using Infinity ALT liquid kits (Sigma-Aldrich, Poole, UK). Serum samples were diluted with 0.9% saline in microtubes according to Table 2.1 and two sets of serum dilution, i.e. either 1:2 and 1:5 or 1:5 and 1:10 were needed for each sample. The dilution of serum sample required for individual sample was depends on degree of hepatotoxicity. If liver is severely damaged, the serum is needed to be more diluted and vice versa. After pre-warming of the ALT solution and the chamber of the plate reader to 37°C (an optimal temperature for liver enzyme activities), 30 µl of diluted sample was added to each well, this was done in duplicate. After placing the well into the plate reader, 300 µl of ALT solution was added using multichannel pipette and the plate was read immediately.

The mean velocity of the plate was read at every 30 sec for 5 min at 340 nm with a Dynex Magellan Bioscience MRX^e reader (Dynex Technologies Inc, Sussex, UK). The

kinetic curve obtained was evaluated and recorded for each individual sample. If no or a very low kinetic curve was obtained, the sample was examined again, using a lower dilution, while with too high readings within short interval, the samples were examined again, using a higher dilution. Then, the value was corrected by subtract it to blank and the actual ALT level was calculated by multiply the obtained value to dilution factor.

Table 2.1. Serum ALT dilution measurement

Ratio	Volume of serum (μ l)	Volume of 0.9% saline (μ l)
Neat	30	0
1:2	15	15
1:5	6	24
1:10	3	27
1:50	5	245

μ l – microlitre.

2.4 Determination of hepatic glutathione (GSH) levels

Thawed liver samples (30-50 mg) were prepared and homogenised with a Retsch MM400 homogeniser (ThermoFisher Scientific, Loughborough, UK) in 800 μ l GSH stock buffer (143 mM Na_2HPO_4 , 6.3 mM EDTA, pH 7.4) with 200 μ l of 6.5% SSA (5-sulfosalicylic acid). The protein was allowed to precipitate on ice for 10 min prior to centrifugation at 14,000 rpm for 5 min. Subsequently, the supernatant was removed, placed into a new tube and subjected to the GSH assay protocol for glutathione determination. Meanwhile, the protein pellet left at the bottom of the tube was dissolved in 1 ml 1 M NaOH at 50-60°C for at least 1 hour and then subjected to the Lowry assay protocol for Lowry-protein correction. The supernatants containing GSH and dissolved protein were stored at -80°C until analysis. Both the GSH and the Lowry assay were performed in 96-well plates.

2.4.1 Glutathione assay

GSH stock buffer was prepared by adding 125 mM $\text{NaH}_2\text{PO}_4 \cdot 2\text{H}_2\text{O}$ and 12.5 mM EDTA (99% pure) and 500 ml sterile water. After that, the pH was adjusted to 7.4 by gradual addition of 5 M NaOH. Subsequently, 1 mM GSH stock solution was prepared by adding 3.07 mg GSH reduced to 10 ml GSH stock buffer. The 1 mM GSH solution was then diluted 1:10 to obtain a 0.1 mM GSH solution. For the preparation of GSH reductase, 154 μl of GSH reductase reagent was added to 10 ml of GSH stock buffer. After that, 20 μl of GSH standards (Table 2.2) or diluted samples (1:20 and 1:50) were added to the wells in duplicates. Then, 20 μl of GSH stock buffer solution were pipetted to each well to neutralise the pH. Daily Assay Reagent was prepared immediately before use by mixing 9.9 mg DTNB, 7.08 mg NADPH and 25 ml GSH stock buffer. Once done, 200 μl of Daily Assay Reagent was added to each individual well and the plate was incubated at room temperature. After a 5 min incubating period, the plate was placed on the plate reader and 50 μl of GSH reductase was added to each well immediately with a multichannel pipette, at the same time removing all bubbles with a needle to avoid interference with the results. Finally, the results were obtained at 415 nm at 1 min interval for 5 min with Revelation software on a Dynex Magellan Bioscience MRX^e reader (Dynex Technologies Inc, Sussex, UK).

Table 2.2. Standards for the glutathione assay.

Standard (Std)	Concentration (nmoles/ml)	Volume of 0.1 mM stock solution (μl)	Volume of GSH stock buffer (μl)
Std 1	0	0	1000
Std 2	1	10	990
Std 3	2	20	980
Std 4	5	50	950
Std 5	10	100	900
Std 6	20	200	800
Std 7	30	300	700
Std 8	40	400	600

Std – standard; nmoles/ml – nanomoles per millilitre; mM – miliMolar; μl – microlitre.

2.4.2 Lowry assay

A standard of the assay was prepared using a stock solution of 1 mg/ml BSA that was diluted in 0.5 M NaOH (5 ml of 0.2 mg/ml solution). Meanwhile, the Lowry reagent was prepared by adding 0.5 ml of 1% $\text{CuSO}_4 \cdot 5\text{H}_2\text{O}$, 0.5 ml of 2% NaK tartrate (2 g NaK tartrate/100 ml dH_2O) and 10 ml 10% Na_2CO_3 in 0.5 M NaOH. 1 ml of Folin's Reagent (yellow phenol reagent, serving as sample indicator to measure levels of amines and amino acids) was added to 9 ml of dH_2O (1:10 ratio) and kept in the dark. After all the reagents were prepared, the standard was diluted (Table 2.3) and each sample diluted 1:100 (10 μl sample with 990 μl 0.5 M NaOH) and 1:200 (5 μl sample with 995 μl of 0.5 M NaOH). After that, 50 μl of either standard or sample were added to wells in duplicate for each standard and individual sample, followed by 50 μl of Lowry reagent. Wells were incubated at room temperature for 15 min. Subsequently, 150 μl Folin's reagent was added to each well and the plate further incubated at room temperature for 30 min, followed by reading on the plate reader at 540 or 570 nm, using Revelation software on a Dynex Magellan Bioscience MRX^e reader (Dynex Technologies Inc, Sussex, UK).

Table 2.3. Standard of Lowry assay

Standard (Std)	Protein (g/ml)	0.2mg/ml BSA (μl)	0.5 M NaOH (μl)
Std 1	0	0	1000
Std 2	20	100	900
Std 3	40	200	800
Std 4	80	400	600
Std 5	100	500	500
Std 6	200	1000	0

g/ml - gram per millilitre; mg/ml – milligram per millilitre; M – Molar; μl – microlitre.

2.4.3 Quantification of glutathione levels

Data obtained from GSH and Lowry assay were calculated from their respective standard curve graph. Finally, total hepatic glutathione (GSH + oxidized glutathione) levels were quantified by normalisation of GSH levels to the hepatic protein content derived from Lowry assay.

2.5 Determination of the hepatic ATP content

Protein free lysates generated for measurement of the hepatic GSH content were also utilised for the determination of the hepatic ATP content with the Sigma ATP bioluminescence kit (Sigma-Aldrich, Poole, UK) that comes with 3 reagents, ATP stock solution, ATP dilution buffer and ATP standard. ATP stock solution was dissolved in 5 ml dH₂O to generate a stock solution with pH 7.8. After gentle mixing, the solution was kept on ice for at least 1 hour to ensure complete dissolution. Then, the ATP assay dilution buffer was prepared by dissolving the buffer solution (ready made in kit) in 50 ml dH₂O. After that, one vial of ATP was dissolved with 1.8 ml sterile water to 1 mM. Then, serial dilutions of ATP standard were prepared (Table 2.4). Subsequently, from each liver sample generated from GSH assay, a 1:10 and 1:20 dilution was prepared. 100 µl of ATP stock solution was put to 96-well plate and allowed to stand for 3 min before rapidly adding 100 µl of either standard or diluted samples to each well. For each sample, duplicates were prepared. Finally, the samples were swirled briskly in order to mix well, followed by measuring the amount of light with a luminometer, Dynex Magellan Bioscience MRX^e reader (Dynex Technologies Inc., Sussex, UK). The hepatic ATP content was recorded as nmol and quantified using ATP standard curve.

Table 2.4. Standard of ATP assay

Standard (Std)	Protein (nM)	ATP standard (1mM)	dH ₂ O (µl)
Std 1	0	0	1000
Std 2	1	100 µl of std 3	900
Std 3	10	100 µl of std 4	900
Std 4	100	100 µl of std 8	900
Std 5	300	3 µl of ATP std	997
Std 6	600	6 µl of ATP std	994
Std 7	800	8 µl of ATP std	992
Std 8	1000	10 µl of ATP std	990

Std – standard; nM – nanoMolar; mM – miliMolar; µl – microlitre.

2.6 Histology and immunohistochemistry for the assessment of hepatotoxicity and regeneration in the liver

2.6.1 Preparation of specimens for histological and immunohistological examinations

Histological specimens from the livers were prepared in the Histology Laboratory, Veterinary Laboratory Services, School of Veterinary Science, University of Liverpool, UK. Samples from the left lateral lobe were fixed in 4% PFA for 24 to 48 hours. Transverse sections were prepared from the fixed samples and placed (cut surface down) into a pre-labelled histology cassette, then routinely paraffin wax embedded using a tissue processor (Tissue-TEK Vacuum Infiltration Processor). Briefly, the tissue was dehydrated with a series of increasing concentrations of ethanol to remove free and bound water. It was then submerged and washed in xylene to remove the ethanol (EtOH). The tissue specimens were then removed from the cassette and embedded into a mould of molten paraffin wax with the trimmed side down. The cassette was then placed on the top of the mould, topped up with wax and allowed to solidify. Sections (3-5 μm) were cut on a microtome, floated onto a clean water bath (45°C) to remove creases, then retrieved and placed on a charged microscope slide and allowed to dry in an oven (60-70°C).

2.6.2 Histological examinations

For the histological assessment, sections were routinely stained with haematoxylin and eosin (HE). The hepatocellular carbohydrate (glycogen) content was assessed on sections routinely stained with the Periodic Acid Schiff (PAS) reaction (Vaquero et al., 2007). All stains were performed by the technical staff in the Histology Laboratory, Veterinary Laboratory Services, School of Veterinary Science, University of Liverpool. For routine histological examination, the liver sections were mounted on plain glass slides (ColorSlides, Solmedia Laboratory Supplies). Slides were then deparaffinized in xylene and dehydrated in graded alcohol. After that, the slides were stained for 5 min with Haematoxylin (VWR International), blueing in running

tap water for 6 min and another 2 min staining with eosin (VWR International). Then, sections were dehydrated again with 95% and 100% EtOH for 1 min before clearing in xylene and mounting with DPX (VWR International).

HE stained sections were examined for any histopathological features and for the identification of apoptotic, necrotic and mitotic hepatocytes. The degree of (predominantly centrilobular) hepatocyte loss was scored (0-5), where 0 indicated no evidence of cell loss (unaltered liver) and 5 extensive cell losses according to the criteria outlined in Table 2.5 (Antoine et al., 2009a). Leukocyte recruitment and infiltration was also assessed and recorded. The histological assessment and scoring was undertaken blindly and independently by Fazila Hamid and Prof Anja Kipar.

Table 2.5. Grading score of histological changes in murine livers.

Grading score	Descriptions
0	Normal – no evidence of hepatocyte necrosis
1	Hepatocyte loss and necrosis – minimal to mild Focal, Limited to centrilobular region Less than ¼ of affected lobules are necrotic Associated with vacuolar degeneration or haemorrhages
2	Hepatocyte loss and necrosis – mild to moderate Focal and multifocal Extends from central to midzonal lobular region ½ of affected lobules are necrotic Associated with vacuolar degeneration or haemorrhages
3	Hepatocyte loss and necrosis – moderate to severe Multifocal, May extends from centrilobular to portal region More than ½ to ¾ of affected lobules are necrotic Associated with vacuolar degeneration or haemorrhages
4	Hepatocyte loss and necrosis – severe Multifocal, More than ¾ of affected lobules are necrotic Associated with vacuolar degeneration or haemorrhages
5	Massive hepatocyte loss and necrosis – severe, involving entire lobules Hepatocytes loss extends from central vein to portal area Hepatocytes loss extends to adjacent lobules (multilobular necrosis) Associated with vacuolar degeneration or haemorrhages

2.6.3 Immunohistological examinations

Immunohistology was applied for the demonstration of cleaved caspase-3 (apoptotic cells) and proliferating cell nuclear antigen (PCNA; proliferating cells) on selected cases, as summarised in Appendix (Table 6.2: CD-1 and Table 6.3: C57BL/6J mice). The staining was performed by Valerie Tilston and Julie Dunn, technical staff in the Histology Laboratory, Veterinary Laboratory Services, School of Veterinary Science, University of Liverpool, UK. Consecutive sections, prepared from the formalin-fixed, paraffin-embedded liver specimens, following those stained with HE and PAS reaction, were used. Sections were deparaffinised in xylene for 10 min followed by rehydration in graded alcohols through each 2 min, twice in 100% EtOH and once in 96% EtOH to remove free and bound water. Then, inactivation of endogenous peroxidase was performed to avoid non-specific background staining, by 30 min incubation in freshly prepared methanol with 0.5% (v/v) H₂O₂ (Perhydrol 30% H₂O₂ P-a, ThermoFisher Scientific) at room temperature, followed by washing twice in dH₂O. Subsequently, antigen retrieval was performed (Table 2.6). For this purpose, sections were incubated at 96-98°C in pre-warmed citrate buffer for 30 min, then cooled at room temperature for 20 min, followed by 5 min washing in TBST (TBS buffer with 0.05% Tween 20). 1xTBST (TBS buffer with 0.05% Tween 20) was prepared by mixing 10xTRIS Stock [60.57 g TRIS, 610 ml dH₂O + 390 ml 1M HCl], 900 ml dH₂O, 7.2 g NaCl and 500 µl Tween 20 and stored in fridge. Citrate buffer pH 4.0/6.0 was prepared by adding 9 ml Stock Solution A [Citric Acid 10.505 g and 500 ml dH₂O] and 41 ml Stock Solution B [Tri-Sodium Citrate 14.705 g and 500 ml dH₂O] and dH₂O with final total volume 500 ml at respective pH 4 or pH 6 and stored in fridge.

Table 2.6. Antigen retrieval methods.

Antigen detection	Antigen retrieval	Retrieval details
Cleaved caspase-3	Citrate buffer, pH 6.0	Incubation at 96-98°C in pre-warmed citrate buffer for 30 min, then cooling at room temperature for 20 min, followed by 5 min TBST wash
PCNA	Citrate buffer, pH 4.0	Incubation at 96-98°C in pre-warmed citrate buffer for 15 min, followed by 20 min cooling at room temperature, followed by 5 min TBST wash

The individual slides were placed into coverplates and Sequenza racks (Thermo Shandon) and washed for 5 min in TBST, followed by blocking of non-specific binding of the antiserum by incubation for 30 min in undiluted goat serum (G9023; Sigma Aldrich, Poole, UK). Then, a further 5 min TBST wash was performed. Sections were then incubated with the primary antibodies at approximately 4°C in fridge) for 15-18 hours, followed by a 5 min TBST wash and incubation with the secondary antibody at room temperature, followed by a further TBST wash. Antibodies and detection systems are listed in Table 2.7.

Table 2.7. Summary of antibodies used, antigen retrieval methods, detection systems and the staining result.

	Cleaved caspase-3	PCNA
Antigen retrieval method	Citrate buffer, pH 6.0	Citrate buffer, pH 4.0
Primary antibody	Rabbit anti-cleaved caspase-3 ^a monoclonal antibody (Asp 1756) (5A1E) 1:50 in TBST at 4°C for overnight	Mouse anti-PCNA ^c , clone PC10, DAKO (M0879); 1:100 in TBST for 30 min at room temperature, followed by TBST wash
Secondary antibody	Goat anti-rabbit biotinylated IgG ^b (BA-1000); 1:100 in TBST for 30 min, followed by 5 min TBST wash	Goat anti mouse Biotin-SP-conjugated Affinipure Fab Fragment IgG ^c (115.067.003) 1:500 in PBS for 20 min at room temperature; and again wash with TBST for 5 min
Detection system	Vectastain ABC kit standard, polyclonal rabbit ^b (PK-4000); 1µl A +1µl B in 100µl TBST for 30 min, followed by TBST wash for 5 min and 4 times dH ₂ O wash	HRP: Horseradish Peroxidase-Streptavidin ^b (SA-5014); 1:500 in PBS for 20 min at room temperature; and last wash with TBST for 5 min
Specificity	Apoptotic cells (Gjorret et al., 2007)	Nuclear expression: Proliferating in early phase G1 and S phases (Kurki et al., 1986) Cytoplasmic expression: Proliferating cells in S phase, late G1 and early G2 phases (Kubben et al., 1994)

^a Obtained from DAKO, Glostrup, Denmark; ^b Obtained from Vector Laboratories Ltd, Peterborough, UK; ^c Obtained from Jackson Immunoresearch Laboratories, Suffolk, UK; TBST- Tris-buffered saline tween; PBS- Phosphate buffered saline.

*PBS- 1 liter (L) of 1XPBS was prepared by adding 8 g of NaCl, 0.2 g KCl, 1.44 g Na₂HPO₄, 0.24 g of KH₂PO₄ to 800 ml of dH₂O and the pH has been adjusted to 7.4 with HCl. Lastly, more dH₂O was added until the total volume is 1000 ml. The solution was dispensed and sterilised by autoclaving at 121°C for 20 min before stored at room temperature.

After removal from the sequenza clips, antibody binding was visualised with diaminobenzidine-tetrahydrochloride (DAB, Fluka Chemie AG, Buchs, Switzerland) with 0.01% H₂O₂ (Perhydrol 30% H₂O₂ P-a, Fisher Scientific) in 0.1 M imidazole buffer (pH 7.1, Fluka Chemie AG) in a 10 min incubation at room temperature, followed by 3 washes with distilled water for each 5 min. After that, slides were counterstained with Papanicolaou's haematoxylin (Merck) for 1 min and then blued in running tap water for 5 min. This was followed by dehydration with ascending EtOH (1 min 96%, 2 min 100% and 3 min 100%), clearing in xylene (2 min 100% and 2 x 3 min 100%) and mounting of cover slips with DPX (BDH brand, VWR International).

2.6.3.1 Quantitative analysis of immunohistological stains

The amount of cleaved caspase 3-positive cells (cytoplasmic staining) was semiquantitatively assessed, based on an estimation of the amount of cells with the morphology of apoptotic cells and showing a specific cytoplasmic reaction (– no positive cells; + scattered positive cells; ++ moderate number of positive cells, and +++ numerous positive cells).

PCNA expression was seen as a nuclear reaction in late G1 phase (faint, stippled) and S phase (intense, uniform) and/or as a cytoplasmic reaction in the G2 phase (stippled, with or without nuclear reaction) and M phase (diffuse reaction, combined with mitotic figures), as previously described (Eldrige et al., 1993). For the quantification of PCNA positive, proliferating cells, ten random fields (at 200x magnification), i.e. non-overlapping areas comprising a minimum of 1,000 hepatocytes, were analysed for each liver. A photomicrograph was taken for each of the 10 random areas for each individual mouse liver, using a Zeiss Axio Imager M2 microscope (Carl Zeiss Ltd, Gottingen, Germany). The total number of hepatocytes, the number of hepatocytes with cytoplasmic PCNA expression, and the total number of PCNA positive hepatocytes (nuclear and/or cytoplasmic reaction) were counted. The mean percentage and standard deviation were calculated for the cells

expressing overall (nuclear and cytoplasmic) PCNA, and the cells showing a cytoplasmic PCNA expression.

2.7 Assessment of cytokine expression in serum, liver and spleen

2.7.1 Measurement of serum cytokine levels by ELISA

For the determination of TNF- α and IL-6 levels in the serum, commercial mouse TNF- α (MTA00B) and IL-6 (M6000B) ELISA assay kits (R&D Laboratories Systems Inc., Abingdon, UK) were used. Mouse kit control, wash buffer and standard solution were prepared according to the manufacturer's protocol. The standard was added with calibrator diluent to prepare serial dilutions and the diluent calibrator served as 0 pg/ml for blank. Assay diluent (50 μ l) provided with the kit was added to each well, followed by 50 μ l of the standard, control or serum sample. Plates were vortexed gently on a shaker to avoid protein degradation. The plate was covered with a sheet of sealing tape to prevent liquid escaping from the wells and was then incubated for 2 hours at room temperature. Subsequently, the sealing tape was removed and discarded. Wash buffer (100 μ l) was added to each well with a squirt bottle for 5 times, inverting the plate and blotting excess liquid in between on a clean paper towel. Subsequently, 100 μ l of conjugate was added to each well which was then covered with a new adhesive strip and incubated at room temperature for 2 hours. During the incubation period, the substrate solution was prepared within 15 min of use to minimise light exposure. After careful removal of the sealing tape and further washing with wash buffer for 5 times, 100 μ l substrate solution was added and the plate incubated for 30 min while covered with clean paper towel to avoid light exposure. Finally, stop solution (100 μ l) was added to each well and the plate gently tapped to ensure thorough mixing. The optical density of each well was determined within 30 min using a microreader Luminex 100 System set to set to 540 nm or 570 nm. The lowest protein concentration of the assay that can be detected is 7.21 pg/mL for TNF- α and 1.8 pg/mL for IL-6 (obtained from manufacturer guideline). Levels below these were assigned a value of zero.

2.7.2 Determination of cytokine transcription levels in liver and spleen

2.7.2.1 RNA extraction

For RNA extraction, frozen liver and spleen specimens with a weight of approximately 50-100 mg were placed in an RNase-free microtube (1.5 ml). 200 µl of Trizol reagent (Sigma-Aldrich) was added and the tissue was homogenised thoroughly with a homogeniser (Retsch® MM400, ThermoFisher Scientific, Loughborough, UK) with frequency of 30/sec for 1 min. A further 800 µl of Trizol reagent was added after full homogenisation was achieved by passing the lysate through a pipette tip. The samples were then incubated at room temperature for 5 min to permit dissociation of nucleoprotein complexes. Each tube was vigorously shaken by hand for 15 sec and then 200 µl of chloroform added to each tube. The tubes were left to incubate for 2 min at room temperature and then spun for 15 min (12,000 x g, 4°C) to separate the solution into an RNA-containing aqueous phase and an organic phase containing DNA and protein. The aqueous phase was then placed into a new 1.5 ml microtube and the other phase discarded. Subsequently, 500 µl of 100% isopropyl alcohol (IPA) was added and the solution incubated for 10 min at room temperature until a white top layer had formed. After that, samples were spun for 10 min (12,000 x g, 4°C). The supernatant was discarded after which the RNA precipitated in a gel-like pellet on the side and bottom of the tube. Pre-chilled (-20°C) 75% EtOH [75 ml EtOH and 25 ml nuclease-free H₂O] was added to each tube which was then agitated for 15 sec and spun for 5 min (7,500 x g, 4°C). The supernatant was again discarded thoroughly and the pellet was allowed to air dry for a minimum of 5-10 min. Finally, the dried pellet was dissolved in approximately 50 µl to 100 µl of nuclease-free H₂O, the amount is depending on the size of the pellet obtained. The RNA was stored at -80°C until DNase treatment was performed later.

2.7.2.2 DNase treatment

An Ambion DNA-free kit (Life Technologies, Paisley, UK) was used to eliminate DNA contamination in the RNA extracts and to obtain pure RNA. To each tube containing 44 μ l RNA solution, 5 μ l of 10x DNase buffer and 1 μ l of 2U rDNase I were added. The tubes were spun at 3,000 rpm (500 g) for 10 sec to remove any bubbles and then placed on a heating block at 37°C for 30 min. After that, 5 μ l of DNase inactivation reagent was added to each tube which was then agitated gently to mix. The tubes were incubated at room temperature for 2 min, followed by centrifugation for 1 min (14,000 rpm or 11,000 g) at room temperature. The resultant supernatant was transferred into new RNase-free tubes (2 ml) and stored at -80°C until reverse transcription (RT) was performed. From each RNA sample, an aliquot of supernatant was used to quantify the RNA with a ND 1000 spectrophotometer (Nanodrop; ThermoFisher Scientific). Samples with good quality RNA values (A₂₆₀/A₂₈₀ ratio of 1.8-2.1 only) were reverse transcribed later. Samples with low quality RNA were not used because it may contain contaminants such as proteins that interfere with the RNA purity. Therefore, RNA was re-extracted from the liver samples until good RNA quality was achieved.

2.7.2.3 Reverse transcription (RT)

The ImProm-II reverse transcriptase kit and Oligo(dT)₁₆ (Promega, Southampton, UK) were used to synthesise cDNA from the total DNA-free RNA. 2.5 μ g of DNA-free RNA was incubated with 1 μ l of 0.5 μ g/ μ l Oligo(dT)₁₆ and nuclease-free H₂O (total volume of 25 μ l) at 70°C for 5 min. The samples were put on ice and the remaining RT components were added: 10 μ l of 5x RT buffer, 8 μ l 25 mM MgCl₂, 1 μ l of 10 mM dNTPs, 2.5 μ l of 10x reverse transcriptase and 3.5 μ l nuclease-free H₂O (final volume of 50 μ l). For each sample, “no RT” reactions (without RT and dNTPs) were included as negative control. The samples were then incubated in a GeneAmp PCR System 9700 (ThermoFisher Scientific, Loughborough, UK) at 25°C for 5 min, followed by 1 hour at 42°C, then 15 min at 70°C and holding at 4°C. After that, 200 μ l of nuclease

free-H₂O was added to each tube to achieve a cDNA concentration of 10 ng/μl and the cDNA was stored at -20°C until the PCR was performed.

2.7.2.4 Conventional PCR

Conventional PCR was performed for the detection of DNA amplification products in agarose gel electrophoresis on selected primers to ensure the PCR has worked. Primers were selected to detect TNF-α, IL-6, IL-10, cyclin-D1, NF-kB and GAPDH mRNA by both the conventional and the qPCR, as listed in Table 2.8.

The gradient temperature was first run starting from 55 to 65°C (based on manufacturer's datasheet) in order to obtain an optimal annealing temperature using the Opticon qPCR machine. After obtaining an optimal temperature (as Table 2.8), these temperature were used both in the conventional PCR and the real-time PCRs.

Table 2.8. Primer sequences for the detection of TNF-α, IL-6, IL-10, cyclin-D1, NF-kB and GAPDH by PCR and real-time PCR.

Target	Primer sequence 5'-3' (F-forward, R-reverse)	Reference of primer sequence	Annealing temperature (°C)	Product length (bp)
TNF-α	F:CCAGTGTGGGAAGCTGTCTT R:AAGCAAAAGAGGAGGCAACA	(McKallip et al., 2013)	62	100
IL-6	F:TAGTCCTTCCTACCCCAATTTCC R:TTGGTCCTTAGCCACTCCTTC	(Sebastian et al., 2011)	62	76
IL-10	F:GGTTGCCAAGCCTTATCGGA R:ACCTGCTCCACTGCCTTGCT	(Yin et al., 2014)	60	191
Cyclin-D1	F:CTACCGCACAAACGCACTTTC R:TAGAAGGCACAGTCGAGG	(Biliran et al., 2005)	56	960
NF-kB	F:CTTGGCAACAGCACAGACC R:GAGAAGTCCATGTCCGCAAT	(Kim et al., 2008b)	65	128
GAPDH	F:GTATGACTCCACTCACGGCAAA R:GGTCTCGCTCCTGGAAGATG	(Zhang et al., 2010)	56-62	101

Reactions were carried out in 0.2 ml thin walled tubes and with a total reaction volume of 50 μ l, containing 10 μ l of cDNA (see Chapter 2.7.2.3), 10 μ l of 10x PCNA buffer, 4 μ l of 1.5 mM MgCl₂, 1 μ l of 10 mM dNTP mixture (Invitrogen), 0.2 μ l of 2U DNA Taq polymerase (Invitrogen), 1 μ l of 40 ng each of sense and antisense primers and 22.8 μ l of nuclease-free H₂O. PCR reactions were performed in a Thermo-Hybrid MBS thermocycler (Thermo Electron Corporation), applying the following cycling conditions: 15 min at 95°C, followed by 35 or 45 cycles of 2 min denaturation at 95°C, 1 min at the annealing temperature (see Table 2.9) and 2 min extension at 72°C, and final extension for 5 min at 72°C. PCR products were electrophoresed through 2% (w/v) agarose gels (Invitrogen) with 2 μ l ethidium bromide (Sigma Aldrich) in TAE Buffer [40 mM Tris-base, 20 mM glacial acetic acid, 1 mM EDTA] and mixed 5:1 with loading buffer [50% v/v glycerol, 100 mM Tris-HCl pH 7.4, 10 mM EDTA, 0.02% w/v orange G]. Electrophoresis was performed in a horizontal electrophoresis chamber (Biorad) filled with TAE buffer at 100 V for 30 min. The gel was examined under UV light (Ultraviolet Transilluminator, Biorad) and the height of the bands from PCR products compared with a 1 kb or 100 bp DNA ladder (Invitrogen) that had been loaded alongside the PCR products.

2.7.2.5 Quantitative Real time PCR (qPCR)

The qPCRs were performed with a final volume of 20 μ l for each sample, containing 5 μ l cDNA of 10 ng/ μ l of reversed transcribed total RNA, 0.4 μ l of 200 nM of each forward and reverse primers for each specific gene (see Table 2.9) and 14.2 μ l of DNA fluorescent dye SYBR Green JumpStartTM (Sigma-Aldrich). An Opticon Monitor 3.0 qPCR machine thermocycler (Bio-Rad) was used, with the cycling conditions provided in Table 2.9. TNF- α , IL-6, NF-kB and GAPDH were run for 35 cycles and cyclin-D1 and IL-10 were quantified at 45 cycles.

Table 2.9. Cycling condition, temperature and time used for qPCR analysis.

Cycling condition	Cycle temperature	Time (min)
Pre-denaturation	95°C	2
Denaturation	95°C	1
Annealing	<i>See Table 2.8</i>	1
Extension	72°C	2
Final Extension	72°C	5
Hold	4°C	Infinity

← 35 or 45 cycles

All reactions were performed in duplicates and run alongside reactions for the reference gene, GAPDH. The melting curve was created to analyse the specificity of the product by measuring the fluorescence at 0.2°C increments, from 65°C to 95°C; the amplification efficiency of the reactions provided together with mRNA transcription by the Opticon qPCR machine (Bio-Rad) were also taken into account. Efficiency (E) is the extent of target DNA or PCR product increase after each cycle where an ideal reaction reaches an efficiency of up to 100%, with acceptable values between 90 to 110% (1.9 to 2.1). Ct value of sample with low E was repeated. Low E indicates poor primer design, inappropriate reaction condition, pipetting errors or other factors. A negative control was included for each sample (“No RT”, see 2.7.2.3) to determine if DNA contamination was present.

Relative quantification was performed. This determines the ratio between the amount of target DNA and the reference amplicon, GAPDH. All values quantified were normalised to the reference gene, GAPDH, and then the calculations are made to obtain fold change by the delta-delta Ct ($2^{-\Delta\Delta Ct}$) formula that also referred to comparative Ct value relative to control animals (reference sample) as calculations below (Schmittgen and Livak, 2008). The transcription values were also compared between fed and fasted animals.

$$\text{Delta Ct} = \text{Ct (target gene)} - \text{Ct (reference gene, GAPDH)}$$

$$2^{\Delta-\text{delta Ct}} (2^{-\Delta Ct}) = 2^{-[\text{Ct (target gene)} - \text{Ct (reference gene, GAPDH)}]}$$

$$2^{\Delta-(\text{delta-delta Ct})} [2^{-\Delta\Delta Ct}] \quad \text{or} \quad \text{Comparative delta-Ct value (Fold change)}$$

$$= 2^{-(\Delta Ct (\text{target sample}) - \Delta Ct (\text{reference sample}))} = \frac{\text{Target sample } 2^{-\Delta Ct}}{\text{Reference sample } 2^{-\Delta Ct}}$$

2.8 Statistical analysis

For statistical analysis of the results, all quantitative values. i.e. values for glutathione (GSH) content, serum ALT level, histological grading score, numbers of PCNA positive cells, serum cytokine levels, relative cytokine mRNA levels, were expressed as mean±standard deviation (SD). Values were analysed for non-normality using a Shapiro-Wilk test. The unpaired t-test was used when normality was indicated, the Mann-Whitney U test used for non-parametric data. Comparisons between multiple groups were performed with One-way ANOVA or Two-way ANOVA, followed by a post hoc Tukey's test, but Dunnett's test was applied to compare to controls. If non-normality was indicated, Kruskal-Wallis test was used. All calculations were performed using StatsDirect statistical software version 2.7.9, results were considered significant when $P < 0.05$ (* $P < 0.05$, ** $P < 0.01$, *** $P < 0.005$).

CHAPTER THREE

RESULTS

CONTENTS

3.1	Effect of fasting in untreated (saline dosed) male CD-1 and C57BL/6J mice	68
3.1.1	Effect of fasting on proportion of body weight	68
3.1.2	Effect of fasting on hepatic glutathione (GSH) contents	70
3.1.2.1	Hepatic GSH levels follow a distinct circadian rhythm, but differ significantly between CD-1 and C57BL/6J mice	70
3.1.2.2	Fasting and refeeding significantly affects the hepatic GSH levels	71
3.1.3	Effect of fasting on hepatic ATP levels	73
3.1.4	Effect of fasting on hepatic GSH and ATP contents	76
3.1.5	Effect of fasting on serum alanine-aminotransferase (ALT) levels	77
3.1.6	Effect of fasting on histological features and hepatocellular glycogen content	80
3.1.7	Effect of fasting on cytokine expression	82
3.1.7.1	Hepatic transcription of TNF- α , IL-6 and IL-10	83
3.1.7.2	Splenic transcription of TNF- α and IL-6	86
3.1.7.3	Serum TNF- α and IL-6 levels	87
3.1.8	Effect of fasting on hepatocellular proliferation	89
3.1.8.1	Assessment of NF- κ B and cyclin-D1 transcription levels as markers of hepatocellular proliferation	89
3.1.8.2	In situ identification of proliferating hepatocytes	91

3.2	Effect of fasting on the response of the liver and/or spleen in CD-1 mice to APAP treatment	93
3.2.1	Hepatic GSH content	93
3.2.2	Hepatic ATP content	97
3.2.3	Hepatic ATP and GSH levels	99
3.2.4	Serum ALT levels	100
3.2.5	Histological features and glycogen content of the liver	103
3.2.6	Overall assessment of liver damage based on all parameters	113
3.2.7	Cytokine transcription in liver and spleen and cytokine levels in the blood of APAP dosed CD-1 mice	115
3.2.7.1	Hepatic transcription of TNF- α , IL-6 and IL-10	115
3.2.7.2	Splenic transcription of TNF- α and IL-6	121
3.2.7.3	Serum TNF- α and IL-6 levels	124
3.2.8	Assessment of liver regeneration based on hepatocellular proliferation	125
3.2.8.1	Hepatic NF-kB mRNA transcription	126
3.2.8.2	Hepatic cyclin-D1 mRNA transcription	128
3.2.8.3	Quantification of PCNA-positive, proliferating hepatocytes	130
3.2.9	Overall assessment of liver regeneration	135

3.3	The response of fed and fasted C57BL/6J mice to APAP overdose and comparison to the response of CD-1 mice	137
3.3.1	Hepatic GSH content	138
3.3.2	Hepatic ATP content	142
3.3.3	Hepatic GSH and ATP levels	145
3.3.4	Serum ALT levels	148
3.3.5	Histological features and hepatocellular glycogen content of the liver	151
3.3.6	Overall assessment and comparison of liver damage in C57BL/6J and CD-1 mice	162
3.3.7	Quantification of cytokine expression in liver, spleen and sera levels	163
3.3.7.1	Hepatic transcription of TNF- α , IL-6 and IL-10	163
3.3.7.2	Splenic transcription of TNF- α and IL-6	172
3.3.7.3	Serum TNF- α and IL-6 levels	174
3.3.8	Assessment of liver regeneration based on hepatocellular proliferation	181
3.3.8.1	Hepatic NF- κ B mRNA transcription	181
3.3.8.2	Hepatic cyclin-D1 mRNA transcription	184
3.3.8.3	Assessment of hepatocyte proliferation based on the immunohistological expression of PCNA	187
3.3.9	Overall assessment of liver regeneration in C57BL/6J and CD-1 mice	192

3.1 Effect of fasting in saline dosed male CD-1 and C57BL/6J mice

Mice that had been deprived of food for 16 or 24 hours and mice that had been fed ad libitum throughout (i.e. prior and post saline administration) were assessed over a 24 hour (CD-1 mice) and 36 hour (C57BL/6J mice) time period to gain information on the effect of fasting on liver function and morphology in two different types of mice commonly used in DILI studies, out-bred CD-1 and in-bred C57BL/6J mice. Several parameters were assessed, including the degree of weight loss, the hepatic glutathione (GSH) and ATP levels, the histological features of the liver, the serum alanine transaminase (ALT) levels and the expression of inflammatory mediators (i.e. cytokines) in liver, spleen and blood as well as the expression of proliferation markers (NF- κ B and cyclin-D1 mRNA, proliferating cell nuclear antigen) in the liver to assess the hepatocellular turnover. These parameters were examined to obtain baseline information on features of potential relevance for the effect of hepatotoxic drugs.

3.1.1 Effect of fasting on proportion of body weight

Body weights of mice were determined immediately prior to saline administration, i.e. at the end of the fasting period of the fasted mice, and, in the case of the fasted mice, also immediately prior to the onset of the fasting period. The body weights of fed mice were similar in both strains (Table 3.1.1). After a 16 hour fasting period, all mice had lost a proportion of body weight, the extent of which was variable depending on the time of day when the animals were first deprived of food (Table 3.1.2, Figure 3.1.1). Onset of fasting during daytime, afternoon and early evening (16:00 to 18:45) led to a mean loss of body weight of just below 10% to almost 12%. With an onset of fasting at midnight, it dropped to 8% on average, though the difference was not statistically significant. When the fasting period was started later in the night (3, 5 or 6 am), the loss of body weight was significantly lower than in the afternoon and early evening and at midnight, below 5% (Figure 3.1.1). The least extensive body weight loss was observed when the fasting period started at 3 am.

Table 3.1.1. Mean body weight (g) of **fed** male CD-1 and C57BL/6J mice at different times of day, immediately prior to saline dosing.

CD-1				C57BL/6J				p-value CD-1 vs C57BL/6J
ToD	Mean	SD	p-value	ToD killing	Mean	SD	p-value	
16:00	28.5	2.3	NS	18:00	28.2	1.5	NS	NS
18:15	28.0	1.7		03:00	29.4	1.0		
18:30	29.6	2.3		05:00	30.2	1.1		
18:45	29.2	1.6		06:00	31.1	1.0		
00:00	29.7	1.9		-	-	-		

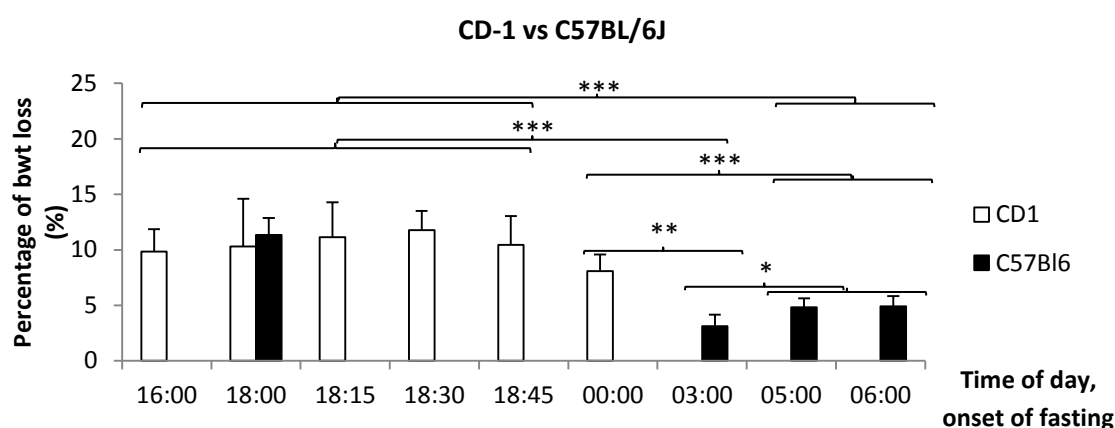
ToD - time of day; SD - standard deviation; NS - not significant.

Table 3.1.2. Mean body weight loss (g), standard deviation and p-value of **fasted** male CD-1 and C57BL/6J mice prior and immediately after the fasting period, at different times of day.

Strains	ToD fasting*	ToD refeeding*	n	Mean	SD	p-value
CD-1	16:00	08:00	5	9.85	2.00	vs 3:00; 0.0001 vs 5:00 & 6:00: 0.0005
	18:00	10:00	4	10.29	4.32	
C57BL/6J	18:00	10:00	6	11.35	1.53	
CD-1	18:15	10:15	5	11.14	3.15	
	18:30	10:30	4	11.77	1.73	
	18:45	10:45	5	10.45	2.59	
	00:00	16:00	5	8.08	1.50	vs 3:00; 0.0087
C57BL/6J	03:00	19:00	6	3.13	1.02	-
	05:00	21:00	6	4.82	0.80	vs 3:00; 0.0102
	06:00	22:00	6	4.91	0.92	vs 0:00; 0.0027

ToD - time of day; n – number of animals used; SD - standard deviation;

* ToD onset of fasting and refeeding, respectively.

**Figure 3.1.1.** Percentage of body weight loss in male CD-1 and C57BL/6J mice after fasting, in relation to the time of day at the onset of the fasting period.

The percentage of body weight loss after a 16 h fasting period that had started at different times of day is illustrated (as listed in Table 3.1.2). Values are expressed as mean±SD (4 to 6 animals per group). ***P<0.005, **P<0.01 and *P<0.05.

3.1.2 Effect of fasting on hepatic glutathione (GSH) content

3.1.2.1 Hepatic GSH levels in fed CD-1 and C57BL/6J mice

Hepatic GSH levels were examined over a 24 hours time period at different times of day in male CD-1 and C57BL/6J mice that had been fed ad libitum to determine the circadian variation in GSH levels. When hepatic GSH levels were assessed from morning to afternoon (10:00 to 15:00), a steady decline was observed in both CD-1 and C57BL/6J mice. In the evening (20:45 in CD-1 mice or 20:00 in C57BL/6J), levels were significantly the lowest (Figure 3.1.2A). If the stress of handling and intraperitoneal application of 0.9% saline did have an effect on food uptake and thereby GSH levels, this was not apparent from 24 hours onwards, as examination of C57BL/6J mice at 24, 30 and 36 hpd, at 10:00 and 14:00, did yield GSH levels similar to those previously obtained at the same time of day (Figure 3.1.2B).

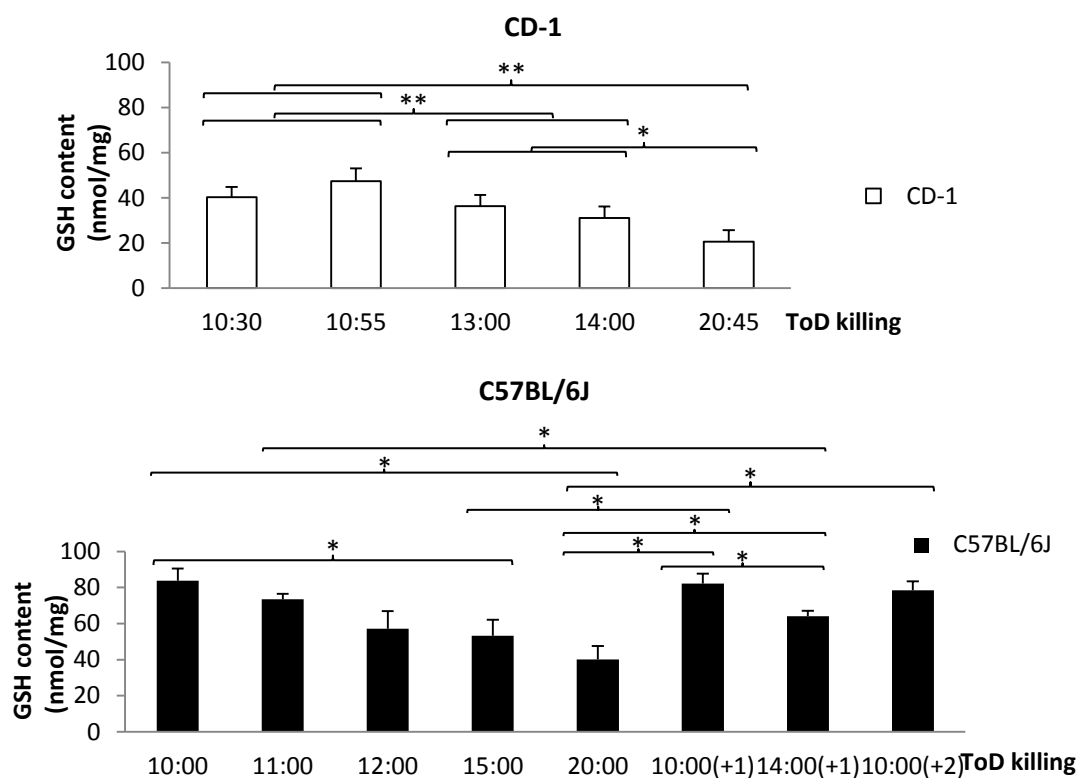


Figure 3.1.2. Hepatic GSH content in fed CD-1 and C57BL/6J mice at different times of day. The hepatic GSH content was assessed at different times of the day in male, fed CD-1 (A) and C57BL/6J (B) mice that had received 0.9% saline i.p. at different time points prior to euthanasia (not shown). Values are expressed as mean \pm SD (4 to 6 animals per group). *** P <0.005, ** P <0.01 and * P <0.05. ToD - time of day; (+1) – time of day on the following day; (+2) – time of day on the next 2 days.

A comparison of GSH levels in both groups of mice showed that the hepatic GSH content was significantly higher in the C57BL/6J mice at all times including morning, midday and evening (Table 3.1.3).

Table 3.1.3. Hepatic GSH levels (nmol/mg) in **fed** male CD-1 and C57BL/6J mice. GSH levels in the liver were determined at different times of day and compared between CD-1 and C57BL/6J mice. Values are expressed as mean±SD (4 to 6 animals per group).

CD-1			C57BL/6J			p-value CD-1 vs C57BL/6J
ToD killing	Mean	SD	ToD killing	Mean	SD	
Morning: 10:30, 10:55	40.34 47.36	4.48 5.75	Morning: 10:00, 11:00, 10:00 (+1), 10:00 (+2)	73.57 83.85 82.26 78.46	2.88 6.65 5.48 4.91	0.0036
Midday: 13:00, 14:00	36.30 31.11	5.04 5.00	Midday: 12:00, 14:00, 15:00	57.16 64.06 53.21	9.79 3.03 8.86	0.0146
Evening: 20:45	20.60	5.13	Evening: 20:00	40.12	7.52	0.0357

ToD - time of day; SD – standard deviation

3.1.2.2 Hepatic GSH levels in fed and fasted CD-1 and C57BL/6J mice

Hepatic GSH levels were also examined over a 24 hour (CD-1 mice) and 36 hour (C57BL/6J mice) time period and at different times of day in male CD-1 and C57BL/6J mice that had been fasted for 16 or 24 hours and then refed for a variable length of time (fasted mice). Intraperitoneal application of 0.9% saline was the event after which the animals were refed. In both groups of mice, upon completion of the fasting period (at 10:00 and 10:30, respectively), the mean hepatic GSH content was significantly lower than in the fed mice, though not lower than in the evening (20:00 and 20:45, respectively) in the fed mice (Figure 3.1.3A,B).

In **CD-1 mice**, GSH levels returned to those of fed animals at 1 hour of refeeding. Interestingly, they appeared to then rise further and at 10 hours of refeeding, reached a peak value almost double of any level in fed mice; this was at 20:00, around the time when the level was at the significantly lower minimum circadian

level in the evening (20:45). After 24 hours of refeeding, levels had dropped to those of fed mice at the same time of day, i.e. in the morning (Figure 3.1.3A).

In **C57BL/6J** mice, GSH levels were still low after 5 hours of refeeding, but increased dramatically thereafter. They were already higher at 10 hours, though not significantly, and peaked at 15 hours of refeeding, when they were significantly higher than in the fed animals at the same time of day (12:00). Levels subsequently dropped and, at 24 hours of refeeding, were significantly lower than in fed animals; at 36 hours, they were similar to those in fed mice (Figure 3.1.3B).

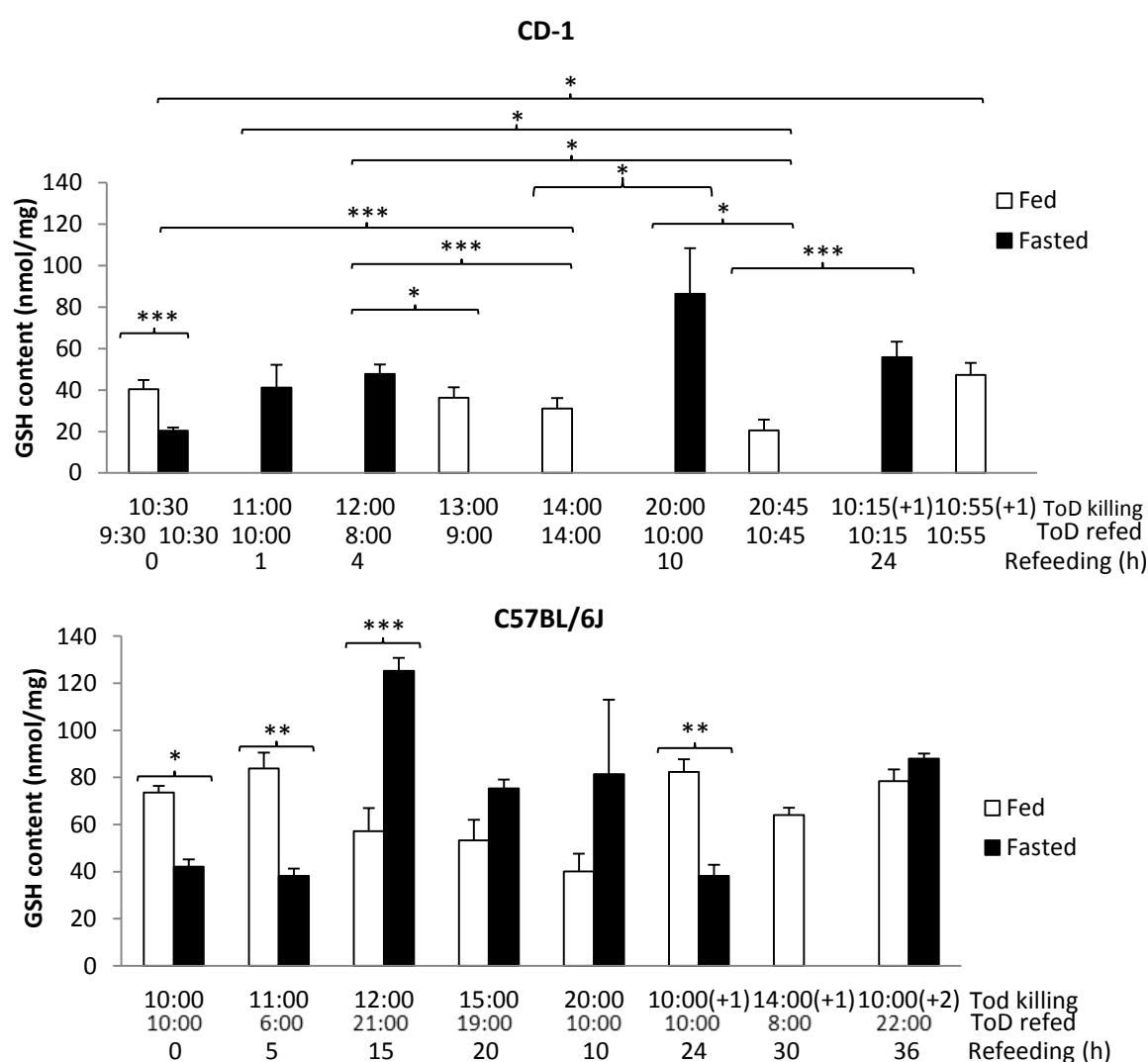


Figure 3.1.3. Hepatic GSH content in male CD-1 and C57BL/6J mice that had been fed or fasted for 16 or 24 h and then refeed for variable time spans.

Both the time of day (ToD) of refeeding (and saline dosing) and of killing are provided to highlight any effect of fasting, the length of refeeding (0 - 24 h) and the time of day on hepatic GSH levels. Values are expressed as mean \pm SD (4 to 6 animals per group). **P<0.005, *P<0.01 and *P<0.05.

3.1.3 Effect of fasting on hepatic ATP levels

The hepatic ATP content was determined to study the effect of fasting on the hepatic energy content. In fed **CD-1 mice**, ATP levels did not vary much over the 24 hour time period, and there was not much variation between individual animals (Table 3.6). After 16 and/or 24 hours of fasting, the ATP content was reduced by almost 90% and increased only minimally within the first hour of refeeding. By 3 hours, the ATP content had increased significantly and reached a peak (at approximately 50% of the levels in fed mice) after 5 hours of refeeding, before it dropped again at 10 hours and 15 hours and increased thereafter. However, by 24 hours, the hepatic ATP content was still only at approximately 50% of the level in fed CD-1 mice (Table 3.1.4, Figure 3.1.4A,B).

Table 3.1.4. Hepatic ATP levels (nmol/mg) in **fed and fasted** CD-1 mice at the different time points post saline application.

Time (hps)	Fed			Fasted			p-value fed vs fasted
	Mean	SD	p-value fed vs fed	Mean	SD	p-value fasted vs fasted	
0	35.4	2.0	NS	4.2	2.6	3 h: 0.0375 5 h: 0.0405	0.0005
0.5	31.3	3.1		4.1	2.7		0.0011
1	32.1	5.6		5.3	3.7		0.0003
3	25.9	4.9		11.0	1.2	10 h: 0.0431	0.0057
5	35.5	4.0		17.1	5.3	15 h: 0.0337	0.0082
10	30.2	6.4		13.7	1.4	5 h: 0.012	0.0094
15	32.7	1.8		10.3	4.1	10 h: NS	0.0060
20	31.8	3.4		14.7	2.3	0, 0.5, 1 h: 0.0058	0.0091
24	33.1	2.1		16.4	3.7		0.0059

hps – hours post saline (and onset of refeeding); SD - standard deviation; NS - not significant.

Hepatic ATP levels were also assessed in **C57BL/6J mice** at selected time points. In fed C57BL/6J mice, ATP levels did not vary much either (Table 3.1.5); however, they were overall 16.3% lower than in the fed CD-1 mice (Figure 3.1.4E). The early time points after the onset of refeeding were not available for the fasted mice, however, over the examined time period (5-36 hours of refeeding), a steady increase in ATP levels was observed, with significant differences between the time points (Table 3.1.5). Different from the CD-1 mice which did not only show a significant drop in

the otherwise rising ATP levels at 15 hours of refeeding, the fasted C57BL/6J mice had reached ATP levels similar to those of fed mice by 20 hours of refeeding (Table 3.1.5, Figure 3.1.4C,D). The difference in the ATP level was statistically significant in comparison to the fasted CD-1 mice at the same time point (Table 3.1.5 and Figure 3.1.4F).

Table 3.1.5. Hepatic ATP levels (nmol/mg) in **fed and fasted** C57BL/6J mice at the different time points post saline application and comparison to time matched CD-1 mice.

Time (hps)	Fed				Fasted				p-value fed vs fasted C57BL/6J
	Mean	SD	p-value vs. fed C57BL/6J	p-value vs. fed CD-1	Mean	SD	p-value vs. fasted C57BL/6J	p-value vs. fasted CD-1	
5	24.6	5.2	NS	NS	12.8	3.5	20 h: 0.0211	NS	0.0265
10	28	4.53			13.95	2.33	36 h: 0.0358	NS	0.0173
15	-	-			19.55	1.63	5 & 10 h: 0.0403	NS	-
20	30.2	3.25			25.2	3.25	5 h: 0.0221	0.009	NS
30	26.75	2.33			-	-	-	-	-
36	24.48	5.26			28.15	4.6	-	-	-

hps – hours post saline (and onset of refeeding); SD-standard deviation, NS- not significant.

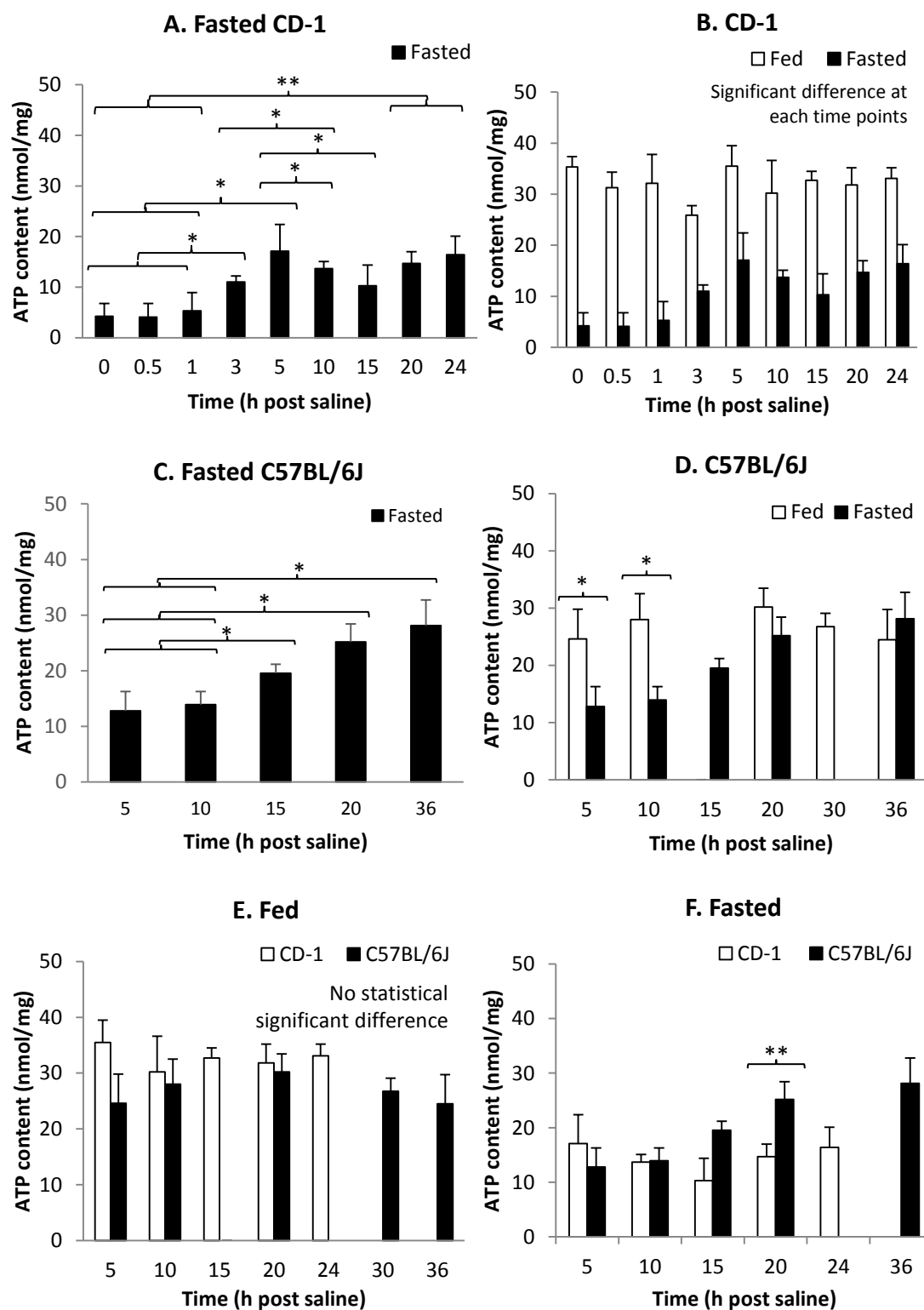


Figure 3.1.4. Hepatic ATP levels in saline dosed male CD-1 and C57BL/6J mice. Hepatic ATP levels in fasted male CD-1 (A) and C57BL/6J (C) mice and comparison to ATP levels in fed mice (C, D). The hepatic ATP contents were also compared between fed (E) and fasted (F) CD-1 and C57BL/6J mice (as listed in Table 3.1.4 and 3.1.5). Values are expressed as mean \pm SD (4 to 6 animals per group). *** P <0.005, ** P <0.01 and * P <0.05.

3.1.4 Effect of fasting on hepatic GSH and ATP contents

We found both hepatic ATP and GSH depleted after the fasting period (see Chapter 3.1.2 and 3.1.3) and wanted to investigate whether there is evidence that the GSH depletion is a consequence of the ATP loss, because a previous study reported that glutathione depletion is inhibited by mitochondrial ATP (Lu, 1999). The values of fasted mice were normalised to time-matched fed mice and the fold change determine as a means to assess whether the GSH or ATP levels were upregulated (>1.0) or downregulated (<1.0) after refeeding. In fasting **CD-1 mice**, the ATP content was reduced throughout the observation period. We observed an increase in hepatic GSH levels at 1 and 4 hps (without significant difference) and a significant increase at 10 hours of refeeding compared to fed mice (Table 3.1.6, Figure 3.1.5A). Similarly, the hepatic ATP of fasted **C57BL/6J mice** was always decreased at 4, 10 and 20 hps compared to fed mice, whereas the GSH level was still low at 4 hps but then increased at 10 to 36 hours of refeeding (except 24 hours), though no significant differences between GSH and ATP levels except at 10 hps (Table 3.1.6).

Table 3.1.6. Hepatic GSH and ATP content after **fasting** in CD-1 and C57BL/6J mice. Fold changes were determined by dividing the values of fasted with time-matched fed mice.

Time (hps)	CD-1						
	GSH (mean)		Fold change	ATP (mean)		Fold change	p-value
	Fed	Fasted		Fed	Fasted		
0	31.1	20.3	0.65	35.4	4.2	0.12	NS
1	40.3	41.3	1.02	32.1	5.3	0.17	NS
4	36.3	47.7	1.32	35.5	17.1	0.48	NS
10	20.6	85.4	4.14	30.2	13.7	0.45	0.007
15	-	-	-	32.7	10.3	0.31	-
20	-	-	-	31.8	14.7	0.46	-
24	47.7	55.9	1.18	33.1	16.4	0.50	NS
Time (hps)	C57BL/6J						
	GSH (mean)		Fold change	ATP (mean)		Fold change	p-value
	Fed	Fasted		Fed	Fasted		
0	73.57	42.07	0.57	-	-	-	-
4	83.9	38.2	0.46	24.6	12.8	0.52	NS
10	40.1	81.38	2.03	28	14.0	0.50	0.047
15	57.2	125.29	2.19	-	19.6	-	-
20	53.2	75.3	1.42	30.2	25.2	0.83	NS
24	82.3	38.23	0.46	-	-	-	-
36	78.46	87.98	1.12	24.48	28.15	1.15	NS

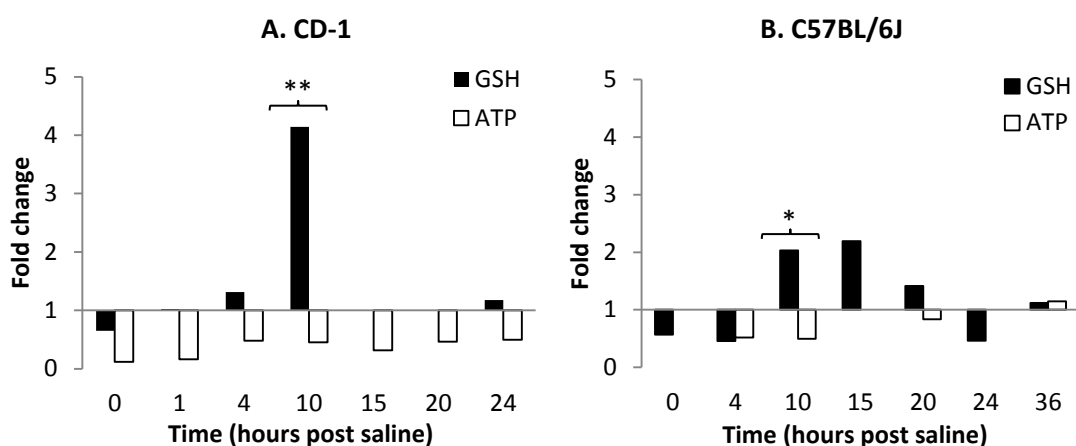


Figure 3.1.5. Hepatic GSH and ATP content (fold changes in comparison to fed mice) in male CD-1 and C57BL/6J mice.

Hepatic GSH and ATP levels were compared after fasting in male CD-1 (A) and C57BL/6J (B) mice at different times of day (ToD) (as listed in Table 3.1.6). Values are expressed as mean \pm SD (4 to 6 animals per group). **P<0.01 and *P<0.05. Fold change= 1: levels in saline dosed fed mice.

3.1.5 Effect of fasting on serum alanine-aminotransferase (ALT) levels

Serum alanine-aminotransaminase (ALT) levels were determined in fed and fasted CD-1 and C57BL/6J mice over a 24 hour (CD-1 mice) and 36 hour (C57BL/6J mice) time period and at different times of day to observe if fasting promotes serum ALT release from the liver.

In fed **CD-1 mice**, ALT levels varied markedly between individuals at most time points, with a maximum standard deviation of more than 60 U/L (Table 3.1.7 and individual data in Table 6.6), ranging from a minimum of 13 U/L to a maximum of 198 U/L. Despite the high variance also between average ALT levels at different times of day (and post saline application), these differences were never significant.

Also in fasted animals, from which samples were taken at the end of the fasting period and after 5 hours and 24 hours of refeeding, marked interindividual variation was observed (Table 3.1.7) and there was no significant difference between ALT levels at the different time points post fasting. Interestingly, however, ALT levels were significantly lower immediately after fasting than with feeding at libitum, and after 24 hours of refeeding they were significantly higher (Figure 3.1.6A).

Table 3.1.7. Serum ALT levels (U/L) in fed and fasted male **CD-1** mice.

Serum ALT enzyme activities are shown together with the number of animals examined at the different time points post saline application (and refeeding of the fasted animals).

Time (hps)	ToD dosing	ToD killing	n	Fed		Fasted		p-value fed vs fasted
				Range	Mean (SD)	Range	Mean (SD)	
0	10:00	10:00	6	45-98	68.33 (20.12)	12-58	41.5 (16.1)	0.042
1	09:30	10:30	4	22-70	51.63 (21.83)	-	-	-
2	09:30	11:30	4	13-90	40.98 (34.69)	-	-	-
4	10:00	13:00	4	20-50	31.17 (13.64)	-	-	-
5	10:00	15:00	6	35-198	78.0 (60.84)	14-85	49.8 (27.5)	NS
8	10:00	18:00	4	14-39	22.55 (10.97)	-	-	-
24	10:00	10:00 (+1)	6	22-37	27.5 (5.39)	36-109	63.2 (22.5)	0.033

hps - hours post saline (and onset of refeeding); ToD - time of day; n - number of mice per group; SD - standard deviation; NS – not significant.

Both in fed and fasted **C57BL/6J** mice, ALT values were less variable (Table 3.1.8) and significantly lower than in the CD-1 mice (Figure 3.1.6B) throughout the experiments. Fasting was not associated with significant changes in ALT levels in the C57BL/6J mice at any time point (Table 3.1.8).

Table 3.1.8. Serum ALT levels (U/L) in fed and fasted **C57BL/6J** mice.

Serum ALT enzyme activities are shown together with the number of animals examined at the different time points post saline application (and refeeding of the fasted animals).

Time (hps)	ToD dosing	ToD killing	n	Fed			Fasted			p-value fed vs fasted
				Range	Mean (SD)	p-value vs CD1	Range	Mean (SD)	p-value vs CD1	
5	10:00	15:00	5	10-35	14.92 (10.41)	NS	10-22	11.67 (7.16)	NS	NS
10	10:00	20:00	5	20-36	29.75 (8.66)	-	20-38	36.03 (8.66)	-	
15	17:00	8:00 (+1)	5	19-29	22.88 (6.70)	-	18-33	29.85 (7.6)	-	
20	11:00	7:00 (+1)	5	20-35	28.00 (7.24)	-	19-26	24.59 (2.90)	-	
24	10:00	10:00 (+1)	5	7-20	8.49 (7.28)	NS	12-25	12.39 (6.81)	NS	
36	7:00	19:00 (+2)	5	10-27	15.78 (7.24)	-	19-33	26.00 (5.61)	-	

hps - hours post saline; ToD - time of day; n - number of mice per group; SD - standard deviation; NS - not significant.

A comparison of ALT enzyme activities between CD-1 and C57BL/6J mice did not reveal any significant differences in either fed or fasted animals at the examined time points (data not shown). Overall, the serum ALT levels of all time points were not significantly different between CD-1 and C57BL/6J mice, both fed and fasted mice (Table 3.1.9, Figure 3.1.6C).

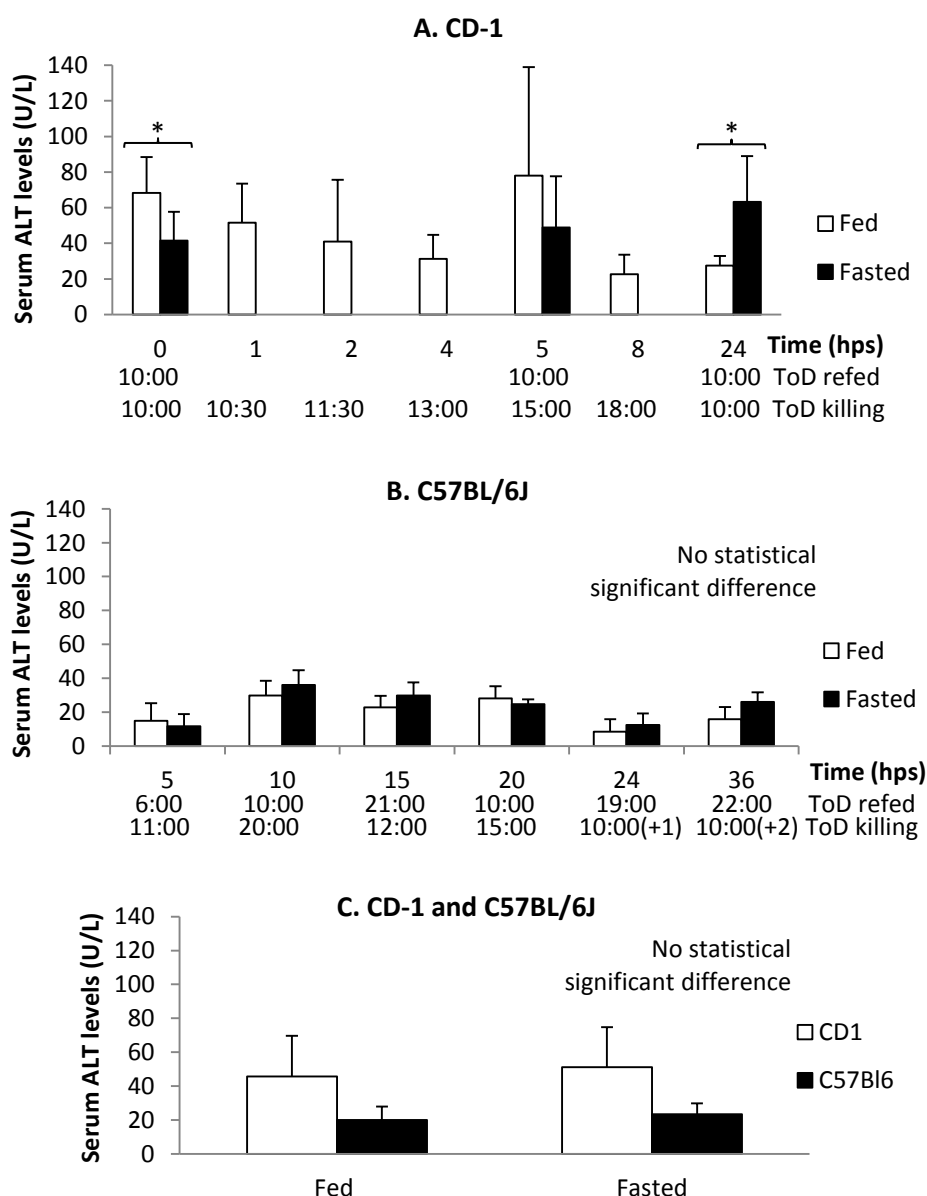


Figure 3.1.6. Serum ALT levels in fed and fasted CD-1 and C57BL/6J mice.

Serum ALT levels in male CD-1 (A) and C57BL/6J (B) mice at different times of day as listed respectively in Tables 3.1.7 and 3.1.8. (C) Pooled serum ALT levels were used for the comparison of ALT levels in fed and fasted CD-1 and C57BL/6J mice (as listed in Table 3.1.9). Animals had received 0.9% saline i.p., after which time point the fasted animals were fed ad libitum again. Values are expressed as mean \pm SD (4 to 6 animals per group). *P<0.05. hps-hour post saline dosing; ToD – Time of day.

Table 3.1.9. Pooled serum ALT levels (U/L) at all time points in saline dosed CD-1 and C57BL/6J mice.

Condition of mice	Strains				p-value CD-1 vs C57BL/6J
	CD-1		C57BL/6J		
	Mean	SD	Mean	SD	
Fed	45.73	23.93	19.97	7.92	NS
Fasted	51.17	23.56	23.42	6.46	NS

SD - standard deviation; NS – not significant.

3.1.6 Effect of fasting on histological features and hepatocellular glycogen content

A histological examination was performed on the liver of the different groups of mice. This did not reveal any histological abnormalities in any of the fed or fasted mice at any time points. In particular, there was also no evidence of hepatocellular degeneration or death. In fed animals and after refeeding, hepatocytes exhibited the typical cloudy cytoplasmic vacuolation indicative of glycogen accumulation (Figure 3.1.7). Staining of the livers for the presence of glycogen, using the PAS reaction, confirmed these findings. In both CD-1 and C57BL/6J mice examined immediately after completion of the 16 or 24 hour fasting period cytoplasmic vacuolation of hepatocytes was not apparent; this indicated the absence of glycogen accumulation and corresponded to the completely negative PAS reaction, providing evidence of complete glycogen depletion (Figure 3.1.7).

After only 0.5 hours of refeeding, there was morphological evidence of glycogen restitution. This was evident by a variable number of random individual PAS-positive hepatocytes in CD-1 mice (Figure 3.1.8A), whereas a weak diffuse PAS reaction was seen in C57BL/6J mice (Figure 3.1.8B). The latter was apparent in the CD-1 mice after 1 hour of refeeding (Figure 3.1.8C), at which time glycogen accumulation appeared to be fully restored in the C57BL/6J mice (Figure 3.1.8D). At 4 hours of refeeding, full glycogen restitution was also apparent in the CD-1 mice.

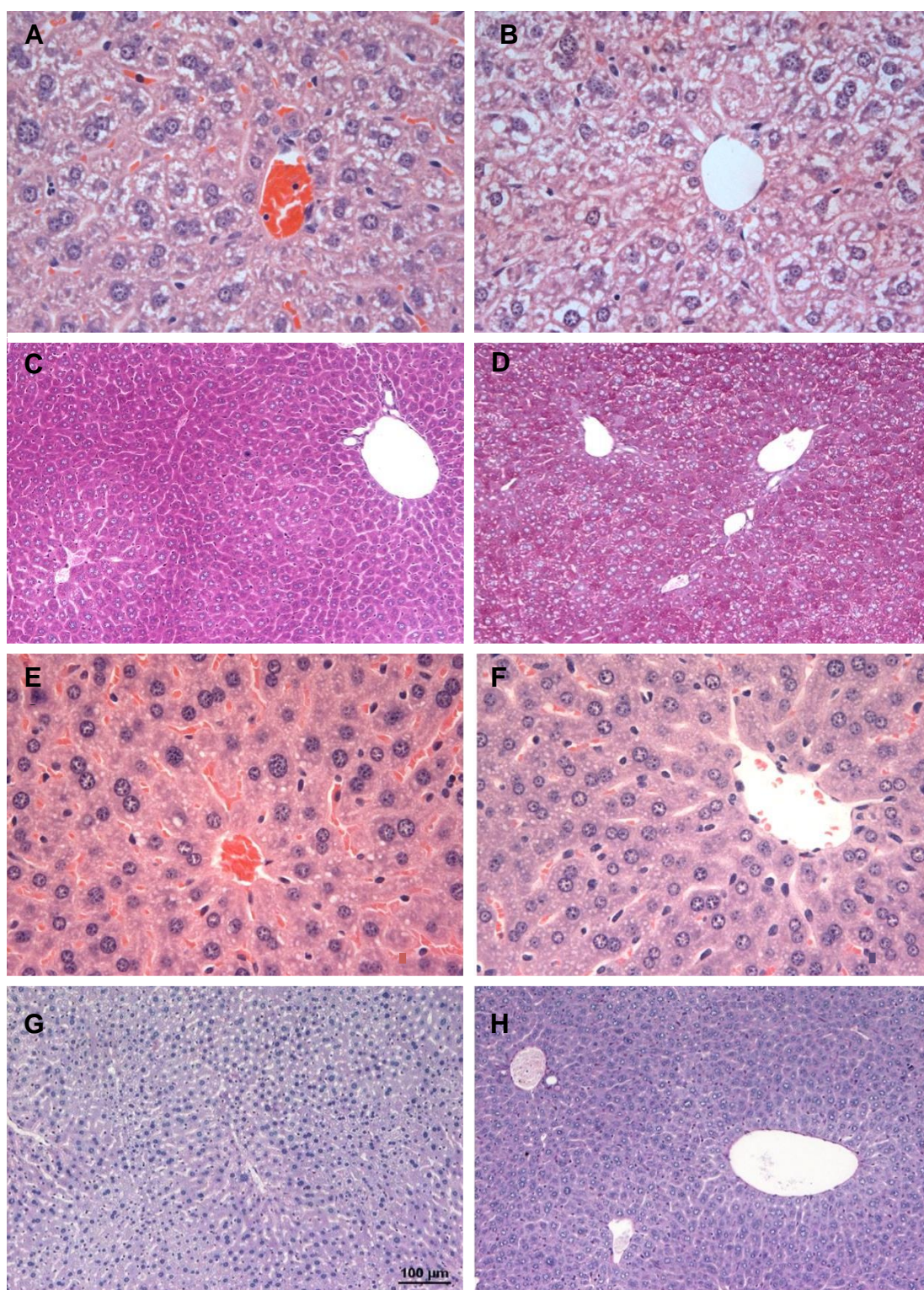


Figure 3.1.7. Histological features and glycogen content in fed and fasted CD-1 and C57BL/6J mice. HE stain and PAS reaction.

A-D: Fed mice. Cytoplasmic vacuolation of all hepatocytes is seen in the HE-stained section (A, B) and the PAS reaction (C, D) confirms the presence of diffuse glycogen in both CD-1 (A, C) and C57BL/6J (B, D) mice. **E-H:** Fasted mice. Immediately after completion of the 16 hour fasting period, the cytoplasmic vacuolation is not apparent in the HE stained sections (E, F), and the PAS reaction (G, H) confirms the complete lack of glycogen in both CD-1 (E, G) and C57BL/6J (F, H) mice. 400x (HE) and 200x (PAS) magnification.

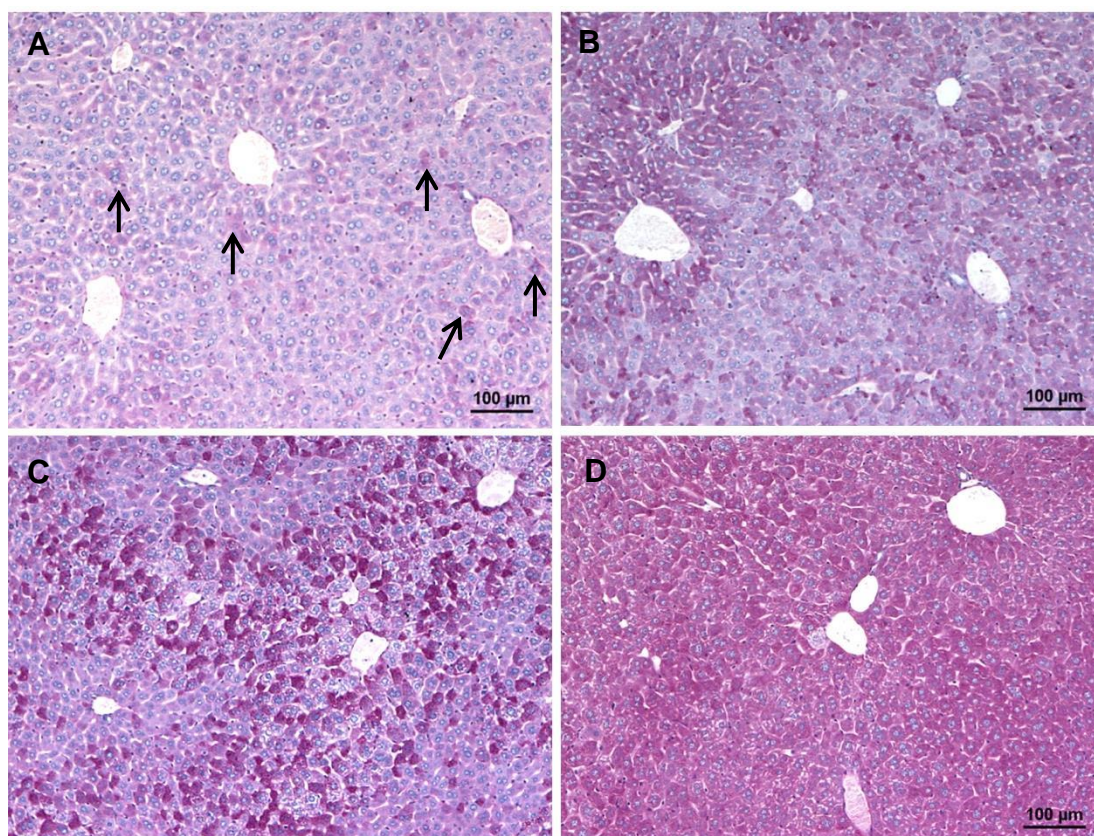


Figure 3.1.8. Hepatocellular glycogen content in CD-1 and C57BL/6J mice that have been refed for 30 and 60 minutes. PAS reaction.

A, B. After 0.5 hour refeeding, random individual PAS-positive hepatocytes (black arrows) are seen in CD-1 mice (A), indicating some glycogen restitution. In C57BL/6J mice (B), the PAS reaction indicates diffuse low level glycogen accumulation. **C, D.** After 1 hour of refeeding, the PAS reaction indicates patchy glycogen restitution in CD-1 mice (C) and diffuse, complete glycogen restitution in C57BL/6J mice (D). 200x magnification.

3.1.7 Effect of fasting on cytokine expression

In an attempt to establish whether fasting has an effect on the hepatic and splenic transcription of cytokines that are responsible for the priming of hepatocytes for proliferation, TNF- α , IL-6, and IL-10 mRNA levels were determined in liver, the TNF- α and IL-6 mRNA levels in the spleen of mice that have been fed or fasted prior to saline dosing. Serum TNF- α and IL-6 levels were also determined in order to detect a potential systemic inflammatory effect of fasting.

3.1.7.1 Hepatic transcription of TNF- α , IL-6 and IL-10

In order to assess the (constitutive) hepatic transcription of hallmark cytokines that are involved in inflammatory and/or regenerative processes in the liver, TNF- α , IL-6 and IL-10 mRNA levels were determined in the liver of both fed and fasted saline dosed control CD-1 (Table 6.7) and C57BL/6J (Table 6.8) mice at different times of day and at different time points of refeeding (0-24 hours). Relative transcription of the cytokines was assessed, using GAPDH as a housekeeping gene to obtain the delta Ct values ($2^{-\Delta Ct}$), and assess the fold change by comparative Ct value method ($2^{-\Delta\Delta Ct}$). The cytokine values obtained from fasted mice were normalised to those of time-matched fed mice to determine the fold change of mRNA levels after fasting. The transcription of a given cytokine was considered as upregulated when a value of >1.0 was obtained for the fasted mice, whereas it was considered as downregulated when the value was <1.0 .

All three cytokines were found to be transcribed in the liver, at very low level for IL-10 and slightly higher levels for IL-6 for both CD-1 and C57BL/6J mice. However, TNF- α seem to transcribe higher than those in C57BL/6J mice (Figure 3.1.9, Tables 6.7: CD-1 and 6.8: C57BL/6J mice).

Showing the fold changes in transcription levels after fasting confirms that fasting did not result in a significant change of TNF- α , IL-6 and IL-10 transcription at any time point in CD-1 and C57BL/6J mice (Figure 3.1.10).

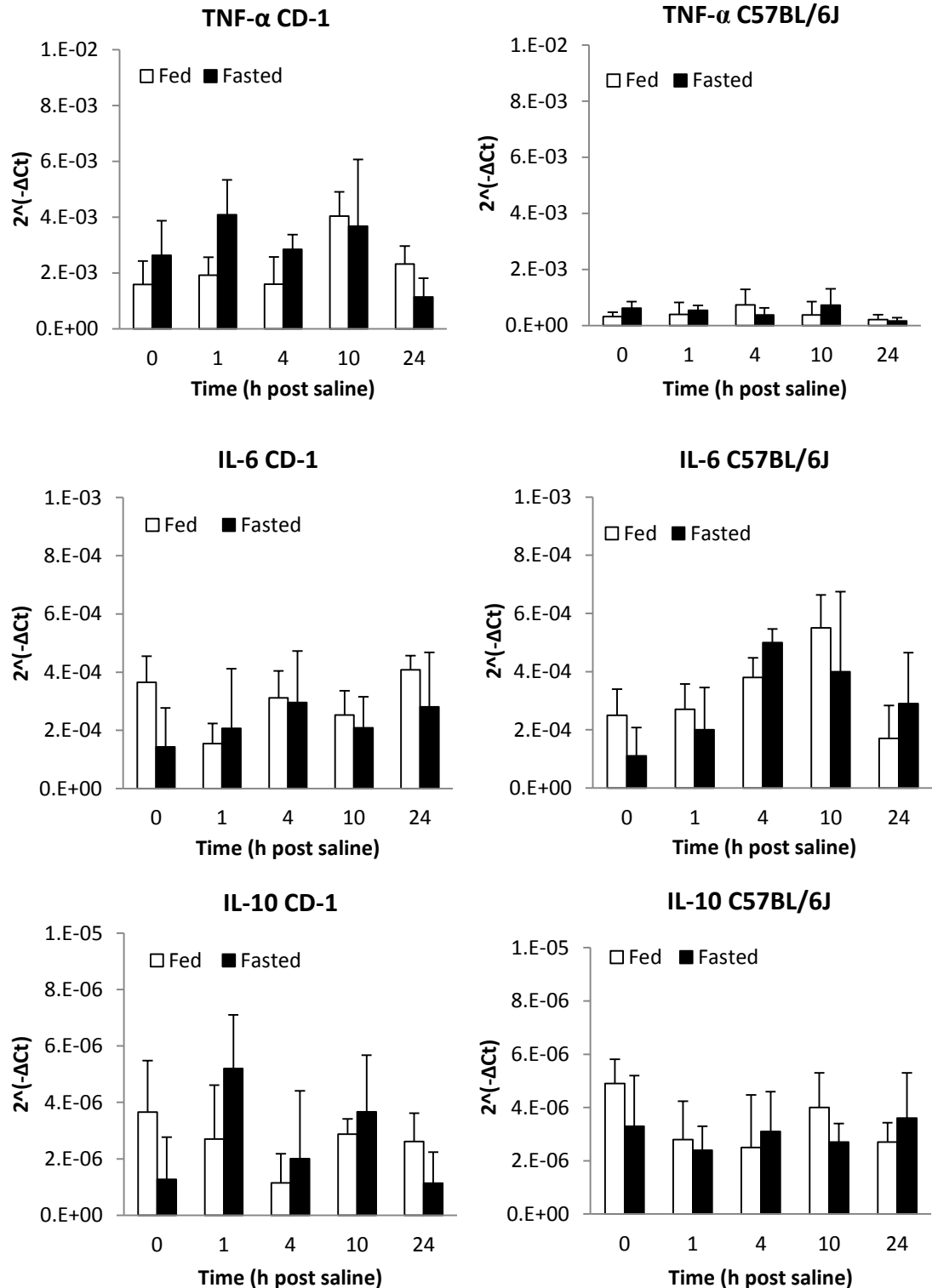


Figure 3.1.9. Hepatic TNF- α , IL-6 and IL-10 transcription in saline dosed CD-1 and C57BL/6J mice (delta Ct value).

TNF- α , IL-6 and IL-10 mRNA levels were determined in fed and fasted male CD1 and C57BL/6J mice at 0, 1, 4 and 24 h post 0.9% i.p. saline administration and compared using delta CT values ($2^{-\Delta Ct}$). Data is given as mean \pm SD (4 to 6 animals per group).

Table 3.1.10. Relative transcription levels of TNF- α , IL-6 and IL-10 in **CD-1 and C57BL/6J** mice using the comparative Ct value method (fold change). Statistical analysis did not identify any significant differences between or within the groups for all examined cytokines.

Time (hps)	TNF- α			IL-6			IL-10		
	CD-1	C57BL/6J	p-value	CD-1	C57BL/6J	p-value	CD-1	C57BL/6J	p-value
0	1.65	1.92	NS	0.39	0.44	NS	0.35	0.67	NS
1	2.13	1.39		1.34	0.85		1.93	0.86	
4/5	1.78	0.51		0.95	1.34		1.75	1.24	
10	0.91	1.95		0.83	0.80		1.28	0.69	
24	0.49	0.76		0.69	1.71		0.44	1.33	

hps – hours post saline (and refeeding); NS – not significant.

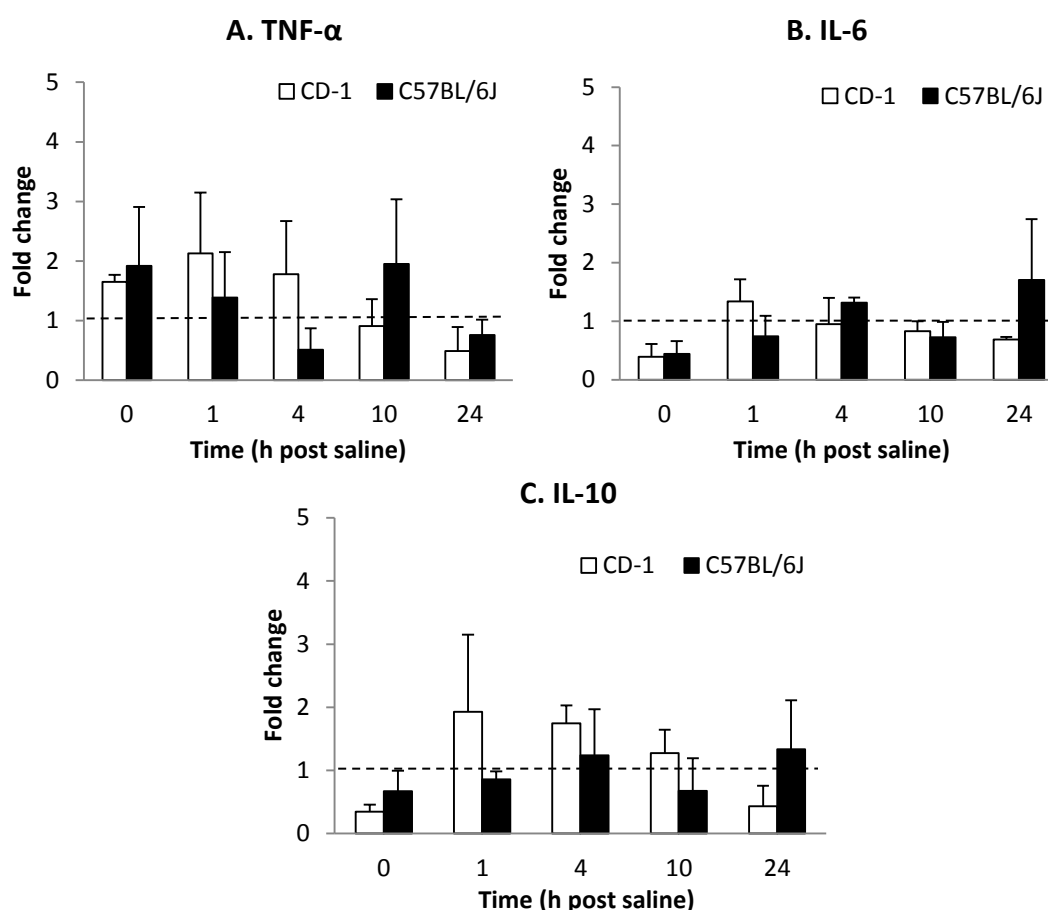


Figure 3.1.10. Hepatic TNF- α , IL-6 and IL-10 transcription in fasted saline dosed CD-1 and C57BL/6J mice (fold change method).

Hepatic TNF- α (A), IL-6 (B) and IL-10 (C) mRNA levels were compared between male CD-1 and C57BL/6J mice at 0, 1, 4 and 24 h post 0.9% i.p. saline administration. Hepatic mRNA levels are calculated using the comparative Ct values, assessing the fold change of fasted mice relative to time-matched fed saline dosed animals ($2^{-\Delta Ct}$ fasted/ $2^{-\Delta Ct}$ fed). Data is given as mean \pm SD (4 to 6 animals per group). Fold change 1 = levels in fed dosed control mice indicated by dashed lines. There is no statistically significant difference in the cytokine levels between CD-1 and C57BL/6J mice at any time points.

3.1.7.2 Splenic transcription of TNF- α and IL-6

In order to gather data on the constitutive transcription of the inflammatory cytokines TNF- α and IL-6 as indicators of a systemic inflammatory response, the real time qPCR for both cytokines was also applied to the spleen. Both cytokines were found to be transcribed at a higher level in the spleen than in the liver, but without significant quantitative differences between fed and fasted CD-1 (Table 3.1.11) and C57BL/6J (Table 3.1.12) mice.

Table 3.1.11. Comparison of mRNA transcription levels ($2^{-\Delta Ct}$) and fold change ($2^{-\Delta Ct}$ fasted/ $2^{-\Delta Ct}$ fed) of TNF- α and IL-6 in the spleen of fed and fasted male **CD-1** mice over a 24 h time period after i.p. application of 0.9% saline (and refeeding).

Time (hps)	ToD dosing	ToD killing	TNF- α				IL-6			
			Fed	Fasted	Fold change	p-value	Fed	Fasted	Fold change	p-value
0	14:00	14:00	0.115	0.101	0.878	NS	0.054	0.01	0.185	NS
1	09:30	10:30	-	0.071	-	-	-	0.038	-	-
10	10:45	20:45	0.031	0.050	1.61	NS	0.024	0.033	-	-
24	10:55	10:55 (+1)	0.024	0.017	0.708	NS	0.024	0.028	1.17	NS

hps – hours post saline (and refeeding); ToD – time of day; SD – standard deviation; NS – not significant.

Table 3.1.12. Comparison of relative transcription levels ($2^{-\Delta Ct}$) and fold change ($2^{-\Delta Ct}$ fasted/ $2^{-\Delta Ct}$ fed) of TNF- α and IL-6 in the spleen of fed and fasted male **C57BL/6J** mice over a 24 h time period after i.p. application of 0.9% saline (and refeeding).

Time (hps)	TNF- α					IL-6				
	Fed	Fasted	Fold change	p-value 5 vs 24 h	p-value to CD-1	Fed	Fasted	Fold change	p-value 5 vs 24 h	p-value to CD-1
5	0.0081	0.0037	0.46	NS	-	0.0083	0.0034	0.42	NS	-
24	0.0012	0.0016	1.13		0.032	0.0064	0.0059	0.92		NS

Time of day of dosing was at 10:00 and of killing at 15:00 (5 h) and 10:00 (+1) (24 h) for both fed and fasted mice. hps – hours post saline (and refeeding); NS – not significant.

3.1.7.3 Serum TNF- α and IL-6 levels

TNF- α and IL-6 levels were determined in the serum using mouse ELISA immunoassay kits at different time points up to 36 hours post saline application (and refeeding) in C57BL/6J mice, and at 5 and 24 hours in CD-1 mice. Fasted mice had been deprived of food for 16 and/or 24 hours prior to refeeding. In all mice, both cytokines were detected in the blood at very low levels. These did not differ significantly between fed and fasted mice at any time point (CD-1 mice: Table 3.1.13, Figure 3.1.11A,C; C57BL/6J mice: Table 3.1.14; Figure 3.1.11B,D).

Table 3.1.13. Serum TNF- α and IL-6 levels (pg/mL) in fed and fasted **CD-1** mice. Comparison of serum TNF- α (A) and IL-6 (B) levels in fed and fasted mice at 5 and 24 h post i.p. application of 0.9% saline (and refeeding).

Time (hps)	ToD dosing	ToD killing	TNF- α			IL-6		
			Mean (SD)		p-value fed vs fasted	Mean (SD)		p-value fed vs fasted
			Fed	Fasted		Fed	Fasted	
5	10:00	15:00	51.4 (12.4)	57.1 (13.3)	NS	25.4 (6.7)	23.1 (4.1)	NS
24	10:00	10:00 (+1)	45.8 (6.4)	63.1 (19.7)	NS	30.1 (2.1)	27.49 (12.6)	NS
p-value 5 vs 24 h			NS	NS		NS	NS	

hps – hours post saline; ToD – time of day; SD – standard deviation; NS – not significant.

Table 3.1.14. Serum TNF- α and IL-6 levels (pg/mL) in saline dosed **C57BL/6J** mice. Comparison of serum TNF- α and IL-6 levels in fed and fasted control mice at 5 h and 24 h post i.p. application of 0.9% saline (and refeeding).

Time (hps)	ToD dosing	ToD killing	TNF- α			IL-6		
			Mean (SD)		p-value fed vs fasted	Mean (SD)		p-value fed vs fasted
			Fed	Fasted		Fed	Fasted	
5	10:00	15:00	3.3 (2.1)	11.3 (6.3)	NS	28.5 (1.9)	19.86 (2.7)	NS
10	10:00	20:00	11.8 (2.8)	26.3 (5.9)	NS	23.2 (5.2)	15.6 (4.6)	NS
15	17:00	08:00	14.6 (3.2)	21.3 (8.1)	NS	25.6 (4.6)	21.5 (3.2)	NS
20	11:00	07:00	15.5 (2.0)	13.8 (2.0)	NS	27.5 (3.2)	19.5 (5.9)	NS
24	10:00	10:00 (+1)	3.6 (4.3)	20.3 (5.1)	NS	14.2 (3.8)	24.5 (8.1)	NS
30	9:00	15:00 (+1)	7.3 (1.2)	-	-	17.1 (1.0)	-	-
36	7:00	19:00 (+2)	10.0 (0.3)	25.4 (5.7)	NS	20.3 (0.6)	16.9 (2.9)	NS

hps – hours post saline; ToD – time of day; SD – standard deviation; NS – not significant.

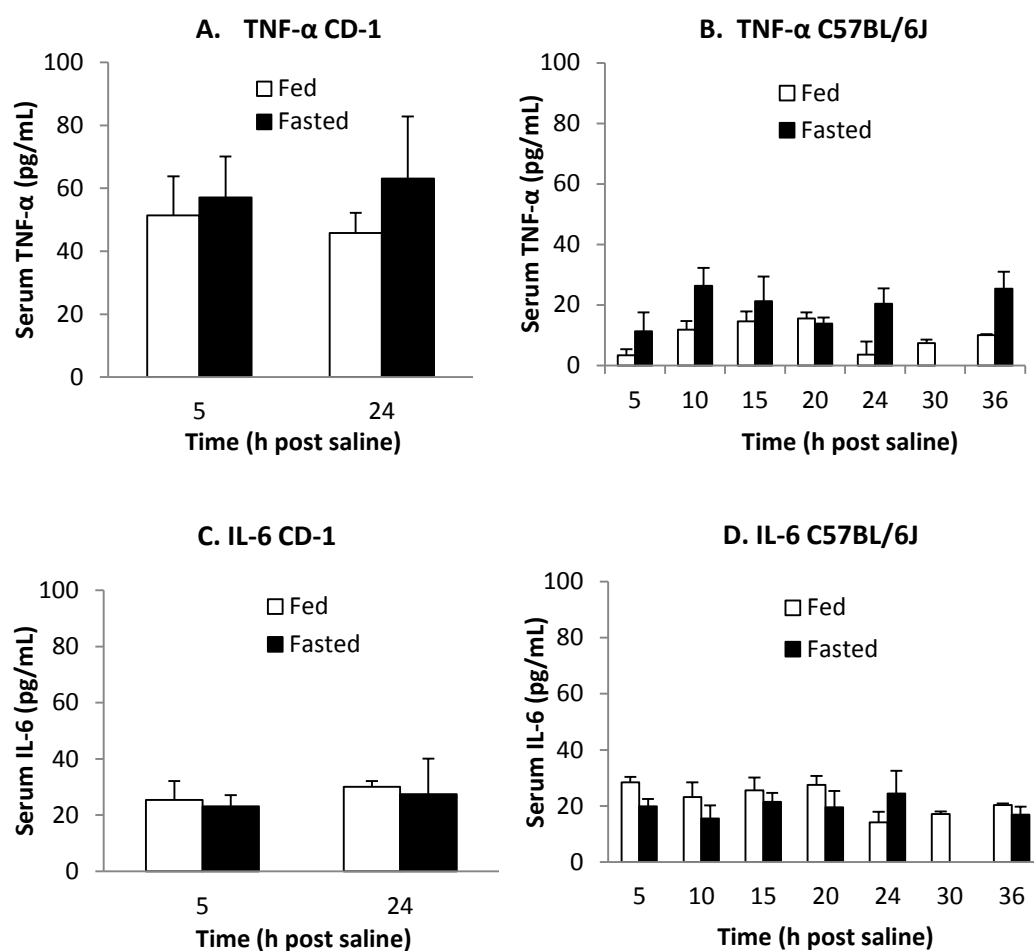


Figure 3.1.11. Serum TNF- α and IL-6 levels in fed and fasted CD-1 and C57BL/6J mice. Cytokine levels were determined in fed and fasted male CD-1 (A, C) and C57BL/6J (B, D) mice at 5 and 24 h (CD-1 mice) and 5 to 36 h (C57BL/6J mice) post 0.9% i.p. saline administration. Data is given as mean \pm SD (4 to 6 animals per group). There is no statistically significant difference in the cytokine levels of both groups at each time point.

However, a comparison of serum TNF- α and IL-6 levels between CD-1 and C57BL/6J mice showed that the TNF- α levels of the fed and fasted CD-1 mice were significantly higher than those of C57BL/6J mice at both tested time points (5 and 24 hours) but the IL-6 levels were similar in both strains (Table 3.1.15).

Table 3.1.15. Comparison of serum TNF- α and IL-6 levels (pg/mL) in fed and fasted **CD-1 and C57BL/6J** mice. The levels were determined in fed and fasted mice at 5 and 24 h post i.p. application of 0.9% saline (and refeeding).

Time (hps)	TNF- α					
	Fed			Fasted		
	CD-1	C57BL/6J	p-value	CD-1	C57BL/6J	p-value
5	51.4	3.3	0.0021	57.1	11.3	0.020
24	45.8	3.6	0.0056	63.1	20.3	0.012
p-value 5 vs 24 h	NS	NS		NS	NS	
Time (hps)	IL-6					
	Fed			Fasted		
	CD-1	C57BL/6J	p-value	CD-1	C57BL/6J	p-value
5	25.4	28.5	NS	23.1	19.86	NS
24	30.1	14.2	NS	27.49	24.5	NS
p-value 5 vs 24 h	NS	NS		NS	NS	

hps – hours post saline; ToD – time of day; NS – not significant.

3.1.8 Effect of fasting on hepatocellular proliferation

3.1.8.1 Assessment of NF-kB and cyclin-D1 transcription levels as markers of hepatocellular proliferation

The constitutive transcription of NF-kB, a transcription factor that is strongly linked with hepatic regenerative processes, and cyclin-D1 as a marker of proliferating hepatocytes in the G phase (Bhushan et al., 2014; Fausto, 2000), were determined in the liver of both fed and fasted saline dosed control CD-1 and C57BL/6J mice at different times of day and at different time points of refeeding (0-24 hours). The relative transcription of both markers was assessed using GAPDH as a housekeeping gene, by the delta Ct value, $2^{-\Delta Ct}$. Overall, CD-1 mice showed higher NF-kB and lower cyclin-D1 transcription levels than C57BL/6J mice. Also, fasting seemed to have no change on the expression of both markers at any time points, as transcription levels were generally similar (Figure 3.1.12A-D).

To compare the effects of fasting on the transcription of NF-kB and cyclin-D1 in CD-1 (Table 6.10) and C57BL/6J mice (Table 6.11), the comparative Ct value (fold change) method was used. No significant difference was seen for any time points for both NF-kB and cyclin-D1 (Figure 3.1.12E,F).

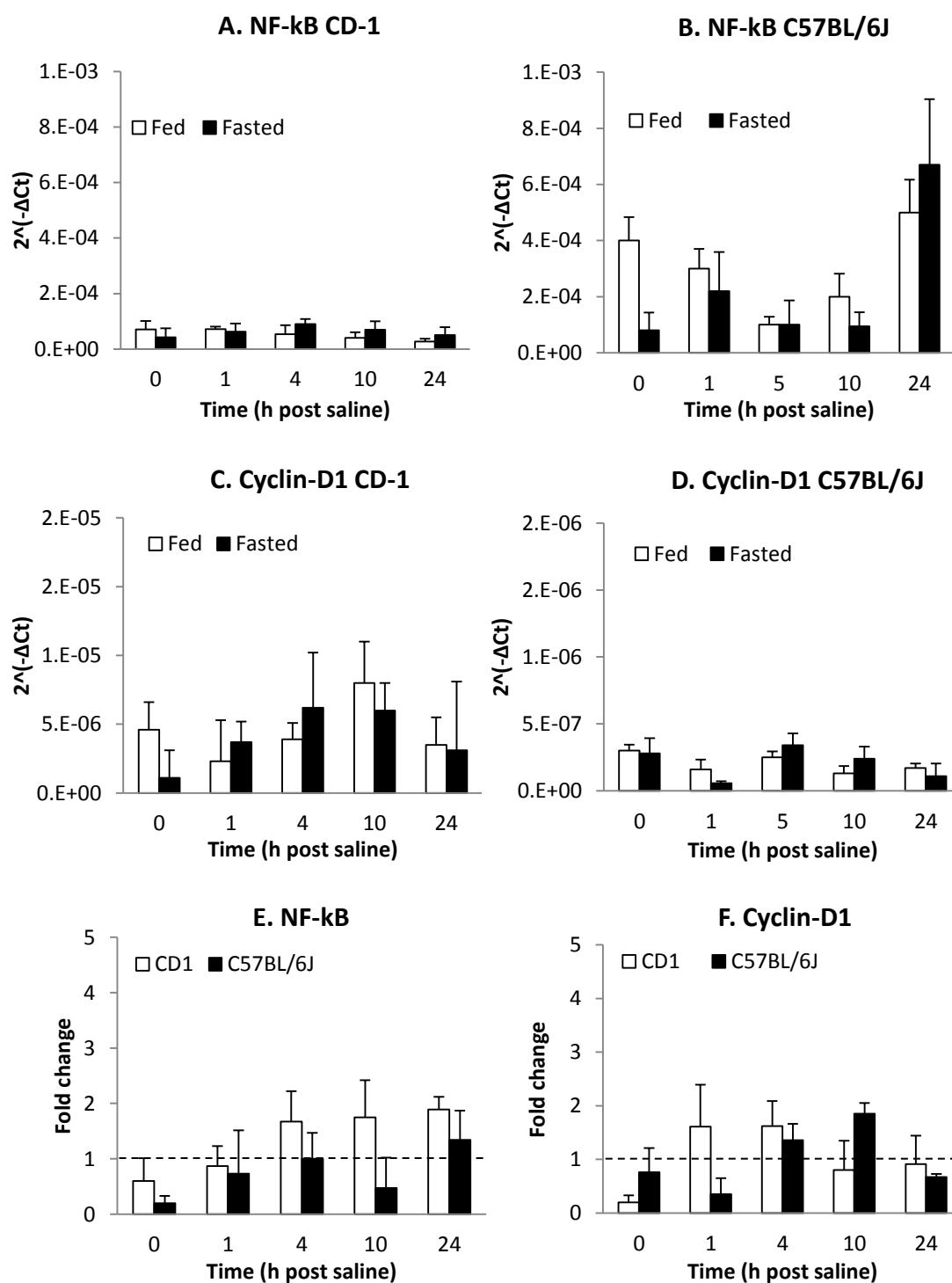


Figure 3.1.12. Changes in hepatic transcription of NF-kB and cyclin-D1 in fasted compared to fed male CD-1 and C57BL/6J mice.

Relative NF-kB and cyclin-D1 mRNA levels were determined in relation to GAPDH mRNA, using the delta Ct, $2^{-\Delta Ct}$ values. The levels of NF-kB and cyclin-D1 using comparative Ct values by fold change ($2^{-\Delta Ct_{fasted}}/2^{-\Delta Ct_{fed}}$) method were also determined. Fold change = 1 : levels in fed dosed control mice as indicated by dashed line. No statistical significant differences were observed at any time point for CD-1 and C57BL/6J mice.

3.1.8.2 In situ identification of proliferating hepatocytes

For the evaluation of the degree of cellular turnover in the unaltered liver of control mice and the potential effect of fasting on this, immunohistology for the expression of proliferating cell nuclear antigen (PCNA) was applied to the liver of fed and fasted control **CD-1 mice** over a 24 hours period after the onset of refeeding the fasted mice. PCNA is a nuclear protein that is involved in DNA synthesis which is expressed in the nucleus in the early phase of the cell cycle, i.e. the G1 and S phases. Immediately prior to and during mitosis, it is (also) expressed in the cytoplasm (Figure 3.1.13; (Kubben et al., 1994; Kurki et al., 1986)).

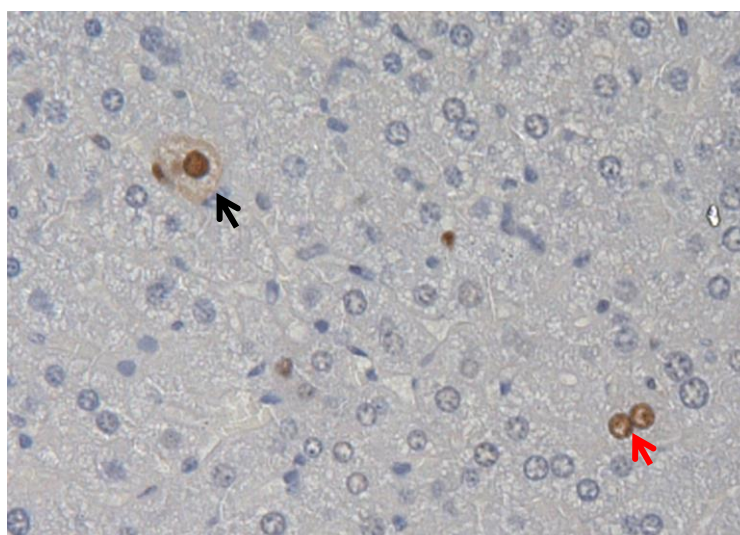


Figure 3.1.13. PCNA expression pattern in hepatocytes.

Liver, fed male CD-1 mouse. PCNA expression in nuclei (red arrow; cells in G1 or S phase) and in the cytoplasm (black arrow; cell at G2 phase immediately prior to mitosis). PAP method, Papanicolaou's haematoxylin counterstain; 400x magnification.

In CD-1 mice, PCNA expression was seen in a relatively variable proportion of cells (average 0.59 - 21% PCNA-positive hepatocytes) with very few cells immediately prior to or in the process of mitosis, as indicated by the cytoplasmic expression of PCNA (0 - 1.19%; Table 6.12). This indicates a various degree of hepatocyte proliferation in the normal liver. Fasting did not result in a significant change in the number of PCNA-positive cells regardless of the length of fasting (16 or 24 hours) and the time span of refeeding (0, 0.5, 1, 5, 10, 15, 20, 24 h), although the

proportion of positive cells was lower in the fasted animals upon completion of the fasting phase (Table 6.12). However, the proportion of cells in the cell cycle (as reflected by their nuclear PCNA expression) sometimes varied significantly over the course of the day, but without any obvious pattern.

Evaluation of proliferating hepatocytes in control **C57BL/6J** mice was only undertaken in fed and fasted animals immediately after saline administration, as this was the only time point at which some differences were seen in the CD-1 mice. While the proportion of PCNA-positive cells was also lower in the fasted C57BL/6J mice, the difference was again not significant (Table 6.13).

A comparison of the figures for CD-1 and C57BL/6J mice showed that the overall amount of proliferating hepatocytes (cells showing nuclear and/or cytoplasmic PCNA expression) was significantly higher in fed CD-1 than in fed C57BL/6J mice; in fasted mice, the difference was still obvious, but it was not significant (Table 3.1.16). There was also no significant difference in the amount of hepatocytes showing cytoplasmic PCNA expression, i.e. hepatocyte immediately prior to or undergoing mitosis, in fed or fasted CD1 and C57BL/6J mice.

Table 3.1.16. Comparison of the amount of proliferating hepatocytes (% nuclear and cytoplasmic PCNA expression; “PCNA+”) and hepatocytes that were prior to/in mitosis (% cytoplasmic PCNA expression; “Cyto+”) in **CD-1 and C57BL/6J** mice that had been fed ad libitum or fasted, immediately after saline dosing (0 hour of refeeding).

Strains	Fed			Fasted		
	ToD killing	% PCNA+ Mean [SD]	% Cyto+ Mean [SD]	ToD killing	% PCNA+ Mean [SD]	% Cyto+ Mean [SD]
CD-1	10:00	21.0 [8.1]	0.66 [0.6]	10:00	6.27 [3.64]	0.16 [0.14]
C57BL/6J	10:00	2.21 [1.41]	0.31[0.52]	10:00	1.18 [0.47]	0.15 [0.09]
p-value		0.0113	NS		NS	NS

ToD – time of day; NS – not significant, Cyto – cytoplasmic.

3.2 Effect of fasting on the response of the liver and/or spleen in CD-1 mice to APAP treatment

In an attempt to evaluate the effect of fasting on the response of the liver to acute toxic injury, male CD-1 mice that had been fed ad libitum (fed mice) and mice that had been fasted for 16 hours or 24 hours received a sublethal dose of APAP intraperitoneally. Saline (0.9%) was applied to control mice. Immediately after dosing, the fasted mice were allowed access to food ad libitum.

None of the dosed animals exhibited clinical signs and resumed and maintained feeding. They were killed at different time points (0-24 hours) after dosing and several serum and liver parameters were assessed in order to monitor the hepatic and systemic effect of APAP overdosing, including serum ALT activity levels, hepatic glutathione levels, hepatic ATP levels and hepatocellular glycogen content as well as histopathological changes in the liver. The inflammatory and regenerative response of hepatocytes was also investigated by relative quantification of cytokine transcription (TNF- α , IL-6, IL-10) and hepatocyte proliferation, assessing NF- κ B, cyclin-D1 transcription and the amount of PCNA expressing hepatocytes. A potential systemic inflammatory response was assessed based on the splenic transcription and serum levels of the pro-inflammatory cytokines TNF- α and IL-6.

3.2.1 Hepatic GSH content

GSH is an antioxidant important for the detoxification of free radicals and oxygen species (Pompella et al., 2003). GSH depletion is long known to be a prerequisite for the onset of APAP hepatotoxicity (Mitchell et al., 1973).

In the present study, the consumption of GSH after acetaminophen administration was assessed by comparing untreated and treated **fed mice** (Table 3.2.1, Figure 3.2.1A). After APAP treatment, the hepatic GSH levels dropped significantly within 1 hour (5.30 ± 3.65 nmol/mg) and had dropped further by 4 hours (4.95 ± 0.56 nmol/mg). However, at 10 hpd, the hepatic GSH content was significantly higher (40.28 ± 0.74 nmol/mg) and almost twice as high as in the control animals (20.6 ± 5.13

nmol/mg) at the same time of day, at 20:45, when these exhibited the lowest circadian value (see Chapter 3.1.2). Also, the amount of GSH was significantly higher at 15 hpd (44.32 ± 12.6 nmol/mg), 20 hpd (35.05 ± 18.49 nmol/mg) and 24 hpd (45.47 ± 10.05 nmol/mg) than at 1 hpd and 4 hpd (Table 3.2.1, Figure 3.2.1B). By 24 hpd, GSH levels were similar to those of the control animals, as those of the latter had doubled from evening to morning. The comparison of hepatic GSH levels at different time points post APAP administration is demonstrated in Table 3.2.1 and Figure 3.2.1B.

Table 3.2.1. Hepatic GSH levels (nmol/mg) in fed control and APAP dosed mice.

Time (hpd)	ToD dosing	ToD killing	Control		APAP		p-value control vs APAP	p-value APAP vs APAP
			Mean	SD	Mean	SD		
0	14:00	14:00	28.81	5.00	-	-	-	1 h: 0.0159
1	9:30	10:30	40.34	4.48	5.30	3.65	0.0286	20 h: 0.0257 24 h: 0.0289
4	9:00	13:00	36.30	5.04	4.95	0.56	0.0286	0 h: 0.0159 , 10 h: 0.0001
10	10:45	20:45	20.60	5.13	40.28	0.74	0.0357	1 h: 0.0002 0 h: 0.0357
15	18:00	9:00(+1)	-	-	44.32	12.64	-	4 h: 0.0471
20	12:20	8:20(+1)	-	-	35.05	18.49	-	4 h: 0.0286
24	10:55	10:55(+1)	47.36	5.75	45.47	10.05	NS	4 h: 0.0356

hpd – hours post dosing; ToD - time of day; SD - standard deviation.

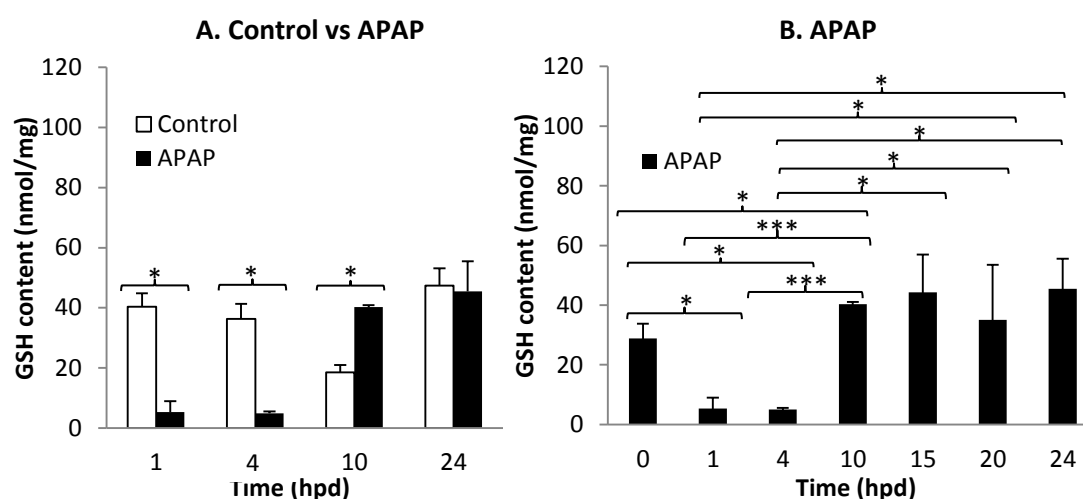


Figure 3.2.1. Hepatic GSH levels in fed male CD-1 mice after APAP treatment.

Hepatic GSH levels were measured in fed mice at different time points (0-24 h) after APAP treatment (530 mg/kg) or 0.9% saline application (control). (A) Comparison of GSH levels in APAP treated and control mice. (B) Comparison of GSH levels in treated animals at different time points post dosing. Values are expressed as mean \pm SD (4 to 6 animals per group). ***P<0.001, **P<0.01 and *P<0.05.

In **fasted APAP treated mice**, GSH levels had significantly dropped within 1 hpd to levels lower than in control animals upon completion of the fasting period (0 hpd). They were significantly lower at 1, 4 and 10 hpd compared to those of control animals after the same time spans of refeeding, where the hepatic GSH levels increased gradually and reached a peak after 10 hours of refeeding before both APAP treated and control mice reached similar levels at 24 hpd (Table 3.2.2, Figure 3.2.2A). The GSH levels of APAP dosed animals were significantly higher at 15 to 24 hpd than earlier time points (Figure 3.2.2B).

Table 3.2.2. Hepatic GSH levels (nmol/mg) in mice that had been **fasted** and then dosed with APAP or 0.9% saline (control mice) and fed ad libitum again, over a 24 hour period.

Time (hpd)	ToD refed	ToD killing	Control		APAP		p-value control vs APAP	p-value APAP vs APAP
			Mean	SD	Mean	SD		
0	10:00	10:00	20.34	3.23	-	-		20 h: 0.0008 5 h: 0.0011
1	10:00	11:00	41.25	10.98	13.67	8.25	0.0286	20 h: 0.0005
4	8:00	12:00	47.70	4.67	4.47	3.57	0.0001	24 h: 0.0142 20 h: 0.0001
10*	10:00	20:00	86.36	22.10	5.28	1.24	0.0001	24 h: 0.0158 0 h: 0.0001
15	16:00	7:00(+1)	-	-	33.98	16.15	-	4 h: 0.0491
20	10:45	6:45(+1)	-	-	49.26	7.82	-	10 h: 0.0002
24	10:15	10:15(+1)	55.85	7.46	50.57	25.22	NS	1 h: 0.0276

10*: The fasted APAP dosed animals that had been killed 10 h after dosing and refeeding had been fasted for 24 h prior to refeeding, whereas all other fasted animals had been fasted for 16 h. Tod - time of day.

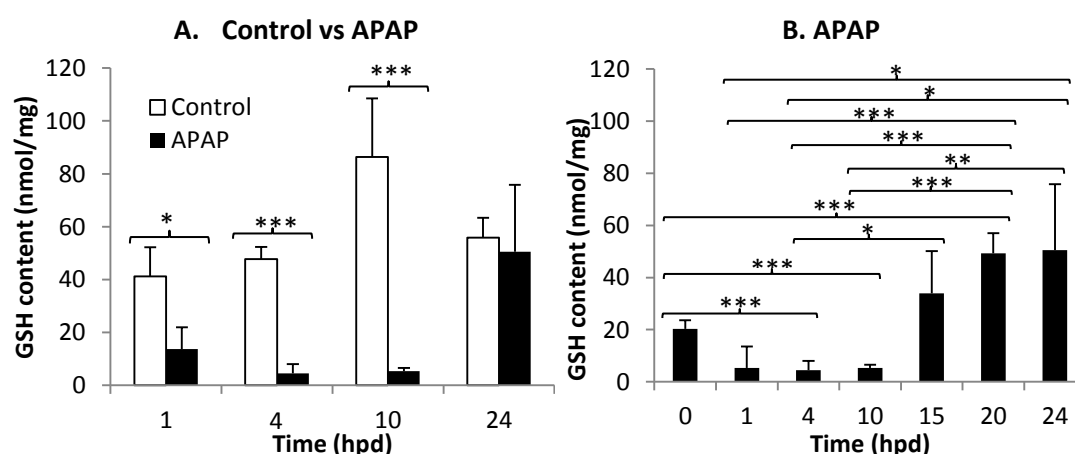


Figure 3.2.2. Hepatic GSH levels in fasted male APAP dosed CD-1 mice.

Hepatic GSH levels were measured in fasted mice at different time points (0-24 h) after APAP treatment (530 mg/kg) or 0.9% saline application (control). (A) Comparison of GSH levels in APAP treated and control mice. (B) Comparison of GSH levels in treated animals at different time points post dosing. Values are expressed as mean±SD (4 to 6 animals per group). ***P<0.005, **P<0.01 and *P<0.05.

Table 3.2.3 illustrates the differences in GSH levels between animals that had been fed or fasted prior to APAP treatment. The time course was similar in both groups, though there were significant differences at 0 and 10 hpd, when levels were significantly lower in the fasted animals. In the latter, the GSH levels had increased to those of fed treated animals from 15 hpd onwards (Table 3.2.3, Figure 3.2.3).

Table 3.2.3. Comparison of mean GSH levels (nmol/mg) in mice that had been **fed or fasted** prior to APAP dosing, over a 24 hours period.

Time (hpd)	Fed				Fasted				p-value fed vs fasted APAP
	ToD dosing	ToD killing	Mean	SD	ToD dosing	ToD killing	Mean	SD	
1	9:30	10:30	5.30	3.65	10:00	11:00	13.67	8.25	NS
4	9:00	13:00	4.95	0.56	8:00	12:00	4.47	3.57	NS
10	10:45	20:45	40.28	0.74	10:00	20:00	5.28	1.24	0.0001
15	18:00	9:00 (+1)	44.32	12.64	16:00	7:00 (+1)	33.98	16.15	NS
20	12:20	8:20 (+1)	35.05	18.49	10:45	6:45 (+1)	49.26	7.82	NS
24	10:55	10:55 (+1)	45.47	10.05	10:15	10:15 (+1)	50.57	25.22	NS

hpd - hours post dosing; ToD - time of day; SD - standard deviation; NS - not significant.

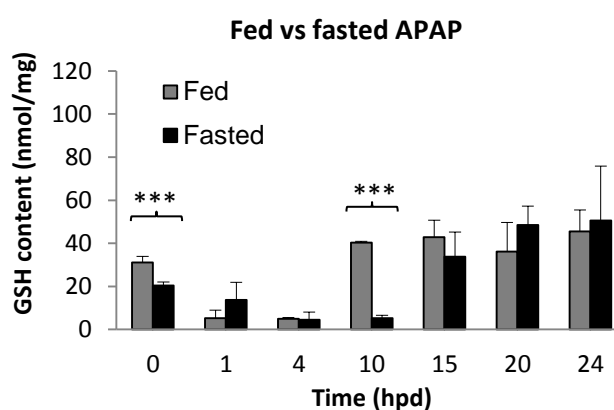


Figure 3.2.3. Comparison of hepatic GSH levels in fed and fasted APAP dosed male CD-1 mice.

Hepatic GSH levels were determined in fed and fasted mice at different time points post APAP treatment. Values are expressed as mean \pm SD (4 to 6 animals per group). ***P<0.005.

3.2.2 Hepatic ATP content

The hepatic ATP content was assessed in **fed mice** after APAP dosing in comparison to saline dosed control animals. APAP dosed mice showed a significantly lower hepatic ATP content at 5 hpd (10.5 ± 2.3 nmol/mg) and 10 hpd (18.3 ± 5.7 nmol/mg) compared to control animals at the same time points (Table 3.2.4, Figure 3.2.4A).

Table 3.2.4. Hepatic ATP levels (nmol/mg) in **fed** CD-1 mice with p-value at the different time points post saline application (control) and APAP dosing.

Time (hpd)	ToD dosing	ToD killing	Control		APAP			p-value control vs APAP
			Mean	SD	Mean	SD	p-value APAP vs APAP	
0	10:00	10:00	35.4	2.0	35.9	1.7	5 h: 0.0069 10 h: 0.0092	NS
1	10:00	11:00	32.1	5.6	31.4	5.1	5 h: 0.0167 10 h: 0.0303	NS
3	10:00	13:00	25.9	4.9	29.8	5.5		NS
5	10:00	15:00	35.5	4.0	10.5	2.3	10 h: NS	0.0056
10	10:00	20:00	30.2	6.4	18.3	5.7	-	0.0405
24	10:00	10:00 (+1)	33.1	2.1	35.4	3.9	5 h: 0.0060 10 h: 0.0277	NS

hpd - hours post dosing; ToD - time of day; SD - standard deviation; NS - not significant.

In the **fasted APAP dosed mice**, the hepatic ATP content was significantly lower than in the fasted control mice, from 3 hpd onwards until the end of the experiment at 24 hpd (Table 3.2.5, Figure 3.2.4B). A comparison of the ATP content in the fasted, APAP treated mice over the time course showed that levels were significantly lower at 1 and 10 hpd than at 24 hpd (Table 3.2.5).

The comparison of ATP values in fed and fasted, APAP treated mice showed significantly lower levels in fasted mice compared to time-matched fed mice at all time points throughout the experiments (Table 3.2.5, Figure 3.2.4C).

Table 3.2.5. Hepatic ATP levels (nmol/mg) in **fasted** CD-1 mice with p-value at the different time points post saline application (control) and APAP dosing.

Time (hpd)	ToD dosing	ToD killing	Control		APAP			p-value control vs APAP	p-value fasted vs fed APAP
			Mean	SD	Mean	SD	p-value		
0	10:00	10:00	4.2	2.6	5.0	2.3	NS	NS	0.0003
1	10:00	11:00	5.3	3.7	4.2	0.9	24 h: 0.024	NS	0.0019
3	10:00	13:00	11.0	1.2	5.6	2.5	NS	0.0398	0.0055
5	10:00	15:00	17.1	5.3	3.5	4.9	NS	0.0087	0.0402
10	10:00	20:00	13.7	1.4	3.4	1.2	24 h: 0.045	0.0060	0.0375
24	10:00	10:00 (+1)	16.4	3.7	8.1	1.3	NS	0.0083	0.0005

hpd - hours post dosing; ToD - time of day; SD - standard deviation; NS - not significant.

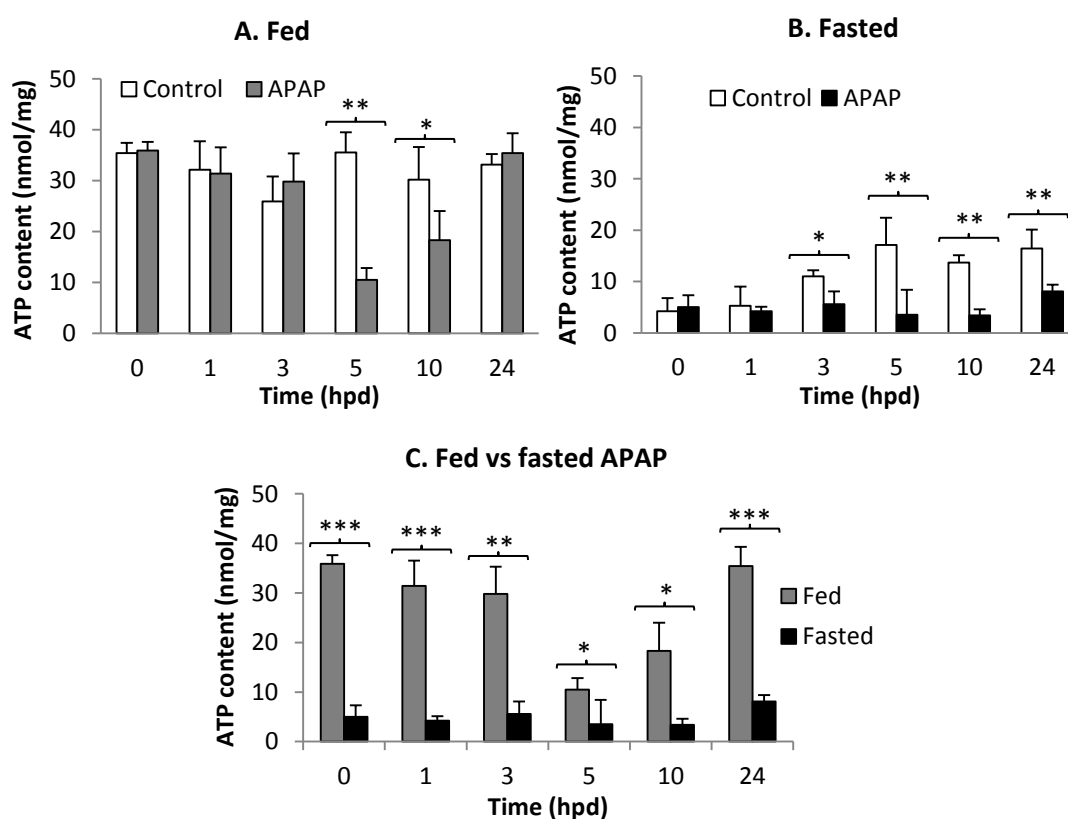


Figure 3.2.4. Hepatic ATP levels after APAP dosing of fed and fasted CD-1 mice. Hepatic ATP levels were measured at different time points (0-24 h) after APAP treatment (530 mg/kg) or 0.9% saline application (control) in fed (A) and fasted (B) mice. (C) Comparison of GSH levels in fed and fasted APAP dosed animals at different time points post treatment. Values are expressed as mean±SD (4 to 6 animals per group). ***P<0.005, **P<0.01 and *P<0.05.

3.2.3 Hepatic ATP and GSH levels

The fold change of hepatic GSH and ATP levels was determined by normalising the values in dosed mice to time-matched control mice that had been fed or fasted prior to dosing.

Following APAP administration in **fed mice**, the GSH levels were reduced significantly more extensively at 1 hpd, but at 10 hpd, it increased significantly compared to hepatic ATP levels. However, at 24 hpd hepatic ATP and GSH levels in fed APAP treated mice were similar to those in control fed mice (Table 3.2.6, Figure 3.2.5A).

In **fasted mice**, although the fold change differences between GSH and ATP levels were insignificant at any time except at 1 hpd, both remained lower in APAP dosed mice compared to respective saline dosed mice throughout the experiment (Table 3.2.6, Figure 3.2.5B).

Table 3.2.6. Comparison of fold changes in hepatic GSH and ATP levels in **fed and fasted**, APAP dosed male CD-1 mice.

Time (hpd)	Fed						
	GSH			ATP			p-value GSH vs ATP
	Control	APAP	Fold change	Control	APAP	Fold change	
1	40.34	5.3	0.13	32.1	31.4	0.98	0.0034
3	-	-	-	25.9	29.8	1.15	-
4	36.3	4.95	0.14	35.5	10.5	0.30	NS
10	20.6	40.28	1.96	30.2	18.3	0.61	0.0005
24	47.36	45.47	0.96	33.1	35.4	1.07	NS
Time (hpd)	Fasted						
	GSH			ATP			p-value GSH vs ATP
	Control	APAP	Fold change	Control	APAP	Fold change	
1	41.25	13.67	0.33	5.3	4.2	0.79	0.0335
3	-	-	-	11.0	5.6	0.51	-
4	47.7	4.47	0.09	17.1	3.5	0.20	NS
10	86.36	5.28	0.06	13.7	3.4	0.25	NS
24	55.85	50.57	0.33	16.4	8.1	0.49	NS

hpd - hours post dosing; ToD - time of day; SD - standard deviation; NS - not significant.

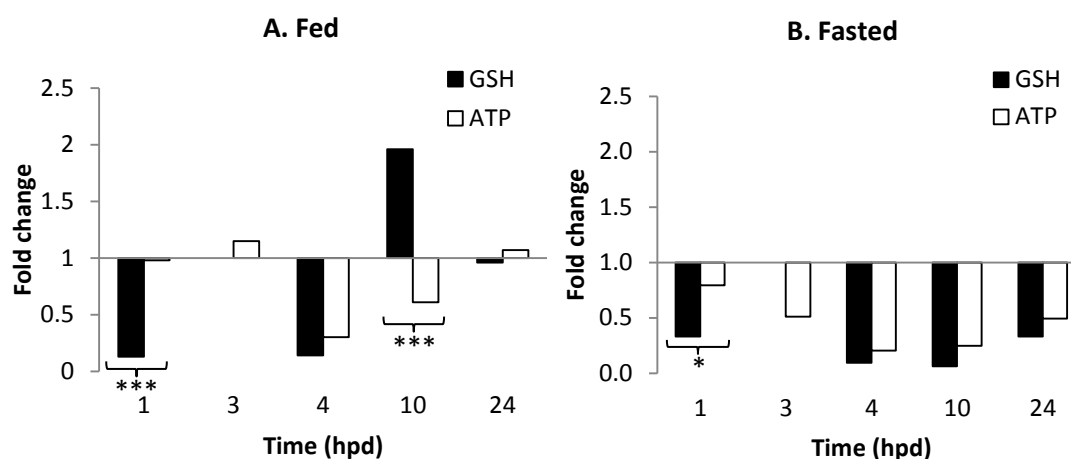


Figure 3.2.5. Hepatic ATP and GSH levels in male CD-1 mice after APAP overdose. Fold changes in ATP and GSH levels in fed (A) and fasted (B) male CD-1 mice after APAP overdose. The levels in APAP dosed mice were normalised to those in time-matched control mice. Values are expressed as mean (4 to 6 animals per group). ** $P < 0.01$ and * $P < 0.05$. Fold change = 1: levels in saline dosed control mice.

3.2.4 Serum ALT levels

The injurious effect of APAP was assessed by measuring a well-established, though non-specific, widely used serum marker of liver damage, the serum ALT activity. In **fed mice**, serum ALT levels were significantly increased at 5, 8 and 24 hpd in comparison to control animals (Table 3.2.7 and Figure 3.2.6A). ALT activities increased progressively and showed significant differences over the time course post APAP dosing: they were significantly higher at 5 hpd than at 1 and 2 hpd. Similarly, they were significantly higher at 24 hpd than at 1, 2 and 4 hpd (Table 3.2.7 and Figure 3.2.6B).

Table 3.2.7. Mean serum ALT levels (U/L) with standard deviation (SD) in **fed** control (0.9% saline) and APAP dosed mice at different times post dosing.

Time (hpd)	ToD dosing	ToD killing	Control		APAP		p value control vs APAP	p-value APAP vs APAP
			Mean	SD	Mean	SD		
1	9:30	10:30	51.63	21.83	477.02	564.23	NS	5 h: 0.0011
2	9:30	11:30	40.98	34.69	198.80	283.87	NS	24 h: 0.0001
4	9:00	13:00	31.17	13.64	698.49	693.98	NS	24 h: 0.0081
5	10:00	15:00	78.20	65.40	2,146.40	1012.30	0.0307	2 h: 0.0286
8	10:00	18:00	22.55	10.97	2333.97	2910.77	0.0074	5 & 24 h: NS
24	10:00	10:00 (+1)	27.5	5.70	2,654.5	334.50	0.0091	1 h: 0.0019

hpd - hours post dosing; ToD - time of day; SD - standard deviation; NS - not significant.

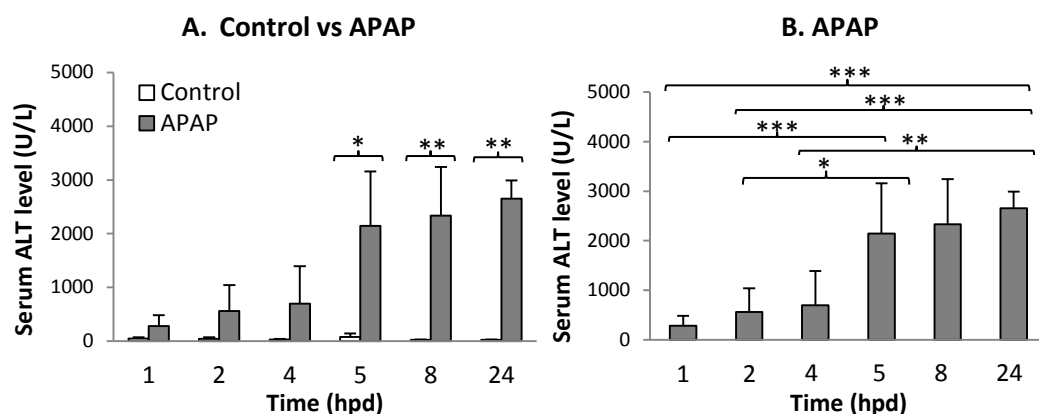


Figure 3.2.6. Serum ALT levels after APAP overdose in male fed CD-1 mice.

The effect of APAP (530 mg/kg) dosing on the serum ALT activity was assessed at different time points up to 24 h after APAP and 0.9% saline (control) dosing (A). Comparison of ALT activity levels at the different time points post APAP dosing (B). Values are expressed as mean±SD (4 to 6 animals per group). ***P<0.005, **P<0.01 and *P<0.05.

The effect of overnight **fasting** on the serum ALT activity after APAP overdose was assessed at two relevant time points, 5 and 24 hpd. At both time points treated mice showed significantly higher serum ALT activities than the respective control animals (Table 3.2.8 and Figure 3.2.7A). Also, in the dosed animals, the activity was significantly higher at 24 hpd than at 5 hpd (Table 3.2.8, Figure 3.2.7B).

Table 3.2.8. Mean serum ALT levels (U/L) with standard deviation (SD) in **fasted** control (0.9% saline) and APAP dosed mice at 5 and 24 hpd.

Time (hpd)	ToD dosing	ToD killing	Control		APAP		p-value control vs APAP
			Mean	SD	Mean	SD	
5	10:00	15:00	49.8	27.5	2,048.6	461.7	0.0086
24	10:00	10:00 (+1)	63.2	22.5	3,603.8	508.8	0.0055
p-value			NS		0.007		

hpd - hours post dosing; ToD - time of day; SD - standard deviation; NS - not significant.

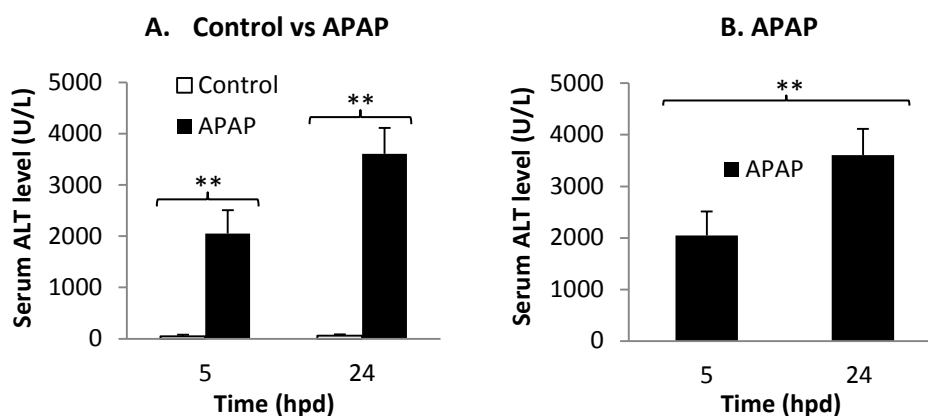


Figure 3.2.7. Serum ALT levels after APAP-induced liver injury in fasted CD-1 mice. (A) Serum ALT levels were measured in fed mice at 5 and 24 h after APAP treatment (530 mg/kg) or 0.9% saline (control) application. (B) Comparison of serum ALT levels in treated animals at 5 and 24 h post APAP treatment. Values are expressed as mean \pm SD (4 to 5 animals per group). **P<0.01.

Subsequently, the serum ALT activity levels at 5 and 24 hpd were compared between mice that been fed or fasted prior to APAP dosing. At 5 hpd, no significant difference was observed, but at 24 hpd, levels were significantly higher in the fasted animals (Table 3.2.9 and Figure 3.2.8).

Table 3.2.9. Mean serum ALT levels (U/L) with standard deviation (SD) in fed and fasted APAP dosed mice at 5 and 24 hpd.

Time (hpd)	Fed APAP		Fasted APAP		p-value fed vs fasted APAP
	Mean	SD	Mean	SD	
5	2,146.4	1012.3	2,048.6	461.7	NS
24	2,654.5	334.5	3,603.8	508.8	0.033

hpd - hours post dosing; SD - standard deviation; NS - not significant.

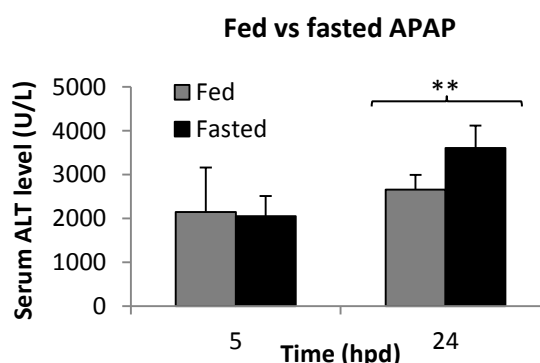


Figure 3.2.8. Serum ALT levels after APAP-induced liver injury in CD-1 mice. Comparison of serum ALT levels at 5 and 24 hpd in APAP treated animals that had been fed or fasted prior to treatment. Values are expressed as mean \pm SD (4 to 6 animals per group). **P<0.01.

3.2.5 Histological features and glycogen content of the liver

The effect of APAP dosing was assessed histologically, using consecutive sections that were stained with haematoxylin-eosin (HE) and underwent the Periodic Acid Schiff (PAS) reaction. The APAP-induced toxic liver changes were scored according to a previously applied scoring system (Antoine et al., 2009b) and the PAS reaction served to evaluate the hepatocellular glycogen content. For the identification of hepatocytes that underwent apoptosis, a further section underwent the immunohistological staining for the demonstration of cleaved caspase-3 (Antoine et al., 2010) in selected cases. All animals had been dosed in the morning (at 9:30 to 10:00). Detailed descriptions of the histological findings and DILI scores of all animals were prepared by Fazila Hamid and Prof Anja Kipar independently and in a blinded fashion. After a consultative discussion, final descriptions and scores were prepared (fed mice: Tables 3.2.10 and 6.14; fasted mice: Tables 3.2.12 and 6.15).

Briefly, in **fed APAP dosed mice**, the earliest histological changes were seen at 2 hpd when a wide, well demarcated rim of hepatocellular glycogen loss was seen at zone 3. The innermost 1-2 centrilobular cell layers often appeared slightly swollen and vacuolated (early hydropic degeneration). By 3 hpd, centrilobular cell loss with numerous apoptotic hepatocytes, confirmed by their expression of cleaved caspase-3 (Figure 3.2.10), was seen; the hepatocellular glycogen had been lost entirely or was only seen in random patchy aggregates of PAS-positive cells. Similar to animals at 3 hpd, mice that had been killed at 4 and 5 hpd showed centrilobular cell loss with minimal neutrophils infiltration, and no glycogen, with numerous cleaved caspase-3 positive apoptotic cells (Figure 3.2.11). At 8 and 10 hpd, mild ongoing cell damage was seen, it was reflected by the presence of occasional apoptotic hepatocytes. Hydropic degeneration was observed in hepatocytes surrounding affected areas, whereas patchy random aggregates of hepatocytes containing glycogen indicated glycogen restitution (Figure 3.2.12). No evidence of ongoing cell damage, but some degree of hydropic degeneration and increased numbers of mitotic figures were seen at 15 and 20 hpd, when almost diffuse hepatocellular glycogen reconstitution was apparent, with the exception of centrilobular areas

with PAS-negative hepatocytes at 20 hpd. By 24 hpd, the livers appeared unaltered with diffuse hepatocellular glycogen accumulation, although with the presence of numerous mitotic figures (Figure 3.2.13).

Table 3.2.10. Histological findings in APAP dosed fed male CD-1 mice (time course). The histological findings are summarised for each group of animals including the number of animals examined at each time point and the range of DILI grading scores for each group. hpd - hours post dosing, n - no of animals used per group; HD - hydropic degeneration, NL - neutrophilic leukocytes, hpc - hepatocytes, CL – centrilobular, CN – coagulative necrosis, CC3 – Cleaved caspase-3, CC3: Negative (-), Positive (+mild,++moderate,+++numerous)hpc.

Time (hpd) [n]	Score range [mean]	Histological findings
0[9]	0	NHAIR; PAS: diffuse hepatocellular glycogen accumulation
0[5]	0	NHAIR; PAS: diffuse hepatocellular glycogen accumulation
1 [9]	0	NHAIR; PAS: diffuse hepatocellular glycogen accumulation (in 6/9 animals evidence of increased glycogen content in CL hpc)
2 [4]	0	CL hpc appear slightly swollen or condensed and partly vacuolated and/or exhibit large nuclei (two most CL cell layers); PAS: wide and well demarcated CL rim (8-10 cell layers) of hepatocellular glycogen loss
3 [5]	0 - 2.5 [1.25]	CL hpc loss (mainly in zone 2), with evidence of apoptotic cells and small NL aggregates; PAS: No glycogen (4/6) or patchy glycogen (2/6); CC3: ++ disseminated in zone 3 and mainly zone 2.
4 [4]	1 - 2.75 [2.44]	CL hpc loss and extending towards zone 2, with several NL and HD of remaining hpc in affected areas; PAS: no glycogen in affected CL areas; CC3: ++/+
5 [13]	0 - 3.25 [2.2]	No evidence of ongoing cell death (5/13), ongoing apoptotic/necrotic CL cell death (8/13), some degree of HD in remaining cells (4/13); PAS: extensive to complete CL glycogen loss; CC3: + (5/13), +++ (4/13), negative (4/13)
8 [4]	0.5 - 4 [1.25]	No evidence of ongoing cell death with no inflammatory infiltrate or evidence of CL coagulative necrosis in few severely affected lobes; PAS: almost diffuse to variable degree of glycogen restoration
10 [11]	0 - 3.25 [1.0]	Slight ongoing CL hpc death (5/6, via apoptosis); HD of hpc surrounding affected areas; PAS: patchy to randomly distributed hpc with glycogen; CC3: scattered individual CL positive hpc
15 [11]	0 - 2.5 [1.125]	Increased mitotic figures, no evidence of ongoing cell death, but some degree of HD and disorderly arrangement of hpc in affected areas; PAS: diffuse glycogen except CL (affected) areas
20 [6]	0-1 [0.65]	Numerous mitotic figures; no ongoing cell death; some HD in affected areas (2/6); PAS: large proportion of CL hpc devoid of glycogen
24 [8]	[0]	Numerous mitotic figures, but otherwise unaltered appearing; PAS: diffuse hepatocellular glycogen accumulation (variable amount); CC3: negative

A summary of the findings with the range of scores and average scores is recorded over the time course in Table 3.2.11 and Figure 3.2.9. DILI scores varied between animals in each group, with individual animals showing a score of 0 even at the time points, when the most severe damage was observed. However, a comparison of the

average DILI scores seen at each time point showed the significantly highest mean scores at 3, 4 and 5 hpd (score 1.25-2.44) and a drop thereafter (Table 3. 2.11).

Table 3.2.11. Histological scores in APAP dosed **fed** CD-1 mice (time course).

Time (hpd)	ToD dosing	ToD killing	n	Score range [mean]	SD	p-value APAP vs APAP
0.5	10:00	10:30	5	[0]	0	0.5,1,2 h: NS
1	9:30	10:30	9	[0]	0	
2	9:30	11:30	4	[0]	0	
3	10:00	13:00	5	0-2.5 [1.25]	1.04	0.5,1,2 h: 0.0318 5 h: NS
4	9:00	13:00	4	1-2.75 [2.44]	1.25	0.5,1,2 h: 0.0093
5	10:00	15:00	13	0-3.25 [2.2]	1.28	0.5,1,2 h: 0.0197
8	10:00	18:00	4	0.5-4 [1.25]	-	-
10	10:00	20:00	11	0-3.25 [1]	0.89	5 h: NS
15	16:00	08:00	11	0-2.5 [1.13]	1.04	10 h: NS
20	10:00	6:00 (+1)	6	0-1 [0.65]	0.27	15 h: NS
24	10:00	10:00 (+1)	4	[0]	0	10 h: NS
			4		-	

hpd – hours post dosing; ToD – time of day, n – number of mice; SD –standard deviation.

Apart from the animals that were killed at 15 hpd which had been dosed at 16:00 in the afternoon, all **fasted animals** had been dosed in the morning (between 8:00 and 10:45). In fasted APAP dosed mice, complete glycogen loss was observed at 0 hour (see Chapter 3.1.6). In fasted mice, at 30 and 60 min after APAP dosing, a low degree of glycogen restitution was seen, represented by a few individual, PAS-positive hepatocytes; this had a lower intensity than in time-matched control mice. No histological abnormality was detected, apart from evidence of early centrilobular hepatocellular hydropic degeneration at 1 hpd (Table 3.2.12). Although fasted mice showed extensive centrilobular cell loss with evidence of scattered necrotic cells and evidence of inflammatory cell (mainly neutrophils) recruitment at 3 to 5 hpd, the average DILI scores were not significantly higher than in fed mice (Figure 3.2.9). There was no evidence of glycogen reconstitution and very occasional scattered cleaved caspase-3 positive apoptotic cells were recorded at 3 and 5 hpd (Table 3.2.12, Figure 3.2.10). By 10 hpd, areas of centrilobular cell loss were surrounded by hepatocytes with mild hydropic degeneration and scattered necrotic cells. At that time, there was either no evidence of hepatocellular

glycogen reconstitution or glycogen accumulation in individual random hepatocytes (Figure 3.2.12). The degree of centrilobular cell loss remained the same but the number of glycogen-containing hepatocytes was higher outside centrilobular regions at 15 hpd (Table 3.2.12). At 20 and 24 hpd, there was evidence of coagulative necrosis of the innermost centrilobular cell layer and diffuse glycogen hepatocellular accumulation outside centrilobular areas with occasionally scattered cleaved caspase-3 positive apoptotic cells (Table 3.2.12, Figure 3.2.13).

Table 3.2.12. Histological findings in APAP dosed fasted male CD-1 mice (time course). The histological findings are summarised for each group of animals including the number of animals examined at each time point and the range of DILI grading scores for each group. hpd - hours post dosing, n - number of animals used per group; HD - hydropic degeneration, NL – neutrophilic leukocytes, hpc - hepatocytes, CL – centrilobular, CN – coagulative necrosis, CC3 – Cleaved caspase-3, CC3: Negative (-), Positive (+mild,++moderate,+++numerous) hpc.

Time (hpd) [n]	Fasting time (h)		Score range [mean]	Histological findings
	16	24		
0 [4]		x	0	NHAIR; complete glycogen loss
0.5 [5]	x		0	NHAIR; PAS: no glycogen (4/5), some degree of glycogen restitution in individuals cells (1/5)
1 [5]	x		0	CL hpc with variably sized cytoplasmic vacuoles (4-5 layers; evidence of early HD), only very mild outside CL; PAS: no glycogen (2/5) or low degree of glycogen restitution in individuals cells (3/5)
3 [5]		x	0.5 - 3 [2.05]	CL hpc loss; CL hpc in particular are vacuolated, several swollen cells with clumped chromatin scattered necrotic cells; PAS: no glycogen. CC3: very occasional scattered pos. cells
4 [4]	x		1 - 3 [2.1]	Marked reduction of CL hpc, HD of remaining hpc; PAS: no glycogen.
5 [5]		x	1 - 3 [2.5]	CL hpc that round up and exhibit loose vacuolation and chromatin clumping; PAS: no glycogen.
10 [5]		x	2 - 4 [2.6]	CL hpc loss surrounded by hpc with HD; occasional NL at transition to unaltered areas; PAS: few cells with/no glycogen. CC3: +
15 [7]	x		0 - 4 [2.15]	In areas without CL cell loss (and scattered necrotic/ apoptotic hpc, with occ. NL) CL 3 hpc layers with homogenous, slightly basophilic cytoplasm (degeneration/early stage of CN), surrounded by hpc with increasing cytoplasmic vacuolation; occasional NL between CL hpc; PAS: diffuse glycogen (variable amount) outside CL areas
20 [10]	x		0 - 5 [2.75]	Disorganised CL hpc with cytoplasm like CN, with some necrotic hpc (5-6 cell layers); a few NL in CV and affected areas; score 5 in subcapsular areas; PAS: diffuse glycogen outside affected CL areas
24 [10]	x		0 - 4 [2.35]	Well delineated CL area of HD with inner layer of hpc with features of CN (and loss of nucleus), 5-6 cell layers, a few NL in CV and affected areas; affected areas surrounded by 1 layer of dense, otherwise unaltered cells; PAS: diffuse glycogen except 2-3 layers of zone 3
[5]		x	1 - 4 [2.4]	CL cell loss, remaining cells often mildly to moderately vacuolated (HD), scattered necrotic cells, small no. of NL within CV, scattered mitotic cells; PAS: diffuse glycogen outside the affected areas; CC3: +/++

Table 3.2.13. Histological scores in APAP dosed **fasted** CD-1 mice (time course).

Time (hpd)	Fasting time (h)		ToD refed	ToD killing	n	Score range [mean]	SD	p-value APAP vs APAP
	16	24						
0.5	x		9:00	9:30	5	[0]	0	-
1	x		8:30	9:30	5	[0]	0	0.5 h: NS
3		x	10:00	13:00	5	0.5-2.75 [2.05]	1.04	0.5 h: 0.0115 1 h: 0.0115
4	x		8:00	12:00	4	1-3 [2.125]	0.48	-
5		x	10:00	15:00	5	1-3 [2.5]	1.41	1 h: NS 3 h: NS
10		x	10:00	20:00	5	2-4 [2.6]	0.42	1 h: 0.0002 5 h: NS
15	x		16:00	7:00 (+1)	5	0-4 [2.15]	0.78	1 h: 0.0036 10 h: NS
20	x		10:45	6:45 (+1)	5	0-5 [2.75]	0.43	1 h: 0.0079 15 h: NS
24		x	10:00	10:00 (+1)	5	1-4 [2.4]	0.89	1 h: 0.0003 20 h: NS 24h (16h): NS
	x		10:15	10:15 (+1)	5	0-4 [2.35]	0.45	

hpd – hours post dosing; ToD – time of day; n – number of animals; SD – standard deviation; NS – not significant; 24h (16h) – 16 hours fasted mice at 24 hpd.

Since the DILI scores in the fasted animals were similar regardless of the length of the fasting period (16 or 24 hpd), the fasted groups were looked at together for the comparison between fed and fasted mice at each time point (Table 3.2.14 and Figure 3.2.9C). This confirmed that the APAP-induced damage was more severe in fasted animals, where the average scores were significantly higher at 10, 20 and 24 hpd (Table 3.2.14, Figure 3.2.9C).

Table 3.2.14. Comparison of histological scores in APAP dosed **fed and fasted** male CD-1 mice (time course).

Time (hpd)	Fed: Mean score [n]	Fasted: Mean score [n]		p-value fed vs fasted APAP
		16 h fasting	24 h fasting	
1	0 [5]	0 [5]	-	NS
3	1.25 [5]	-	2.05 [5]	NS
4	2.44 [4]	2.125 [4]	-	NS
5	2.2 [13]	-	2.5 [5]	NS
10	1 [11]	-	2.6 [5]	0.0406
15	1.125 [11]	2.15 [5]	-	NS
20	0.65 [6]	2.75 [5]	-	0.0043
24	0 [4]	2.35 [5]	-	0.0160
	0 [4]	-	2.4 [5]	0.0159
	-	2.35 [5]	2.4 [5]	NS
	0 [4]	2.375 [10]		0.0001

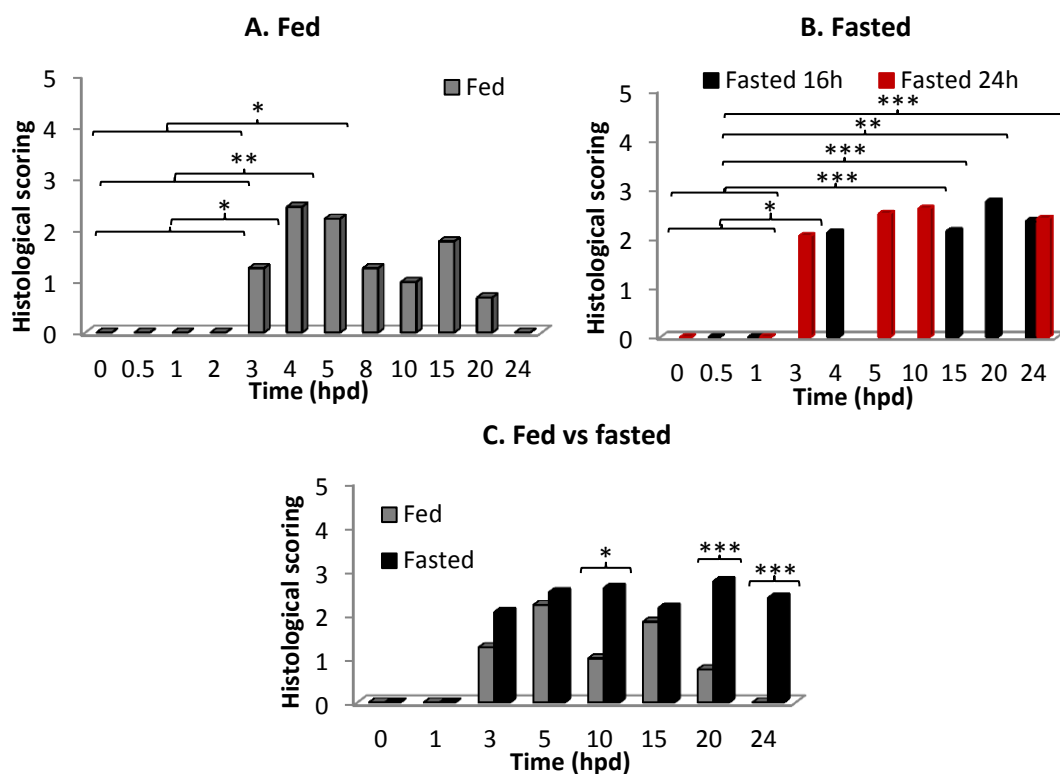


Figure 3.2.9. Histological scoring in CD-1 mice after APAP overdose. Histological scoring after APAP overdose (530 mg/kg) over 0-24 hpd in fed (A) and 16 or 24 h fasted (B) mice. (C) Comparison between fed and fasted mice (combined 16 and 24 h fasted mice) with regards to the histological grading score. Data represent mean±SD (4 to 13 animals per group). ***P<0.005, **P<0.01 and *P<0.05.

The histopathological features of the liver in fed and fasted APAP dosed mice were compared at 3 hpd (Figure 3.2.10), 5 hpd (Figure 3.2.11), 10 hpd (Figure 3.2.12) and 24 hpd (Figure 3.2.13). At early time points, both fed and fasted mice showed a similar degree of centrilobular cell loss, but with more evidence of neutrophils in the fasted mice. At later time points, there was no evidence of further hepatocyte damage in fed mice, and the liver parenchyma appeared unaltered, suggesting that the liver damage had subsided and almost complete regeneration and diffuse glycogen restoration had taken place by 24 hpd. At the same time point, in fasted mice, there was still evidence of ongoing cell damage, while glycogen was restored outside the affected centrilobular areas. The semiquantitative assessment of the amount of cleaved caspase-3 positive apoptotic cells showed that numerous cells in the affected centrilobular areas died of apoptosis in fed mice at 3 hpd (++) and even more at 5 hpd (+/+++ (Figure 3.2.10). In contrast, in fasted mice no or only few apoptotic cells (-/+ at centrilobular areas were seen at the same time points.

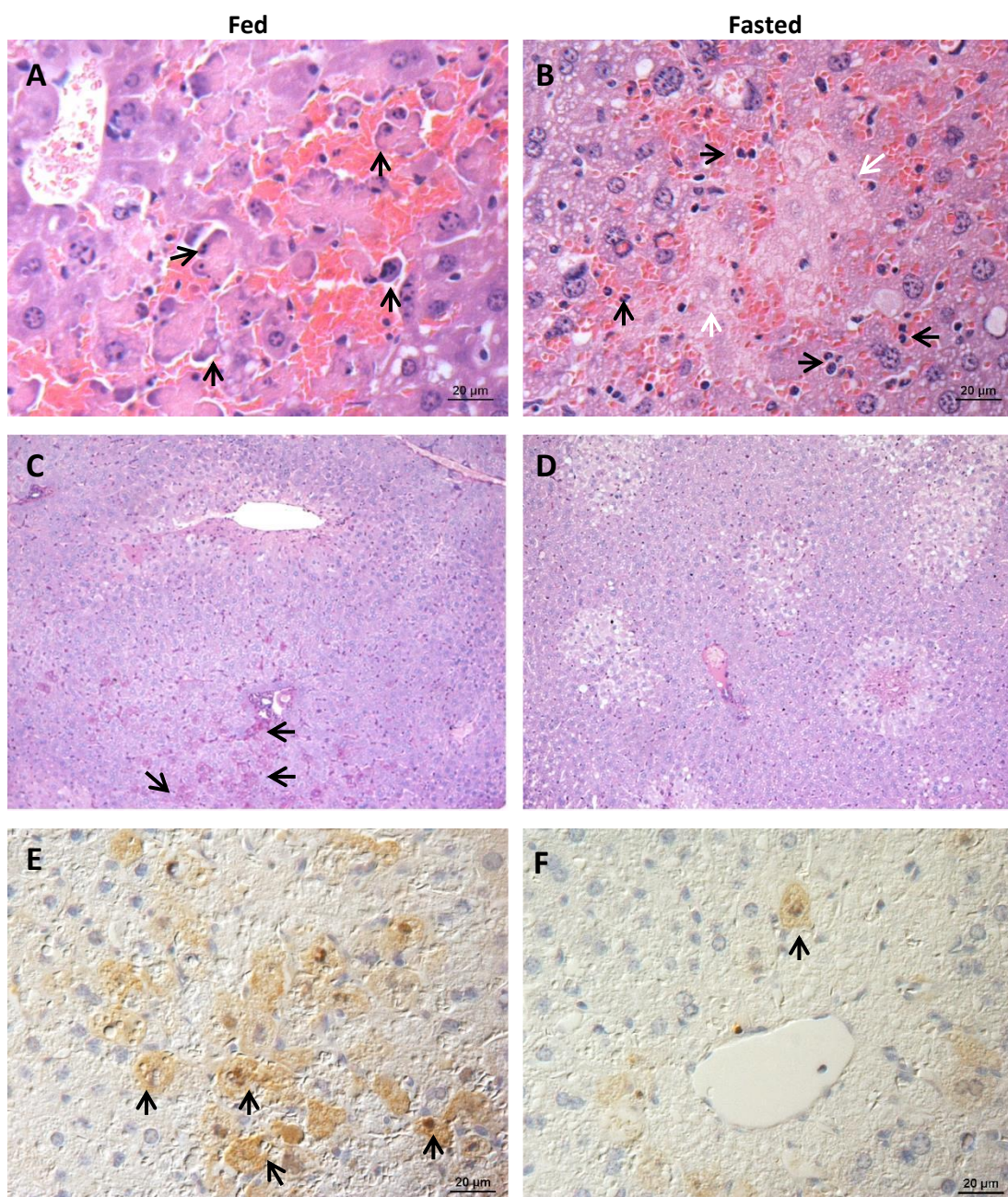


Figure 3.2.10. Assessment of histopathological features and glycogen content in fed and fasted male CD-1 mice at 3 h post APAP (530 mg/kg) treatment.

In fed animals, there was centrilobular cell loss (score 1.25) (A) and no evidence of hepatocellular glycogen reconstitution apart from in a few individual PAS-positive cells (black arrows) (C). In fasted mice, the centrilobular damage was more intense (score 2.05) and there were necrotic cells (white arrows) with moderate infiltration of neutrophils (black arrows) (B) and no evidence of hepatocellular glycogen reconstitution (D). In fed mice, the presence of a large number of centrilobular apoptotic cells was confirmed by staining for cleaved caspase-3 (black arrows) (E); their number was much lower in fasted mice (F). A, B: HE stain; C, D: PAS reaction; E, F: PAP method, Papanicolaou's haematoxylin counterstain. Magnification x400 (A, B, E, F) and x100 (C, D).

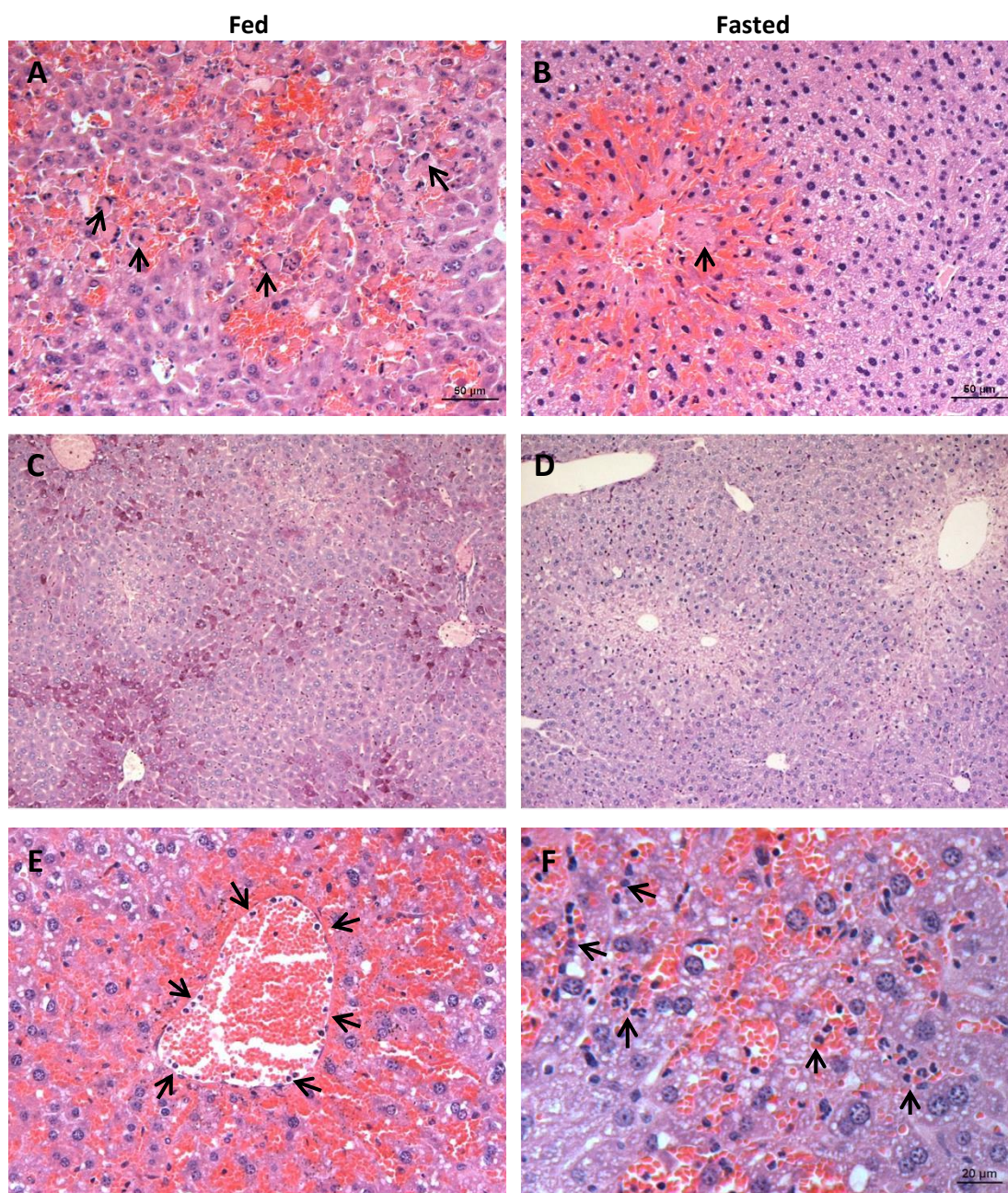


Figure 3.2.11. Assessment of histopathological features and glycogen content in fed and fasted male CD-1 mice at 5 h post APAP (530 mg/kg) treatment.

In fed mice, centrilobular hepatocyte loss (score 2.2) is seen, affecting zones 3 and 2 (A). Patchy random aggregates of hepatocytes with glycogen accumulation are present (C), representing glycogen reconstitution. In fasted mice, more intense centrilobular hepatocyte loss (score 2.5) and necrotic cells (black arrow) are seen (B), and there is no evidence of hepatocellular glycogen reconstitution (D). The higher magnification shows some neutrophils rolling along the endothelium of a central vein (black arrows) in a fed mouse (E), whereas in a fasted mouse numerous neutrophils are seen infiltrating the sinuses adjacent to the affected centrilobular area (black arrows) (F). A, B, E, F: HE stain; C, D: PAS reaction. Magnification x200 (A, B, E), x100 (C, D) and x400 (F).

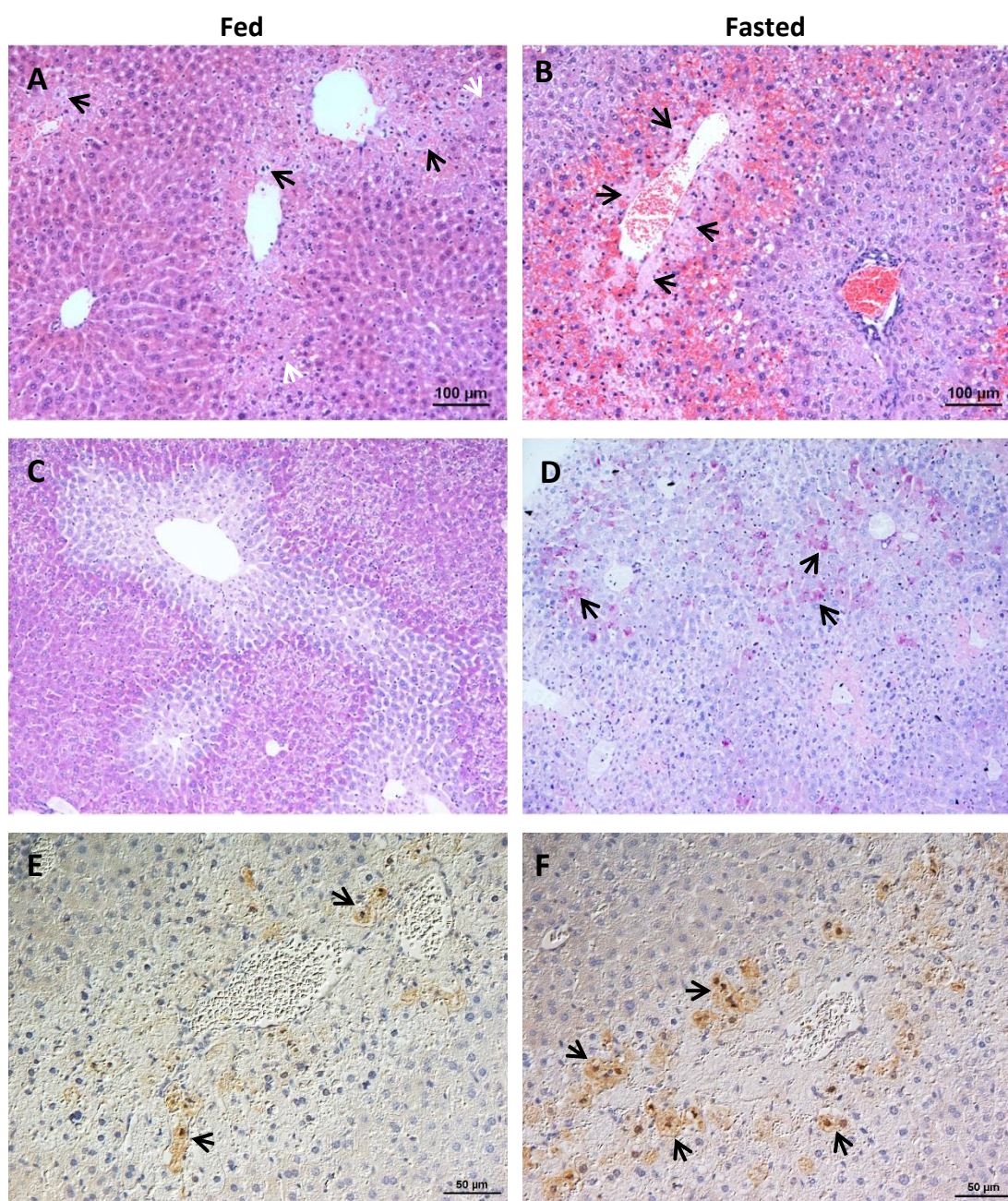


Figure 3.2.12. Assessment of histopathological features and glycogen content in fed and fasted male CD-1 mice at **10 h post APAP** (530 mg/kg) treatment.

In fed mice (A), there is still evidence of centrilobular cell loss (score 1), but to a lesser degree than at the earlier time points with evidence of hydroptic degeneration of a few hepatocytes (black arrows) and mitotic figures (white arrows). There is evidence of complete hepatocellular glycogen reconstitution outside affected areas of centrilobular region (C). In fasted mice (B), extensive centrilobular cell loss (score 2.6) and necrosis of hepatocytes (black arrows) as well as moderate neutrophil infiltration is seen (B). Only scattered random individual hepatocytes show evidence of glycogen accumulation (D). Staining for cleaved caspase-3 reveals a few apoptotic hepatocytes in affected centrilobular areas (black arrows) in fed mice (E). Their number was substantially higher in fasted mice (F). A, B: HE stain; C, D: PAS reaction; E, F: PAP method, Papanicolaou's haematoxylin counterstain. Magnification x100 (A, B, C, D) and x200 (E, F).

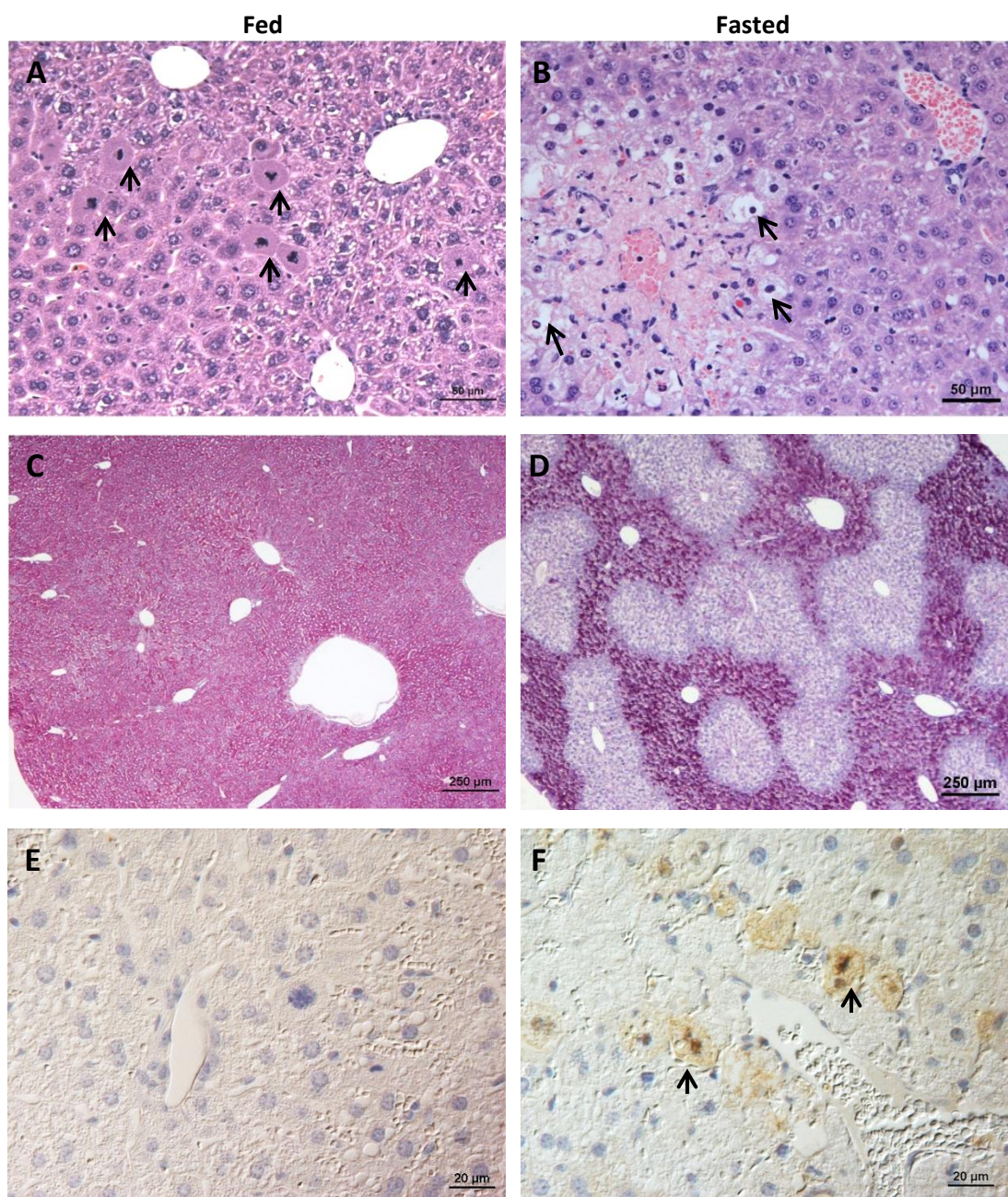


Figure 3.2.13. Assessment of histopathological features and glycogen content in fed and fasted male CD-1 mice at **24 h post APAP (530 mg/kg)** treatment.

In fed mice, there is no evidence of cell loss (score 0), suggesting complete hepatic regeneration; numerous mitotic figures are seen (black arrows) (A). There is diffuse hepatocellular glycogen accumulation (C). In fasted mice, there are well delineated centrilobular areas of swollen hepatocytes undergoing hydropic degeneration (score 2.4) (black arrows) and coagulative necrosis of cells in the innermost layer (B), with diffuse hepatocellular glycogen restitution outside the affected centrilobular layers (D). A, B: HE stain; C, D: Absent of apoptosis in fed mice (E), but presence of several centrilobular apoptotic cells which was confirmed by cleaved caspase-3 staining (black arrows) (F). PAS reaction: E, F: PAP method, Papanicolaou's haematoxylin counterstain. Magnification x200 (A, B), x40 (C, D) and x400 (E, F).

3.2.6 Overall assessment of liver damage based on all parameters

We combined the data obtained testing the various parameters (levels of hepatic GSH, ATP, serum ALT and DILI score) in order to have better illustration of overall degree of liver damage following APAP overdosing in fed and fasted CD-1 mice over 24 hours (Table 3.2.15, Figure 3.2.14). Data are presented as fold change relative to time matched control mice, except for the DILI scores (raw data). In fed mice, depletion of GSH and ATP at early time points coincides with histological evidence of acute liver injury (scores) and high serum ALT activity. The damage subsides at the end of the study period when GSH and ATP levels return to control animal levels (Figure 3.2.14A).

In contrast, fasted mice showed prolonged depletion of hepatic GSH and ATP which coincides with the morphological evidence of more pronounced liver injury and higher serum ALT activity (Figure 3.2.14B). Briefly, over the 24 hour time course fasted CD-1 mice had higher DILI scores and higher serum ALT levels with more intense hepatic GSH and ATP depletion than fed mice (Table 3.2.15, Figure 3.2.14C).

Table 3.2.15. Comparison of GSH, ATP, ALT fold changes and DILI scores in fed and fasted male CD-1 mice following APAP overdose.

Time (hpd)	GSH		ATP		ALT		DILI score	
	Fed	Fast	Fed	Fast	Fed	Fast	Fed	Fast
1	0.13	0.33	0.98	0.79	9.24	-	0	0
3	-	-	1.15	0.51	-	-	1.25	2.05
4	0.14	0.09	0.3	0.2	22.41	-	2.44	2.13
5	-	-	-	-	27.45	41.14**	2.2	2.5
10	1.96***	0.06	0.61	0.25	-	-	1	2.6*
15	-	-	-	-	-	-	1.12 5	2.15
20	-	-	-	-	-	-	0.65	2.75***
24	0.96	0.33	1.07	0.49	96.53***	57.02	0	2.4***

Statistical significant, *P<0.05, **P<0.01 and ***P<0.005 are seen in comparison between fed and fasted APAP dosed CD-1 mice. hpd - hours post dosing.

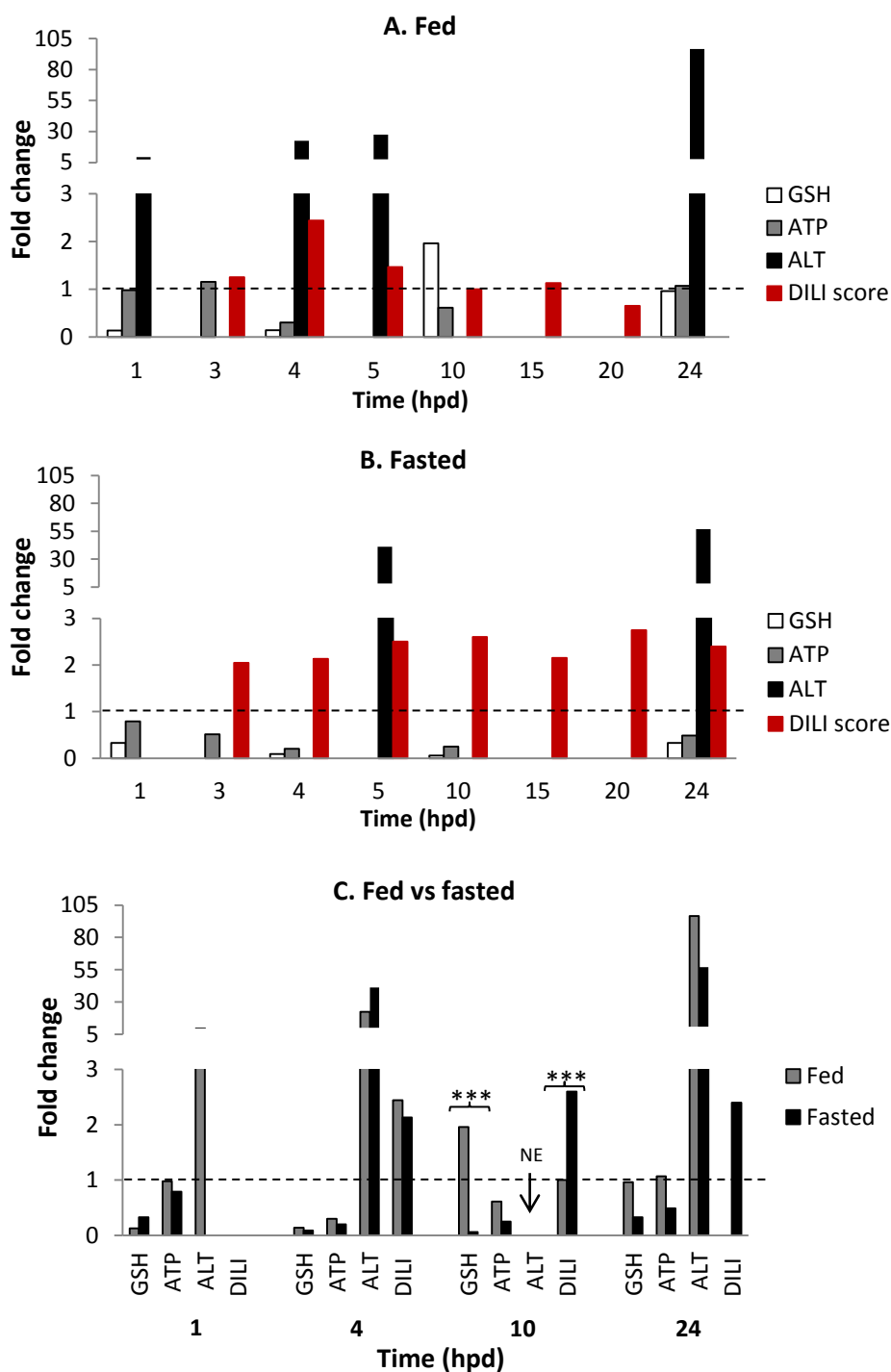


Figure 3.2.14. Assessment of liver damage in fed and fasted male CD-1 mice following APAP overdose.

The liver GSH and ATP and the serum ALT levels and the DILI scores were compared over 1-24 h in animals that had been fed (A) or fasted (B) prior to APAP administration. The levels were also compared between fed and fasted CD-1 mice (C). The values of GSH, ATP and ALT are assessed by fold change that is calculated on relative to time-matched control mice, on exemption of DILI score (as listed in Table 3.2.15). Data represent mean (4 to 6 animals per group). Fold change = 1: levels in saline dosed control mice indicated by dashed lines. NE – not examined.

3.2.7 Cytokine transcription in liver and spleen and cytokine levels in the blood of APAP dosed CD-1 mice

3.2.7.1 Hepatic transcription of TNF- α , IL-6 and IL-10

The relative transcription of TNF- α , IL-6 and IL-10 in the liver and spleen of APAP dosed mice was assessed in relation to the constitutive transcription levels in fed and fasted control mice, using the values for the housekeeping gene GAPDH as initial reference values, using the delta Ct values, $2^{-\Delta Ct}$ to compare the transcription activities of control and APAP dosed mice (Figure 3.2.15). Overall, mRNA levels of all cytokines are highly expressed in APAP dosed mice than those in controls.

In both fed and fasted CD-1 mice, increased TNF- α transcription was observed at 1, 4 and 10 hpd in comparison to time-matched control mice, at 24 hpd, it was lower (Figure 3.2.15). In fed mice, IL-6 and IL-10 transcription levels increased gradually and peaked at 15 hpd (for IL-10) and 20 hpd (for IL-6). At 24 hpd, levels were lower again, but still higher than in the control mice (Table 6.16, Figure 3.2.15C,E), but the no substantial change was seen in fasted mice (Table 6.18, Figure 3.2.15D,F). Details of the hepatic TNF- α , IL-6 and IL-10 mRNA levels using the delta Ct and comparative Ct value method are provided in the Appendix (fed mice: Table 6.16; fasted mice: Table 6.18).

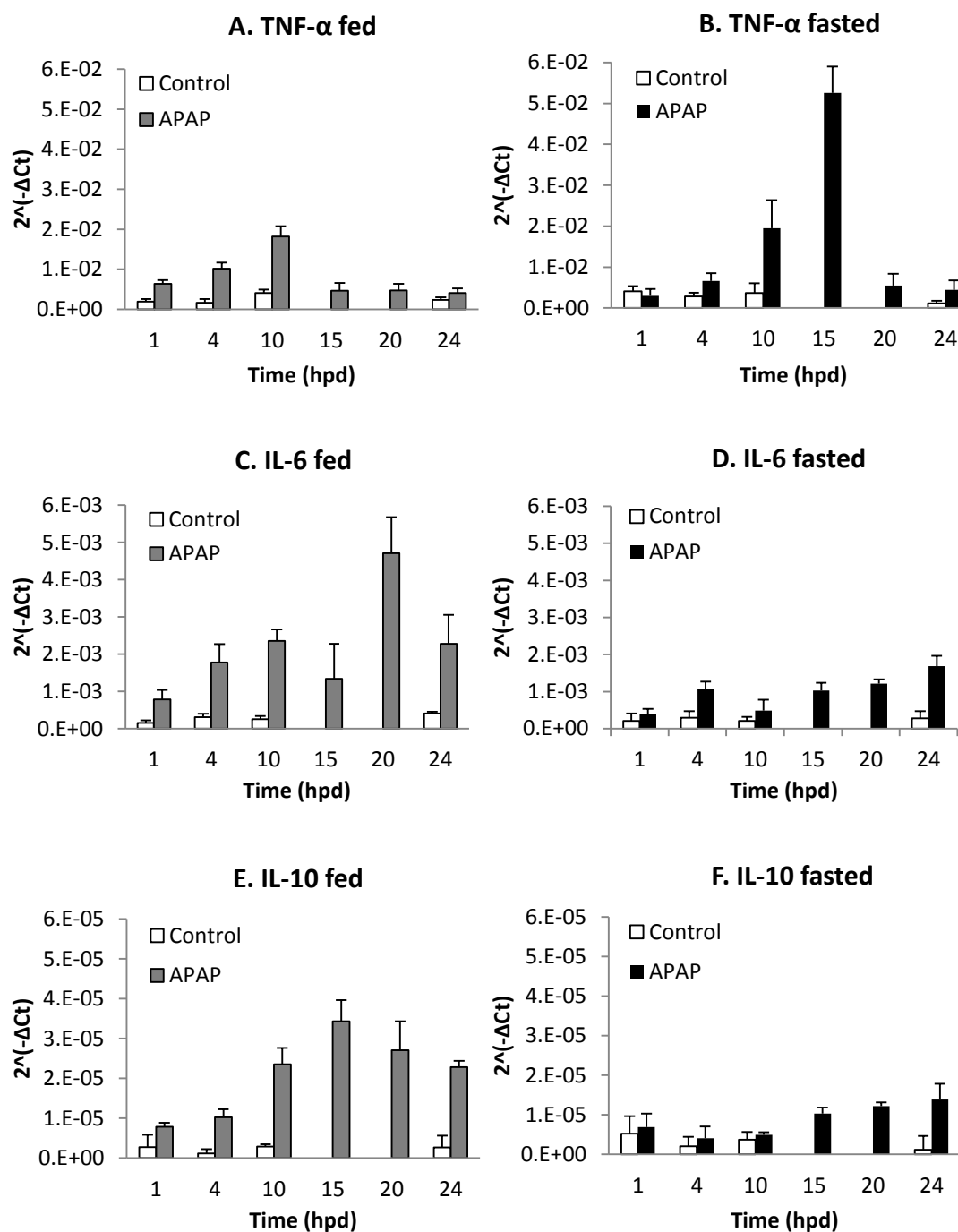


Figure 3.2.15. Hepatic TNF- α , IL-6 and IL-10 transcription levels after APAP dosing of fed and fasted male CD-1 mice.

The hepatic mRNA levels of cytokines TNF- α (A, B), IL-6 (C, D) and IL-10 (E, F) were compared between 0.9% saline (control) and 530 mg/kg APAP dosed fed and fasted mice. Hepatic mRNA levels are calculated using the Ct value formula, $2^{-\Delta Ct}$. Data represent mean \pm SD (4 to 6 animals per group).

Comparison of the transcription levels was carried out by comparative Ct value method, assessing the fold change of treatment groups after normalising to controls. Statistical analysis was determined by the fold change in treated vs. time matched control mice. Details of the cytokines transcription were prepared in Appendix (fed mice: Tables 6.16-17 and fasted mice: Tables 6.18-19).

TNF- α mRNA levels showed a significant 6-fold peak increase at 4 hpd and 4.5-fold increase at 10 hpd and had returned to control mouse levels at 24 hpd in fed mice (Figure 3.2.16A, Table 6.16). In fasted mice, TNF- α mRNA levels were not significantly increased at 1 and 4 hpd, but were statistically higher at 10 hpd (5.3-fold) and 24 hpd (3.9-fold) compared to those in control mice (Figure 3.2.16B). In APAP dosed mice, TNF- α showed a gradual increase at 4 hpd (2.3-fold) and 10 hpd (5.3-fold) and reached a peak at 15 hpd (14.3-fold) before it went down significantly and was 4.8-fold higher at 20 hpd and 3.9-fold higher at 24 hpd (Table 6.18).

In fed animals, although quite variable, **IL-6** mRNA levels were significantly increased in APAP dosed mice throughout the experiment, with the following fold changes: 1 hpd (5-fold), 4 hpd (5.7-fold), 10 hpd (9.3-fold), and 24 hpd (5.6-fold) (Figure 3.2.16C, Table 6.16). In fasted mice, the IL-6 mRNA expression was upregulated consistently over the entire study period, with a significant increase at 4 hpd (3.6-fold), 10 hpd (2.3-fold), and 24 hpd (6-fold) (Figure 3.2.16D, Table 6.18).

IL-10 mRNA levels showed a significant 8-fold increase in fed APAP dosed mice at 4, 10 and 24 hpd compared to the time matched control mice. Moreover, the levels reached a peak at 15 hpd (12-fold) before decreasing slightly, reaching an 8.7-fold higher level than control mice at 24 hpd, a difference that was not statistically significant upon comparison with the 4 to 24 hpd fold changes (Figure 3.2.16E, Table 6.16). In fasting mice, IL-10 transcription levels were similar to those observed in control mice at the earlier time points, but were increased significantly at 20 hpd (10.6-fold) and 24 hpd (12-fold) (Figure 3.2.16F, Table 6.18).

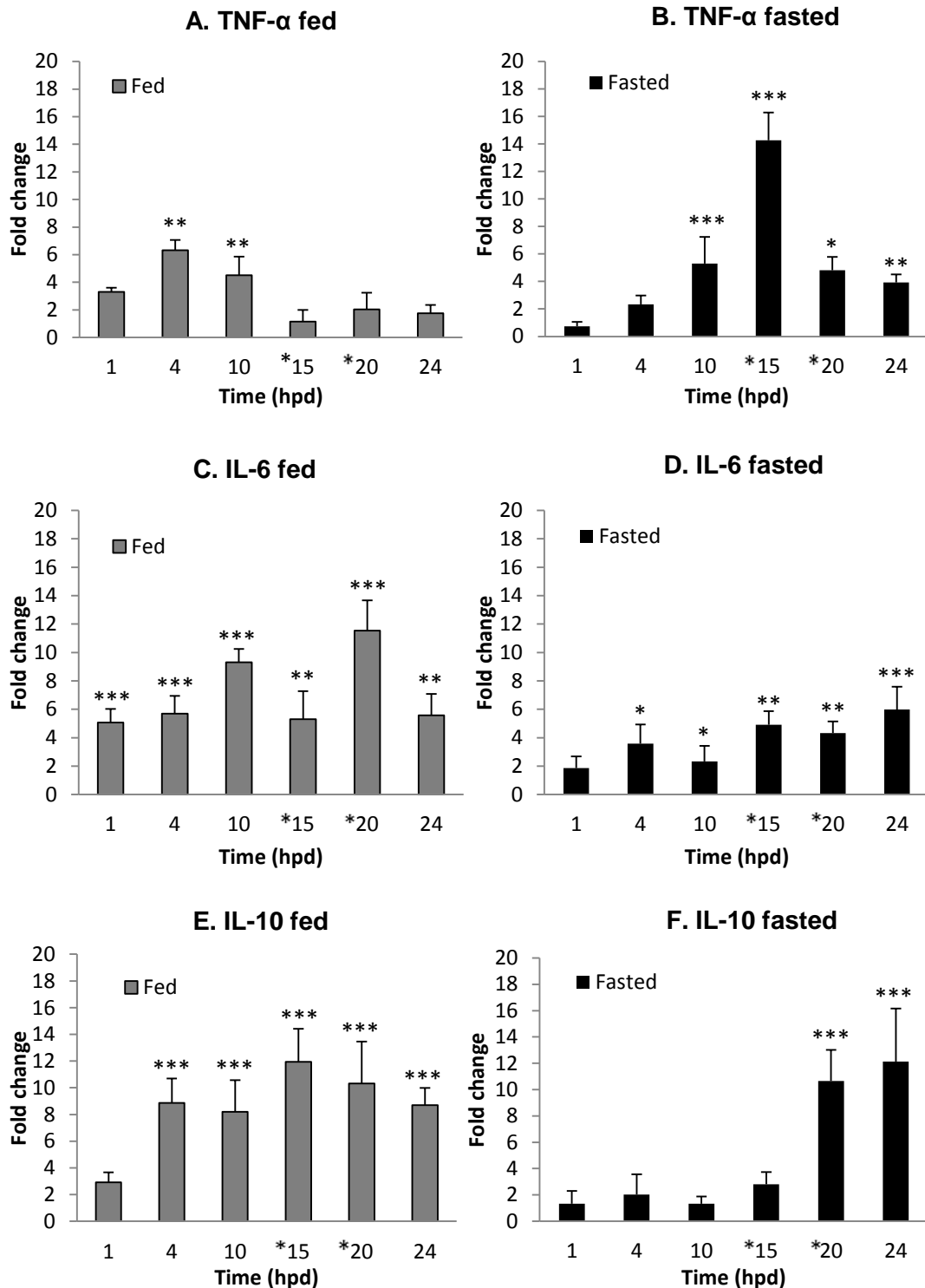


Figure 3.2.16. Hepatic TNF- α , IL-6 and IL-10 transcription levels in fed and fasted male CD-1 mice after APAP dosing.

The hepatic mRNA levels of cytokines TNF- α (A, B), IL-6 (C, D) and IL-10 (E, F) are shown in fed and fasted CD-1 mice after 530 mg/kg APAP administration. Hepatic mRNA levels are calculated using the comparative Ct values, assessing the fold change relative to respective time matched control mice, except *15 (relative to 10 h post saline) and *20 hpd (relative to 24 h post saline). Data represent mean \pm SD (4 to 6 animals per group). *** P <0.005, ** P <0.01 and * P <0.05.

In order to assess the changes in cytokine levels in APAP dosed mice over the entire time period, we compared those to pooled values where different time-matched of all control mice had been taken together because we had not identified any statistical significant difference in their values over the study period (see Chapter 3.1.7.1). This approach also detected a statistically significant difference in the hepatic TNF- α , IL-6 and IL-10 levels at different time points. Details of mRNA levels of these cytokines are provided in Appendix (fed: Table 6.17 and fasted: Table 6.19).

In fed mice, the previous results were confirmed (see also Figure 3.2.16A) and TNF- α mRNA levels were found to be significantly increased at 4 hpd (6.3-fold) and 10 hpd (4.5-fold) before returning to basal levels at 15 to 24 hpd (Table 6.17). In fasted mice, similar to the previous results, significantly higher TNF- α mRNA levels were only observed at 10 hpd (6.8-fold) and 15 hpd (18.3-fold) (Table 6.19). While hepatic TNF- α mRNA levels were increased significantly at 4 hpd in fed mice, fasted mice had a sharp peak at 15 hpd before returned to controls thereafter (Figure 3.2.17A).

IL-6 mRNA levels were found to be significantly increased in fed APAP dosed mice at 4 hpd (6-fold), 10 hpd (7.9-fold), 20 hpd (15.8-fold), and 24 hpd (7.6-fold) while the previous results showed a significant increase also at 15 hpd (Table 6.17). In fasted mice, the IL-6 mRNA expression was upregulated gradually over the entire study period, with a significant increase at 4 hpd (4.7-fold), 20 hpd (5.3-fold) and 24 hpd (7.4-fold) (Table 6.19), but the previous results (see Figure 3.2.16D) had a significant increase at 10 and 15 hpd. Meanwhile, hepatic IL-6 transcription was significantly higher at 10 hpd and much higher at 20 hpd in fed mice compared to fasted mice, before both reached a similar level at 24 hpd (Figure 3.2.17B).

In fed animals, IL-10 mRNA levels were significantly increased in APAP dosed mice at 4 hpd (3.9-fold), 10 hpd (9-fold) and reached a peak at 15 hpd (13.2-fold) before decreasing slowly at 20 hpd (10.4-fold) and 24 hpd (8.8-fold) compared to pooled control mice (Table 6.17), which was similar to the previous results (Figure 3.2.16E). In fasting mice, different from the previous results (see Figure 3.2.16F), IL-10 mRNA levels was increased significantly at 20 hpd (4.6-fold) and 24 hpd (5.2-fold) only

(Table 6.19). Following APAP treatment, transcription of IL-10 was significantly higher in fed mice at 10, 15 and 20 hpd compared to fasted mice (Figure 3.2.17C).

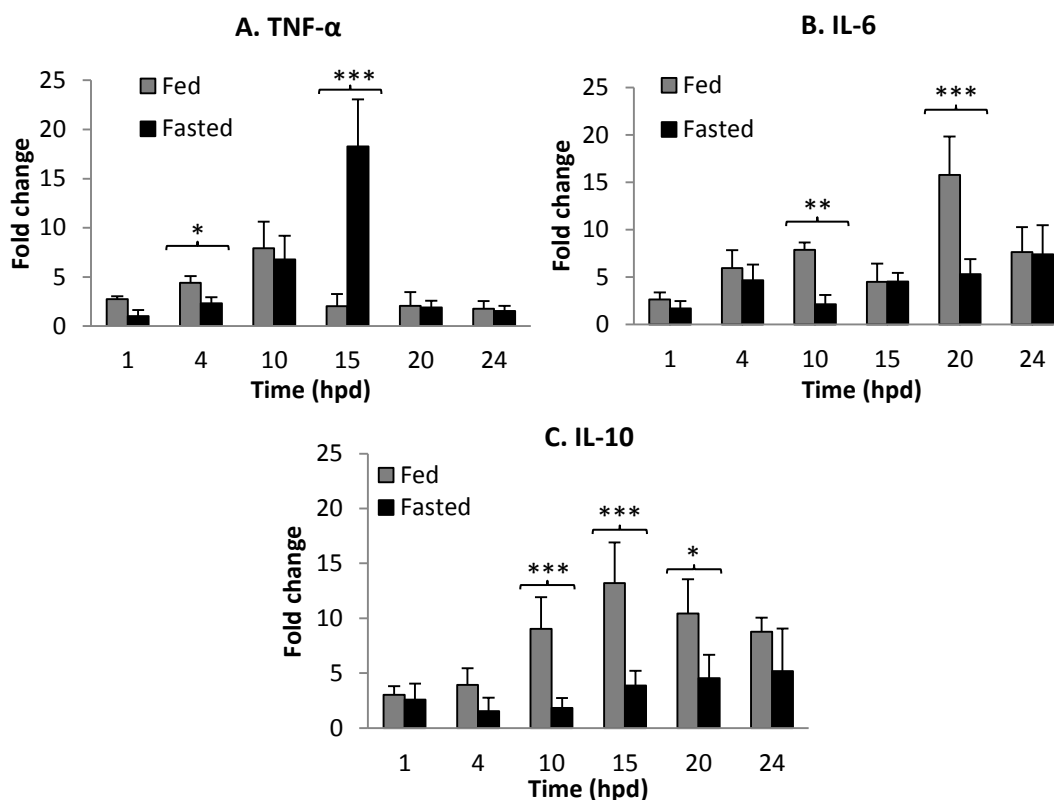


Figure 3.2.17. Hepatic TNF- α , IL-6 and IL-10 transcription levels in fed and fasted male CD-1 mice after APAP dosing.

Hepatic TNF- α (A), IL-6 (B) and IL-10 (C) transcription levels are compared between fed and fasted APAP dosed male CD-1 mice. Hepatic mRNA levels are calculated using the comparative Ct values, assessing the fold change relative to pooled control animals. Data is given as mean \pm SD (4 to 6 animals per group). ***P<0.005, **P<0.01 and *P<0.05.

3.2.7.2 Splenic transcription of TNF- α and IL-6

In order to assess whether APAP overdosing leads to a systemic inflammatory response as a consequence of hepatic damage, the splenic TNF- α and IL-6 transcription was assessed at 10 to 24 hpd, using the delta Ct value and fold change method to compare the levels in fed and fasted treated and control mice (Table 6.20, Figure 3.2.18).

In **fed animals**, splenic TNF- α transcription levels were significantly higher at 10 hpd (3.9-fold) in APAP dosed mice and were found to have declined after that. IL-6 mRNA levels were significantly higher at 20 hpd (3.9-fold) and 24 hpd (3.7-fold) compared to control mice and APAP dosed mice at earlier time-points (Table 6.20). In **fasted mice**, TNF- α transcription levels were significantly higher at 15 hpd (4.3-fold), 20 hpd (7.2-fold) and 24 hpd (6.3-fold). In contrast, the IL-6 mRNA levels did not differ significantly from those of control animals at any time point (Table 6.20).

The comparison of fed and fasted mice did not identify a statistically significant difference in the transcription of both TNF- α and IL-6 at 10 and 15 hpd; after that, at 20 and 24 hpd, the TNF- α mRNA levels were significantly higher and the IL-6 mRNA levels were significantly lower in fasted mice (Table 6.20, Figure 3.2.18E,F).

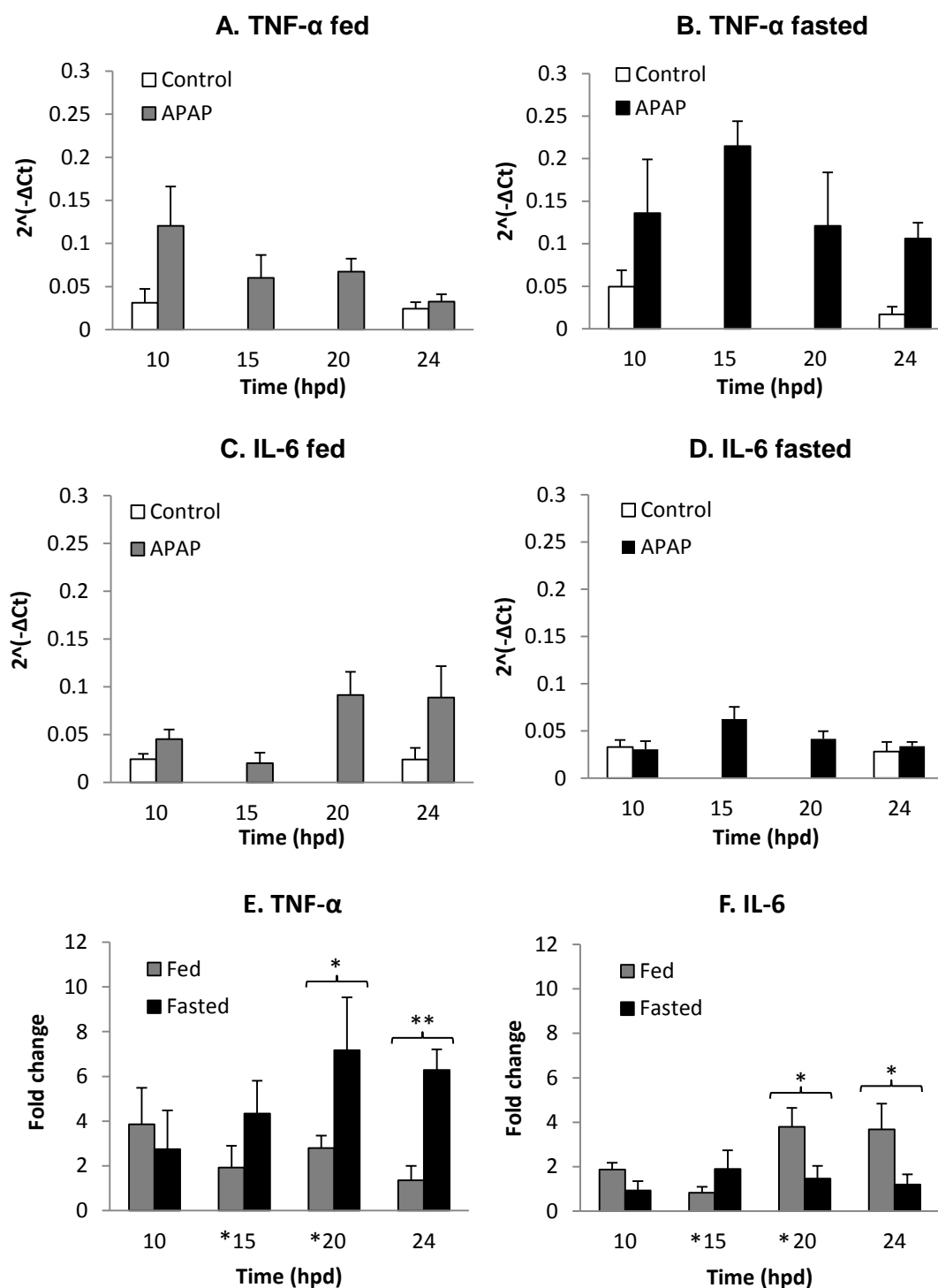


Figure 3.2.18. Splenic TNF- α and IL-6 transcription in male CD-1 mice that had been either fed or fasted prior to APAP dosing.

TNF- α and IL-6 mRNA levels were determined in fed (A, C) and fasted (B, D) CD-1 mice using the delta Ct value, $2^{-\Delta Ct}$. A comparison of levels in fed and fasted mice was undertaken using the comparative Ct value as fold change relative to respective to time-matched control mice, except *15 (relative to 10 h post saline) and *20 hpd (relative to 24 h post saline) for TNF- α (E) and IL-6 (F). Data represent mean \pm SD (4 to 6 animals per group). *** $P < 0.005$, ** $P < 0.01$ and * $P < 0.05$.

We also assessed the mRNA cytokine levels using **pooled control** values for the compare with those of APAP dosed mice at different time points, because we had not identified any statistical significant difference in the values of control animals over the entire time course (see Chapter 3.1.7.2). In fed animals, a statistical significant increase of splenic TNF- α transcription than pooled control mice was only seen at 10 hpd (4.4-fold) (Table 6.21). However, in fasted mice, the levels were always significantly higher at 10 hpd (4.1-fold), more extensively at 15 hpd (6.5-fold) and then reduced gradually at 20 (3.6-fold) and 24 hpd (3.2-fold). The comparison of values in fed and fasted mice did not recognise significant differences in TNF- α mRNA levels at 10 and 20 hpd, but a significant increase at 15 and 24 hpd in fasted compared to fed mice (Table 6.21, Figure 3.2.19A), but the levels was also significant at 20 hpd (see Figure 3.2.18E).

In contrast to splenic TNF- α , the IL-6 mRNA levels in the spleen were significantly increased at 20 hpd (3.8-fold) and 24 hpd (3.7-fold) in APAP dosed fed mice, but not at any time point in fasted treated animals. The comparison of both groups showed that splenic IL-6 mRNA levels were significantly higher at 20 and 24 hpd (both were approximately 3.8-fold) in the fed APAP dosed mice (Table 6.21, Figure 3.2.19B) as similar results shown previously (see Figure 3.2.18F).

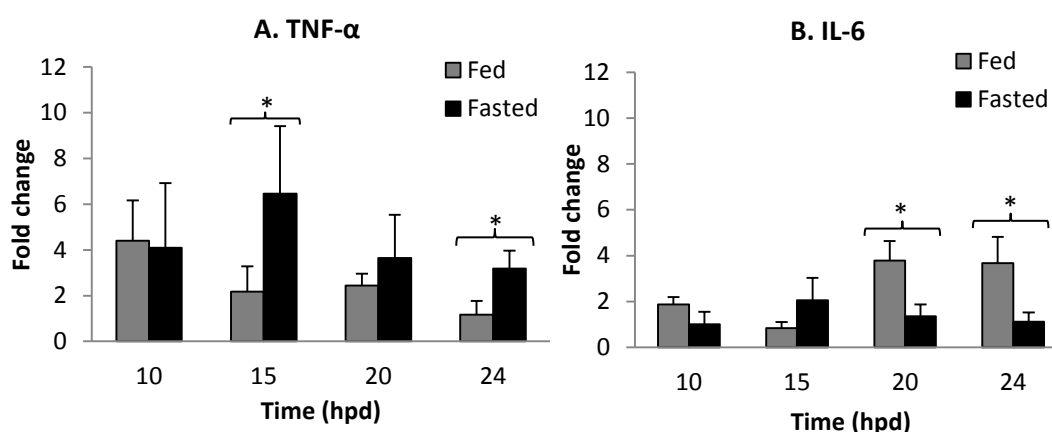


Figure 3.2.19. Splenic TNF- α and IL-6 transcription of in APAP dosed CD-1 mice. Splenic TNF- α and IL-6 mRNA levels are compared between fed and fasted APAP dosed male CD-1 mice. Splenic mRNA levels were compared using the comparative Ct value as fold change relative to pooled control animals. Data is given as mean \pm SD (4 to 6 animals per group). ***P<0.005, **P<0.01 and *P<0.05.

3.2.7.3 Serum TNF- α and IL-6 levels

Serum TNF- α and IL-6 levels were measured at 5 and 24 hpd. In fed mice, **TNF- α** levels were similar to those of the control mice at 5 hpd, but were significantly higher at 24 hpd (95.0 ± 14.1 pg/mL) (Figure 3.2.20A). In fasted mice, serum TNF- α levels were significantly higher (227.8 ± 53.6 pg/mL) at the same time point in comparison to control animals (63.1 ± 19.7 pg/mL) (Figure 3.2.20B), these levels were also significantly higher than those of the fed mice at 24 hpd (Table 3.2.16).

Serum **IL-6** levels were significantly higher in both fed (203.0 ± 39.61 pg/mL) and fasted (96.4 ± 35.2 pg/mL) APAP dosed mice in comparison to control mice (27.5 ± 12.6 pg/mL) at 5 and 24 hpd (Figure 3.2.20C,D). The comparison of fed and fasted dosed mice showed that the IL-6 levels were significantly higher in the fed mice (Table 3.2.17).

Table 3.2.16. Comparison of serum **TNF- α** and **IL-6** levels (pg/mL) in control and APAP treated fed and fasted CD1 mice. Data is given as mean SD of 4 mice per group.

Time (hpd)	ToD dosing	ToD killing	Fed			Fasted			p-value fed vs fasted APAP
			Control (SD)	APAP (SD)	p-value control vs APAP	Control (SD)	APAP (SD)	p-value control vs APAP	
5	10:00	15:00	51.4 (12.4)	62.1 (13.5)	NS	57.1 (13.3)	101.2 (40.1)	NS	NS
24	10:00	10:00 (+1)	45.8 (6.4)	95.0 (14.1)	0.010	63.1 (19.7)	227.8 (53.6)	0.007	0.022
p-value			NS	NS		NS	0.039		

Time (hpd)	ToD dosing	ToD killing	Fed			Fasted			p-value fed vs fasted APAP
			Control (SD)	APAP (SD)	p-value control vs APAP	Control (SD)	APAP (SD)	p-value control vs APAP	
5	10:00	15:00	25.4 (6.7)	54.3 (10.2)	0.045	23.1 (4.1)	35.4 (10.5)	0.049	0.039
24	10:00	10:00 (+1)	30.1 (2.08)	203.0 (39.6)	0.007	27.49 (12.6)	96.4 (35.2)	0.020	0.009
p-value			NS	0.006		NS	NS		

hpd - hours post dosing, ToD - time of day, SD - standard deviation, NS - not significant.

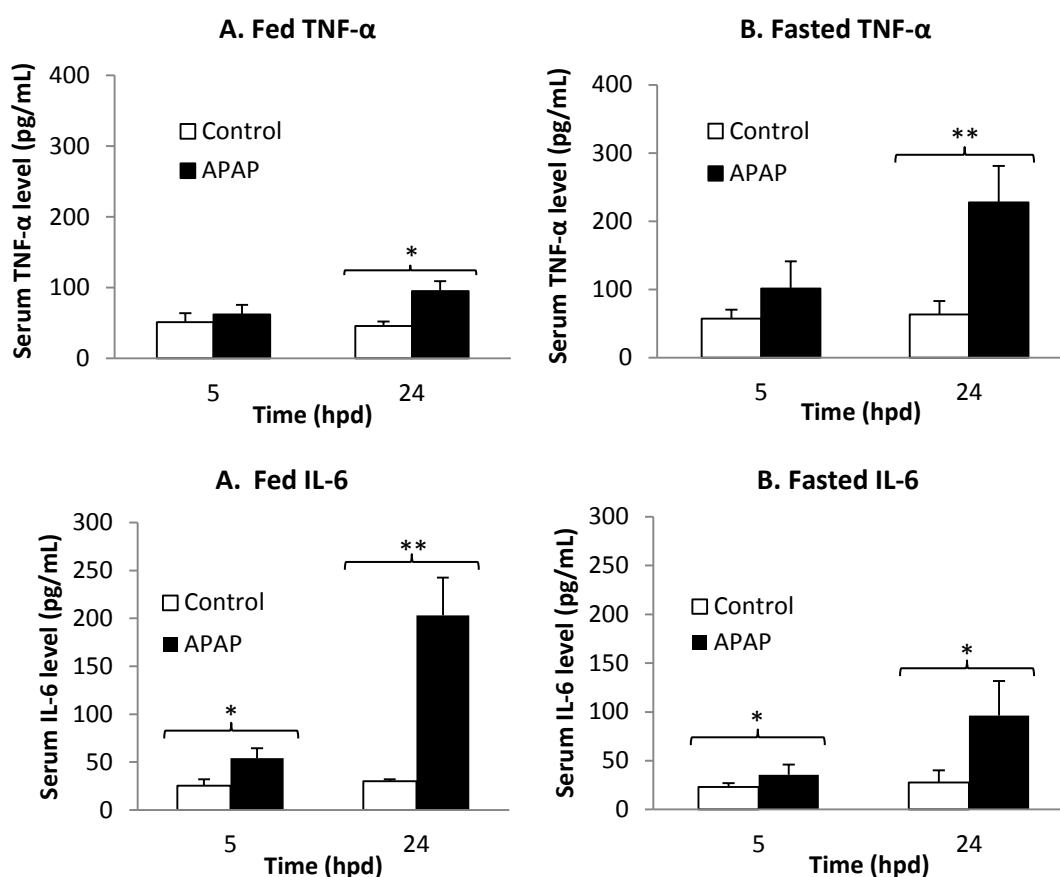


Figure 3.2.20. Serum TNF- α and IL-6 levels in control and APAP dosed male CD-1 mice. Serum TNF- α levels were determined after the administration of 530 mg/kg APAP or 0.9% saline (controls) in fed (A) and fasted (B) mice. Levels are compared between fed and fasted APAP dosed mice (C). Data is given as mean \pm SD (4 to 6 animals per group). **P<0.01 and *P<0.05.

3.2.8 Assessment of liver regeneration based on hepatocellular proliferation

Liver regeneration after acute APAP induced injury was assessed on the basis of three parameters: 1) NF- κ B mRNA expression, as NF- κ B appears to be a transcription factor that is upregulated by TNF- α and able to promote liver regeneration (Bhushan et al., 2014), 2) the transcription of cyclin-D1, a protein expressed in cells that have passed the G1 restriction point and entered the G1 phase (Fausto, 2000), and 3) the expression of PCNA, a protein expressed in cells that have entered the cell cycle and head towards mitosis (Kurki et al., 1986).

3.2.8.1 Hepatic NF- κ B mRNA transcription

In fed APAP dosed mice, hepatic NF- κ B mRNA levels were higher than in **time matched saline dosed mice** in the delta Ct method (Figure 3.2.21A), when the fold changes were assessed, NF- κ B mRNA levels were found to be significantly increased at 4 hpd (4.7-fold), 10 hpd (17.6-fold), 15 hpd (13-fold), and 20 hpd (18.6-fold). After that they dropped, but were still 11.7-fold higher than in control animals at 24 hpd (Table 6.22).

In fasted mice, NF- κ B transcription levels were not as high as in fed mice, but they were higher than in time matched fasted control animals at all time points (Figure 3.2.21B). Comparative assessment of fold change showed the mRNA levels were similar at 15, 20 and 24 hpd and significantly higher than in the control animals (up to 6-fold), and they were significantly higher than the levels at 1, 4 and 10 hpd where an up to 3-fold increase was seen (Table 6.22). A comparison between fed and fasted mice showed that the NF- κ B mRNA levels were significantly higher in the fed mice from 10 hpd until the end of experiment at 24 hpd (Table 6.22, Figure 3.2.21C).

The NF- κ B mRNA levels of APAP dosed animals were also assessed relative to **pooled control** mice values because values had been found to be similar in saline dosed mice over the entire time course (see Chapter 3.1.8.1). Fed animals showed a statistically significant rapid increase in NF- κ B mRNA levels at 10 hpd (13.3-fold) before decreasing slightly at 15 hpd (9.9-fold), 20 hpd (9.5-fold) and 24 hpd (6.1-fold) (Table 6.23). In fasted mice, a significant increase was only recognised at 20 and 24 hpd (both 4.7-fold). However, NF- κ B mRNA levels were significantly higher in the fed mice at 10, 15 and 20 hpd compared to the fasted mice following APAP dosing (Table 6.23, Figure 3.2.21D), similar to the previous results for all time points apart from 24 hpd (see Figure 3.2.21C).

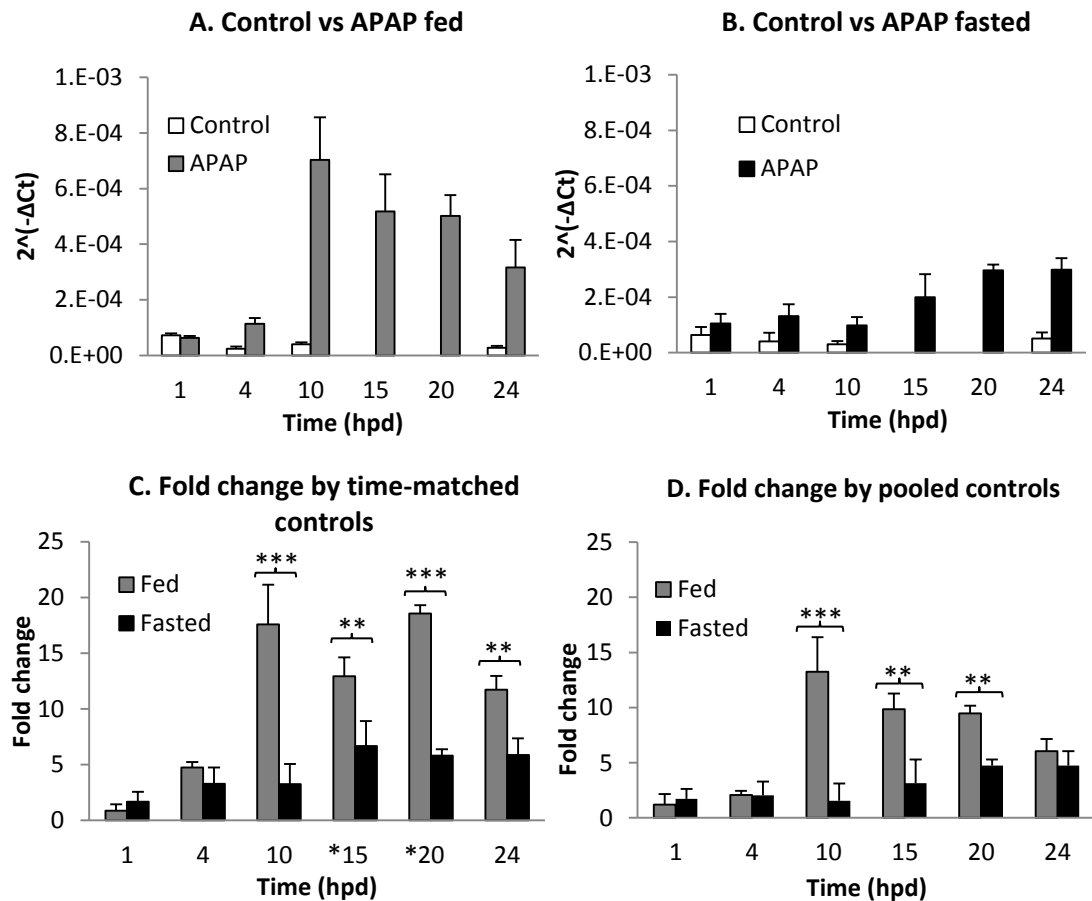


Figure 3.2.21. Hepatic NF- κ B transcription in control and APAP dosed CD-1 mice. Hepatic NF- κ B mRNA levels in fed (A) and fasted (B) were calculated using the delta Ct value, $2^{-\Delta Ct}$. NF- κ B mRNA levels in fed and fasted (C) were compared using the comparative Ct values, assessing the fold change relative to respective time matched control mice, except *15 (relative to 10 h post saline) and *20 hpd (relative to 24 h post saline). Hepatic mRNA levels are also calculated using the comparative Ct values, assessing the fold change relative to pooled control animals (D). Data is given as mean \pm SD (4 to 6 animals per group). *** $P < 0.005$, ** $P < 0.01$ and * $P < 0.05$.

3.2.8.2 Hepatic cyclin-D1 transcription

Hepatic cyclin-D1 transcription was also assessed as an indirect tool to quantify the proliferating hepatocytes, i.e. hepatocytes that are committed to DNA replication.

Similar to NF- κ B, cyclin-D1 transcription was significantly increased at 4, 10 and 24 hpd in fed APAP dosed mice compared to saline dosed **time matched control** mice (Table 6.24). By using the fold change method, the significant increase at 4 hpd (8.6-fold) was confirmed; after that the fold changes were less high, at 10 hpd (4.9-fold) and 15 hpd (3.9-fold), though the difference was still significant. However, at 20 hpd it had increased again and a peak (16-fold increase) was seen which was maintained, though at a slightly lower level, until 24 hpd (12.4-fold).

In fasted mice, significantly increased cyclin-D1 mRNA levels were observed at 15 hpd (6-fold), 20 hpd (4.3-fold) and 24 hpd (7.6-fold) compared to time matched saline dosed mice (Table 6.24). These levels were significantly higher than the 1, 4 and 10 hpd levels, when a less than 3.0-fold change was observed in the APAP dosed animals. Over the time course, a significantly higher transcription level was seen in fed mice at 4 hpd, with no difference to fasted mice at 10 and 15 hpd, but significantly higher levels again at 20 and 24 hpd (Figure 3.2.22C).

When the cyclin-D1 mRNA levels in APAP dosed animals were compared to **pooled control** animal values, the hepatic cyclin-D1 transcription was found to be significantly increased in fed treated animals as early as 4 hpd (8.1-fold), but also at 10 and 15 hpd and even more at 20 hpd before it was slightly lower, but still significantly than in control mice at 24 hpd (Table 6.25). In fasted mice, however, a significant increase was only observed at 15 hpd (9-fold) and 24 hpd (6-fold). A comparison between fed and fasted APAP dosed animals confirmed that the cyclin-D1 mRNA levels in fed mice were significantly higher at 4, 20 and 24 hpd (Table 6.25, Figure 3.2.22D; see also Figure 3.2.22C).

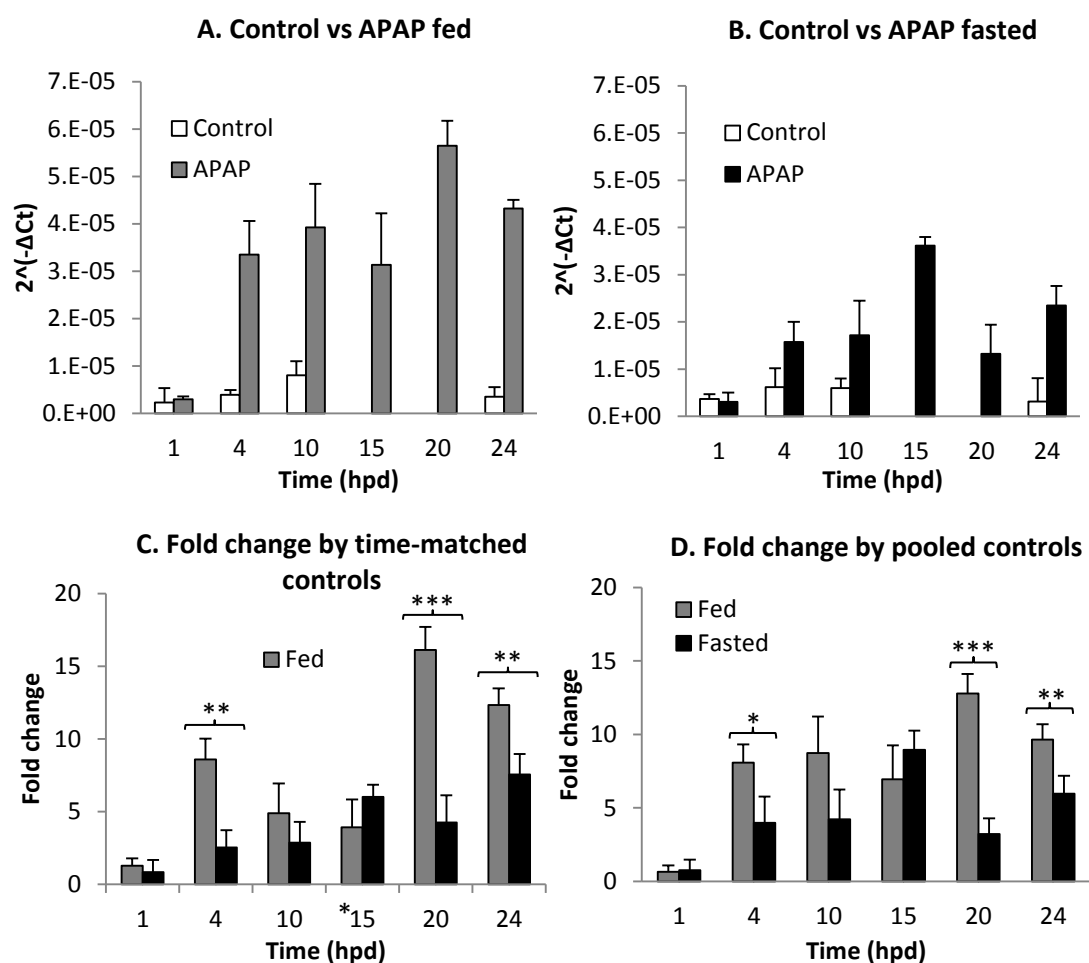


Figure 3.2.22. Hepatic transcription of cyclin-D1 in male CD-1 mice.

Hepatic cyclin-D1 mRNA levels in fed (A) and fasted (B) were determined using the delta Ct value, $2^{-\Delta Ct}$. Cyclin-D1 mRNA levels in fed and fasted (C) were compared using the comparative Ct values, assessing the fold change relative to respective time matched control mice, except *15 (relative to 10 h post saline) and *20 hpd (relative to 24 h post saline). Hepatic mRNA levels are also calculated using the comparative Ct values, assessing the fold change relative to pooled control animals (D). Data is given as mean \pm SD (4 to 6 animals per group). ***P<0.005, **P<0.01 and *P<0.05.

3.2.8.3 Quantification of PCNA-positive, proliferating hepatocytes

PCNA is a nuclear protein that is expressed in late G1 and throughout the S phase of the mitotic cycle, with translocation from the nucleus to the cytoplasm during the G2 and M phase (Kubben et al., 1994). The quantitative analysis of hepatocytes showing PCNA expression in immunohistologically stained sections was used to compare the degree of hepatocyte regeneration in fed and fasted APAP dosed mice. The pooled PCNA values of the saline dosed control animals served as control values, since no relevant differences in the amount of PCNA positive cells were seen throughout the time course (see Chapter 3.1.8.2).

In **fed APAP treated mice**, the amount of PCNA-positive hepatocytes (both nuclear and cytoplasmic staining) was increased in comparison to control animals over the entire time course except at 15 hpd. APAP treatment induced increased PCNA expression in hepatocytes as early as 1 hpd (7.92% vs 7.39% in controls), though the difference was not significant. Interestingly, this was followed by a significant peak at 3 hpd (25.96%), a time when hepatocyte death (represented by the presence of apoptotic cells) and loss was seen. The level was reduced when tested at 5 and 10 hpd, before it was found to have dropped substantially by 15 hpd, when the amount of PCNA-positive cells was lower than in control animals, though not significantly. After that, a progressively higher, significant increase was seen at 20 and 24 hpd (Tables 6.26 and 6.27, Figure 3.2.24A).

In **fasted mice**, the amount of PCNA-positive, proliferating hepatocytes was already increased slightly, but not significantly, at 0.5 hpd (10.42%) and 1 hpd (10.25%) (both groups of mice had been fasted for 16 hours prior to APAP dosing) in comparison to the control mice (5.3%). At 3, 5 and 10 hpd, mice that had been fasted for 24 hours prior to dosing were examined. In these, the PCNA levels were all slightly, but not significantly lower (at approximately 3%) than in the control mice. At the later time points, when 16 hour fasted mice were examined, at 15 hpd (9.3 %), 20 hpd (15.7%) and 24 hpd (13.1%), the number of PCNA-positive proliferating cells was found to be significantly increased in comparison to the control mice (Figure 3.2.24B). Interestingly, when a group of mice that had fasted

for 24 hours prior to APAP dosing was examined at 24 hpd, the amount of PCNA-positive cells was significantly lower than in the mice that had fasted for 16 hours (Tables 6.26 and 6.27, Figure 3.2.24B).

A comparison between fed and fasted CD-1 mice showed that the amount of PCNA expressing cells was significantly higher in fed mice at 3, 5 and 10 hpd (Figures 3.2.24C, Table 6.27). The high amount of PCNA positive cells can be seen in fed but none in fasted mice at 5 hpd (Figure 3.2.23A,B). However, at 24 hpd, the PCNA expressing cells were obvious in both groups (Figure 3.2.23C,D).

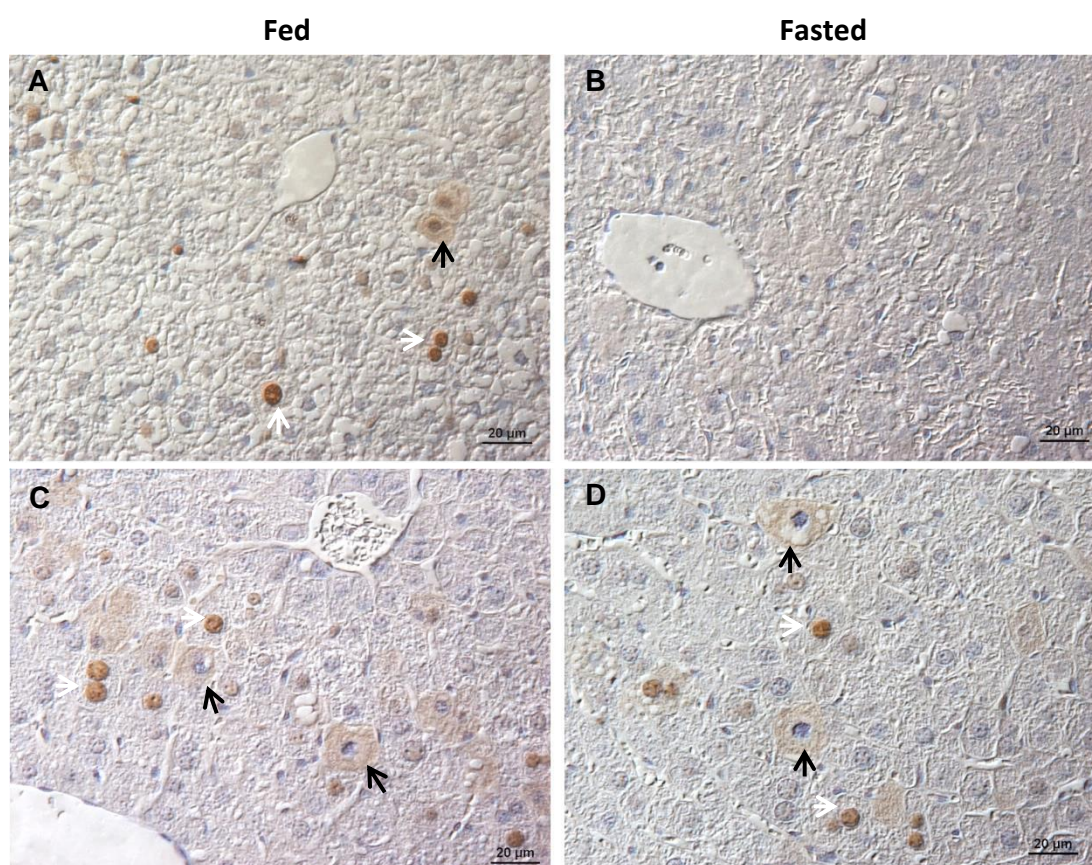


Figure 3.2.23. Immunohistological demonstration of PCNA expression in the liver of fed and fasted APAP dosed male CD-1 mice.

In fed mice, a large number of hepatocytes exhibit nuclear (white arrows), cytoplasmic (black arrows) PCNA expression at 5 hpd (A) and 24 hpd (C). In contrast, fasted mice show no PCNA-positive hepatocytes at 5 hpd (B), but a high amount at 24 hpd (D). PAP method, Papanicolaou's haematoxylin counterstain; Magnification 400x.

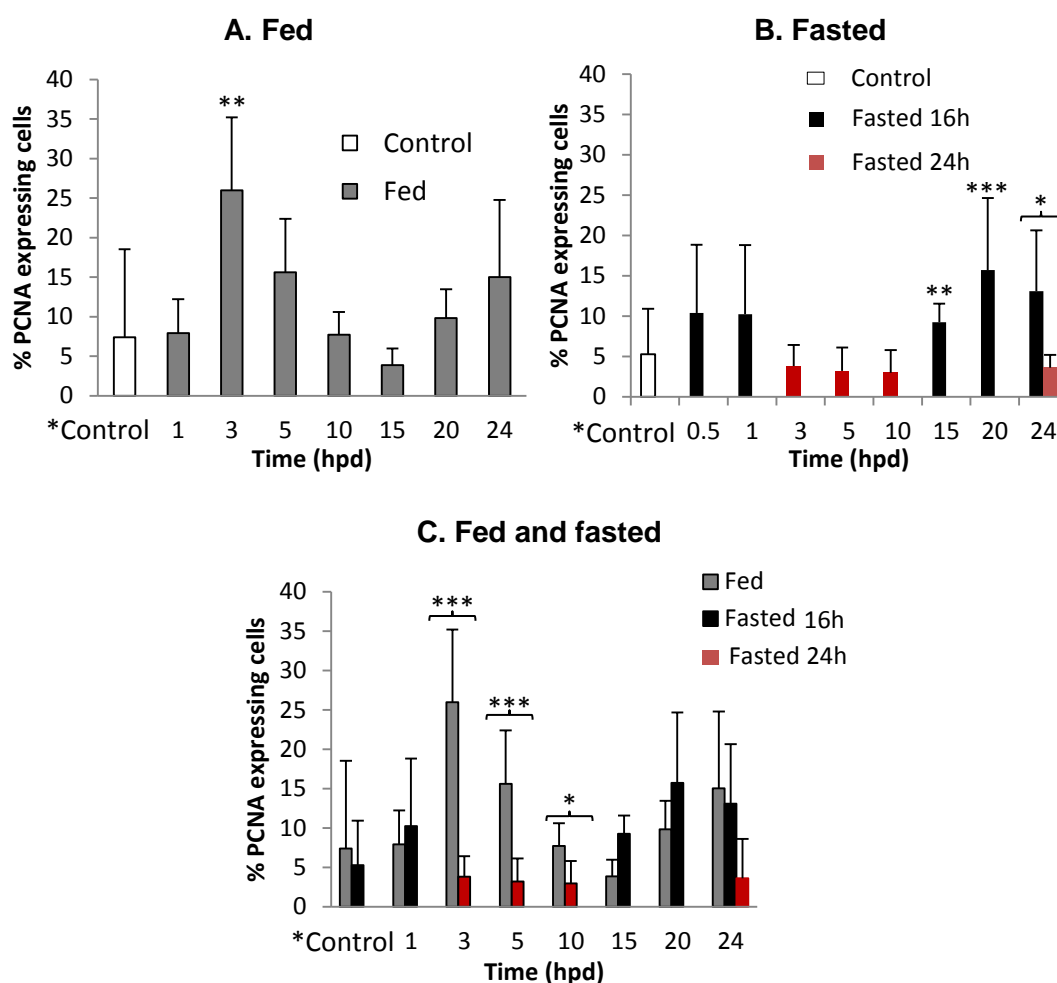


Figure 3.2.24. Assessment of proliferating hepatocytes, based on the expression of proliferating cell nuclear antigen (PCNA).

Quantification (%) of PCNA-positive hepatocytes (nuclear and cytoplasmic expression) in fed (A) and fasted (B) control and APAP dosed male CD-1 mice. The amount was also compared between fed and fasted treated mice (C). *Control – pooled control animals (fed: 0 + 10 h post saline; fasted 0 – 24 h post saline). Data represent means \pm SD (4 to 6 animals per group). ***P<0.005, **P<0.01 and *P<0.05.

Fed mice showed a step-wise increase in the number of cells exhibiting cytoplasmic PCNA expression (i.e. cells immediately prior to or undergoing mitosis), which was significant and at a peak at 5 hpd (1.02%). The amount of positive cells had dropped at 10 hpd and was again significantly increased at 20 hpd (1.04%) and 24 hpd (0.94%) compared to control animals (Table 6.29, Figure 3.2.25A). This was associated with an increase in histologically evident mitotic figures. In contrast, in fasted APAP dosed mice, we observed a rapid and significant increase in hepatocytes showing cytoplasmic PCNA expression compared to control animals as early as 0.5 hpd and until 5 hpd. Similar to fed animals, after a drop at 10 hpd, the

amount of positive cells progressively increased until 24 hpd (Figure 3.2.25B, Table 6.29).

Over the entire time period, the difference between fed and fasted APAP treated mice in the number of hepatocytes with cytoplasmic PCNA expression was not significant, apart from at 10 hpd, when their number was significantly higher in fed mice (0.27%) than in fasted mice (0.06%) (Figure 3.2.25C, Table 6.29).

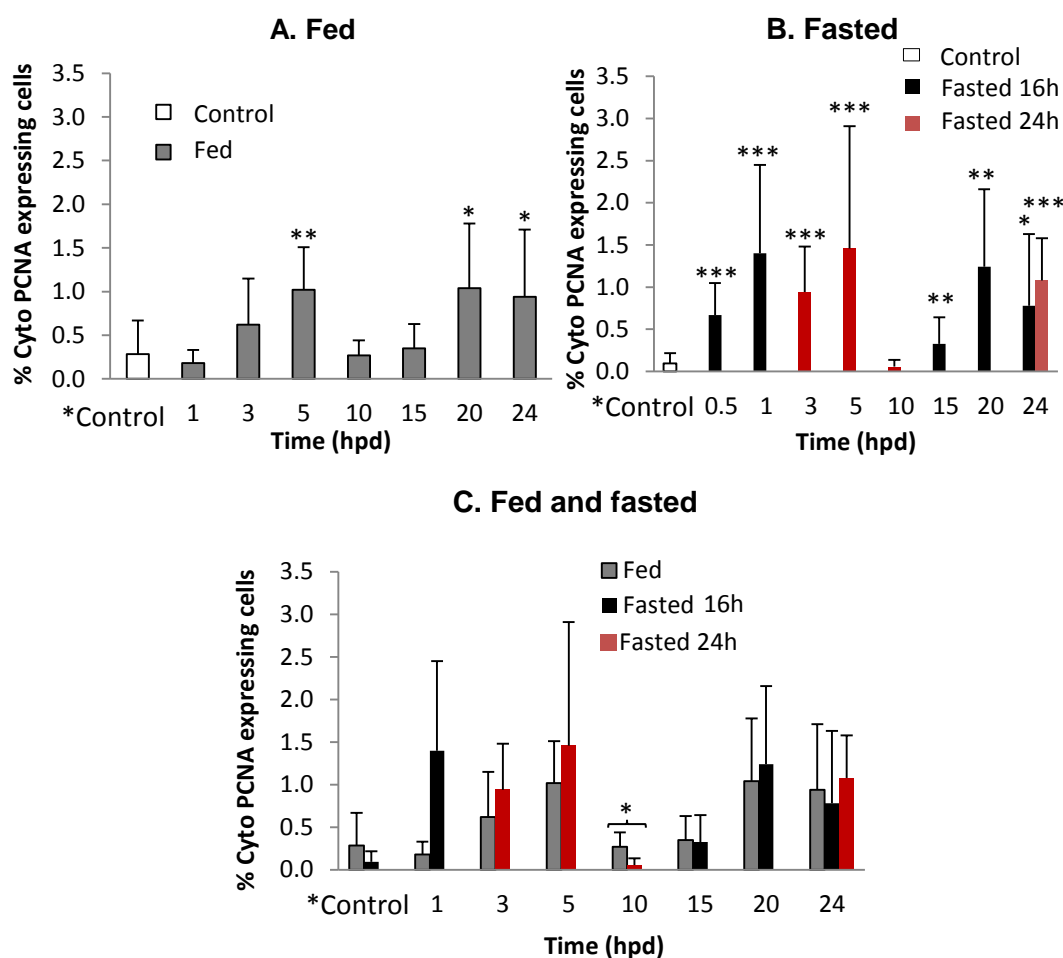


Figure 3.2.25. Assessment of hepatocytes exhibiting cytoplasmic PCNA expression. Quantification (%) of hepatocytes with cytoplasmic PCNA expression in fed (A) and fasted (B) APAP dosed male CD-1 mice. The percentage of positive hepatocytes was also compared between fed and fasted mice (C). *Control – pooled control animals (fed: 0 + 10 h post saline; fasted 0 – 24 h post saline); Cyto – cytoplasmic. Data represent means \pm SD (4 to 5 animals per group). **P<0.01 and *P<0.05.

Assessment of PCNA expression in fed mice over the entire time course shows a first peak of PCNA-positive cells at 3 hpd, indicating that a substantial proportion of remaining cells entered the cell cycle immediately after onset of hepatocellular cell loss. A first peak in the number of cells with cytoplasmic PCNA, i.e. prior to or in mitosis, was seen a bit later, at 5 hpd, subsequently, both numbers declined steadily until 10 hpd, indicating that the first cell cycle, i.e. wave of cell proliferation in response to APAP induced damage was completed. It also indicates that new hepatocytes then entered the cell cycle, leading to an increase in PCNA-positive cells after 15 hpd and a second wave of cell division towards 24 hpd (Table 6.27, Figure 3.2.26).

However, in fasted mice, the first wave of PCNA expression, i.e. cell proliferation is not seen and there is evidence that proliferation only sets in after 10 hpd. Instead, the immediate increase in cytoplasmic PCNA expression, i.e. the number of cells prior to or within mitosis, that is seen between 1 and 5 hpd indicates that cells that were in the cell cycle when injury occurred (their amount would be represented by the number of PCNA-positive cells in control animals) are induced to rapidly complete the cell cycle upon injury (Table 6.29, Figure 3.2.26A,B).

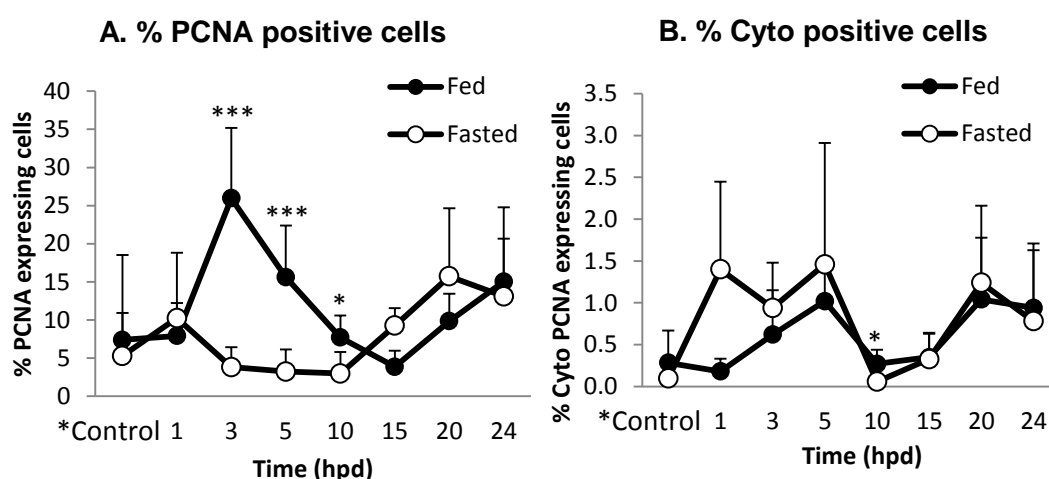


Figure 3.2.26. Assessment of hepatocytes exhibiting PCNA expression.

The amount (%) of PCNA-positive cells (nuclear and cytoplasmic expression) (A) and of hepatocytes with cytoplasmic PCNA expression (B) was compared between fed and fasted APAP-dosed male CD-1 mice. *Control – pooled control animals (fed: 0 + 10 h post saline; fasted 0 – 24 h post saline); Cyto – cytoplasmic. Data represent means \pm SD (4 to 6 animals per group). *** $P < 0.005$, ** $P < 0.01$ and * $P < 0.05$.

3.2.9 Overall assessment of liver regeneration

In this present study, we gathered quantitative data on parameters that provide information on the extent and capacity of the liver to regenerate, i.e. the transcription of TNF- α , IL-6 and IL-10), NF-kB and cyclin-D1 and the extent of PCNA expression to evaluate the effect of fasting on the capacity of liver to regenerate following APAP injury of CD-1 mice. To allow a comparative assessment of the data, the fold changes of each parameter was determined over the entire time course.

In **fed mice**, an initial increment of TNF- α level was followed by an almost progressive increase in the transcription of IL-6 and IL-10, with a peak at 20 and 15 hpd, respectively. By 10 hpd, a peak upregulation of TNF- α was accompanied by increased NF-kB and subsequently cyclin-D1 transcription that reached the highest levels at 20 hpd before all these markers reduced slightly at 24 hpd when complete regeneration appeared to have taken place. However, at this stage these levels were still significantly higher than in control mice. Meanwhile, hepatocytes showed an increased overall and cytoplasmic PCNA expression at 4 hpd and at the end of experiment, 20 and/or 24 hpd (Table 3.2.18).

In contrast, in **fasted mice**, hardly any relevant changes were observed at early time points except for an increase in hepatocytes showing cytoplasmic PCNA expression. At 10 and 15 hpd, TNF- α upregulation was seen accompanied by the production of other markers, including IL-6, IL-10, NF-kB and cyclin-D1 and an increase in hepatocytes exhibiting cytoplasmic PCNA expression prior to its subsequent reduction to levels that were nonetheless still significantly higher than those of control mice. Briefly, although values in fed and fasted mice did not differ much at 4 hpd, fed mice showed higher expression of regeneration markers at 10 hpd which goes alongside the morphological evidence of better liver regeneration in the fed mice (Table 3.2.18, Figure 3.2.27).

Table 3.2.18. Fold change in the levels of TNF- α , IL-6, IL-10, NF-kB, cyclin-D1 and PCNA expression in fed and fasted male CD-1 mice following APAP dosing.

Fed							
Time (hpd)	TNF- α	IL-6	IL-10	NF-kB	Cyclin-D1	PCNA	
						Nuclear + Cyto	Cyto
1	2.76	2.6	3.0	1.2	0.7	1.07	0.64
4	4.4 \dagger	6.0**	3.9*	2.1	8.1** \dagger	2.11** $\#\#$	3.64**
10	7.9**	7.9** $\#\#$	9.0** $\#\#$	13.3***	8.7**	1.04 \dagger	0.96 \dagger
15	2.0	4.5	13.2*** $\#\#$	9.85*** $\#\#$	7.0*	0.52	1.25
20	2.1	15.8*** $\#\#$	10.4*** \dagger	9.5*** $\#\#$	12.8*** $\#\#$	1.33	3.71*
24	1.77	7.6*	8.8**	6.1**	9.6** $\#\#$	2.03*	3.36*
Fasted							
Time (hpd)	TNF- α	IL-6	IL-10	NF-kB	Cyclin-D1	PCNA	
						Nuclear + Cyto	Cyto
1	1.0	1.7	2.6	1.7	0.8	1.94	5.38***
4	2.3	4.7*	1.5	2.1	4.0	0.61	5.62***
10	6.8*	2.2	1.8	1.5	4.2	0.56	0.23
15	18.3*** $\#\#$	4.5	3.9	3.2	9.0***	2.20**	14.92**
20	1.9	5.3*	4.6*	4.7*	3.2	2.97***	4.77**
24	1.5	7.4**	5.2*	4.7*	6.0*	1.58*	3.54***

Statistical significant, ***P<0.005, **P<0.01 and *P<0.05 are seen in the comparison to the pooled control mice; whereas \dagger P<0.05, $\#\#$ P<0.01, and $\#\#\#$ P<0.005 are observed in comparison to fed and fasted APAP dosed CD-1 mice. hpd – hours post dosing; Cyto – cytoplasmic.

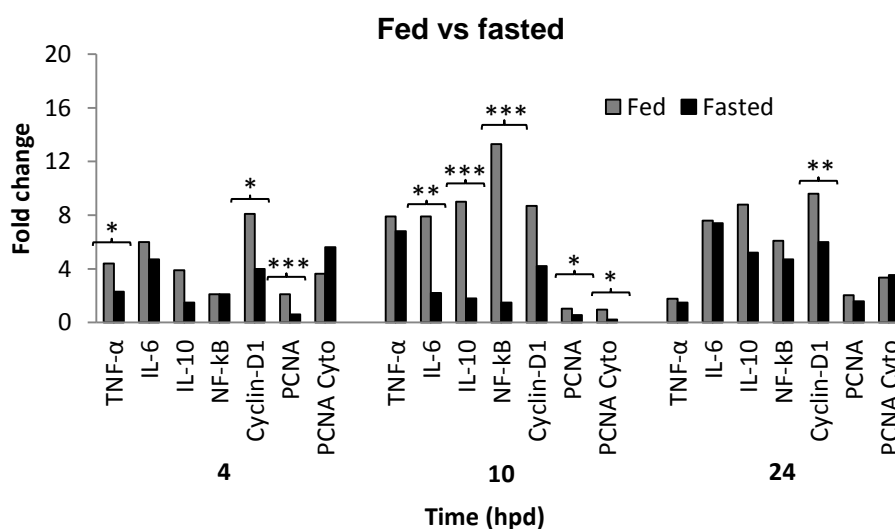


Figure 3.2.27. Assessment of liver regeneration in fed and fasted male CD-1 mice. The levels of hepatic TNF- α , IL-6, IL-10, NF-kB and cyclin-D1 mRNA and PCNA expression were evaluated over 1-24 h in animals that had been fed (A) or fasted (B) prior to APAP administration. A comparison of fed and fasted mice following APAP dosing is shown for each marker (as listed in Table 3.2.18). Fold changes are calculated relative to pooled control mice. Cyto – cytoplasmic. Data represent mean (4 to 6 animals per group). ***P<0.005, **P<0.01 and *P<0.05.

3.3 The response of fed and fasted C57BL/6J mice to APAP overdose and comparison to the response of CD-1 mice

To test the response of C57BL/6J mice to APAP, in a similar fashion to the CD-1 mice, male C57BL/6J mice that had been fed ad libitum throughout (fed mice) or had been fasted for 16 hours (fasted mice) received a sublethal dose of APAP or 0.9% saline (control mice) intraperitoneally. The fasted mice were allowed access to food ad libitum immediately after dosing. This approach was taken for two reasons: a) to assess the potential differences in the response of the two groups of mice to APAP overdose with regards to the type and degree of acute liver injury and regeneration, and b) to assess the effect of fasting on the response in the C57BL/6J mice.

None of the animals exhibited clinical signs, all resumed feeding after fasting and/or treatment. Groups of mice were euthanised at different time points between 0 and 36 hpd, and, like in the CD-1 mice, several serum and liver parameters were assessed in order to monitor the hepatic and systemic effect of APAP dosing including serum ALT activity levels, hepatic GSH and ATP levels and the hepatocellular glycogen content as well as histopathological changes of the liver. The inflammatory and proliferative response of hepatocytes was also assessed by measuring the transcription levels of cytokines TNF- α , IL-6 and IL-10, and of the transcription factors NF- κ B and cyclin-D1. The amount of PCNA-positive, proliferating hepatocytes was also assessed.

3.3.1 Hepatic GSH content

In **fed APAP dosed C57BL/6J mice**, GSH levels had significantly dropped as early as 30 minutes after APAP dosing, then showed a slight, but not significant further decrease at 1 hpd and reached the lowest value by 3 hpd. After that, the GSH content increased gradually from 5 to 30 hpd. At 24 hpd, it was still significantly lower than in control animals at the same time of day, while it was significantly higher at 30 hpd, a time of day, when levels were comparatively low in control mice. At 36 hpd, levels were similar to those of control mice (Table 3.3.1, Figure 3.3.1A; see also Chapter 3.1.2 for the circadian control mouse values).

Table 3.3.1. Mean GSH content (nmol/mg) with standard deviation (SD) in **fed** control (saline dosed) and APAP dosed male C57BL/6J mice at different times post dosing, with a comparison to the values obtained in CD-1 mice.

Time (hpd)	C57BL/6J					CD-1		
	ToD dosing	ToD killing	Mean (SD)		p-value control vs APAP	p-value APAP vs APAP	Mean (SD) APAP	p-value vs APAP C57BL/6J
			Control	APAP				
0	10:00	10:00	-	73.57 (2.88)	-	0.5 h: 0.0004 1 h: 0.0001 5 h: 0.0002 10,15 h: 0.0035	28.81 (5.0)	NS
0.5	10:00	10:30	-	31.94 (3.76)	-	5 h: 0.0004 3 h: 0.0006	-	-
1	10:00	11:00	-	25.42 (7.28)	-	3 h: 0.0047	5.30 (3.65)	0.0286 ↓
3	9:00	12:00	-	1.68 (0.85)	-	5 h: 0.003 10 h: 0.0025	-	-
*5	10:00	15:00	83.85 (6.65)	17.78 (8.77)	0.006	20 h: 0.0021	4.95 (0.56)	NS
10	10:00	20:00	40.12 (7.52)	31.28 (6.45)	NS	3 h: 0.0027 5 h: 0.0013	40.28 (0.74)	NS
15	17:00	8:00	46.66 (8.19)	38.00 (2.80)	NS	5 h: 0.0016 20 h: 0.0199	44.32 (12.64)	NS
20	11:00	7:00	53.21 (8.86)	61.30 (11.0)	NS	30 h: 0.0072 10 h: 0.019	35.05 (18.49)	0.0294 ↓
24	10:00	10:00 (+1)	82.26 (5.48)	69.75 (7.86)	0.034	36 h: 0.0457 15 h: 0.0283 5 h: 0.0193	45.47 (10.05)	0.0002 ↓
30	9:00	15:00 (+1)	64.06 (3.03)	99.13 (14.61)	0.014	5 h: 0.0009	-	24 h: 0.0014 ↓
36	7:00	19:00 (+2)	60.46 (4.91)	75.45 (13.25)	NS	15 h: 0.0088	-	24 h: 0.0128 ↓

hpd - hours post dosing; ToD - time of day; SD - standard deviation; NS – not significant; *5 – values of 5 h C57BL/6J was compared to 4 h CD-1 mice.

In comparison to time-matched APAP dosed CD-1 mice, the GSH levels were significantly higher at 1, 20 and 24 hpd in the C57BL/6J mice which were examined at the same time of day (Figure 3.3.1C).

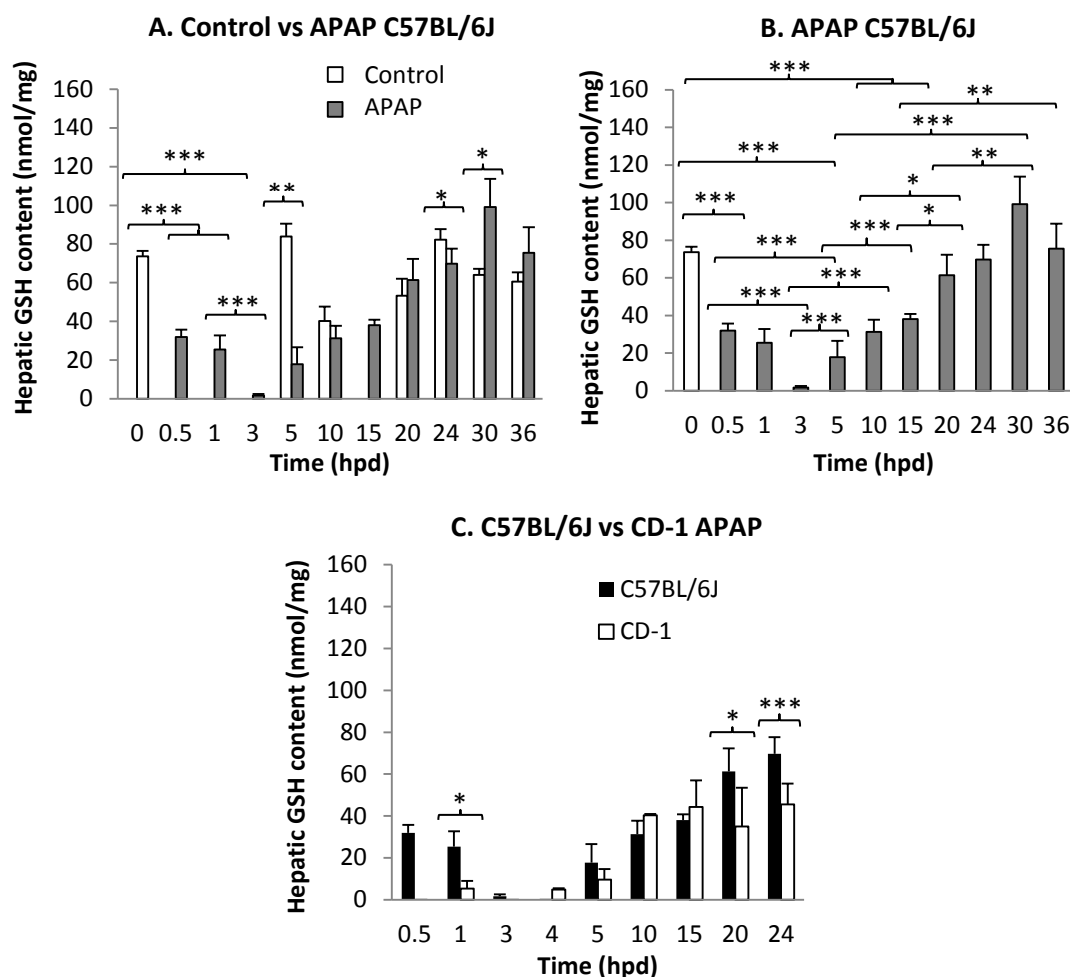


Figure 3.3.1. Hepatic GSH levels in fed male C57BL/6J mice after APAP treatment and comparison to fed CD-1 mice.

Hepatic GSH levels were measured in fed mice at different time points (0-36 hpd) after APAP treatment (530 mg/kg) or 0.9% saline application (controls). (A) Comparison of GSH levels in APAP treated and control mice. (B) Comparison of GSH levels in treated C57BL/6J animals at different time points post treatment. (C) Comparison of GSH levels in fed APAP dosed C57BL/6J and CD-1 mice (as listed in Table 3.3.1). Values were expressed as mean \pm SD (4 to 6 animals per group). ***P<0.005, **P<0.01 and *P<0.05.

APAP treatment of **fasted mice** also led to an immediate drop in GSH levels as early as 30 minutes (Table 3.3.2, Figure 3.3.2A) compared to mice at 0 hpd which exhibited low GSH value due to the preceding fasting (see Chapter 3.1.2). The lowest level was again reached at 3 hpd, after which a gradual increase with until 20

hpd, followed by a slight, possibly time of day-related drop at 24 hpd but still significantly lower than basal levels. After that, it reach a peak at 36 hpd and only had a same levels to controls (Table 3.3.2, Figure 3.3.2A); at both latter time points values did not differ significantly from those of the control animals at the same time of day. Over the time course post dosing, the values in treated animals varied significantly between time points (Table 3.3.2, Figure 3.3.2B).

Table 3.3.2. Mean hepatic GSH content (nmol/mg) with standard deviation (SD) in control and APAP treated **fasted** C57BL/6J at different times post dosing, with p-value to CD-1 APAP dosed mice.

Time (hpd)	C57BL/6J						CD-1		
	ToD dosing	ToD killing	Mean (SD)		p value control vs APAP	p-value APAP vs APAP	p-value fasted vs fed	Mean (SD) APAP	p-value vs APAP C57BL/6J
			Control	APAP					
0	10:00	10:00	-	41.52 (6.85)	-	0.5 h: 0.0002 3 h: 0.0001 36 h: 0.0005	0.034	20.34 (3.23)	NS
0.5	10:00	10:30	-	15.30 (4.83)	-	3 h: 0.0054 24 h: 0.0116 36 h: 0.0001	0.042	[1 h] 13.67 (8.25)	0.5 h: NS 3 h: 0.0134 ↑
3	9:00	12:00	-	2.02 (0.14)	-	15 h: 0.0087 20 h: 0.0256 36 h: 0.0001	NS	-	-
5	10:00	15:00	38.20 (3.09)	4.18 (0.7)	0.036	15 h: 0.0122 36 h: 0.0001	0.034	[4 h] 4.47 (3.57)	5 h: NS
10	10:00	20:00	81.38 (31.63)	13.65 (6.91)	0.0001	36 h: 0.0002	0.017	5.28 (1.24)	NS
15	17:00	8:00	125.29 (5.45)	22.04 (6.47)	0.0008	36 h: 0.0003	0.010	33.98 (16.15)	NS
20	11:00	7:00	75.30 (3.82)	36.49 (16.47)	0.014	0 h: 0.0028 5 h: 0.029	0.049	49.26 (7.82)	NS
24	10:00	10:00 (+1)	38.23 (4.6)	29.94 (3.77)	0.045	0 h: 0.0397 5 h: 0.0044	0.006	[24 h] 50.57 (25.22)	NS
36	7:00	19:00 (+2)	87.98 (2.12)	72.43 (1.38)	NS	20 h: 0.0227	NS		36 h: NS

hpd - hours post dosing; ToD - time of day; SD - standard deviation; NS – not significant; [1 h] – values of CD-1 mice were obtained at 1 hpd; [4 h] – values of CD-1 mice were obtained at 4 hpd; [24 h] - values of CD-1 mice were obtained at 24 hpd.

The comparison of GSH levels in fed and fasted APAP dosed mice which were always dosed and killed at the same time of day showed significantly lower GSH levels in the fasted mice at the early time points (0 and 5 hpd). However, at 10, 15 and 20 hpd, the GSH content was significantly higher in the fasted mice (Table 3.3.2, Figure 3.3.2C). The comparison of GSH levels in fasted, APAP dosed C57BL/6J and CD-1 mice did not show any significant differences (Figure 3.3.2D).

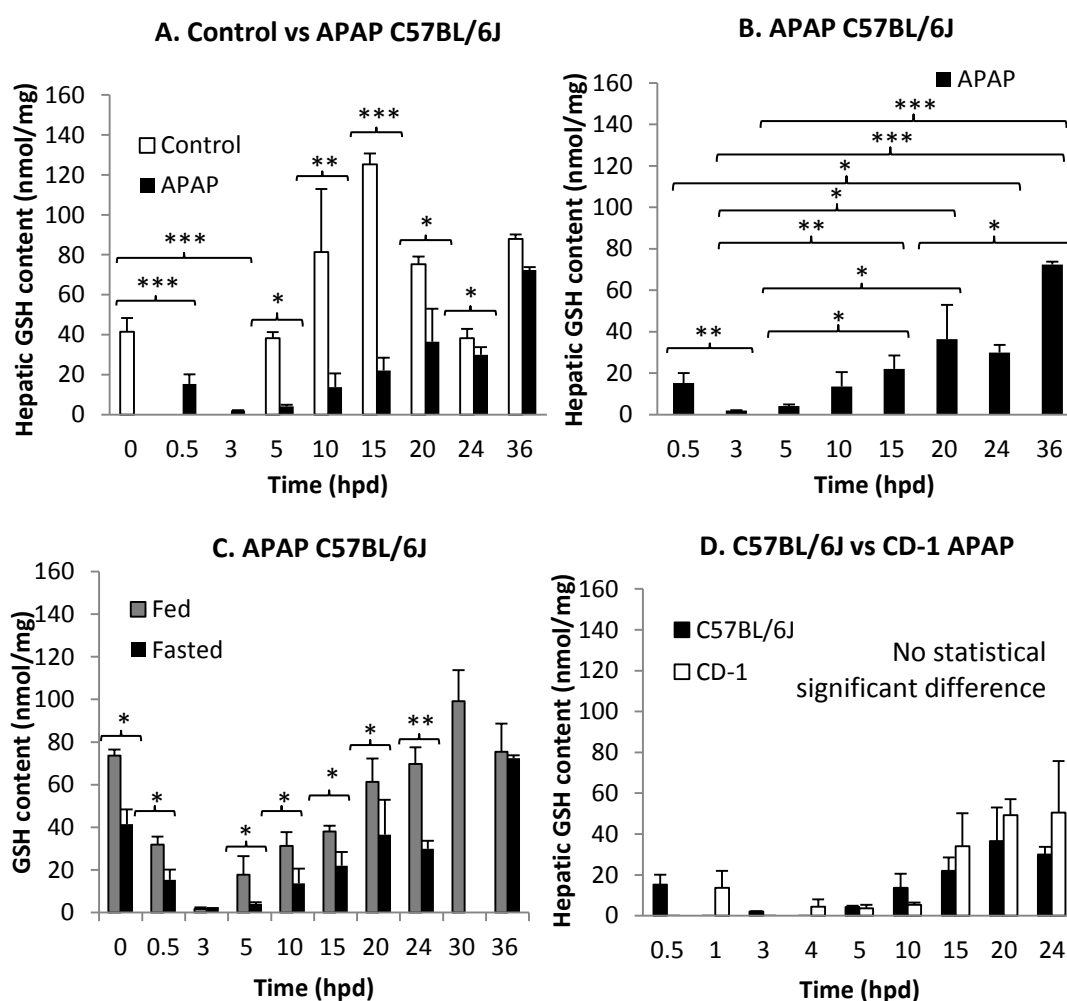


Figure 3.3.2. Hepatic GSH levels in fasted male C57BL/6J after APAP treatment and comparison to fasted CD-1 mice.

Hepatic GSH levels were measured in fasted mice at different time points (0-36 h) after APAP treatment (530 mg/kg) or 0.9% saline application (controls). (A) Comparison of APAP treated and control C57BL/6J mice. (B) Comparison of GSH levels in treated C57BL/6J mice at different time points. (C) Comparison of hepatic GSH content to that of fed APAP treated C57BL/6J mice), and also to fasted APAP treated CD-1 mice (D) (as listed in Table 3.3.2). Values were expressed as mean \pm SD (4 to 6 animals per group). ***P<0.005, **P<0.01 and *P<0.05.

3.3.2 Hepatic ATP content

In APAP treated **fed C57BL/6J mice**, hepatic ATP levels were determined between 5 and 36 hpd compared to pooled control mice as no statistical significant was observed in control mice at any time points (see Chapter 3.1.3). At 5, 10 and 15 hpd, they were significantly lower than those in the control mice (Figure 3.3.3A), reaching levels similar to those of control animals at the same time of day by 20 hpd (Table 3.3.3). Looking at the time course, a significant increase in the ATP levels was seen from 5 to 20 hpd, after which the levels remained stable (Figure 3.3.3B). There was no difference in ATP levels between C57BL/6J and CD-1 mice except at 5 hpd when they were significantly higher in CD-1 mice (Table 3.3.3, Figure 3.3.3C).

Table 3.3.3. Hepatic ATP content (nmol/mg) with standard deviation (SD) in **fed** control (saline) and APAP dosed mice at different time points post dosing.

Time (hpd)	C57BL/6J					CD-1		
	ToD dosing	ToD killing	Mean (SD)		p-value control vs APAP	p-value APAP vs APAP	Mean (SD) APAP	p-value vs APAP C57BL/6J
			Control	APAP				
5	10:00	15:00	-	4.95 (2.47)	-	10 h: 0.0487 15 h: 0.0032	10.5 (2.3)	0.0057 ↑
10	10:00	20:00	28.0 (4.53)	14.03 (3.26)	0.034	15 h: 0.025	18.3 (5.7)	NS
15	17:00	8:00	-	21.10 (3.47)	-	20 h: 0.0151 36 h: 0.0094	-	-
20	11:00	7:00	30.2 (3.25)	29.38 (4.82)	NS	5 h: 0.0015 10 h: 0.0053 15 h: 0.026	-	-
24	10:00	10:00 (+1)	-	26.70 (5.37)	-		35.4 (3.9)	NS
30	9:00	15:00 (+1)	26.75 (2.33)	24.98 (5.25)	NS		-	-
36	7:00	19:00 (+2)	24.48 (5.26)	29.50 (1.97)	NS		-	-
Pooled control	-	-	25.36 (3.84)	-	5 h: 0.0001 10 h: 0.0051 15 h: 0.0253 20, 24, 30, 36 h: NS	-	-	-

hpd - hours post dosing; ToD - time of day; SD - standard deviation; NS – not significant.

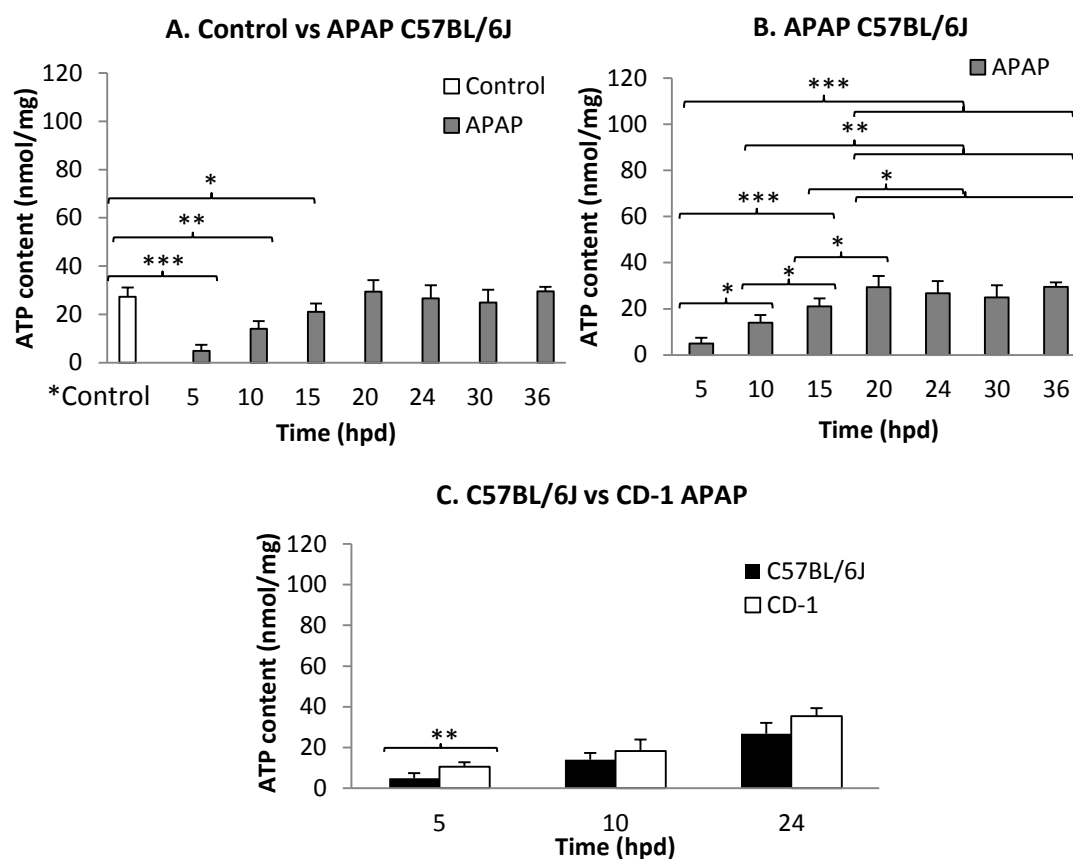


Figure 3.3.3. Hepatic ATP levels in fed male C57BL/6J mice after APAP treatment and comparison to fed CD-1 mice.

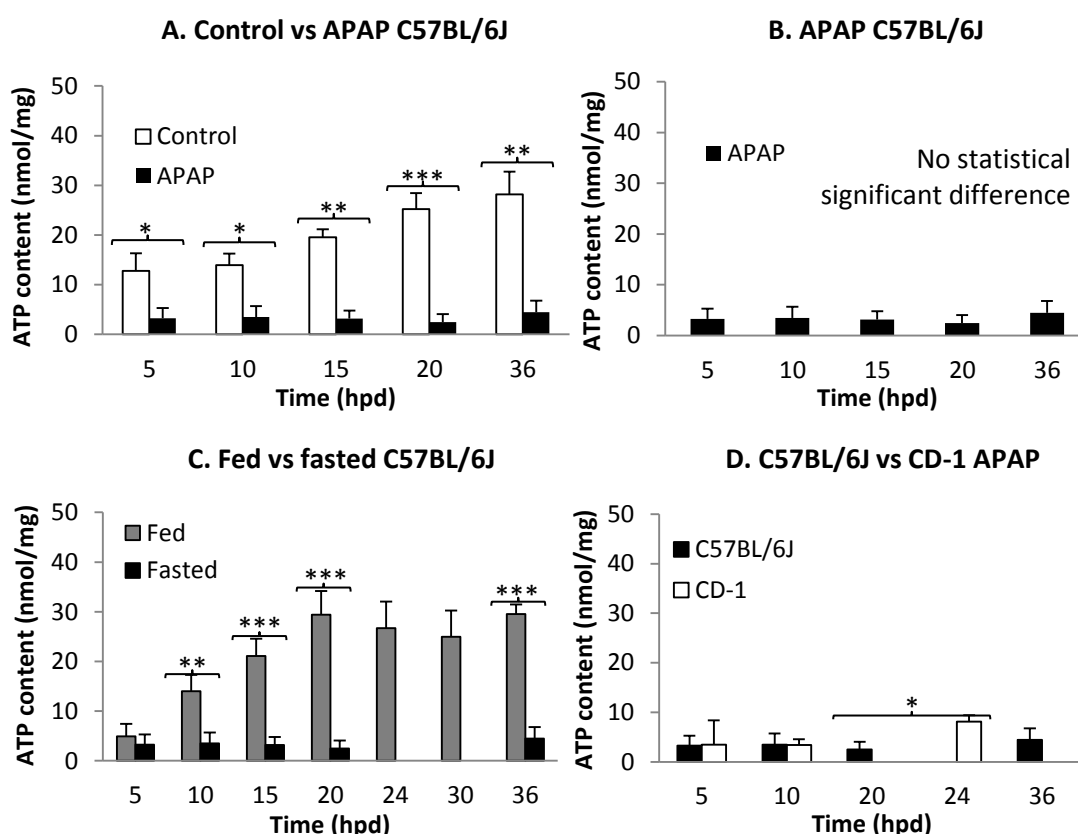
Hepatic ATP levels were measured in fed C57BL/6J mice at different time points (5-36 h) after APAP treatment (530 mg/kg) or 0.9% saline application (controls). (A) Comparison of APAP treated and control C57BL/6J mice. (B) Comparison of ATP levels in treated C57BL/6J animals at different time points post treatment. (C) Comparison of hepatic ATP levels in APAP dosed C57BL/6J and CD-1 mice at 5, 10 and 24 hpd (as listed in Table 3.3.3). *Control - pooled control values. Values were expressed as mean \pm SD (4 to 6 animals per group). *** $P < 0.005$, ** $P < 0.01$ and * $P < 0.05$.

In **fasted C57BL/6J mice**, hepatic ATP levels were measured between 5 and 36 hpd, the latter being the time point when the values returned to those of control mice in the fed APAP dosed group. After APAP dosing, ATP levels in fasted mice remained very low over the entirely time period and were significantly lower than in the respective time-matched control mice (Table 3.3.4, Figure 3.3.4A), remaining at the same very low level throughout (Figure 3.3.4B). There was a significant difference between ATP levels in fed and fasted C57BL/6J mice, as the ATP levels in the fed mice had rapidly recovered post APAP insult (Figure 3.3.4C). For a comparison to CD-1 mice, only a few values were available. These indicate that the liver of fasted CD-1 mice regains ATP faster than the liver of C57BL/6J mice (Figure 3.3.4D).

Table 3.3.4. Hepatic ATP content (nmol/mg) with standard deviation (SD) in **fasted** control (saline) and APAP dosed C57BL/6J mice at different times post dosing (10-36 hpd).

Time (hpd)	C57BL/6J					CD-1			
	ToD dosing	ToD killing	Mean (SD)		p-value control vs APAP	p-value vs APAP fasted	p-value fasted vs fed	Mean (SD) APAP	p-value vs APAP C57BL/6J
			Control	APAP					
5	10:00	15:00	12.8 (3.5)	3.27 (2.03)	0.0389	NS at any time point	NS	3.5 (4.9)	NS
10	10:00	20:00	13.95 (2.33)	3.48 (2.23)	0.0405		0.0067	3.4 (1.2)	NS
15	17:00	8:00	19.55 (1.63)	3.18 (1.60)	0.0079		0.0042	-	-
20	11:00	7:00	25.2 (3.25)	2.48 (1.59)	0.0023		0.0038	[24 h] 8.1 (1.3)	20 h: 0.010 ↑
36	7:00	19:00 (+2)	28.15 (4.60)	4.48 (2.31)	0.0056		0.0025		36 h: NS

hpd - hours post dosing; ToD - time of day; SD - standard deviation; NS – not significant; [24 h] – values of CD-1 mice were obtained at 24 hpd.

**Figure 3.3.4.** Hepatic ATP levels in fasted male C57BL/6J mice after APAP treatment and comparison to CD-1 mice.

Hepatic ATP levels were measured in fasted C57BL/6J mice at different time points (10-36 h) after APAP treatment (530 mg/kg) or 0.9% saline application (controls). (A) Comparison of APAP dosed and control mice. (B) Comparison of ATP levels in APAP treated C57BL/6J mice at different time points. (C) Hepatic ATP levels in fed and fasted APAP dosed C57BL/6J mice. (D) Comparison of ATP levels in fasted APAP dosed C57BL/6J and CD-1 mice. Values were expressed as mean±SD (4 to 6 animals per group). ***P<0.005, **P<0.01 and *P<0.05.

3.3.3 Hepatic GSH and ATP levels

Similar to CD-1 mice (see Chapter 3.2.3), the fold changes in hepatic GSH and ATP levels were assessed in APAP dosed C57BL/6J mice and subsequently compared to those in APAP dosed CD-1 mice. APAP treatment of **fed C57BL/6J mice** resulted in a drop in hepatic GSH and ATP levels, with a similar fold change between 5 and 15 hpd. At 20 and 24 hpd, levels had returned to levels close to those of control mice. At 30 hpd, while ATP levels were still low, the GSH levels were significantly higher than in controls (see also Figure 3.3.1A); by 36 hpd, both ATP and GSH levels were higher than in control animals (Table 3.3.5, Figure 3.3.5A). A comparison with fed CD-1 mice showed that at 10 hpd the GSH fold change was significantly higher in the CD-1 than in the C57BL/6J mice, while the ATP content was at a similar level in both strains (Figure 3.3.5B). However, at 24 hpd, ATP and GSH levels in both strains were similar to each other and to the time matched saline control mice (Table 3.3.5, Figure 3.3.5B).

In **fasted APAP dosed C57BL/6J mice**, both GSH and ATP levels did not recover within 30 hours post dosing, though the GSH levels increased but ATP level was still significantly depleted (Figure 3.3.5C). The tendency was similar in fasted CD-1 mice, when the values at 10 hpd and the GSH values at 24 hpd were compared. Interestingly, at the end of the experiment, i.e. at 24 hpd in CD-1 mice and at 36 hpd in C57BL/6J mice, the value was still lower in the C57BL/6J mice, though without statistical significance (Table 3.3.5, Figure 3.3.5D).

Table 3.3.5. Comparison of GSH and ATP levels in fed and fasted male C57BL/6J mice after APAP overdose and comparison to CD-1 mice.

Time (hpd)	Fed								
	GSH				ATP				p-value GSH vs ATP C57BL/6J
	Control	APAP	Fold change	p-value vs CD-1	Control	APAP	Fold change	p-value vs CD-1	
5	83.85	17.78	0.21	-	-	4.95	(0.18)	-	NS
10	40.12	31.28	0.78	0.01	28.00	14.03	0.50	NS	NS
15	46.66	38.00	0.81	-	29.00	21.10	0.75	-	NS
20	53.21	61.30	1.15	-	30.20	29.38	0.97	-	NS
24	82.26	69.75	0.85	NS	28.00	26.70	1.00	NS	NS
30	64.06	99.13	1.55	-	26.75	24.98	0.93	-	NS
36	60.46	75.45	1.25	-	24.48	29.50	1.21	-	NS
Time (hpd)	Fasted								
	GSH				ATP				p-value GSH vs ATP C57BL/6J
	Control	APAP	Fold change	p-value vs CD-1	Control	APAP	Fold change	p-value vs CD-1	
10	81.38	13.65	0.17	NS	13.95	3.48	0.25	NS	NS
15	125.3	22.04	0.18	-	19.55	3.18	0.16	-	NS
20	75.30	36.49	0.48	-	25.20	2.48	0.10	-	NS
24	38.23	29.94	0.78	NS	-	-	-	-	-
36	87.98	72.43	0.82	-	28.15	4.48	0.16	(24h) NS	0.027

(24 h) - 24 hpd values of CD-1 mice were compared with the 36 hpd values of fasted C57BL/6J mice; (0.18) - fold change ATP obtained at 5 h post APAP was normalised to 10 h post saline.

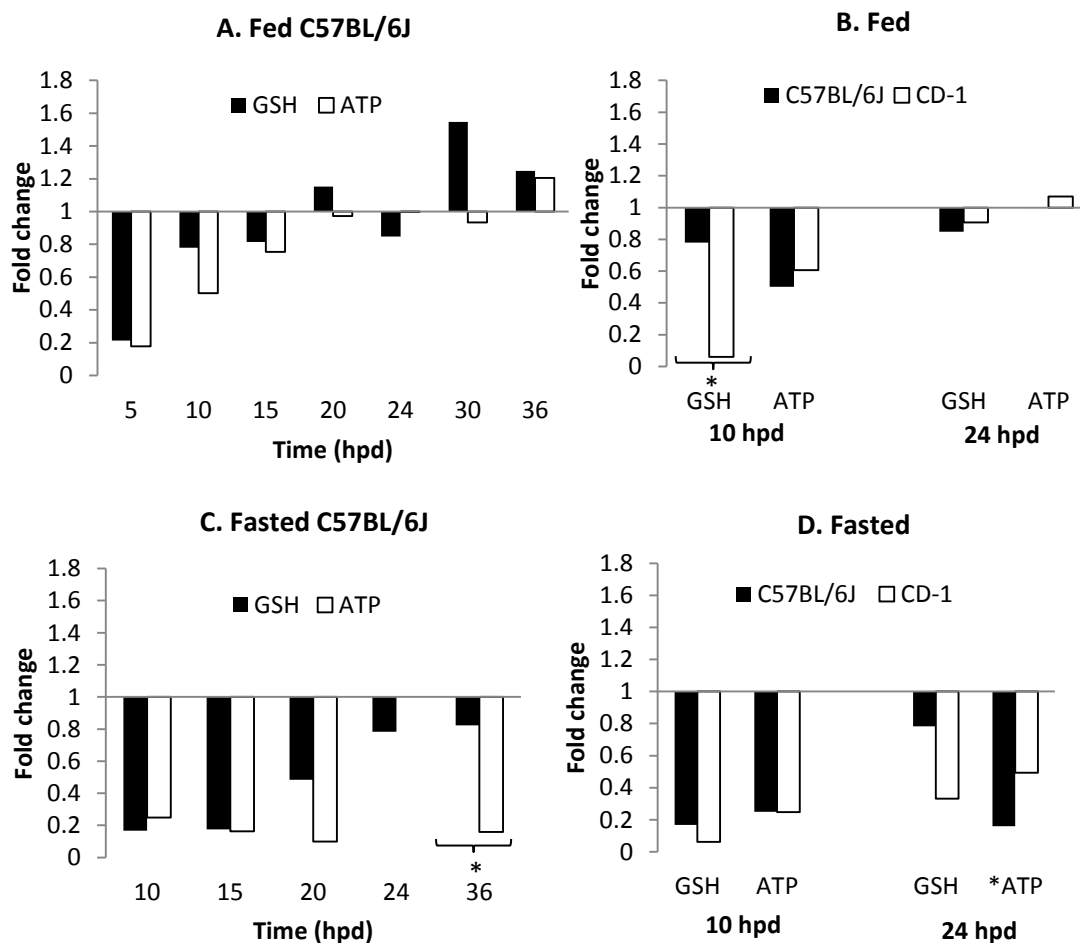


Figure 3.3.5. Hepatic ATP and GSH levels in male C57BL/6J mice after APAP overdose and comparison to CD-1 mice.

The fold change in hepatic ATP and GSH levels was determined in male C57BL/6J mice after APAP treatment of fed (A) and fasted (C) mice. The fold changes were also compared between C57BL/6J and CD-1 mice at 10 and 24 hpd in animals that had been fed (B) or fasted (D) prior to dosing (as listed in Table 3.3.5). The fold changes in APAP dosed mice were normalised to control mice. *ATP – ATP values obtained at 36 hpd in C57BL/6J mice and at 24 hpd in CD-1 mice. Values were expressed as mean (4 to 6 animals per group). *** $P < 0.005$, ** $P < 0.01$ and * $P < 0.05$. Fold change = 1 : Levels in saline dosed control mice.

3.3.4 Serum ALT levels

Following APAP dosing, **fed C57BL/6J mice** exhibited significantly elevated ALT throughout the entire examination period, between 3 and 36 hpd (Table 3.3.6 and Figure 3.3.6A). Looking at the time course it becomes obvious that after the initial raise in serum ALT towards 3 hpd, the increase towards 5 hpd was again significant. Between 5 and 15 hpd, values remained at a similar level, after which they increased further and reached a peak at 24 hpd, followed by a significant drop towards 36 hpd (Figure 3.3.6B). ALT values were available from CD-1 mice at 5 and 24 hpd, these were very similar to those of the C57BL/6J mice (Figure 3.3.6C).

Table 3.3.6. Mean serum ALT levels (U/L) with standard deviation (SD) in **fed** control (saline) and APAP dosed male C57BL/6J mice at different times post dosing, including comparison to values in CD-1 mice.

Time (hpd)	ToD dosing	ToD killing	Control		APAP		p-value control vs APAP	p-value APAP vs APAP	p-value vs APAP CD-1
			Mean	SD	Mean	SD			
3	9:00	12:00	-	-	1004.74	252.56	-	5 h: 0.0286	-
5	10:00	15:00	14.92	10.41	2056.82	214.47	0.012	20 h: 0.0233 24 h: 0.0024	NS
10	10:00	20:00	29.75	8.66	2066.58	79.56	0.016	-	-
15	17:00	8:00	22.88	6.7	1964.11	246.04	0.022	24 h: 0.0024	-
20	11:00	7:00	28.00	7.24	2598.31	217.24	0.008	-	-
24	10:00	10:00 (+1)	8.49	7.28	2709.49	231.65	0.004	36 h: 0.0491	NS
36	7:00	19:00 (+2)	15.78	7.24	1763.94	539.04	0.042	-	-
Pooled control	-	-	18.86	7.54	-	-	3 h: 0.0059 5 h: 0.0033 10 h: 0.0002 15 h: 0.0031 20 h: 0.0006 24 h: 0.0001 36 h: 0.0078	-	-

hpd - hours post dosing; ToD - time of day; SD - standard deviation; NS – not significant; Pooled control – average of all values from control animals at all different time points.

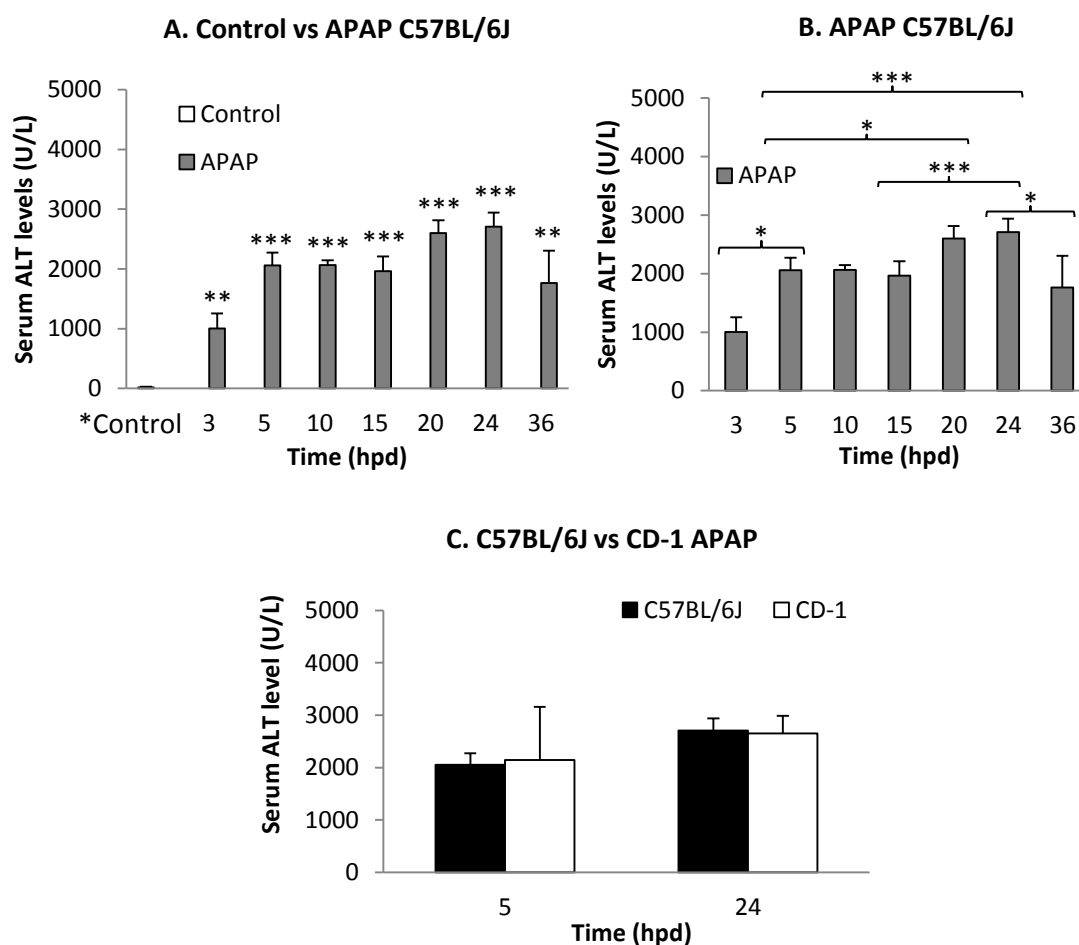


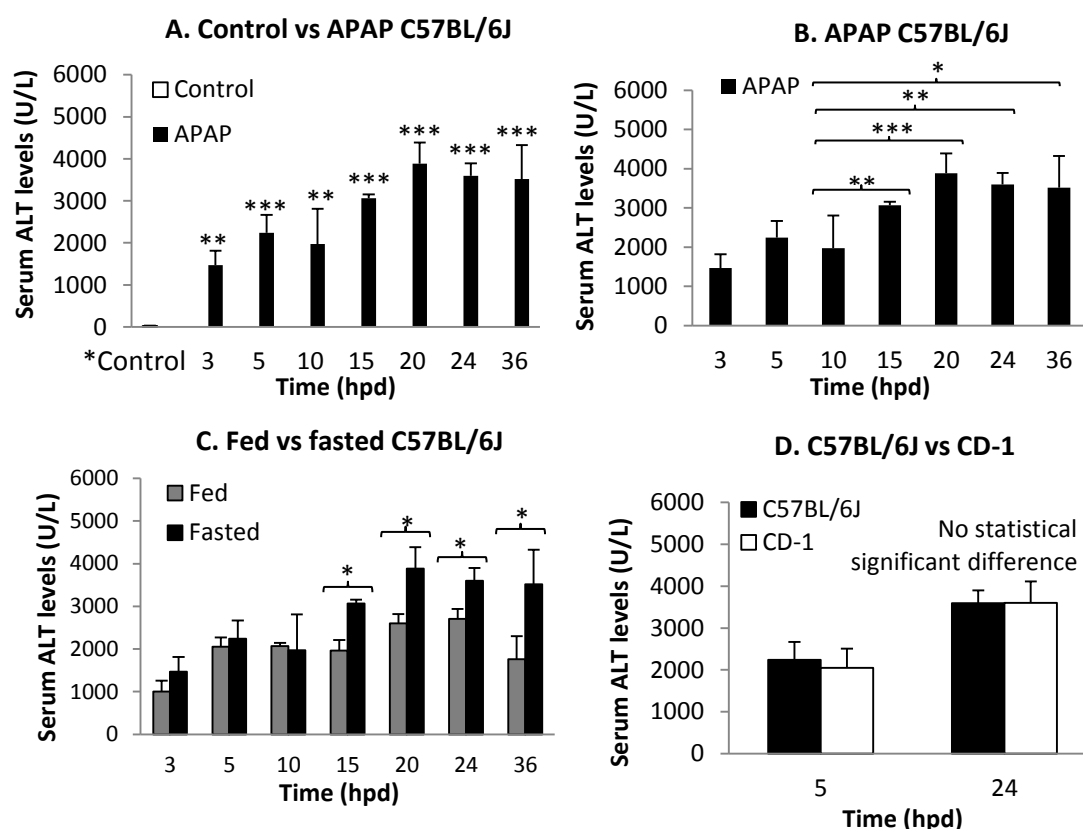
Figure 3.3.6. Serum ALT levels in male fed C57BL/6J mice after APAP overdose and comparison to fed CD-1 mice.

The serum ALT levels in fed C57BL/6J mice were assessed over 3-36 h in 0.9% saline (control) and APAP (530 mg/kg) dosed mice. (A) Comparison of APAP dosed and control mice. (B) Comparison of ALT levels in treated C57BL/6J animals over time and (C) comparison to fed APAP treated CD-1 mice (as listed in Table 3.3.6). *Control – pooled control values. Values were expressed as mean \pm SD (4 to 6 animals per group). *** P <0.005, ** P <0.01 and * P <0.05.

In **fasted C57BL/6J mice**, a similar increase in ALT activity was observed after APAP dosing, with significantly elevated levels throughout the entire examination period, i.e. between 3 and 36 hpd (Figure 3.3.7A). Early after APAP dosing, at 3, 5 and 10 hpd, levels in fasted mice were similar to those in fed mice; however, at the later time points, they were significantly higher than in the fed mice and had only dropped minimally towards 36 hpd (Table 3.3.7 and Figure 3.3.7B,C). Again, ALT values in fasted CD-1 mice which were available at 5 and 24 hpd, were very similar to those of the C57BL/6J mice (Figure 3.3.7D).

Table 3.3.7. Mean serum ALT levels (U/L) with standard deviation (SD) in **fasted** control (saline) and APAP dosed C57BL/6J mice and comparison to CD-1 mice.

Time (hpd)	Control		APAP		p-value control vs APAP	p-value APAP vs APAP	p-value fasted vs fed APAP	p-value vs APAP CD-1
	Mean	SD	Mean	SD				
3	-	-	1470.74	345.02	-	5 h: NS	NS	-
5	11.67	7.16	2240.83	425.04	0.0057	24 h: 0.0133	NS	NS
10	36.03	8.66	1972.96	836.01	0.0238	15 h: 0.0087 36 h: 0.0288	NS	-
15	29.85	7.6	3064.23	91.18	0.0018	24 h: NS	NS	-
20	24.59	2.9	3886.12	501.14	0.0047	10 h: 0.0039	0.0494	-
24	12.39	6.81	3597.04	299.46	0.0016	10 h: 0.0064	0.0386	NS
36	26.00	5.61	3518.25	805.54	0.0006	5 h: NS	0.0462	-
Pooled control	22.82	6.90	-	-	3 h: 0.0083 5 h: 0.0026 10 h: 0.0059 15 h: 0.0019 20 h: 0.0004 24 h: 0.0001 36 h: 0.0009	-	-	-

**Figure 3.3.7.** Serum ALT levels in fasted C57BL/6J mice after APAP overdose and comparison to fasted CD-1 mice.

The serum ALT levels in fasted C57BL/6J mice were assessed over 3-36 h in 0.9% saline (control) and APAP (530 mg/kg) dosed mice. (A) Comparison of APAP treated and control mice. (B) Comparison of ALT levels in treated C57BL/6J mice over time and (C) comparison to fed mice. (D) Comparison of serum ALT levels to fasted APAP dosed CD-1 mice (as listed in Table 3.3.7). *Control – pooled control values. Values were expressed as mean±SD (4 to 6 animals per group). ***P<0.005, **P<0.01 and *P<0.05.

3.3.5 Histopathological features and glycogen content of the liver

Similar to CD-1 mice (see Chapter 3.2.5), the effect of APAP dosing in C57BL/6J mice was also assessed histologically, using HE-stained liver sections and those stained with the PAS reaction. All of animals had been dosed in the morning (10:00), except 15 hpd (17:00). Detailed descriptions of the histological findings and DILI scores of all animals were prepared by Fazila Hamid and Prof Anja Kipar independently and in a blinded fashion. After a consultative discussion, final descriptions and scores were prepared (fed mice: Tables 3.3.8 and 6.31; fasted mice: Tables 3.3.10 and 6.32).

In **fed C57BL/6J mice**, at 0, 0.5 and 1 hpd, no histopathological changes and diffuse hepatocellular glycogen accumulation were observed. At 3 hpd, centrilobular cell loss with no or very few apoptotic hepatocytes was seen (Figure 3.3.10A). The presence of apoptotic cells was confirmed by their cleaved caspase-3 expression. Alongside this, the presence of several neutrophils in centrilobular areas suggested recruitment of inflammatory cells. In these areas, some hepatocytes appeared slightly swollen and vacuolated (early hydropic degeneration) and the hepatocellular glycogen had been lost.

Mice that had been killed at 5 hpd showed more extensive centrilobular cell loss than those at 3 hpd while there were no or only very occasional cleaved caspase-3 positive apoptotic cells, and marked neutrophil infiltration with erythrocytes filling up the areas of hepatocytes loss; no hepatocellular glycogen was seen in the affected zone 3. At 10 hpd, ongoing cell damage with morphological features of apoptosis was still present, but to a lesser extent, and few mitotic figures were seen in hepatocytes. Mice that had been killed at 15 hpd showed more centrilobular cell loss and PAS-negative centrilobular hepatocytes than at 10 hpd; however, these mice had been dosed in the late afternoon (17:00) whereas all other mice had been dosed between 7:00 to 11:00 in the morning. At 20 hpd, ongoing centrilobular cell death was seen, as reflected by the presence of occasional apoptotic hepatocytes similarly as morphological observed at 24 hpd (Figure 3.3.11A). At this stage, diffuse hepatocellular glycogen accumulation was seen, sparing the innermost centrilobular cell layers. Hydropic degeneration was seen in hepatocytes surrounding the

affected area. At 30 and 36 hpd, the innermost centrilobular cell layer exhibited coagulative necrosis and a few apoptotic cells as well as a few infiltrating neutrophils, but almost complete glycogen deposition (Table 3.3.8, Figure 3.3.14).

Table 3.3.8. Histological findings in APAP dosed **fed** C57BL/6J mice (time course). The histological findings are summarised for each group of animals examined at each time point and the range of DILI grading scores of each group (4 to 6 animals per group). CL – centrilobular; HD - hydropic degeneration, hpc - hepatocytes, CN - coagulative necrosis, NL – neutrophilic leukocytes; CC3 – Cleaved caspase-3; haemorrhage – erythrocytes filling up the space in areas of hepatocyte loss.

Time (hpd)	Score range [mean]	Histological findings
0	0	NHAIR; PAS: Diffuse glycogen
0.5	0	NHAIR; PAS: Diffuse glycogen
1	0	NHAIR; PAS: Diffuse glycogen
3	0.5-2 [1.25]	CL hpc loss and haemorrhage with several infiltrating NL; no or very occasional apoptotic hpc and HD of remaining cells in affected CL areas; PAS: loss of glycogen in hpc surrounding affected areas; CC3: +
5	1-4 [2.75]	More extensive CL hpc loss with haemorrhage and marked NL infiltration; PAS: loss of glycogen in hpc surrounding affected areas; CC3: +
10	1-2.5 [1.5]	CL hpc loss with moderate NL infiltration; scattered mitotic figures; PAS: no glycogen in 3-4 layers of hpc in affected CL areas
15	1-2.5 [2.17]	CL hpc loss with haemorrhage and moderate NL infiltration at zone 3 and 2; PAS: no glycogen in affected CL areas.
20	0-2.5 [1.3]	CN and HD of remaining CL hpc with evidence of apoptotic cells and NL infiltration; PAS: no glycogen in hpc in affected CL areas.
24	1-1.5 [1.15]	CN and HD of remaining CL hpc with mild NL infiltration; PAS: no glycogen in 2-3 CL hpc layers; CC3: +/++
30	0-1.5 [0.75]	2-3 innermost CL hpc layers with CN and few infiltrating NL; PAS: no glycogen in CL hpc layers; CC3: +
36	0-1.5 [0.8]	CN of 1-2 innermost CL hpc layers with some apoptotic cells; PAS: diffuse glycogen in hpc surrounding the CN layers; CC3: +

A summary of the findings with the range of scores and average scores is recorded over the time course in Table 3.3.9 and Figure 3.3.8. The earliest histological damage was seen at 3 hpd. At 5 hpd, the most severe changes were observed, with a drop thereafter (Figure 3.3.8A), except at 15 hpd, which was the group of animals that had been dosed at 17:00.

Although DILI scores in C57BL/6J mice were always higher than in CD-1 mice, statistically significant differences were only identified at 24 hpd; the differences were also significant at 30 and 36 hpd, in which liver damage was still present in fed C57BL/6J mice compared to CD-1 mice at 24 hpd (0 score) where complete

regeneration was observed (Figure 3.3.8B). In the C57BL/6J mice, ongoing cell damage was represented by the presence of cleaved caspase-3 positive apoptotic cells and cells with morphological features of coagulative necrosis in the innermost centrilobular hepatocyte layers, surrounded by a layer of cells with hydropic degeneration; this was accompanied by a lack of hepatocellular glycogen accumulation in affected areas (Figure 3.3.12A,C,E). In the fed CD-1 mice, the histological features suggested complete regeneration and complete glycogen restitution at 24 hpd (Figure 3.3.12B,D,F), whereas the pictures in the fed C57BL/6J mice was similar to that seen in the fasted CD-1 at this time point (see also Figure 3.2.13).

Table 3.3.9. Histological DILI scores in APAP dosed **fed** C57BL/6J mice (time course) and comparison to CD-1 mice.

Time (hpd)	C57BL/6J					CD-1		
	ToD dosing	ToD killing	n	Score range [mean]	SD	p-value APAP fed	Mean score	p-value to fed APAP to C57BL/6J
0	10:00	10:00	4	0	0	Score 0 vs: 3 h: 0.0286 5 h: 0.0206 20 h: 0.0028 24 h: 0.023 36 h: 0.0286	0	NS
0.5	10:00	10:30	4	0	0		0	NS
1	10:00	11:00	4	0	0		0	NS
3	9:00	12:00	4	0.5-2 [1.25]	0.58	-	1.25	NS
5	10:00	15:00	6	1-4 [2.75]	1.22	24 h: 0.0405	2.2	NS
10	10:00	20:00	9	1-2.5 [1.5]	0.5	-	1	NS
15	17:00	8:00	8	1-2.5 [2.17]	0.58	20 h: 0.0273	1.125	NS
20	11:00	7:00	9	0-2.5 [1.3]	0.61	24 h: 0.0357	0.65	NS
24	10:00	10:00 (+1)	5	1-1.5 [1.15]	0.47	15 h: 0.0263	0	0.0231
30	9:00	15:00 (+1)	4	0-1.5 [0.75]	0.61	5 h: 0.0383	-	~ 0.0447
36	7:00	19:00 (+2)	4	0-1.5 [0.8]	0.13	15 h: 0.0471 5 h: 0.0435	-	~ 0.0095

hpd – hours post dosing; ToD – time of days; n - number of animals used per group; SD – standard deviation; NS – not significant; ~ - p-value of histological score at 30 or 36 hpd in C57BL/6J mice compared to 24 hpd scores in CD-1 mice.

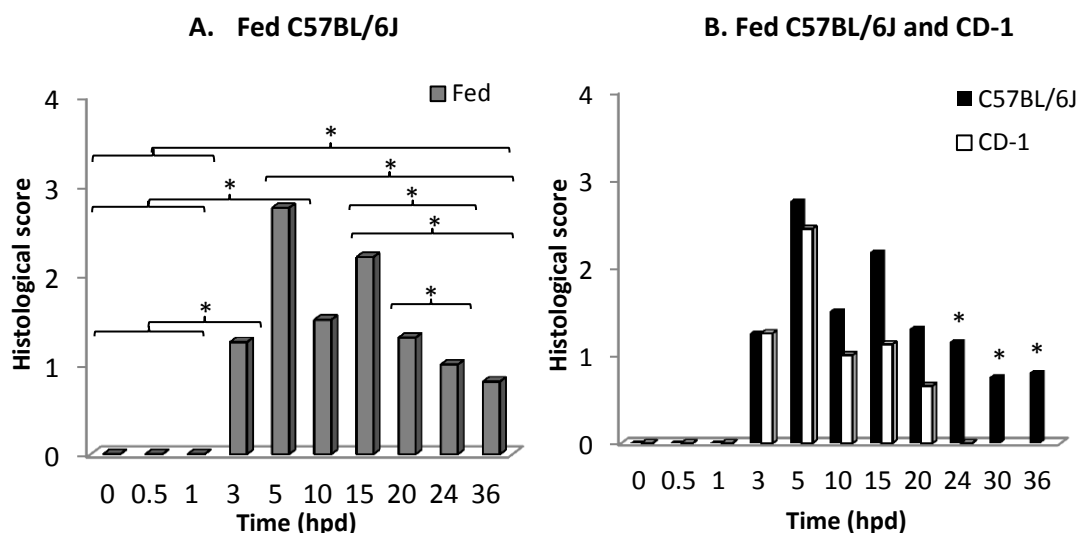


Figure 3.3.8. Histological scoring in fed C57BL/6J mice after APAP overdose and comparison to the scores in CD-1 mice.

(A) Average histological grading scores in fed C57BL/6J mice over 0-36 hpd. (B) Comparison of scores in fed C57BL/6J and CD-1 mice (as listed in Table 3.3.9). Data represent mean \pm SD (4 to 9 animals per group). * P <0.05, and histological score at 30 or 36 hpd in C57BL/6J mice compared to 24 hpd scores in CD-1 mice (B).

In **fasted C57BL/6J mice**, no histological abnormalities were detected up to 3 hpd (Figures 3.3.8 and 3.3.10B). While complete glycogen cell loss was seen immediately after fasting (at 0 hpd; see Chapter 3.1.6), a low degree of glycogen restitution was seen at 30 minutes up to 3 hpd (Figure 3.3.10D). However, by 5 hpd, fasted mice showed the highest DILI scores (score 3.25) with extensive centrilobular cell loss and bridging necrosis. Meanwhile, PAS-positive cells were hardly seen except in some periportal regions. Centrilobular cell loss associated with scattered apoptotic cells and no or few hepatocytes that contained glycogen were seen at 10 and 15 hpd, with similar DILI scores to fed mice. At 20 and 24 hpd, there was evidence of coagulative necrosis of the innermost centrilobular cell layers and hydropic degeneration surrounding the areas of cell loss, whereas glycogen was accumulated in hepatocytes outside the affected areas (Figure 3.3.13C). At 36 hpd, the degree of centrilobular cell loss was slightly less intense and diffuse hepatocellular glycogen accumulation was seen outside the centrilobular areas with still some evidence of apoptotic cells centrilobularly (Figure 3.3.14).

Table 3.3.10. Histological findings in APAP dosed **fasted** C57BL/6J mice (time course). The histological findings are summarised for each group of animals examined at each time point and the range of grading scores of each group (4-6 animals per group). hpd – hours post dosing; NHAIR – no histological abnormality is recognised; CL - centrilobular; hpc – hepatocytes; NL – neutrophilic leukocytes; HD - hydrophic degeneration; CN – coagulative necrosis; CC3 – Cleaved caspase-3.

Time (hpd)	Score range [mean]	Histological findings
0	0	NHAIR; PAS: No glycogen
0.5	0	NHAIR; PAS: Diffuse glycogen (relatively low amount)
1	0	NHAIR; PAS: Diffuse glycogen
3	0	NHAIR; PAS: Diffuse glycogen with variable intensity
5	2-4 [3.25]	CL cell loss with bridging necrosis of innermost CL hpc layers and numerous NL; PAS: diffuse glycogen loss, except in some periportal hpc with variable amount
10	1-3 [2.13]	CL cell loss with NL infiltration, few apoptotic cells; PAS: scattered random hpc containing glycogen
15	1-2 [1.75]	CL cell loss with a few scattered apoptotic cells and substantial NL infiltration; PAS: no glycogen
20	1-3 [2]	CN of innermost 2-3 CL hpc layers with HD of few remaining hpc at zone 2 (between affected and unaffected areas); few apoptotic cells; PAS: no glycogen except in a few scattered random individual hpc
24	2-2.5 [2.1]	Similar to 20 hpd; CN, HD and occasional apoptosis of remaining hpc in affected CL areas; PAS: no glycogen in affected CL areas of zone 3. CC3: ++
36	1-2 [1.5]	CN of innermost 2-3 CL hpc layers with moderate NL infiltration and some apoptotic hpc; PAS: diffuse glycogen outside affected areas. CC3: +

The comparison between fed and fasted C57BL/6J mice showed that fed C57BL/6J mice started to show cell loss and a score at 3 hpd, whereas the fasted mice showed still no morphological abnormality (Figure 3.3.10A-D); but the first evidence of APAP-induced damage only at 5 hpd, however, at this time point, the most severe damage was observed (highest scores), before the scores dropped again. Fasted mice showed more severe liver injury than fed mice, with significantly higher average scores at 24 hpd (Figure 3.3.11). By 36 hpd, centrilobular cell loss with morphological features of coagulative necrosis, and glycogen loss was more extensive in fasted mice with evidence of cleaved caspase-3 positive cells centrilobularly (Figure 3.3.14A-F).

Table 3.3.11. Histological scores in APAP dosed **fasted** C57BL/6J mice (time course) and comparison to CD-1 mice.

Time (hpd)	C57BL/6J						CD-1		
	Time dosing	Time killing	n	Mean score	SD	p-value APAP vs APAP	p-value fasted vs fedAPAP	Mean score	p-value vs APAP C57BL/6J
0	10:00	10:00	4	0	0	Score 0 vs: 5 h: 0.0159 10 h: 0.0109 15 h: 0.0002 20 h: 0.0122 24 h: 0.0286 36 h: 0.047	NS	0	NS
0.5	10:00	10:30	4	0	0		NS	0	-
1	10:00	11:00	4	0	0		NS	0	NS
3	9:00	12:00	4	0	0		0.0286	2.05	0.0111 ↑
5	10:00	15:00	4	3.25	0.5	-	NS	2.5	NS
10	10:00	20:00	4	2.13	0.75	-	NS	2.6	NS
15	17:00	08:00	4	1.75	0.29	24 h: 0.032	NS	2.15	NS
20	11:00	07:00	4	2	0.74	-	0.0493	2.75	NS
24	10:00	10:00(+1)	5	2.1	0.14	36 h: 0.0357	0.0079	2.38	NS
36	7:00	19:00(+2)	4	1.5	0	-	NS	-	-

hpd – hours post dosing; n - number of animals in group; SD – standard deviation; NS – not significant.

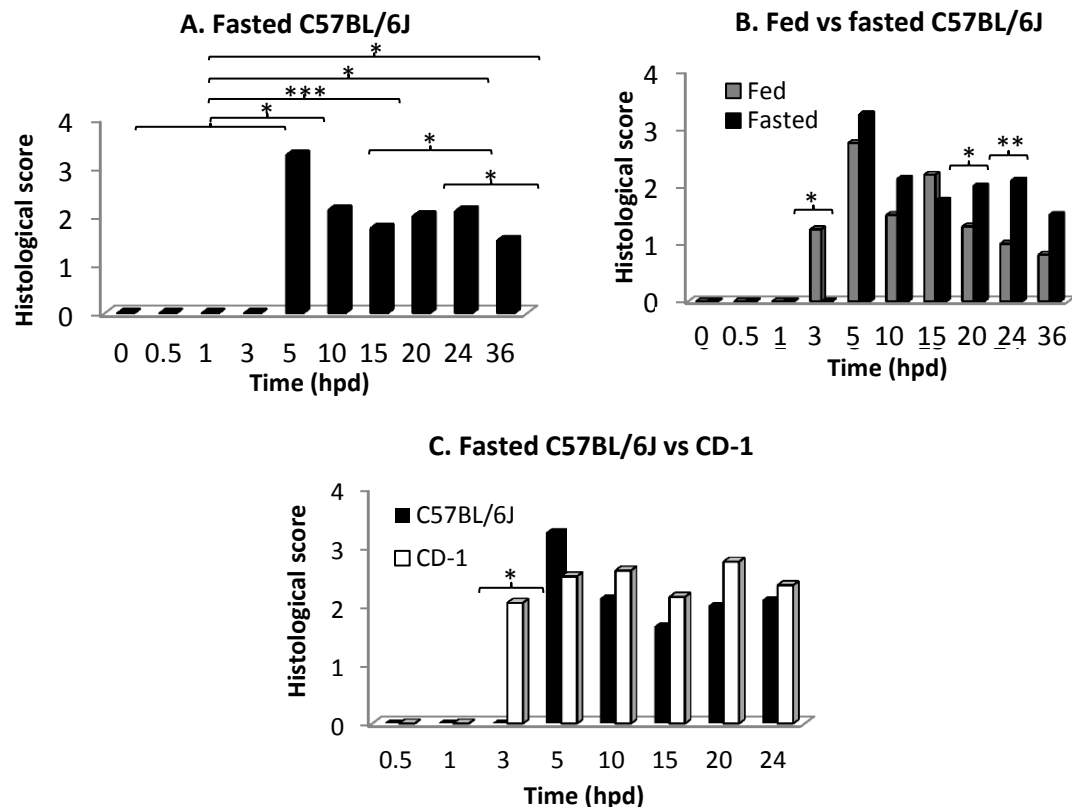


Figure 3.3.9. Histological scoring in fasted C57BL/6J and CD-1 mice after APAP overdose. (A) Histological grading score in fasted C57BL/6J mice over 0-36 hpd. (B) Comparison of APAP scores in fed and fasted APAP treated C57BL/6J mice. (C) Scores in fasted APAP treated C57BL/6J mice were compared to those in CD-1 mice (as listed in Table 3.3.11). Data represent mean±SD (4 to 9 animals per group). ***P<0.005, **P<0.01 and *P<0.05.

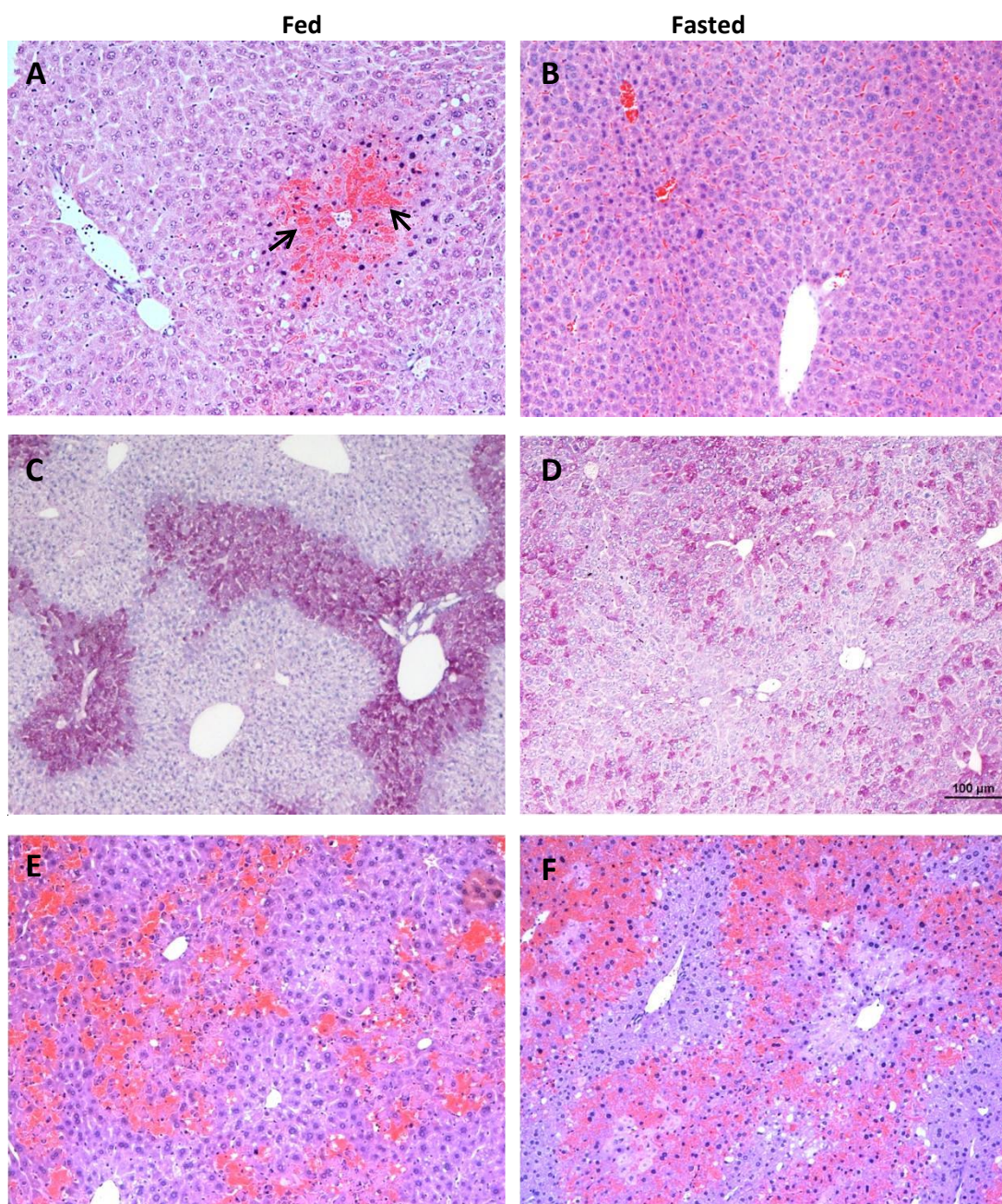


Figure 3.3.10. Assessment of histopathological features and glycogen content in fed and fasted C57BL/6J mice with comparison to CD-1 mice at **3 hours post APAP** (530 mg/kg) treatment.

There is centrilobular hepatocyte loss (score 1.25) with haemorrhage (black arrows) in fed C57BL/6J mice (A), together with a loss of hepatocellular glycogen at affected areas (C). In fasted C57BL/6J mice, no histological abnormality is identified (score 0) (B), and the almost diffuse glycogen accumulation (D) indicates glycogen restitution after the fasting period. At the same time point, CD-1 mice showed similar degree of hepatocytes loss (score 1.25) in fed (E) and more intense centrilobular cell loss (score 2.05) in fasted (F) animals (see also Figure 3.2.10). A, B, E, F: HE stain; C, D: PAS reaction. Magnification 100x.

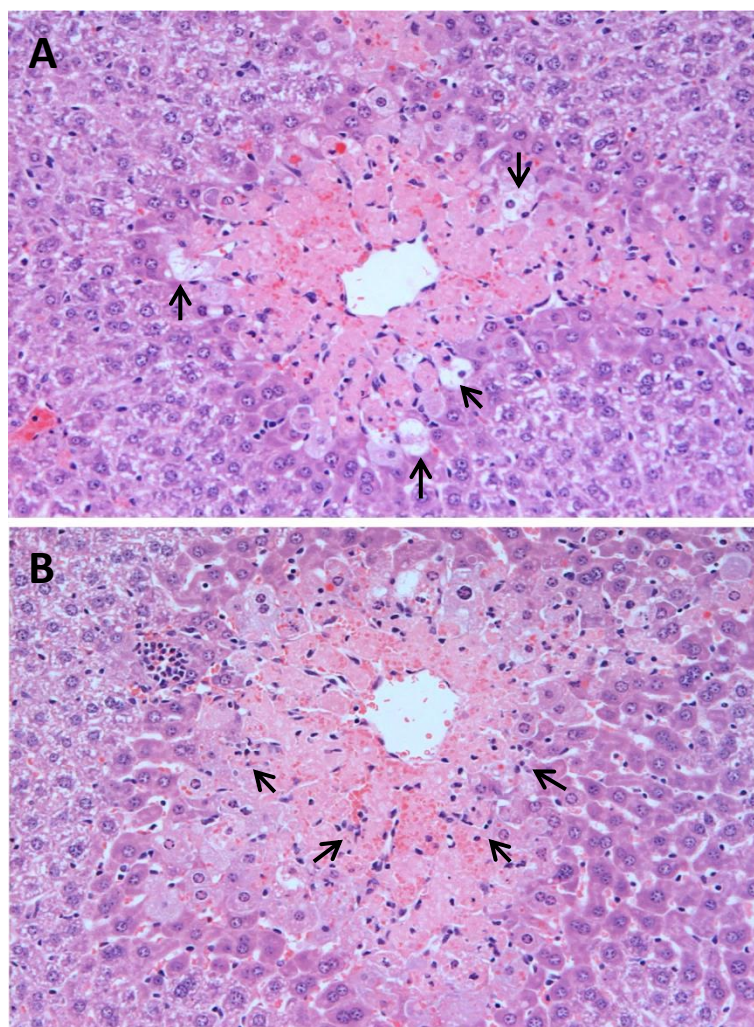


Figure 3.3.11. Assessment of histopathological features and glycogen content in fed and fasted C57BL/6J mice at **24 h post APAP** (530 mg/kg) treatment. Fed mice (A) showed centrilobular hepatocyte loss and coagulative necrosis (score 1.15), surrounded by a layer of hepatocytes with hydropic degeneration (black arrows). In fasted mice (B), changes were similar but generally more extensive (score 2.1) with marked neutrophil infiltration (black arrows) was seen. HE stain. Magnification x200 (A, B).

Comparison of average scores in fasted animals of both strains showed higher DILI scores in CD-1 mice from 10 to 24 hpd, but without statistically significant difference. The latter was only found at 3 hpd, as fasted CD-1 mice exhibited liver damage earlier than fasted C57BL/6J mice. In fasting animals, hepatocellular damage that reflected by coagulative necrosis was similar in C57BL/6J mice and CD-1 mice with no glycogen at affected region, but more neutrophils infiltration was seen in C57BL/6J mice (Figure 3.3.13A-D; see also Figure 3.3.11B). Meanwhile, evidence of ongoing cell death by expression of positive cleaved caspase-3 was also not differ in both CD-1 and C57BL/6J mice (Figure 3.3.13E,F).

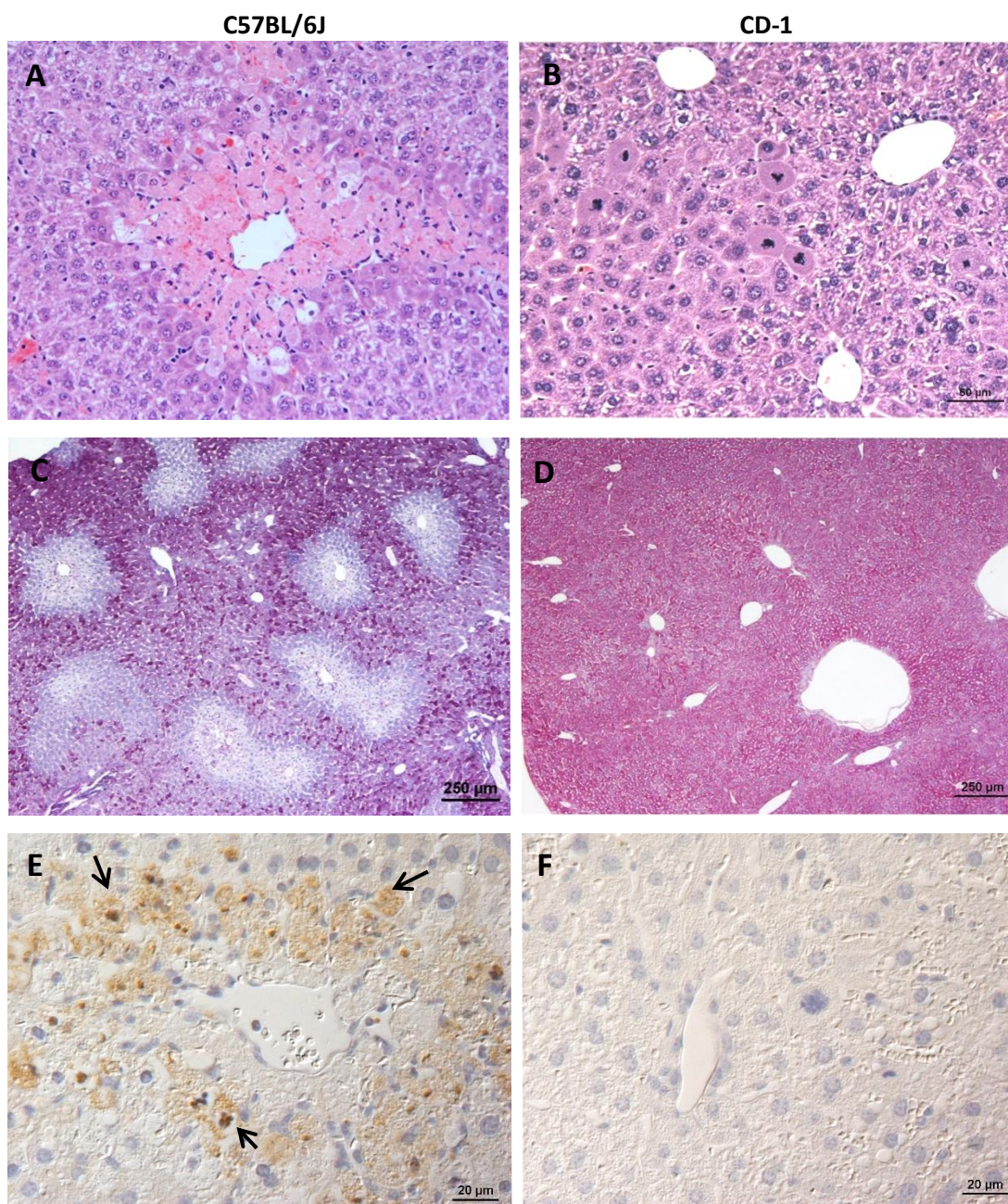


Figure 3.3.12. Assessment of histopathological features and glycogen content in **fed C57BL/6J** and **CD-1** mice at 24 h post APAP (530 mg/kg) treatment.

In C57BL/6J mice, there is evidence of ongoing centrilobular cell death (score 1.15) (via coagulative necrosis and apoptosis (A, E) and degeneration (A; see also Figure 3.3.11A) and a lack of hepatocellular glycogen in affected areas (C). In contrast, livers of CD-1 mice appeared unaltered and showed evidence of complete regeneration with evidence of numerous mitotic figures (score 0) (B) and diffuse glycogen restitution (D) and without evidence of apoptosis (F). A, B: HE stain: C, D: PAS reaction. E, F: Staining for cleaved caspase-3, PAP method, Papanicolaou's haematoxylin counterstain. Magnification x200 (A, B), x40 (C, D) and x400 (E, F).

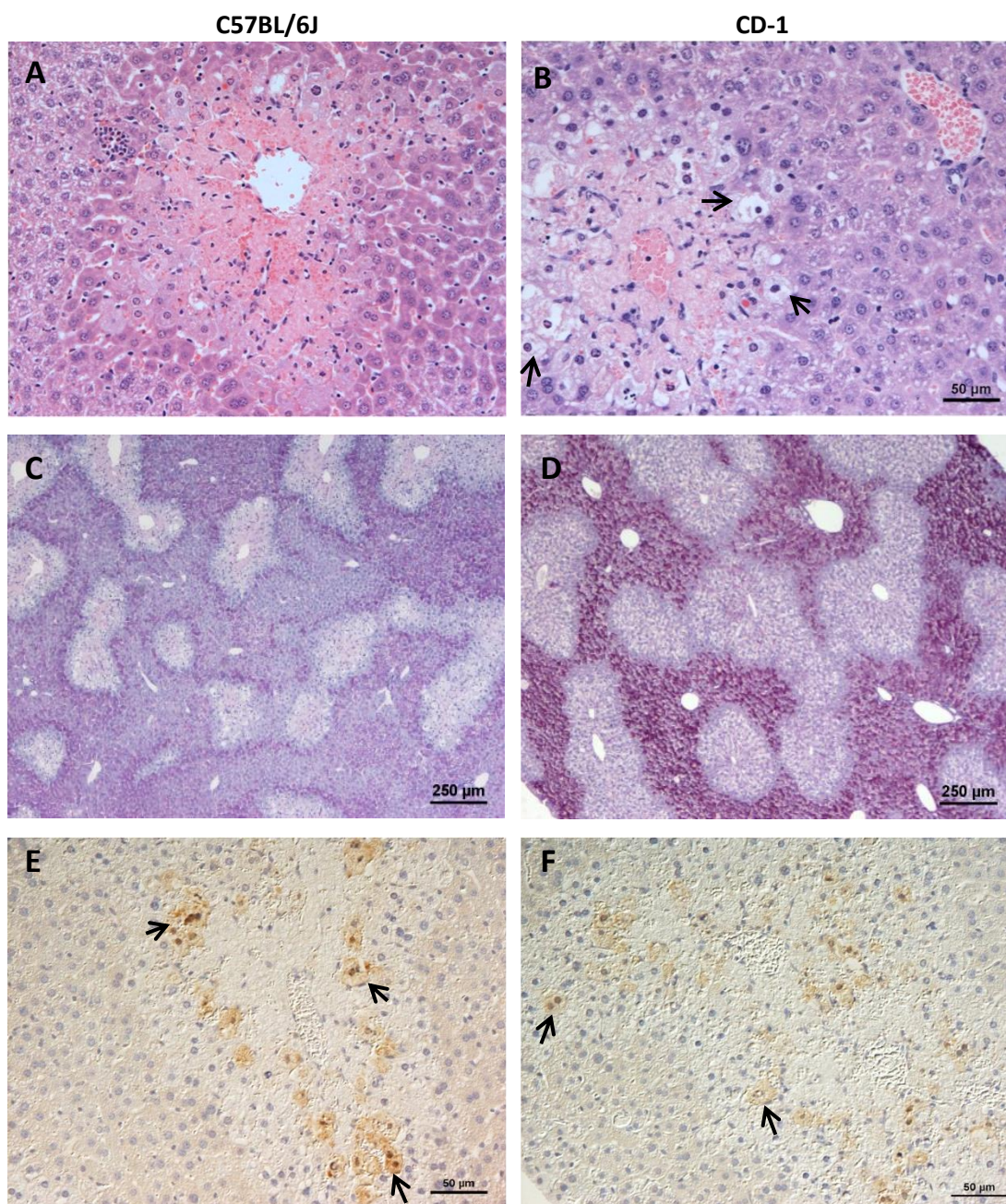


Figure 3.3.13. Assessment of histopathological features and glycogen content in **fasted C57BL/6J and CD-1 mice** at 24 h post APAP (530 mg/kg) treatment.

In C57BL/6J mice, there is centrilobular hepatocyte loss (score 2.1), surrounded by layers of coagulative necrosis (A) and apoptotic cells death (E). Affected centrilobular areas lack glycogen and the amount of glycogen outside these areas is low and variable (C). In CD-1 mice, coagulative necrosis of the innermost centrilobular hepatocyte layer is seen (score 2.38), surrounded by hepatocytes undergoing hydropic degeneration (black arrows) (B), intermingled with a few apoptotic cells (F). There is diffuse glycogen restitution outside the affected centrilobular areas (D). A, B: HE stain; C, D: PAS reaction; E, F: Staining for cleaved caspase-3, PAP method, Papanicolaou's haematoxylin counterstain. Magnification x200 (A, B, E, F) and x100 (C, D).

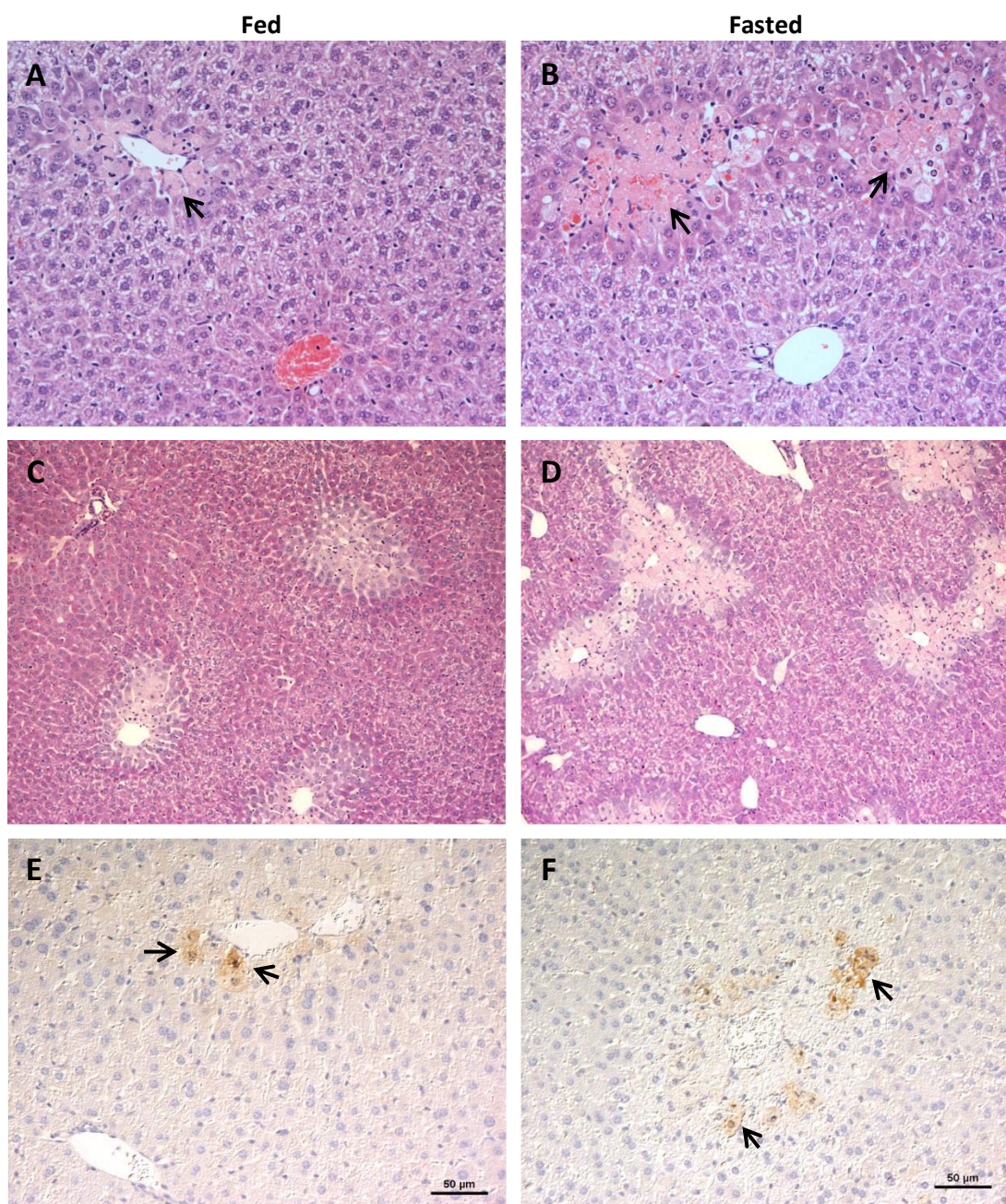


Figure 3.3.14. Assessment of histopathological features and glycogen content in fed and fasted C57BL/6J at 36 h post APAP (530 mg/kg) treatment.

In fed mice, mild centrilobular coagulative necrosis (score 0.8) (A; black arrow) and occasional hepatocyte apoptosis (E; black arrows) is seen. There is diffuse glycogen accumulation outside a centrilobular, approximately 2-3 cell layer wide area (C). In fasted mice, ongoing centrilobular cell death was more extensive (score 1.5), with innermost layers of coagulative necrosis (B; black arrows) and apoptosis (F; black arrows). There is diffuse hepatocellular glycogen accumulation outside the affected centrilobular areas (D). A, B: HE stain; C, D: PAS reaction; E, F: Staining for cleaved caspase-3, PAP method, Papanicolaou's haematoxylin counterstain (E). Magnification x200 (A, B, E, F) and x100 (C, D).

3.3.6 Overall assessment and comparison of liver damage in C57BL/6J and CD-1 mice

The degree of liver damage following APAP overdose was assessed in male C57BL/6J and CD-1 mice based on the levels of hepatic GSH and ATP and serum ALT, together with the DILI scores at 5, 10 and 24 hpd (Table 3.3.12). Data are presented as fold change relative to time-matched control animals, except for the DILI scores (use of raw data).

In control animals, serum ALT levels in C57BL/6J mice were generally lower than in CD-1 mice, although the difference was not significant (see Chapter 1, Figure 3.1.6). Following APAP treatment of **fed mice**, however, significant differences were found between both strains. The fold change of the increase was significantly higher in the C57BL/6J mice at both examined time points (5 and 24 hpd). A comparison between hepatic GSH levels was possible at 10 and 24 hpd, and the fold change of increase was significantly higher in the CD-1 mice at 10 hpd (Figure 3.3.15A).

In **fasted mice**, the difference was restricted to serum ALT, where the fold changes were significantly higher in the C57BL/6J mice at both available time points, 5 and 24 hpd (Figure 3.3.15B).

Table 3.3.12. Comparison of GSH, ATP, ALT and DILI score in male C57BL/6J and CD-1 mice in animals that had been fed or fasted prior to APAP dosing using comparative value, assessing fold change relative to control animals.

Time (hpd)	Mice	GSH		ATP		ALT		DILI score	
		C57BL/6J	CD-1	C57BL/6J	CD-1	C57BL/6J	CD-1	C57BL/6J	CD-1
5	Fed	0.21	-	0.18	-	137.9***	27.45	2.75	2.2
	Fasted	-	-	-	-	192.0***	41.14	3.25	2.5
10	Fed	0.78	1.96*	0.50	0.61	69.5	-	1.5	1.0
	Fasted	0.17	0.06	0.25	0.25	54.8	-	2.13	2.6
24	Fed	0.85	0.96	1.00	1.07	319.1***	96.53	1.15*	0
	Fasted	0.78	0.33	-	0.49	290.3***	57.02	2.1	2.4

Statistical significant, *P<0.05 and ***P<0.005 are seen in the comparison between C57BL/6J and CD-1 mice that had been either fed or fasted prior to APAP dosing; hpd – hours post dosing.

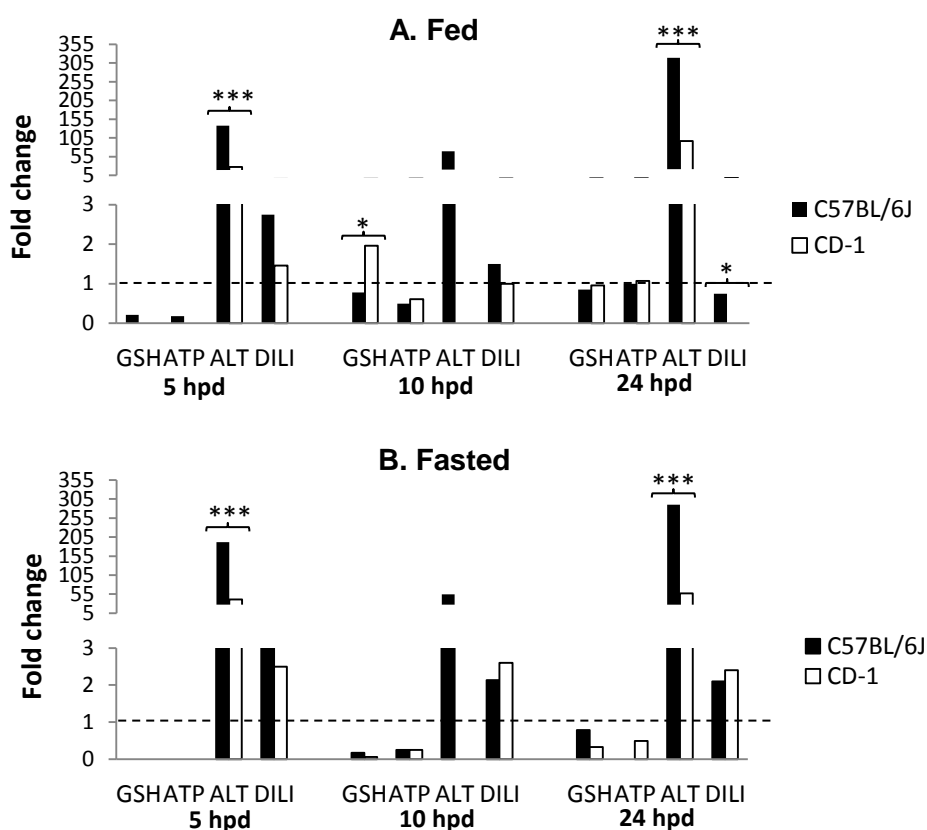


Figure 3.3.15. Assessment of liver damage in fed and fasted male C57BL/6J and CD-1 mice after APAP dosing.

The hepatic GSH and ATP levels, serum ALT levels and DILI scores were compared between C57BL/6J and CD-1 at 5, 10 and 24 hpd in animals that had been fed (A) or fasted (B) prior to 530 mg/kg APAP dosing (as listed in Table 3.3.12). The GSH, ATP and ALT values are assessed as fold change relative to the levels in time-matched control mice, the DILI scores as raw data. Data represents mean (4 to 6 animals per group). *** $P < 0.005$ and * $P < 0.05$. Fold change = 1 : levels in saline dosed control mice indicated by dashed lines.

3.3.7 Quantification of cytokine expression in liver, spleen and sera levels in C57BL/6J mice and comparison to CD-1 mice

3.3.7.1 Hepatic transcription of TNF- α , IL-6 and IL-10

An evidence of upregulation of TNF- α , IL-6 and IL-10 cytokines at several time points of post APAP dosing showed that the transcription was obviously seen in fed rather than fasted mice, like it was also observed in the CD-1 mice (see Chapter 3.2.7), by using delta Ct values normalised to the housekeeping gene GAPDH (fed mice: Table 6.33; fasted mice: Table 6.35; Figure 3.3.16).

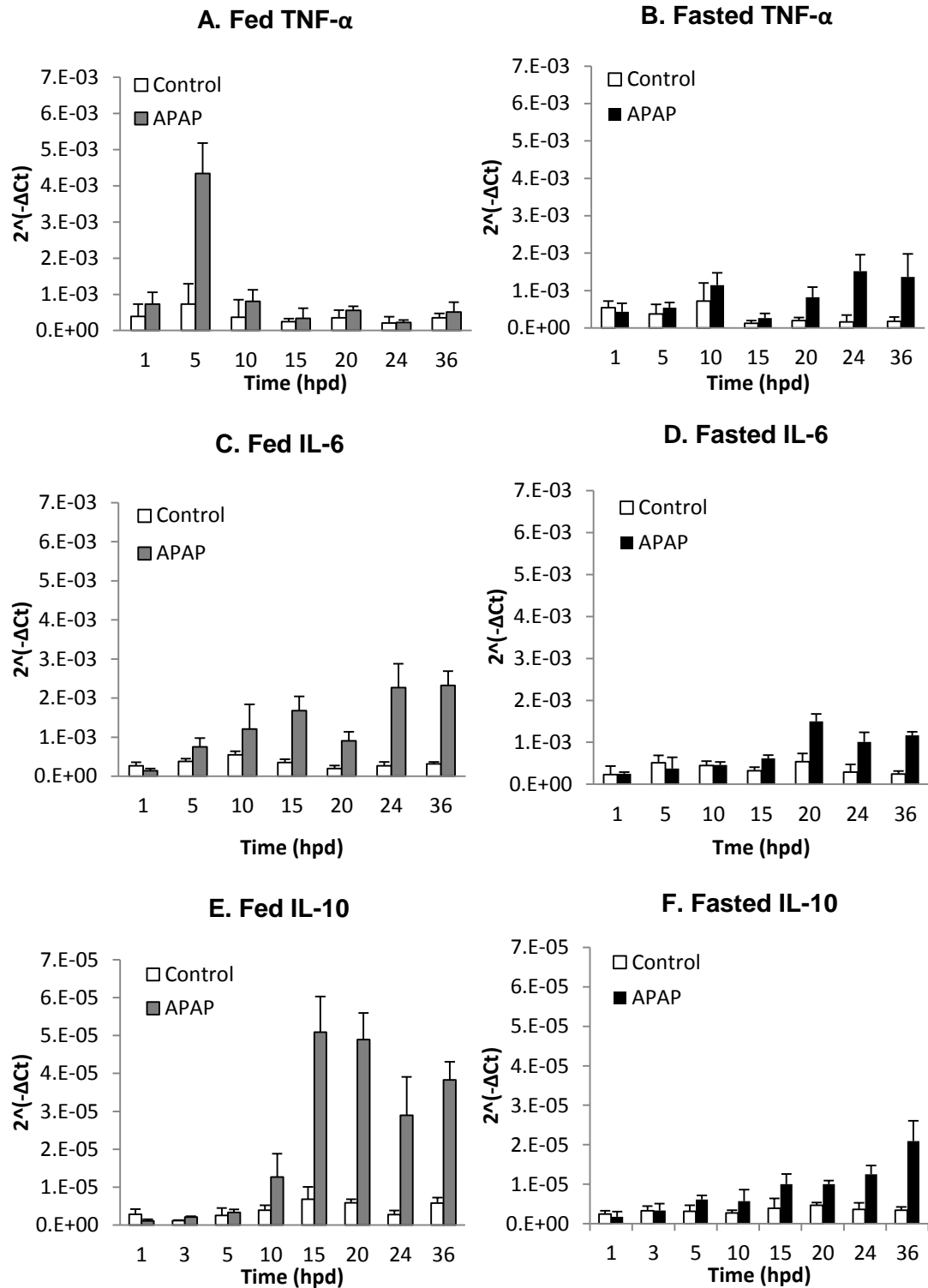


Figure 3.3.16. Hepatic TNF- α , IL-6 and IL-10 mRNA levels in control and APAP dosed fed and fasted male C57BL/6J mice over 1-36 hpd.

The hepatic mRNA levels of cytokines TNF- α (A, B), IL-6 (C, D) and IL-10 (E, F) were compared between 0.9% saline (control mice) and 530 mg/kg APAP dosed fed and fasted C57BL/6J mice. Hepatic mRNA levels were calculated using the delta Ct value formula, $2^{-\Delta Ct}$. Data represent mean \pm SD (4 to 6 animals per group).

Thus, similar to CD-1 mice (see Chapter 3.2.7), the cytokine transcription levels were assessed by the comparative Ct value as fold change relative to time-matched control C57BL/6J mice. In fed C57BL/6J mice, a significant, 6-fold increase in hepatic **TNF- α** transcription in comparison to **time-matched control** animals was seen at 5 hpd (Figure 3.3.17A). In fasted mice, significant fold changes in TNF- α mRNA levels were observed at later time points, i.e. at 20 hpd (4.2-fold), 24 hpd (9.6-fold) and 36 hpd (7.9-fold). Comparing fed and fasted C57BL/6J mice, we observed that the TNF- α transcription was significantly higher in the fed mice at 5 hpd (6-fold increase) and then dropped again (Table 6.33), whereas fasted C57BL/6J mice showed upregulation of TNF- α transcription from 20 hpd onwards, with the highest fold change at 24 hpd before a slight drop was seen at 36 hpd, over this time period, fold changes were significantly higher than in fed mice at the same time points (Table 6.35, Figure 3.3.17A).

The comparison of fed APAP dosed mice over the time course showed a significantly higher increase in CD-1 than in C57BL/6J mice at 10 hpd (4.5-fold), but at other time points a similar pattern and comparable fold change was seen in both groups of mice (Table 6.33, Figure 3.3.17B). In fasting mice, at 10 and 15 hpd, the TNF- α upregulation was significantly more intense in CD-1 mice (10 hpd: 1.6-fold vs 5.3-fold increase in C57BL/6J and CD-1 mice, respectively). In the CD-1 mice, a further increase was seen from 10 to 15 hpd, when the peak was seen (14.3-fold upregulation). Transcription levels then dropped in the CD-1 mice, whereas another increase was seen in the C57BL/6J mice, with a peak at 24 hpd, when the fold changes were significantly higher in the C57BL/6J mice (9.6-fold in C57BL/6J vs. 3.9-fold in CD-1 mice) (Table 6.35, Figure 3.3.17C).

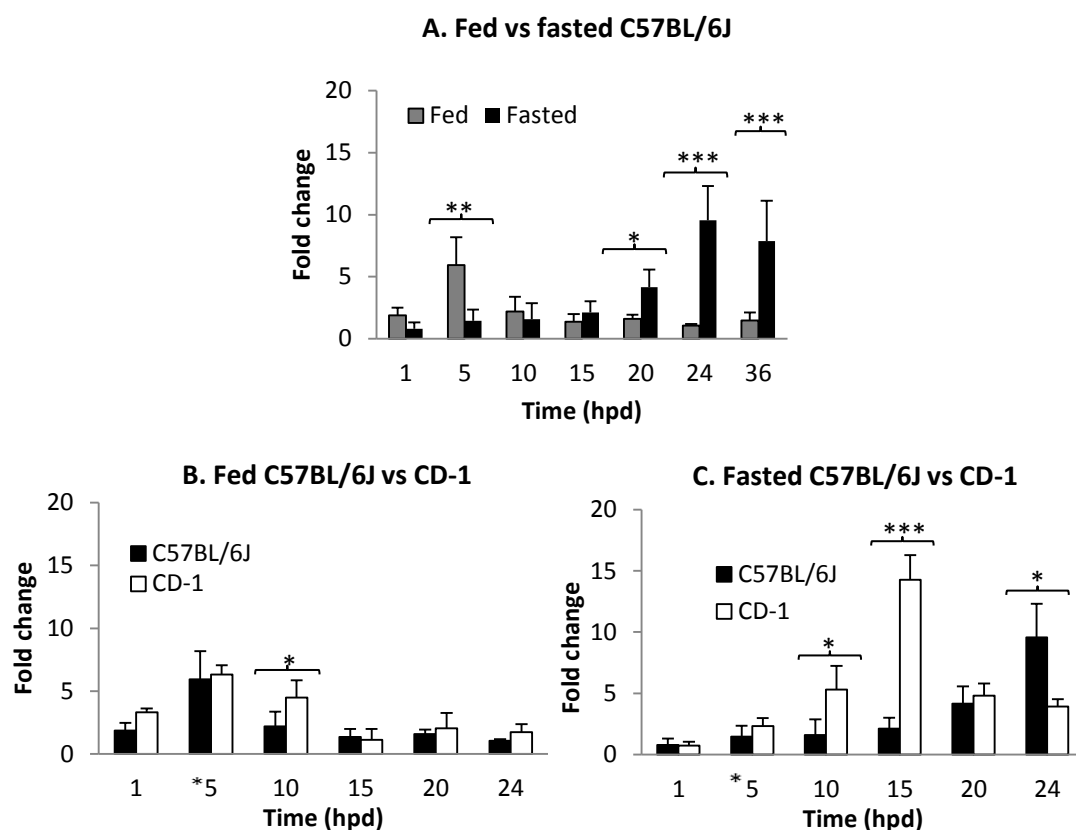


Figure 3.3.17. Fold changes in hepatic TNF- α transcription levels in fed and fasted APAP dosed C57BL/6J mice and comparison to CD-1 mice.

Hepatic TNF- α transcription levels were determined after APAP (530 mg/kg; 1-36 hpd) dosing of fed and fasted male C57BL/6J mice (A). The levels were also compared between C57BL/6J and CD-1 mice in either fed (B) or fasted (C) mice prior to APAP dosing. Hepatic TNF- α mRNA levels are calculated using the comparative Ct values, assessing the fold change relative time-matched control animals. Data is given as mean \pm SD (4 to 6 animals per group). *** P <0.005, ** P <0.01 and * P <0.05.

Hepatic mRNA transcription levels were also assessed by the comparative Ct value as fold change relative to the **pooled control** levels as no significant differences were seen in the control animal levels at any time point (fed mice: Table 6.34; fasted mice: Table 6.36). This confirmed the significant fold change in hepatic TNF- α mRNA level in fed APAP dosed mice at 5 hpd (11.7-fold) and a significant upregulation in fasted mice at 20 hpd (2.3-fold), 24 hpd (4.2-fold) and 36 hpd (3.8-fold) (Table 6.36, Figure 3.3.18A) as similar result obtained in Figure 3.3.17A. Comparing these results with those from CD-1 mice (APAP overdose at each time point vs pooled control values) significant differences were seen in the fed mice. In C57BL/6J, the fold change was significantly higher at 5 hpd (11.7-fold vs 4.4-fold), but significantly lower at 10 hpd (7.9-fold vs 2.2-fold) (Table 6.34, Figure 3.3.18B). In

fasted mice, the results were the same as those obtained with the time matched controls (Table 6.36, Figure 3.3.18C; for comparison, see Figure 3.3.17C).

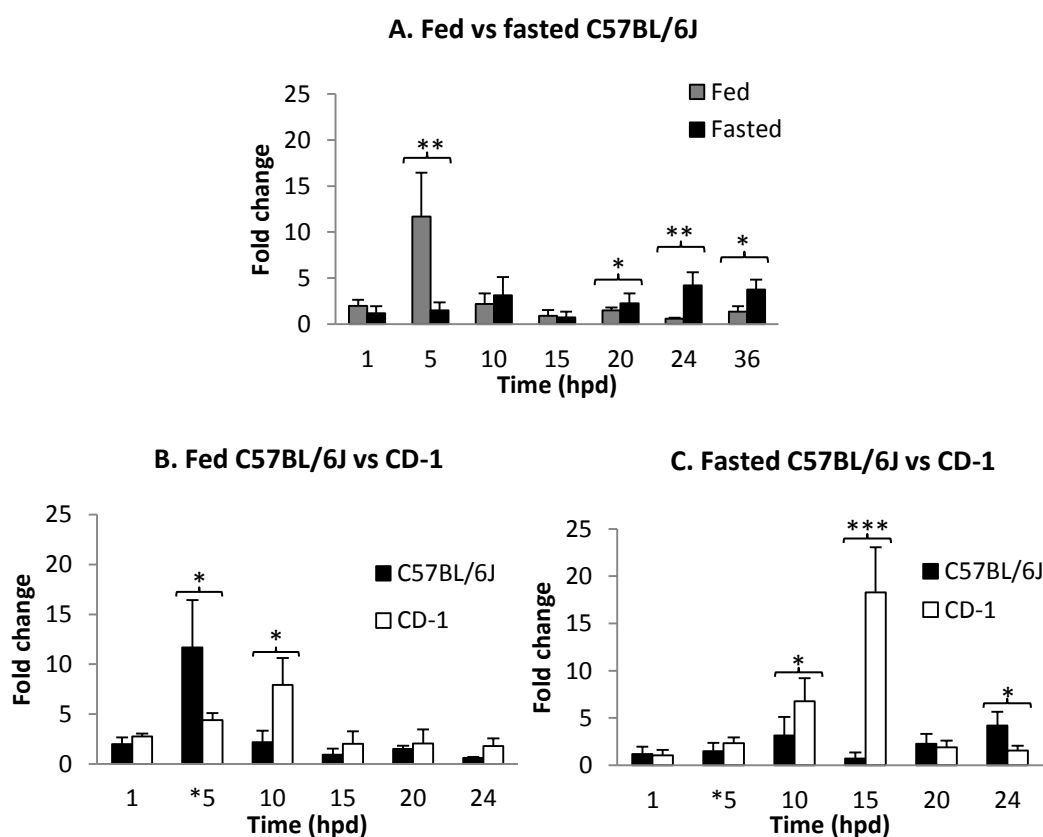


Figure 3.3.18. Fold changes in hepatic TNF- α transcription levels in fed and fasted APAP dosed C57BL/6J mice and comparison to CD-1 mice.

Hepatic TNF- α transcription levels were determined after APAP (530 mg/kg; 1-36 hpd) dosing of fed and fasted male C57BL/6J mice (A). Comparison of fold changes in fed (B) and fasted (C) APAP dosed C57BL/6J and CD-1 mice. Hepatic mRNA levels are calculated using the comparative Ct values, assessing the fold change relative pooled control animals. *5 - values of 5 h C57BL/6J was compared to 4 h CD-1 mice. Data is given as mean \pm SD (4 to 6 animals per group). ***P<0.005, **P<0.01 and *P<0.05.

In fed APAP dosed C57BL/6J mice, the IL-6 level was found to have increased by 4.6-fold in comparison to **time-matched control** mice at 15 and 20 hpd. At 24 hpd (8.5-fold), it reached a peak, and then dropped slightly towards 36 hpd (7.3-fold); the difference was significant from 15 to 36 hpd (Table 6.33). In fasted C57BL/6J mice, IL-6 mRNA levels rose steadily, and the upregulation was significant at 24 hpd (3.5-fold) and 36 hpd (4.8-fold) (Figure 3.3.20B). However, the fold changes were consistently lower in the fasted mice, and the difference was significant at 15 and 24 hpd. While at the latter time point the peak value was seen in the fed mice, it was not yet the case in the fasted mice (Table 6.35, Figure 3.3.19A).

In comparison to fed CD-1 mice, the hepatic IL-6 upregulation was almost consistently significantly less intense in fed C57BL/6 mice and appeared to be delayed, still rising at 24 hpd, while the CD-1 mice exhibited a significant increase as early as 1 hpd, with increasing fold changes over 5 hpd (5-fold), 10 hpd (9.3-fold) and 20 hpd (11.5-fold), with a peak at the latter time point (Table 6.33, Figure 3.3.19B) when histological evidence of ongoing liver damage had subsided in CD-1 mice whereas in C57BL/6J mice, ongoing cell death was observed (see Chapter 3.2.6). In fasted mice, a similar pattern, with a steady increase was observed, but the fold changes were consistently higher in the CD-1 mice. This difference was significant at 4/5 hpd (CD-1 mice: 4 hpd (3.6-fold); C57BL/6J mice: 5 hpd (0.7-fold)) and 15 hpd (5.3-fold in C57BL/6J) (Table 6.35, Figure 3.3.19C).

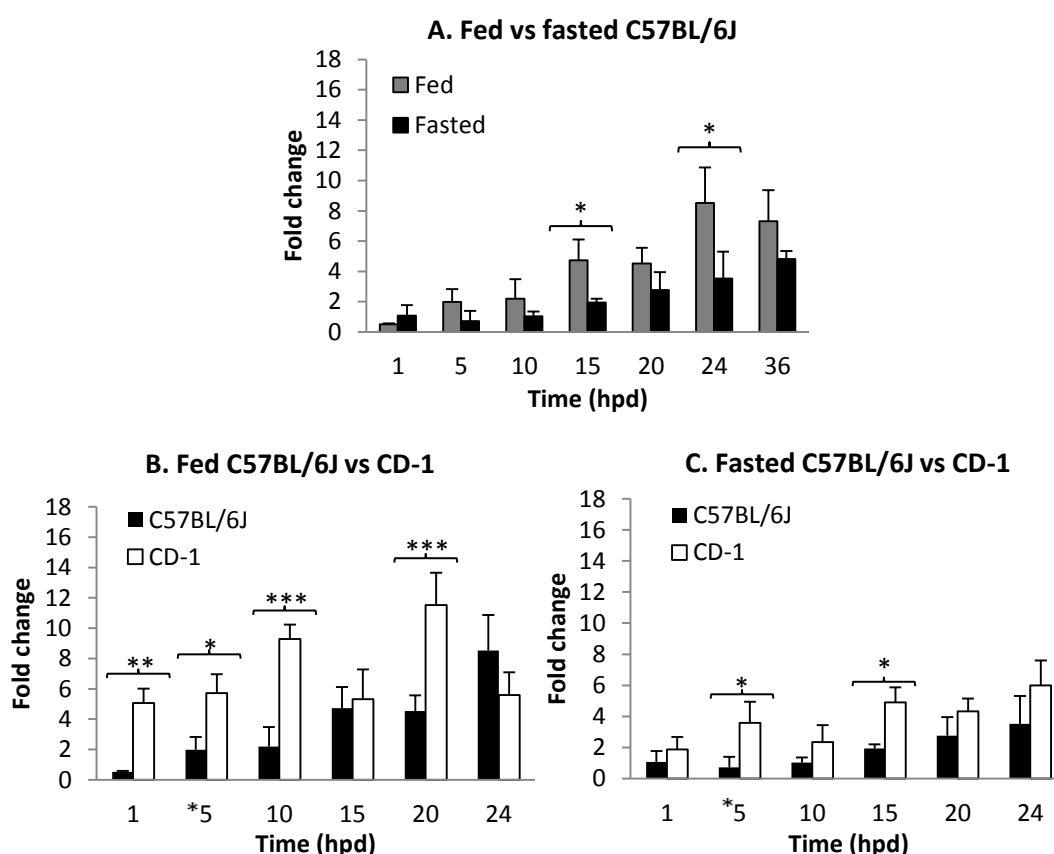


Figure 3.3.19. Fold changes in hepatic IL-6 transcription levels in fed and fasted APAP dosed C57BL/6J mice and comparison to CD-1 mice.

Hepatic IL-6 transcription levels were determined after APAP (530 mg/kg; 1-36 hpd) dosing of fed and fasted male C57BL/6J mice (A). Comparison of fold changes in fed (B) and fasted (C) APAP dosed C57BL/6J and CD-1 mice. Hepatic mRNA levels are calculated using the comparative Ct values, assessing the fold change relative time-matched control animals. Data is given as mean \pm SD (4 to 6 animals per group). ***P<0.005, **P<0.01 and *P<0.05.

Looking at the fold changes relative to **pooled control** mouse values, the significantly higher increase in IL-6 transcription level in the fed C57BL/6J mice at 15 and 24 hpd was confirmed, and a significantly higher fold change was additionally detected at 36 hpd (7.2-fold) in comparison to the fasted mice (Table 6.36, Figure 3.3.20A). The comparison of fed mice of both groups did not confirm the significantly higher increase in the CD-1 at 1 hpd which was detected before (Table 6.34, Figure 3.3.20B; for comparison, see Figure 3.3.19B). In the fasted mice, the previous results were confirmed (Table 6.36, Figure 3.3.20C; for comparison, see Figure 3.3.19C).

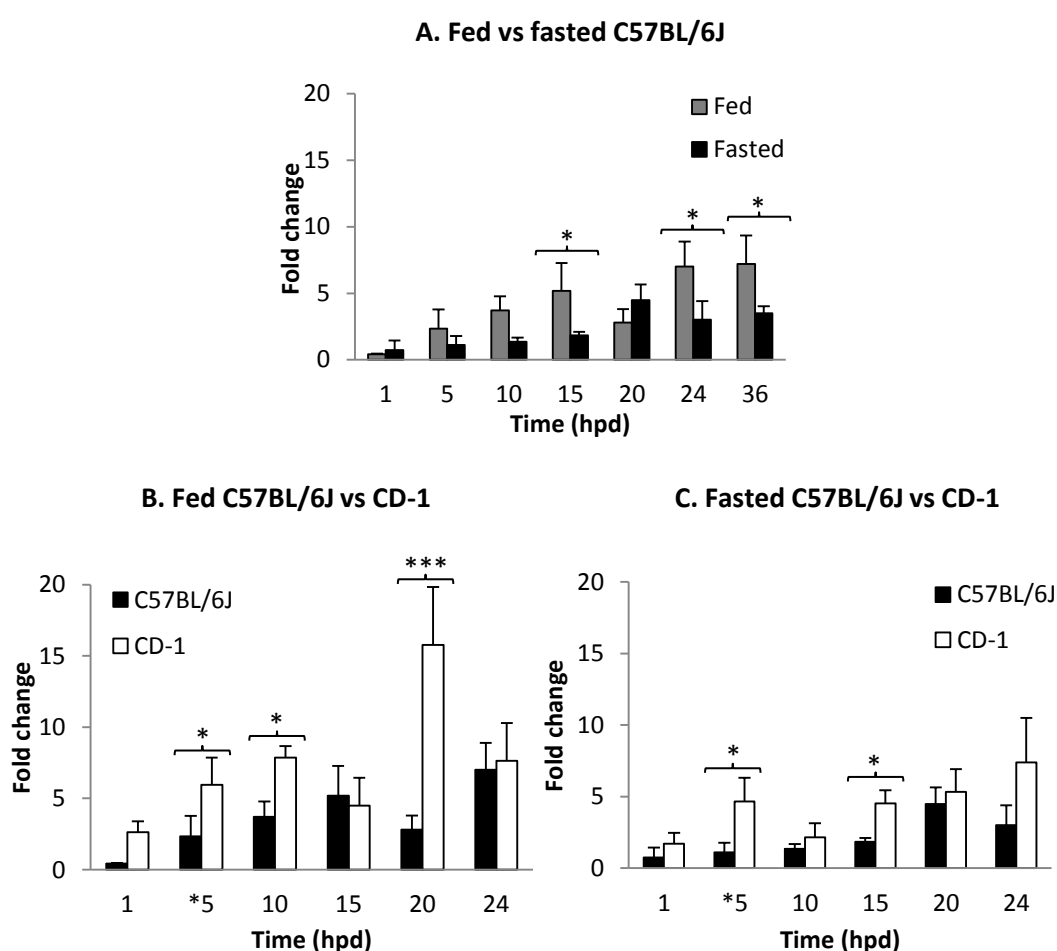


Figure 3.3.20. Fold changes in hepatic IL-6 transcription levels in fed and fasted APAP dosed C57BL/6J mice and comparison to CD-1 mice.

Hepatic IL-6 transcription levels were determined after APAP (530 mg/kg; 1-36 hpd) dosing of fed and fasted male C57BL/6J mice (A). Comparison of fold changes in fed (B) and fasted (C) APAP dosed C57BL/6J and CD-1 mice. Hepatic mRNA levels are calculated using the comparative Ct values, assessing the fold change relative pooled control animals. *5- values of 5 h C57BL/6J was compared to 4 h CD-1 mice. Data is given as mean±SD (4 to 6 animals per group). ***P<0.005, **P<0.01 and *P<0.05.

In fed animals, the hepatic **IL-10** transcription increased steadily and was significantly upregulated in APAP dosed C57BL/6J mice in comparison to **time-matched control** mice at 15 hpd (7.5-fold), 20 hpd (8.4-fold), 24 hpd (10.6-fold) and 36 hpd (6.6-fold) (Table 6.33). In fasted C57BL/6J mice, the fold changes in IL-10 transcriptions levels were much lower, with a significant difference to saline-dosed mice at 24 hpd (3.5-fold) and 36 hpd (6.1-fold) only (Table 6.35). By 36 hpd, the fold change was similar to that one seen in fed APAP dosed mice, while the fold changes were significantly higher at the earlier time points (15, 20 and 24 hpd) in the fed mice (Table 6.36, Figure 3.3.21A).

The comparison to CD-1 mice showed that the upregulation in these mice occurred earlier and at a higher level (significant difference at at 4/5 hpd (8.9-fold vs. 1.3-fold) and 10 hpd (8.2-fold vs. 3.2-fold). In CD-1 mice, the peak fold change in IL-10 transcription was at 15 hpd after which time point a mild decline was seen, whereas in the C57BL/6J a later and steady increase was observed, with the peak at 24 hpd (Table 6.33, Figure 3.3.21B; see also Figure 3.3.20B). In fasted CD-1 mice, IL-10 mRNA fold changes were equally low during the early phase post APAP dosing. However, at 20 hpd (10.6-fold vs. 2.2-fold) and 24 hpd (12.1-fold vs. 3.5-fold) a marked upregulation was seen and the difference to the IL-10 transcription level in C57BL/6J mice was significant (Table 6.35, Figure 3.3.21C).

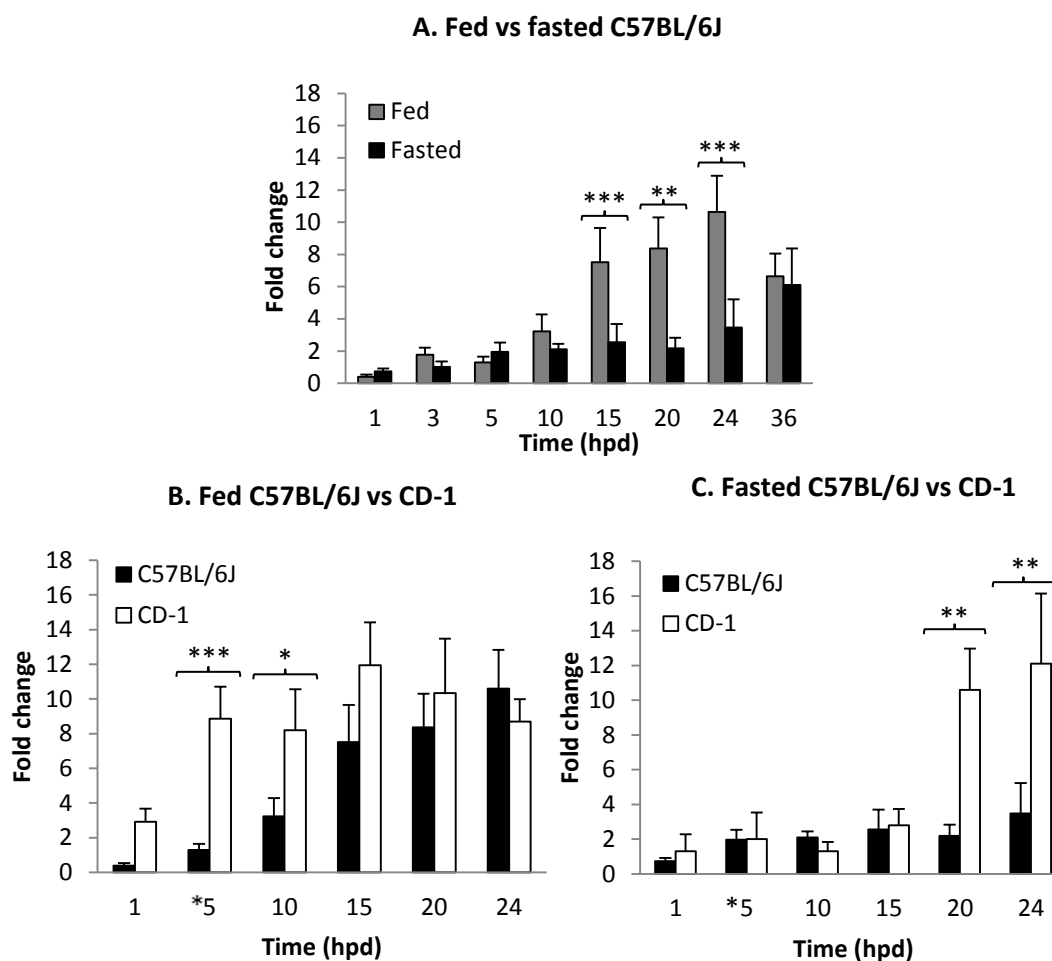


Figure 3.3.21. Fold changes in hepatic IL-10 transcription levels in fed and fasted APAP dosed C57BL/6J mice and comparison to CD-1 mice.

Hepatic IL-10 transcription levels were determined after APAP (530 mg/kg; 1-36 hpd) dosing of fed and fasted male C57BL/6J mice (A). Comparison of fold changes in fed (B) and fasted (C) APAP dosed C57BL/6J and CD-1 mice. Hepatic mRNA levels are calculated using the comparative Ct values, assessing the fold change relative time-matched control animals. Data is given as mean \pm SD (4 to 6 animals per group). *** P <0.005, ** P <0.01 and * P <0.05.

However, when the fold change relative to the **pooled control** values was assessed, the significant increase in hepatic IL-10 mRNA levels in fed C57BL/6J mice at 15 and 20 hpd was confirmed, without a difference to fasted mice at 24 hpd (Tables 6.34 and 6.36, Figure 3.3.22A). The comparison of fed animals of both groups confirmed the previous findings (Table 6.34, Figure 3.3.22B; for comparison see Figure 3.3.21B). However, in the fasted groups, a significant upregulation of IL-10 was detected in CD-1 mice at 20 hpd (4.6-fold vs. 3.0-fold), whereas the significantly higher increase at 24 hpd in the CD-1 mice was not confirmed (Table 6.36, Figure 3.3.22C; for comparison see Figure 3.3.21C).

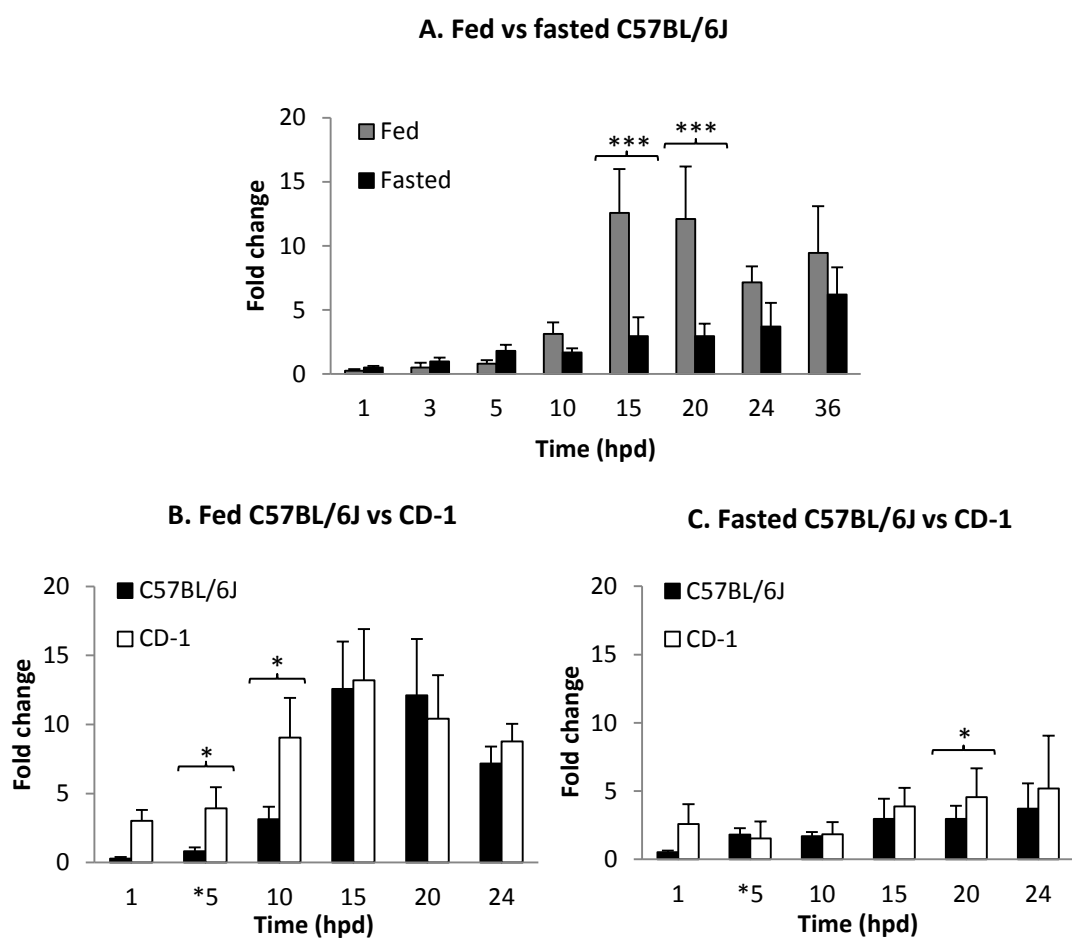


Figure 3.3.22. Fold changes in hepatic IL-10 transcription levels in fed and fasted APAP dosed C57BL/6J mice and comparison to CD-1 mice.

Hepatic IL-10 transcription levels were determined after APAP (530 mg/kg; 1-36 hpd) dosing of fed and fasted male C57BL/6J mice (A). Comparison of fold changes in fed (B) and fasted (C) APAP dosed C57BL/6J and CD-1 mice. Hepatic mRNA levels are calculated using the comparative Ct values, assessing the fold change relative pooled control animals. *5-values of 5 h C57BL/6J was compared to 4 h CD-1 mice. Data is given as mean \pm SD (4 to 6 animals per group). ***P<0.005, **P<0.01 and *P<0.05.

3.3.7.2 Splenic transcription of TNF- α and IL-6

For the quantitative assessment of splenic TNF- α and IL-6 transcription levels at 5 and 24 hpd in C57BL/6J mice the fold change method was applied. At 5 hpd, no treatment induced fold changes were observed in either fed or fasted mice; this was also the case in fed mice at 24 hpd (Table 6.37). In contrast, a significant, up to 10-fold increase in splenic TNF- α transcription was observed in fasted mice at 24 hpd compared to fed control and APAP dosed mice (Table 6.37, Figure 3.3.23A). At 24 hpd, splenic TNF- α mRNA level was significantly higher in fasted than in fed mice

in both strains (Table 6.37), however, there was no difference between C57BL/6J mice and CD-1 in either the fed or fasted group (Figure 3.3.23B).

In contrast, IL-6 transcription was significantly upregulated in fed C57BL/6J mice at 5 hpd in comparison to control and fasted APAP dosed mice (Table 6.37). In fasted C57BL/6J mice, the IL-6 transcription was instead significantly upregulated at 24 hpd (8.6-fold), however, this upregulation was far less pronounced than that observed in fed C57BL/6J mice at 5 hpd (7.9-fold) (Figure 3.3.23C). Interestingly, by 24 hpd, it was also significantly (i.e. almost 4-fold) higher in the fed CD-1 mice, whereas in the fasted mice at this time point, IL-6 transcription was a significant 8.6-fold change higher than in the fed C57BL/6J mice and fasted CD-1 mice (Figure 3.3.23D).

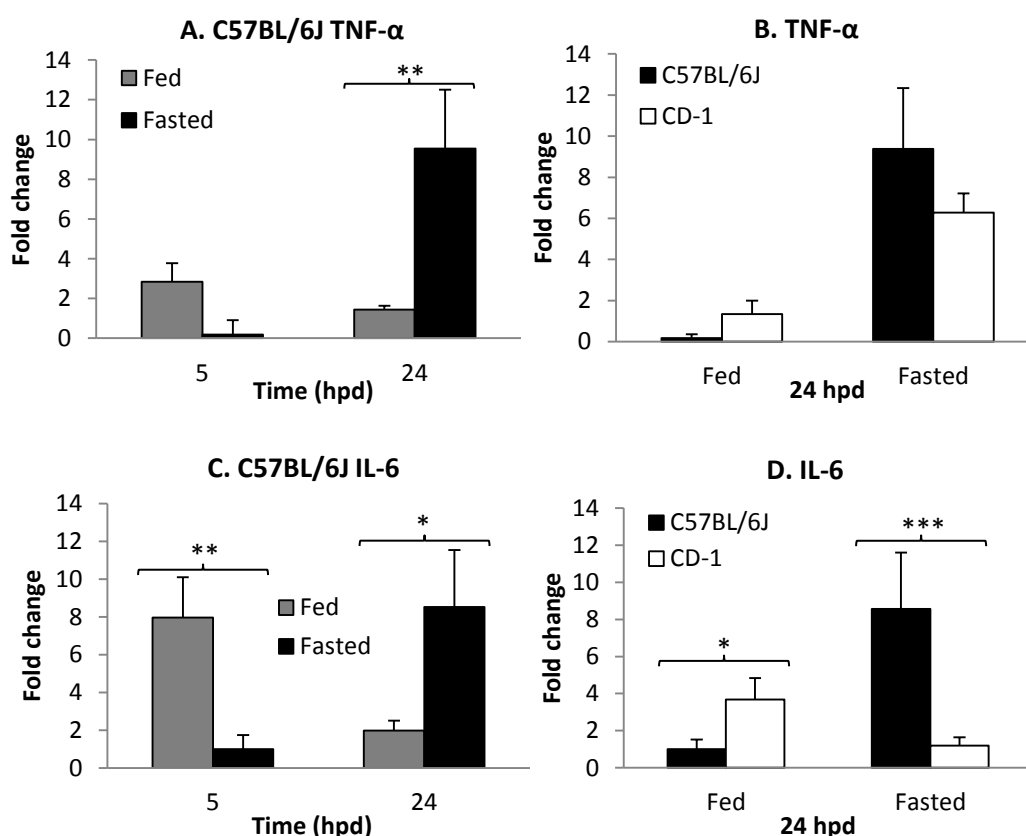


Figure 3.3.23. Fold change in splenic TNF- α and IL-6 transcription levels after APAP dosing in C57BL/6J mice and comparison to CD-1 mice.

Splenic TNF- α and IL-6 transcription levels were assessed after APAP (530 mg/kg) dosing of fed and fasted male C57BL/6J mice (A, C) at 5 and 24 hpd. Comparison of splenic TNF- α (B) and IL-6 (D) at 24 hpd in APAP dosed C57BL/6J and CD-1 mice. Hepatic mRNA levels are calculated using comparative Ct values, assessing fold change relative to time-matched control animals. Values were expressed as mean \pm SD (4 to 6 animals per group). *** P <0.005, ** P <0.01 and * P <0.05.

3.3.7.3 Serum TNF- α and IL-6 levels

Serum TNF- α and IL-6 levels were measured over a 0-36 hpd time course in both fed and fasted APAP dosed and time-matched (for 5-36 hpd) and pooled saline control C57BL/6J mice. In fed APAP dosed mice, **TNF- α level** increased steadily up to 10 hpd and then declined until the end of the experiment at 36 hpd; however, they were always significantly higher than in the time matched as well as in the pooled controls (Table 3.3.13, Figure 3.3.24A,B).

Table 3.3.13. TNF- α serum levels (pg/mL) in control and APAP treated **fed** C57BL/6J mice with p-value and comparison to levels in fed CD-1 mice.

Time (hpd)	Control		APAP		p-value control vs APAP	p-value APAP vs APAP	p-value vs fed APAP CD-1
	Mean	SD	Mean	SD			
0	-	-	22.86	6.95	-	1 h: 0.0095 3 h: 0.0001 5 h: 0.0004 10 h: 0.0001 15 h: 0.0037	-
0.5	-	-	20.14	3.65	-	20h: 0.0009 24h: 0.0005 30h: 0.0026 36h: 0.0069	-
1	-	-	39.01	2.69	-	3 h: 0.0008 10 h: 0.0009	-
3	-	-	67.52	9.07	-	10 h: 0.0057	-
5	3.3	2.09	74.37	7.13	0.0066	10 h: 0.004 30 h: 0.0418	NS
10	11.83	2.83	104.36	17.37	0.0094	20 h: 0.0234 36 h: 0.0069	-
15	14.58	3.25	94.75	31.70	0.0407	30 h: 0.042 36 h: 0.0228	-
20	15.50	2.01	72.13	10.31	0.0323	36 h: 0.0225	-
24	3.60	4.33	75.86	7.94	0.0250	30 h: 0.023 36 h: 0.006	NS
30	7.33	1.2	62.75	5.30	0.0171	36 h: 0.046	-
36	10.04	0.29	56.29	0.88	0.0078	0 h: 0.0005	-
Pooled control	11.09	3.12	-	-	1 h: 0.0480 3 h: 0.0125 5 h: 0.0109 10 h: 0.0012 15 h: 0.0073 20 h: 0.0052 24 h: 0.0066 30 h: 0.0207 36 h: 0.0195	-	-

hpd – hours post dosing; SD – standard deviation; NS – not significant.

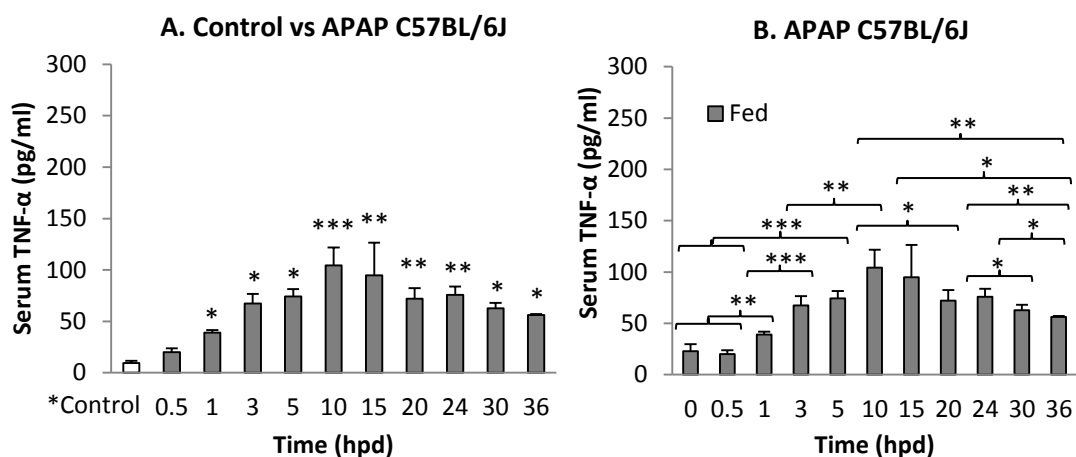


Figure 3.3.24. Serum TNF- α level in fed male C57BL/6J mice.

(A) Serum TNF- α levels at different time points after 0.9% saline (control) and 530mg/kg APAP administration to fed C57BL/6J mice. (B) Serum TNF- α level over 36 h post APAP dosing in fed C57BL/6J mice (as listed in Table 3.3.12). *Control – pooled control. Values were expressed as mean \pm SD (4 to 6 animals per group). ***P<0.005, **P<0.01 and *P<0.05.

In fasted APAP dosed mice, serum TNF- α level was also significantly higher than the time-matched and pooled control mouse values throughout the experiment (Table 3.3.14, Figure 3.3.25A). However, the time course differed from the one found in the fed APAP treated mice, as the serum TNF- α levels were increased, but remained similar between 3 and 15 hpd, afterwards showing a further, significant increase (up to 250 pg/mL) from 20 to 36 hpd (Figure 3.3.25B). At the latter time points, the serum TNF- α level of the fasted mice were significantly higher than those of the fed mice post APAP dosing (Figure 3.3.25C).

A comparison of the serum TNF- α level in fed and fasted, APAP dosed C57BL/6J and CD-1 mice at 5 and 24 hpd showed similar levels in both groups of mice (Figure 3.3.25D).

Table 3.3.14. TNF- α serum levels (pg/mL) in control and APAP treated **fasted** C57BL/6J mice with p-value and comparison to levels in fasted CD-1 mice.

Time (hpd)	Control		APAP		p-value control vs APAP	p-value APAP vs APAP	p-value fasted vs fed APAP	p-value vs fasted APAP CD-1
	Mean	SD	Mean	SD				
0	-	-	18.2	7.21	-	1 h: 0.0004	NS	-
0.5	-	-	20.31	6.41	-	36 h: 0.0002	NS	-
1	-	-	62.34	8.52	-	3 h: 0.0001	NS	-
3	-	-	145.32	17.84	-	3,5,10,15 h: NS (a)	NS	-
5	11.25	6.31	123.94	23.73	0.0001	0,0.5 h vs (a): 0.0053	NS	NS
10	26.29	5.89	122.17	18.85	0.0018	24 h: 0.0043	NS	-
15	21.25	8.13	144.04	26.93	0.0014	20 h: 0.0134 36 h: 0.0048	NS	-
20	13.83	2.01	212.00	5.30	0.0028	20,24,30,36 h: NS (b)	0.0093	-
24	20.33	5.1	249.81	39.55	0.0023	(a) vs (b): 0.034	0.0108	NS
36	25.36	5.65	226.86	22.12	0.0045	10 h: 0.0007	0.0024	-
Pooled control	19.37	5.80	-	-	1 h: 0.034 3 h: 0.0003 5 h: 0.0018 10 h: 0.0059 15 h: 0.0005 20 h: 0.0001 24 h: 0.0001 36 h: 0.0001	-	-	-

hpd – hours post dosing; SD – standard deviation; NS – not significant.

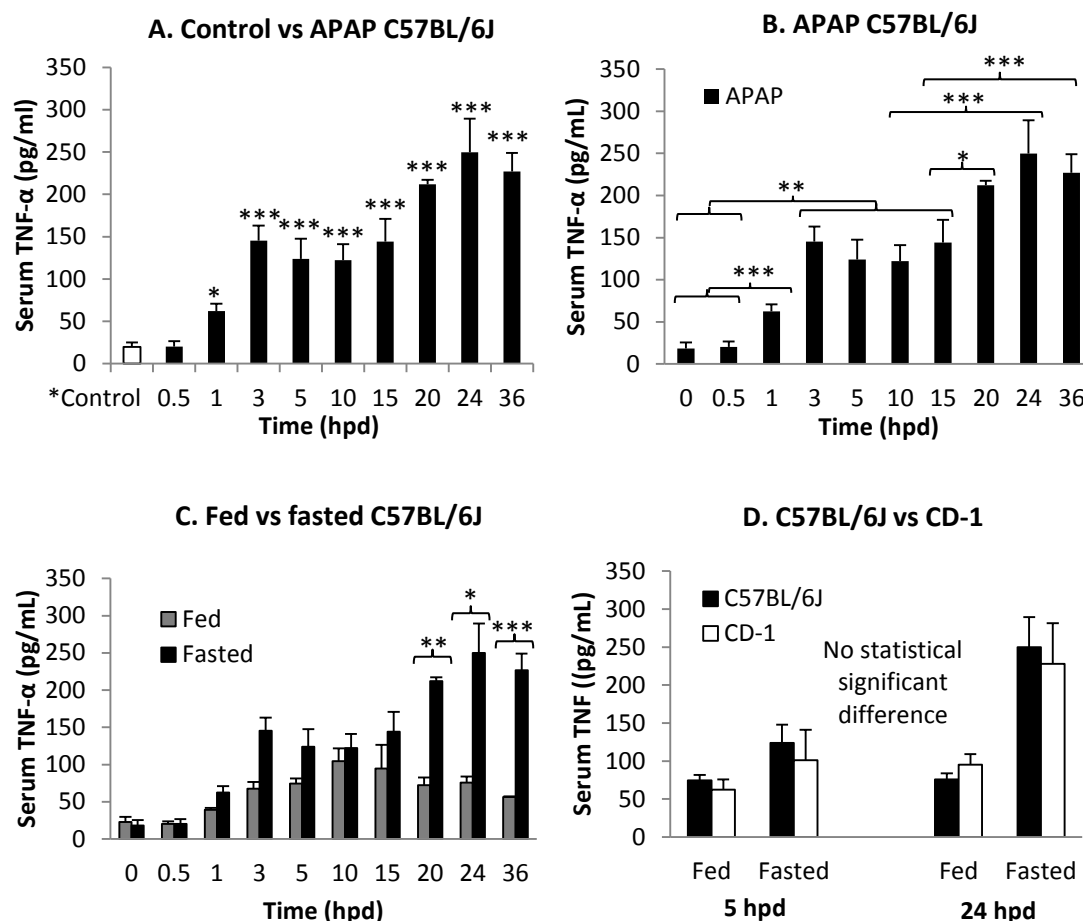


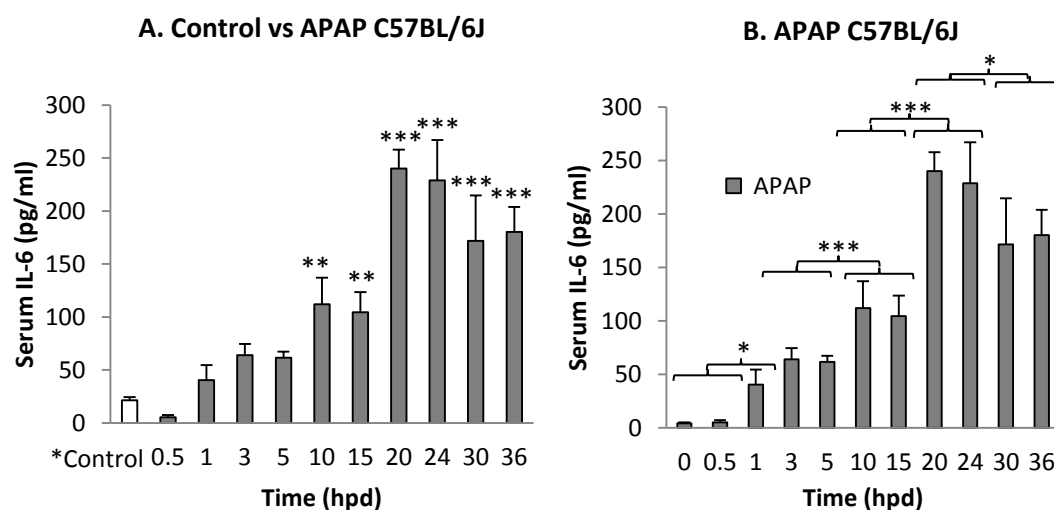
Figure 3.3.25. Serum TNF- α level in C57BL/6J mice, and comparison to CD-1 mice. (A) Serum TNF- α level at different time points after 0.9% saline (control) and 530 mg/kg APAP administration in fasted male C57BL/6J mice. (B) Serum TNF- α level over 36 h post APAP dosing in fasted C57BL/6J mice. (C) Comparison to fed APAP dosed C57BL/6J mice. Comparison of serum TNF- α level in fed and fasted APAP dosed C57BL/6J and CD-1 mice (D) (as listed in Table 3.3.13). *Control – pooled control. Values were expressed as mean \pm SD (4 to 6 animals per group). *** $P < 0.005$, ** $P < 0.01$ and * $P < 0.05$.

Similar to serum TNF- α levels, serum **IL-6 levels** were also significantly increased in comparison to time matched and pooled control mice over the entire time course (Table 3.3.15, Figure 3.3.26A). They reached a peak at 20 and 24 hpd, being twice as high as at 10 and 15 hpd before a slight drop was seen at 30 and 36 hpd (Figure 3.3.26B). Fed treated C57BL/6J mice showed a similar serum IL-6 profile to CD-1 mice at 5 and 24 hpd (Table 3.3.15, Figure 3.3.27D).

Table 3.3.15. IL-6 serum levels (pg/mL) in control and APAP treated **fed** C57BL/6J mice with p-value and comparison to levels in fed CD-1 mice.

Time (hpd)	C57BL/6J					CD-1		
	Control		APAP		p-value control vs APAP	p-value APAP vs APAP	APAP Mean (SD)	p-value vs APAP C57BL/6J
	Mean	SD	Mean	SD				
0	-	-	4.15	1.02	-	1 h: 0.031	-	-
0.5	-	-	5.32	2.1	-	3, 5 h: 0.0019	-	-
1	-	-	40.49	14.21	-	3 h: 0.0405	-	-
3	-	-	64.02	10.63	-	10, 15 h: 0.0010	-	-
5	-	-	61.69	5.75	-	20, 24 h: 0.0003	54.3 (10.2)	NS
10	23.24	5.24	111.9	25.19	0.0314	20, 24 h: 0.0046	-	-
15	25.62	4.58	104.53	19.07	0.0164	30, 36 h: 0.0232	-	-
20	27.52	3.2	240.02	17.92	0.0001	0, 0.5 h: 0.0001 30, 36 h: 0.0457	-	-
24	14.2	3.8	228.83	38.25	0.0004		203 (39.6)	NS
30	17.05	0.95	171.71	42.96	0.0026	3, 5 h: 0.0002	-	-
36	20.3	0.6	180.14	23.72	0.0009	10, 15 h: 0.0051	-	-
Pool ed control	20.03	3.16	-	-	10 h: 0.0069 15 h: 0.0092 20 h: 0.0001 24 h: 0.0007 30 h: 0.0012 36 h: 0.0001	-	-	-

hpd - hours post dosing; SD - standard deviation; NS – not significant.

**Figure 3.3.26.** Serum IL-6 levels in fed male C57BL/6J mice.

(A) Serum IL-6 levels at different time points after 0.9% saline (control) and 530 mg/kg APAP administration to fed C57BL/6J mice. (B) Serum IL-6 levels over 36 h post APAP dosing in fed C57BL/6J mice (as listed in Table 3.3.15). *Control – pooled control. Values were expressed as mean±SD (4 to 6 animals per group). ***P<0.005, **P<0.01 and *P<0.05.

In fasted C57BL/6J mice, serum IL-6 levels were significantly increased in comparison to levels in time matched control animals from 15 hpd onwards, in comparison to pooled control animal levels from 20 hpd (Table 3.3.16, Figure 3.3.27A), showing similar levels between 1 and 15 hpd, and another, but significantly higher level plateau between 20 and 36 hpd (Figure 3.3.27B).

Overall, serum IL-6 levels were lower in fasted than in fed APAP dosed mice, with a significant difference at 15, 20 and 24 hpd (Figure 3.3.27C). Also, fasted mice did not show an obvious peak level throughout the experiment. Similarly, fasted treated C57BL/6J and CD-1 mice also showed a similar serum IL-6 profile at 5 and 24 hpd (Figure 3.3.27D).

Table 3.3.16. IL-6 serum levels (pg/mL) in control and APAP treated **fasted** C57BL/6J mice with p-value and comparison to levels in fasted CD-1 mice.

Time (hpd)	C57BL/6J						CD-1		
	Control		Fasted APAP		p-value control vs APAP	p-value APAP vs APAP	p-value fasted vs fed	Mean (SD) APAP	p-value vs fasted APAP C57BL/6J
	Mean	SD	Mean	SD					
0	-	-	17.25	5.62	-	1,3 h: 0.026	NS	-	-
0.5	-	-	19.21	6.51	-		NS	-	-
1	-	-	43.75	8.63	-	5,10, 15 h: NS 20,24 h: 0.0035 36 h: 0.0055	NS	-	-
3	-	-	41.28	10.65	-		NS	-	-
5	-	-	56.29	12.34	-	0,0.5 h: 0.0031	NS	35.4 (10.5)	NS
10	15.63	4.59	40.25	34.94	NS	-	NS	-	-
15	21.45	3.15	52.08	15.35	0.0057	20,24,36 h: 0.0177	0.027	-	-
20	19.46	5.92	103.15	23.24	0.0003	0,0.5 h: 0.0002 1,3 h: 0.0009	0.002	-	-
24	24.51	8.1	94.31	35.72	0.0019	5 h: 0.0016	0.001	96.4 (35.2)	NS
36	16.95	2.88	130.88	51.2	0.0045	20,24 h: NS 1,3 h: 0.0007	NS	-	-
Pooled control	19.29	5.14	-	-	20 h: 0.0029 24 h: 0.0044 36 h: 0.0007	-	-	-	-

hpd - hours post dosing; SD - standard deviation; NS – not significant.

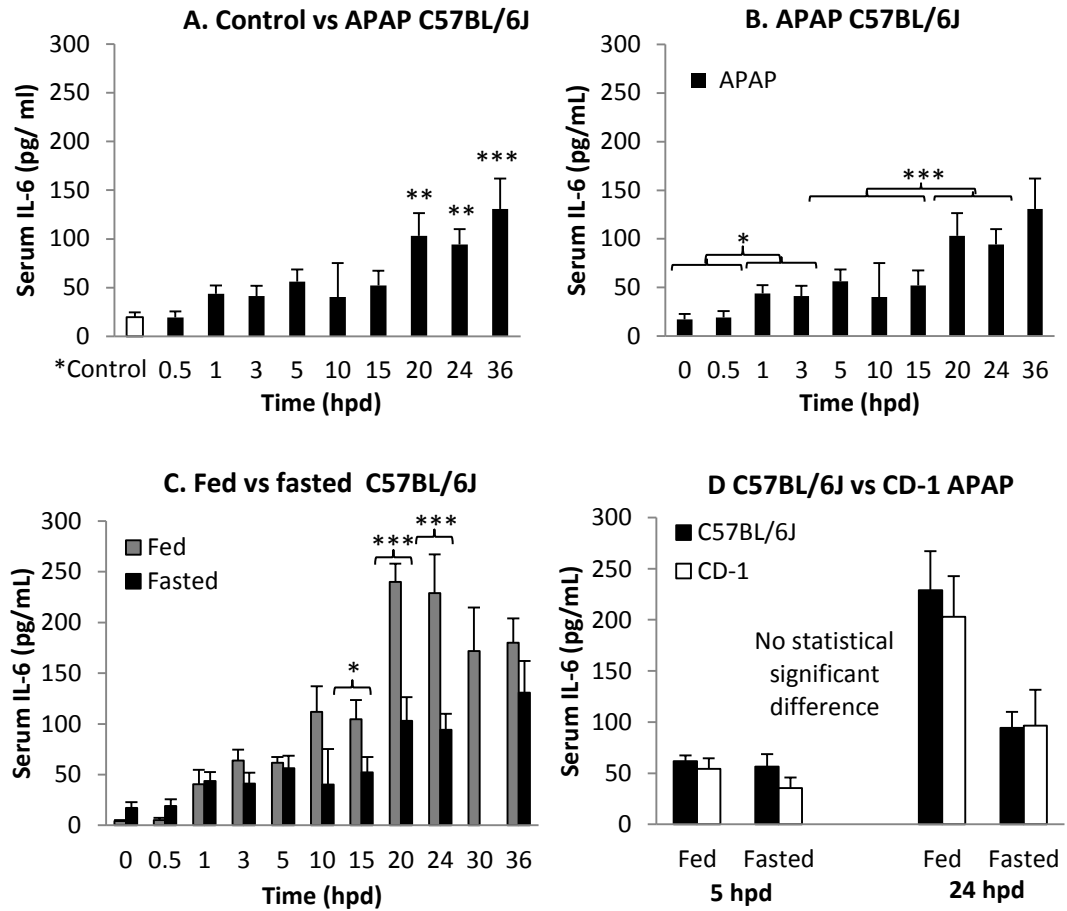


Figure 3.3.27. Serum IL-6 levels in C57BL/6J mice, and comparison to CD-1 mice. (A) Serum IL-6 levels at different time points after 0.9% saline (control) and 530 mg/kg APAP administration in fasted male C57BL/6J mice. (B) Serum TNF- α level over 36 h post APAP dosing in fasted C57BL/6J mice. (C) Comparison to fed APAP dosed C57BL/6J mice. Comparison of serum TNF- α level in fed and fasted APAP dosed C57BL/6J and CD-1 mice (D) (as listed in Table 3.3.16). *Control – pooled control. Values were expressed as mean \pm SD (4 to 6 animals per group). *** P <0.005, ** P <0.01 and * P <0.05.

3.3.8 Assessment of liver regeneration based on hepatocellular proliferation

3.3.8.1 Hepatic NF- κ B mRNA transcription

There was an upregulation of hepatic NF- κ B at later time points both in fed and fasted mice when assessing transcription levels of NF- κ B by delta Ct method (Figure 3.3.31A,B).

When the fold change was used as a basis for the statistical evaluation, a significant increase in NF- κ B transcription was observed in fed APAP dosed C57BL/6J mice compared to **time-matched control** animals; this was, for example, 2.7-fold at 5 hpd, 5.7-fold at 10 hpd, 6.9-fold at 15 hpd and still 4.7-fold at 36 hpd (Table 6.38, Figure 3.3.31C). In fasted APAP dosed mice, significant upregulation of the NF- κ B transcription in comparison to control animals was seen from 15 until 36 hpd (Figure 3.3.31D). However, transcription levels were significantly higher in the fed animals when levels peaked at 10 and 15 hpd (Table 6.38, Figure 3.3.31E).

The comparison of NF- κ B transcription levels in fed APAP dosed C57BL/6J and CD-1 mice showed a significantly more intense upregulation in CD-1 mice at 10, 15, 20 and 24 hpd (Figure 3.3.32A). In the fasted APAP dosed mice, however, transcription levels were slightly higher in the CD-1 mice, though never with a significant difference (Table 6.38, Figure 3.3.32B).

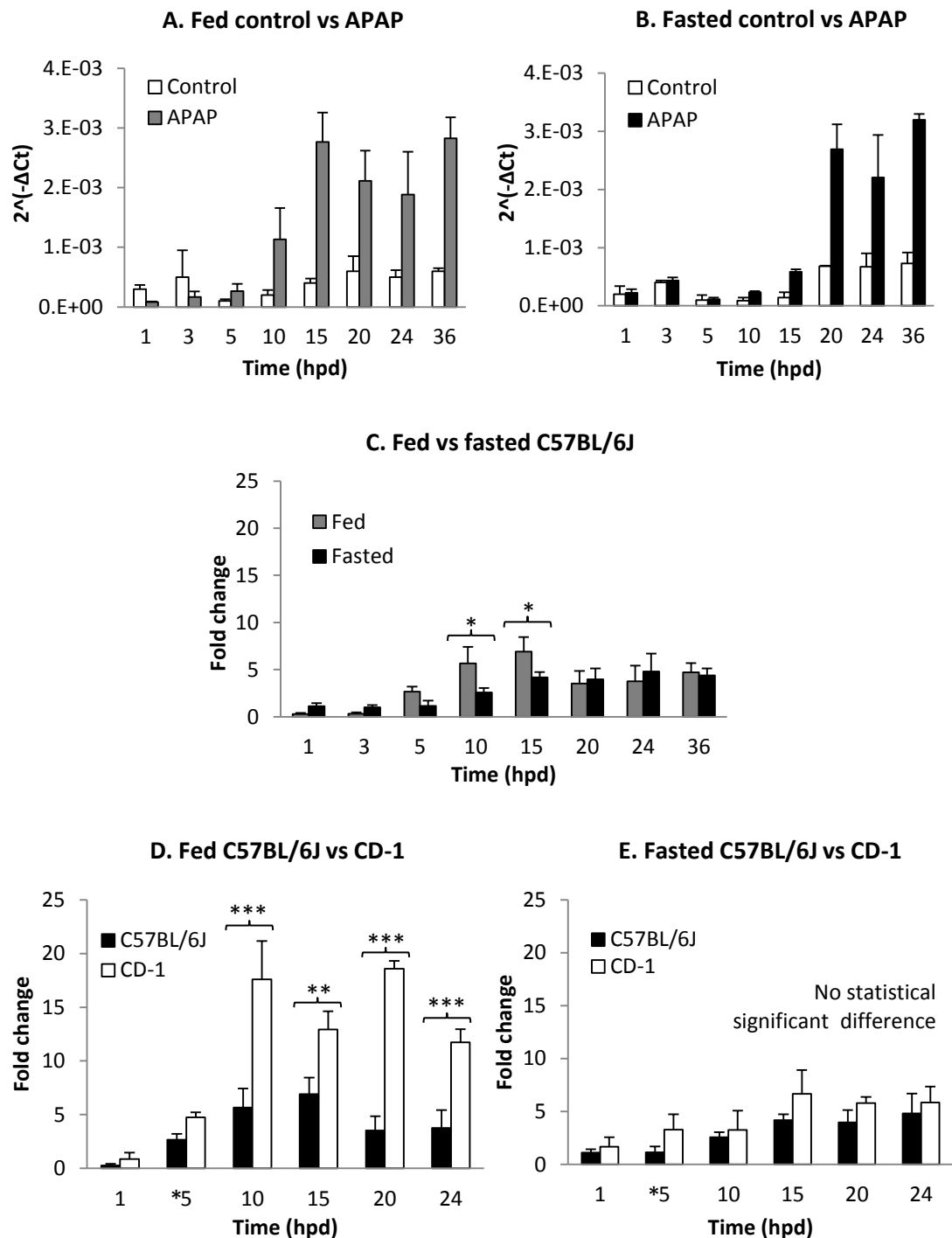


Figure 3.3.28. Hepatic NF- κ B transcription in fed and fasted C57BL/6J mice and comparison to CD-1 mice.

Hepatic NF- κ B transcription levels in (A) fed and (B) fasted control and APAP dosed C57BL/6J mice were determined using the delta Ct value, $2^{-\Delta Ct}$. The hepatic NF- κ B mRNA levels were also calculated in fed and fasted C57BL/6J mice (C), using the comparative Ct value method, assessing the fold change relative to time-matched control animals. The levels were also compared in fed (D) and fasted (E) APAP dosed C57BL/6J and CD-1 mice. Values were expressed as mean \pm SD (4 to 6 animals per group). *** $P < 0.005$, ** $P < 0.01$ and * $P < 0.05$. *5- values of 5 h C57BL/6J was compared to 4 h CD-1 mice.

The values in APAP dosed mice were also compared to **pooled control** animal values as we did not recognise any differences in controls over the time course (see Chapter 3.1.8.1). In fed mice, similar to Figure 3.3.28D, the upregulation of hepatic NF- κ B mRNA transcription was significant from 10 hpd onwards, in fasted mice the upregulation was significant from at 20 hpd onwards (Table 6.39). The comparison of fed and fasted animals showed similar results as seen with the time matched controls (Table 6.39, Figure 3.3.29A; see also Figure 3.3.28C). The findings were also compared to CD-1 mice. The latter had higher levels throughout, and the difference was significant in fed mice at 10 (2.8-fold in C57BL/6J vs 13.3-fold in CD-1 mice) and 20 hpd (5.3-fold in C57BL/6J vs 9.5-fold in CD-1 mice) (Table 6.39, Figure 3.3.29A), whereas no significant differences were seen in fasted mice at any time post APAP dosing (Figure 3.3.29B).

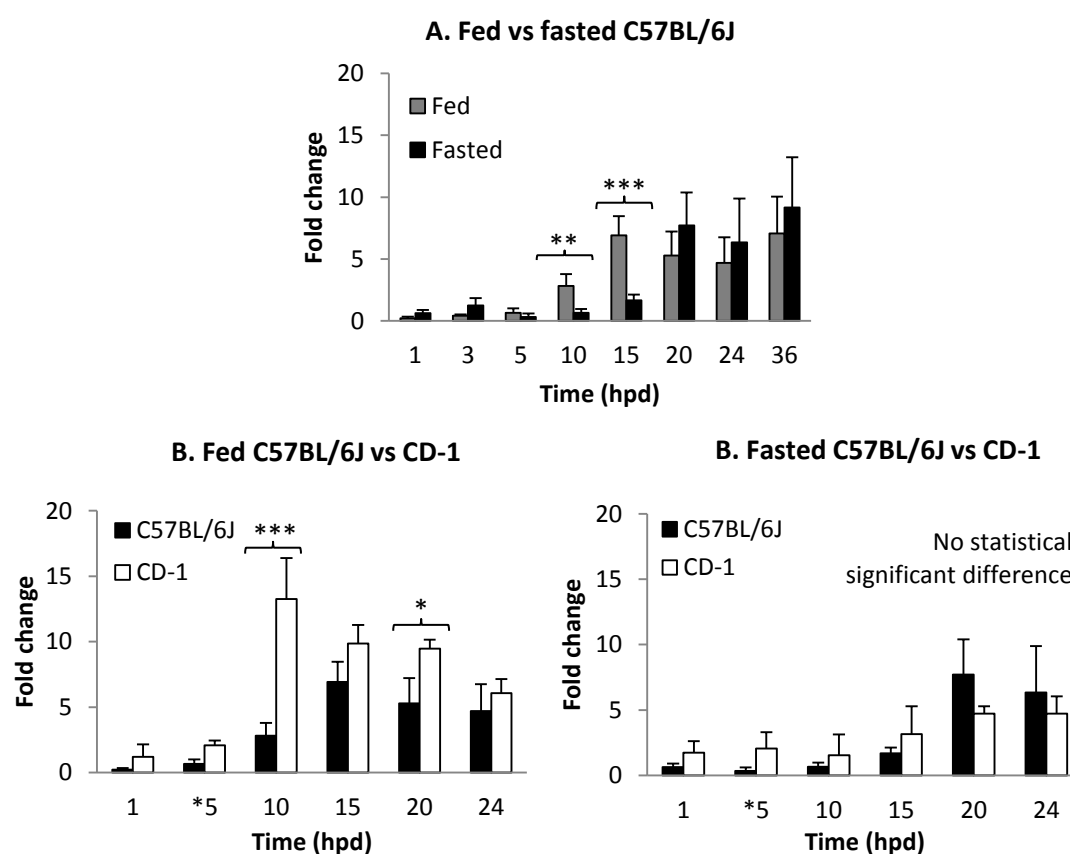


Figure 3.3.29. Hepatic NF- κ B transcription in APAP dosed male C57BL/6J mice.

Hepatic NF- κ B transcription levels were determined after 530 mg/kg APAP administration in fed and fasted C57BL/6J mice (A). Comparison of fed (B) and fasted (C) APAP dosed C57BL/6J and CD-1 mice. Hepatic mRNA levels are calculated using the comparative Ct values, assessing the fold change relative to pooled control animals. Data is given as mean \pm SD (4 to 6 animals per group). *** P <0.005, ** P <0.01 and * P <0.05. *5- values of 5 h C57BL/6J was compared to 4 h CD-1 mice.

3.3.8.2 Hepatic cyclin-D1 transcription

By delta Ct method, fed APAP dosed mice generally showed higher cyclin-D1 mRNA levels than time-matched control mice from 15 hpd onwards (Figure 3.3.30A). In fasted mice, a peak was seen at 36 hpd (Table 6.40, Figure 3.3.30B).

Using comparison of the delta Ct method, in **fed APAP dosed C57BL/6J** mice, upregulation of cyclin-D1 transcription was seen from 5 hpd onwards, with a significant difference to control mice at the later time points, i.e. 15 hpd (9-fold), 20 hpd (6-fold), 24 hpd (6.6-fold) and 36 hpd (5.4-fold) (Table 6.40).

In **fasted mice**, the difference to control mice was significant at 24 hpd (3.2-fold) and 36 hpd (4.6-fold) (Figure 3.35D). In general, however, mRNA levels were lower in the fasted mice, and the difference was significant at 10 to 24 hpd (Table 6.40).

A comparison of the cyclin-D1 transcription in fed and fasted APAP dosed C57BL/6J and CD-1 mice showed an overall higher fold change in CD-1 mice (Figure 3.3.30C). In the fed animals, the difference was significant at 4/5 hpd (8.6-fold), at 20 hpd (16-fold), when a peak was seen in the CD-1 mice, and at 24 hpd (12.4-fold) (Table 6.40, Figure 3.3.30D). In the fasted mice, it was significant between 15 hpd (6-fold) and 24 hpd (7.6-fold) (Figure 3.3.30E).

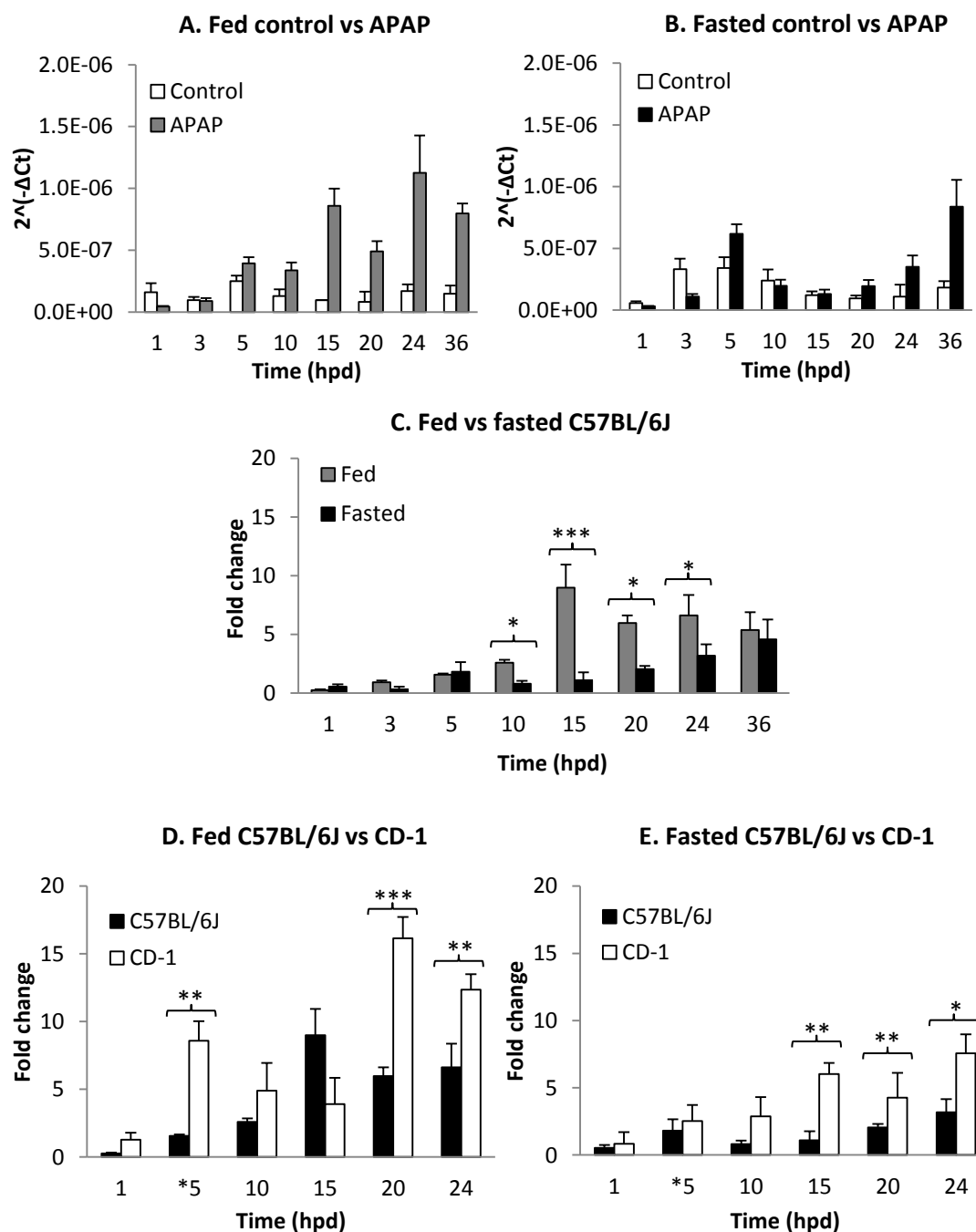


Figure 3.3.30. Hepatic cyclin-D1 transcription in fed and fasted C57BL/6J mice and comparison to CD-1 mice.

Hepatic cyclin-D1 transcription levels in (A) fed and (B) fasted control and APAP dosed C57BL/6J mice were determined using the delta Ct value, $2^{-\Delta Ct}$. The hepatic cyclin-D1 mRNA levels were also calculated in fed and fasted C57BL/6J mice (C), using the comparative Ct value method, assessing the fold change relative to time-matched control animals. The levels were also compared in fed (D) and fasted (E) APAP dosed C57BL/6J and CD-1 mice. Values were expressed as mean \pm SD (4 to 6 animals per group). *** P <0.005, ** P <0.01 and * P <0.05. *5- values of 5 h C57BL/6J was compared to 4 h CD-1 mice.

As no differences in cyclin-D1 mRNA levels were observed in control animals over the entire time course (see Chapter 3.1.8.1), all saline dosed animal values were gathered as pooled control values. This approach confirmed the previous results, whereas in fasted mice, only the 36 hpd level was found to be significantly higher with this approach (Table 6.41). The comparison of fed and fasted APAP dosed mice recognised statistical difference at 15, 20 and 24 hpd only (Table 6.41, Figure 3.3.31A). The hepatic cyclin-D1 mRNA levels in APAP dosed CD-1 mice were significantly higher at 4/5 hpd (8.1-fold), 10 and 20 hpd in fed animals (Table 6.41, Figure 3.3.31B) and at 15 (9-fold) to 24 hpd in fasted animals than those in C57BL/6J mice (Figure 3.3.31C).

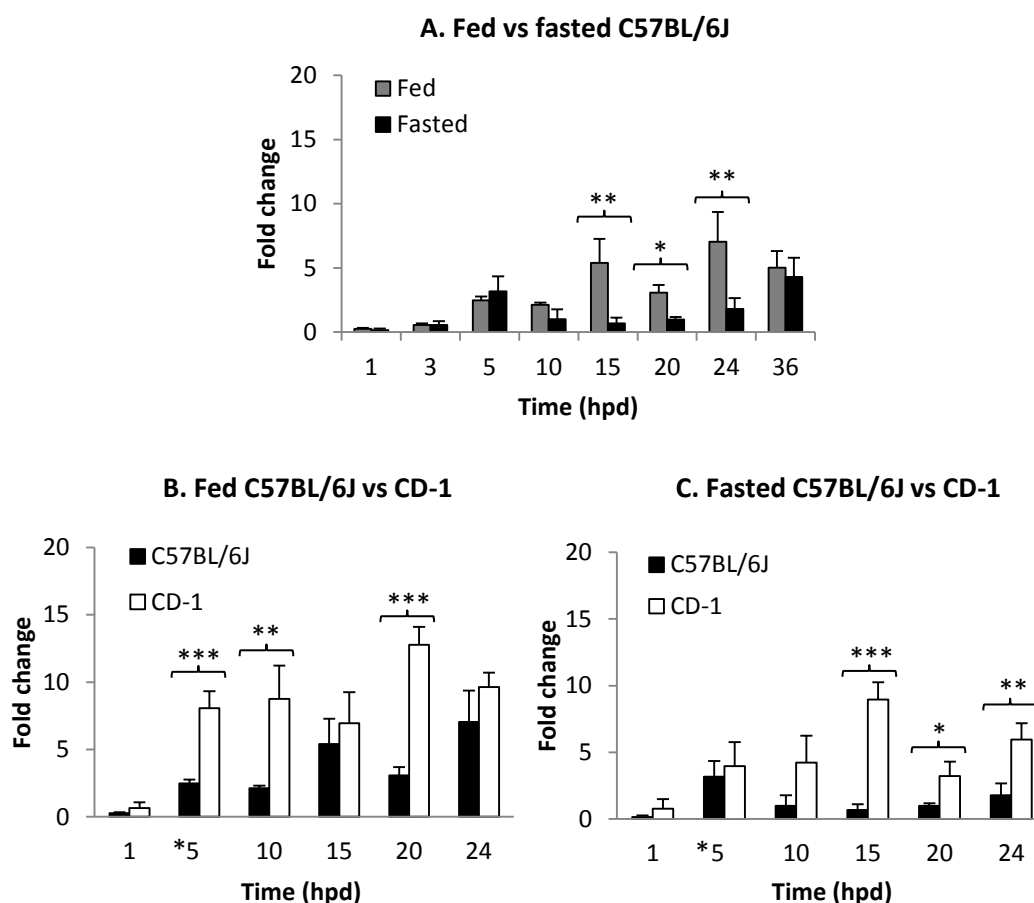


Figure 3.3.31. Hepatic cyclin-D1 transcription in APAP dosed C57BL/6J mice and comparison to CD-1 mice.

Hepatic cyclin-D1 transcription levels were determined after 530 mg/kg APAP administration between fed and fasted APAP dosed male CD-1 mice (A). The levels were compared in fed (B) and fasted (C) APAP dosed C57BL/6J and CD-1 mice. Hepatic mRNA levels are calculated using the comparative Ct values, assessing the fold change relative to pooled control animals. Data is given as mean \pm SD (4 to 6 animals per group). ***P<0.005, **P<0.01 and *P<0.05. *5- values of 5 h C57BL/6J was compared to 4 h CD-1 mice.

3.3.8.3 Assessment of hepatocyte proliferation based on the immunohistological expression of PCNA

In C57BL/6J mice, the potential changes in the number of proliferating PCNA-positive hepatocytes were assessed in APAP dosed mice at 5 to 36 hpd. In **fed APAP dosed C57BL/6J mice**, the number of PCNA-positive proliferating hepatocytes was found to rise steadily after 5 hpd, at 10 to 36 hpd, when it reached a peak with around 25% positive cells (Table 3.3.17). In **fasted APAP dosed mice**, an increase was only seen from 20 hpd onwards, and it was significant compared to controls from then until 36 hpd (Table 3.3.17). However, the extent of the increase was less intense in fasted mice, with a significant difference in the number of PCNA-positive cells from 15 to 36 hpd (Table 3.3.17, Figure 3.3.33A).

Table 3.3.17. Range and average amount (%) of PCNA-positive, proliferating cells in fed control mice at 0 h and in APAP dosed C57BL/6J mice at different time points post dosing. The values were also compared to those obtained in CD-1 mice.

Time (hpd)	Fed			Fasted			p-value fed vs fasted C57BL/6J
	Mean (SD)	p-value APAP C57BL/6J	p-value C57BL/6J vs CD-1	Mean (SD)	p-value APAP C57BL/6J	p-value C57BL/6J vs CD-1	
Control 0	2.21 (1.41)	-	(NS)	1.18 (0.47)	-	(NS)	NS
5	2.11 (1.79)	15 h: 0.016	0.0008 ↑	1.20 (0.3)	20 h: 0.027	NS	NS
10	5.53 (1.22)		NS	2.84 (2.26)	24 h: 0.013	NS	NS
15	8.04 (1.67)	20 h: 0.018	NS	1.02 (0.13)	20 h: 0.025	0.014 ↑	0.0159
20	19.53 (0.76)	5 h: 0.029	0.0009 ↓	5.98 (2.4)	24 h: NS	NS	0.0007
24	23.15 (1.95)	15 h: 0.025	NS	13.02 (6.55)	5 h: 0.0092 15 h: 0.0098	NS	0.0493
36	24.97 (7.49)	15 h: 0.014	24 h: NS	12.7 (2.68)	5 h: 0.034 10 h: 0.029 15 h: 0.034	24h (24): 0.0411 ↓ 24h (16): 0.0472 ↓	0.0419

(NS) - p-value of 0 h C57BL/6J vs pooled control values of all time points in CD-1; hpd – hours post dosing; SD – standard deviation; 24h (24) – 24 h fasting period at 24 hours post dosing; 24h (16) – 16-h fasting period at 24 hours post dosing.

The results were then compared to CD-1 mice (see Chapter 3.2.8.3). By 24 hpd, amount of PCNA expressing hepatocytes were higher in fed in both strains (Figure 3.3.32). Fed and fasted mice of both strains showed significantly higher amounts of PCNA-positive hepatocytes in the fed CD-1 mice at 5 hpd. However, it needs to be noted that the number of PCNA-positive hepatocytes was also higher in the controls (see Chapter 3.1.8.2, Table 3.1.16). At 10 and 15 hpd, the amounts were similar to those in the fed C57BL/6J mice in which no substantial increase had so far been seen. At the later time points (20 and 24 hpd), the amount of proliferating cells was higher in the C57BL/6J mice, although a significant difference was only seen at 20 hpd (Figure 3.3.33B). In fasted mice, the amount was similarly low in both groups of mice up to 10 hpd. At 15 and 20 hpd, it was higher in the CD-1 mice, with a significant difference at 15 hpd. At 24 hpd, the amount was higher in the C57BL/6J mice, though without a significant difference (Table 3.3.17, Figure 3.3.33C).

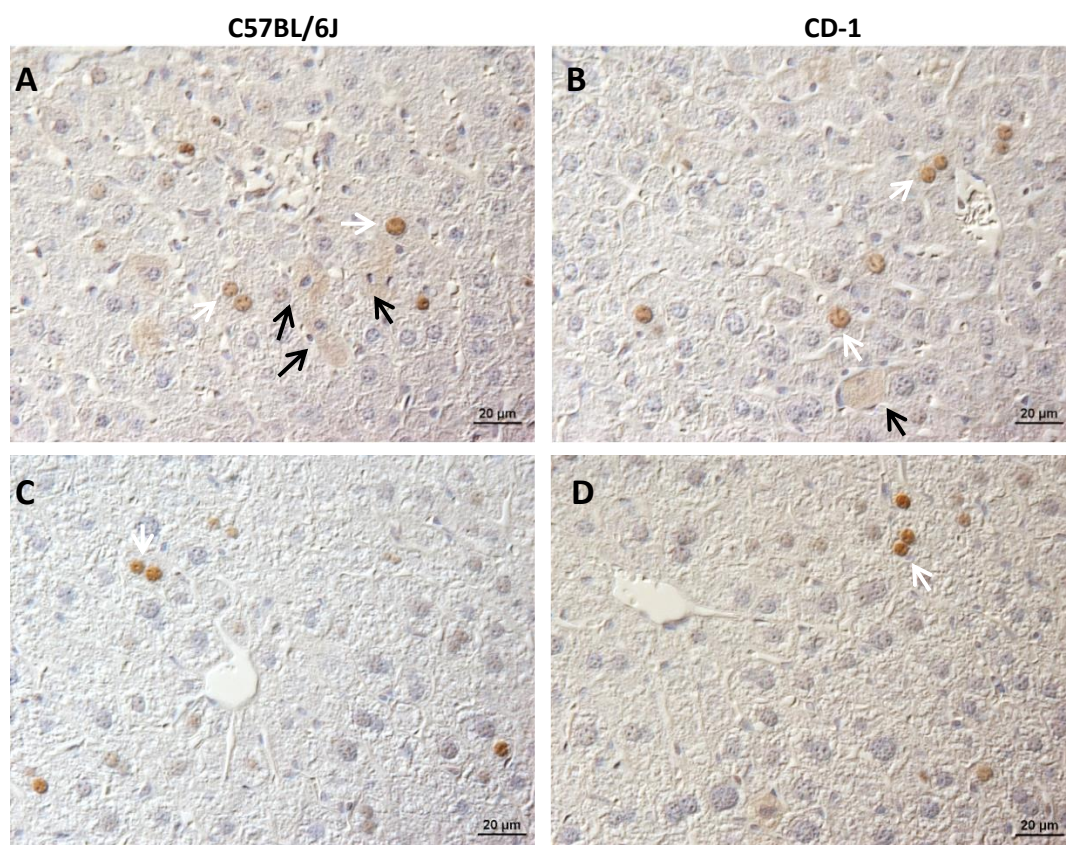


Figure 3.3.32. Immunohistological demonstration of PCNA expression in the liver of fed and fasted male C57BL/6J and CD-1 mice at 24 hpd.

In fed mice, a large number of hepatocytes exhibit nuclear (white arrows) and cytoplasmic (black arrows) PCNA expression in both C57BL/6J (A) and CD-1 (B) mice. In fasted mice the amounts of PCNA-positive hepatocytes were much lower in both strains (C, D). PAP method, Papanicolaou's haematoxylin counterstain. Magnification 400x.

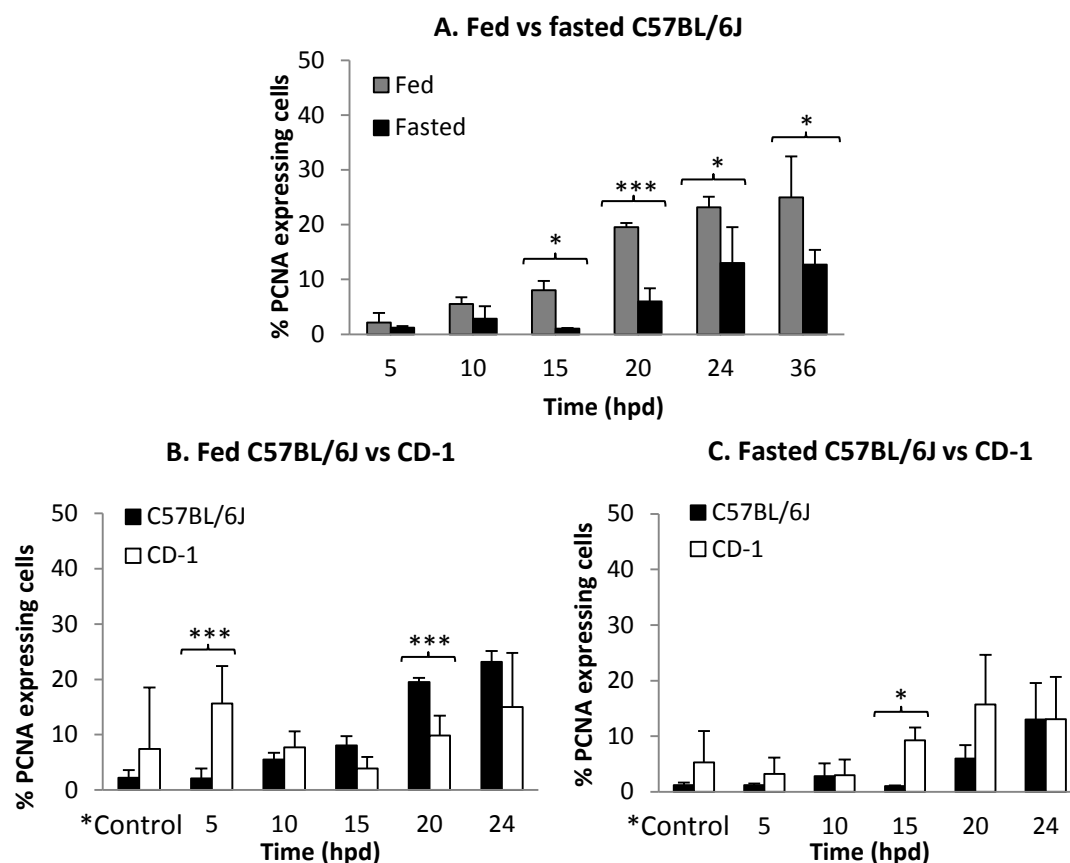


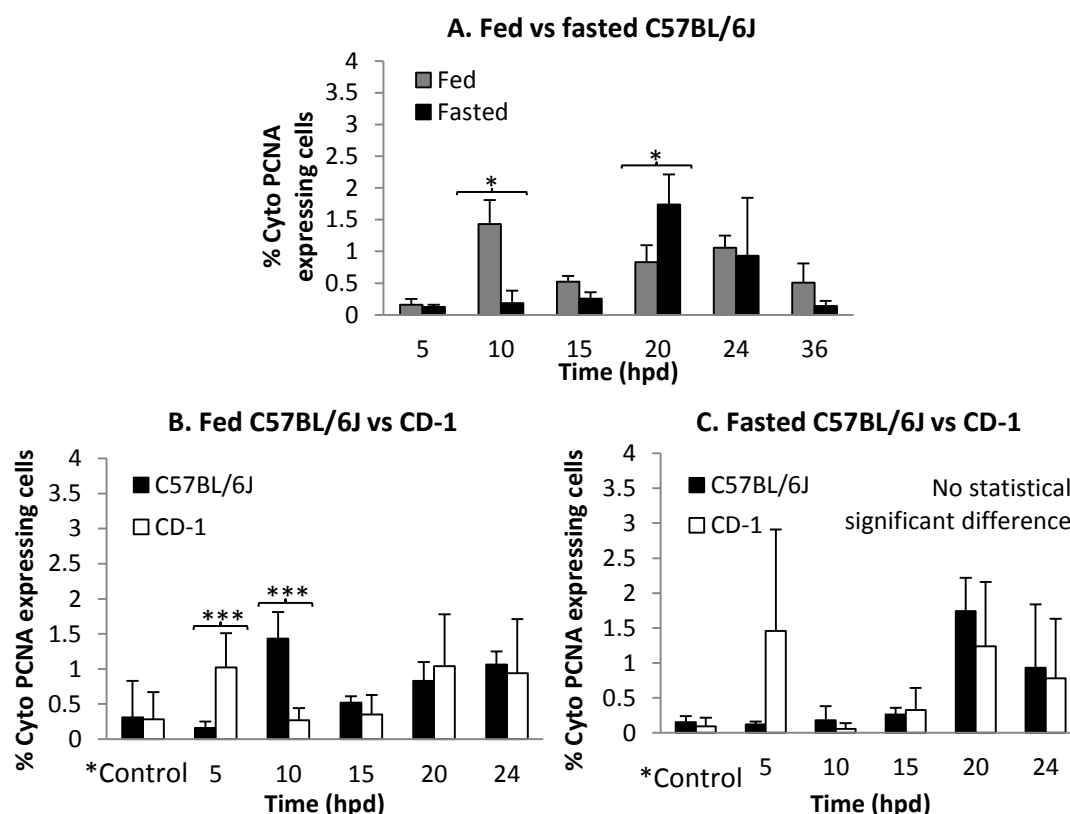
Figure 3.3.33. Assessment of proliferating hepatocytes, based on the expression of proliferating cell nuclear antigen (PCNA) and comparison to CD-1 mice. Quantification (percentage) of PCNA-positive hepatocytes (nuclear and cytoplasmic expression) in fed and fasted APAP dosed C57BL/6J mice (A). Percentages of PCNA-positive hepatocytes in fed (A) and fasted (B) C57BL/6J and CD-1 mice (as listed in Table 3.3.17). Data represent means \pm SD (4 to 6 animals per group). *** P <0.005, ** P <0.01 and * P <0.05.

Over the entire time course, the amount of hepatocytes with cytoplasmic PCNA expression (i.e. cells in the G2 or M phase) did not vary significantly in fed APAP dosed C57BL/6J mice in comparison to saline dosed mice (0 hour) (Table 3.3.18, Figure 3.3.34A). In fasted C57BL/6J mice, however, a significant increase (up to 2% positive cells) was seen at 20 hpd, but the numbers dropped thereafter (Figure 3.3.34B). In comparison, the fed mice exhibited a significantly higher number of hepatocytes with cytoplasmic PCNA expression at 10 hpd, whereas the number was significantly higher in the fasted C57BL/6J mice at 20 hpd (Figure 3.3.34C). There was no statistical significant difference in the amount of hepatocytes with cytoplasmic PCNA expression between fed and fasted APAP dosed C57BL/6J and CD-1 mice with the exception of the 5 hpd time point in the fed mice, where the number was significantly higher in the CD-1 mice, and at 10 hpd, when it was significantly lower (Table 3.3.18).

Table 3.3.18. Average amount (%) of hepatocytes with cytoplasmic PCNA expression in fed and fasted APAP dosed male C57BL/6J mice and comparison to the amount in CD-1 mice.

Time (hpd)	Fed			Fasted			p-value fed vs fasted C57BL/6J
	Mean (SD)	p-value APAP C57BL/6J	p-value C57BL/6J vs CD-1	Mean (SD)	p-value APAP C57BL/6J	p-value C57BL/6J vs CD-1	
Control 0	0.31 (0.52)	All NS at any time points	NS	0.15 (0.09)	-	NS	NS
5	0.16 (0.09)		0.0008 ↑	0.12 (0.04)	20 h: 0.0063	NS	NS
10	1.43 (0.38)		0.0021 ↓	0.18 (0.2)	20 h: 0.0088	NS	0.013
15	0.52 (0.09)		NS	0.26 (0.1)	20 h: 0.0069	NS	NS
20	0.83 (0.27)		NS	1.74 (0.48)	36 h: 0.0061	NS	0.0222
24	1.06 (0.19)		NS	0.93 (0.91)	-	NS	NS
36	0.51 (0.30)		-	0.14 (0.08)	-	-	NS

hpd – hours post dosing; SD – standard deviation; NS – not significant.

**Figure 3.3.34.** Assessment of hepatocytes exhibiting cytoplasmic PCNA expression and comparison to CD-1 mice.

Quantification % of cytosolic PCNA expressing hepatocytes in fed and fasted APAP dosed male C57BL/6J mice (A) (as listed in Table 3.3.18). Percentages of cytoplasmic PCNA-positive hepatocytes in fed (A) and fasted (B) C57BL/6J and CD-1 mice following APAP dosing. *Control – C57BL/6J at 0 hpd, CD-1 is pooled control (0+10 h post saline). Data represent means±SD (4 to 6 animals per group). ***P<0.005, **P<0.01 and *P<0.05.

The time course of PCNA expression in C57BL/6J and CD-1 mice was compared to identify any differences in the length of the cell cycle and the onset of proliferation after APAP dosing. In fed APAP dosed CD-1 mice, a first peak of PCNA expression was seen at 5 hpd, with a second peak at 24 hpd, suggesting a cell cycle of approximately 19 hours (Figure 3.3.35A). As C57BL/6J mice showed a progressive increase of overall PCNA expression, it is difficult to define the onset of proliferation (Figure 3.3.35C). Only at 10 hpd, cytoplasmic PCNA expression was significantly higher in the C57BL/6J mice, whereas it was significantly higher in the CD-1 mice at 5 hpd, before both were similar again at 15 hpd and thereafter (Figure 3.3.35B). However, PCNA-positive hepatocytes increased later in fasted than in fed mice, with a first peak at 20 hpd. Although PCNA expressions follow each other in both strains, the percentages of PCNA-positive cells in C57BL/6J mice seem to increase later and were significantly lower than in the CD-1 mice at 15 hpd (Figure 3.3.35C). Moreover, we observed that the cytoplasmic PCNA expression in fasting mice started to rise at later time points, with same levels in both strains (Figure 3.3.35D).

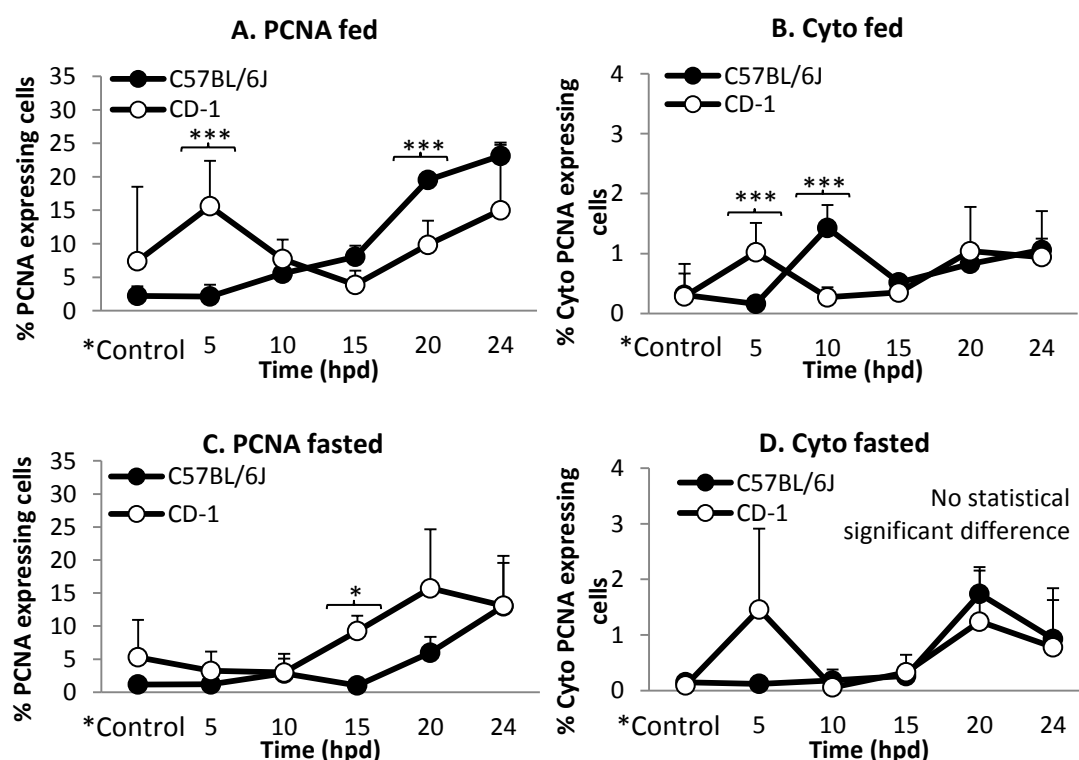


Figure 3.3.35. Assessment of hepatocytes exhibiting PCNA and cytoplasmic PCNA expression in C57BL/6J and CD-1 mice after APAP dosing.

Quantification % of overall and cytoplasmic PCNA-positive hepatocytes in fed (A, C) and fasted (B, D) C57BL/6J and CD-1 mice after APAP dosing. *Control – C57BL/6J at 0 hpd, CD-1 is pooled control (0+10 h post saline). Data represent means \pm SD (4 to 6 animals per group). *** P <0.005, ** P <0.01 and * P <0.05. Cyto – cytoplasmic.

3.3.9 Overall assessment of liver regeneration in C57BL/6J and CD-1 mice

The extent of liver regeneration following APAP overdose in C57BL/6J and CD-1 mice was comparatively assessed by several parameters at 4/5, 10 and 24 hpd including TNF- α , IL-6, IL-10, NF-kB, cyclin-D1 and PCNA expression (Table 3.3.19, Figure 3.3.36). Fed CD-1 showed significantly higher hepatic IL-6, IL-10, NF-kB and cyclin-D1 mRNA upregulation at 4/5 hpd, and higher levels at 10 hpd, before both strains showed a similar level at 24 hpd. However, while the amount of PCNA-positive hepatocytes was significantly higher at 4/5 hpd in CD-1 mice, this was reversed at 10 and 24 hpd (Figure 3.3.36A). However, at 24 hpd, while IL-6 and cyclin-D1 were highly transcribed in the liver, the amount of PCNA-positive hepatocytes was significantly lower in CD-1 mice (Table 3.3.19, Figure 3.3.36B).

Table 3.3.19. Assessment of liver regeneration of the levels of TNF- α , IL-6, IL-10, NF-kB, cyclin-D1 and PCNA expression in the liver by comparative value, assessing the fold change relative to pooled control animals.

Fed						
Time (hpd)	*5		10		24	
Liver parameters	C57BL/6J	CD-1	C57BL/6J	CD-1	C57BL/6J	CD-1
TNF- α	11.7	4.4*	2.18	7.9*	0.59	1.77
IL-6	2.33	6.0*	3.71	7.9*	7.02	7.6
IL-10	0.81	3.9*	3.14	9.0*	7.17	8.8
NF-kB	0.67	2.1	2.83	13.3***	4.70	6.1
Cyclin-D1	2.48	8.1***	2.12	8.7**	7.04	9.6
PCNA	0.95	2.11*	2.5	1.04	10.5	2.03**
PCNA Cyto	0.65	3.64*	4.5	0.96*	3.5	3.36

Fasted						
Time (hpd)	*5		10		24	
Liver parameters	C57BL/6J	CD-1	C57BL/6J	CD-1	C57BL/6J	CD-1
TNF- α	1.49	2.3	3.14	6.8*	4.19	1.5*
IL-6	1.11	4.7*	1.36	2.2	3.01	7.4*
IL-10	1.81	1.5	1.69	1.8	3.71	5.2
NF-kB	0.33	2.1	0.66	1.5	6.33	4.7
Cyclin-D1	3.17	4.0	1.01	4.2	1.80	6.0**
PCNA	1.0	0.61	2.4	0.56	11.0	1.58***
PCNA Cyto	0.67	5.62**	1.3	0.23	6.0	3.54

Statistical significant differences (***P<0.005, **P<0.01 and *P<0.05) are seen in CD-1 mice in comparison to C57BL/6J mice after APAP dosing. hpd – hours post dosing; Cyto – cytoplasmic; *5 - values of 5 h C57BL/6J was compared to 4 h CD-1 mice.

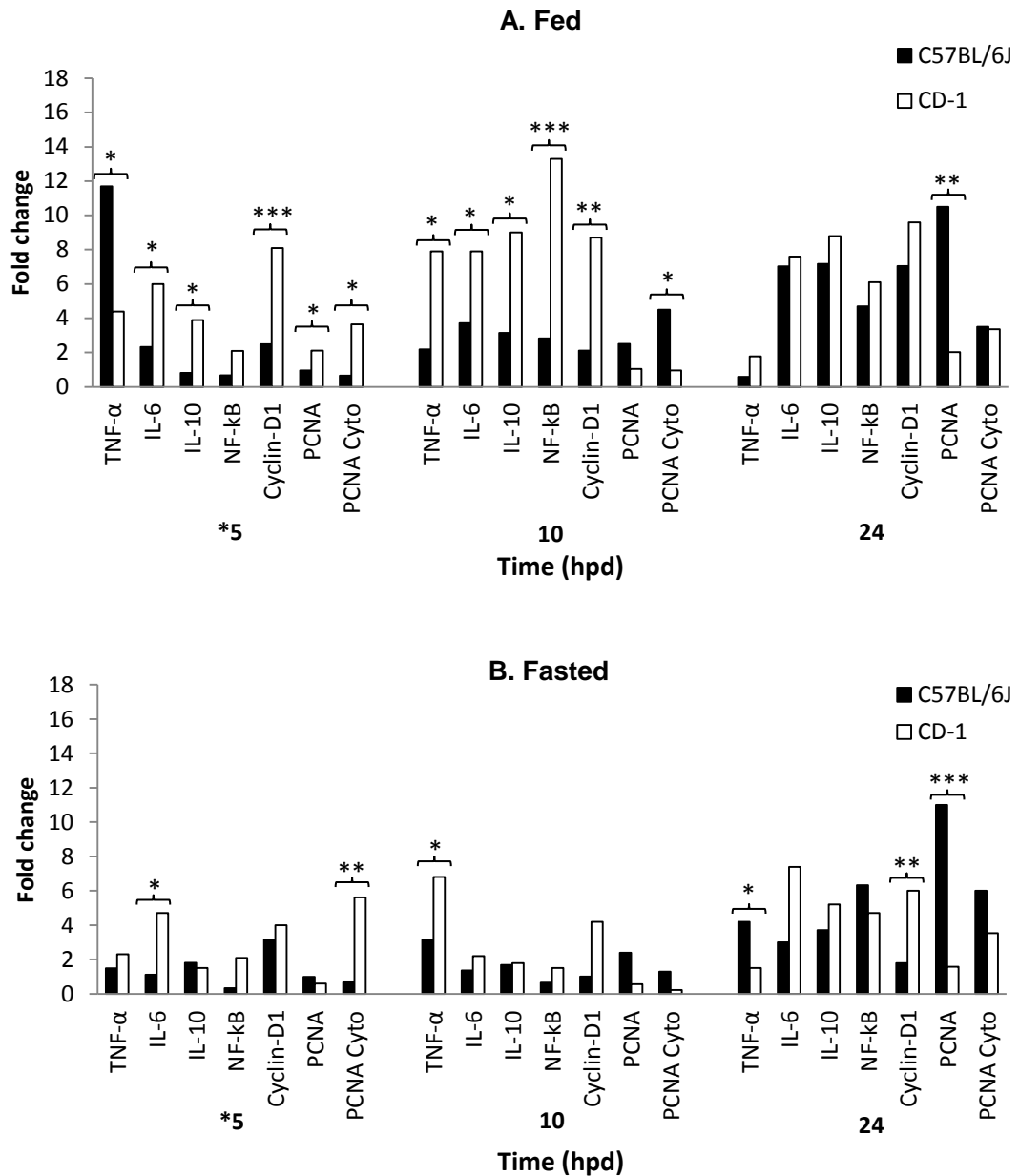


Figure 3.3.36. Assessment of liver regeneration in male fed and fasted C57BL/6J and CD-1 mice after APAP dosing.

The levels of hepatic TNF- α , IL-6, IL-10, NF-kB, cyclin-D1 and PCNA expression were evaluated at 5, 10 and 24 hpd in animals that had been fed (A) or fasted (B) prior to APAP administration (as listed in Table 3.3.19). Fold changes are calculated relative to pooled control mice. Data represent mean (4 to 6 animals per group). *5- values of 5 h C57BL/6J was compared to 4 h CD-1 mice. Cyto-cytoplasmic.

CHAPTER FOUR

DISCUSSION AND CONCLUSIONS

4	DISCUSSION	196
4.1	Effects of fasting in saline dosed control male CD-1 and C57BL/6J mice	197
4.2	Effect of fasting in the response of male CD-1 and C57BL/6J mice to APAP overdose	204
4.2.1	Drug-induced liver injury after APAP overdose	204
4.2.2	Inflammatory response and regeneration of the liver after APAP induced liver injury in male CD-1 mice and C57BL/6J mice	213
4.2.3	Differences in the response to APAP injury and the subsequent regenerative process in fed and fasted CD-1 and C57BL/6J mice	225
4.3	CONCLUSIONS	227

4 DISCUSSION

Despite the extensive use of laboratory mice in DILI research, data on baseline values in commonly used out-bred and in-bred strains with regards to their response to fasting is still lacking. This is particularly inconvenient, since variable approaches are used by researchers, often accompanied by only limited information on the feeding and fasting protocols that were applied, thus reducing the reproducibility and applicability of the results and ultimately counteracting the 3R concepts.

The aims of this thesis were to gather relevant basic information on the inflammatory and regenerative response in commonly used *in vivo* models of DILI, assessing and characterising them by a chosen set of quantifiable liver parameters on two strains of mice, the out-bred CD-1 and the more commonly used in-bred C57BL/6J mice. A recent study reported an impaired regenerative capacity after high dose (600 mg/kg) APAP treatment, however, this experiment was carried out in male C57BL/6J mice that had been fasted for 12 hours only (Bhushan et al., 2014). Taking this into consideration, we wanted to establish whether fasting or strain differences profoundly change the potential of the liver to regenerate. Hence, the studies in this thesis have been undertaken to investigate the effects of fasting on acute hepatotoxicity and regeneration in mice of these two strains.

To characterise the APAP models of hepatotoxicity, markers of toxicity and necrosis (serum ALT and histopathology), apoptosis (cleaved caspase-3), relevant metabolic processes (hepatic GSH content) and energy levels (hepatic ATP content) were evaluated in both fed and fasted CD-1 and C57BL/6J control and APAP dosed mice. As hypothesis had fully fulfilled, that The degree of hepatic regenerative capacity was assessed by the immunohistological demonstration of PCNA-positive, proliferating hepatocytes and the transcription levels of relevant cytokines (TNF- α , IL-6, IL-10) and relevant transcription factor (NF- κ B) and cell-cycle protein (cyclin-D1); the inflammatory cytokines TNF- α and IL-6 also provided information on the (systemic) inflammatory response after APAP induced liver injury.

In untreated control mice, the hypothesis was partly proven correct although some differences in basal levels were identified between both fed and fasted CD-1 and C57BL/6J mice. As expected, the response to APAP differed between fed and fasted mice; in both strains fasting prior to APAP overdose resulted in more extensive liver damage, thereby leading to lesser hepatic regeneration. Surprisingly, the assessment of APAP dosed fed animals of both strains indicates that CD-1 mice have a higher regenerative capacity than C57BL/6J mice.

4.1 Effects of fasting in saline dosed control male CD-1 and C57BL/6J mice

Before the impact of fasting on APAP induced liver injury was investigated, CD-1 and C57BL/6J mice that had been fed and fasted prior to 0.9% saline dosing were assessed for the effect of fasting on relevant liver parameters. Fasting is defined as the withdrawal of food from animals which still have free access to water (Jensen et al., 2013). After fasting periods, mice generally show a substantial reduction of their body weight since the drinking activity corresponds to the food intake and is therefore reduced alongside (Kurokawa et al., 2000). It is known that mice consume about two thirds of their daily food and water ratio during the scotophase, with a 5-fold increase of the eating rate in the evening (Petersen, 1978).

Our data also showed that the **body weights** were basically equal in CD-1 and C57BL/6J mice fed ad libitum at any time of study although it has been reported that body weight and food intake can vary between mouse strains (Bachmanov et al., 2002). While this may be the case, it appears not to affect the average body weight loss that is seen after fasting: both the CD-1 and C57BL/6J mice showed a similar range of weight loss after 16 hours fasting, when the onset of fasting was at the same time of day. The lowest degree of body weight loss was seen when the fasting period had started at 3 am, indicating that the highest food intake took place in the first half of the night. The circadian rhythm of food consumption is well known in mice (Petersen, 1978), but it has also previously been shown that the body weight of mice undergoes a circadian rhythm (Eckel-Mahan and Sassone-Corsi, 2013; Schnell et al., 1984), a finding that the results of our study support.

Interestingly, the body weight loss after fasting did not result in changes in body mass and liver weight (Jensen et al., 2013). It is therefore important to consider this variance when starting an experiment with fasted mice, in particular since mice that have already lost more than 10% of their body weight will reach the endpoint of a permitted experiment after a moderate additional weight loss due to treatment.

The **hepatic GSH** level peaks at the end of the scotophase (night cycle) when mice have taken up the bulk of their daily food ration, and are lowest when mice sleep, at the end of the prolonged light period (Schnell et al., 1984); they show a diurnal variation (Jaeschke and Wendel, 1985). Our results confirm that the hepatic GSH content follows the circadian rhythm of the mice as levels were significantly higher in the morning than in the afternoon and at night time (20:45) in both CD-1 and C57BL/6J mice. It has previously been shown that fasting of mice results in reduced hepatic glutathione levels (Brooks and Pong, 1981; Strubelt et al., 1981b). As predicted, in the present study the GSH level was significantly reduced after fasting, but returned to levels similar to those of fed mice within 24 hours refeeding in CD-1 mice. However, after the first 10 hours of refeeding, at a time of day when the GSH level in fed mice had decreased due to the circadian rhythm (20:00), the GSH level in the fasted mice was significantly higher and seemed to overshoot far above the normal maximum level, apparently overriding also the circadian rhythm. It was similar in C57BL/6J mice at the same time of day and length of refeeding and progressed to an even higher value after 15 hours of refeeding. Overshooting of GSH level was likely due to overeating when feeding was resumed (Bare and Cicala, 1960). While GSH levels of CD-1 mice return to basal levels after 24 hours of refeeding, C57BL/6J mice took much longer and reached the levels observed in fed mice at 36 hours of feeding. The rate of GSH synthesis depends on the availability of cysteine provided with the diet (Lu, 1999). A study suggested that the enzymes involved in GSH synthesis are unaffected by fasting, which confirms that it strongly depends on the food intake (Tateishi et al., 1974). Due to rapid GSH turnover in this study, the mice might have changed their diurnal rhythm in order to restore the hepatic GSH level, but why it then overshoots remains to be clarified. It can also not be explained, why there is a strain differences in the speed of GSH replenishing

after starvation. It was also interesting to note that GSH levels were always significantly higher in the fed C57BL/6J mice than in the fed CD-1 mice. This appears not to indicate that C57BL/6J mice have a higher detoxification potential than CD-1 mice, as a previous study has shown that the antioxidant capability depends on the threshold of GSH to detoxify free radicals (Casini et al., 1984). For example, although both CD-1 and C57BL/6J mice were induced with the same dose of APAP, fed CD-1 had higher caspase activation which initiate apoptosis than fed C57BL/6J mice (Acton, 2013).

The amount of **hepatic ATP** is critical in particular during toxic insults, as it is essential for cells to die via apoptosis instead of necrosis, thereby protecting the liver from the pathological consequences of necrosis following APAP administration (James et al., 2003b). Furthermore, GSH synthesis also requires ATP (Lu, 1999), ATP thereby being a prerequisite to ensure optimal detoxification capacity. Interestingly, despite the circadian fluctuation of food intake and hepatic GSH, similar fluctuations in the hepatic ATP content were not observed. In our study, hepatic ATP levels were always lower in C57BL/6J than CD-1 in fed mice, though did not differ significantly. A previous study has showed that lower sensitivity to tissue injury in in-bred A/J mice than C57BL/6J mice is due to downregulation of ATP-gated P2X receptor as a pain sensor when ATP leaked from damaged tissue (Tsuda et al., 2002). It indicated the difference of ATP levels could be strain-specific. As expected, however, fasting of mice resulted in substantial depletion of overall hepatic ATP in CD-1 (64%) and C57BL/6J (38%) mice. Surprisingly, the ATP content did not return to the level in fed animals even after 24 hours of refeeding in the CD-1 mice, whereas in C57BL/6J mice, a gradual increase in the ATP content was observed after refeeding until it reached a level similar to fed mice after 20 hours. Starvation is believed to inhibit ATP production and further depletes the substrates used to synthesise ATP (Berg JM, 2002; Fry, 2010).

Since hepatic **GSH synthesis and ATP content** can be expected to be associated, we investigated their fold changes alongside each other. Theoretically, GSH synthesis is depending on the availability of cysteine and the activity of the enzyme γ -glutamylcysteine synthetase (GCS). It includes two ATP-requiring steps; [1] L-

glutamate + L-cysteine + ATP \rightarrow γ -glutamyl-L-cysteine + ADP + Pi (inorganic phosphate) and [2] γ -glutamyl-L-cysteine + L-glycine + ATP \rightarrow GSH + ADP + Pi (Lu, 1999). In our study, while ATP levels remained low after the onset of refeeding throughout the experiment, we observed a significant increase of hepatic GSH after 10 hours of refeeding, which indicates that the level of hepatic GSH may not correlate with the level of hepatic ATP, suggesting that the synthesis of GSH still occurs when a basic, though overall insufficient amount of ATP is present. Also, glycogen is synthesised when sufficient glucose and ATP are available, with one ATP molecule being required per glucose molecule that is incorporated into the polymeric branched structure of glycogen (Berg et al., 2002). The rapid refilling of glycogen stores that was observed in the present study makes it likely that the ATP is used up in this manner. Consequently, after fasting, ATP cannot be stored and is utilised as soon as it has been synthesised; this would explain the low ATP levels over such a long period of refeeding in the fasted mice.

Serum ALT activities were measured as a means to detect potential liver damage as a consequence of fasting. ALT is widely used as a clinically proven, though not sensitive indicator of liver damage (Kim et al., 2008a). Intriguingly, our data revealed average ALT activities in C57BL/6J mice to always be significantly lower than those of CD-1 mice and to show less variance. The wide interindividual variation among the out-bred CD-1 mice, however, makes it difficult to formulate reference values and impossible to interpret subtle changes. Such variation in CD-1 is likely due to their relatively high degree of genetic dissimilarity. In any case, the lack of a distinctive increase of ALT activities after fasting in either strain of mice confirms that fasting does not induce substantial damage to the liver.

As expected, the **histological assessment** did not identify any abnormal morphological changes or any significant inflammatory cell recruitment as a consequence of fasting in CD-1 and C57BL/6J mice except the apparent lack of cytoplasmic vacuolation of hepatocytes that can be visualised histologically at higher magnification immediately after fasting. This confirms the results of a previous study that reported the liver structure and zonation, including periportal and pericentral areas, was still preserved after 72 hours of fasting (Sokolovic et al.,

2008). Together, glycogen stores within hepatocytes appear completely lost after the fasting period in both strains. In agreement with this, a previous study reported a 90% reduction in hepatic glycogen was in C57BL/6J mice after 18 hours compared to 5 hours of fasting which only resulted in a 10% loss, but does not compromise the glycogen content in muscles (Ayala et al., 2006). It is important to note that liver glycogen stores is important to maintain glucose homeostasis (Klover and Mooney, 2004), and recent studies have shown that the expression of a number of genes involved in the hepatic glucose metabolism is under circadian regulation (Panda et al.; Storch et al., 2002; Ueda et al., 2002). During fasting, glycogen stored in the liver are mobilised in order to replenish blood glucose and conserve energy (ATP) via glycogenolysis (Fry, 2010), which explains the apparent complete hepatocellular glycogen depletion immediately after the fasting period. However, when feeding is resumed, the excess of insulin promotes the glucose conversion into glycogen for storage in the liver to quickly maintain its homeostatic functions. After reintroduction of food at a similar time of day, we found evidence of rapid glycogen restitution in both groups of mice. However, while it seemed to be completely restored after only 30 minutes in C57BL/6J mice, glycogen restitution seemed to take 4 hours in the CD-1 mice. This suggests that C57BL/6J mice either consumed food more rapidly or in larger amounts once it was reintroduced or that they have a more rapid glycogen reserve capacity once blood glucose levels are maintained.

Although some studies have quantified the transcription of **TNF- α** , **IL-6** and **IL-10** in the liver as potential indicators of inflammatory or regenerative responses following chemical intoxication (i.e. APAP, CCl₄ or GalN) (Masubuchi et al., 2003a; Mehendale, 2005; Peschon et al., 1998), study on the potential effects of starvation alone on their hepatic transcription and thereby the induction or reduction of a (pro-) inflammatory state still needs to be studied. Thus, we were interested in gathering baseline information on such a potential effect of fasting. However, no evidence was found of changes in the transcription of TNF- α , IL-6 and IL-10 in the liver or spleen due to fasting in CD-1 and/or C57BL/6J mice, although these cytokines were found to be constitutively transcribed in the spleen and, at a lower level, the liver. Overall, the TNF- α transcription was higher than that of IL-6 and IL-10, and it was

found to be transcribed at a higher level in the C57BL/6J mice. These findings provide baseline information to suggest that different mouse strains with their own genetic backgrounds can develop a different degree of immune cell activation during toxic insults and inflammatory responses. It should be noted that the serum TNF- α levels were always higher in the CD-1 mice, a feature that has so far not been reported. However, serum IL-6 did not differ in either strain (C57BL/6J or CD-1) in response to fasting, which indicates that fasting does not influence the release of this cytokine.

Similarly, fasting appeared not to have an effect on hepatocyte turnover, since hepatic **NF- κ B and cyclin-D1 transcription** levels were not altered after fasting. Furthermore, there was no evidence of circadian changes in their transcription. The results of the quantitative assessment of proliferating, PCNA-expressing hepatocytes confirm these findings at the in situ level. PCNA is a well-accepted indicator of liver regeneration and hepatocyte proliferation (Bravo et al., 1987). The liver mass is maintained by self-replicating hepatocytes during normal liver turnover (Malato et al., 2011). In both fed and fasted CD-1 and C57BL/6J mice a relatively low, but varying (in CD-1 mice) amount of PCNA-positive hepatocytes was seen. The observed overall higher number in fed CD-1 mice than in fed C57BL/6J mice at the time of saline application (0 h) suggests that the liver of CD-1 mice has a higher basal cellular turnover than that of C57BL/6J mice (Table 3.1.16).

In summary, the present study shows that fasting alone has substantial effects on some liver parameters that might be of relevance for (and monitored in) any study in which fasted mice are used. In particular also the circadian effects that influence the parameters not only in fed, but also in fasted mice need to be considered as well. Also, while they were apparently not influenced directly by a circadian rhythm or fasting, other parameters including liver morphology, ALT activity, PCNA expression and cytokine transcription, might be of relevance. Therefore, the present study provides insight into differences in baseline levels in different mouse strains and in their response to fasting, which need to be considered before conducting a mouse study.

4.2 Effect of fasting in the response of male CD-1 and C57BL/6J mice to APAP overdose

4.2.1 Drug-induced liver injury after APAP overdose

The literature provides evidence that diet restriction prior to APAP dosing can increase the degree of hepatic injury (Strubelt et al., 1981a). The purpose of the present study was to systematically assess the influence of fasting on the extent and degree of APAP-induced liver damage and subsequent liver regeneration in out-bred (CD-1) and in-bred (C57BL/6J) mice and assess whether the presence and extent of inflammation differs in fed and fasted animals. Accordingly, a range of parameters (hepatic GSH, ATP, serum ALT and histology, i.e. DILI score) were examined in male CD-1 and C57BL/6J mice that had been fed ad libitum or fasted for 16 hours (or 24 hours) prior to receiving a sublethal APAP dose.

In both CD-1 and C57BL/6J mice fed ad libitum, **hepatic GSH levels** dropped significantly after APAP dosing, confirming the results of previous studies (Antoine et al., 2010; Williams et al., 2011). The drop occurred as early as 1 hpd in CD-1 mice and at 3 hpd in C57BL/6J mice. This might be due to the generally higher basal GSH content in C57BL/6J mice, which was seen when control animals of both strains were compared; this could allow the liver of C57BL/6J mice to initially detoxify a higher amount of APAP prior to succumbing to the toxic injury (Strubelt et al., 1981a). Interestingly, GSH levels were subsequently increased significantly (at 10 hpd) in treated CD-1 mice compared to control mice at the same time of killing, 20:45. This suggests that the physiological circadian hepatic GSH rhythm can be interrupted as a consequence of GSH depletion, like in APAP overdose, due to excessive glutathione production in the liver in response to the loss of GSH. In CD-1 mice, GSH returned to basal levels at the end of the study (at 24 hpd), similar to what was seen in Swiss Webster (SW) mice (Williams et al., 2011). In contrast, the GSH levels in C57BL/6J mice were similar in control and APAP dosed mice at 10 hpd (time of killing, 20:00). Although the levels in APAP dosed mice were increasing, they still did not reach control animal levels, where GSH was increased at 24 h saline dosed mice but not statistically higher than the 0 hpd values, with time of killing was at 10:00 in both. Meanwhile, over-production of GSH was also seen in

C57BL/6J mice at 30 hpd, with levels were higher than in CD-1 mice at 20 and 24 hpd, at the same time points, and exceeding control animal levels at 30 hpd before returning to control animal levels at 36 hpd. Such fluctuating GSH levels might be the result of over production in order to compensate for the GSH consumption after APAP dosing. The difference to control animal levels cannot readily be explained but could theoretically also indicate further utilise of GSH due to the presence of APAP insult. However, this is unlikely as the half-life of metabolised APAP in the blood is about 4-6 hours in hepatotoxic doses (Pyrsoopoulos, 2014).

As mentioned earlier, overnight fasting of the mice resulted in significantly decreased basal hepatic GSH levels, indicating that the animals had a decreased antioxidant defence and detoxification capacity at the time of APAP dosing. Therefore, higher amounts of the reactive metabolite NAPQI can be expected to be generated, enhancing the hepatotoxic effect of an APAP dose (Brooks and Pong, 1981; Strubelt et al., 1981b). As overnight fasting of mice does not only reduce hepatic glutathione levels, but also alter the diurnal GSH variation, it has been commonly used in studies of APAP-induced hepatotoxicity, allowing the induction of hepatotoxic injury at more moderate doses (Jaeschke and Wendel, 1985). The results of our study not only show that hepatic GSH levels are significantly lower in fasted than in fed mice of both strains at the same time of day, they also show that levels do not differ much between both strains despite the differences in the fed counterparts, confirming the results of previous studies (Hinson et al., 2010). Consequently, fasted animals developed a distinctly more intense early degree of liver injury following APAP administration. In line with this, the restoration of hepatic glutathione levels after APAP administration of C57BL/6J mice occurred more rapidly in fed mice (at 10 hpd) than in fasted mice where it was first seen at 36 hpd. Interestingly, fasted, APAP treated CD-1 mice reached hepatic GSH levels similar to those in saline treated control mice by 24 hpd, whereas C57BL/6J had not fully recovered at 24 hpd, a feature also reported previously (Williams et al., 2011). They were only returned to basal levels at 36 hpd. At these end time points, fasted mice of both strains showed ongoing centrilobular damage which reduces the capability of hepatocytes to produce GSH (Hinson et al., 2010). These results

confirm that in the mouse, GSH depletion is a prerequisite for the onset of toxicity following APAP overdose (Davis et al., 1974). At toxic APAP doses, the reactive metabolite has been shown to deplete the glutathione content by up to 80-90%. Increased formation of reactive oxygen and nitrogen species, i.e. NAPQI in hepatocytes induced by APAP, can reduce the GSH content. It has been shown that the degree of covalent binding of the reactive metabolite to proteins determines the outcome of hepatocyte damage until glutathione is almost completely depleted (Mitchell et al., 1973; Nelson, 1990). The capability of an individual mouse to detoxify NAPQI determines the severity of the APAP hepatotoxicity (Hinson et al., 2010). Furthermore, the fact that the hepatic GSH content had reached control levels in both strains at the end of the study period suggests that either physiological adaptation or regeneration had taken place within the liver, enabling hepatocytes to synthesise glutathione (Lu, 1999).

Following APAP treatment, **ATP levels** were also severely depleted in fed CD-1 and C57BL/6J mice (at 5 and 10 hpd). By 24 hpd, ATP levels had returned to basal control animal levels in both strains. However, fed C57BL/6J mice appear to generate ATP earlier than CD-1 mice following APAP toxicity, and the ATP loss is greater in fed CD-1 mice than in fed C57BL/6J mice at 5 hpd. While in our study ATP levels in fed C57BL/6J mice returned to control animal levels after 20 hpd, a previous study reported that in fed C57BL/6J mice ATP levels returned to basal levels (0 hpd) at 3 hpd. In SW mice, however, they remained low (Williams et al., 2011). Although the APAP dose applied intraperitoneally was identical in both studies (530 mg/kg), the basal control mouse levels in our study based on the pooled values of more than 20 control mice and not on only 4-6 animals at 0 hpd in the previous study (Williams et al., 2011) which could have hampered the statistical analysis. APAP dosed fasted mice showed a significant ATP reduction compared to both saline dosed fasted and APAP dosed fed mice for both strains from 5 hpd onwards, a finding that is in agreement with the results of other studies (Antoine et al., 2010; Lee et al., 1988). Moreover, another study also reported hepatic ATP reduction by 50% in mice after overnight fasting, APAP dosing of the fasted mice resulted in an additional decline to around 70% in both C57BL/6J and SW mice

(Williams et al., 2011), however the study claimed that the amount of ATP was still sufficient to promote caspase activation and apoptosis, though this appeared not to be the case in the study by Antoine et al. (2010). Unfortunately, the study did not mention specifically the time of day and length of fasting, as fasting alone influences the ATP levels and could therefore have influenced the results. Loss of mitochondrial membrane potential due to mitochondrial permeability transition as a consequence of increased oxidative stress due to NAPQI would reduce the ability of mitochondria to synthesise ATP (Hinson et al., 2010). Usually, ATP is produced by glycolysis, where glycogen is degraded to produce glucose which is then used to generate pyruvate, ATP, NADH and H⁺ (Berg JM, 2002). In addition, pyruvate and NADH derived from glycolysis also provide substrates to further synthesise ATP during the mitochondrial citric acid cycle (Berg JM, 2002; Fry, 2010). Furthermore, an in vitro study has demonstrated that APAP-induced apoptosis of hepatocytes does also rely on ATP produced by glycolysis (Kon et al., 2007).

Although it is known that both hepatic **GSH and ATP contents** are depleted after APAP overdose (Antoine et al., 2010; Saito et al., 2010), very little is known about the potential association between GSH and ATP in the liver. In CD-1 mice, the hepatic GSH reduction was remarkably more intense than the ATP level reduction at 1 hpd, however by 10 hpd, the GSH content had significantly increased whereas the ATP level was still low. In C57BL/6J mice, as expected, the hepatic ATP level was proportional to the GSH level, without significant differences in the fold change at all times in fed or fasted mice. In fed C57BL/6J mice, GSH and ATP levels became similar to those of control animals by 24 hpd, like in fed CD-1 mice, but then a slight increase was observed at 36 hpd. However, both GSH and ATP levels were lower in fasted mice of both strains at all time points, although at 36 hpd in C57BL/6J mice. Because the toxic effect of APAP was still more apparent in fasted compared to fed mice at 24 hpd, both GSH and ATP levels were still lower than in control mice at this point. Reduced hepatic ATP production could also result from reduced hepatic GSH levels, as GSH depletion results in an increased production of a reactive APAP metabolite, NAPQI that increases the oxidative stress and can induce mitochondrial permeability transition (Hinson et al., 2010).

Although **ALT activity** levels are more liver specific than aspartate aminotransferase (AST) levels (Giannini et al., 2005), AST is not a specific marker for APAP-induced liver damage because it is also highly present in skeletal, cardiac muscle and kidneys (Lindblom et al., 2007). Nevertheless, both are not sensitive marker for hepatotoxicity as also been released in other non-toxic liver diseases, such as viral infections, alcoholic and steatohepatitis (Jadhao et al., 2004). Furthermore, the serum half-life of ALT is long, ranging from 37 to 60 hours, leading to consistently elevated levels after peak liver damage (Hawker, 1991; Seneviratne et al., 2006). This explains why the serum ALT level was still significantly elevated in fed CD-1 mice at 24 hpd, when the histological examination of the liver suggested complete recovery. Nonetheless, the serum ALT activity is a well-established indicator of APAP-induced acute liver damage (Giannini et al., 2005; Jaeschke et al., 2014); in the present studies, while a time dependent increase in APAP hepatotoxic changes was seen in the early phase in both fed and fasted CD-1 and C57BL/6J mice, the ALT activity was higher at later phases in fasted than fed for both strains (CD-1 mice: 24 hpd; C57BL/6J mice: 20, 24 and 36 hpd), in the latter reflecting the ongoing damage that was seen in the histological specimens. Serum ALT levels were compared at 5 and 24 hpd and were similar in fed and fasted APAP dosed mice of both strains, at these time points, suggesting that the extent of liver injury after APAP was the same; this was, but, not confirmed by the histological examination.

The type of **liver change** induced by APAP in mice, i.e. centrilobular cell loss/necrosis, is well known (Gujral et al., 2002; Jaeschke et al., 2003); however, information on the mode of cell death is still partly controversial, and both apoptosis and necrosis are being mentioned (Guicciardi et al., 2013; Gujral et al., 2002). The literature has demonstrated that fasting of mice prior to dosing can elevate the level of hepatic necrosis, thereby increasing the severity of liver damage in animal models (Strubelt et al., 1981a); already in an older study it was stated that in fasted mice, apoptotic cell death is less likely to be found because it is an energy dependent process (Kerr et al., 1972). Other literature considered apoptosis as less likely to be a key feature of APAP induced liver injury because of the rapid drop in ATP and the oxidative stress that do not facilitate caspase activation (Cover et al.,

2005; Gujral et al., 2002; Gunawan et al., 2006; Lawson et al., 2000). However, these studies were all done in animals that had been fasted prior to dosing. In a study in fed CD-1 mice it was clearly shown that apoptosis is a relevant form of cell death in the early stage, i.e. as early as 3 hours after APAP overdose. The histological and immunohistological findings were supported by biochemical markers of apoptosis, i.e. cytokeratin 18 cleavage, DNA laddering and procaspase-3 processing (Antoine et al., 2010). In contrast, a subsequent study demonstrated that hepatic ATP contents did not correlate with APAP-induced caspase activation in SW and C57BL/6J mice and concluded that its activation to promote apoptosis is strain specific (Williams et al., 2011).

The present study shows that there are again differences between the two mouse strains. In CD-1 mice, relatively numerous apoptotic cells were seen in fed animals at 3 and 5 hpd, these were not observed in the fasted animals. As discussed above, in fed mice, we identified a significant drop in hepatic ATP content only at 5 hpd, which suggests that apoptotic cell death at the early time points is possible due to sufficient ATP amounts. A previous study reports contradicting results, i.e. the absence of apoptotic cells at 3 and 5 hours post APAP dosing, but early evidence of oncotic, i.e. swelling necrosis with features of karyolysis and loss of membrane integrity using TUNEL staining in both fed and fasted out-bred SW mice, with no difference in the type and extent of injury in both groups (Williams et al., 2011). Although apoptosis was not observed histologically, Williams et. al. showed an increase in caspase-3 activity at 3 hpd, but not at 5 hpd in fed SW mice, a feature not seen in the fasted mice which corresponds to earlier findings in the study by Antoine et. al. (Antoine et al., 2010). However, at 24 hpd, the authors reported morphological features of oncotic necrosis but no evidence of apoptosis in both fed and fasted SW and C57BL/6J mice (Williams et al., 2011). These results could be due to the mouse strain used, though this needs to be investigated further. At 10 hpd, we still observed centrilobular hepatocyte necrosis, although the DILI score decreased after 5 hpd (apart from at 15 hpd, which was a group of mice dosed accidentally at 17:00) and intriguingly, at 24 hpd, the histological features of the liver in CD-1 mice suggested complete regeneration, with presence of numerous

mitotic figures as also been reported previously, where normal liver architecture was restored after 24 hours of 500 mg/kg APAP dosed CD-1 mice (Apte et al., 2009b). Also, in the fed mice there was no histological evidence of substantial inflammatory cell influx at any time point. These results are in accordance with a previous study on APAP induced hepatotoxicity in fed CD-1 mice (Antoine et al., 2010). They provide further evidence that regeneration is the final outcome of drug-induced liver toxicity including APAP toxicity, as has been claimed previously based on rodent models (Apte et al., 2009b; Mehendale, 2005). It was hypothesised that with the metabolism of APAP unaffected by fasting in these systems, the decrease in basal GSH would not play a major role in the inhibition of later events during APAP hepatotoxicity, such as apoptosis. Low ATP content that we observed previously in fasted mice could explain the dominance of necrosis that we observed histologically. Rather, depletion of ATP due to fasting to below a threshold level can lead to reduction of apoptotic cell death and switch to necrosis (Antoine et al., 2010). Moreover, it also has been claimed that genes which facilitate apoptosis were down-regulated in mice after restricted feeding (Matthias et al., 2004).

In contrast to CD-1 mice, fed C57BL/6J mice still showed centrilobular cell loss, neutrophil infiltration and ongoing cell degeneration and death via apoptosis and coagulative necrosis at later time points. The extent of the ongoing damage was apparently slowly decreasing, indicated by the drop in the average DILI score from 1.15 at 24 hpd to 0.75 at 30 hpd and 0.8 at 36 hpd, whereas the fed CD-1 did not show any evidence of centrilobular damage at 24 hpd. This indicates that the primary mode of cell death at these later time points is apoptosis followed or accompanied by necrosis; however, the cause for this ongoing centrilobular injury is still unclear and needs to be investigated. However, it cannot be excluded that low energy levels due to mitochondrial damage could be a reason that contributes to prolonged cell death following APAP dosing. A comparative study of resistant and susceptible strains (i.e. SJL and C57BL/6J mice) by genomic and proteomic approaches revealed that C57BL/6J mice had a lesser cytoprotective gene like HSP (heat shock protein) 70, and more prototoxicant gene (i.e. osteopontin), thereby contributing to intense hepatotoxicity following APAP overdose (Welch et al., 2006).

Interestingly, morphological evidence of liver damage was seen later in fasted (at 5 hpd) than in fed (at 3 hpd) C57BL/6J mice, which was also later than in fed and fasted CD-1 mice, where liver damage was obvious at 3 hpd. It is possible that the delay in the fasted C57BL/6J mice to respond to the toxic insult might be due to very high ATP levels in association with refeeding at a time point before 5 hpd (these were not examined in this study), because we could see in saline dosed fasted C57BL/6J mice that their hepatic ATP levels recovered earlier than that of CD-1 mice. Over time, marked centrilobular cell loss and evidence of coagulative necrosis of the innermost remaining hepatocyte layer and hydropic degeneration of hepatocytes surrounding the latter was present in both fasted CD-1 and C57BL/6J mice; a feature also seen at the later time points in fed C57BL/6J mice and in a previous study (Williams et al., 2011). The extent of liver damage was significantly higher in fasted CD-1 mice at 10, 20 and 24 hpd. In C57BL/6J mice, the damage also persisted in the fasted mice and was found to be more extensive even at 30 hpd (score 2.1) and 36 hpd (score 1.5), when it was found to decrease as well. It has previously been suggested that the hepatic ATP reduction in fasted mice promotes necrotic cell death in response to APAP overdose, leading to the release of reduced HMGB-1 which triggers the recruitment of inflammatory cells and the formation of pro-inflammatory cytokines (Antoine et al., 2010; Robertson et al., 2000). Release of these proteins from the cells during necrosis into the extracellular space attracts leukocytes to damaged areas (Robertson et al., 2000). Accordingly, neutrophils were found in the affected areas in fasted APAP dosed mice until the end of the study period, which was more pronounced in the C57BL/6J mice. A similar study also reported more neutrophils in the liver of C57BL/6J than in SW mice (Williams et al., 2011). While the authors observed a comparable degree of injury and neutrophil infiltration at 3 and 5 hpd in both fed and fasted C57BL/6J mice, they observed less extensive necrosis in the fed mice at 24 hpd, similar to our study. However, there was no evidence of decreasing neutrophil infiltration, as high amounts of neutrophils were located between the necrotic cells (Williams et al., 2011). In conjunction with the finding, Williams et al. also observed no upregulation of caspase-3 activity at 3, 5 and 24 hpd. Alongside the morphological evidence of centrilobular hepatocyte necrosis, we used staining for cleaved caspase-3 to

confirm the presence of a few apoptotic cells alongside these until 36 hpd in our study. As mentioned previously, this indicates that both necrosis and apoptosis occur simultaneously; also, the amount of apoptotic cells might even be underestimated, because it is likely that cells undergoing coagulative necrosis remain visible longer than apoptotic cells/bodies which are rapidly phagocytosed (Corcoran et al., 1994; Sahota et al., 2013).

The extent of hepatic carbohydrate or **glycogen content** within hepatocytes was assessed by staining with the PAS reaction. This is a crude method, since it does not allow precise quantification, but has the advantage of allowing comments on the distribution of glycogen-containing hepatocytes. In the present study, we used the PAS reaction to examine the liver of fed CD-1 mice over the entire time course, but in particular also in the early phase after APAP overdose (0, 0.5, 1, 2 and 3 hpd). The glycogen content was reduced already at 1 hpd and was completely lost apart from a few scattered individual PAS-positive cells at 3 and 5 hpd. This suggests that the animals had not resumed food consumption immediately after APAP treatment, when food was reintroduced. Thereafter, glycogen started to accumulate again throughout the parenchyma, except for the innermost centrilobular areas where it was still generally absent at 10 to 20 hpd. In fed mice, complete glycogen restitution was indicated at 24 hpd in CD-1 mice, where morphological evidence of complete liver regeneration, whereas C57BL/6J mice revealed consistently PAS-negative in cell damage of centrilobular hepatocytes until 36 hpd. In fasted mice, we observed a different scenario: At the time of dosing, i.e. immediately after completion of the 16 or 24 hour fasting period, there was no evidence of hepatocellular glycogen content. This is in accordance with a previous publication that suggested near complete depletion of hepatic glycogen stores and thereby reduced generation of cellular ATP through glycolysis and the citric acid cycle as a prominent biochemical feature of fasting (Strubelt et al., 1981a). The hepatocellular glycogen was gradually restored outside the affected centrilobular areas in APAP treated animals, sparing the centrilobular areas with ongoing hepatocellular damage in both strains.

4.2.2 Inflammatory response and regeneration of the liver after APAP induced liver injury in male CD-1 mice and C57BL/6J mice

Many DILI studies have demonstrated compensatory liver regeneration as its final outcome (Anand et al., 2003; Apte et al., 2009a; Hu and Colletti, 2008). Nevertheless, knowledge about the mechanism of liver regeneration following APAP toxicity is limited, and still needs to be further elucidated. The present study did not only undertake a quantitative assessment of liver regeneration after APAP-induced DILI, but also continued to define the role played by inflammatory cytokines that are believed to be produced (Bhushan et al., 2014). To determine the time frame of the onset of inflammation and/or regeneration in our model, the degree of TNF- α , IL-6 and IL-10 transcription in the liver was assessed alongside the histological changes of liver toxicity and any other pathological response. To assess the associated systemic response, the TNF- α and IL-6 transcription levels in the spleen and their serum protein levels were also measured, as these would indicate cytokine production in tissues/cells outside the liver known to potentially contribute to systemic changes. After liver injury, many other cells are also responsible for serum protein levels including circulating monocytes, splenic or enteric macrophages (Abbas et al., 2015), whereby the levels have been shown to correspond to mRNA expression levels (Okubo et al., 2013).

All examined cytokines were expressed at mRNA level in the examined tissues of fed and fasted control mice of both strains, albeit at very low relative levels, and without significant differences at any time point (after refeeding). In contrast, changes were observed following APAP overdose. The comparative Ct value, $2^{-\Delta\Delta Ct}$ was employed to assess the relative gene transcription. Previous studies have assessed the hepatic mRNA transcription levels of a range of cytokines after APAP overdose relative to 0 h or pooled control livers (Apte et al., 2009b; Bhushan et al., 2014; Fisher et al., 2013). In the present study, the mRNA transcription after APAP overdose was assessed in comparison to both time-matched and pooled controls. The results of these two approaches were not same, which might be due to the variability between individual and total number of animals used. However, the expression pattern did not vary much, ensuring that the evaluations are valid.

After APAP overdose, hepatic **TNF- α** mRNA levels were upregulated and peaked early (5 hpd) in fed animals of both strains, before the levels in fasted mice increased more pronounced and reached a peak at 15 hpd in CD-1 mice and 24 hpd in C57BL/6J mice (Figure 3.3.18), which confirmed the results of a previous study (Bhushan et al., 2014). Similarly, splenic mRNA and serum protein TNF- α levels were significantly higher in fasted mice of both strains (and at similar levels) at the end of the study period. TNF- α upregulation would activate leukocytes and vascular endothelial cell activation, increasing the adhesion of leucocytes to endothelial cells via increased adhesion molecule expression, which would lead to the recruitment of leukocytes into the liver and, potentially, a systemic inflammatory response. Therefore, leucocytes infiltration contributed to more tissue necrosis (Blazka et al., 1996b; Blazka et al., 1995). The nucleic acids of necrotic cells is believed to leak into the circulation (Fournie et al., 1995; Jahr et al., 2001; Melkonyan et al., 2008), and HMGB-1 released by necrotic cells can generate an inflammatory response, in the liver by activating Kupffer cells through binding of TLR-4 receptors on the cell surface, leading to the release of cytokines (i.e. TNF- α) (Scaffidi et al., 2002; Tsung et al., 2005), and in other tissues, like the spleen (Yin et al., 2011), leading to a systemic inflammatory response. This study also showed that both hepatic and splenic cytokine transcription is a consistent feature after partial hepatectomy. Previous studies have suggested that the up-regulation of TNF- α in the liver is a result of the cumulative activation of neutrophils and Kupffer cells following APAP treatment (Jaeschke, 2006b; Su et al., 2005). However, we saw TNF- α upregulation also in the liver of fed mice, and early after APAP injury, without any remarkable influx of neutrophils. This strongly indicates that TNF- α is expressed by liver cells, i.e. likely also hepatocytes which have anyway previously been shown to produce cytokines, i.e. after endotoxin stimulation (Panesar et al., 1999). In fasted mice the hepatic TNF- α expression increased further at later time points, when the observed, though still low level, neutrophil influx and delayed regeneration was observed. While the expression of TNF- α in the liver was then decreasing, further upregulation was seen in the spleen at 24 hpd (6.5-fold; CD-1 mice and 9.4-fold; C57BL/6J mice) of fasted mice. A previous study has reported that in C57BL/6J mice at 24 hpd, liver injury and TNF- α expression in the liver is also higher than in Balb/c mice

(Masubuchi et al., 2009), confirming that C57BL/6J mice are apparently more prone to APAP induced DILI than other strains. Splenic TNF- α release could account for or at least contribute substantially to the observed elevation of the serum TNF- α level, confirming the systemic release of TNF- α following APAP induced liver injury also reported previously (Antoine et al., 2010; Walker et al., 1982).

The role of **IL-6** in liver injury and regeneration is complex, as it has been claimed to have both pro- and anti-inflammatory properties (Heinrich et al., 2003; Hirano, 1998). In the present study, in fed mice, IL-6 mRNA levels peaked substantially later than TNF- α mRNA levels in both strains (CD-1: 20 hpd, C57BL/6J: 36 hpd), accompanied by a significant increase in splenic IL-6 transcription (CD-1 mice: 20 and 24 hpd (splenic IL-6 levels before 10 hpd were not examined); C57BL/6J: 5 hpd) compared to fasted mice. However, splenic IL-6 upregulation was not seen in fasted CD-1 mice until the end of the study period at 24 hpd, whereas it was increased (8.6-fold) in fasted C57BL/6J mice at 24 hpd. A previous study has shown that the increase in hepatic IL-6 mRNA levels after APAP administration is induced by TNF- α (Masubuchi et al., 2003c). Both, IL-6 and TNF- α , have been shown to be important for priming hepatocytes to enter the cell cycle (Chiu et al., 2003; Fausto, 2000). A previous study in APAP dosed (600 mg/kg) fasted C57BL/6J mice revealed an upregulation of hepatic IL-6 from 3 hpd onwards and a peak at 12 hpd, followed by a drop at 24 hpd (Bhushan et al., 2014). In the present study, hepatic IL-6 transcription was upregulated at much lower levels after APAP overdose in fasted mice of both strains (and levels were similar in both) than in fed mice. However, this confirms that IL-6 signalling was not interrupted and liver regeneration possible, though consistent with the apparent lower regeneration activity in the fasted mice, as indicated by the significantly lower number of PCNA-positive, proliferating hepatocytes at most time points. Interestingly, the IL-6 expression patterns were similar in spleen and serum in both groups of mice, showing IL-6 production at later time points and a significant upregulation only in the fed mice, correlating with the transcription levels in the liver. The serum IL-6 does likely result from the release by both liver and spleen (Khalil et al., 1996; Kitamura et al., 1997). IL-6 binds to its receptor, gp130 at the cell membrane, which results in the phosphorylation and

nuclear translocation of STAT-3, inducing the transcription of many target genes (Cressman et al., 1995). IL-6 is considered to play a major role in the initiation of repair processes and to promote regeneration of the liver after APAP overdose (Fausto, 2000). The results of a previous study provide evidence that after the peak of injury, i.e. within 12-24 hours of APAP overdose, infiltrating macrophages and Kupffer cells generate IL-6 to downregulate inflammation and promote tissue recovery and have a high chance of phagocytosis (Laskin and Laskin, 2009).

While the role of TNF- α and IL-6 in the progression or regression of APAP induced hepatotoxicity has been widely studied, little is known about the role of **IL-10**, an anti-inflammatory cytokine that has also been shown to play a role in liver regeneration in the partial hepatectomy (PHx) model (Yin et al., 2011). In the present study, significant upregulation of hepatic IL-10 mRNA was observed in fed APAP dosed mice (CD-1 mice: from 10 hpd onwards; C57BL/6J mice: from 15 hpd onwards) and continued to increase until the end of study. In fasted CD-1 mice, a similar tendency was observed, but the upregulation started later and was apparent only at 20 and 24 hpd. In fasted C57BL/6J mice, it was only apparent at 24 hpd and increased towards 36 hpd. The earlier upregulation of IL-10 transcription in the fed mice corresponds to the observed earlier evidence of liver regeneration in these animals (for example, in CD-1 mice, regeneration appeared to be almost complete by 24 hpd, after upregulation of IL-10 transcription from 10 hpd onwards) and suggests a role of IL-10 in liver regeneration also after toxic insults. A previous study reported increased susceptibility to APAP hepatotoxicity in IL-10 KO mice (Bourdi et al., 2002), and another study confirmed the role of IL-10 in promoting liver regeneration (Huang et al., 2006). However, IL-10 deficient mice can still show enhanced liver regeneration via STAT-3 activation after partial hepatectomy (Yin et al., 2011). However, the depletion of these cells reduced the IL-10 expression in regenerating liver after PHx (Yin et al., 2011), but in our study IL-10 was upregulated at later time points after APAP hepatotoxicity.

In the present study, we assessed the expression of **NF-kB** in the APAP DILI model, as it is believed to be activated by TNF- α (Schutze et al., 1995). Following APAP dosing, we observed an increase in NF-kB transcription (13-fold at 10 hpd) in fed

CD-1 mice which remained elevated until the end of the experiment; this was associated with histological evidence of better liver regeneration than in the time-matched fasted mice. In the latter, a significant rise in NF- κ B transcription in comparison to controls was seen at the end of the study, but no difference between both strains. It shows that increased NF- κ B transcription correlates with the stimulation of liver recovery in fed APAP dosed mice and is in line with another study which indicated that NF- κ B is able to generate a pro-regenerative response by inducing the expression of survival genes like BCL_{XL} and AP1, thereby improving liver regeneration after injury (Fausto, 2000; Malhi et al., 2006).

We further studied the transcription and expression of proteins that are expressed during the cell cycle, **cyclin-D1 and proliferating cell nuclear antigen (PCNA)**. Cyclin-D1 is responsible for the regulation of cell cycle entry and is widely used as a marker of proliferating hepatocytes that passed the G1 restriction point and are committed to DNA replication (Fausto, 2000). In our study, cyclin-D1 transcription was first seen to be upregulated in fed CD-1 mice as early as 4 hpd, and it was even higher at 20 hpd, when hepatocellular damage had subsided, confirming the increase in the amount of hepatocytes that had started DNA proliferation. However, in fed C57BL/6J mice, a similar upregulation was only seen from 15 hpd onwards, which coincided with the lower degree of proliferation (8% overall and 0.5% cytoplasmic PCNA-expressing cells vs. 3.9% and 0.35% in CD-1 mice) and the comparatively delayed IL-6 and IL-10 mRNA upregulation in this group of mice. In fasted mice of both strains, where ongoing hepatocellular damage was still observed after 24 hours, cyclin-D1 upregulation was seen from 15 hpd (CD-1 mice) and 24 hpd (C57BL/6J mice) onwards, and at lower levels than in fed mice of both strains. Therefore, this data also confirms that cyclin-D1 transcription is a good marker for liver regeneration (Yang et al., 2009a; Yang et al., 2012c). A study on mice also reported that DNA synthesis starts within 12-16 hours after PHx (Michalopoulos, 1990), but the peak of DNA synthesis is seen later, at 36-40 hours, depending on the strains (Taub, 2004). The increase in DNA synthesis appeared well synchronised and started in periportal hepatocytes, then moving towards centrilobular areas (Taub, 2004). However, toxic agents can have different effects. For example, after massive

liver necrosis or apoptosis induced by CCl₄, DNA synthesis was observed, but the cell-cycle response was not synchronised, different from the response to PHx (Fausto, 1999; Koniaris et al., 2003). Hepatocytes seem to have a variable regenerative capability, only few hepatocytes are needed to regenerate the liver and restore its function after pronounced liver injury (Satyanarayana et al., 2004).

Some authors believed that the necrosis of hepatocytes results in a growth factor and cytokine response similar to that seen in the PHx model (Dabeva and Shafritz, 1993). The results of the present study suggest a peak in DNA synthesis in fed APAP dosed CD-1 mice at 3 hpd, followed by a gradual decrease towards 5 and 10 hpd, followed by a further increase between 15 and 24 hpd. In fed C57BL/6J mice, a gradual increase was seen until 36 hpd. This suggests strain-specific differences. The cyclin-D1 results are complemented by the results of the PCNA staining. These indicate that fed CD-1 mice react to hepatocyte loss with a brief priming phase in which a significant proportion of hepatocytes (approximately 25%) enter the cell cycle. The latter appears to be completed at around 10 hpd, the time when hepatocytes most likely completed the S phase which has been shown to occur after about 8 hours in mice (Alberts et al., 2002). A second replication cycle occurs after this, with a peak at or after 24 hpd. In comparison, fasting prior to the toxic insult does not allow the first peak to occur and it appears that entry of cells from the G₀ phase into the cell cycle is delayed. This might be, because the more pronounced liver injury and marked cell death inhibits the entry of hepatocytes into the cell cycle at an early stage. A study has reported inhibition of liver regeneration following APAP overdose in fasted C57BL/6J mice as a result of p21 protein induction, an active inhibitor of the cell cycle, due to increased cellular stress (Bhushan et al., 2014). The results of the present study indicate that at this early stage (up to 5 hpd), regeneration in fasted APAP dosed mice does entirely rely on cells that were in the cell cycle at the time of injury, as cytoplasmic PCNA expression was significantly increased. At the later stage, the extent of hepatic regeneration, as represented by both nuclear and cytoplasmic hepatocellular PCNA expression, appear to be similar in fed and fasted mice. The lack of the initial proliferation peak after fasting would then explain the still apparent hepatocyte loss at 24 hpd.

The amount of **cytoplasmic PCNA expression** was also assessed to identify hepatocytes that had entered the M and/or G2 phase of the cell cycle. In regenerating hepatocytes, the exact mechanism that could restrict hepatocytes to enter the M phase still needs to be further studied (Miyaoaka and Miyajima, 2013). The amount of cells in the M phase (mitosis) was always lower than that of the cells in the early, i.e. G1/S phase of the cell cycle. Upon completion of DNA synthesis, hepatocytes need to pass the G2 checkpoints, ensuring that genome stability is maintained before they undergo mitosis (Stark and Taylor, 2004). In the present study, cytoplasmic PCNA expression was seen earlier in fed CD-1 mice than in fed C57BL/6J mice. Intriguingly, we also observed a rapid (as early as 0.5 hpd until 5 hpd) and significant increase in hepatocytes showing cytoplasmic PCNA expression in fasted CD-1 mice compared to control animals, which likely represents cells that were in the G1 phase at the time of injury and were activated rapidly to undergo mitosis. However, in fasted C57BL/6J mice, the increase in overall PCNA-positive hepatocytes started later, suggesting a further delay in DNA synthesis (from 15 hpd onwards) in comparison to fasted CD-1 mice (at 10 hpd onwards). The findings in fasted mice are in line with another study in rats where hepatocyte proliferation was reduced after a fasting period but increased after food was resumed (Kouda et al., 2004). A previous study on C57BL/6J mice exposed to different APAP doses showed delayed onset of liver proliferation with more intense liver damage after fasting, which was believed to be due to the suppression of many proteins involved in the regulation of the cell cycle, including cyclins and cyclin-dependent kinases, or the inhibition of cell cycle progression, such as p21 or p38 (Bhushan et al., 2014).

The following sequence of actions of liver regeneration is likely: TNF α -TNFR1-NFkB-IL6-IL10. Animals deficient in TNF receptor 1 (TNFR1) that received TNF- α neutralising antibodies show a reduction in hepatic DNA synthesis and STAT3 activation after APAP overdose (Diehl, 1995; Gardner et al., 2003; Yamada et al., 1997). Despite the fact that TNF- α has a pro-inflammatory role, studies in TNFR1-deficient mice have shown that TNFR1 is important for liver regeneration following APAP injury in the mouse (Chiu et al., 2003). A modest elevation of hepatic TNF- α would increase the binding of TNF- α to TNFR1 which would result in nuclear

translocation of NF- κ B and its activation, which could in turn prevent further cell death and promote a proliferative response by increasing cell progression in the G1 and S phase (Yamada and Fausto, 1998; Yamada et al., 1997). This mechanism could be responsible for the high cyclin-D1 and PCNA expression and thereby the regeneration seen in fed animals in our study. Our data showed TNF- α /NF- κ B transcription was upregulated earlier in fed than in fasted mice; this would suggest that TNF- α indeed has a role in liver regeneration following APAP overdose, as indicated in previous studies (Bhushan et al., 2014; Hinson et al., 2010). At the same time, NF- κ B activation can enhance the hepatic IL-6 transcription, which will stimulate the JAK/STAT pathway to initiate and trigger STAT-3 activation (Cressman et al., 1996; Wuestefeld et al., 2003). STAT-3 is a signal transduction factor that activates a large number of genes, i.e. cfos, IRF-1 or AP1 for hepatocyte regeneration (Li et al., 2002). IL-6/STAT-3 signalling has promitotic effects on various cells for hepatic regeneration and improves cell survival (Kovalovich et al., 2001; Michalopoulos and DeFrances, 1997). Accordingly, the upregulation of IL-6 transcription that we observed after the upregulation of TNF- α and NF- κ B in the fed APAP dosed mice suggests that this pathway is also active in the regenerative processes after APAP induced liver injury.

Cyclin-D1 is an important transcriptional target of NF- κ B, activating its expression (Guttridge et al., 1999). Furthermore, IL-6 also increases the expression of IL-10 as IL-6 alone is unable to stimulate the proliferation of hepatocytes in vivo (Bourdi et al., 2002). Without a potent stimulation towards liver recovery, IL-10 does regulate regeneration and inhibit inflammation by attenuating ROS and peroxynitrite production (Krenkel et al., 2014). Our data suggest that the less extensive transcription of NF- κ B in the liver may be one of the reasons for the observed less intense cyclin-D1 transcription and delayed/less intense hepatic regeneration in fasted APAP dosed mice as seen in our study. Thus, our results indicate that depending on the conditions, a given APAP dose can be toxic, inducing only brief damage to the liver, as regeneration rapidly restores the integrity, or leading to a more prolonged damage, with delayed regeneration and a systemic inflammatory response, providing a scenario in which further (functional) challenges to the liver

would likely be more harmful (Prescott, 2000). In any case, our data clearly indicate that fasted mice have a reduced regenerative capacity of the liver, likely due to delayed and less intense activation of the TNF- α /NF- κ B, IL-6/STAT3 and IL-10 pathways and a subsequent delayed and reduced induction of cyclin-D1 and PCNA expression, leading to reduced cell proliferation. Multiple mechanisms are likely involved in the facilitation of liver regeneration following toxic injury, in which the above mentioned appear to play significant roles (Figure 4.1).

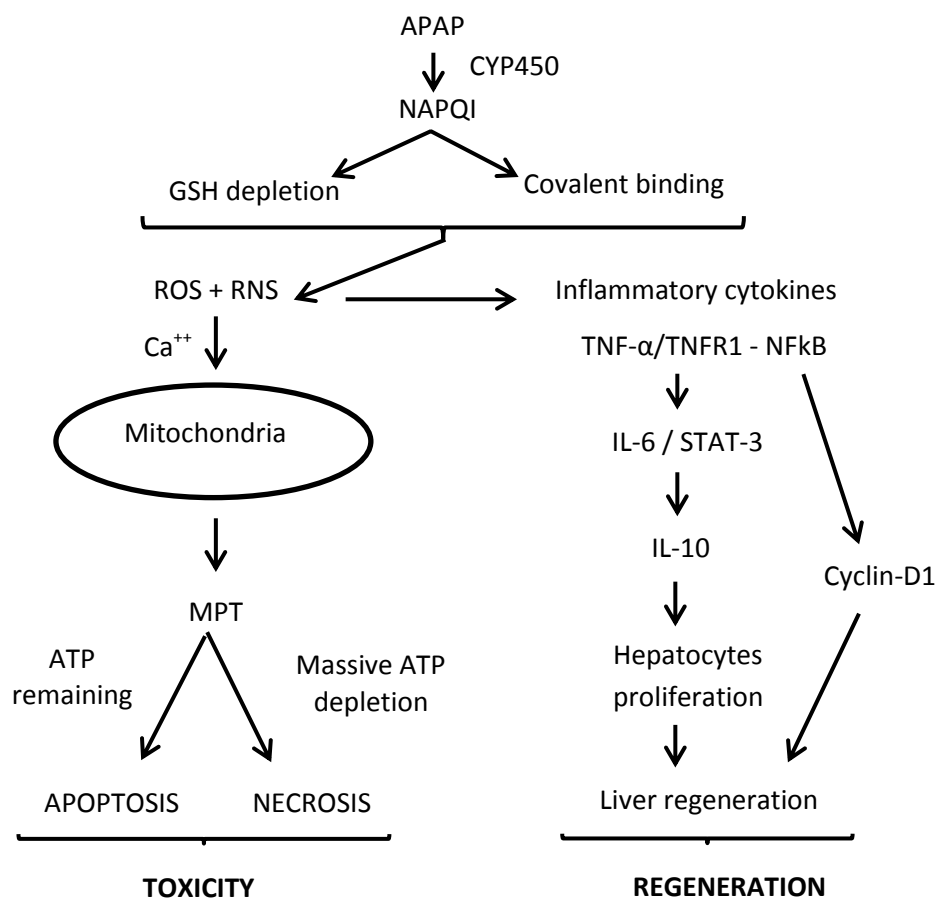


Figure 4.1. Schematic diagramme of mechanisms involved in APAP induced toxic liver injury and subsequent regeneration.

APAP is metabolised by cytochrome P450 (CYP450) to NAPQI which binds to and thereby depletes glutathione (GSH) and covalently binds to proteins. Loss of GSH leads to oxidative stress by increasing the formation of reactive oxygen species (ROS) and reactive nitrogen species (RNS) that alter the calcium metabolism of mitochondria. This initiates mitochondrial permeability transition (MPT) that inhibits the mitochondrial membrane potential and thereby the synthesis of ATP. Consequently, hepatocytes die either via apoptosis or necrosis, depending on the availability of ATP. Cytokines like TNF- α is released after inflammatory cells are sensitised as a consequence of, among others (i.e. HMGB-1), ROS and RNS. The TNF- α /NF- κ B pathway is activated, followed by IL-6/STAT-3, cyclin-D1 and IL-10 expression which promote hepatocyte proliferation and thereby liver regeneration.

4.2.3 Differences in the response to APAP injury and the subsequent regenerative process in fed and fasted CD-1 and C57BL/6J mice

The present study represents a thorough comparative investigation into the time course and events following APAP overdose in fed and fasted male CD-1 and C57BL/6J mice, covering the period from immediately after dosing to a time point when in fed CD-1 mice there was evidence of full regeneration at 24 hpd, these were considered as the “standard” for the study which is believed to correlate with the levels of GSH, ATP, ALT and DILI score. A comparison of fed and fasted mice of each strain and an overall comparison between both strains is provided in the Appendix (Table 6.30: CD-1; Table 6.42: C57BL/6J; Table 6.43: both strains).

In summary, in **fed CD-1 mice**, first evidence of centrilobular cell loss due to cell death via apoptosis and necrosis and minimal neutrophil infiltration, accompanied by loss of glycogen stores, is seen at 3 hpd and intensified at 5 hpd; this coincides with GSH and ATP depletion. In conjunction with these findings, PCNA expressing hepatocytes were increased in number at the same time points, indicating that a proportion of remaining intact cells entered the cell cycle immediately after the onset of cell loss, which was also supported by the observed upregulation of cyclin-D1 and TNF- α transcription. At the same time, IL-6, IL-10 and NF- κ B transcription also showed onset of a progressive increase. While GSH and ATP depletion was still evident at 10 hpd, centrilobular damage and inflammatory response had declined and the number of PCNA-positive proliferating cells was very low, indicating that the first cell cycle after injury was already completed by then. From 15 hpd onwards, the PCNA expression increased again and was correlated with an elevation in hepatic cyclin-D1 transcription. DILI scores decreased further and complete regeneration with numerous mitotic figures and diffuse hepatocellular glycogen restitution by 24 hpd, the time when GSH and ATP levels had returned to control mice, and only ALT activities remaining high. At this time, the transcription of all examined cytokines and transcription factors had started to decline. Briefly, **fed C57BL/6J mice** differed from CD-1 mice in the response to APAP overdose in so far, that the extent of injury and inflammatory cell recruitment was more pronounced and prolonged. Even at 36 hpd, the liver had not completely recovered

and showed ongoing centrilobular hepatocyte degeneration and death, even though GSH and ATP levels had returned to those of control animals. Moreover, the expression of markers of regeneration (NF- κ B, cyclin-D1 and PCNA) was lower at the early time points, then increased over time and finally reached levels similar to CD-1 mice. These findings are consistent with strain specific differences in the response to APAP overdose that could lead to very different results and interpretations depending on the type of study and parameters tested.

In **fasted animals** of both strains, higher DILI scores and more pronounced neutrophil infiltration was seen, with impaired glycogen restitution was seen as early as 3 to 5 hpd. This was associated with higher serum ALT levels than in fed mice. This correlated with marked depletion of the levels of GSH, ATP and glycogen stores that had already been diminished significantly due to the prior fasting alone. This confirms that fasting compromises the hepatic detoxification capacity due to GSH depletion, leading to increased susceptibility to APAP hepatotoxicity (Larson, 2007). Coupled with the prolonged reduction of hepatic ATP, this contributes to the increased ALT activities and exacerbates hepatocellular damage (Antoine et al., 2010; Walker et al., 1982). Thereafter, DILI scores declined in both strains over time until the end of the experiment. The observed TNF- α upregulation at later time points correlates with the neutrophil influx and the larger extent of hepatocyte necrosis. Both strains also showed an increase of IL-6, IL-10, NF- κ B and cyclin-D1 transcription, again more pronounced at the later time points. Accordingly, the increase in hepatocyte proliferation was also delayed, with a first peak in overall PCNA-positive hepatocytes only at 20 hpd; there was only minimal histological evidence of liver regeneration until the end of the study period at 24 and 36 hpd, respectively. These differences can explain the delay of liver recovery in the fasted groups, where very similar results were obtained for both strains. They are of quantitative or time-related nature, without evidence of major mechanistic differences. To date, the cause for the difference in susceptibility to APAP overdose in various mouse strains is not fully understood. However, it was believed that the differences of basal gene expression including drug metabolism, innate immune and

stress response could influence the response (Jaeschke et al., 2012) Jaeschke et al., 2012).

4.3 CONCLUSIONS

Fasting prior to dosing is a routine procedure in scientific experimentation. However, thorough investigations to address the potential implications of fasting in each animal model and whether these might compromise animal welfare or generate an unintended variability in some parameters that would interfere with the study outcome have so far not reported. The present study has addressed this knowledge gap and provides insight into differences in baseline levels between an example out-bred (CD-1) and an in-bred (C57BL/6J) mouse strain and in their response to fasting, which need to be considered before conducting a mouse study. Our study revealed that fed C57BL/6J mice had higher GSH levels but lower ATP content than CD-1 mice. While fed mice of both strains showed GSH-oriented circadian rhythm, fasting mice had produced GSH excessively after 10 hours of refeeding. Meanwhile, refeeding C57BL/6J mice exhibited better ATP recovery and glycogen restitution than those in CD-1 mice. The response exhibited by different mouse strain could not be ignored. The background information of different mouse model could provide better understanding on choice of mouse model for DILI studies.

The present study also provides further insight into the processes and mechanisms leading to toxic liver changes after APAP overdose, covering the period of acute liver injury to full regeneration. Our findings confirm that fasting prior to APAP overdose has a substantial effect on the GSH and ATP content, the extent of liver damage and serum ALT activities and the presence and extent of a systemic inflammatory response. Fasting also delays the onset and extent of liver regeneration. In fed animals, a less intense and short-lived upregulation of TNF- α transcription in combination with IL-6 and IL-10, NF-kB and cyclin-D1 mRNA upregulation as well as a more pronounced hepatocellular PCNA expression reflects

the better hepatic regenerative capacity as it was indicated by the histological examination. The quantitative differences in the transcription of the listed markers appear informative to evaluate the degree of liver damage and regeneration in the murine model of APAP hepatotoxicity. Therefore, further studies using respective knock-out mice would be beneficial to clarify the role played by these cytokines in particular in the regeneration of the liver after toxic injury.

The present study also confirms that different mouse strains respond differently to the same APAP dose. However, the differences were almost exclusively restricted to the time-related and quantitative aspects of the response to APAP overdose. Fed C57BL/6J mice showed evidence of a higher susceptibility to APAP toxicity than fed CD-1 mice, and accordingly delays in the subsequent regenerative processes; this does, however, not suggest differences in the principle toxic and regenerative mechanisms. It would be interesting to extend the study to assess the time required for complete liver regeneration in fasted CD-1 as well as fed and fasted C57BL/6J mice. Additionally, further investigations would be required to fully illustrate the mechanisms involved in the delay of the hepatic recovery and also to explain the differences between mouse strains. Documentation of the latter would allow researchers to optimise their experimental approach by choosing the most suitable mouse model. Hence, this could minimise the risk of highly variable and/or controversial results and further enhance the validity of the studies. Since the liver has a major regenerative capacity that is triggered by several cytokines and growth factors, future investigations are needed to provide more insight into signalling pathways that are important for liver regeneration, as a tool to identify novel targets for the treatment of acetaminophen intoxication.

CHAPTER FIVE

BIBLIOGRAPHY

- Abbas, A.K., Lichtman, A.H.H., Pillai, S., (2015) Basic Immunology: Functions and Disorders of the Immune System. *Elsevier Limited, Oxford*, 29-38.
- Abshagen, K., Eipel, C., Kalff, J.C., Menger, M.D., Vollmar, B., (2007) Loss of NF-kappaB activation in Kupffer cell-depleted mice impairs liver regeneration after partial hepatectomy. *Am J Physiol Gastrointest Liver Physiol* **292**, G1570-1577.
- Acton, Q.A., (2013) Acetanilides—Advances in Research and Application: 2013 Edition. *Scholarly Editions*, 13-15.
- Adams, D.H., Ju, C., Ramaiah, S.K., Uetrecht, J., Jaeschke, H., (2010) Mechanisms of Immune-Mediated Liver Injury. *Toxicological Sciences* **115**, 307-321.
- Agarwal, R., MacMillan-Crow, L.A., Rafferty, T.M., Saba, H., Roberts, D.W., Fifer, E.K., James, L.P., Hinson, J.A., (2011) Acetaminophen-induced hepatotoxicity in mice occurs with inhibition of activity and nitration of mitochondrial manganese superoxide dismutase. *J Pharmacol Exp Ther* **337**, 110-116.
- Alberts B, Johnson A, Lewis J, et al. Bruce Alberts, Alexander Johnson, Julian Lewis, Martin Raff, Keith Roberts, and Peter Walter Molecular Biology of the Cell. 4th edition. New York: Garland Science; 2002. The Initiation and Completion of DNA Replication in Chromosomes. Aller, M.A., Arias, J.L., Sanchez-Patan, F., (2006) The inflammatory response: an efficient way of life. *Med Sci Monit* **12**, RA225-234.
- Amacher, D.E., (1998) Serum transaminase elevations as indicators of hepatic injury following the administration of drugs. *Regul Toxicol Pharmacol* **27**, 119-130.
- Anand, S.S., Murthy, S.N., Vaidya, V.S., Mumtaz, M.M., Mehendale, H.M., (2003) Tissue repair plays pivotal role in final outcome of liver injury following chloroform and allyl alcohol binary mixture. *Food and Chemical Toxicology* **41**, 1123-1132.
- Antoine, D.J., Williams, D.P., Kipar, A., Jenkins, R.E., Regan, S.L., Sathish, J.G., Kitteringham, N.R., Park, B.K., (2009) High-mobility group box-1 protein and keratin-18, circulating serum proteins informative of acetaminophen-induced necrosis and apoptosis in vivo. *Toxicol Sci* **112**, 521-531.
- Antoine, D.J., Williams, D.P., Kipar, A., Laverty, H., Park, B.K., (2010) Diet Restriction Inhibits Apoptosis and HMGB1 Oxidation and Promotes Inflammatory Cell Recruitment during Acetaminophen Hepatotoxicity. *Molecular Medicine* **16**, 1-490.
- Apte, U., (2009) Hepatic defenses against toxicology: Liver regeneration and tissue repair. *Comprehensive Toxicology* 339-367.
- Apte, U., Gkretsi, V., Bowen, W.C., Mars, W.M., Luo, J.H., Donthamsetty, S., Orr, A., Monga, S.P., Wu, C., Michalopoulos, G.K., (2009a) Enhanced liver regeneration following changes induced by hepatocyte-specific genetic ablation of integrin-linked kinase. *Hepatology* 50.
- Apte, U., Singh, S., Zeng, G., Cieply, B., Virji, M.A., Wu, T., Monga, S.P.S., (2009) Beta-Catenin Activation Promotes Liver Regeneration after Acetaminophen-Induced Injury. *The American Journal of Pathology* **175**, 1056-1065.
- Ashkenazi, A., Dixit, V.M., (1998). Death Receptors: Signaling and Modulation. *Science (Classic)* **281**, 1305-1308.
- Ayala, J.E., Bracy, D.P., McGuinness, O.P., Wasserman, D.H., (2006) Considerations in the Design of Hyperinsulinemic-Euglycemic Clamps in the Conscious Mouse. *Diabetes* **55**, 390-397.
- Bari, K., Fontana, R.J., (2014) Acetaminophen overdose: What practitioners need to know. *Clinical Liver Disease* **4**, 17-21.
- Bartolone, J.B., Birge, R.B., Sparks, K., Cohen, S.D., Khairallah, E.A., (1988) Immunochemical analysis of acetaminophen covalent binding to proteins. *Biochemical pharmacology* **37**, 4763-4774.

- Bare, J.K., Cicala, G., (1960) Deprivation and time of testing as determinants of food intake. *J Comp Physiol Psychol* **53**, 151-154.
- Bauer, M., Hamm, A.C., Bonaus, M., Jacob, A., Jaekel, J., Schorle, H., Pankratz, M.J., Katzenberger, J.D., (2004) Starvation response in mouse liver shows strong correlation with life-span-prolonging processes. *Physiol Genomics* **17**, 230-244.
- Beck, J.A., Lloyd, S., Hafezparast, M., Lennon-Pierce, M., Eppig, J.T., Festing, M.F., Fisher, E.M., (2000) Genealogies of mouse inbred strains. *Nature genetics* **24**, 23-25.
- Becketta, G.J., Dyson, E.H., Chapman, B.J., Templeton, A.J., Hayes, J.D., (1985) Plasma glutathione S-transferase measurements by radioimmunoassay: a sensitive index of hepatocellular damage in man. *Clinica chemica acta* **146**, 11-19.
- Berg, J.M., Tymoczko, J.L., Stryer, L., (2002) Biochemistry. 5th edition. *W.H. Freeman, New York*. Section 16.1, Glycolysis Is an Energy-Conversion Pathway in Many Organisms.
- Bhushan, B., Walesky, C., Manley, M., Gallagher, T., Borude, P., Edwards, G., Monga, S.P.S., Apte, U., (2014) Pro-Regenerative Signaling after Acetaminophen-Induced Acute Liver Injury in Mice Identified Using a Novel Incremental Dose Model. *The American Journal of Pathology* **184**, 3013-3025.
- Biron, C.A., Nguyen, K.B., Pien, G.C., Cousens, L.P., Salazar-Mather, T.P., (1999) Natural killer cells in antiviral defense: function and regulation by innate cytokines. *Annu Rev Immunol* **17**, 189-220.
- Bj, P., Yang, M.U., Yang, M.U., (1982) Refeeding after fasting in the rat: effects on body composition and food efficiency. *The American Journal of Clinical Nutrition* **36**, 444-449.
- Blazka, M.E., Elwell, M.R., Holladay, S.D., Wilson, R.E., Luster, M.I., (1996) Histopathology of Acetaminophen-Induced Liver Changes: Role of Interleukin 1 alpha and Tumor Necrosis Factor alpha. *Toxicologic Pathology* **24**, 181-189.
- Blazka, M.E., Wilmer, J.L., Holladay, S.D., Wilson, R.E., Luster, M.I., (1995) Role of Proinflammatory Cytokines in Acetaminophen Hepatotoxicity. *Toxicology and Applied Pharmacology* **133**, 43-52.
- Boelsterli, U.A., Lim, P.L., (2007) Mitochondrial abnormalities--a link to idiosyncratic drug hepatotoxicity? *Toxicol Appl Pharmacol* **220**, 92-107.
- Boess, F., Bopst, M., Althaus, R., Polsky, S., Cohen, S.D., Eugster, H., Pietro, Boelsterli, U.A., (1998) Acetaminophen hepatotoxicity in tumor necrosis factor/lymphotoxin-alpha; gene knockout mice. *Hepatology* **27**, 1021-1029.
- Bolder, U., Trang, N.V., Hagey, L.R., Schteingart, C.D., Ton-nu, H., Cerre, C., Oude Elferink, R.P.J., Hofmann, A.F., (1999) Sulindac is excreted into bile by a canalicular bile salt pump and undergoes a cholehepatic circulation in rats. *Gastroenterology* **117**, 962-971.
- Borst, P., Elferink, R.O., (2002) Mammalian ABC Transporters in Health and Disease. *Annual Review of Biochemistry* **71**, 537-592.
- Bossy-Wetzel, E., Green, D.R., (1999). Apoptosis: checkpoint at the mitochondrial frontier. *Mutat Res* **434**, 243-251.
- Botta, D., Shi, S., White, C.C., Dabrowski, M.J., Keener, C.L., Srinouanprachanh, S.L., Farin, F.M., Ware, C.B., Ladiges, W.C., Pierce, R.H., Fausto, N., Kavanagh, T.J., (2006) Acetaminophen-induced liver injury is attenuated in male glutamate-cysteine ligase transgenic mice. *J Biol Chem* **281**, 28865-28875.
- Botting, R., (2000) Paracetamol-inhibitable COX-2. *J Physiol Pharmacol* **51**, 609-618.

- Bour, E.S., Ward, L.K., Cornman, G.A., Isom, H.C., (1996) Tumor necrosis factor-alpha-induced apoptosis in hepatocytes in long-term culture. *The American Journal of Pathology* **148**, 485-495.
- Bourdi, M., Masubuchi, Y., Reilly, T.P., Amouzadeh, H.R., Martin, J.L., George, J.W., Shah, A.G., Pohl, L.R., (2002) Protection against acetaminophen-induced liver injury and lethality by interleukin 10: Role of inducible nitric oxide synthase. *Hepatology* **35**, 289-298.
- Boutaud, O., Aronoff, D.M., Richardson, J.H., Marnett, L.J., Oates, J.A., (2002) Determinants of the cellular specificity of acetaminophen as an inhibitor of prostaglandin H2 synthases. *Proceedings of the National Academy of Sciences* **99**, 7130-7135
- Bradham, C.A., Plumpe, J., Manns, M.P., Brenner, D.A., Trautwein, C., (1998) Mechanisms of hepatic toxicity. I. TNF-induced liver injury. *Am J Physiol* **275**, G387-392.
- Bravo, R., Frank, R., Blundell, P.A., Macdonald-Bravo, H., (1987) Cyclin/PCNA is the auxiliary protein of DNA polymerase-delta. *Nature* **326**, 515-517.
- Brooks, R.R., Pong, S.F., (1981) Effects of fasting, body weight, methylcellulose, and carboxymethylcellulose on hepatic glutathione levels in mice and hamsters. *Biochemical pharmacology* **30**, 589-594.
- Buki, A., Okonkwo, D.O., Wang, K.K., Povlishock, J.T., (2000) Cytochrome c release and caspase activation in traumatic axonal injury. *J Neurosci* **20**, 2825-2834.
- Casini, A.F., Pompella, A., Comporti, M., (1984) Glutathione depletion, lipid peroxidation, and liver necrosis following bromobenzene and iodobenzene intoxication. *Toxicol Pathol* **12**, 295-299.
- Chia, R., Achilli, F., Festing, M.F., Fisher, E.M., (2005) The origins and uses of mouse outbred stocks. *Nat Genet* **37**, 1181-1186.
- Chiu, H., Gardner, C.R., Dambach, D.M., Durham, S.K., Brittingham, J.A., Laskin, J.D., Laskin, D.L., (2003) Role of tumor necrosis factor receptor 1 (p55) in hepatocyte proliferation during acetaminophen-induced toxicity in mice. *Toxicology and Applied Pharmacology* **193**, 218-227.
- Claassen, V. (1994) In "Neglected factors in Pharmacology and Neuroscience Research". Elsevier, 290-320.
- Cohen, G.M., (1997) Caspases: the executioners of apoptosis. *Biochemical Journal* **326**, 1-16.
- Coles, B., Wilson, I., Wardman, P., Hinson, J.A., Nelson, S.D., Ketterer, B., (1988) The spontaneous and enzymatic reaction of N-acetyl-p-benzoquinonimine with glutathione: A stopped-flow kinetic study. *Archives of biochemistry and biophysics* **264**, 253-260.
- Corcoran, G.B., Fix, L., Jones, D.P., Moslen, M.T., Nicotera, P., Oberhammer, F.A., Buttyan, R., (1994) Apoptosis: molecular control point in toxicity. *Toxicol Appl Pharmacol* **128**, 169-181.
- Cover, C., Mansouri, A., Knight, T.R., Bajt, M.L., Lemasters, J.J., Pessayre, D., Jaeschke, H., (2005) Peroxynitrite-induced mitochondrial and endonuclease-mediated nuclear DNA damage in acetaminophen hepatotoxicity. *J Pharmacol Exp Ther* **315**, 879-887.
- Cressman, D.E., Diamond, R.H., Taub, R., (1995) Rapid activation of the Stat3 transcription complex in liver regeneration. *Hepatology* **21**, 1443-1449.
- Cressman, D.E., Greenbaum, L.E., DeAngelis, R.A., Ciliberto, G., Furth, E.E., Poli, V., Taub, R., (1996) Liver Failure and Defective Hepatocyte Regeneration in Interleukin-6-Deficient Mice. *Science (Classic)* **274**, 1379-1383.

- Dabeva, M.D., Shafritz, D.A., (1993) Activation, proliferation, and differentiation of progenitor cells into hepatocytes in the D-galactosamine model of liver regeneration. *The American Journal of Pathology* **143**, 1606-1620.
- Dahlin, D.C., Miwa, G.T., Lu, A.Y., Nelson, S.D., (1984) N-acetyl-p-benzoquinone imine: a cytochrome P-450-mediated oxidation product of acetaminophen. *Proceedings of the National Academy of Sciences* **81**, 1327-1331.
- Dai, G., He, L., Chou, N., Wan, Y.J., (2006) Acetaminophen metabolism does not contribute to gender difference in its hepatotoxicity in mouse. *Toxicol Sci* **92**, 33-41.
- Dallman, M.F., Akana, S.F., Strack, A.M., Hanson, E.S., Sebastian, R.J., (1995) The Neural Network that Regulates Energy Balance Is Responsive to Glucocorticoids and Insulin and Also Regulates HPA Axis Responsivity at a Site Proximal to CRF Neurons. *Annals of the New York Academy of Sciences* **771**, 730-742.
- David Josephy, P., (2005) The Molecular Toxicology of Acetaminophen. *Drug Metabolism Reviews* **37**, 581-594.
- Davies, M.H., (1986) Acetaminophen toxicity in isolated hepatocytes. *Advances in Experimental Medicine and Biology* **197**, 993-1003.
- Davis, D.C., Potter, W.Z., Jollow, D.J., Mitchell, J.R., (1974) Species differences in hepatic glutathione depletion, covalent binding and hepatic necrosis after acetaminophen. *Life sciences* **14**, 2099-2109.
- Dean, M., Rzhetsky, A., Allikmets, R., (2001) The Human ATP-Binding Cassette (ABC) Transporter Superfamily. *Genome Research* **11**, 1156-1166.
- Decker, K., (1990) Biologically active products of stimulated liver macrophages (Kupffer cells). *European Journal of Biochemistry* **192**, 245-261.
- Deli, A., Kreidl, E., Santifaller, S., Trotter, B., Seir, K., Berger, W., Schulte-Hermann, R., Rodgarkia-Dara, C., Grusch, M., (2008) Activins and activin antagonists in hepatocellular carcinoma. *World Journal of Gastroenterology : WJG* **14**, 1699-1709.
- Diehl, A., (1995) Tumor necrosis factor-alpha modulates CCAAT/enhancer binding proteins-DNA binding activities and promotes hepatocyte-specific gene expression during liver regeneration 1. *Hepatology* **22**, 252-261.
- Dietze, E.C., Schafer, A., Omichinski, J.G., Nelson, S.D., (1997) Inactivation of Glyceraldehyde-3-phosphate Dehydrogenase by a Reactive Metabolite of Acetaminophen and Mass Spectral Characterization of an Arylated Active Site Peptide. *Chemical Research in Toxicology* **10**, 1097-1103.
- Donahower, B.C., McCullough, S.S., Hennings, L., Simpson, P.M., Stowe, C.D., Saad, A.G., Kurten, R.C., Hinson, J.A., James, L.P., (2010) Human recombinant vascular endothelial growth factor reduces necrosis and enhances hepatocyte regeneration in a mouse model of acetaminophen toxicity. *Journal of Pharmacology and Experimental Therapeutics* **334**, 33-43.
- Dossing, M., Sonne, J., (1993) Drug-induced hepatic disorders. Incidence, management and avoidance. *Drug Saf* **9**, 441-449.
- Douni, E., Kollias, G., (1998) A Critical Role of the p75 Tumor Necrosis Factor Receptor (p75TNF-R) in Organ Inflammation Independent of TNF, Lymphotoxin α , or the p55TNF-R. *Journal of Experimental Medicine* **188**, 1343-1352.
- Dumitriu, I.E., Baruah, P., Manfredi, A.A., Bianchi, M.E., Rovere-Querini, P., (2005) HMGB1: guiding immunity from within. *Trends in Immunology* **26**, 381-387.
- Eguchi, Y., Shimizu, S., Tsujimoto, Y., (1997) Intracellular ATP levels determine cell death fate by apoptosis or necrosis. *Cancer Res* **57**, 1835-1840.
- El-Hassan, H., Anwar, K., Macanas-Pirard, P., Crabtree, M., Chow, S.C., Johnson, V.L., Lee, P.C., Hinton, R.H., Price, S.C., Kass, G.E., (2003) Involvement of mitochondria in

- acetaminophen-induced apoptosis and hepatic injury: roles of cytochrome c, Bax, Bid, and caspases. *Toxicol Appl Pharmacol* **191**, 118-129.
- Eldrige, S.R., Butterworth, B.E., Goldsworthy, T.L., (1993) Proliferating cell nuclear antigen: a marker for hepatocellular proliferation in rodents. *Environ Health Perspect* **5**, 211-218.
- Ellacott, K.L.J., Morton, G.J., Woods, S.C., Tso, P., Schwartz, M.W., (2010) Assessment of Feeding Behavior in Laboratory Mice. *Cell Metabolism* **12**, 10-17.
- Elmore, S., (2007) Apoptosis: a review of programmed cell death. *Toxicol Pathol* **35**, 495-516.
- Evans, J., (1993) Liver failure induced by paracetamol. *British Medical Journal* **306**, 717-718.
- Faouzi, S., Burckhardt, B.E., Hanson, J.C., Campe, C.B., Schrum, L.W., Rippe, R.A., Maher, J.J., (2001) Anti-Fas induces hepatic chemokines and promotes inflammation by an NF-kappa B-independent, caspase-3-dependent pathway. *J Biol Chem* **276**, 49077-49082.
- Fausto, N., (1999) Lessons from genetically engineered animal models. V. Knocking out genes to study liver regeneration: present and future. *Am J Physiol* **277**, G917-921.
- Fausto, N., (2000) Liver regeneration. *J Hepatol* **32**, 19-31.
- Ferret, P.J., Hammoud, R., Tulliez, M., Tran, A., Trebeden, H., Jaffray, P., Malassagne, B., Calmus, Y., Weill, B., Batteux, F., (2001) Detoxification of reactive oxygen species by a nonpeptidyl mimic of superoxide dismutase cures acetaminophen-induced acute liver failure in the mouse. *Hepatology* **33**, 1173-1180.
- Festing, M.F.W., (2010) Invited review: Inbred strains should replace outbred stocks in toxicology, safety testing, and drug development. *Toxicologic Pathology* **38**, 681-690.
- Fiers, W., (1991) Tumor necrosis factor Characterization at the molecular, cellular and in vivo level. *FEBS letters* **285**, 199-212.
- Fisher, J.E., McKenzie, T.J., Lillegard, J.B., Yu, Y., Juskewitch, J.E., Nedredal, G.I., Brunn, G.J., Yi, E.S., Malhi, H., Smyrk, T.C., Nyberg, S.L., (2013) Role of Kupffer cells and toll-like receptor 4 in acetaminophen-induced acute liver failure. *J Surg Res* **180**, 147-155.
- Fournie, G.J., Courtin, J.P., Laval, F., Chale, J.J., Pourrat, J.P., Pujazon, M.C., Lauque, D., Carles, P., (1995) Plasma DNA as a marker of cancerous cell death. Investigations in patients suffering from lung cancer and in nude mice bearing human tumours. *Cancer Lett* **91**, 221-227.
- Francavilla, A., Makowka, L., Polimeno, L., Barone, M., Demetris, J., Prelich, J., Van Thiel, D.H., Starzl, T.E., (1989) A dog model for acetaminophen-induced fulminant hepatic failure. *Gastroenterology* **96**, 470-478.
- Franco, R., Cidlowski, J.A., (2009) Apoptosis and glutathione: beyond an antioxidant. *Cell Death Differ* **16**, 1303-1314.
- Friedman, J.R., Kaestner, K.H., (2011) On the origin of the liver. *The Journal of Clinical Investigation* **121**, 4630-4633.
- Froy, O., Miskin, R., (2010) Effect of feeding regimens on circadian rhythms: implications for aging and longevity. *Aging (Albany NY)* **2**, 7-27.
- Froy, O., Miskin, R., (2007) The interrelations among feeding, circadian rhythms and ageing. *Progress in Neurobiology* **82**, 142-150.
- Fry, M. (2010) Essential biochemistry for medicine (Chichester, West Sussex, Wiley-Blackwell), 13-17.

- Galun, E., Axelrod, J.H., (2002) The role of cytokines in liver failure and regeneration: potential new molecular therapies. *Biochimica et Biophysica Acta (BBA) - Molecular Cell Research* **1592**, 345-358.
- Gao, B., Radaeva, S., Park, O., (2009) Liver natural killer and natural killer T cells: immunobiology and emerging roles in liver diseases. *J Leukoc Biol* **86**, 513-528.
- Gardner, C.R., Laskin, J.D., Dambach, D.M., Chiu, H., Durham, S.K., Zhou, P., Bruno, M., Gerecke, D.R., Gordon, M.K., (2003) Exaggerated hepatotoxicity of acetaminophen in mice lacking tumor necrosis factor receptor-1 Potential role of inflammatory mediators. *Toxicology and Applied Pharmacology* **192**, 119-130.
- Gavrilova, O., Leon, L.R., Marcus-Samuels, B., Mason, M.M., Castle, A.L., Refetoff, S., Vinson, C., Reitman, M.L., (1999) Torpor in mice is induced by both leptin-dependent and -independent mechanisms. *Proceedings of the National Academy of Sciences* **96**, 14623-14628.
- Gazzard, B.G., Hughes, R.D., Mellon, P.J., Portmann, B., Williams, R., (1975) A dog model of fulminant hepatic failure produced by paracetamol administration. *Br J Exp Pathol* **56**, 408-411.
- Giannini, E.G., Testa, R., Savarino, V., (2005) Liver enzyme alteration: a guide for clinicians. *CMAJ : Canadian Medical Association Journal* **172**, 367-379.
- Gjorret, J.O., Fabian, D., Avery, B., Maddox-Hyttel, P., (2007) Active caspase-3 and ultrastructural evidence of apoptosis in spontaneous and induced cell death in bovine in vitro produced pre-implantation embryos. *Mol Reprod Dev* **74**, 961-971.
- Goldin, R.D., Ratnayaka, I.D., Breach, C.S., Brown, I.N., Wickramasinghe, S.N., (1996) Role of macrophages in acetaminophen (paracetamol)-induced hepatotoxicity. *Journal of Pathology* **179**, 432-435.
- Goldring, C.E., Kitteringham, N.R., Elsbey, R., Randle, L.E., Clement, Y.N., Williams, D.P., McMahon, M., Hayes, J.D., Itoh, K., Yamamoto, M., Park, B.K., (2004) Activation of hepatic Nrf2 in vivo by acetaminophen in CD-1 mice. *Hepatology* **39**, 1267-1276.
- Greenwell, A., Foley, J.F., Maronpot, R.R., (1991) An enhancement method for immunohistochemical staining of proliferating cell nuclear antigen in archival rodent tissues. *Cancer Lett* **59**, 251-256.
- Grillo, M.P., Hua, F., Knutson, C.G., Ware, J.A., Li, C., (2003) Mechanistic studies on the bioactivation of diclofenac: identification of diclofenac-S-acyl-glutathione in vitro in incubations with rat and human hepatocytes. *Chem Res Toxicol* **16**, 1410-1417.
- Gross, A., McDonnell, J.M., Korsmeyer, S.J., (1999) BCL-2 family members and the mitochondria in apoptosis. *Genes Dev* **13**, 1899-1911.
- Guengerich, F.P., (2003) Cytochromes P450, Drugs, and Diseases. *Molecular interventions* **3**, 194-204.
- Guengerich, F.P., Liebler, D., Reed, D., (1985) Enzymatic activation of chemicals to toxic metabolites. *Critical Reviews in Toxicology* **14**, 259-307.
- Guengerich, F.P., Shimada, T., (1991) Oxidation of toxic and carcinogenic chemicals by human cytochrome P-450 enzymes. *Chemical Research in Toxicology* **4**, 391-407.
- Guicciardi, M.E., Gores, G.J., (2009) Life and death by death receptors. *Faseb J* **23**, 1625-1637.
- Guicciardi, M.E., Malhi, H., Mott, J.L., Gores, G.J., (2013) Apoptosis and Necrosis in the Liver. *Comprehensive Physiology* **3**, 977-1010.
- Gujral, J.S., Knight, T.R., Farhood, A., Bajt, M.L., Jaeschke, H., (2002) Mode of Cell Death after Acetaminophen Overdose in Mice: Apoptosis or Oncotic Necrosis? *Toxicological Sciences* **67**, 322-328.

- Gunawan, B., Kaplowitz, N., (2004) Clinical Perspectives on Xenobiotic; Induced Hepatotoxicity. *Drug Metabolism Reviews* **36**, 301-312.
- Gunawan, B.K., Liu, Z., Han, D., Hanawa, N., Gaarde, W.A., Kaplowitz, N., (2006) c-Jun N-Terminal Kinase Plays a Major Role in Murine Acetaminophen Hepatotoxicity. *Gastroenterology* **131**, 165-178.
- Guttridge, D.C., Albanese, C., Reuther, J.Y., Pestell, R.G., Baldwin, A.S., Jr., (1999) NF-kappaB controls cell growth and differentiation through transcriptional regulation of cyclin D1. *Mol Cell Biol* **19**, 5785-5799.
- Hagenbuch, B., Meier, P.J., (1994) Molecular cloning, chromosomal localization, and functional characterization of a human liver Na⁺/bile acid cotransporter. *Journal of Clinical Investigation* **93**, 1326-1331.
- Hall, P.A., Woods, A.L., (1990) Immunohistochemical markers of cellular proliferation: achievements, problems and prospects. *Cell Tissue Kinet* **23**, 505-522.
- Harrill, A.H., Watkins, P.B., Su, S., Ross, P.K., Harbourt, D.E., Stylianou, I.M., Boorman, G.A., Russo, M.W., Sackler, R.S., Harris, S.C., Smith, P.C., Tennant, R., Bogue, M., Paigen, K., Contractor, T., Wiltshire, T., Rusyn, I., Threadgill, D.W., (2009) Mouse population-guided resequencing reveals that variants in CD44 contribute to acetaminophen-induced liver injury in humans. *Genome Res* **19**, 1507-1515.
- Hart, S.G., Beierschmitt, W.P., Wyand, D.S., Khairallah, E.A., Cohen, S.D., (1994) Acetaminophen nephrotoxicity in CD-1 mice. I. Evidence of a role for in situ activation in selective covalent binding and toxicity. *Toxicol Appl Pharmacol* **126**, 267-275.
- Hawker, F., (1991) Liver dysfunction in critical illness. *Anaesth Intensive Care* **19**, 165-181.
- Hayes, J., McLellan, L., (1999) Glutathione and glutathione-dependent enzymes represent a co-ordinately regulated defence against oxidative stress. *Free Radical Research* **31**, 273-300.
- Hazelton, G.A., Hjelle, J.J., Klaassen, C.D., (1986) Effects of cysteine pro-drugs on acetaminophen-induced hepatotoxicity. *J Pharmacol Exp Ther* **237**, 341-349.
- Heijboer, A.C., Donga, E., Voshol, P.J., Dang, Z.C., Havekes, L.M., Romijn, J.A., Corssmit, E.P.M., (2005) Sixteen hours of fasting differentially affects hepatic and muscle insulin sensitivity in mice. *The Journal of Lipid Research* **46**, 582-588.
- Heinrich, P.C., Behrmann, I., Haan, S., Hermanns, H.M., Muller-Newen, G., Schaper, F., (2003) Principles of interleukin (IL)-6-type cytokine signalling and its regulation. *Biochem J* **374**, 1-20.
- Henderson, N.C., Pollock, K.J., Frew, J., Mackinnon, A.C., Flavell, R.A., Davis, R.J., Sethi, T., Simpson, K.J., (2007) Critical role of c-jun (NH2) terminal kinase in paracetamol-induced acute liver failure. *Gut* **56**, 982-990.
- Henne-Bruns, D., Artwohl, J., Broelsch, C., Kremer, B., (1988) Acetaminophen-induced acute hepatic failure in pigs: Controversial results to other animal models. *Res Exp Med* **188**, 463-472.
- Hinson, J.A., Pohl, L.R., Monks, T.J., Gillette, J.R., (1981) Acetaminophen-induced hepatotoxicity. *Life Sci* **29**, 107-116.
- Hinson, J.A., Mays, J.B., Cameron, A.M., (1983) Acetaminophen-induced hepatic glycogen depletion and hyperglycemia in mice. *Biochemical pharmacology* **32**, 1979-1988.
- Hinson, J.A., Roberts, D.W., James, L.P., (2010) Mechanisms of acetaminophen-induced liver necrosis. *Handb Exp Pharmacol* 369-405.

- Hirano, T., (1998) Interleukin 6 and its Receptor: Ten Years Later. *International Reviews of Immunology* **16**, 249-284.
- Hirao, J., Arakawa, S., Watanabe, K., Ito, K., Furukawa, T., (2006) Effects of restricted feeding on daily fluctuations of hepatic functions including p450 monooxygenase activities in rats. *J Biol Chem* **281**, 3165-3171.
- Hong, F., Kim, W.H., Tian, Z., Jaruga, B., Ishac, E., Shen, X., Gao, B., (2002) Elevated interleukin-6 during ethanol consumption acts as a potential endogenous protective cytokine against ethanol-induced apoptosis in the liver: involvement of induction of Bcl-2 and Bcl-xL proteins. *Oncogene* **21**, 32-43.
- Hori, O., Brett, J., Slattery, T., Cao, R., Zhang, J., Chen, J.X., Nagashima, M., Lundh, E.R., Vijay, S., Nitecki, D., (1995) The Receptor for Advanced Glycation End Products (RAGE) Is a Cellular Binding Site for Amphoterin mediation of neurite outgrowth and co-expression of rage and amphoterin in the developing nervous system. *Journal of Biological Chemistry* **270**, 25752-25761.
- Howell, S.R., Klaassen, C., (1991) Circadian variation of hepatic UDP-glucuronic acid and the glucuronidation of xenobiotics in mice. *Toxicol Lett* **57**, 73-79.
- Howie, D., Adriaenssens, P.I., Prescott, L.F., (1977) Paracetamol metabolism following overdose: application of high performance liquid chromatography. *J Pharm Pharmacol* **29**, 235-237.
- Hu, B., Colletti, L.M., (2008) Stem cell factor and c-kit are involved in hepatic recovery after acetaminophen-induced liver injury in mice. *American Journal of Physiology - Gastrointestinal and Liver Physiology* **295**, G45-G53.
- Hu, Y., Ingelman-Sundberg, M., Lindros, K.O., Yin, H., Ingelman-Sundberg, M., Lindros, K.O., (1995) Induction mechanisms of cytochrome P450 2E1 in liver: Interplay between ethanol treatment and starvation. *Biochemical pharmacology* **50**, 155-161.
- Huang, W., Ma, K., Zhang, J., Qatanani, M., Cuvillier, J., Liu, J., Dong, B., Huang, X., Moore, D.D., (2006) Nuclear receptor-dependent bile acid signaling is required for normal liver regeneration. *Science* 312.
- Imamura, R., Konaka, K., Matsumoto, N., Hasegawa, M., Fukui, M., Mukaida, N., Kinoshita, T., Suda, T., (2004) Fas ligand induces cell-autonomous NF-kappaB activation and interleukin-8 production by a mechanism distinct from that of tumor necrosis factor-alpha. *J Biol Chem* **279**, 46415-46423.
- Ishida, Y., Kondo, T., Kimura, A., Tsuneyama, K., Takayasu, T., Mukaida, N., (2006) Opposite roles of neutrophils and macrophages in the pathogenesis of acetaminophen-induced acute liver injury. *European Journal of Immunology* **36**, 1028-1038.
- Ishikawa, T., (1992) The ATP-dependent glutathione S-conjugate export pump. *Trends in biochemical sciences* **17**, 463-468.
- Ito, Y., Bethea, N.W., Abril, E.R., McCuskey, R.S., (2003) Early hepatic microvascular injury in response to acetaminophen toxicity. *Microcirculation* **10**, 391-400.
- Iverson, S.L., Uetrecht, J.P., (2001) Identification of a Reactive Metabolite of Terbinafine: Insights into Terbinafine-Induced Hepatotoxicity. *Chemical Research in Toxicology* **14**, 175-181.
- Jadhao, S.B., Yang, R.Z., Lin, Q., Hu, H., Anania, F.A., Shuldiner, A.R., Gong, D.W., (2004) Murine alanine aminotransferase: cDNA cloning, functional expression, and differential gene regulation in mouse fatty liver. *Hepatology* **39**, 1297-1302.
- Jaeschke, H., Wendel, A., (1985) Diurnal fluctuation and pharmacological alteration of mouse organ glutathione content. *Biochemical pharmacology* **34**, 1029-1033.

- Jaeschke, H., (1990) Glutathione disulfide formation and oxidant stress during acetaminophen-induced hepatotoxicity in mice in vivo: the protective effect of allopurinol. *J Pharmacol Exp Ther* **255**, 935-941.
- Jaeschke, H., (2006) How relevant are neutrophils for acetaminophen hepatotoxicity? *Hepatology* **43** (6):1191-4.
- Jaeschke, H., Gores, G.J., Cederbaum, A.I., Hinson, J.A., Pessayre, D., Lemasters, J.J., (2002) Mechanisms of Hepatotoxicity. *Toxicological Sciences* **65**, 166-176.
- Jaeschke, H., Knight, T.R., Bajt, M.L., (2003) The role of oxidant stress and reactive nitrogen species in acetaminophen hepatotoxicity. *Toxicology Letters* **144**, 279-288.
- Jaeschke, H., Williams, C.D., Ramachandran, A., Bajt, M.L., (2012) Acetaminophen hepatotoxicity and repair: the role of sterile inflammation and innate immunity. *Liver Int* **32**, 8-20.
- Jaeschke, H., Xie, Y., McGill, M.R., (2014) Acetaminophen-induced Liver Injury: from Animal Models to Humans. *Journal of Clinical and Translational Hepatology* **2**, 153-161.
- Jahr, S., Hentze, H., Englisch, S., Hardt, D., Fackelmayer, F.O., Hesch, R.D., Knippers, R., (2001) DNA fragments in the blood plasma of cancer patients: quantitations and evidence for their origin from apoptotic and necrotic cells. *Cancer Res* **61**, 1659-1665.
- James, L.P., Lamps, L.W., McCullough, S., Hinson, J.A., (2003a) Interleukin 6 and hepatocyte regeneration in acetaminophen toxicity in the mouse. *Biochemical and Biophysical Research Communications* **309**, 857-863.
- James, L.P., Mayeux, P.R., Hinson, J.A., (2003b) Acetaminophen-induced hepatotoxicity. *Drug Metab Dispos* **31**, 1499-1506.
- Jensen, T., Kiersgaard, M., Sorensen, D., Mikkelsen, L., (2013) Fasting of mice: a review. *Laboratory Animals* **47**, 225-240.
- Jewell, S.A., Monte, D., Gentile, A., Guglielmi, A., Altomare, E., Albano, O., (1986) Decreased hepatic glutathione in chronic alcoholic patients. *Journal of Hepatology* **3**, 1-6.
- Jollow, D.J., Mitchell, J.R., Potter, W.Z., Davis, D.C., Gillette, J.R., Brodie, B.B., (1973) Acetaminophen-induced hepatic necrosis. II. Role of covalent binding in vivo. *The Journal of Pharmacology and Experimental Therapeutics* **187**, 195-202.
- Ju, C., Reilly, T.P., Bourdi, M., Radonovich, M.F., Brady, J.N., George, J.W., Pohl, L.R., (2002) Protective role of Kupffer cells in acetaminophen-induced hepatic injury in mice. *Chem Res Toxicol* **15**, 1504-1513.
- Karin, M., Lin, A., (2002) NF-kappa B at the crossroads of life and death. *Nature immunology* **3**, 221-227.
- Kerb, R., Hoffmeyer, S., Brinkmann, U., (2001) ABC drug transporters: hereditary polymorphisms and pharmacological impact in MDR1, MRP1 and MRP2. *Pharmacogenomics* **2**, 51-64.
- Kerr, F., Dawson, A., Whyte, I.M., Buckley, N., Murray, L., Graudins, A., Chan, B., Trudinger, B., (2005) The Australasian Clinical Toxicology Investigators Collaboration randomized trial of different loading infusion rates of N-acetylcysteine. *Ann Emerg Med* **45**, 402-408.
- Kerr, J.F.R., Wyllie, A.H., Currie, A.R., (1972) Apoptosis: A Basic Biological Phenomenon with Wideranging Implications in Tissue Kinetics. *British Journal of Cancer* **26**, 239-257.

- Khalil, R.M., Hultner, L., Mailhammer, R., Luz, A., Moeller, J., Mohamed, A.A., Omran, S., Dormer, P., (1996) Kinetics of interleukin-6 production after experimental infection of mice with *Schistosoma mansoni*. *Immunology* **89**, 256-261.
- Kim, S.H., Hyun, S.H., Choung, S.Y., (2006) Anti-diabetic effect of cinnamon extract on blood glucose in db/db mice. *Journal of Ethnopharmacology* **104**, 119-123.
- Kim, W.R., Flamm, S.L., Di Bisceglie, A.M., Bodenheimer, H.C., (2008a) Serum activity of alanine aminotransferase (ALT) as an indicator of health and disease. *Hepatology* **47**, 1363-1370.
- Kim, Y.E., Kang, H.B., Park, J.A., Nam, K.H., Kwon, H.J., Lee, Y., (2008b) Upregulation of NF-kappaB upon differentiation of mouse embryonic stem cells. *BMB Rep* **41**, 705-709.
- Kinoshita, M., Igarashi, S., Kume, E., Saito, N., Arakawa, K., (2000) Fasting induces impairment of gastric mucosal integrity in non-insulin-dependent diabetic (db/db) mice. *Alimentary Pharmacology & Therapeutics* **14**, 359-366.
- Kitamura, H., Konno, A., Morimatsu, M., Jung, B.D., Kimura, K., Saito, M., (1997) Immobilization stress increases hepatic IL-6 expression in mice. *Biochem Biophys Res Commun* **238**, 707-711.
- Kitteringham, N.R., Powell, H., Clement, Y.N., Dodd, C.C., Tettey, J.N., Pirmohamed, M., Smith, D.A., McLellan, L.I., Kevin Park, B., (2000) Hepatocellular response to chemical stress in CD-1 mice: Induction of early genes and γ -glutamylcysteine synthetase. *Hepatology* **32**, 321-333.
- Klover, P.J., Mooney, R.A., (2004) Hepatocytes: critical for glucose homeostasis. *The International Journal of Biochemistry & Cell Biology* **36**, 753-758.
- Knight, T.R., Kurtz, A., Bajt, M.L., Hinson, J.A., Jaeschke, H., (2001) Vascular and hepatocellular peroxynitrite formation during acetaminophen toxicity: role of mitochondrial oxidant stress. *Toxicol Sci* **62**, 212-220.
- Kon, K., Ikejima, K., Okumura, K., Aoyama, T., Arai, K., Takei, Y., Lemasters, J.J., Sato, N., (2007) Role of apoptosis in acetaminophen hepatotoxicity. *J Gastroenterol Hepatol* **22**, S49-52.
- Koniaris, L.G., McKillop, I.H., Schwartz, S.I., Zimmers, T.A., (2003) Liver regeneration. *J Am Coll Surg* **197**, 634-659.
- Kouda, K., Nakamura, H., Kohno, H., Ha-Kawa, S.K., Tokunaga, R., Sawada, S., (2004) Dietary restriction: effects of short-term fasting on protein uptake and cell death/proliferation in the rat liver. *Mech Ageing Dev* **125**, 375-380.
- Kovalovich, K., DeAngelis, R.A., Li, W., Furth, E.E., Ciliberto, G., Taub, R., (2000) Increased toxin-induced liver injury and fibrosis in interleukin-6-deficient mice. *Hepatology* **31**, 149-159.
- Kovalovich, K., Li, W., DeAngelis, R., Greenbaum, L.E., Ciliberto, G., Taub, R., (2001) Interleukin-6 Protects against Fas-mediated Death by Establishing a Critical Level of Anti-apoptotic Hepatic Proteins FLIP, Bcl-2, and Bcl-xL. *Journal of Biological Chemistry* **276**, 26605-26613.
- Krenkel, O., Mossanen, J.C., Tacke, F., (2014) Immune mechanisms in acetaminophen-induced acute liver failure. *Hepatobiliary Surg Nutr* **3**, 331-343.
- Kubben, F.J., Peeters-Haesevoets, A., Engels, L.G., Baeten, C.G., Schutte, B., Arends, J.W., Stockbrügger, R.W., Blijham, G.H., (1994) Proliferating cell nuclear antigen (PCNA): a new marker to study human colonic cell proliferation. *Gut* **35**, 530-535.
- Kumar, V., Robbins, S.L. (2007) Robbins basic pathology (Philadelphia, PA, Saunders/Elsevier), 29-40.

- Kurki, P., Vanderlaan, M., Dolbeare, F., Gray, J., Tan, E.M., (1986) Expression of proliferating cell nuclear antigen (PCNA)/cyclin during the cell cycle. *Exp Cell Res* **166**, 209-219.
- Kurokawa, M., Akino, K., Kanda, K., (2000) A new apparatus for studying feeding and drinking in the mouse. *Physiology & Behavior* **70**, 105-112.
- Kvittingen, E.A., Rootwelt, H., Berger, R., Brandtzaeg, P., (1994) Self-induced correction of the genetic defect in tyrosinemia type I. *J Clin Invest* **94**, 1657-1661.
- Lakehal, F., Dansette, P.M., Becquemont, L., Lasnier, E., Delelo, R., Balladur, P., Poupon, R., Beaune, P.H., Housset, C., (2001) Indirect Cytotoxicity of Flucloxacillin toward Human Biliary Epithelium via Metabolite Formation in Hepatocytes. *Chemical Research in Toxicology* **14**, 694-701.
- Larrey, D., (2000) Drug-induced liver diseases. *J Hepatol* **32**, 77-88.
- Larson, A.M., (2007) Acetaminophen hepatotoxicity. *Clin Liver Dis* **11**, 525-548.
- Larson, A.M., Polson, J., Fontana, R.J., Davern, T.J., Lalani, E., Hynan, L.S., Reisch, J.S., Schiodt, F.V., Ostapowicz, G., Shakil, A.O., Lee, W.M., (2005) Acetaminophen-induced acute liver failure: results of a United States multicenter, prospective study. *Hepatology* **42**, 1364-1372.
- Laskin, D.L., (2009) Macrophages and Inflammatory Mediators in Chemical Toxicity: A Battle of Forces. *Chemical Research in Toxicology* **22**, 1376-1385.
- Laskin, D.L., Laskin, J.D., (2001) Role of macrophages and inflammatory mediators in chemically induced toxicity. *Toxicology* **160**, 111-118.
- Laskin, D.L., Pilaro, A.M., Ji, S., (1986) Potential role of activated macrophages in acetaminophen hepatotoxicity. *Toxicology and Applied Pharmacology* **86**, 216-226.
- Lasser, K.E., Allen, P.D., Woolhandler, S.J., Himmelstein, D.U., Wolfe, S.M., Bor, D.H., (2002) Timing of new black box warnings and withdrawals for prescription medications. *Jama* **287**, 2215-2220.
- Latta, M., Kunstle, G., Leist, M., Wendel, A., (2000) Metabolic Depletion of ATP by Fructose Inversely Controls Cd95- and Tumor Necrosis Factor Receptor 1-Mediated Hepatic Apoptosis. *Journal of Experimental Medicine* **191**, 1975-1985.
- Laurent, S., Horsmans, Y., Starkel, P., Leclercq, I., Sempoux, C., Lambotte, L., (2005) Disrupted NF-kappa B activation after partial hepatectomy does not impair hepatocyte proliferation in rats. *World J Gastroenterol* **11**, 7345-7350.
- Lawson, J.A., Farhood, A., Hopper, R.D., Bajt, M.L., Jaeschke, H., (2000) The Hepatic Inflammatory Response after Acetaminophen Overdose: Role of Neutrophils. *Toxicological Sciences* **54**, 509-516.
- Lazarou, J., Pomeranz, B.H., Corey, P.N., (1998) Incidence of adverse drug reactions in hospitalized patients: a meta-analysis of prospective studies. *Jama* **279**, 1200-1205.
- Lee, R.G., Clouse, M.E., Lanir, A., (1988) Liver adenosine triphosphate and pH in fasted and well-fed mice after infusion of adenine nucleotide precursors. *Liver* **8**, 337-343.
- Lee, S.S.T., Buters, J.T.M., Pineau, T., Fernandez-Salguero, P., Gonzalez, F.J., (1996) Role of CYP2E1 in the Hepatotoxicity of Acetaminophen. *Journal of Biological Chemistry* **271**, 12063-12067.
- Lee, W.M., Senior, J.R., (2005) Recognizing Drug-Induced Liver Injury: Current Problems, Possible Solutions. *Toxicologic Pathology* **33**, 155-164.
- Leist, M., Single, B., Castoldi, A.F., Kuhnle, S., Nicotera, P., (1997) Intracellular adenosine triphosphate (ATP) concentration: a switch in the decision between apoptosis and necrosis. *J Exp Med* **185**, 1481-1486.
- Lemasters, J.J., (1999) V. Necrapoptosis and the mitochondrial permeability transition: shared pathways to necrosis and apoptosis. *Am J Physiol* **276**, G1-6.

- Lemasters, J.J., Qian, T., Bradham, C.A., Brenner, D.A., Cascio, W.E., Trost, L.C., Nishimura, Y., Nieminen, A.L., Herman, B., (1999) Mitochondrial dysfunction in the pathogenesis of necrotic and apoptotic cell death. *J Bioenerg Biomembr.* **31**, 305-319.
- Libermann, T.A., Baltimore, D., (1990) Activation of interleukin-6 gene expression through the NF-kappa B transcription factor. *Molecular and Cellular Biology* **10**, 2327-2334.
- Li, W., Liang, X., Kellendonk, C., Poli, V., Taub, R., (2002) STAT3 Contributes to the Mitogenic Response of Hepatocytes during Liver Regeneration. *Journal of Biological Chemistry* **277**, 28411-28417.
- Lindblom, P., Rafter, I., Copley, C., Andersson, U., Hedberg, J.J., Berg, A.L., Samuelsson, A., Hellmold, H., Cotgreave, I., Glinghammar, B., (2007) Isoforms of alanine aminotransferases in human tissues and serum--differential tissue expression using novel antibodies. *Arch Biochem Biophys* **466**, 66-77.
- Liu, Z.X, Han, D., Gunawan, B., Kaplowitz, N., (2006) Neutrophil depletion protects against murine acetaminophen hepatotoxicity. *Hepatology* **43**, 1220-1230.
- Liu, Z.X., Govindarajan, S., Kaplowitz, N., (2004) Innate immune system plays a critical role in determining the progression and severity of acetaminophen hepatotoxicity. *Gastroenterology* **127**, 1760-1774.
- Liu, Z.X., Govindarajan, S., Okamoto, S., Dennert, G., (2000) NK cells cause liver injury and facilitate the induction of T cell-mediated immunity to a viral liver infection. *J Immunol* **164**, 6480-6486.
- Liu, Z.X., Kaplowitz, N., (2006) Role of innate immunity in acetaminophen-induced hepatotoxicity. *Expert Opin Drug Metab Toxicol* **2**, 493-503.
- Lu, S.C., (1999) Regulation of hepatic glutathione synthesis: current concepts and controversies. *Faseb J* **13**, 1169-1183.
- Luster, M.I., Simeonova, P.P., Gallucci, R.M., Bruccoleri, A., Blazka, M.E., Yucesoy, B., (2001) Role of inflammation in chemical-induced hepatotoxicity. *Toxicology Letters* **120**, 317-321.
- Mackay, I.R., (2002) Hepatoimmunology: a perspective, **80** (1) : 36-40.
- Malato, Y., Ehedego, H., Al-Masaoudi, M., Cubero, F.J., Bornemann, J., Gassler, N., Liedtke, C., Beraza, N., Trautwein, C., (2012) NF-kappaB essential modifier is required for hepatocyte proliferation and the oval cell reaction after partial hepatectomy in mice. *Gastroenterology* **143**, 1597-1608.
- Malato, Y., Naqvi, S., Schurmann, N., Ng, R., Wang, B., Zape, J., Kay, M.A., Grimm, D., Willenbring, H., (2011) Fate tracing of mature hepatocytes in mouse liver homeostasis and regeneration. *J Clin Invest* **121**, 4850-4860.
- Malhi, H., Gores, G.J., Lemasters, J.J., (2006) Apoptosis and necrosis in the liver: A tale of two deaths? *Hepatology* **43**, S31-S44.
- Mangipudy, R.S., Chanda, S., Mehendale, H.M., (1995) Tissue repair response as a function of dose in thioacetamide hepatotoxicity. *Environ Health Perspect* **103**, 260-267.
- Mariathasan, S., Weiss, D.S., Newton, K., McBride, J., O'Rourke, K., Roose-Girma, M., Lee, W.P., Weinrauch, Y., Monack, D.M., Dixit, V.M., (2006) Cryopyrin activates the inflammasome in response to toxins and ATP. *Nature* **440**, 228-232.
- Marin, J.J., (2012) Plasma membrane transporters in modern liver pharmacology. *Scientifica* **14**, 428139.

- Martin-Murphy, B.V., Holt, M.P., Ju, C., (2010) The role of damage associated molecular pattern molecules in acetaminophen-induced liver injury in mice. *Toxicol Lett* **192**, 387-394.
- Martinez-Hernandez, A., Amenta, P.S., (1995) The extracellular matrix in hepatic regeneration. *Faseb J* **9**, 1401-1410.
- Masson, M.J., Carpenter, L.D., Graf, M.L., Pohl, L.R., (2008) Pathogenic role of natural killer T and natural killer cells in acetaminophen-induced liver injury in mice is dependent on the presence of dimethyl sulfoxide. *Hepatology* **48**, 889-897.
- Masubuchi, Y., Bourdi, M., Reilly, T.P., Graf, M.L., George, J.W., Pohl, L.R., (2003) Role of interleukin-6 in hepatic heat shock protein expression and protection against acetaminophen-induced liver disease. *Biochem Biophys Res Commun* **304**, 207-212.
- Masubuchi, Y., Sugiyama, S., Horie, T., (2009) Th1/Th2 cytokine balance as a determinant of acetaminophen-induced liver injury. *Chem Biol Interact* **179**, 273-279.
- Matsuo, T., Yamaguchi, S., Mitsui, S., Emi, A., Shimoda, F., Okamura, H., (2003) Control mechanism of the circadian clock for timing of cell division in vivo. *Science* **302**, 255-259.
- Matthias, B., C, H.A., Melanie, B., Andrea, J., Jens, J., Hubert, S., J, P.M., D, K.J., Bauer, M., (2004) Starvation response in mouse liver shows strong correlation with life-span-prolonging processes. *Physiological Genomics* **17**, 230-244.
- McCarver, D.G., Hines, R.N., (2002) The ontogeny of human drug-metabolizing enzymes: phase II conjugation enzymes and regulatory mechanisms. *J Pharmacol Exp Ther* **300**, 361-366.
- McClain, C.J., Kromhout, J.P., Peterson, F.J., Holtzman, J.L., (1980) Potentiation of Acetaminophen Hepatotoxicity by Alcohol. *Jama* **244**, 251-253.
- McConnachie, L.A., Mohar, I., Hudson, F.N., Ware, C.B., Ladiges, W.C., Fernandez, C., Chatterton-Kirchmeier, S., White, C.C., Pierce, R.H., Kavanagh, T.J., (2007) Glutamate cysteine ligase modifier subunit deficiency and gender as determinants of acetaminophen-induced hepatotoxicity in mice. *Toxicol Sci* **99**, 628-636.
- McGill, M.R., Sharpe, M.R., Williams, C.D., Taha, M., Curry, S.C., Jaeschke, H., (2012a) The mechanism underlying acetaminophen-induced hepatotoxicity in humans and mice involves mitochondrial damage and nuclear DNA fragmentation. *J Clin Invest* **122**, 1574-1583.
- McGill, M.R., Williams, C.D., Xie, Y., Ramachandran, A., Jaeschke, H., (2012b) Acetaminophen-induced liver injury in rats and mice: comparison of protein adducts, mitochondrial dysfunction, and oxidative stress in the mechanism of toxicity. *Toxicol Appl Pharmacol* **264**, 387-394.
- McKallip, R.J., Hagele, H.F., Uchakina, O.N., (2013) Treatment with the hyaluronic acid synthesis inhibitor 4-methylumbelliferone suppresses SEB-induced lung inflammation. *Toxins (Basel)* **5**, 1814-1826.
- McNaughton, R., Huet, G., Shakir, S., (2014) An investigation into drug products withdrawn from the EU market between 2002 and 2011 for safety reasons and the evidence used to support the decision-making. *BMJ* **4**, e004221.
- Mehendale, H.M., (2005) Tissue repair: an important determinant of final outcome of toxicant-induced injury. *Toxicol Pathol* **33**, 41-51.
- Melkonyan, H.S., Feaver W.F., Meyer, E., Shekhtman, E.M., Xin, Z., Umansky, S.R., (2008) Transrenal nucleic acids: from proof of principle to clinical tests. *Ann N Y Acad Sci* **1137**, 73-81.

- Meyer, U.A., (1996) Overview of enzymes of drug metabolism. *Journal of Pharmacokinetics and Pharmacodynamics* **24**, 449-459.
- Michalopoulos, G.K., (1990) Liver regeneration: molecular mechanisms of growth control. *Faseb J* **4**, 176-187.
- Michalopoulos, G.K., (2010) Liver Regeneration after Partial Hepatectomy: Critical Analysis of Mechanistic Dilemmas. *The American Journal of Pathology* **176**, 2-13.
- Michalopoulos, G.K., (2013) Principles of liver regeneration and growth homeostasis. *Comprehensive Physiology* **3**, 485-513.
- Michalopoulos, G.K., DeFrances, M.C., (1997) Liver regeneration. *Science* **276**, 60-66.
- Miller, D.J., Hickman, R., Fratter, R., Terblanche, J., Saunders, S.J., (1976) An animal model of fulminant hepatic failure: a feasibility study. *Gastroenterology* **71**, 109-113.
- Mitchell, J.R., Jollow, D.J., Potter, W.Z., Davis, D.C., Gillette, J.R., Brodie, B.B., (1973) Acetaminophen-induced hepatic necrosis. I. Role of drug metabolism. *The Journal of Pharmacology and Experimental Therapeutics* **187**, 185-194.
- Miyaoka, Y., Miyajima, A., (2013) To divide or not to divide: revisiting liver regeneration. *Cell Division* **8**, 1-12.
- Mizuno, N., Niwa, T., Yotsumoto, Y., Sugiyama, Y., (2003) Impact of Drug Transporter Studies on Drug Discovery and Development. *Pharmacological Reviews* **55**, 425-461.
- Mossanen, J.C., Tacke, F., (2015) Acetaminophen-induced acute liver injury in mice. *Lab Anim* **49**, 30-36.
- Mudter, J., Neurath, M.F., (2007) Il-6 signaling in inflammatory bowel disease: Pathophysiological role and clinical relevance. *Inflammatory Bowel Diseases* **13**, 1016-1023.
- Muldrew, K.L., James, L.P., Coop, L., McCullough, S.S., Hendrickson, H.P., Hinson, J.A., Mayeux, P.R., (2002) Determination of acetaminophen-protein adducts in mouse liver and serum and human serum after hepatotoxic doses of acetaminophen using high-performance liquid chromatography with electrochemical detection. *Drug Metab Dispos* **30**, 446-451.
- Nathan, C., (2002) Points of control in inflammation. *Nature* **420**, 846-852.
- Nejak-Bowen, K.N., Monga, S.P.S. (2015) Chapter 6 - Developmental Pathways in Liver Regeneration-I, In: Apte, U. (Ed.) Liver Regeneration. *Academic Press Boston* 77-101.
- Nelson, S., (1990) Molecular Mechanisms of the Hepatotoxicity Caused by Acetaminophen. *Seminars in Liver Disease* **10**, 267-278.
- Nicotera, P., Leist, M., Ferrando-May, E., (1998) Intracellular ATP, a switch in the decision between apoptosis and necrosis. *Toxicol Lett* **103**, 139-142.
- Nowell, N.W., (1970) Circadian rhythm of glucose tolerance in laboratory mice. *Diabetologia* **6**, 488-492.
- Okubo, S., Miyamoto, M., Takami, K., Kanki, M., Ono, A., Nakatsu, N., Yamada, H., Ohno, Y., Urushidani, T., (2013) Identification of Novel Liver-Specific mRNAs in Plasma for Biomarkers of Drug-Induced Liver Injury and Quantitative Evaluation in Rats Treated With Various Hepatotoxic Compounds. *Toxicological Sciences* **132**, 21-31.
- Ostapowicz, G., Fontana, R.J., Schiolslash, F.V., Larson, A., Davern, T.J., Han, S.H., McCashland, T.M., Shakil, A.O., Hay, J.E., Hynan, L., Crippin, J.S., Blei, A.T., Samuel, G., Reisch, J., Lee, W.M., (2002) Results of a Prospective Study of Acute Liver Failure at 17 Tertiary Care Centers in the United States. *Annals of Internal Medicine* **137**, 947-954.

- Pachkoria, K., Isabel Lucena, M., Molokhia, M., Cueto, R., Serrano Carballo, A., Carvajal, A., Andrade, R., (2007) Genetic and Molecular Factors in Drug-Induced Liver Injury: A Review. *Current Drug Safety* **2**, 97-112.
- Panesar, N., Tolman, K., Mazuski, J.E., (1999) Endotoxin stimulates hepatocyte interleukin-6 production. *J Surg Res* **85**, 251-258.
- Park, B.K., Kitteringham, N.R., Maggs, J.L., Pirmohamed, M., Williams, D.P., (2005) The role of metabolic activation in drug-induced hepatotoxicity. *The Annual Review of Pharmacology and Toxicology* **45**, 177-202.
- Park, D.R., Thomsen, A.R., Frevert, C.W., Pham, U., Skerrett, S.J., Kiener, P.A., Liles, W.C., (2003) Fas (CD95) induces proinflammatory cytokine responses by human monocytes and monocyte-derived macrophages. *J Immunol* **170**, 6209-6216.
- Penicaud, L., Le Magnen, J., (1980) Recovery of body weight following starvation or food restriction in rats. *Neuroscience & Biobehavioral Reviews* **4**, 47-52.
- Perkins, N.D., (2000) The Rel/NF- κ B family: Friend and foe. *Trends in biochemical sciences* **25**, 434-440.
- Peschon, J.J., Torrance, D.S., Stocking, K.L., Glaccum, M.B., Otten, C., Willis, C.R., Charrier, K., Morrissey, P.J., Ware, C.B., Mohler, K.M., (1998) TNF receptor-deficient mice reveal divergent roles for p55 and p75 in several models of inflammation. *J Immunol* **160**, 943-952.
- Pessayre, D., Dolder, A., Artigou, J.Y., Wandscheer, J.C., Descatoire, V., Degott, C., Benhamou, J.P., (1979) Effect of fasting on metabolite-mediated hepatotoxicity in the rat. *Gastroenterology* **77**, 264-271.
- Petersen, S., (1978) Feeding, blood glucose and plasma insulin of mice at dusk. *Nature* **275**, 647-649.
- Pirmohamed, M., James, S., Meakin, S., Green, C., Scott, A.K., Walley, T.J., Farrar, K., Park, B.K., Breckenridge, A.M., (2004) Adverse drug reactions as cause of admission to hospital: prospective analysis of 18 820 patients. *Bmj* **329**, 15-19.
- Pompella, A., Visvikis, A., Paolicchi, A., De Tata, V., Casini, A.F., (2003) The changing faces of glutathione, a cellular protagonist. *Biochem Pharmacol* **66**, 1499-1503.
- Prescott, L.F., (2000) Paracetamol, alcohol and the liver. *British Journal of Clinical Pharmacology* **49**, 291-301.
- Price, V.F., Miller, M.G., Jollow, D.J., (1987) Mechanisms of fasting-induced potentiation of acetaminophen hepatotoxicity in the rat. *Biochem Pharmacol* **36**, 427-433.
- Pritchard, M.T., Apte, U., (2015) Chapter 2 - Models to Study Liver Regeneration, In : Apte, U. (Ed.) *Liver Regeneration. Academic Press Boston* 15-40.
- Pyrsoopoulos, N., (2014) Drug hepatotoxicity, 587-607.
- Quintana, F.J., Cohen, I.R., (2005) Heat Shock Proteins as Endogenous Adjuvants in Sterile and Septic Inflammation. *The journal of immunology* **175**, 2777-2782.
- Rabinovitch, A., (1998) An update on cytokines in the pathogenesis of insulin-dependent diabetes mellitus. *Diabetes Metab Rev* **14**, 129-151.
- Raffray, M., Cohen, G.M., (1997) Apoptosis and necrosis in toxicology: a continuum or distinct modes of cell death? *Pharmacol Ther* **75**, 153-177.
- Raucci, A., Palumbo, R., Bianchi, M.E., (2007) HMGB1: A signal of necrosis : Review. *Autoimmunity* **40**, 285-289.
- Raucy, J.L., Lasker, J.M., Lieber, C.S., Black, M., (1989) Acetaminophen activation by human liver cytochromes P450IIE1 and P450IA2. *Biochemistry and biophysics* **271**, 270-283.

- Ray, S.D., Mumaw, V.R., Raje, R.R., Fariss, M.W., (1996) Protection of acetaminophen-induced hepatocellular apoptosis and necrosis by cholesteryl hemisuccinate pretreatment. *J Pharmacol Exp Ther* **279**, 1470-1483.
- Riehle, K.J., Campbell, J.S., McMahan, R.S., Johnson, M.M., Beyer, R.P., Bammler, T.K., Fausto, N., (2008) Regulation of liver regeneration and hepatocarcinogenesis by suppressor of cytokine signaling 3. *J Exp Med* **205**, 91-103.
- Roberts, D.W., Pumford, N.R., Potter, D.W., Benson, R.W., Hinson, J.A., (1987) A sensitive immunochemical assay for acetaminophen-protein adducts. *The Journal of Pharmacology and Experimental Therapeutics* **241**, 527-533.
- Roberts, R.L., Mulder, R.T., Joyce, P.R., Luty, S.E., Kennedy, M.A., (2004) No evidence of increased adverse drug reactions in cytochrome P450 CYP2D6 poor metabolizers treated with fluoxetine or nortriptyline. *Hum Psychopharmacol* **19**, 17-23.
- Robertson, J.D., Orrenius, S., (2000) Molecular Mechanisms of Apoptosis Induced by Cytotoxic Chemicals. *Critical Reviews in Toxicology* **30**, 609-627.
- Robinson, S.M., Mann, D.A., (2010) Role of nuclear factor kappaB in liver health and disease. *Clin Sci (Lond)* **118**, 691-705.
- Rock, K.L., Kono, H., (2008) The Inflammatory Response to Cell Death. *Annual Review of Pathology Mechanisms of Disease* **3**, 99-126.
- Rubartelli, A., Lotze, M.T., (2007) Inside, outside, upside down: damage-associated molecular-pattern molecules (DAMPs) and redox. *Trends in Immunology* **28**, 429-436.
- Sahota, P.S., Popp, J.A., Hardisty, J.F., Gopinath, C., (2013) Toxicologic Pathology: Nonclinical Safety Assessment. *Taylor & Francis*, 55-62.
- Saito, C., Zwingmann, C., Jaeschke, H., (2010) Novel mechanisms of protection against acetaminophen hepatotoxicity in mice by glutathione and N-acetylcysteine. *Hepatology* **51**, 246-254.
- Satyanarayana, A., Manns, M.P., Rudolph, K.L., (2004) Telomeres and telomerase: a dual role in hepatocarcinogenesis. *Hepatology* **40**, 276-283.
- Savill, J., Gregory, C., Haslett, C., (2003) CELL BIOLOGY: Eat Me or Die. *Science (Classic)* **302**, 1516-1517.
- Scaffidi, P., Misteli, T., Bianchi, M.E., (2002) Release of chromatin protein HMGB1 by necrotic cells triggers inflammation. *Nature* **418**, 191-195.
- Schlingmann, F., Van de Weerd, H.A., Baumans, V., Remie, R., Van Zutphen, L.F.M., (1998) A Balance Device for the Analysis of Behavioural Patterns of the Mouse. *Animal welfare* **7**, 177-188.
- Schmittgen, T.D., Livak, K.J., (2008) Analyzing real-time PCR data by the comparative C(T) method. *Nat Protoc* **3**, 1101-1108.
- Schnell, R.C., Bozigan, H.P., Davies, M.H., Merrick, B.A., Park, K.S., McMillan, D.A., (1984) Factors influencing circadian rhythms in acetaminophen lethality. *Pharmacology* **29**, 149-157.
- Schutze, S., Wiegmann, K., Machleidt, T., Kronke, M., (1995) TNF-induced activation of NF-kappa B. *Immunobiology* **193**, 193-203.
- Sebastian, B.M., Roychowdhury, S., Tang, H., Hillian, A.D., Feldstein, A.E., Stahl, G.L., Takahashi, K., Nagy, L.E., (2011) Identification of a cytochrome P4502E1/Bid/C1q-dependent axis mediating inflammation in adipose tissue after chronic ethanol feeding to mice. *J Biol Chem* **286**, 35989-35997.
- Seeff, L.B., Cuccherini, B.A., Zimmerman, H.J., Adler, E., Benjamin, S.B., (1986) Acetaminophen Hepatotoxicity in Alcoholics : A Therapeutic Misadventure. *Annals of Internal Medicine* **104**, 399-404.

- Selzner, M., Camargo, C.A., Clavien, P.A., (1999) Ischemia impairs liver regeneration after major tissue loss in rodents: protective effects of interleukin-6. *Hepatology* **30**, 469-475.
- Seneviratne, S.L., Malavige, G.N., de Silva, H.J., (2006) Pathogenesis of liver involvement during dengue viral infections. *Trans R Soc Trop Med Hyg* **100**, 608-614.
- Shimizu, M., Morita, S., Mitsuru, S., Shigeru, M., (1992) Effects of feeding and fasting on hepatolobular distribution of glutathione and cadmium-induced hepatotoxicity. *Toxicology* **75**, 97-107.
- Sigal, S.H., Rajvanshi, P., Gorla, G.R., Sokhi, R.P., Saxena, R., Gebhard, D.R., Jr., Reid, L.M., Gupta, S., (1999) Partial hepatectomy-induced polyploidy attenuates hepatocyte replication and activates cell aging events. *Am J Physiol* **276**, G1260-1272.
- Simpson, K.J., Lukacs, N.W., McGregor, A.H., Harrison, D.J., Strieter, R.M., Kunkel, S.L., (2000) Inhibition of tumour necrosis factor alpha does not prevent experimental paracetamol-induced hepatic necrosis. *The Journal of Pathology* **190**, 489-494.
- Sokolovic, M., Sokolovic, A., Wehkamp, D., Ver Loren van Themaat, E., de Waart, D.R., Gilhuijs-Pederson, L.A., Nikolsky, Y., van Kampen, A.H., Hakvoort, T.B., Lamers, W.H., (2008) The transcriptomic signature of fasting murine liver. *BMC Genomics* **9**, 1471-2164.
- Srirangan, S., Choy, E.H., (2010) The Role of Interleukin 6 in the Pathophysiology of Rheumatoid Arthritis. *Therapeutic Advances in Musculoskeletal Disease* **2**, 247-256.
- Storch, K.-F., Lipan, O., Leykin, I., Viswanathan, N., Davis, F.C., Wong, W.H., Weitz, C.J., (2002) Extensive and divergent circadian gene expression in liver and heart. *Nature* **417**, 78-83.
- Strubelt, O., Dost-Kempf, E., Siegers, C.P., Younes, M., Volpel, M., Preuss, U., Dreckmann, J.G., (1981) The influence of fasting on the susceptibility of mice to hepatotoxic injury. *Toxicol Appl Pharmacol* **60**, 66-77.
- Su, G.L., Gong, K.Q., Fan, M.H., Kelley, W.M., Hsieh, J., Sun, J.M., Hemmila, M.R., Arbabi, S., Remick, D.G., Wang, S.C., (2005) Lipopolysaccharide-binding protein modulates acetaminophen-induced liver injury in mice. *Hepatology* **41**, 187-195.
- Sun, B., Karin, M., (2008) NF-kappaB signaling, liver disease and hepatoprotective agents. *Oncogene* **27**, 6228-6244.
- Szentirmai, E., Kapas, L., Sun, Y., Smith, R.G., Krueger, J.M., (2010) Restricted feeding-induced sleep, activity, and body temperature changes in normal and preproghrelin-deficient mice. *Am J Physiol Regul Integr Comp Physiol* **298**, R467-477.
- Tacke, F., Luedde, T., Trautwein, C., (2009) Inflammatory pathways in liver homeostasis and liver injury. *Clinical Reviews in Allergy and Immunology* **36**, 4-12.
- Tartaglia, L.A., Rothe, M., Hu, Y.-F., Goeddel, D.V., (1993) Tumor necrosis factor's cytotoxic activity is signaled by the p55 TNF receptor. *Cell* **73**, 213-216.
- Tartaglia, L.A., Weber, R.F., Figari, I.S., Reynolds, C., Palladino, M.A., Goeddel, D.V., (1991) The two different receptors for tumor necrosis factor mediate distinct cellular responses. *Proceedings of the National Academy of Sciences* **88**, 9292-9296.
- Tateishi, N., Higashi, T., Shinya, S., Naruse, A., Sakamoto, Y., (1974) Studies on the regulation of glutathione level in rat liver. *J Biochem* **75**, 93-103.
- Taub, R., (1996) Transcriptional control of liver regeneration. *FASEB Journal* **10**, 413-427.
- Taub, R., (2004) Liver regeneration: From myth to mechanism. *Nature Reviews Molecular Cell Biology* **5**, 836-847.

- Theocharis, S.E., Skopelitou, A.S., Margeli, A.P., Pavlaki, K.J., Kittas, C., (1994) Proliferating cell nuclear antigen (PCNA) expression in regenerating rat liver after partial hepatectomy. *Dig Dis Sci* **39**, 245-252.
- Thummel, K.E., Lee, C.A., Kunze, K.L., Nelson, S.D., Slattery, J.T., (1993) Oxidation of acetaminophen to N-acetyl-p-aminobenzoquinone imine by Human CYP3A4. *Biochemical pharmacology* **45**, 1563-1569.
- Tian, J., Avalos, A.M., Mao, S.Y., Chen, B., Senthil, K., Wu, H., Parroche, P., Drabic, S., Golenbock, D., Sirois, C., Hua, J., An, L.L., Audoly, L., La Rosa, G., Bierhaus, A., Naworth, P., Marshak-Rothstein, A., Crow, M.K., Fitzgerald, K.A., Latz, E., Kiener, P.A., Coyle, A.J., (2007) Toll-like receptor 9;dependent activation by DNA-containing immune complexes is mediated by HMGB1 and RAGE. *Nature immunology* **8**, 487-496.
- Trautwein, C., Rakemann, T., Niehof, M., Rose-John, S., Manns, M.P., (1996) Acute-phase response factor, increased binding, and target gene transcription during liver regeneration. *Gastroenterology* **110**, 1854-1862.
- Tsokos-Kuhn, J.O., Hughes, H., Smith, C.V., Mitchell, J.R., (1988) Alkylation of the liver plasma membrane and inhibition of the Ca²⁺ ATPase by acetaminophen. *Biochemical pharmacology* **37**, 2125-2131.
- Tsuda, M., Shigemoto-Mogami, Y., Ueno, S., Koizumi, S., Ueda, H., Iwanaga, T., Inoue, K., (2002) Downregulation of P2X₃ receptor-dependent sensory functions in A/J inbred mouse strain. *Eur J Neurosci* **15**, 1444-1450.
- Tsung, A., Sahai, R., Tanaka, H., Nakao, A., Fink, M.P., Lotze, M.T., Yang, H., Li, J., Tracey, K.J., Geller, D.A., Billiar, T.R., (2005) The nuclear factor HMGB1 mediates hepatic injury after murine liver ischemia-reperfusion. *J Exp Med* **201**, 1135-1143.
- Tsuneki, H., Sugihara, Y., Honda, R., Wada, T., Sasaoka, T., Kimura, I., (2002) Reduction of blood glucose level by orexins in fasting normal and streptozotocin-diabetic mice. *Eur J Pharmacol* **448**, 245-252.
- Tsung, A., Sahai, R., Tanaka, H., Nakao, A., Fink, M.P., Lotze, M.T., Yang, H., Li, J., Tracey, K.J., Geller, D.A., Billiar, T.R., (2005) The nuclear factor HMGB1 mediates hepatic injury after murine liver ischemia-reperfusion. *J Exp Med* **201**, 1135-1143.
- Tucci, V., Hardy, A., Nolan, P.M., (2006) A comparison of physiological and behavioural parameters in C57BL/6J mice undergoing food or water restriction regimes. *Behavioural Brain Research* **173**, 22-29.
- Ueda, H.R., Chen, W., Adachi, A., Wakamatsu, H., Hayashi, S., Takasugi, T., Nagano, M., Nakahama, K.-i., Suzuki, Y., Sugano, S., Iino, M., Shigeyoshi, Y., Hashimoto, S., (2002) A transcription factor response element for gene expression during circadian night. *Nature* **418**, 534-539.
- Uetrecht, J., (2003) Screening for the potential of a drug candidate to cause idiosyncratic drug reactions. *Drug Discov Today* **8**, 832-837.
- Ulloa, L., Ochani, M., Yang, H., Tanovic, M., Halperin, D., Yang, R., Czura, C.J., Fink, M.P., Tracey, K.J., (2002) Ethyl pyruvate prevents lethality in mice with established lethal sepsis and systemic inflammation. *Proc Natl Acad Sci USA* **99**, 12351-12356.
- Vabulas, R.M., Ahmad-Nejad, P., da Costa, C., Miethke, T., Kirschning, C.J., Wagner, H., (2001) Endocytosed HSP60s Use Toll-like Receptor 2 (TLR2) and TLR4 to Activate the Toll/Interleukin-1 Receptor Signaling Pathway in Innate Immune Cells. *Journal of Biological Chemistry* **276**, 31332-31339.
- Vaquero, J., Bélanger, M., James, L., Herrero, R., Desjardins, P., Côté, J., Blei, A.T., Butterworth, R.F., (2007) Mild Hypothermia Attenuates Liver Injury and Improves Survival in Mice With Acetaminophen Toxicity. *Gastroenterology* **132**, 372-383.

- Wajant, H., Pfizenmaier, K., Scheurich, P., (2003) Tumor necrosis factor signaling. *Cell Death and Differentiation* **10**, 45-65.
- Walker, R.M., Massey, T.E., McElligott, T.F., Racz, W.J., (1982) Acetaminophen toxicity in fed and fasted mice. *Canadian Journal of Physiology and Pharmacology* **60**, 399-404.
- Wang, J.H., Redmond, H.P., Watson, R.W., Bouchier-Hayes, D., (1995) Role of lipopolysaccharide and tumor necrosis factor-alpha in induction of hepatocyte necrosis. *Am J Physiol* **269**, G297-304.
- Webb, G.P., Jagot, S.A., Jakobson, M.E., (1982) Fasting-induced torpor in *Mus musculus* and its implications in the use of murine models for human obesity studies. *Comp Biochem Physiol* **72**, 211-219.
- Whyte, I.M., Francis, B., Dawson, A.H., (2007) Safety and efficacy of intravenous N-acetylcysteine for acetaminophen overdose: analysis of the Hunter Area Toxicology Service (HATS) database. *Curr Med Res Opin* **23**, 2359-2368.
- Williams, C.D., Koerner, M.R., Lampe, J.N., Farhood, A., Jaeschke, H., (2011) Mouse strain-dependent caspase activation during acetaminophen hepatotoxicity does not result in apoptosis or modulation of inflammation. *Toxicol Appl Pharmacol* **257**, 449-458.
- Wood, C.E., Hukkanen, R.R., Sura, R., Jacobson-Kram, D., Nolte, T., Odin, M., Cohen, S.M., (2015) Scientific and Regulatory Policy Committee (SRPC) Review*: Interpretation and Use of Cell Proliferation Data in Cancer Risk Assessment. *Toxicol Pathol* **43**, 760-775.
- Wuestefeld, T., Klein, C., Streetz, K.L., Betz, U., Lauber, J., Buer, J., Manns, M.P., Muller, W., Trautwein, C., (2003) Interleukin-6/glycoprotein 130-dependent pathways are protective during liver regeneration. *J Biol Chem* **278**, 11281-11288.
- Yabuuchi, H., Tamai, I., Morita, K., Kouda, T., Miyamoto, K., Takeda, E., Tsuji, A., (1998) Hepatic sinusoidal membrane transport of anionic drugs mediated by anion transporter Npt1. *J Pharmacol Exp Ther* **286**, 1391-1396.
- Yamada, Y., Fausto, N., (1998) Deficient liver regeneration after carbon tetrachloride injury in mice lacking type 1 but not type 2 tumor necrosis factor receptor. *The American Journal of Pathology* **152**, 1577-1589.
- Yamada, Y., Kirillova, I., Peschon, J.J., Fausto, N., (1997) Initiation of liver growth by tumor necrosis factor: deficient liver regeneration in mice lacking type I tumor necrosis factor receptor. *Proc Natl Acad Sci USA* **94**, 1441-1446.
- Yang, L., Magness, S.T., Bataller, R., Rippe, R.A., Brenner, D.A., (2005) NF-kappaB activation in Kupffer cells after partial hepatectomy. *Am J Physiol Gastrointest Liver Physiol* **289**, G530-538.
- Yang, Q., Shi, Y., He, J., Chen, Z., (2012a) The evolving story of macrophages in acute liver failure. *Immunol Lett* **147**, 1-9.
- Yang, R., Miki, K., He, X., Killeen, M.E., Fink, M.P., (2009a) Prolonged treatment with N-acetylcysteine delays liver recovery from acetaminophen hepatotoxicity. *Critical Care* **13**, R55.
- Yang, R., Zhang, S., Cotoia, A., Oksala, N., Zhu, S., Tenhunen, J., (2012b) High mobility group B1 impairs hepatocyte regeneration in acetaminophen hepatotoxicity. *BMC Gastroenterology* **12**, 45.
- Yang, R., Zhang, S., Kajander, H., Zhu, S., Koskinen, M.L., Tenhunen, J., (2011) Ringer's lactate improves liver recovery in a murine model of acetaminophen toxicity. *BMC Gastroenterology* **11**, 125.

- Yang, R., Zou, X., Koskinen, M.L., Tenhunen, J., (2012c) Ethyl pyruvate reduces liver injury at early phase but impairs regeneration at late phase in acetaminophen overdose. *Critical Care* **16**, R9.
- Yang, R., Zou, X., Tenhunen, J., Zhu, S., Kajander, H., Koskinen, M.L., Tonnessen, T.I., (2014) HMGB1 neutralization is associated with bacterial translocation during acetaminophen hepatotoxicity. *BMC Gastroenterology* **14**, 66.
- Yee, S.B., Bourdi, M., Masson, M.J., Pohl, L.R., (2007) Hepatoprotective Role of Endogenous Interleukin-13 in a Murine Model of Acetaminophen-Induced Liver Disease. *Chemical Research in Toxicology* **20**, 734-744.
- Yin, S., Wang, H., Park, O., Wei, W., Shen, J., Gao, B., (2011) Enhanced Liver Regeneration in IL-10-Deficient Mice after Partial Hepatectomy via Stimulating Inflammatory Response and Activating Hepatocyte STAT3. *The American Journal of Pathology* **178**, 1614-1621.
- Yin, T., He, S., Ye, T., Shen, G., Wan, Y., Wang, Y., (2014) Antiangiogenic therapy using sunitinib combined with rapamycin retards tumor growth but promotes metastasis. *Transl Oncol* **7**, 221-229.
- Yu, M., Wang, H., Ding, A., Golenbock, D.T., Latz, E., Czura, C.J., Fenton, M.J., Tracey, K.J., Yang, H., (2006) HMGB1 signals through toll-like receptor (tlr) 4 and tlr2. *Shock* **26**, 174-179.
- Yuko, I., Toshikazu, K., Tohru, O., Hiromi, F., Yoichiro, I., Naofumi, M., Ishida, Y., (2002) A pivotal involvement of IFN-gamma in the pathogenesis of acetaminophen-induced acute liver injury. *The FASEB Journal* **16**, 1227-1236.
- Zajicek, G., Oren, R., Weinreb, M.J., (1985) The streaming liver. *Liver* **5**, 293-300.
- Zamek-Gliszczyński, M.J., Hoffmaster, K.A., Nezasa, K.-i., Tallman, M.N., Brouwer, K.L.R., (2006) Integration of hepatic drug transporters and phase II metabolizing enzymes: Mechanisms of hepatic excretion of sulfate, glucuronide, and glutathione metabolites. *European Journal of Pharmaceutical Sciences* **27**, 447-486.
- Zhang, F., Qian, L., Flood, P.M., Shi, J.S., Hong, J.S., Gao, H.M., (2010) Inhibition of I κ B Kinase- β Protects Dopamine Neurons Against Lipopolysaccharide-Induced Neurotoxicity. *The Journal of Pharmacology and Experimental Therapeutics* **333**, 822-833.
- Zhang, L., Brett, C.M., Giacomini, K.M., (1998) Role of organic cation transporters in drug absorption and elimination. *The Annual Review of Pharmacology and Toxicology* **38**, 431-460.
- Zhou, S., Chan, E., Duan, W., Huang, M., Chen, Y.Z., (2005) Drug Bioactivation Covalent Binding to Target Proteins and Toxicity Relevance. *Drug Metabolism Reviews* **37**, 41-213.

CHAPTER SIX

APPENDIX

Table 6.1. List of experiments from which samples for the current study were recruited.

Time (hpd)	CD-1						C57BL/6J			
	Fed		Fasted				Fed		16 h fasting	
	Control	APAP	16 h fasting		24 h fasting		Control	APAP	Control	APAP
			Control	APAP	Control	APAP				
0	1, 5	1, 5	5	5	1	1	2	2	2	2
0.5	1	1	-	-	1	1	2	2	2	2
1	1, 3	1, 3	5	4	1	1	2	2	2	2
2	3	3	-	-	-	-	-	-	-	-
3	1	1	-	-	1	1	2	2	2	2
4	3, 5	3, 5	5	5	-	-	-	-	-	-
5	1	1	-	-	1	1	2	2	2	2
8	3	3	-	-	-	-	-	-	-	-
10	1, 5	1, 5	-	-	2	2	5	2, 5	5	5
15	1, 5	1, 5	5	5	1	1	5	2, 5	5	5
20	1, 5	1, 5	5	5	1	1	5	2, 5	5	5
24	1, 5	1, 5	5	5	1	1	2	2	2	2
30	-	-	-	-	-	-	5	5	-	-
36	-	-	-	-	-	-	5	5	5	5

Legend: Experiments performed by 1 - Daniel Antoine (2009/2010), 2 - Craig Benson (2011), 3 - Phil Starkey Lewis (2011), 4 - Harley Webb (2013) and 5 - Fazila Hamid (2013/2014). hpd – hours post dosing; h – hours.

Table 6.2. List of tests performed on samples from **CD-1 mice** according to the respective studies.

Time (hpd)	Liver GSH	Liver ATP	Serum ALT	Histopathological examination				Serum protein levels		Relative quantification of cytokine transcription						
				Histology		Immunohistology				Liver					Spleen	
				HE	PAS	Caspase-3	PCNA	TNF- α	IL-6	TNF- α	IL-6	IL-10	NF-kB	Cyclin-D1	TNF- α	IL-6
0	1, 5	1, 5	1, 5	1, 5	1, 5	-	1, 5	-	-	5	5	5	5	5	-	-
0.5	-	-	-	1, 4	1, 4	-	1	-	-	-	-	-	-	-	-	-
1	1, 3	1	1, 3	1,3,4	1,3,4	-	1	-	-	3	3	3	3	3	-	-
2	-	-	3	3	3	-	-	-	-	-	-	-	-	-	-	-
3	-	1	-	1	1	1	1	-	-	-	-	-	-	-	-	-
4	3, 5	-	3, 5	3, 5	3, 5	-	-	-	-	3, 5	3, 5	3, 5	3, 5	3, 5	-	-
5	-	1	1	1	1	1	1	1	1	-	-	-	-	-	-	-
8	-	-	3	3	3	-	-	-	-	-	-	-	-	-	-	-
10	2, 5	1	2, 5	1, 2, 5	1, 2, 5	1, 2, 5	1	5	5	2, 5	2, 5	2, 5	2, 5	2, 5	5	5
15	5	-	5	1, 4, 5	1, 4, 5	-	5	5	5	5	5	5	5	5	5	5
20	5	-	5	1, 4, 5	1, 4, 5	-	5	5	5	5	5	5	5	5	5	5
24	1, 5	1	1, 5	1, 4, 5	1, 4, 5	1, 5	1, 5	1, 5	1, 5	5	5	5	5	5	5	5

Legend: Experiments performed by 1 - Daniel Antoine (2009/2010), 2 - Craig Benson [fasted only] (2011), 3 - Phil Starkey Lewis [fed only] (2011), 4 - Harley Webb [fasted only] (2013), and 5 - Fazila Hamid (2013/2014).

Table 6.3. List of tests performed on samples from **C57BL/6J mice** according to the respective studies.

Time (hpd)	Liver GSH	Liver ATP	Serum ALT	Histopathological examination				Serum protein levels		Relative quantification of cytokine transcription						
				Histology		Immunostaining		TNF- α	IL-6	Liver					Spleen	
				HE	PAS	Caspase-3	PCNA			TNF- α	IL-6	IL-10	NF-kB	Cyclin-D1	TNF- α	IL-6
0	2	-	2	2	2	-	-	2	2	2	2	2	2	2	-	-
0.5	2	-	2	2, 4	2, 4	-	-	2	2	2	2	2	2	2	-	-
1	2	-	2	2	2	-	-	2	2	2	2	2	2	2	-	-
3	2	-	2	2	2	2	-	2	2	2	2	2	2	2	-	-
5	2	2	2	2	2	2	2	2	2	2	2	2	2	2	-	-
10	5	5	5	4, 5	4, 5	5	5	5	5	5	5	5	5	5	5	5
15	5	5	5	4, 5	4, 5	5	5	5	5	5	5	5	5	5	5	5
20	5	5	5	4, 5	4, 5	5	5	5	5	5	5	5	5	5	5	5
24	2	-	2	2	2	2	5	2	2	2	2	2	2	2	-	-
30	5	5	5	5	5	5	-	5	5	5	5	5	5	5	5	5
36	5	5	5	5	5	5	5	5	5	5	5	5	5	5	5	5

Legend: Experiments performed by 2 - Craig Benson (2011), 4 - Harley Webb [fed only] (2013), and 5 - Fazila Hamid (2013/2014).

Table 6.4. List of experiments performed in **CD-1 mice**, with time of day of dosing (controls: 0.9 % saline; treated: or 530 mg/kg APAP) and endpoint, that had been fed ad libitum or fasted for 16 or 24 h prior to dosing.

Time (hpd)	Exp	Fed		16 h Fasting			24 h Fasting		
		ToD dosing	ToD killing	ToD fasting	ToD dosing	ToD killing	ToD fasting	ToD dosing	ToD killing
0	1	10:00	10:00	-	-	-	10:00	10:00 (+1)	10:00
	5	14:00	14:00	18:00	10:30 (+1)	10:30	-	-	-
0.5	1	10:00	10:30	-	-	-	10:00	10:00(+1)	10:30
	4	-	-	17:00	09:00 (+1)	09:30	-	-	-
1	1	10:00	11:00	18:00	10:00	11:00	10:00	10:00 (+1)	11:00
	4	-	-	16:30	08:30 (+1)	09:30	-	-	-
	3	09:30	10:30	-	-	-	-	-	-
2	3	09:30	11:30	-	-	-	-	-	-
3	1	10:00	13:00	-	-	-	10:00	10:00 (+1)	13:00
4	3	09:00	13:00	-	-	-	-	-	-
	5	-	-	16:00	08:00 (+1)	12:00	-	-	-
5	1	10:00	15:00	-	-	-	10:00	10:00 (+1)	15:00
8	3	10:00	18:00	-	-	-	-	-	-
10	1	10:00	20:00	-	-	-	10:00	10:00 (+1)	20:00
	2	-	-	-	-	-	10:00	10:00 (+1)	20:00
	5	10:45	20:45	-	-	-	-	-	-
15	1	10:00	01:00	-	-	-	10:00	10:00 (+1)	01:00 (+1)
	4	-	-	16:08	08:08 (+1)	23:08	-	-	-
	5	18:00	09:00 (+1)	00:00	16:00	07:00 (+1)	-	-	-
20	1	10:00	06:00 (+1)	-	-	-	10:00	10:00 (+1)	06:00 (+1)
	4	-	-	17:07	09:07 (+1)	05:07 (+1)	-	-	-
	5	12:20	08:20 (+1)	18:45	10:45 (+1)	06:45 (+1)	-	-	-
24	1	10:00	10:00 (+1)	-	-	-	10:00	10:00 (+1)	10:00 (+1)
	4	-	-	16:23	08:23 (+1)	08:23 (+1)	-	-	-
	5	10:55	10:55 (+1)	18:15	10:15 (+1)	10:15 (+1)	-	-	-

Exp – Experiments performed by 1 - Daniel Antoine (2009/2010), 2 - Craig Benson (2011), 3 - Phil Starkey Lewis (2011), 4 - Harley Webb (2013), and 5 - Fazila Hamid (2013/2014). hpd - hours post dosing; ToD – time of day; (+1) - time of day on the following day.

Table 6.5. List of experiments performed in **C57BL/6J mice**, with time of day of dosing (controls: 0.9 % saline; treated: or 530 mg/kg APAP) and endpoint, that had been fed ad libitum or fasted for 16 h prior to dosing.

Time (hpd)	Exp	Fed		16 h Fasting		
		ToD dosing	ToD killing	ToD fasting	ToD dosing	ToD killing
0	2	10:00	10:00	18:00	10:00 (+1)	10:00
0.5	4	09:00	09:30	-	-	-
	2	10:00	10:30	18:00	10:00 (+1)	10:30
1	2	10:00	11:00	18:00	10:00 (+1)	11:00
3	2	09:00	12:00	17:00	09:00 (+1)	12:00
5	2	10:00	15:00	18:00	10:00 (+1)	15:00
10	4	08:00	18:00	-	-	-
	5	10:00	20:00	18:00	10:00 (+1)	20:00
15	4	08:00	23:00	-	-	-
	5	17:00	08:00 (+1)	01:00	17:00	08:00 (+1)
20	4	09:00	05:00 (+1)	-	-	-
	5	11:00	07:00 (+1)	19:00	11:00 (+1)	07:00 (+1)
24	2	10:00	10:00 (+1)	18:00	10:00 (+1)	10:00 (+1)
30	5	09:00	15:00 (+1)	-	-	-
36	5	07:00	19:00 (+1)	15:00	07:00 (+1)	19:00 (+1)

Exp – Experiments carried out by 2 - Craig Benson (2011), 4 - Harley Webb (2013), and 5 - Fazila Hamid (2013/2014).

hpd – hours post dosing; ToD – time of day; (+1) - time of day on the following day.

A. 0.9% saline dosed (control) CD-1 and C57BL/6J mice

Table 6.6. Individual serum ALT values of fed CD-1 mice at different time points post saline application (control animals).

Animal ID	Time (hpd)						
	0	1	2	4	5	8	24
1	71	22	22	50	198	20	25
2	45	49	39	20	80	18	22
3	80	70	13	32	41	14	37
4	47	66	90	23	58	39	27
5	69	-	-	-	35	-	24
6	98	-	-	-	56	-	30
Mean (SD)	68.33 20.12	51.63 21.83	40.98 34.69	31.17 13.64	78.0 60.84	22.55 10.97	27.5 5.39

Table 6.7. Relative transcription levels (illustrated as $2^{-\Delta Ct}$ relative to GAPDH) of TNF- α , IL-6 and IL-10 in **fed and fasted male CD-1 mice** over a 24 h time period after i.p. application of 0.9% saline. The fold change was assessed to explore changes in the transcription levels due to fasting by dividing the $2^{-\Delta Ct}$ value of fasted by the $2^{-\Delta Ct}$ values of time-matched fed animals.

Time (hps)	ToD dosing	ToD killing	TNF- α			IL-6			IL-10		
			Fed	Fasted	Fold change	Fed	Fasted	Fold change	Fed	Fasted	Fold change
0	14:00	14:00	1.59E-03	2.64E-03	1.65	3.65E-04	1.43E-04	0.39	3.66E-06	1.27E-06	0.35
1	09:30	10:30	1.92E-03	4.09E-03	2.13	1.55E-04	2.07E-04	1.34	2.7E-06	5.2E-06	1.93
4	09:00	13:00	1.60E-03	2.85E-03	1.78	3.12E-04	2.96E-04	0.95	1.15E-06	2.01E-06	1.75
10	10:45	20:45	4.04E-03	3.68E-03	0.91	2.53E-04	2.09E-04	0.83	2.87E-06	3.67E-06	1.28
24	10:55	10:55 (+1)	2.32E-03	1.14E-03	0.49	4.08E-04	2.81E-04	0.69	2.62E-06	1.14E-06	0.44

Table 6.8. Relative transcription levels (illustrated as $2^{-\Delta Ct}$ relative to GAPDH) of TNF- α , IL-6 and IL-10 in **fed and fasted male C57BL/6J mice** over a 24 h time period after i.p. application of 0.9% saline. The fold change was assessed to explore changes in the transcription levels due to fasting by dividing the $2^{-\Delta Ct}$ value of fasted by the $2^{-\Delta Ct}$ values of time-matched fed animals.

Time (hps)	ToD dosing	ToD killing	TNF- α			IL-6			IL-10		
			Fed	Fasted	Fold change	Fed	Fasted	Fold change	Fed	Fasted	Fold change
0	10:00	10:00	3.20E-04	6.14E-04	1.92	2.50E-04	1.10E-04	0.44	4.9E-06	3.3E-06	0.67
1	10:00	11:00	3.90E-04	5.41E-04	1.39	2.70E-04	2.30E-04	0.85	2.8E-06	2.4E-06	0.86
5	10:00	15:00	7.30E-04	3.73E-04	0.51	3.80E-04	5.10E-04	1.34	2.5E-06	3.1E-06	1.24
10	10:00	20:00	3.70E-04	7.21E-04	1.95	5.50E-04	4.40E-04	0.8	3.9E-06	2.7E-06	0.69
24	10:00	10:00 (+1)	2.10E-04	1.59E-04	0.76	1.70E-04	2.90E-04	1.71	2.7E-06	3.6E-06	1.33

Table 6.9. Relative transcription levels ($2^{-\Delta Ct}$) of TNF- α , IL-6 and IL-10 in comparison of **CD-1 and C57BL/6J mice** that had either been fed or fasted prior to saline dosing. *5- values of 5 h C57BL/6J was compared to 4 h CD-1 mice.

Time (hps)	TNF- α				IL-6				IL-10			
	Fed		Fasted		Fed		Fasted		Fed		Fasted	
	CD-1	C57BL/6J	CD-1	C57BL/6J	CD-1	C57BL/6J	CD-1	C57BL/6J	CD-1	C57BL/6J	CD-1	C57BL/6J
0	1.59E-03	3.20E-04	2.64E-03	6.14E-04	3.65E-04	2.50E-04	1.43E-04	1.10E-04	3.66E-06	4.9E-06	1.27E-06	3.3E-06
1	1.92E-03	3.90E-04	4.09E-03	5.41E-04	1.55E-04	2.70E-04	2.07E-04	2.30E-04	2.7E-06	2.8E-06	5.2E-06	2.4E-06
*5	1.60E-03	7.30E-04	2.85E-03	3.73E-04	3.12E-04	3.80E-04	2.96E-04	5.10E-04	1.15E-06	2.5E-06	2.01E-06	3.1E-06
10	4.04E-03	3.70E-04	3.68E-03	7.21E-04	2.53E-04	5.50E-04	2.09E-04	4.40E-04	2.87E-06	3.9E-06	3.67E-06	2.7E-06
24	2.32E-03	2.10E-04	1.14E-03	1.59E-04	4.08E-04	1.70E-04	2.81E-04	2.90E-04	2.62E-06	2.7E-06	1.14E-06	3.6E-06

Table 6.10. Relative transcription levels (illustrated as $2^{-\Delta Ct}$ relative to GAPDH) and fold change ($2^{-\Delta\Delta Ct}$) of NF-kB and cyclin-D1 in **fed and fasted CD-1 mice** over a 24 h time period after i.p. application of 0.9% saline and refeeding of the fasted animals. The fold change was assessed to explore changes in the transcription levels due to fasting by dividing the $2^{-\Delta Ct}$ value of fasted by the $2^{-\Delta Ct}$ values of time-matched fed animals.

Time (hps)	NF-kB								Cyclin-D1					
	ToD dosing	ToD killing	Fed		Fasted		Fold change	SD	Fed		Fasted		Fold change	SD
			Mean	SD	Mean	SD			Mean	SD	Mean	SD		
0	14:00	14:00	7.1E-05	3.0E-05	4.3E-05	3.2E-05	0.61	0.41	4.6E-06	2E-06	1.1E-06	2E-06	0.24	0.13
1	09:30	10:30	7.2E-05	9.3E-06	6.3E-05	2.9E-05	0.88	0.36	2.3E-06	3E-06	3.7E-06	1E-06	1.61	0.78
4	09:00	13:00	5.4E-05	3.2E-05	9.0E-05	1.8E-05	1.67	0.55	3.9E-06	1E-06	6.2E-06	4E-06	1.59	0.47
10	10:45	20:45	4.0E-05	2.1E-05	7.0E-05	3.0E-05	1.75	0.67	8.0E-06	3E-06	6.0E-06	2E-06	0.75	0.55
24	10:55	10:55 (+1)	2.7E-05	1.1E-05	5.1E-05	2.8E-05	1.89	0.23	3.5E-06	2E-06	3.1E-06	5E-06	0.89	0.53

Table 6.11. Relative transcription levels (illustrated as $2^{-\Delta Ct}$ relative to GAPDH) and fold change ($2^{-\Delta\Delta Ct}$) of NF-kB and cyclin-D1 in **fed and fasted C57BL/6J mice** over a 24 h time period after i.p. application of 0.9% saline and refeeding of the fasted animals. The fold change was assessed to explore changes in the transcription levels due to fasting by dividing the $2^{-\Delta Ct}$ value of fasted by the $2^{-\Delta Ct}$ values of time-matched fed animals.

Time (hps)	ToD dosing	ToD killing	NF-kB						Cyclin-D1					
			Fed		Fasted		Fold change	SD	Fed		Fasted		Fold change	SD
			Mean	SD	Mean	SD			Mean	SD	Mean	SD		
0	10:00	10:00	4.0E-04	8.4E-05	8.0E-05	6.4E-05	0.21	0.11	3E-07	4.5E-08	2.8E-07	1.1E-07	0.93	0.35
1	10:00	11:00	3.0E-04	7.0E-05	2.2E-04	1.4E-04	0.67	0.43	1.6E-07	7.2E-08	5.7E-08	1.5E-08	0.36	0.11
5	10:00	15:00	1.0E-04	2.8E-05	1.0E-04	8.7E-05	1.00	0.50	2.5E-07	4.5E-08	3.4E-07	8.9E-08	1.36	0.68
10	10:00	20:00	2.0E-04	8.2E-05	9.0E-05	5.0E-05	0.45	0.22	1.3E-07	5.4E-08	2.4E-07	8.9E-08	1.85	0.66
24	10:00	10:00 (+1)	5.0E-04	1.2E-04	6.7E-04	2.3E-04	1.34	0.23	1.7E-07	3.3E-08	1.1E-07	9.5E-08	0.65	0.22

Table 6.12. Comparison of the amount (%) of proliferating hepatocytes (nuclear and cytoplasmic PCNA expression; “PCNA+”) and hepatocytes that exhibited cytoplasmic PCNA expression (“Cyto+”) in **fed and fasted CD-1 mice** over a course of 24 h post 0.9% saline dosing and refeeding of the fasted animals. n – number of animals used per group; NS - not significant; Cyto – cytoplasmic.

Time (hps)	Fed				Fasted						p-value fed vs fasted %PCNA+	p-value fed vs fasted %Cyto+
	n	ToD killing	%PCNA+ Range [mean]	% Cyto+ Range [mean]	Fasting time (h)		n	ToD killing	% PCNA+ Range [mean]	% Cyto+ Range [mean]		
					16	24						
0	4	10:00	15.3 - 26.7 [21.0]	0.27-1.05 [0.66]		x	4	10:00	2.27 - 9.4 [6.27]	0 - 0.27 [0.16]	NS	NS
0.5	-	-	-	-	x		5	09:30	2.58 - 19.05 [6.75]	0.08 - 2.42 [1.19]	-	-
1	-	-	-	-	x		5	09:30	0.8 - 5.6 [2.89]	0 - 0.46 [0.18]	-	-
5	-	-	-	-		x	5	15:00	0.77 - 1.12 [1.89]	0.14 - 0.3 [0.22]	-	-
10	5	20:00	0.31 - 0.73 [0.59]	0 - 0.16 [0.1]		x	5	20:00	0.08 - 2.7 [1.26]	0	NS	NS
15	-	-	-	-	x		5	23:08	2.79 - 22.4 [7.9]	0	-	-
20	-	-	-	-	x		5	05:07	2.69 - 21.0 [10.34]	0 - 0.19 [0.05]	-	-
24	-	-	-	-	x		5	08:23	1.54 - 16.4 [6.34]	0.06 - 0.21 [0.11]	-	-
p-value (time points)		10:00 vs 20:00: NS		10:00 vs 20:00: NS					10 vs 15h: 0.0075** Others: NS	0.5 vs 1 h: 0.0125 10 vs 24 h: 0.0073 15 vs 24 h: 0.0079 Others: NS	-	-

Table 6.13. Comparison of the amount (%) of proliferating hepatocytes (nuclear and cytoplasmic PCNA expression; “PCNA+”) and hepatocytes that exhibited cytoplasmic PCNA expression (“Cyto+”) in **fed and fasted C57BL/6J mice** over a course of 24 h post 0.9% saline dosing and refeeding of the fasted animals. n – number of animals used per group; NS - not significant; Cyto – cytoplasmic.

Time (hps)	Fed mice			Length of fasting	Fasted mice			p-value fed vs fasted
	n	% PCNA+ (average [SD])	% Cyto+ (average [SD])		n	% PCNA+ (average [SD])	% Cyto+ (average [SD])	
0	4	2.21 [1.41]	0.31 [0.52]	16 h	4	1.18 [0.47]	0.15 [0.09]	% PCNA: NS % Cyto: NS

B. APAP dosed CD-1 mice

Table 6.14. Histological findings in APAP dosed **fed CD-1 mice** (time course). The histological findings and average grading scores for individual animals at each time point were recorded over a 24 h time course. hpd - hours post dosing; NHAIR - no histological abnormality is recognised; CL – centrilobular; HD - hydropic degeneration; NL - neutrophilic leukocytes; hpc – hepatocytes; pos. – positive; neg. – negative; occ. - occasional; ind. - individual; CC3 – cleaved caspase-3; mod. – moderate; CV – central vein; apop. – apoptosis; nec. – necrosis.

Time (hpd)	Case no.	Score range [mean]	Histological descriptions	Exp	
1	11L-4456	0	NHAIR; PAS: Diffuse glycogen	4	
	11L-4457	0	NHAIR; PAS: Diffuse glycogen		
	11L-4458	0	NHAIR; PAS: Diffuse glycogen		
	11L-4459	0	NHAIR; PAS: Diffuse glycogen		
	11L-4460	0	NHAIR; PAS: Diffuse glycogen		
		Summary	[0]	NHAIR; PAS: Diffuse glycogen	
	11L-4571	0	NHAIR; PAS: Diffuse glycogen	3	
	11L-4572	0	NHAIR; PAS: Diffuse glycogen		
	11L-4573	0	NHAIR; PAS: Diffuse glycogen		
	11L-4574	0	NHAIR; PAS: Diffuse glycogen		
	Summary	[0]	NHAIR; PAS: Diffuse hepatocellular glycogen accumulation (in 6/9 animals evidence of increased glycogen content in CL of hpc)		
3	09L-993	0-1	CL cell loss mainly in zone 2/3, very numerous apop. cells (all zones especially zone 2); several mitotic figures and also NL aggregates. CC3: ++ (disseminated; no obvious necrotic cells; also pos. cells with normal appearing nuclei); PAS: No glycogen except very few ind. hpc	1	
	09L-994	1-2	Similar to 09L-993, but more apparent of cell loss. CC3: ++; PAS: Patchy aggregates of pos. hpc		
	09L-995	2	Similar to 09L-993 and 994, with distinct cell loss mainly in zone 2; obvious loss of cells, but no necrotic cells seen. CC3: ++ (more intense staining than 993 and 994). PAS: No glycogen		
	09L-996	0-1	Increased CL cell loss; lesser apop. cells. CC3: Scattered pos. cells. PAS: Vacuolated cells (CL) neg., other cells patchy pos. with variable intensity distributed randomly		
	09L-997	0-1	Mild CL cell loss and increased NL between hepatic cords; occ. degenerate/ cell death in zone 2; some degree of vacuolation at remaining hpc. CC3: Small no. of disseminated pos. hpc. PAS: No glycogen		
		Summary	[1.25]		CL cell loss mainly at zone 2 with evidence of apoptotic cells with small NL aggregates; CC3: ++ disseminated at zone 3 and mainly zone 2; PAS: No glycogen (4/6) or patchy glycogen (2/6).
4	11L-4587	2-3	CL cell loss, with hydropic swelling of remaining hpc. Some NL infiltration and transit to unaffected area. CC3: +; PAS: No glycogen at affected area of zone 3	3	
	11L-4588	2-3	Similar to 11L-4587		

	11L-4589	1-3	CL cell loss with few NL at CL; CC3:+; PAS: Variable amount of glycogen outside zone 3	
	11L-4590	2-3	Increased CL cell loss and extend to zone 2, HD of remaining hpc; CC3:++; PAS: No glycogen at zone 3	
	Summary	[2.44]	Cell loss centrilobularly and several NL extending towards zone 2, with HD of remaining hpc in affected areas; CC3: ++/+; PAS: No glycogen in affected CL areas	
5	07L-3572	2-3	Focal subcapsular haemorrhage; vacuolated cells adjacent to cell loss; mild increase in NL between hepatic cords and at border to cell loss; occ. necrotic/apoptotic cells; increased mitotic figures. CC3: + (scattered pos. cells); PAS: No glycogen	1
	07L-3573	0-2	CL loss; numerous mitotic figures; small NL aggregates; occ. necrotic cells. CC3: +; PAS: Few pos. hpc.	
	07L-3576	2-3	Hepatocellular vacuolation at border to cell loss; very mild NL increase; some mitotic cells (border); no nec./apop. cells. CC3: + (Very occ. pos. hpc). PAS: No glycogen	
	07L-3577	2-3	Few vacuolation of hpc at border; scattered dying hpc; some mitotic figures. CC3: + (Occ. pos. hpc).	
	07L-4218	0-1	Vacuolated cells in zones 1 and 2; increased mitotic figures (mainly zone 3). CC3: Neg.	
	07L-4219	0-1	Same to 4218, but more mitotic figures; CL have no vacuolation and very dense cytoplasm. CC3: Neg.	
	07L-4220	1-2	Cell loss CL, but not apop. or nec. cells seen; mitotic figures in particular at border. CC3: Neg. PAS: Patchy glycogen outside affected areas of zone 3	
	07L-4221	1	Almost random numerous apoptotic/necrotic hpc; some small NL aggregates; increased mitotic figures. CC3: ++/+++ PAS: Occ. pos. hpc outside affected areas of zone 3	
	07L-4222	2-3	Numerous apoptotic/necrotic cells, like wide band in zone 2; increased mitotic figures. CC3:++/+++ PAS: Occ. pos. hpc outside affected areas of zone 3	
	07L-4223	2-3	Similar to 07L-4222	
	07L-4224	1-2	Similar, but slightly less severe than 07L-4222 and 4223; occ. hpc that have phagocytosed apoptotic cells; small NL aggregates. CC3: +/+++ PAS: Scattered glycogen to ind. hpc randomly	
	08L-619	2	No dying cells, just cell loss with hyperaemia/haemorrhage CL, scattered pos. NL. CC3: ++ PAS: Occ. scattered pos. hpc	
	08L-620	2-3	No dying cells, just cell loss with hyperaemia/haemorrhage CL. CC3: Neg. PAS: diffuse patchy glycogen	
	Summary	[1.46]	No evidence of ongoing cell death (4/13), ongoing apoptotic/necrotic cell death (9/13), some degree of HD in remaining cells (4/13); CC3: + (4/13), +++ (5/13), negative (4/13). PAS: extensive to complete glycogen loss centrilobularly	
10	09L-892	1	CL cell loss; in zone 3: hpc with dense, rounded nuclei, hpc with vacuoles, appear irregularly arranged; often a few NL in zone 2 or at transition to unaltered parenchyma; occ. scattered or small groups of apoptotic and necrotic hpc. CC3: + (Occ. 1-3 pos. hpc). PAS: Patchy pos. cells mainly in zone 1; cells with vacuoles in zone 3 neg.	1
	09L-893	2	CL cell loss, no obvious dying cells; hpc adjacent to loss with vacuoles; some NL in CV with some rolling; CC3: + (Very occ. ind. pos. hpc); PAS: patchy glycogen at hpc randomly	
	09L-894	1	CL cell loss with vacuolated hpc and occ. dense nuclei (see 09L-892); scattered apop. cells and nec. cells (some small degree of CN); increased NL in CV, rolling between adjacent hpc.; mild portal infiltration; increased mitosis. CC3: +(Scattered ind. pos. hpc); PAS: Mod. pos. hpc. distributed randomly	
	09L-895	1	CL cell loss and hpc. vacuolation; some small NL aggregates and NL rolling in CV; very occ. dying (apoptotic/necrotic) cells. CC3: + (Scattered ind. pos. hpc). PAS: Ind. pos. hpc	
	09L-896	1-2	CL cell loss; hpc vacuolation adjacent to cell loss, occ. dying (necrotic) hpc. CC3: Negative	
	09L-897	0-1	CL slight cell loss apparent, with vacuolated hpc; some hpc with dark condensed nuclei (see 892) at CL; scattered apoptotic and necrotic hpc. CC3: + (Scattered ind. pos. hpc). PAS: Ind. pos. hpc	

Appendix

	13L-1443	1	CL cell loss with vacuolated hpc, scattered apop./nec. Cells; few NL at CL; CC3: +; PAS: Ind. pos. hpc.	5
	13L-1444	2	Similar to 13L-1443 but the cell loss is more intense.	
	13L-1445	1	CL cell loss with some hpc with HD and PAS: Diffuse glycogen except 4-5 layers of zone 3	
	13L-1446	1	CL loss (4-6 cell layers); some NL rolling in CV and affected areas. PAS: Patchy to diffuse glycogen except 2-3 layer of zone 3	
	13L-1447	0-4	CL cell loss with scattered apop./nec. cells; CC3: +; PAS: Patchy to diffuse glycogen except zone 3	
	Summary	[1.0]	Slight ongoing hpc death (5/6, via apoptosis); HD of hpc surrounding affected areas; CC3: scattered individual CL positive hpc. PAS: patchy to randomly distributed hpc with glycogen.	
15	09L-898	1-2	Some CL cell loss, with several vacuolated hpc in that area; numerous mitotic figures, also with bizarre large nuclei (in periphery of previously affected zone); no dying cells; a few NL (and small aggregates) between hepatic cords. PAS: Diffuse glycogen with variable intensity except 2-3 layers of CL	1
	09L-899	0-1	Irregular arrangement at CL; some NL aggregates between cords and some NL rolling in CV; numerous mitotic figures; PAS: Patchy to diffuse glycogen except affected area of zone 3	
	09L-900	1-2	CL cell loss, but evidence of "filling up" with swollen hpc that often exhibit vacuoles; no dying cells; only mild increase in NL and NL rolling in CV. PAS: Low density of glycogen outside affected areas	
	09L-901	1-2	CL cell loss with only low amount of "filling up", but by vacuolated hpc; increased mitotic figures, also immediately adjacent to cell loss. PAS: No glycogen at affected areas with variable amount	
	09L-902	1	Very similar to 899, but mitotic figures not too numerous; scattered multinucleated cells	
	09L-903	0-1	CL cell loss but evidence of "filling up" with swollen hpc that often exhibit vacuoles; no dying cells; some NL aggregates and NL rolling in CV; numerous mitotic figures, also along necrotic area	5
	13L-1993	0-2	CL cell loss with blood with vacuolated hpc surrounded the affected areas; No ongoing cell death is seen. Few evidence of mitotic figures. PAS: No glycogen at affected areas of zone 3.	
	13L-1994	1-3	CL cell loss few evidence of CN, with HD of remaining hpc and rim around affected area; PAS: No glycogen outside affected areas of zone 3	
	13L-1995	0-2	Similar to 13L-1993	
	13L-1996	2-3	CL cell loss with blood; vacuoles in cells outside affected areas; PAS: No glycogen at affected areas.	
	13L-1997	1-2	Some areas with central 1 layer of early CN of hpc; some evidence of mitotic figures. PAS: Diffuse glycogen except 4-6 layers of CL	
Summary	[1.125]	CL cell loss with some degree of HD and disorderly arrangement of hpc in affected areas; increased mitotic figures, no evidence of ongoing cell death; PAS: Diffuse glycogen except CL (affected) areas		
20	09L-904	0	No apparent reduced cell nos., but possibly CL swollen hpc and some irregular arrangement; numerous mitotic figures. PAS: Large proportion of CL hpc devoid of glycogen	1
	09L-905	0-1	Reduced cell no. CL and irregularly arranged hpc; hpc in general relatively vacuolated; numerous mitotic figures. PAS: Most hpc positive (in vacuoles)	
	09L-906	0-1	Some degree of CL irregular arrangement; numerous mitotic figures. PAS: diffuse glycogen with variable amount except affected areas	
	09L-907	0-1	Some degree of CL irregular arrangement; numerous mitotic figures and occ. giant nuclei; PAS: almost diffuse glycogen at low amount	
	09L-908	0	Some degree of CL irregular arrangement; numerous mitotic figures; PAS: Large proportion of CL hpc devoid of glycogen	
	09L-909	0	Similar to 09L-908	

	Summary	[0.65]	Numerous mitotic figures; no ongoing cell death; some HD in affected areas (2/6); PAS: large proportion of CL hpc devoid of glycogen	
24	09L-910	0	Numerous mitotic figures, but otherwise unaltered appearing. PAS: Most hpc. pos. with variable amount (in vacuoles); cells in mitosis partly neg.	1
	09L-911	0	Numerous mitotic figures (or these large dense ovoid nuclei), otherwise unaltered appearing; CC3: Neg.PAS: Diffuse glycogen	
	09L-912	0	Numerous mitotic figures, otherwise unaltered appearing. PAS: Diffuse glycogen	
	09L-913	0	Numerous mitotic figures, otherwise unaltered appearing. PAS: Diffuse glycogen	
	13L-1453	0	Reduced cellularity of 1-2 cell layers CL, CC3: Neg. PAS: Diffuse glycogen except 1-2 layer of zone 3	5
	13L-1454	0	Similar to 13L-1453 but diffuse glycogen is seen	
	13L-1455	0	Some area is intact but some still evidence of small rim (1 cell layer) of hpc necrosis CL and NL along CV and between cords; PAS: Diffuse glycogen except 3-4 cell layers of CL	
	13L-1456	0	Similar to 13L-1455 but less intense and all CL are almost intact. PAS: Diffuse except 1-2 layer of zone 3	
	Summary	[0]	Numerous mitotic figures, but otherwise unaltered appearing and almost similar to controls; CC3: Negative; PAS: Diffuse hepatocellular glycogen accumulation	

Exp – Experiments performed by 1 - Daniel Antoine (2009/2010), 2 - Craig Benson (2011), 3 - Phil Starkey Lewis (2011), 4 - Harley Webb (2013), and 5 - Fazila Hamid (2013/2014).

Table 6.15. Histological findings in APAP dosed **fasted CD-1 mice** (time course). The histological findings and average grading scores for individual animals at each time point were recorded over a 24 h time course. hpd - hours post dosing; NHAIR - no histological abnormality is recognised; CL – centrilobular; HD - hydropic degeneration; NL - neutrophilic leukocytes; hpc – hepatocytes; pos. – positive; neg. – negative; occ. - occasional; ind. - individual; CC3 – cleaved caspase-3; mod. – moderate; CV – central vein; apop. – apoptosis; nec. – necrosis.

Time (hpd)	Case no.	Score range [mean]	Histological descriptions	Exp
0.5	11L-4431	0	Hpc with slight and distinct small cyto vacuoles. PAS: Disseminated small no. of hpc with glycogen	4
	11L-4432	0	Hpc with variable sized cyto vacuoles and few distinct small vacuoles (>intense CL). PAS: No glycogen	
	11L-4433	0	Hpc with variable sized cyto vacuoles CL (4-5 cell layers), very mild outside this. PAS: No glycogen	
	11L-4434	0	Hpc with variable sized cyto vacuoles CL (4-5 cell layers), very mild outside this. PAS: No glycogen	
	11L-4435	0	Hpc with variable sized cyto vacuoles CL (4-5 cell layers), outside this less intense. PAS: No glycogen	
		Summary	[0]	
1	11L-4436	0	Hpc with variable sized cyto vacuoles CL (4-5 cell layers), outside this less intense; scattered small aggregates of NL with ind. apoptotic/necrotic hpc. PAS: No glycogen	4
	11L-4437	0	Hpc with variable sized cyto vacuoles CL (4-5 cell layers; early HD), only very mild outside this (obvious transition). PAS: Disseminated small number of hpc with glycogen (outside CL areas)	

Appendix

	11L-4438	0	Hpc with variable sized cyto vacuoles CL (up to 50% of lobe; early HD), only very mild outside this (obvious transition). PAS: Outside CL areas disseminated mod. no. of hpc with glycogen	
	11L-4439	0	Hpc with variable sized cyto CL (4-5 cell layers), outside this less intense. PAS: No glycogen	
	11L-4440	0	Hpc with variable sized cyto vacuoles CL (4-5 cell layers), outside this less intense (slight transition). PAS: Outside CL areas disseminated scattered hpc with glycogen	
	Summary	[0]	NHAIR, except evidence of hpc with variable sized cytoplasmic vacuoles CL (4-5 layers; evidence of early HD), only very mild outside CL; PAS: no glycogen (2/5) or low degree of glycogen restitution in individuals cells (3/5)	
3	09L-988	1-2	Cell loss in zone 2; no dying cells; occ. small NL aggregates. CC3: Very occ. pos. cell; few pos. cells also in zone 2. PAS: No glycogen	1
	09L-989	2-3	Cell loss mainly in zone 2; extending to zone 3 (CL); occ. dying cells; some swollen/vacuolated cells immediately adjacent to area of cell loss. CC3: Scattered pos. cells in zones of cell loss. PAS: Neg.	
	09L-990	0-1	Mild CL cell loss; CL cells in particular are vacuolated, several swollen cells with clumped chromatin; few scattered necrotic cells. CC3: Scattered pos. cells, swollen cells are neg. PAS: Neg.	
	09L-991	2-3	Some swollen cells (see 09L-990) still present, CL cell loss; cells with swollen vacuoles close to necrosis; some necrotic cells; some small NL aggregates. CC3: Scattered pos. cells. PAS: Neg.	
	09L-992	2-3	Cell loss CL at zone 2; vacuolated and swollen cells CL (see 990). CC3: Very occ. pos. cell. PAS: Neg.	
	Summary	[2.05]	CL cell loss; CL cells in particular are vacuolated, several swollen cells with clumped chromatin; scattered necrotic cells; PAS: no glycogen. CC3: Very occasional scattered pos. cells	
4	13L-1729	1-3	CL cell loss and filled with blood, with HD of remaining hpc and occ. ind. nec. cell. PAS: No glycogen	5
	13L-1730	0-3	CL cell loss and filled with blood, with hydropic swelling of remaining hpc. PAS: No glycogen	
	13L-1731	1-3	Same as above	
	13L-1732	1-3	Same as above	
	Summary	[2.125]	Marked reduction of hpc and blood at CL, hydrophic swelling of remaining hpc; PAS: Neg.	
5	08L-611	3	CL cell loss; no dying cells; vacuole cell close to area of cell loss; CC3: Few pos CL hpc. PAS: Neg.	1
	08L-612	1-3	Cells with vacuole close to area of cell loss. CC3: Negative. PAS: No glycogen	
	08L-613	2	CL hpc that round up and exhibit loose vacuolation and chromatin clumping; CC3: Neg.; PAS: Neg.	
	08L-614	2	Similar to 08L-613, occ. necrotic hpc, CC3: Neg. PAS: Neg.	
	08L-615	1-3	Scattered necrotic cells; occ. cells as in 08L-613; increased no. of NL. CC3: Neg. PAS: Neg.	
	Summary	[2.5]	CL hpc round up and loose vacuolation and chromatin clumping; some vacuoles; PAS: Neg.	
10	10L-722	3-4	More extensive CL cell loss; HD surrounding affected areas; occ. NL at transition to unaltered areas. PAS: Pos. at ind. hpc	2
	10L-723	3-4	Similar to 10L-722. PAS: no glycogen except some scattered ind. hpc	
	10L-724	3-4	Similar to 10L-723; some NL in affected areas (transition to unaltered ones). PAS: No glycogen	
	10L-725	2-4	Mod. no. of NL and occ. necrotic cells in affected areas (transition). PAS: No glycogen except few hpc	
	10L-726	2-3	Occ. NL at transition to normal areas. PAS: No glycogen in affected areas	
	Summary	[2.6]	CL cell loss surrounded by hpc with HD; occasional NL at transition to unaltered areas; CC3: +; PAS: No glycogen except few scattered ind. hpc	
15	11L-4441	0-2	In areas without CL cell loss (and scattered necrotic/apoptotic hpc, with occ. NL. CL zone (3 cell layers) of hpc with homogenous, slightly basophilic cyto (degeneration/early stage of CN), surrounded by hpc with cyto vacuolation; occ. NL. PAS: Diffuse glycogen	4

			outside affected CL areas	
	11L-4442	1-4	Surrounding areas with almost complete cell loss is rim with changes described in 11L-4441 (among those scattered necrotic and apoptotic cells) and then normal appearing hpc with some vacuoles; a few NL in affected areas. PAS: Hpc outside affected areas with variable amount of glycogen	
	11L-4443	0-4	Surrounding areas with almost complete cell loss is rim with changes described in 11L-4441 (among those scattered nec. and apop. cells) and then normal appearing hpc with some vacuoles; some NL in affected areas, occ. as small aggregates. PAS: Diffuse glycogen outside affected CL areas	
	11L-4444	2-4	Surrounding areas with almost complete cell loss is rim with changes described in 11L-4441 (among those scattered necrotic and apoptotic cells) and then normal appearing hpc with some vacuoles; some NL in affected areas, occ. as small aggregates, some NL in CV. PAS: No glycogen	
	11L-4445	1	CL disorganised hpc with cyto like CN, with scattered necrotic hpc (3-5 cell layers); a few NL in CV and in affected areas. PAS: Diffuse glycogen (variable amount) outside affected CL areas.	
	13L-1733	3-4	CL cell loss and CN with variable degree of HD in remaining hpc. PAS: No glycogen at affected areas.	
	13L-1734	0-2	CL CN with HD between and surrounding necrotic cells, PAS: 3-4 inner layers with glycogen loss.	
	13L-1735	1-2	CL swelling and CN with most hpc still in place; PAS: No glycogen at affected areas of zone 3	
	13L-1736	3-4	CL cell loss with blood and HD of remaining hpc; otherwise DG. PAS: No glycogen at affected areas	5
	Summary	[2.15]	In areas without CL cell loss (and scattered necrotic/ apoptotic hpc, with occ. NL) CL zone (3 cell layers) of hpc with homogenous, slightly basophilic cytoplasm (degeneration/ early stage of CN), surrounded by hpc with increasing cytoplasmic vacuolation; occasional NL between CL hpc; PAS: Diffuse glycogen (variable amount) outside CL areas	
20	11L-4446	1-5	CL disorganised hpc with cyto like CN, with some nec. hpc (5-6 cell layers); a few NL in CV and some in affected areas; large random blood pools; score 5 in subcapsular areas. PAS: No glycogen	
	11L-4447	1-2	CL disorganised hpc with cyto like CN, with several necrotic hpc (5-6 cell layers; inner 1-2 cell layers apparent complete CN). PAS: Mod. no. of hpc in unaltered areas with glycogen	
	11L-4448	1-2	CL disorganised hpc with cyto like CN, with few necrotic hpc (5-6 cell layers; inner 1(-2) cell layers apparent complete CN); scattered NL in CV & affected areas. PAS: Diffuse glycogen outside zone 3	4
	11L-4449	1-2	Similar as in 11L-4448. PAS: Numerous hpc with glycogen in unaltered areas	
	11L-4450	1-5	CL disorganised hpc with cytoplasm like CN, with some necrotic hpc (5-6 cell layers); a few NL in CV and some to several in affected areas; score 5 in subcapsular areas. PAS: Pos. at unaffected areas	
	13L-1738	0-1	CL swelling and CN and/or apoptosis, with most hpc still in place; outside DG; some CV with a few NL; PAS: 1-2 layers affected area with glycogen loss	
	13L-1739	1-2	CL swelling and CN and/or apoptosis with most hpc still in place; often with several NL between cords, at border to intact hpc; surrounded by 1-2 layers with HD; PAS: No glycogen at affected areas	
	13L-1740	0-1	CL swelling and CN and/or apoptosis, PAS: 1-2 layers affected area with glycogen loss	
	13L-1741	0-4	Some intense areas of CL cell loss with blood with innermost layer of CN; still ongoing cell death and NL infiltration; PAS: No glycogen at affected areas	5
	13L-1742	0-4	Similar to 13L-1742. PAS: Diffuse glycogen except 2-3 layer of zone 3	
	Summary	[2.75]	CL disorganised hpc with cytoplasm like CN, with few necrotic hpc (5-6 cell layers); few NL in CV & affected areas; score 5 in subcapsular areas; PAS: diffuse glycogen outside affected CL areas	

Appendix

24	11L-4451	1	Well delineated CL area of HD with inner layer of hpc with features of CN (and loss of nucleus), 5-6 cell layers. PAS: Diffuse glycogen in unaltered areas, but 1 layer without glycogen around affected areas	4
	11L-4452	1-2	CL cell loss, then layer of cells with HD, scattered nec. and apop. cells; some blood pools; 5-6 cell loss layers surrounded by 1 layer of dense, otherwise unaltered cells. PAS: No glycogen at affected areas	
	11L-4453	1-4	Well delineated CL area of HD with inner layer of hpc with features of CN (and loss of nucleus), 5-6 cell layers; score 5 is patchy (random); a few NL in CV and affected areas; affected areas surrounded by 1 layer of dense, otherwise unaltered cells. PAS: Diffuse glycogen outside the layer of dense cells	
	11L-4454	2-3	Few remaining intact cells in affected areas otherwise with HD (or vacuoles). PAS: Neg. at zone 3	
	11L-4455	1-2	CL areas (4-6 cell layers) with HD and scattered nec. cells; NL in affected areas (some aggregates); one layer rim of dense, otherwise unaltered hpc. PAS: Diffuse glycogen outside the layer of dense cells	
	Summary	[2.4]	Well delineated CL area of HD with inner layer of hpc with features of CN (and loss of nucleus), 5-6 cell layers, a few NL in CV and affected areas; affected areas surrounded by 1 layer of dense, otherwise unaltered cells; PAS: Diffuse glycogen except 2-3 layers of zone 3, (1 no glycogen)	
	13L-1743	1-3	CL swelling and CN and/or apoptosis, with most hpc still in place; surrounded by 1-2 layers with glycogen loss; some affected areas with NL; CC3: +; PAS: Diffuse glycogen except 1-2 layer of zone 3	5
	13L-1744	1-3	CL CN with frequent apop. cells, with most hpc. still in place; surrounded by 1-2 layers with glycogen loss; some affected areas with NL; CC3: +; PAS: Diffuse glycogen except 2-3 layers of zone 3	
	13L-1745	0-3	CL CN and/or apoptosis, with most hpc still in place; surrounded by 1-2 layers with glycogen loss; some affected areas with a few NL between cords; CC3: +; PAS: Diffuse glycogen except 2-3 layer of zone 3	
	13L-1746	0-4	CL CN with apoptotic cells, surrounded by a layer with HD; outside DG; sometimes several NL aligned between cords. CC3: ++; PAS: Diffuse glycogen except 2-3 layers of zone 3	
	13L-1747	1-3	CL CN and present of apoptotic/necrotic cells; most hpc. still in place; surrounded by a layer with HD; CC3: +; PAS: No glycogen at zone 3	
	Summary (Mean 2.375)	[2.35]	CL cell loss, remaining cells are mild to moderately vacuolated (HD), scattered nec./apop. cells, few NL in CV, few mitotic cells; CC3: +/++; PAS: Diffuse glycogen outside the affected areas	

Exp – Experiments performed by 1 - Daniel Antoine (2009/2010), 2 - Craig Benson (2011), 3 - Phil Starkey Lewis (2011), 4 - Harley Webb (2013), and 5 - Fazila Hamid (2013/2014).

Table 6.16. Hepatic cytokine transcription of TNF- α , IL-6 and IL-10 in **time-matched control and APAP treated fed CD-1 mice**, using the delta Ct method, $2^{-\Delta Ct}$ and also the comparative Ct value method, i.e. the fold change with p-value. *15- relative to 10 h post saline; *20- relative to 24 h post saline. Statistical significant (p-value control vs APAP) is seen in comparison between fold change APAP and fold change control ($2^{-\Delta Ct \text{ individual value}}/2^{-\Delta Ct \text{ mean}}$).

TNF- α								
Time (hpd)	Control		APAP				p-value control vs APAP	
	Mean	SD	Mean	SD	Fold change	SD		p-value fed APAP vs APAP
1	1.92E-03	6.45E-04	6.34E-03	9.44E-04	3.31	0.31	4 h: 0.0065	NS
4	1.60E-03	9.74E-04	1.01E-02	1.54E-03	6.32	0.75	10 h: 0.0407 , 15 h: 0.0023 , 20 h: 0.0305 , 24 h: 0.0419	0.0077
10	4.04E-03	8.64E-04	1.82E-02	2.55E-03	4.50	1.36	15 h: 0.0152	0.0098
*15	-	-	4.63E-03	1.97E-03	1.14	0.85	15, 20 & 24 h : NS	NS
*20	-	-	4.73E-03	1.67E-03	2.04	1.22		NS
24	2.32E-03	6.45E-04	4.07E-03	1.14E-03	1.75	0.63		NS
IL-6								
Time (hpd)	Control		APAP				p-value control vs APAP	
	Mean	SD	Mean	SD	Fold change	SD		p-value fed APAP vs APAP
1	1.55E-04	6.90E-05	7.85E-04	2.51E-04	5.06	0.96	4, 15 or 24 h: NS, 10 h: 0.016 , 20 h: 0.0002	0.0030
4	3.12E-04	9.30E-05	1.78E-03	4.91E-04	5.71	1.25	10 h: 0.0073 , 20 h: 0.0019	0.0006
10	2.53E-04	8.30E-05	2.35E-03	3.12E-04	9.29	0.95	15 h: 0.0069 , 20 h: 0.0009 24 h: 0.0077	0.0001
*15	-	-	1.34E-03	9.34E-04	5.31	1.97	20 h: 0.0089	0.0097
*20	-	-	4.71E-03	9.70E-04	11.53	2.13	24 h: 0.0065	0.0001
24	4.08E-04	4.90E-05	2.28E-03	7.76E-04	5.59	1.5	15 h: NS	0.0056
IL-10								
Time (hpd)	Control		APAP				p-value control vs APAP	
	Mean	SD	Mean	SD	Fold change	SD		p-value fed APAP vs APAP
1	2.70E-06	3.14E-06	7.85E-06	9.66E-07	2.91	0.76	4 h: 0.0011 , 10 h: 0.0026 , 15 h: 0.0006 , 20 h: 0.0009 , 24 h: 0.0046	NS
4	1.15E-06	1.03E-06	1.02E-05	1.99E-06	8.87	1.84	15 h: 0.0433	0.0041
10	2.87E-06	5.43E-07	2.35E-05	4.12E-06	8.19	2.37	10, 15, 20 & 24h: NS	0.0008
*15	-	-	3.43E-05	5.37E-06	11.95	2.47		0.0022
*20	-	-	2.71E-05	7.26E-06	10.34	3.13		0.0010
24	2.62E-06	2.97E-06	2.28E-05	1.62E-06	8.70	1.28		0.0006

Table 6.17. Hepatic cytokine transcription of TNF- α , IL-6 and IL-10 in **pooled liver samples of fed control CD-1 mice and in APAP treated fed CD-1 mice**, using the delta Ct method, $2^{-\Delta Ct}$ and also the comparative Ct value method, i.e. the fold change with p-value. Statistical significant (p-value control vs APAP) is seen in comparison between fold change APAP and fold change control ($2^{-\Delta Ct \text{ individual value}} / 2^{-\Delta Ct \text{ mean}}$).

TNF- α								
Time (hpd)	Control		APAP				p-value control vs APAP	
	Mean	SD	Mean	SD	Fold change	SD		p-value fed APAP vs APAP
1	2.30E-03	7.8E-04	6.34E-03	9.44E-04	2.76	0.27	10 h: 0.0015 , 15,20,24 h: NS	NS
4			1.01E-02	1.54E-03	4.40	0.7	1 h: 0.0316	0.0315
10			1.82E-02	2.55E-03	7.93	2.68	15,20,24 h: 0.0017	0.0055
15			4.63E-03	1.97E-03	2.02	1.25	4 h: 0.0397 15,20,24 h: NS	NS
20			4.73E-03	1.67E-03	2.06	1.4		NS
24			4.07E-03	1.14E-03	1.77	0.79		NS
IL-6								
Time (hpd)	Control		APAP				p-value control vs APAP	
	Mean	SD	Mean	SD	Fold change	SD		p-value fed APAP vs APAP
1	2.99E-04	7.4E-05	7.85E-04	2.51E-04	2.63	0.77	4 h: 0.0288 , 10 h: 0.0076 , 20 h: 0.0002	NS
4			1.78E-03	4.91E-04	5.96	1.89	10 h: 0.0051 , 20 h: 0.0012	0.0087
10			2.35E-03	3.12E-04	7.87	0.8	15 h: 0.0069 , 20 h: 0.0058 24 h: NS	0.0056
15			1.34E-03	9.34E-04	4.49	1.95	20 h: 0.0001 1 h: NS	NS
20			4.71E-03	9.70E-04	15.77	4.06	24 h: 0.0070	0.0001
24			2.28E-03	7.76E-04	7.64	2.65	15 h: 0.0233	0.0102
IL-10								
Time (hpd)	Control		APAP				p-value control vs APAP	
	Mean	SD	Mean	SD	Fold change	SD		p-value fed APAP vs APAP
1	2.6E-06	1.9E-06	7.85E-06	9.66E-07	3.02	0.78	10, 20 h: 0.0076	NS
4			1.02E-05	1.99E-06	3.92	1.52	15 h: 0.0020 , 24 h: 0.0093	0.0411
10			2.35E-05	4.12E-06	9.04	2.88	15 h: 0.0491	0.0083
15			3.43E-05	5.37E-06	13.19	3.73	24 h: 0.0088	0.0003
20			2.71E-05	7.26E-06	10.42	3.14	10 h: NS, 15 h: 0.0289 , 24 h: 0.0406	0.0018
24			2.28E-05	1.62E-06	8.77	1.28	10,20 h: NS	0.0010

Table 6.18. Hepatic cytokine transcription of TNF- α , IL-6 and IL-10 in **time-matched control and APAP treated male CD-1 mice** had been fasted for 16/24 h prior to dosing using delta Ct method, $2^{-\Delta Ct}$ and also the comparative Ct value method, i.e. the fold change with p-value. *15- relative to 10 h post saline; *20- relative to 24 h post saline. Statistical significant (p-value control vs APAP) is seen in comparison between fold change APAP and fold change control ($2^{-\Delta Ct \text{ individual value}}/2^{-\Delta Ct \text{ mean}}$).

TNF- α									
Time (hpd)	Control		APAP				p-value control vs APAP	p-value fasted vs fed APAP	
	Mean	SD	Mean	SD	Fold change	SD			p-value fasted APAP vs APAP
1	4.09E-03	1.25E-03	2.99E-03	1.64E-03	0.73	0.32	4 h: 0.0094 , 10 h: 0.0330 , 15 h: 0.0001 , 20 h: 0.0059 ,	NS	0.0134
4	2.85E-03	8.74E-04	6.65E-03	1.85E-03	2.33	0.65	10 h: NS, 15 h: 0.0047 , 20/24 h: NS	NS	0.0093
10	3.68E-03	2.38E-03	1.95E-02	6.87E-03	5.3	1.95	15 h: 0.0025 , 20 or 24 h: NS	0.0033	NS
*15	-	-	5.26E-02	6.44E-03	14.27	2.02	20 h: 0.0013 , 24 h: 0.0009	0.0003	0.0005
*20	-	-	5.47E-03	2.89E-03	4.81	0.98	24 h: NS	0.0404	0.0373
24	1.14E-03	6.74E-04	4.46E-03	2.32E-03	3.92	0.60	1 h: 0.0055	0.0087	0.0477
IL-6									
Time (hpd)	Control		APAP				p-value control vs APAP	p-value fasted vs fed APAP	
	Mean	SD	Mean	SD	Fold change	SD			p-value fasted APAP vs APAP
1	2.07E-04	2.05E-04	3.87E-04	1.43E-04	1.87	0.81	4 h: 0.0453 , 15 h: 0.0105 , 20 h: 0.0266 , 24 h: 0.0089	NS	0.0110
4	2.96E-04	1.77E-04	1.06E-03	2.07E-04	3.59	1.35	24 h: 0.0255	0.0286	NS
10	2.09E-04	1.07E-04	4.89E-04	2.96E-04	2.34	1.09	24 h: 0.0109	0.0487	0.0057
*15	-	-	1.03E-03	2.09E-04	4.91	0.95	15, 20 or 24 h: NS	0.0074	NS
*20	-	-	1.21E-03	1.16E-04	4.32	0.82		0.0090	0.0079
24	2.81E-04	1.87E-04	1.68E-03	2.81E-04	5.99	1.6		0.0049	NS
IL-10									
Time (hpd)	Control		APAP				p-value control vs APAP	p-value fasted vs fed APAP	
	Mean	SD	Mean	SD	Fold change	SD			p-value fasted APAP vs APAP
1	5.20E-06	4.40E-06	6.87E-06	3.41E-06	1.3	0.97	1,4,10 & 15 h: NS	NS	NS
4	2.01E-06	2.40E-06	4.06E-06	2.92E-06	2.0	1.54		NS	0.0090
10	3.67E-06	2.00E-06	4.89E-06	6.99E-07	1.3	0.54		NS	0.0068
*15	-	-	1.03E-05	1.56E-06	2.8	0.94		NS	0.0047
*20	-	-	1.21E-05	9.96E-07	10.6	2.37	1,4,10,15 h: 0.0018 , 24 h: NS	0.0032	NS
24	1.14E-06	3.50E-06	1.38E-05	4.01E-06	12.1	4.05		0.0001	NS

Table 6.19. Hepatic cytokine transcription of TNF- α , IL-6 and IL-10 in **pooled liver samples of fasted control CD-1 mice and in APAP treated fasted CD-1 mice**, using the delta Ct method, $2^{-\Delta Ct}$ and also the comparative Ct value method, i.e. the fold change with p-value. Statistical significant (p-value control vs APAP) is seen in comparison between fold change APAP and fold change control ($2^{-\Delta Ct \text{ individual value}} / 2^{-\Delta Ct \text{ mean}}$).

TNF- α									
Time (hpd)	Control		APAP				p-value fasted APAP vs APAP	p-value control vs APAP	p-value fasted vs fed APAP
	Mean	SD	Mean	SD	Fold change	SD			
1	2.88E-03	1.19E-04	2.99E-03	1.64E-03	1.04	0.59	10 h: 0.0340 , 15 h: 0.0001	NS	NS
4			6.65E-03	1.85E-03	2.31	0.62		NS	0.0193
10			1.95E-02	6.87E-03	6.78	2.43	20,24 h: 0.0278	0.0292	NS
15			5.26E-02	6.44E-03	18.28	4.79	10 h: 0.0085	0.0001	0.0015
20			5.47E-03	2.89E-03	1.90	0.7	1,4 h: NS, 15 h: 0.0001	NS	NS
24			4.46E-03	2.32E-03	1.55	0.52		NS	NS
IL-6									
Time (hpd)	Control		APAP				p-value fasted APAP vs APAP	p-value control vs APAP	p-value fasted vs fed APAP
	Mean	SD	Mean	SD	Fold change	SD			
1	2.27E-04	1.52E-04	3.87E-04	1.43E-04	1.70	0.76	10 h: NS, 4 h: 0.0221 24 h: 0.0098	NS	NS
4			1.06E-03	2.07E-04	4.67	1.65	15,20 h: NS	0.0130	NS
10			4.89E-04	2.96E-04	2.15	0.98	15 h: 0.0411	NS	0.0060
15			1.03E-03	2.09E-04	4.53	0.9	24 h: 0.0209	NS	NS
20			1.21E-03	1.16E-04	5.33	1.59	24 h: NS	0.0183	0.0007
24			1.68E-03	2.81E-04	7.39	3.1	10 h: 0.0194	0.0069	NS
IL-10									
Time (hpd)	Control		APAP				p-value fasted APAP vs APAP	p-value Control vs APAP	p-value fasted vs fed APAP
	Mean	SD	Mean	SD	Fold change	SD			
1	2.66E-06	2.01E-06	6.87E-06	3.41E-06	2.58	1.45	4,10 h: NS	NS	NS
4			4.06E-06	2.92E-06	1.53	1.24	10 h: NS	NS	NS
10			4.89E-06	6.99E-07	1.84	0.89	15 h: 0.0408	NS	0.0011
15			1.03E-05	1.56E-06	3.88	1.35	20 h: NS	NS	0.0046
20			1.21E-05	9.96E-07	4.55	2.12	10 h: 0.0272	0.0445	0.0347
24			1.38E-05	4.01E-06	5.19	3.87	10 h: 0.0485	0.0302	NS

Table 6.20. Comparison of splenic TNF- α and IL-6 cytokine transcription in fed and fasted control and APAP treated CD-1 mice in a 24 h period using delta Ct value, $2^{-\Delta Ct}$ and the comparative Ct value, i.e. fold change as compared to **time-matched control** mice. *15- relative to 10 h post saline; *20- relative to 24 h post saline. Statistical significant (p-value control vs APAP) is seen in comparison between fold change APAP and fold change control ($2^{-\Delta Ct \text{ individual value}} / 2^{-\Delta Ct \text{ mean}}$).

Time (hpd)	TNF- α														
	Fed							Fasted							p-value APAP fed vs fasted
	Control		APAP		Fold change	SD	p-value fed APAP	Control		APAP		Fold change	SD	p-value fasted APAP	
	Mean	SD	Mean	SD				Mean	SD	Mean	SD				
10	0.031	0.016	0.121	0.046	3.86	1.63	24 h: 0.028	0.0496	0.0192	0.1360	0.063	2.74	1.73	24 h: 0.0117	
*15	-	-	0.060	0.027	1.92	0.98	NS	-	-	0.2148	0.0293	4.33	1.47	20 h: 0.0296	NS
*20	-	-	0.067	0.015	2.79	0.56	NS	-	-	0.1210	0.063	7.17	2.37	10 h: 0.0103	0.0152
24	0.024	0.0077	0.032	0.0086	1.35	0.65	NS	0.0169	0.009	0.1060	0.0187	6.28	0.93	20 h: NS	0.0075
Time (hpd)	IL-6														
	Fed							Fasted							p-value APAP fed vs fasted
	Control		APAP		Fold change	SD	p-value fed APAP	Control		APAP		Fold change	SD	p-value fasted APAP	
	Mean	SD	Mean	SD				Mean	SD	Mean	SD				
10	0.0242	0.0056	0.0452	0.01	1.87	0.31	20 h: 0.023 24 h: 0.041	0.033	0.007	0.0308	0.0085	0.93	0.42	NS	
*15	-	-	0.0202	0.011	0.84	0.26	20 h: 0.013 24 h: 0.022	-	-	0.0628	0.0127	1.90	0.84	NS	NS
*20	-	-	0.0915	0.024	3.79	0.85	24 h: NS	-	-	0.0416	0.0083	1.47	0.57	NS	0.034
24	0.0241	0.0120	0.0887	0.033	3.68	1.16	-	0.0284	0.01	0.0341	0.0044	1.20	0.45	NS	0.029

Table 6.21. Comparison of splenic TNF- α and IL-6 cytokine transcription in fed and fasted control and APAP treated mice in a 24 h period using delta Ct value, $2^{-\Delta Ct}$ and the comparative Ct value, i.e. fold change as compared to **pooled liver samples of the control** mice. Statistical significant (p-value control vs APAP) is seen in comparison between fold change APAP and fold change control ($2^{-\Delta Ct \text{ individual value}}/2^{-\Delta Ct \text{ mean}}$).

Time (hpd)	TNF- α														p-value APAP fed vs fasted
	Fed							Fasted							
	Control		APAP		Fold change	SD	p-value control vs APAP	Control		APAP		Fold change	SD	p-value control vs APAP	
	Mean	SD	Mean	SD				Mean	SD	Mean	SD				
10	0.0275	0.0119	0.121	0.046	4.40	1.77	0.0232	0.0333	0.0141	0.1360	0.063	4.09	2.83	0.0456	NS
15			0.060	0.027	2.18	1.10	NS			0.2148	0.0293	6.46	2.96	0.0067	0.0308
20			0.067	0.015	2.44	0.53	NS			0.1210	0.0630	3.64	1.89	0.0152	NS
24			0.032	0.0086	1.16	0.60	NS			0.1060	0.0187	3.19	0.78	0.0434	0.0255
Time (hpd)	IL-6														p-value APAP fed vs fasted
	Fed							Fasted							
	Control		APAP		Fold change	SD	p-value fed control vs APAP	Control		APAP		Fold change	SD	p-value control vs APAP	
	Mean	SD	Mean	SD				Mean	SD	Mean	SD				
10	0.0242	0.0088	0.0452	0.010	1.87	0.32	NS	0.0307	0.0085	0.0308	0.0085	1.00	0.55	NS	NS
15			0.0202	0.011	0.84	0.26	NS			0.0628	0.0127	2.05	0.98	NS	NS
20			0.0915	0.024	3.79	0.85	0.0130			0.0416	0.0083	1.36	0.52	NS	0.0449
24			0.0887	0.033	3.67	1.15	0.0319			0.0341	0.0044	1.11	0.41	NS	0.0370

Table 6.22. Comparison of hepatic NF- κ B transcription in fed and fasted control and APAP treated CD-1 mice in a 24 h period using delta Ct value, $2^{-\Delta Ct}$ and the comparative Ct value, i.e. fold change as compared **to time-matched control** mice. *15- relative to 10 h post saline; *20- relative to 24 h post saline. Statistical significant (p-value control vs APAP) is seen in comparison between fold change APAP and fold change control ($2^{-\Delta Ct \text{ individual value}} / 2^{-\Delta Ct \text{ mean}}$).

Fed									
Time (hpd)	Control		APAP				p-value fed APAP vs APAP	p-value control vs APAP	
	Mean	SD	Mean	SD	Fold change	SD			
1	7.2E-05	7.3E-06	6.3E-05	6.3E-06	0.88	0.58	4 h: 0.032 , 10 h: 0.0013 , 15 h: 0.0059 , 20 h: 0.0003 , 24 h: 0.0008	NS	
4	2.4E-05	8.2E-06	1.1E-04	2.1E-05	4.74	0.49	10 h: 0.0015 , 15 h: 0.0027 , 20 h: 0.0005 , 24 h: 0.0016	NS	
10	4.0E-05	7.1E-06	7.0E-04	1.5E-04	17.60	3.56	15 h: 0.0441 , 24 h: 0.0285	0.0001	
*15	-	-	5.2E-04	1.4E-04	12.93	1.68	20 h: 0.0388	0.0019	
*20	-	-	5.0E-04	7.5E-05	18.57	0.73	24 h: 0.0102	0.0001	
24	2.7E-05	7.3E-06	3.2E-04	9.9E-05	11.73	1.23	15 h: NS	0.0003	
Fasted									
Time (hpd)	Control		APAP				p-value fasted APAP vs APAP	p-value control vs APAP	p-value APAP fed vs fasted
	Mean	SD	Mean	SD	Fold change	SD			
1	6.3E-05	2.9E-05	1.1E-04	3.4E-05	1.67	0.90	1, 4 or 10 h: NS, 15, 20 and 24 h: 0.0047	NS	NS
4	4.0E-05	3.2E-05	1.3E-04	4.3E-05	3.29	1.46		NS	NS
10	3.0E-05	1.1E-05	9.8E-05	3.1E-05	3.26	1.82		NS	0.0008
*15	-	-	2.0E-04	8.2E-05	6.67	2.25	15, 20 or 24 h: NS	0.0059	0.0058
*20	-	-	3.0E-04	2.2E-05	5.80	0.58		0.0020	0.0013
24	5.1E-05	2.2E-05	3.0E-04	4.1E-05	5.85	1.50		0.0173	0.0089

Table 6.23. Comparison of hepatic NF-kB transcription in fed and fasted control and APAP treated mice in a 24 h period using delta Ct value, $2^{-\Delta Ct}$ and the comparative Ct value, i.e. fold change as compared to **pooled liver samples of the control** mice. Statistical significant (p-value control vs APAP) is seen in comparison between fold change APAP and fold change control ($2^{-\Delta Ct \text{ individual value}} / 2^{-\Delta Ct \text{ mean}}$).

Fed									
Time (hpd)	Control		APAP				p-value fed APAP vs APAP	p-value control vs APAP	
	Mean	SD	Mean	SD	Fold change	SD			
1	5.28E-05	2.07E-05	6.3E-05	6.3E-06	1.19	0.96	10 h: 0.0001 , 15 h: 0.0012 , 20 h: 0.0045 , 24 h: 0.0075	NS	
4			1.1E-04	2.1E-05	2.08	0.37		NS	
10			7.0E-04	1.5E-04	13.26	3.12	15 h: 0.030	0.0001	
15			5.2E-04	1.4E-04	9.85	1.42	20 h: NS	0.0001	
20			5.0E-04	7.5E-05	9.47	0.69	10 h: 0.0129	0.0034	
24			3.2E-04	9.9E-05	6.06	1.08	20 h: 0.0061	0.0063	
Fasted									
Time (hpd)	Control		APAP				p-value control vs APAP	p-value APAP fed vs fasted	
	Mean	SD	Mean	SD	Fold change	SD			
1	6.34E-05	2.74E-05	1.1E-04	3.4E-05	1.74	0.88	15h: NS, 20 h: 0.0317	NS	NS
4			1.3E-04	4.3E-05	2.05	1.25		NS	NS
10			9.8E-05	3.1E-05	1.55	1.57		NS	0.0012
15			2.0E-04	8.2E-05	3.15	2.13	20 h: NS	NS	0.0072
20			3.0E-04	2.2E-05	4.73	0.55	15 h: NS, 10 h: 0.0445	0.0199	0.0055
24			3.0E-04	4.1E-05	4.73	1.32		0.0308	NS

Table 6.24. Comparison of hepatic cyclin-D1 transcription in fed and fasted control and APAP treated CD-1 mice in a 24 h period using delta Ct value, $2^{-\Delta Ct}$ and the comparative Ct value, i.e. fold change as compared **to time-matched control** mice. *15- relative to 10 h post saline; *20- relative to 24 h post saline. Statistical significant (p-value control vs APAP) is seen in comparison between fold change APAP and fold change control ($2^{-\Delta Ct \text{ individual value}} / 2^{-\Delta Ct \text{ mean}}$).

Fed									
Time (hpd)	Control		APAP				p-value fed APAP vs APAP	p-value control vs APAP	
	Mean	SD	Mean	SD	Fold change	SD			
1	2.3E-06	3.00E-06	2.9E-06	6.4E-07	1.28	0.52	4 h: 0.0018 , 10 h: 0.0402 , 20 h: 0.0003 , 24 h: 0.0005	NS	
4	3.9E-06	1.00E-06	3.6E-05	7.1E-06	8.59	1.44	15 h: 0.0156 , 20 h: 0.0105 , 24 h: 0.032	0.0025	
10	8.0E-06	3.00E-06	3.9E-05	9.2E-06	4.90	2.05	20 h: 0.0034 , 24 h: 0.0075	0.0097	
*15	-	-	3.1E-05	1.1E-05	3.92	1.92		0.0060	
*20	-	-	5.7E-05	5.3E-06	16.14	1.57	24 h: 0.0493	0.0001	
24	3.5E-06	2.00E-06	4.3E-05	1.8E-06	12.35	1.15	-	0.0001	
Fasted									
Time (hpd)	Control		APAP				p-value fasted APAP vs APAP	p-value control vs APAP	p-value APAP fed vs fasted
	Control	SD	APAP	SD	Fold change	SD			
1	3.7E-06	1.00E-06	3.1E-06	1.9E-06	0.84	0.86	1,4 or 10 h: NS, 15 h: 0.0105 , 20 h: 0.0480 , 24 h: 0.00634	NS	NS
4	6.2E-06	4.00E-06	1.6E-05	4.3E-06	2.53	1.20		NS	0.0086
10	6.0E-06	2.00E-06	1.7E-05	7.3E-06	2.87	1.43		NS	NS
*15	-	-	3.6E-05	1.8E-06	6.02	0.83	15, 20 & 24 h: NS	0.0077	NS
*20	-	-	1.3E-05	6.2E-06	4.26	1.86		0.0094	0.0010
24	3.1E-06	5.00E-06	2.4E-05	4.1E-06	7.57	1.40		0.0055	0.0077

Table 6.25. Comparison of hepatic NF-kB transcription in fed and fasted control and APAP treated mice in a 24 h period using delta Ct value, $2^{-\Delta\Delta Ct}$ and the comparative Ct value, i.e. fold change as compared to **pooled liver samples of the control** mice. Statistical significant (p-value control vs APAP) is seen in comparison between fold change APAP and fold change control ($2^{-\Delta Ct \text{ individual value}} / 2^{-\Delta Ct \text{ mean}}$).

Fed									
Time (hpd)	Control		APAP				p-value fed APAP vs APAP	p-value control vs APAP	
	Mean	SD	Mean	SD	Fold change	SD			
1	4.46E-06	2.2E-06	2.9E-06	6.4E-07	0.65	0.43	4,10,24 h: 0.0010 , 20 h: 0.0001	NS	
4			3.6E-05	7.1E-06	8.07	1.26	10,24 h: NS, 20 h: 0.0056	0.0074	
10			3.9E-05	9.2E-06	8.74	2.48	20 h: 0.011 , 24 h: NS	0.0052	
15			3.1E-05	1.1E-05	6.95	2.30	24 h: NS	0.0209	
20			5.7E-05	5.3E-06	12.78	1.33	24 h: 0.0122	0.0003	
24			4.3E-05	1.8E-06	9.64	1.05	1 h: 0.0015	0.0066	
Fasted									
Time (hpd)	Control		APAP				p-value control vs APAP	p-value fed vs fasted APAP	
	Mean	SD	Mean	SD	Fold change	SD			
1	4.02E-06	2.8E-06	3.1E-06	1.9E-06	0.77	0.72	15 h: 0.0001 , 24 h: 0.0055	NS	NS
4			1.6E-05	4.3E-06	3.98	1.79	1 h: 0.0029 , 20 h: NS	NS	0.0391
10			1.7E-05	7.3E-06	4.23	2.03		NS	NS
15			3.6E-05	1.8E-06	8.96	1.30	4,10 h: 0.0018 , 20 h: 0.0004	0.0011	NS
20			1.3E-05	6.2E-06	3.23	1.06	24 h: 0.0330	NS	0.0009
24			2.4E-05	4.1E-06	5.97	1.21	15 h: 0.0021	0.0273	0.0089

Table 6.26. Range and average amount (%) of PCNA-positive, proliferating cells in fed and 16 or 24 h fasted control (saline) and APAP dosed mice at different time points post dosing.

Time (hpd)	Fed				Fasted					
	n	% PCNA+ (range; [mean])		p-value control vs APAP	Fasting time (h)		n	% PCNA+ (range; [mean])		p-value control vs APAP
		Control	APAP		16	24		Control	APAP	
0	4	15.3-26.7 [21.0]	-	-		x	4	2.27-9.4 [6.27]	-	-
0.5	-	-	-	-	x		5	2.58-19.05 [6.75]	3.31-22.5 [10.42]	0.0095
1	5	-	3.55-14.4 [7.92]	0 h: NS, 10 h: 0.0158	x		5	0.8 - 5.6 [2.89]	3.45-20.9 [10.25]	NS
3	5	-	11.95-34.9 [25.96]	0 h: NS, 10 h: 0.0036		x	5	-	1.08-7.79 [3.82]	-
5	6	-	7.35-26.9 [15.62]	0 h: NS, 10 h: 0.0007		x	5	0.77 - 1.12 [1.89]	0.4-6.98 [3.23]	NS
10	6	0.31-0.73 [0.59]	5.7-13.4 [7.71]	0 h: NS, 10 h: 0.0095		x	5	0.08 - 2.7 [1.26]	0.29-6.87 [2.98]	NS
15	6	-	1.54-24.3 [3.86]	0 h: NS, 10 h: 0.0095	x		5	2.79 - 22.4 [7.9]	6.76-21.2 [11.65]	0.0404
20	6	-	2.96-13.48 [9.84]	0 h: NS, 10 h: NS	x		5	2.69 - 21.0 [10.34]	8.1-28.3 [15.73]	0.0297
24	4	-	4-24.2 [15.02]	0 h: NS, 10 h: NS	x		5	1.54 - 16.4 [6.34]	2.04-19.9 [13.09]	0.0188
						x	5	-	1.67-4.86 [3.62]	NS
					x	x	10	1.54 - 16.4 [6.34]	1.67-19.9 [8.36]	NS

Table 6.27. Range and average amount (%) of PCNA-positive, proliferating cells in fed and 16/24 h fasted **pooled control** (saline) and APAP dosed CD-1 mice at different time points post dosing.

Time (hpd)	Fed				Fasted						
	n	Control Mean (SD)	APAP Range [mean]	p-value control vs APAP	Fasting time (h)		n	Control Mean (SD)	APAP Range [mean]	p-value control vs APAP	p-value fed vs fasted APAP
					16	24					
1	5	7.39 (11.14)	3.55-14.4 [7.92]	All NS at any time points	x		5	5.29 (5.63)	3.45-20.9 [10.25]	NS	NS
3	5		11.95-34.9 [25.96]			x	5		1.08-7.79 [3.82]	NS	0.0044
5	6		7.35-26.9 [15.62]			x	5		0.4-6.98 [3.23]	NS	0.0011
10	6		5.7-13.4 [7.71]			x	5		0.29-6.87 [2.98]	NS	0.0303
15	6		1.54-24.3 [3.86]			x	5		6.76-21.2 [11.65]	0.0090	NS
20	6		2.96-13.48 [9.84]			x	5		8.1-28.3 [15.73]	0.0019	NS
24	4	4-24.2 [15.02]			x		5	2.04-19.9 [13.09]	0.0405	NS	
						x	5	1.67-4.86 [3.62]	NS	NS	
					x	x	10	1.67-19.9 [8.36]	NS	NS	

Table 6.28. Range and average amount (%) of cytoplasmic PCNA-positive, proliferating mitotic cells in fed and fasted time-matched control (saline) and APAP dosed CD-1 mice at different time points post dosing. hpd – hours post dosing; n – no of animal per group; NS not significant; Cyto – cytoplasmic.

Time (hpd)	Fed				Fasted					
	n	% Cyto+ (range; [mean])		p-value control vs APAP	Fasting time (h)		n	% Cyto+ (range; [mean])		p-value control vs APAP
		Control	APAP		16	24		Control	APAP	
0	4	0.27-1.05 [0.66]	-			x	4	0-0.27 [0.16]	-	-
0.5	-	-	-	-	x		5	0.08 – 2.42 [1.19]	0.15-1.16 [0.67]	NS
1	5	-	0-0.39 [0.18]	0 h: NS, 10 h: NS	x		5	0 – 0.46 [0.18]	0.38-3.02 [1.40]	NS
3	5	-	0-1.18 [0.62]	0 h: NS, 10 h: NS		x	5	-	0.16-1.62 [0.94]	-
5	6	-	0.7-2.07 [1.02]	0 h: NS, 10 h: 0.0006		x	5	0.14 – 0.3 [0.22]	0.17-3.9 [1.46]	NS
10	6	0-0.16 [0.1]	0.05-0.56 [0.27]	0 h: NS, 10 h: 0.0472		x	5	0	0-0.19 [0.056]	NS
15	6	-	0.14-0.91 [0.35]	0 h: NS, 10 h: 0.0275	x		5	0	0.12-13.5 [3.88]	0.0079
20	6	-	0.24-2.12 [1.04]	0 h: NS, 10 h: 0.0433	x		5	0 – 0.19[0.05]	0-2.54 [1.24]	NS
24	4	-	0.37-2.07 [0.94]	0 h: NS, 10 h: NS,	x		5	0.06 – 0.21 [0.11]	0-1.97 [0.78]	NS
						x	5	-	0.17-1.87 [1.08]	0.0159
					x	x	10	0.06 – 0.21 [0.11]	0-1.97 [0.92]	0.0360

Table 6.29. Range and average amount (%) of cytoplasmic PCNA-positive, proliferating mitotic cells in fed and fasted **pooled control** (saline) and APAP dosed CD-1 mice at different time points post dosing. hpd – hours post dosing; n - no of animal per group; NS not significant; Cyto – cytoplasmic.

Time (hpd)	Fed				Fasted						
	n	Control Mean (SD)	APAP Range [mean]	p-value control vs APAP	Fasting time (h)		n	Control Mean (SD)	APAP Range [mean]	p-value control vs APAP	p-value fed vs fasted APAP
					16	24					
1	5	0.28 (0.39)	0-0.39 [0.18]	NS	x		5	0.095 (0.121)	0.38-3.02 [1.40]	0.0001	NS
3	5		0-1.18 [0.62]	NS		x	5		0.16-1.62 [0.94]	0.0004	NS
5	6		0.7-2.07 [1.02]	0.0082		x	5		0.17-3.9 [1.46]	0.0003	NS
10	6		0.05-0.56 [0.27]	NS		x	5		0-0.19 [0.056]	NS	0.0216
15	6		0.14-0.91 [0.35]	NS	x		5		0.12-13.5 [3.88]	0.0057	NS
20	6		0.24-2.12 [1.04]	0.0411	x		5		0-2.54 [1.24]	0.0092	NS
24	4	0.37-2.07 [0.94]	0.0446		x		5	0-1.97 [0.78]	0.0438	NS	
						x	5	0.17-1.87 [1.08]	0.0005	NS	
					x	x	10	0-1.97 [0.92]	0.0011	NS	

Table 6.30. A summary comparison of the examined parameters for the assessment of APAP hepatotoxicity in **fed and fasted CD-1 mice** (1-24 hpd). Statistically significant differences were observed between the fasted and fed mice that had received APAP intraperitoneally. Hepatic or splenic mRNA levels were summarised based on fold change relative to pooled control animals. 4/5- Studies done at 5 hpd are serum ALT and PCNA, others are at 4 hpd. *P<0.005, <0.01 or <0.05.

	Time (hours post APAP dosing)											
	1		4/5		10		15		20		24	
	Fed	Fast	Fed	Fast	Fed	Fast	Fed	Fast	Fed	Fast	Fed	Fast
Hepatic GSH	5.3 (3.65)	13.7(8.3)	4.95(0.6)	4.47(3.6)	40.3(0.7)	5.3(1.2)*	44.3(12.6)	33.98(16.2)	35.1(18.5)	49.3(7.8)	45.5 (10)	50.6(25.2)
Hepatic ATP	31.4 (5.1)	4.2 (0.9)*	10.5 (2.3)	3.5 (4.9)*	18.3 (5.7)	3.4 (1.2)*	-	-	-	-	35.4(3.9)	8.1 (1.3)*
Fold change												
1- GSH	0.13	0.33	0.14	0.09	1.96	0.06	-	-	-	-	0.96	0.33
2- ATP	0.98*	0.79*	0.30	0.20	0.61*	0.25	-	-	-	-	1.07	0.49
Serum ALT	-	-	2146.4 (1012.3)	2048.6 (461.7)	-	-	-	-	-	-	2654.5 (334.5)	3603.8 (508.8)*
HE score	0 (0)	0 (0)	2.4(0.25)	2.5 (1.41)	1 (1.31)	2.6(0.42)	1.13(1.24)	2.15 (0.78)	0.65(0.67)	2.75 (0.4)*	0 (0)	2.38(0.7)*
TNF- α												
1- Liver	2.76(0.3)	1.0(0.6)	4.4(0.7)	2.3 (0.6)*	7.9 (2.7)	6.8 (2.4)	2.0 (1.3)	18.3 (4.8)*	2.1 (1.4)	1.9 (0.7)	1.77(0.8)	1.5 (0.5)
2- Spleen	-	-	-	-	4.4 (1.8)	4.9 (2.0)	2.2 (1.1)	7.8 (1.6)*	2.4 (0.5)	4.4 (1.9)	1.2(0.6)	3.9 (0.8)*
3- Serum	-	-	62 (13.5)	101.2(40)	-	-	-	-	-	-	95 (14)	228 (54)*
IL-6												
1- Liver	2.6 (0.8)	1.7 (0.8)	6.0 (1.9)	4.7 (1.7)	7.9 (0.8)	2.2 (1.0)*	4.5 (2.0)	4.5 (0.9)	15.8 (4.0)	5.3 (1.6)*	7.6 (2.7)	7.4 (3.1)
2- Spleen	-	-	-	-	1.9 (0.3)	1.0 (0.6)	0.8 (0.3)	2.0 (1.0)	3.8 (0.9)	1.4 (0.5)*	3.7 (1.2)	1.1 (0.4)*
3- Serum	-	-	54.3(10)	35.4(11)*	-	-	-	-	-	-	203(40)	96(35.2)*
Hepatic IL-10	3.0 (0.8)	2.6 (1.5)	3.9 (1.5)	1.5 (1.2)	9.0 (2.9)	1.8 (0.9)*	13.2(3.7)	3.9 (1.4)*	10.4(3.1)	4.6(2.1)*	8.8 (1.3)	5.2 (3.9)
Hepatic NF-kB	1.19 (0.96)	1.74 (0.9)	2.1 (0.4)	2.1 (1.3)	13.3(3.1)	1.5 (1.6)*	9.85(1.4)	3.2 (2.1)*	9.5(0.7)	4.7 (0.6)*	6.1 (1.1)	4.7 (1.3)
Liver cyclin-D1	0.7 (0.4)	0.8 (0.7)	8.1 (1.3)	4.0 (1.8)*	8.7 (2.5)	4.2 (2.0)	7.0 (2.3)	9.0 (1.3)	12.8 (1.3)	3.2 (1.1)*	9.6 (1.1)	6.0 (1.2)*
IH PCNA (%)												
1- Overall	7.92	10.25	15.62	3.23*	7.71	2.98*	3.86	11.65	9.84	15.73	15.02	8.36
2- Cyto+	0.18	1.40	1.02	1.46	0.27	0.06*	0.35	3.88	1.04	1.24	0.94	0.92

C. APAP dosed C57BL/6J mice

Table 6.31. Histological findings in APAP dosed fed C57BL/6J mice (time course). The histological findings and average grading scores for individual animals at each time point were recorded over a 36 h time course. hpd - hours post dosing; NHAIR - no histological abnormality is recognised; CL – centrilobular; HD - hydropic degeneration; NL - neutrophilic leukocytes; hpc – hepatocytes; pos. – positive; neg. – negative; occ. - occasional; ind. - individual; CC3 – cleaved caspase-3; mod. – moderate; CV – central vein; apop. – apoptosis; nec. – necrosis.

Time (hpd)	Case no.	Score range [mean]	Histological descriptions	Exp
0	09L-3233	0	Hepatocellular vacuolation; NHAIR; PAS: Diffuse glycogen	2
	09L-3234	0	NHAIR; PAS: diffuse glycogen	
	09L-3235	0	NHAIR; PAS: diffuse glycogen	
	09L-3236	0	NHAIR; PAS: diffuse glycogen	
	Summary	[0]	NHAIR; PAS: Diffuse glycogen in hpc	
1	09L-3249	0	NHAIR; PAS: diffuse glycogen	
	09L-3250	0	NHAIR; PAS: diffuse glycogen	
	09L-3251	0	NHAIR; PAS: diffuse glycogen	
	09L-3252	0	NHAIR; PAS: diffuse glycogen	
	Summary	[0]	NHAIR; PAS: Diffuse glycogen in hpc	
3	09L-3257	0.5-1	Mild CL cell loss; very few apoptotic hpc and increase amount of NL at CL, HD of some hpc at CL. PAS: Glycogen only at zone 1	
	09L-3258	0.5-1	Mild CL cell loss; intense cytoplasm of hpc at CL and increase NL infiltration centrilobularly, some aggregate to cell death. Very few apoptotic hpc. PAS: Loss of glycogen at zone 3	
	09L-3259	1.5-2	CL cell loss and haemorrhage with NL infiltration. No evidence of cell death. PAS: Pos. outside zone 3	
	09L-3260	1.5-2	Similar to 09L-3259	
	Summary	[1.25]	CL cell loss and haemorrhage with several NL infiltration; no or very occ. apop. hpc and HD of remaining cells in affected CL areas; PAS: Loss of glycogen in hpc surrounding affected areas	
5	09L-3265	1-1.5	HD at inner CL surrounded by intense cytoplasm, moderate NL at zone 3. PAS: only glycogen at zone 1	
	09L-3266	2-2.5	Extensive CL cell loss with high NL at affected area of zone 3, some evidence of NL at affected areas and CV. PAS: Glycogen at unaffected area of zone 1 only	
	09L-3267	3.5-4	More extensive CL cell loss with haemorrhage, marked NL infiltration. PAS: No glycogen at affected areas CL	
	09L-3268	3.5-4	Similar to 09L-3267	
	13L-5205	1-3	CL cell loss with some NL infiltration with few aggregate to ind cell death, PAS: Glycogen at outside zone 3	
	13L-5206	2-3	More extensive cell loss with some NL infiltration. PAS: No glycogen at affected areas	
	Summary	[2.75]	More extensive centrilobular cell loss with haemorrhage and marked NL infiltration; PAS: Loss of glycogen in hpc surrounding affected areas	
10	11L-4466	1	Mild cell loss; scattered hpc death with aggregation of NL. Increase no of NL between hepatic cord, few hpc at CL underwent degeneration. PAS: Glycogen at area of unaffected area of zone 2 and 1	4

Appendix

	11L-4467	0-1	Very mild CL cell loss; hpc with fine vacuoles at 3-4 layers of CL; slight to mild LC infiltrates at CL; PAS: hpc with variable amount of glycogen at zone 2 and 1 only. (no glycogen at 4-5 layers of CL)	5
	11L-4468	1.5	Some CL cell loss with increased no of NL, some NL aggregate to ind. cell death hpc. PAS: hpc with variable amount of glycogen except zone 3 and zone 2	
	11L-4469	0-2	CL cell loss; mild infiltration of NL at CL; hpc with no vacuolation at CL region (a few cell loss). PAS: hpc with glycogen with variable amount except zone 3	
	11L-4470	1.5	CL cell loss with evidence of scattered apoptotic/necrotic cell and mitotic figures of hpc (moderate); mild NL infiltration between zone 3 & 2. PAS: Disseminated hpc with variable amount of glycogen at zone 2	
	14L-0689	1-1.5	CL cell loss with few scattered mitotic figures; mild NL with haemorrhage at zone 3; NL aggregate to cell death. CC3: +; PAS: Very mild scattered ind. hpc. with glycogen	
	14L-0690	1-1.5	Similar to 14L-0689	
	14L-0691	2-2.5	Extensive CL cell loss and moderate NL at zone 3 & 2, mitotic figure; evidence of moderate NL. CC3: very few pos. hpc. PAS: Moderate hpc with glycogen (almost diffuse)	
	14L-0692	1-1.5	CL cell loss; aggregation of NL to ind. cell death; high haemorrhage at zone 3 with still present of hpc nucleus. CC3: ++; PAS: Diffuse glycogen except 3-4 layers of zone 3	
	Summary	[1.5]	CL cell loss with moderate NL infiltration and scattered evidence of mitotic figures; CC3: +/++; PAS: No glycogen in 3-4 layers of hpc in affected zones areas with variable density	
15	11L-4471	1	Rounded hpc with very few aggregation of NL to ind. cell death. PAS: Disseminated hpc with glycogen with variable density except some few layers of zone 3 and 1	4
	11L-4472	1-2	Reduced cellularity of CL with some NL aggregate to individual cell death; mild CL cell loss; PAS: Disseminated hpc with variable density of glycogen except affected region of zone 3	
	11L-4473	1	One evidence of mitotic figures; a few scattered aggregation of NL to individual hpc cell death; reduced cellularity of some CL; minimal NL infiltrate between hepatic cord; PAS: Scattered ind. glycogen with variable density distribute randomly in all zones	
	11L-4474	1	Very few scattered ind. cell death with NL aggregation, mild NL infiltrate between hepatic cord; PAS: Scattered individual glycogen hpc distribute randomly at all zones especially zone	
	11L-4475	1-2	Mild mitotic figures and aggregation of NL to hpc cell death, mild CL cell loss, infiltration of NL at zone 3 and 2. Hpc with variable sized cyto. vacuoles CL (4-5 cell layers), outside this less intense. PAS: Diffuse glycogen with variable density except 3-5 layers of zone 3	5
	14L-0693	2-3	CL cell loss (almost all lobe) with high haemorrhage and moderate NL at zone 3 and 2; CC3: +; Neg.; PAS: No glycogen at affected areas of zone 3	
	14L-0695	4-5	Dead- exclude from study	
	14L-0696	1-2	CL cell loss and few scattered cell death; some NL infiltration at affected areas; no mitotic figures. CC3: +; PAS: No glycogen at affected areas of zone 3	
	14L-0697	2-3	Similar to 14L-0693	
Summary	[2.17]	CL cell loss with haemorrhage and moderate NL infiltration at zone 3 & 2; CC3: +; PAS: No glycogen in affected zones with some disseminated hpc with glycogen with variable amount		
20	11L-4476	0-2	Mild to moderate CL cell loss and some variable sized cyto vacuoles at CL; Infiltration of NL at CL and zone 2 (some aggregate to ind. cell death); some evidence of mitotic figures at CL and zone 2. PAS: few scattered ind. variable intensity of glycogen randomly at all zones except CL	4

	11L-4477	1	Mild CL cell loss and cell death; NL infiltration at CL and zone 2 (some aggregate to nec./ apop hpc). PAS: few scattered ind. variable intensity of glycogen randomly at all zones except CL	5
	11L-4478	1-2	Swollen and vacuolated cytoplasmic (HD) Mild CL cell loss with few necrotic hpc in some CL accompanied with NL aggregation; some NL circulated at zone 2 and 3. PAS: Diffuse glycogen except 3-5 layers of zone 3	
	11L-4479	1-2	Mild to moderate CL cell loss and scattered NL aggregation to necrotic cell death; NL recruit out of CV to CL; some vacuolated hpc at CL; PAS: No glycogen	
	11L-4480	0-1	Reduced & disorganised CL cellularity; some mild CL cell loss; some aggregation of NL to ind. apop./nec. cell. CC3: ++; PAS: Few scattered hpc with glycogen randomly distributed except zone 3	
	14L-0701	1-1.5	Ongoing cell damage, evidence of apoptosis with low amount of NL at zone 3. CC3: +; PAS: Diffuse glycogen except 5-6 layers of zone 3	
	14L-0702	1-1.5	CL cell loss; with evidence of apoptosis/necrotic cells; some aggregation of NL to ind cell death. CC3: ++; PAS: Diffuse glycogen except 3-4 layers of zone	
	14L-0703	0-1	Mild CL cell loss; CC3: +; PAS: Diffuse glycogen except 1-2 layer of zone 3 (almost intact).	
	14L-0704	2-2.5	Moderate no of scattered apoptotic cell at zone 3 with some NL aggregate to death cell. CC3: +/++; PAS: Diffuse glycogen except affected 2-3 layers of zone 3	
	Summary	[1.3]	CN and HD of remaining CL hpc with and evidence of apoptotic cell with NL infiltration; CC3; +/++; PAS: No glycogen in hpc in affected zones; few scattered ind. hpc, (1/5) no glycogen	
24	09L-3273	1-1.5	CN of some hpc, few scattered apop. at zone 3, HD of hpc at affected and unaffected areas, few NL with aggregate to cell death. CC3: ++; PAS: Diffuse glycogen except 5-6 layers of affected areas	2
	09L-3274	1	Some CL with HD on remaining hpc and aggregation of NL to cell death. CC3: +; PAS: No glycogen at affected areas of zone 3	
	09L-3275	1	Numerous apoptosis to some CL with moderate no of NL to cell death, few CL are intact; CC3: +; PAS: Neg. at affected areas of CL	
	13L-5207	0.5-1.5	Some CL with 1-2layer of cell loss and few NL infiltration centrilobularly, CC3: Neg.; PAS: diffuse glycogen except 2-3 layer of zone 3	
	13L-5208	0.5-1	CL 1-2 layer of cell loss with mild NL infiltration. PAS: Scattered ind hpc with low glycogen amount	
Summary	[1.15]	CN and HD of remaining CL hpc with mild NL infiltration; CC3: +/++; PAS: Neg. in 2-3 CL layers		
30	13L-5211	0-1	Some CL with 1-2 layer of cell loss and few NL infiltration. CC3: very few pos. hpc; PAS: Neg. at CL	5
	13L-5212	1-1.5	2-3 layers of CN with some NL (few aggregate to cell death between affected & unaffected areas) CC3: +; PAS: No glycogen at affected areas	
	13L-5213	1-1.5	2-3 layers of CL with CN and moderate NL infiltration; CC3: +; PAS: No glycogen at affected areas	
	13L-5214	0	NHAIR. CC3: Neg. PAS: no glycogen at 2-3 layer of zone 3	
	Summary	[0.75]	2-3 innermost CL hpc layers with CN and few infiltrating NL; CC3: +; PAS: Neg. in CL hpc layers	
36	14L-0709	1	Inner zone 3 with CN surrounded by swollen cell (HD); CC3: + (Occ. pos. hpc) PAS: Diffuse glycogen except 1-2 layer of zone 3	5
	14L-0710	1	CN with 1-2 layer of zone 1 surrounded by intense cyto of hpc. CC3: +; PAS: Diffuse glycogen except affected area of zone 3	
	14L-0711	0-1.5	Similar to 14L-0710 but CN is slightly more intense. PAS: Glycogen only on unaffected area	
	14L-0712	1	CN with 1-2 layer of zone 1; few apop. hpc, some NL infiltration with its aggregation to cell death. CC3: + (scattered ind. pos. at CL); PAS: Diffuse glycogen except affected areas of zone 3	
Summary	[0.8]	CN at 1-2 innermost CL hpc layers with some apoptotic cells; CC3: +; PAS: Diffuse glycogen surrounding the CN layers (3-4 layer of zone 3)		

Exp – Experiments performed by 2 - Craig Benson (2011), 4 - Harley Webb (2013), and 5 - Fazila Hamid (2013-14).

Table 6.32. Histological findings in APAP dosed **fasted C57BL/6J mice** (time course). The histological findings and average grading scores for individual animals at each time point were recorded over a 36 h time course. hpd - hours post dosing; NHAIR - no histological abnormality is recognised; CL – centrilobular; HD - hydropic degeneration; NL - neutrophilic leukocytes; hpc – hepatocytes; pos. – positive; neg. – negative; occ. - occasional; ind. - individual; CC3 – cleaved caspase-3; mod. – moderate; CV – central vein; apop. – apoptosis; nec. – necrosis.

Time (hpd)	Case no.	Score range [mean]	Histological descriptions	Exp
0	10L-2368	0	NHAIR; PAS: No glycogen	2
	10L-2369	0	NHAIR; PAS: No glycogen	
	10L-2370	0	NHAIR; PAS: No glycogen	
	10L-2371	0	NHAIR; PAS: No glycogen	
	Summary	[0]	NHAIR; PAS: No glycogen	
0.5	10L-2376	0	NHAIR; PAS: Diffuse glycogen with low amount	
	10L-2377	0	NHAIR; PAS: Diffuse glycogen with low amount	
	10L-2378	0	NHAIR; PAS: Glycogen loss at CL	
	10L-2379	0	NHAIR; PAS: Diffuse glycogen with low amount	
	Summary	[0]	NHAIR; PAS: Diffuse glycogen (relatively low amount; one animal with CL loss of glycogen)	
1	10L-2384	0	NHAIR; PAS: Diffuse glycogen but relatively low amount	
	10L-2385	0	NHAIR; PAS: Diffuse glycogen but relatively low amount	
	10L-2386	0	NHAIR; PAS: Diffuse glycogen but relatively very low amount	
	10L-2387	0	NHAIR; PAS: No glycogen	
	Summary	[0]	NHAIR; No glycogen, one animal with centrilobular HD	
3	10L-2392	0	NHAIR; few NL at zone 3 and few HD of CL hpc. PAS: Extensive CL glycogen loss except few area with low amount	
	10L-2393	0	NHAIR; PAS: Glycogen at variable amount	
	10L-2394	0	NHAIR; PAS: PAS: Glycogen at variable amount, less intense at CL	
	10L-2395	0	NHAIR; PAS: Glycogen at variable amount, less intense at CL	
	Summary	[0]	NHAIR; PAS: Diffuse glycogen with variable intensity	
5	10L-2400	2-3	Coagulative bridging necrosis between CL with numerous NL between affected area with some evidence of apoptotic hpc. PAS: Glycogen at some area of zone 1 with variable amount	
	10L-2401	3-4	More extensive CL cell loss with bridging necrosis. Numerous NL infiltration mainly zone 3. PAS; No glycogen except scattered ind hpc at variable intensity	
	10L-2402	3-4	Same as in 10L-2401, PAS; glycogen with variable amount only at zone 1	
	10L-2403	3-4	CN of innermost zone 3, and bridging necrosis, high NL at affected area. PAS: Pos. with variable amount at zone 1	
	Summary	[3.25]	CL cell loss with bridging necrosis of innermost CL layers with numerous NL; PAS: Diffuse glycogen loss, except in some periportal hpc with variable amount	
10	14L-0937	1-2	CL loss with high no of NL (some aggregate to ind. cell death), few apoptotic cell and inflammatory cells. CC3: +/++; PAS: No glycogen	5

			except scattered ind. hpc	
	14L-0938	1-2	Same as in 14L-0937	
	14L-0939	2-3	More intense CL loss with high NL and few evidence of apop. cells. CC3: +; PAS: Glycogen to few ind. hpc	
	14L-0940	3	Same as in 14L-0939 with increase amount of NL aggregates to ind. cell death. CC3: +; PAS: Glycogen at ind. hpc scattered to all zone	
	Summary	[2.13]	CL cell loss with NL infiltration; few apop. cells; CC3: +/+++; PAS: Scattered random hpc containing glycogen	
15	14L-0943	1.5-2	CL cell loss, few scattered apop. with high NL between affected & unaffected area. CCL: +/+++; PAS: Neg.	
	14L-0944	1-2	CL cell loss with high NL between affected/unaffected zone, with few apoptotic cells. CC3: +; PAS: Scattered glycogen at zone 1 with variable amount	
	14L-0945	2	Same as in 14L-0943. PAS: No glycogen except few scattered individual hpc	
	14L-0946	1.5-2	Evidence of a few apoptotic cells. PAS: No glycogen	
	Summary	[1.75]	CL cell loss with a few scattered apoptotic cells and substantial NL infiltration; CC3: +; PAS: Neg.	
20	14L-0949	1-1.5	CL cell loss with numerous NL at zone 3. Scattered ind. glycogen randomly with variable density mainly zone 1 & 2. CC3: +; PAS: scattered glycogen randomly with variable amount	
	14L-0950	1.5-2	CN of inner 2-3 layers of CL with numerous NL infiltrations between affected and unaffected areas. CC3: +/+++; PAS: Glycogen with variable amount only at some area of zone 1	
	14L-0951	3	More extensive than 14L-0950. PAS: No glycogen	
	14L-0952	1-3	Similar as in 14L-0951/52. CC3: +; PAS: No glycogen except scattered randomly ind. hpc with glycogen	
	Summary	[2]	CN of innermost 2-3 CL hpc layers with few HD of remaining hpc at zone 2 between affected and unaffected areas; few apoptotic cells; CC3: +/+++; PAS: Neg. except few scattered random ind. hpc	
24	10L-2409	2-2.5	CN of CL, and moderate no of apoptosis at zone 3, moderate amount of NL. CC3: +/+++; PAS: No glycogen at zone 3	2
	10L-2410	2	CN of CL; few apop, high NL between affected and unaffected area. CC3: +; PAS: No glycogen at affected areas	
	10L-2411	2	Aggregation of NL to death cell, few scattered apoptosis at affected area. CC3: ++; PAS: Neg. at affected areas	
	10L-2412	2-2.5	CN, HD of remaining cells, few scattered apoptotic body, some NL infiltration. CC3: +; PAS: Neg. at affected areas	
	10L-2413	2	CN of CL, moderate apoptosis, some NL with aggregate to ind. cell death. CC3: ++; PAS: Neg. at affected areas	
	Summary	[2.1]	Similar to 20 hpd; CN, HD and occasional apoptosis of remaining hpc in affected areas; CC3: ++; PAS: No glycogen in affected areas of zone 3	
36	14L-0955	2	CN of innermost layer of zone 3 and few scattered apoptotic cells; few NL at affected areas. CC3: +; PAS: Diffuse glycogen outside affected areas	5
	14L-0956	2	Similar to 14L-0955	
	14L-0957	1-2	CN of 2-3 layers of inner CL, some apoptotic hpc at CL. CC3: +/+++; PAS: Glycogen at unaffected area of zone 2 & 1	
	14L-0958	1-2	Inner 2-3 layers of CN at CL, some apoptotic hpc and moderate NL between affected and unaffected areas. CC3: +; PAS: Glycogen at unaffected area of zone 2 and 1	
	Summary	[1.5]	CN of innermost 2-3 CL hpc layers with moderate NL infiltration and some apoptotic hpc; CC3: +; PAS: Diffuse glycogen outside affected areas	

Exp – Experiments performed by 2 - Craig Benson (2011) and 5 - Fazila Hamid (2013/2014).

Table 6.33. Hepatic cytokine transcription of TNF- α , IL-6 and IL-10 in **time-matched control and APAP treated fed C57BL/6J mice**, using the delta Ct method, $2^{-\Delta Ct}$ and also the comparative Ct value method, i.e. the fold change with p-value. The fold change values of APAP dosed C57BL/6J mice were also compared to APAP dosed CD-1 mice. *5- values of 5 h C57BL/6J was compared to 4 h CD-1 mice. In CD-1 mice only (*15- relative to 10 h post saline; *20- relative to 24 h post saline).

TNF- α								
Time (hpd)	Control		APAP				p-value control vs APAP	p-value vs APAP CD-1
	Mean	SD	Mean	SD	Fold change	SD		
1	3.90E-04	3.40E-04	7.30E-04	3.30E-04	1.87	0.62	NS	NS
*5	7.30E-04	5.60E-04	4.34E-03	8.45E-04	5.95	2.23	0.0065	NS
10	3.70E-04	4.80E-04	8.10E-04	3.13E-04	2.19	1.18	NS	0.0229
15	2.50E-04	7.80E-05	3.40E-04	2.80E-04	1.36	0.63	NS	NS
20	3.50E-04	2.12E-04	5.60E-04	1.12E-04	1.60	0.34	NS	NS
24	2.10E-04	1.70E-04	2.20E-04	6.80E-05	1.05	0.14	NS	NS
36	3.50E-04	1.23E-04	5.10E-04	2.74E-04	1.46	0.66	NS	-
IL-6								
Time (hpd)	Control		APAP				p-value control vs APAP	p-value vs APAP CD-1
	Mean	SD	Mean	SD	Fold change	SD		
1	2.68E-04	6.89E-05	1.38E-04	6.20E-05	0.52	0.06	NS	0.0052
*5	3.80E-04	9.26E-05	7.55E-04	2.20E-04	1.99	0.84	NS	0.0309
10	5.50E-04	8.33E-05	1.20E-03	6.36E-04	2.19	1.29	NS	0.0001
15	3.55E-04	7.40E-05	1.68E-03	3.60E-04	4.73	1.38	0.0225	NS
20	2.00E-04	1.03E-04	9.07E-04	2.30E-04	4.54	1.03	0.0095	0.004
24	2.66E-04	4.85E-05	2.27E-03	6.08E-04	8.52	2.34	0.0030	NS
36	3.18E-04	2.38E-04	2.33E-03	3.60E-04	7.31	2.05	0.0011	-
IL-10								
Time (hpd)	Control		APAP				p-value control vs APAP	p-value vs APAP CD-1
	Mean	SD	Mean	SD	Fold change	SD		
1	2.78E-06	1.43E-06	1.10E-06	3.84E-07	0.39	0.14	NS	NS
3	1.16E-06	1.45E-07	2.06E-06	2.58E-07	1.78	0.44	NS	-
*5	2.54E-06	1.97E-06	3.29E-06	8.54E-07	1.29	0.36	NS	0.0005
10	3.92E-06	1.30E-06	1.27E-05	6.14E-06	3.23	1.05	NS	0.0102
15	6.78E-06	3.31E-06	5.09E-05	9.42E-06	7.51	2.14	0.0068	NS
20	5.85E-06	9.70E-07	4.90E-05	7.00E-06	8.37	1.94	0.0056	NS
24	2.72E-06	1.13E-06	2.90E-05	1.01E-05	10.60	2.24	0.0005	NS
36	5.76E-06	1.50E-06	3.83E-05	4.78E-06	6.64	1.41	0.0017	-

Table 6.34. Hepatic cytokine transcription of TNF- α , IL-6 and IL-10 in **pooled liver samples of fed control C57BL/6J mice and in APAP treated fed C57BL/6J mice**, using the delta Ct method, $2^{-\Delta Ct}$ and also the comparative Ct value method, i.e. the fold change with p-value. The fold change values of APAP dosed C57BL/6J mice were also compared to APAP dosed CD-1 mice. *5- values of 5 h C57BL/6J was compared to 4 h CD-1 mice.

TNF- α								
Time (hpd)	Control		APAP				p-value control vs APAP	p-value vs APAP CD-1
	Mean	SD	Mean	SD	Fold change	SD		
1	3.71E-04	2.80E-04	7.30E-04	3.30E-04	1.97	0.68	NS	NS
*5			4.34E-03	8.45E-04	11.7	4.75	0.0004	0.0292
10			8.10E-04	3.13E-04	2.18	1.16	NS	0.0391
15			3.40E-04	2.80E-04	0.92	0.63	NS	NS
20			5.60E-04	1.12E-04	1.51	0.30	NS	NS
24			2.20E-04	6.80E-05	0.59	0.11	NS	NS
36			5.10E-04	2.74E-04	1.37	0.59	NS	-
IL-6								
Time (hpd)	Control		APAP				p-value control vs APAP	p-value vs APAP CD-1
	Mean	SD	Mean	SD	Fold change	SD		
1	3.23E-04	1.01E-04	1.38E-04	6.20E-05	0.43	0.05	NS	NS
*5			7.55E-04	2.20E-04	2.33	1.45	NS	0.0204
10			1.20E-03	6.36E-04	3.71	1.07	0.0112	0.0492
15			1.68E-03	3.60E-04	5.20	2.08	0.0103	NS
20			9.07E-04	2.30E-04	2.80	1.00	NS	0.0003
24			2.27E-03	6.08E-04	7.02	1.87	0.0025	NS
36			2.33E-03	3.60E-04	7.21	2.15	0.0009	-
IL-10								
Time (hpd)	Control		APAP				p-value control vs APAP	p-value vs APAP CD-1
	Mean	SD	Mean	SD	Fold change	SD		
1	4.05E-06	1.47E-06	1.10E-06	3.84E-07	0.27	0.12	NS	NS
3			2.06E-06	2.58E-07	0.51	0.38	NS	-
*5			3.29E-06	8.54E-07	0.81	0.28	NS	0.0278
10			1.27E-05	6.14E-06	3.14	0.89	NS	0.0302
15			5.09E-05	9.42E-06	12.6	3.42	0.0001	NS
20			4.90E-05	7.00E-06	12.1	4.09	0.0001	NS
24			2.90E-05	1.01E-05	7.17	1.23	0.0005	NS
36	3.83E-05	4.78E-06	9.47	3.64	0.0001	-		

Table 6.35. Hepatic cytokine transcription of TNF- α , IL-6 and IL-10 in **time-matched control and APAP treated male C57BL/6J mice** had been fasted for 16 h prior to dosing using delta Ct method, $2^{-\Delta Ct}$ and also the comparative Ct value method, i.e. the fold change with p-value. The fold change values of APAP dosed C57BL/6J mice were also compared to APAP dosed CD-1 mice. *5- values of 5 h C57BL/6J was compared to 4 h CD-1 mice. In CD-1 mice only (*15- relative to 10 h post saline; *20- relative to 24 h post saline).

TNF- α									
Time (hpd)	Control		APAP				p-value control vs APAP	p-value fasted vs fed C57BL/6J	p-value vs APAP CD-1
	Mean	SD	Mean	SD	Fold change	SD			
1	5.41E-04	1.75E-04	4.30E-04	2.30E-04	0.79	0.51	NS	NS	NS
*5	3.73E-04	2.56E-04	5.40E-04	1.38E-04	1.45	0.89	NS	0.0083	NS
10	7.21E-04	4.84E-04	1.14E-03	3.30E-04	1.58	1.29	NS	NS	0.0300
*15	1.23E-04	7.40E-05	2.60E-04	1.25E-04	2.11	0.90	NS	NS	0.0006
*20	1.97E-04	8.39E-05	8.20E-04	2.74E-04	4.16	1.41	0.0450	0.0323	NS
24	1.59E-04	1.82E-04	1.52E-03	4.40E-04	9.56	2.75	0.0010	0.0001	0.0137
36	1.73E-04	1.19E-04	1.36E-03	6.20E-04	7.86	3.26	0.0032	0.0015	-
IL-6									
Time (hpd)	Control		APAP				p-value control vs APAP	p-value fasted vs fed C57BL/6J	p-value vs APAP CD-1
	Mean	SD	Mean	SD	Fold change	SD			
1	2.30E-04	2.05E-04	2.49E-04	3.74E-05	1.08	0.7	NS	NS	NS
*5	5.10E-04	1.77E-04	3.72E-04	2.74E-04	0.73	0.67	NS	NS	0.0360
10	4.44E-04	1.07E-04	4.56E-04	7.65E-05	1.03	0.32	NS	NS	NS
*15	3.19E-04	8.47E-05	6.18E-04	7.37E-05	1.94	0.27	NS	0.0289	0.0151
*20	5.41E-04	1.92E-04	1.50E-03	1.80E-04	2.77	1.18	NS	NS	NS
24	2.86E-04	1.87E-04	1.01E-03	2.30E-04	3.53	1.78	0.0280	0.0329	NS
36	2.42E-04	7.30E-05	1.17E-03	8.14E-05	4.83	0.53	0.0059	NS	-
IL-10									
Time (hpd)	Control		APAP				p-value control vs APAP	p-value fasted vs fed C57BL/6J	p-value vs APAP CD-1
	Mean	SD	Mean	SD	Fold change	SD			
1	2.39E-06	9.00E-07	1.74E-06	1.28E-06	0.73	0.18	NS	NS	NS
3	3.28E-06	1.15E-06	3.32E-06	1.74E-06	1.01	0.35	NS	NS	-
*5	3.12E-06	1.50E-06	6.11E-06	1.05E-06	1.96	0.58	NS	NS	NS
10	2.70E-06	7.00E-07	5.68E-06	2.92E-06	2.10	0.35	NS	NS	NS
*15	3.90E-06	2.47E-06	9.98E-06	2.60E-06	2.56	1.13	NS	0.0044	NS
*20	4.61E-06	7.41E-07	1.00E-05	8.48E-07	2.18	0.66	NS	0.0070	0.0056
24	3.60E-06	1.70E-06	1.25E-05	2.28E-06	3.47	1.75	0.0410	0.0015	0.0063
36	3.42E-06	7.98E-07	2.09E-05	5.14E-06	6.11	2.26	0.0012	NS	-

Table 6.36. Hepatic cytokine transcription of TNF- α , IL-6 and IL-10 in **pooled liver samples of fasted control C57BL/6J mice and in APAP treated fasted C57BL/6J mice**, using the delta Ct method, $2^{-\Delta Ct}$ and also the comparative Ct value method, i.e. the fold change with p-value. The fold change values of APAP dosed C57BL/6J mice were also compared to APAP dosed CD-1 mice. *5- values of 5 h C57BL/6J was compared to 4 h CD-1 mice.

TNF- α									
Time (hpd)	Control		APAP				p-value control vs APAP	p-value fasted vs fed C57BL/6J	p-value vs APAP CD-1
	Mean	SD	Mean	SD	Fold change	SD			
1	3.63E-04	1.96E-04	4.30E-04	2.30E-04	1.19	0.76	NS	NS	NS
*5			5.40E-04	1.38E-04	1.49	0.86	NS	0.0052	NS
10			1.14E-03	3.30E-04	3.14	1.97	NS	NS	0.0399
15			2.60E-04	1.25E-04	0.72	0.64	NS	NS	0.0003
20			8.20E-04	2.74E-04	2.26	1.06	NS	0.0417	NS
24			1.52E-03	4.40E-04	4.19	1.44	0.0462	0.0058	0.0381
36			1.36E-03	6.20E-04	3.75	1.08	0.0370	0.0454	-
IL-6									
Time (hpd)	Control		APAP				p-value control vs APAP	p-value fasted vs fed C57BL/6J	p-value vs APAP CD-1
	Mean	SD	Mean	SD	Fold change	SD			
1	3.35E-04	1.47E-04	2.49E-04	3.74E-05	0.74	0.7	NS	NS	NS
*5			3.72E-04	2.74E-04	1.11	0.67	NS	NS	0.0337
10			4.56E-04	7.65E-05	1.36	0.32	NS	NS	NS
15			6.18E-04	7.37E-05	1.84	0.27	NS	0.0380	0.0208
20			1.50E-03	1.80E-04	4.47	1.18	0.0409	NS	NS
24			1.01E-03	2.30E-04	3.01	1.39	0.0280	0.0183	NS
36			1.17E-03	8.14E-05	3.49	0.53	0.0362	0.0170	-
IL-10									
Time (hpd)	Control		APAP				p-value control vs APAP	p-value fasted vs fed C57BL/6J	p-value vs APAP CD-1
	Mean	SD	Mean	SD	Fold change	SD			
1	3.37E-06	1.24E-06	1.74E-06	1.28E-06	0.52	0.13	NS	NS	NS
3			3.32E-06	1.74E-06	0.99	0.3	NS	NS	NS
*5			6.11E-06	1.05E-06	1.81	0.48	NS	NS	NS
10			5.68E-06	2.92E-06	1.69	0.32	NS	NS	NS
15			9.98E-06	2.60E-06	2.96	1.47	NS	0.0001	NS
20			1.00E-05	8.48E-07	2.97	0.96	NS	0.0001	0.0490
24			1.25E-05	2.28E-06	3.71	1.85	0.0252	NS	NS
36	2.09E-05	5.14E-06	6.20	2.12	0.0083	NS	-		

Table 6.37. Comparison of splenic TNF- α and IL-6 cytokine transcription in fed and fasted control and APAP treated C57BL/6J mice at 5 and 24 hpd using delta Ct value, $2^{-\Delta Ct}$ and the comparative Ct value, i.e. fold change as compared to **time-matched control** mice. The fold change values of APAP dosed C57BL/6J mice were also compared to APAP dosed CD-1 mice. *5- values of 5 h C57BL/6J was compared to 4 h CD-1 mice.

TNF- α											
Time (hpd)	Fed					Fasted					p-value fed vs fasted C57BL/6J
	Mean		Fold change (SD)	p-value APAP 5 vs 24 h	p-value vs APAP CD-1	Mean		Fold change (SD)	p-value APAP 5 vs 24 h	p-value vs APAP CD-1	
	Control	APAP				Control	APAP				
*5	8.4E-04	2.4E-03	2.86 (0.93)	NS	-	3.7E-03	5.4E-03	1.46 (0.73)	0.0003	-	NS
24	1.2E-03	2.2E-04	0.18 (0.19)		NS	1.6E-04	1.5E-03	9.38 (2.96)		NS	0.0075
IL-6											
Time (hpd)	Fed					Fasted					p-value fed vs fasted C57BL/6J
	Mean		Fold change (SD)	p-value APAP 5 vs 24 h	p-value vs APAP CD-1	Mean		Fold change (SD)	p-value APAP 5 vs 24 h	p-value vs APAP CD-1	
	Control	APAP				Control	APAP				
*5	8.2E-05	6.5E-04	7.93 (2.13)	0.0043	-	3.4E-04	6.8E-04	1.99 (0.74)	0.0067	-	0.0087
24	6.4E-05	6.4E-05	1.00 (0.52)		0.039	2.8E-05	2.4E-04	8.57 (3.02)		0.0013	0.0254

Table 6.38. Comparison of hepatic NF- κ B transcription in fed and fasted control and APAP treated C57BL/6J mice in a 36 h period using delta Ct value, $2^{-\Delta Ct}$ and the comparative Ct value, i.e. fold change as compared to **time-matched control** mice. The fold change values of APAP dosed C57BL/6J mice were also compared to APAP dosed CD-1 mice. *5- values of 5 h C57BL/6J was compared to 4 h CD-1 mice. In CD-1 mice only (*15- relative to 10 h post saline; *20- relative to 24 h post saline).

Fed										
Time (hpd)	Control		APAP				p-value control vs APAP	p-value vs APAP CD-1		
	Mean	SD	Mean	SD	Fold change	SD				
1	3.00E-04	7.00E-05	8.43E-05	7.63E-06	0.28	0.14	NS	NS		
3	5.00E-04	4.52E-04	1.67E-04	9.44E-05	0.33	0.14	NS	-		
*5	1.00E-04	2.80E-05	2.67E-04	1.19E-04	2.67	0.53	0.0490	NS		
10	2.00E-04	8.22E-05	1.13E-03	5.25E-04	5.66	1.77	0.0035	0.0030		
*15	4.00E-04	7.47E-05	2.77E-03	4.91E-04	6.92	1.54	0.0020	0.0052		
*20	6.00E-04	2.53E-04	2.11E-03	5.04E-04	3.52	1.33	0.0424	0.0001		
24	5.00E-04	1.17E-04	1.88E-03	7.15E-04	3.77	1.66	0.0280	0.0038		
36	6.00E-04	5.09E-05	2.83E-03	3.49E-04	4.71	0.97	0.0063	-		
Fasted										
Time (hpd)	Control		APAP				p-value control vs APAP	p-value fasted vs fed C57BL/6J	p-value vs APAP CD-1	
	Mean	SD	Mean	SD	Fold change	SD				
1	2.00E-04	1.40E-04	2.23E-04	6.13E-05	1.12	0.32	NS	NS	NS	
3	4.00E-04	3.62E-05	4.35E-04	5.43E-05	1.01	0.24	NS	NS	-	
*5	1.00E-04	8.65E-05	1.14E-04	2.97E-05	1.14	0.56	NS	NS	NS	
10	9.00E-05	5.00E-05	2.32E-04	1.82E-05	2.58	0.46	NS	0.0409	NS	
*15	1.40E-04	9.09E-05	5.85E-04	4.14E-05	4.18	0.56	0.0114	0.0253	NS	
*20	6.80E-04	1.26E-05	2.69E-03	4.30E-04	3.96	1.18	0.0203	NS	NS	
24	6.70E-04	2.33E-04	2.21E-03	7.31E-04	4.81	1.88	0.0417	NS	NS	
36	7.30E-04	1.88E-04	3.20E-03	1.03E-04	4.38	0.76	0.0084	NS	-	

Table 6.39. Comparison of hepatic NF- κ B transcription in fed and fasted control and APAP treated C57BL/6J mice in a 36 h period using delta Ct value, $2^{-\Delta Ct}$ and the comparative Ct value, i.e. fold change as compared to **pooled liver samples of the control** mice. The fold change values of APAP dosed C57BL/6J were also compared to APAP dosed CD-1 mice. *5- values of 5 h C57BL/6J was compared to 4 h CD-1 mice.

Fed									
Time (hpd)	Control		APAP		Fold change	SD	p-value control vs APAP	p-value vs APAP CD-1	
	Mean	SD	Mean	SD					
1	4.0E-04	1.35E-04	8.43E-05	7.63E-06	0.21	0.14	NS	NS	
3			1.67E-04	9.44E-05	0.42	0.11	NS	NS	
*5			2.67E-04	1.19E-04	0.67	0.34	NS	NS	
10			1.13E-03	5.25E-04	2.83	0.96	0.0303	0.0003	
15			2.77E-03	4.91E-04	6.93	1.54	0.0015	NS	
20			2.11E-03	5.04E-04	5.28	1.95	0.0075	0.0256	
24			1.88E-03	7.15E-04	4.70	2.06	0.0083	NS	
36			2.83E-03	3.49E-04	7.08	2.97	0.0097	-	
Fasted									
Time (hpd)	Control		APAP		Fold change	SD	p-value control vs APAP	p-value vs APAP CD-1	p-value fasted vs fed C57BL/6J
	Mean	SD	Mean	SD					
1	3.5E-04	1.0E-04	2.23E-04	6.13E-05	0.64	0.25	NS	NS	NS
3			4.35E-04	5.43E-05	1.25	0.59	NS	NS	NS
*5			1.14E-04	2.97E-05	0.33	0.28	NS	NS	NS
10			2.32E-04	1.82E-05	0.66	0.30	NS	NS	0.0052
15			5.85E-04	4.14E-05	1.68	0.44	NS	NS	0.0036
20			2.69E-03	4.30E-04	7.71	2.68	0.0011	NS	NS
24			2.21E-03	7.31E-04	6.33	3.55	0.0066	NS	NS
36			3.20E-03	1.03E-04	9.17	4.04	0.0058	-	NS

Table 6.40. Comparison of hepatic cyclin-D1 transcription in fed and fasted control and APAP treated C57BL/6J mice in a 36 h period using delta Ct value, $2^{-\Delta Ct}$ and the comparative Ct value, i.e. fold change as compared to **time-matched control** mice. The fold change values of APAP dosed C57BL/6J mice were also compared to APAP dosed CD-1 mice. *5- values of 5 h C57BL/6J was compared to 4 h CD-1 mice; In CD-1 mice only (*15- relative to 10 h post saline; *20- relative to 24 h post saline).

Fed											
Time (hpd)	Control				APAP				p-value control vs APAP	p-value vs APAP CD-1	
	Mean	SD	Fold change	SD	Mean	SD	Fold change	SD			
1	1.60E-07	7.24E-08	0.36	0.13	4.27E-08	5.44E-09	0.27	0.07	NS	NS	
3	9.60E-08	2.48E-08	3.45	2.94	8.99E-08	2.32E-08	0.94	0.14	NS	-	
*5	2.50E-07	4.51E-08	1.36	1.19	3.94E-07	5.03E-08	1.57	0.09	NS	0.0064	
10	1.30E-07	5.40E-08	1.85	1.08	3.37E-07	6.26E-08	2.59	0.26	NS	NS	
*15	9.54E-08	4.43E-08	1.26	0.22	8.58E-07	1.39E-07	8.99	1.95	0.0012	NS	
*20	8.21E-08	8.13E-08	1.14	0.77	4.91E-07	8.18E-08	5.98	0.64	0.0011	0.0017	
24	1.70E-07	5.33E-08	0.65	0.64	1.12E-06	3.03E-07	6.62	1.74	0.0093	0.0069	
36	1.48E-07	6.66E-08	1.24	0.70	7.97E-07	2.03E-07	5.37	1.53	0.0070	-	
Fasted											
Time (hpd)	Control				APAP				p-value control vs APAP	p-value fasted vs fed C57BL/6J	p-value vs APAP CD-1
	Mean	SD	Fold change	SD	Mean	SD	Fold change	SD			
1	5.7E-08	1.50E-08	0.36	0.13	3.10E-08	3.10E-09	0.54	0.21	NS	NS	NS
3	3.31E-07	8.61E-08	3.45	2.94	1.09E-07	2.02E-08	0.33	0.23	NS	NS	-
*5	3.40E-07	8.84E-08	1.36	1.19	6.18E-07	7.72E-08	1.82	0.83	NS	NS	NS
10	2.40E-07	8.90E-08	1.85	1.08	1.96E-07	5.09E-08	0.82	0.25	NS	0.0155	NS
*15	1.20E-07	3.12E-08	1.26	0.22	1.31E-07	7.51E-08	1.09	0.69	NS	0.0036	0.0070
*20	9.38E-08	2.44E-08	1.14	0.77	1.93E-07	5.02E-08	2.06	0.25	NS	0.0445	0.0057
24	1.10E-07	9.50E-08	0.65	0.64	3.50E-07	9.11E-08	3.18	0.98	0.0180	0.0301	0.0280
36	1.83E-07	5.17E-08	1.24	0.70	8.37E-07	2.18E-07	4.58	1.69	0.0106	NS	-

Table 6.41. Comparison of hepatic cyclin-D1 transcription in fed and fasted control and APAP treated C57BL/6J mice in a 36 h period using delta Ct value, $2^{-\Delta Ct}$ and the comparative Ct value, i.e. fold change as compared to **pooled liver samples of the control** mice. The fold change values of APAP dosed C57BL/6J mice were also compared to APAP dosed CD-1 mice. *5- values of 5 h C57BL/6J was compared to 4 h CD-1 mice. hpd – hours post dosing; SD – standard deviation; NS not significant.

Fed									
Time (hpd)	Control		APAP		Fold change	SD	p-value control vs APAP	p-value vs APAP CD-1	
	Mean	SD	Mean	SD					
1	1.6E-07	4.96E-08	4.27E-08	5.44E-09	0.27	0.07	NS	NS	
3			8.99E-08	2.32E-08	0.57	0.12	NS	-	
*5			3.9E-07	5.03E-08	2.48	0.29	NS	0.0005	
10			3.4E-07	6.26E-08	2.12	0.19	NS	0.0073	
15			8.6E-07	1.39E-07	5.39	1.88	0.0093	NS	
20			4.9E-07	8.18E-08	3.09	0.60	0.0480	0.0001	
24			1.1E-06	3.03E-07	7.04	2.32	0.0069	NS	
36			8.0E-07	2.03E-07	5.01	1.30	0.0135	-	
Fasted									
Time (hpd)	Control		APAP		Fold change	SD	p-value control vs APAP	p-value vs APAP CD-1	p-value fasted vs fed C57BL/6J
	Mean	SD	Mean	SD					
1	1.95E-07	5.69E-08	3.10E-08	3.1E-09	0.16	0.12	NS	NS	NS
3			1.09E-07	2.02E-08	0.56	0.30	NS	-	NS
*5			6.18E-07	7.72E-08	3.17	1.19	NS	NS	NS
10			1.96E-07	5.09E-08	1.01	0.78	NS	NS	NS
15			1.31E-07	7.51E-08	0.67	0.45	NS	0.0002	0.0066
20			1.93E-07	5.02E-08	0.99	0.20	NS	0.0127	0.0211
24			3.5E-07	9.11E-08	1.80	0.87	NS	0.0068	0.0061
36			8.37E-07	2.18E-07	4.29	1.51	0.0079	-	NS

Table 6.42. A summary comparison of the examined parameters for the assessment of APAP hepatotoxicity in **fed and fasted C57BL/6J mice** (5-36 hpd). Statistically significant differences were observed between the fasted and fed mice that had received APAP intraperitoneally. Hepatic or splenic mRNA levels were summarised based on fold change relative to pooled control animals. *P<0.005, <0.01 or <0.05.

	Time (hours post APAP dosing)											
	5		10		15		20		24		36	
	Fed	Fast	Fed	Fast	Fed	Fast	Fed	Fast	Fed	Fast	Fed	Fast
Hepatic GSH	17.8 (9)	4.2 (0.7)*	31 (6.5)	13.7(6.9)*	38 (2.8)	22 (6.5)*	61.3 (11)	36.5 (16.5)*	69.8 (7.9)	29.9(3.8)*	75.5 (13)	72.4 (1.4)
Hepatic ATP	5.0 (2.5)	3.27 (2.0)	14 (3.3)	3.5 (2.2)*	21 (3.5)	3.2 (1.6)*	29.4 (4.8)	2.5 (1.6)*	26.7 (5.4)	-	29.5 (2.0)	4.48(2.3)*
Fold change												
1- GSH	0.21	-	0.78	0.17	0.81	0.18	1.15	0.48	0.85	0.78	1.25	0.82
2- ATP	0.18	-	0.50	0.25	0.75	0.16	0.97	0.10	1.00	-	1.21	0.16*
Serum ALT	2056.8 (214.5)	2240.8 (425)	2066.6 (79.6)	1972.96 (836)	1964.1 (246)	3064.2 (91.18)*	2598.3 (217.2)	3886.1 (501.1)*	2709.5 (231.7)	3597 (299.5)*	1763.9 (539)	3518.3 (805.5)*
HE score	2.75 (1.22)	3.25 (0.5)	1.5 (0.5)	2.13 (0.75)	2.17 (0.58)	1.75 (0.29)	1.3 (0.61)	2.0 (0.74)*	1.15 (0.47)	2.1 (0.14)*	0.8 (0.13)	1.5 (0)
TNF- α												
1- Liver	11.7(4.8)	1.5(0.9)*	2.2(1.2)	3.1(2.0)	0.9(0.6)	0.7(0.6)	1.5(0.3)	2.3(1.1)*	0.6(0.1)	4.2(1.4)*	1.4 (0.6)	3.8(1.1)*
2- Spleen	2.9(0.9)	1.5(0.7)	-	-	-	-	-	-	0.2(0.19)	9.38(3.0)*	-	-
3- Serum	74.4(7)	124(24)	104(17)	122(18.9)	95(31.7)	144(27)	72 (10.3)	212(5.3)*	75.9(7.9)	250(40)*	56.3(0.9)	227(22)*
IL-6												
1- Liver	2.3(1.5)	1.1(0.7)	3.7(1.1)	1.4(0.3)	5.2(2.1)	1.8(0.3)*	2.8(1.0)	4.5(1.2)	7.0(1.9)	3.0(1.4)*	7.2(2.2)	3.5(0.5)*
2- Spleen	7.9(2.1)	2.0(0.7)*	-	-	-	-	-	-	1.0(0.5)	8.6(3.0)*	-	-
3- Serum	61.7(6)	56.3(12)	112(25)	40.3(35)	105(19)	52(15.4)*	240(18)	103.2(23)*	229(38)	94(35.7)*	180(24)	131 (51)
Hepatic IL-10	0.8(0.3)	1.8(0.5)	3.1(0.9)	1.7(0.3)	12.6(3.4)	3.0(1.5)*	12.1(4.1)	3.0(1.0)*	7.2(1.2)	3.7(1.9)	9.5(3.6)	6.2(2.1)
Hepatic NF-kB	0.7(0.5)	0.3(0.3)	2.8(1.0)	0.7(0.3)*	6.9(1.5)	1.7(0.4)*	5.3(2.0)	7.7(2.7)	4.7(2.1)	6.3(3.6)*	7.1(3.0)	9.2(4.0)
Hepatic cyclin-D1	2.5(0.3)	3.2(1.2)	2.1(0.2)	1.0 (0.8)*	5.4(1.9)	0.7(0.5)*	3.1(0.6)	1.0 (0.2)*	7.0(2.3)	1.8(0.9)*	5.0(1.3)	4.3(1.5)
IH PCNA (%)												
1- Overall	2.1(1.8)	1.2(0.3)	5.5(1.2)	2.8(2.3)	8.0(1.7)	1.0(0.1)*	19.5(0.8)	6.0(2.4)*	23.2(2.0)	13.0(6.6)*	25(7.5)	12.7(2.7)*
2- Cyto	0.2(0.1)	0.1(0.1)	1.4(0.4)	0.2(0.2)*	0.5(0.1)	0.3(0.1)	0.8(0.3)	1.7(0.5)*	1.1(0.2)	0.9(0.9)	0.5(0.3)	0.1(0.1)

Table 6.43. A summary comparison of the examined parameters for the assessment of APAP hepatotoxicity in **fed and fasted CD-1 and C57BL/6J mice** at *5, 10 and 24 hpd. Statistically significant differences were observed between CD-1 and C57BL/6J mice that had received APAP intraperitoneally in either fed or fasted groups. Hepatic and/or splenic mRNA levels were summarised based on fold change relative to pooled control animals. *5- values of 5 h C57BL/6J was compared to 4 h CD-1 mice for measurement of hepatic and/or splenic TNF- α , IL-6, IL-10, NF-kB and cyclin-D1. *P<0.005, <0.01 or <0.05.

	Time (hours post APAP dosing)											
	*5				10				24			
	Fed		Fasted		Fed		Fasted		Fed		Fasted	
	CD-1	C57BL/6J	CD-1	C57BL/6J	CD-1	C57BL/6J	CD-1	C57BL/6J	CD-1	C57BL/6J	CD-1	C57BL/6J
Hepatic GSH	4.95 (0.56)	17.8 (9)	4.47 (3.6)	4.2 (0.7)	40 (0.7)	31 (6.5)	5.28 (1.2)	13.7 (6.9)	45.5(10)	69.8 (7.9)*	50.6 (25)	29.9 (3.8)
Hepatic ATP	10.5 (2.3)	5.0 (2.5)*	3.5 (4.9)	-	18 (5.7)	14 (3.3)	3.4 (1.2)	3.5 (2.2)	35.4 (3.9)	26.7 (5.4)	8.1 (1.3)	-
Fold change												
1- GSH	0.14	0.21	0.09	-	1.96	0.78*	0.06	0.17	0.96	0.85	0.33	0.78
2- ATP	0.30	0.18	0.20	-	0.61	0.50	0.25	0.25	1.07	1.00	0.49	-
Serum ALT	2146.4 (1012.3)	2056.8 (214.5)	2048.6 (461.7)	2240.8 (425)	-	2066.6 (79.6)	-	1972.96 (836)	2654.5 (334.5)	2709.5 (231.7)	3603.8 (508.8)	3597 (299.5)
HE score	2.44 (1.25)	2.75 (1.22)	2.5 (1.41)	3.3 (0.5)	1 (0.89)	1.5 (0.5)	2.6 (0.42)	2.13 (0.8)	0 (0)	1.15(0.5)*	2.38(0.7)	2.1(0.14)
TNF- α												
1- Liver	4.4(0.7)	11.7(4.8)*	2.3 (0.6)	1.5(0.9)*	7.9 (2.7)	2.2(1.2)*	6.8 (2.4)	3.1(2.0)*	1.77(0.8)	0.6(0.1)	1.5 (0.5)	4.2(1.4)*
2- Spleen	-	2.9(0.9)	-	1.5(0.7)	4.4 (1.8)	-	4.9 (2.0)	-	1.2(0.6)	0.2(0.19)	3.2 (0.8)	9.38(3.0)*
3- Serum	62 (13.5)	74.4(7)	101.2(40)	124(24)	-	104(17)	-	122(18.9)	95 (14)	75.9(7.9)	228 (54)	250(40)
IL-6												
1- Liver	6.0 (1.9)	2.3(1.5)*	4.7 (1.7)	1.1(0.7)	7.9 (0.8)	3.7(1.1)*	2.2 (1.0)	1.4(0.3)	7.6 (2.7)	7.0(1.9)	7.4 (3.1)	3.0(1.4)
2- Spleen	-	7.9(2.1)	-	2.0(0.7)	1.9 (0.3)	-	1.0 (0.6)	-	3.7(1.2)	1.0(0.5)*	1.1 (0.4)	8.6(3.0)*
3- Serum	54.3(10)	61.7(6)	35.4(11)	56.3(12)	-	112(25)	-	40.3(35)	203(40)	229(38)	96(35.2)	94(35.7)
Hepatic IL-10	3.9 (1.5)	0.8(0.3)*	1.5 (1.2)	1.8(0.5)	9.0 (2.9)	3.1(0.9)*	1.8 (0.9)	1.7(0.3)	8.8 (1.3)	7.2(1.2)	5.2 (3.9)	3.7(1.9)
Hepatic NF-kB	2.1 (0.4)	0.7(0.5)	2.1 (1.3)	0.3(0.3)	13.3(3.1)	2.8(1.0)*	1.5 (1.6)	0.7(0.3)	6.1 (1.1)	4.7(2.1)	4.7 (1.3)	6.3(3.6)
Hepatic cyclin-D1	8.1 (1.3)	2.5(0.3)*	4.0 (1.8)	3.2(1.2)	8.7 (2.5)	2.1(0.2)*	4.2 (2.0)	1.0 (0.8)*	9.6 (1.1)	7.0(2.3)	6.0 (1.2)	1.8(0.9)*
IH PCNA (%)												
1- Overall	15.62	2.1(1.8)*	3.23	1.2(0.3)	7.71	5.5(1.2)	2.98	2.8(2.3)	15.02	23.2(2.0)	8.36	13.0(6.6)
2- Cyto	1.02	0.2(0.1)*	1.46	0.1(0.1)	0.27	1.4(0.4)*	0.06	0.2(0.2)	0.94	1.1(0.2)	0.92	0.9(0.9)

